
Evaluation and improvement of the sPC-SAFT equation of state for complex mixtures

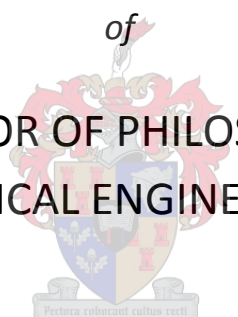
by

Adriaan Jacobus de Villiers

Dissertation presented for the Degree

of

DOCTOR OF PHILOSOPHY
(CHEMICAL ENGINEERING)



in the Faculty of Engineering
at Stellenbosch University

Supervisor

Prof. A.J. Burger

December 2011

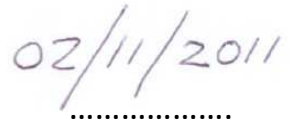
Declaration

By submitting this dissertation electronically, I declare that the entirety of the work contained therein is my own, original work, that I am the sole author thereof (save to the extent explicitly otherwise stated), that reproduction and publication thereof by Stellenbosch University will not infringe any third party rights and that I have not previously in its entirety or in part submitted it for obtaining any qualification.



.....

Signature



.....

Date

Copyright © 2011 Stellenbosch University

All rights reserved

Abstract

Efficient process design commonly relies on equation-of-state (EOS) models to provide reliable estimates of thermodynamic properties. The accuracy of EOS models, in turn, depends on the extent to which they account for intermolecular forces. The aim of this project was to improve the simplified Perturbed Chain - Statistical Associating Fluid Theory (sPC-SAFT), enabling it to account more accurately for complex molecular interactions. The more simple SAFT-based Cubic-Plus-Association (CPA) model was evaluated along similar lines for comparative purposes.

A literature review showed that both sPC-SAFT and CPA have been widely applied in phase equilibria problems, but not extensively for the prediction of other thermodynamic properties. Consequently, an initial evaluation was performed on the ability of sPC-SAFT and CPA to predict first- and second-order thermodynamic properties. The properties of non-polar, polar and hydrogen bonding fluids were considered, showing that:

- a) sPC-SAFT and CPA generally predict first-order properties with the same accuracy, but sPC-SAFT provides improved predictions of second-order properties. Significant errors are, however, still observed with sPC-SAFT.
- b) A parameter regression study with sPC-SAFT, using model parameters obtained by including second-order properties in the regression function, results in poor predictions of the saturated vapour pressure and liquid density.
- c) Treating strong polar and dispersive forces together as *Van der Waals* forces results in many properties being poorly predicted by both sPC-SAFT and CPA.
- d) The major limitation of the association term in both CPA and sPC-SAFT is its inability to account for the influence of bond co-operativity, especially in alcohol/water mixtures.

Based on these findings, the following improvements could be made:

- a) The development of a new association scheme for 1-alcohols, denoted the 2C association scheme.
- b) The extension of sPC-SAFT with the polar theories of *Jog & Chapman* (JC) and *Gross & Vrabec* (GV) to obtain sPC-SAFT-JC and sPC-SAFT-GV.
- c) The extension of CPA with modified versions of the aforementioned polar theories to obtain CPA-JC and CPA-GV.
- d) The development of a new 'universal' cross-association approach.

The new 2C association scheme consists of one bipolar association site and one negative electron donor site and is a combination of the 1A and 2B/3B association schemes. Modelling 1-alcohols with the 2C scheme in sPC-SAFT results in improved VLE predictions of alcohol/water and alcohol/alcohol mixtures, but alcohol/alkane VLE is predicted less accurately compared to the 2B and 3B association schemes.

sPC-SAFT-JC and sPC-SAFT-GV provide improved VLE predictions of mixtures with non-associating polar components compared to sPC-SAFT. VLE of polar/alkane and polar/polar systems can be represented accurately with no or only very small binary interaction parameters (BIPs). CPA-JC and CPA-GV also enable improved VLE predictions of the polar/alkane and polar/polar mixtures compared to CPA. sPC-SAFT-GV and sPC-SAFT-JC were also applied to several mixtures of associating components including alcohol/alkane, alcohol/alcohol and alcohol/water systems. New alcohol model parameters for both sPC-SAFT-GV and sPC-SAFT-JC based on the 2C, 2B and 3B association schemes were determined. The predictions of both sPC-SAFT-GV and sPC-SAFT-JC, based on any of the three association schemes, provide similar alcohol/alkane and alcohol/alcohol VLE representations, but the best phase equilibria predictions of water/alcohol systems are obtained when alcohols are modelled with the newly proposed 2C association scheme.

The usefulness of a new ‘universal’ cross-association approach was demonstrated with both sPC-SAFT-GV and sPC-SAFT-JC. The philosophy behind the new approach is to set the association volume value of the solvating component equal to the cross-associating volume value of the 1-alcohol of the same molecular size and to determine an association energy value from binary VLE data. This approach aims to characterize the solvating behaviour of the cross-associating component. Preliminary results are demonstrated with systems containing acetone, propyl formate and ethyl acetate.

Other thermodynamic properties, such as excess enthalpy and excess volume can be described with the new polar sPC-SAFT and CPA models. In the majority of cases, improvements are observed compared to the normal sPC-SAFT and CPA models, but BIPs are still required to obtain accurate correlations. However, these BIPs cannot be used in phase equilibria calculations and are generally property-specific.

To summarise: Through the development of the 2C scheme, and the incorporation of polar terms into the sPC-SAFT model structure, notable improvement in the VLE predictions of polar (non-hydrogen bonding)/alkane, alcohol/alkane, alcohol/water and polar/alcohol systems could be obtained if compared to the original sPC-SAFT EOS. As such, the research presented in this thesis encapsulates some significant novel contributions, viz.:

- a) A systematic evaluation of sPC-SAFT and CPA, providing better insight into their ability to predict thermodynamic properties.
- b) The development of the new 2C association scheme for 1-alcohols, as published in *Ind. Eng. Chem. Res.* **2011**, 50, 8711–8725.
- c) The extension of sPC-SAFT with the polar theories of JC and GV, with application to non-associating components, as published in *Fluid Phase Equilib.* **2011**, 305, 174–184.
- d) The extension of CPA with the JC and GV polar theories, as published in *Fluid Phase Equilib.* **2011**, 312, 66–78.
- e) The application of sPC-SAFT-GV and sPC-SAFT-JC to associating components, including results with the new 2C association scheme.
- f) The development of the new ‘universal’ cross-association approach.

Opsomming

Doeltreffende prosesontwerp steun grotendeels op toestandvergelykings (EOS) om goeie skattings van vloeistofeienskappe te voorspel. Die akkuraatheid van hierdie modelle word bepaal deur hoe goed hulle die invloed van molekulêre kragte kan naboots. Die doel van hierdie projek was dus om die 'simplified Perturbed Chain-Statistical Associating Fluid Theory' (sPC-SAFT) te verbeter, sodat dit komplekse molekulêre kragte beter kan beskryf. Die meer vereenvoudigde SAFT-gebaseerde 'Cubic-Plus-Association' (CPA) model was ook geëvalueer vir vergelykende doeleindes.

'n Literatuurstudie het getoon dat beide sPC-SAFT en CPA reeds wyd toegepas is in fase ewewig probleme, maar nie vir ander termodinamiese eienskappe nie. Gevolglik, is 'n aanvanklike ondersoek uitgevoer waarin die vermoë van sPC-SAFT en CPA om eerste- en tweede-orde termodinamiese eienskappe te voorspel, geëvalueer is. Die eienskappe van nie-polêre, polêre en waterstof-bindende komponente is oorweeg en die hoof bevindinge uit hierdie ondersoek is:

- a) sPC-SAFT en CPA voorspel oor die algemeen eerste-orde eienskappe met dieselfde akkuraatheid, maar sPC-SAFT bied verbeterde voorspellings van tweede-orde eienskappe. Beduidende foute is egter steeds teenwoordig in die voorspellings van sPC-SAFT.
- b) 'n Model parameter regressie studie met sPC-SAFT het getoon dat deur tweede-orde eienskappe ook in die regressie-funksie in te sluit, swak skattings van die eienskappe wat nodig is vir 'n goeie fase-ewewig voorspellings, verkry word.
- c) Die gesamentlike behandeling van sterk polêre en dispersie kragte as *Van der Waals* kragte, lei tot swak voorspellings van baie eienskappe deur sPC-SAFT en CPA.
- d) Die hoof beperking van die assosiasie term wat gebruik word deur beide CPA en sPC-SAFT, is die term se onbekwaamheid om die invloed van verbinding-samewerkings te beskryf, veral in mengsels van alkohole met water.

Hierdie bevindings het as basis gedien om die volgende verbeterings aan te bring:

- a) Die ontwikkeling van 'n nuwe assosiasie skema vir 1-alkohole: die 2C-assosiasie skema.
- b) Die uitbreiding van sPC-SAFT met die polêre teorieë van *Jog & Chapman* (JC) en *Gross & Vrabec* (GV) om sPC-SAFT-JC en sPC-SAFT-GV onderskeidelik te kry.
- c) Die uitbreiding van CPA met gewysigde weergawes van die polêre teorieë om CPA-JC en CPA-GV te kry.
- d) Die ontwikkeling van 'n nuwe 'universele' kruis-assosiasie benadering.

Die nuut-voorgestelde 2C assosiasie skema bestaan uit een bipolêre assosiasie sone en een negatiewe elektron skenker sone en is 'n kombinasie van die 1A en 2B/3B assosiasie skemas. Die modellering van 1-alkohole met die 2C skema in sPC-SAFT lei tot 'n verbetering in damp-vloeistof ewewig (VLE) voorspellings van alkohol/water en alkohol/alkohol sisteme, maar vir alkohol/alkaan sisteme is minder akkurate voorspellings verkry in vergelyking met die 2B en 3B assosiasie skemas.

sPC-SAFT-JC en sPC-SAFT-GV lewer beter VLE voorspellings van mengsels met nie-assosiërende polêre komponente in vergelyking met sPC-SAFT. Die VLE van polêre/alkaan en polêre/polêre stelsels kan akkuraat beskryf word deur beide modelle wanneer geen of baie klein binêre interaksie parameters (BIPs) gebruik word. CPA-JC en CPA-GV lewer ook verbeterde VLE voorspellings van polêre/alkaan en polêre/polêre mengsels in vergelyking met CPA. sPC-SAFT-GV en sPC-SAFT-JC is ook toegepas op verskeie assosiërende mengsels, insluitend: alkohol/alkaan, alkohol/alkohol en alkohol/water stelsels. Nuwe alkohol parameters is vir beide sPC-SAFT-GV en sPC-SAFT-JC bepaal gebaseer op die 2C, 2B en 3B assosiasie skemas. Die voorspellings van sPC-SAFT-GV en sPC-SAFT-JC, gebaseer op enigeen van die drie assosiasie skemas, lewer soortgelyke alkohol/alkaan en alkohol/alkohol VLE voorspellings, maar die beste fase-ewewig voorspellings vir water/alkohol sisteme is verkry wanneer alkohole gemodelleer word met die 2C assosiasie skema.

Die nuwe 'universele' kruis-assosiasie benadering is gedemonstreer met beide sPC-SAFT-GV en sPC-SAFT-JC. Die filosofie agter die nuwe benadering is om die assosiasie volume waarde van die solverende komponent gelyk te stel aan die kruis-assosiasie volume waarde van die 1-alkohol met dieselfde molekulêre massa. Die assosiasie energie waarde word dan bepaal vanaf binêre VLE data. Hierdie benadering poog om die solverende gedrag van die kruis-assosiërende komponent meer akkuraat te karakteriseer. Voorlopige resultate met mengsels van asetoon, propiel formaat en etiel asetaat dui aan dat merkwaardige verbeterings in VLE voorspellings gekry word.

Ander termodinamiese eienskappe, soos oortollige entalpie en oortollige volume, is ook ondersoek met die nuwe polêre sPC-SAFT en CPA-modelle. In meeste gevalle word verbeterde resultate gekry in vergelyking met die oorspronklike sPC-SAFT en CPA modelle, maar groot BIPs word steeds benodig om aanvaarbare korrelasies te kry. Hierdie BIPs kan egter nie gebruik word vir fase-ewewig voorspellings nie en is eienskap-spesifiek.

Om op te som: deur die ontwikkeling van die 2C skema, en insluiting van die polêre terme in die sPC-SAFT model struktuur, is merkwaardige verbeterings in die VLE voorspellings van polêre/alkaan, alkohol/alkaan, alkohol/water en polêre/alkohol sisteme gekry in vergelyking met die oorspronklike sPC-SAFT EOS. Die navorsing voorgelê in hierdie tesis het dus gelei tot die volgende nuwe bydraes:

- a) Die sistematiese evaluering van die vermoë van sPC-SAFT en CPA om termodinamiese eienskappe te voorspel.
- b) Die ontwikkeling van die nuwe 2C assosiasie skema vir 1-alkohole soos gepubliseer in *Ind. Eng. Chem. Res.* **2011**, 50, 8711–8725.
- c) Die uitbreiding van sPC-SAFT met die polêre teorieë van JC en GV soos gepubliseer in *Fluid Phase Equilib.* **2011**, 305, 174–184.
- d) Die uitbreiding van CPA met die polêre teorieë van JC en GV soos gepubliseer in *Fluid Phase Equilib.* **2011**, 312, 66–78.
- e) Die toepassing van hierdie nuwe modelle op assosiërende komponente, insluitend resultate met die nuwe 2C skema.
- f) Die ontwikkeling van 'n nuwe kruis-assosiasie benadering.

Acknowledgements

The financial assistance of Sasol Technology (Pty) Ltd towards this research is hereby acknowledged. Opinions expressed and conclusions arrived at are those of the author and are not necessarily to be attributed to the sponsors.

The author would like to thank the following people who greatly assisted the work presented in this thesis:

- Prof. A.J. Burger, for his excellent supervision and guidance.
- Dr. C.E. Schwarz, for her invaluable help and encouragement.
- Prof. G.M. Kontogeorgis, for his many insightful discussions.
- Dr. C. Crause, for suggesting the project and assisting in the coding of the program.
- My wife, Inge, for all her love, support, encouragement and patience.
- My parents, for their continual encouragement and love.
- Lord Jesus, for giving me the ability and helping me to do the work.

Table of contents

CHAPTER 1	INTRODUCTION	1
1.1	PROJECT RELEVANCE AND PROBLEM STATEMENT.....	1
1.2	INTRODUCTION TO SAFT	3
1.2.1	TRADITIONAL EOS MODELS	3
1.2.2	THE SAFT-APPROACH	5
1.3	OBJECTIVES AND AIMS	6
1.4	SCOPE AND LIMITATIONS	7
1.4.1	EOS MODELS CONSIDERED	7
1.4.2	COMPONENTS CONSIDERED	7
1.4.3	THERMODYNAMIC REGION	8
1.5	THESIS LAYOUT AND SIGNIFICANT CONTRIBUTIONS	8
CHAPTER 2	LITERATURE REVIEW	11
2.1	PC-SAFT AND SIMPLIFIED PC-SAFT.....	11
2.1.1	CONCEPT.....	11
2.1.2	MODEL DESCRIPTION.....	12
2.1.3	APPLICATION OF PC-SAFT AND SPC-SAFT	19
2.1.4	SHORTCOMINGS OF PC-SAFT AND SPC-SAFT	21
2.2	CUBIC-PLUS-ASSOCIATION (CPA)	22
2.2.1	CONCEPT.....	22
2.2.2	MODEL DESCRIPTION.....	23
2.2.3	APPLICATION OF CPA.....	25
2.2.4	SHORTCOMINGS OF CPA	27
2.3	ACCOUNTING FOR CROSS-ASSOCIATION IN SAFT MODELS.....	27
2.4	SIGNIFICANCE OF PARAMETER REGRESSION AND FITTING PROCEDURES	29
2.4.1	RELATIONSHIPS BETWEEN PROPERTIES AND PARTIAL DERIVATIVE OF THE STATE FUNCTION.....	29
2.4.2	DATA IN CURRENT REGRESSION PROCEDURES.....	31
2.5	CHAPTER SUMMARY	34
CHAPTER 3	MODELLING PROPERTIES OF PURE COMPONENTS	37
3.1	PURE COMPONENT PARAMETERS USED.....	38
3.2	NON-POLAR COMPONENTS	39
3.2.1	MASS DENSITY	41
3.2.2	PRESSURE-VOLUME DERIVATIVE	43
3.2.3	ISOTHERMAL HEAT CAPACITY	45

3.2.4	ISOBARIC HEAT CAPACITY	48
3.2.5	PRESSURE-TEMPERATURE DERIVATIVE	50
3.2.6	HEAT CAPACITY RATIO	52
3.2.7	SPEED OF SOUND	53
3.2.8	SECTION HIGHLIGHTS.....	54
3.3	POLAR (NON-HB) COMPONENTS	55
3.3.1	MASS DENSITY	56
3.3.2	PRESSURE-VOLUME DERIVATIVE	57
3.3.3	ISOBARIC HEAT CAPACITY	58
3.3.4	PRESSURE-TEMPERATURE DERIVATIVE	59
3.3.5	SPEED OF SOUND	60
3.3.6	SECTION HIGHLIGHTS.....	62
3.4	HYDROGEN BONDING COMPONENTS.....	62
3.4.1	MASS DENSITY	64
3.4.2	PRESSURE-VOLUME DERIVATIVE	67
3.4.3	ISOCORIC HEAT CAPACITY	69
3.4.4	ISOBARIC HEAT CAPACITY	70
3.4.5	PRESSURE-TEMPERATURE DERIVATIVE	73
3.4.6	HEAT CAPACITY RATIO	74
3.4.7	SPEED OF SOUND	75
3.4.8	SECTION HIGHLIGHTS.....	77
3.5	LIMITS OF PARAMETER REGRESSION WITH SPC-SAFT	78
3.6	CHAPTER SUMMARY	82
3.6.1	OVERVIEW OF COMPARISON BETWEEN MODELS	82
3.6.2	CHAPTER HIGHLIGHTS	84
CHAPTER 4	MODELLING PROPERTIES OF BINARY MIXTURES	87
4.1	NON-POLAR/NON-POLAR SYSTEMS.....	87
4.1.1	MASS DENSITY	88
4.1.2	EXCESS VOLUME	88
4.1.3	EXCESS ENTHALPY	90
4.1.4	EXCESS ISOBARIC HEAT CAPACITY	92
4.1.5	SECTION HIGHLIGHTS.....	92
4.2	NON-POLAR/POLAR (NON-HB) SYSTEMS	93
4.2.1	MASS DENSITY	93
4.2.2	EXCESS VOLUME	94
4.2.3	EXCESS ENTHALPY	97
4.2.4	SECTION HIGHLIGHTS.....	97
4.3	NON-POLAR/HYDROGEN BONDING SYSTEMS.....	98
4.3.1	MASS DENSITY	98
4.3.2	EXCESS VOLUME	99
4.3.3	EXCESS ENTHALPY	101
4.3.4	ISOBARIC HEAT CAPACITY	102
4.3.5	EXCESS ISOBARIC HEAT CAPACITY	103

4.3.6	SECTION HIGHLIGHTS.....	104
4.4	HYDROGEN BONDING / HYDROGEN BONDING SYSTEMS.....	104
4.4.1	MASS DENSITY	105
4.4.2	EXCESS VOLUMES.....	109
4.4.3	EXCESS ENTHALPY	109
4.4.4	SPEED OF SOUND	111
4.4.5	EXCESS ISOBARIC HEAT CAPACITY	112
4.4.6	SECTION HIGHLIGHTS.....	114
4.5	CHAPTER SUMMARY	115
<u>CHAPTER 5 IMPROVEMENT OF SPC-SAFT</u>		<u>117</u>
5.1	POSSIBLE AREAS OF IMPROVEMENT	117
5.1.1	ACCOUNTING FOR POLAR FORCES	117
5.1.2	DESCRIPTION OF HYDROGEN BONDING BETWEEN WATER AND ALCOHOLS	117
5.1.3	DEFICIENCY IN TEMPERATURE DEPENDENCY OF MODELS	118
5.1.4	IMPROVEMENT OF THE REFERENCE TERM	118
5.2	SCOPE OF PROJECT	119
<u>CHAPTER 6 A NEW ASSOCIATION SCHEME FOR ALCOHOLS</u>		<u>121</u>
6.1	CURRENT STATUS OF SPC-SAFT IN PREDICTING PHASE EQUILIBRIUM OF ALCOHOL/WATER SYSTEMS.....	122
6.2	DEVELOPMENT OF A NEW ASSOCIATION SCHEME	123
6.3	MODEL PARAMETERS.....	126
6.4	VLE AND VLE OF ALCOHOL/WATER MIXTURES	129
6.5	VLE OF ALCOHOL/ALCOHOL MIXTURES	134
6.6	VLE AND LLE OF ALCOHOL/<i>N</i>-ALKANE MIXTURES.....	137
6.7	MULTI-COMPONENT PHASE EQUILIBRIA.....	141
6.8	CHAPTER SUMMARY.....	143
6.8.1	SCIENTIFIC CONTRIBUTION	144
<u>CHAPTER 7 EXTENDING SPC-SAFT AND CPA WITH DIPOLAR TERMS: APPLICATION TO NON-ASSOCIATING COMPONENTS</u>		<u>145</u>
7.1	PERTURBATION THEORY FOR DIPOLAR FLUIDS	146
7.1.1	MOLECULAR-APPROACH AND SEGMENT-APPROACH	146
7.1.2	JOG AND CHAPMAN'S POLAR (JC).....	147
7.1.3	GROSS AND VRABEC'S DIPOLAR (GV).....	150
7.2	APPLICATION AND SHORTCOMINGS OF POLAR TERMS.....	153
7.2.1	PHASE EQUILIBRIA.....	153
7.2.2	OTHER THERMODYNAMIC DERIVATIVE PROPERTIES	154
7.2.3	SHORTCOMINGS OF POLAR TERMS	155
7.3	REGRESSION AND MODEL PARAMETER DETERMINATION	156
7.3.1	METHOD AND DATA INCLUDED.....	156

7.3.2	NEW MODEL PARAMETERS FOR SPC-SAFT-GV AND SPC-SAFT-JC.....	157
7.3.3	NEW MODEL PARAMETERS FOR CPA.....	161
7.4	NON-POLAR/POLAR (NON-HB) SYSTEMS	163
7.4.1	VAPOUR-LIQUID EQUILIBRIA	163
7.4.2	EXCESS ENTHALPY	173
7.4.3	EXCESS VOLUME	176
7.4.4	SECOND-ORDER PROPERTIES.....	177
7.5	POLAR (NON-HB)/POLAR (NON-HB)	178
7.5.1	VAPOUR-LIQUID EQUILIBRIA	178
7.5.2	EXCESS ENTHALPY	180
7.5.3	EXCESS VOLUME	181
7.6	MULTI-COMPONENT VLE	182
7.7	CHAPTER SUMMARY.....	183
7.7.1	SPC-SAFT-GV AND SPC-SAFT-JC.....	183
7.7.2	CPA-GV AND CPA-JC.....	184
7.7.3	SCIENTIFIC CONTRIBUTION	185
CHAPTER 8	APPLICATION OF POLAR SPC-SAFT AND POLAR CPA TO ASSOCIATING COMPONENTS	187
8.1	ASSOCIATION SCHEMES AND MODEL PARAMETERS	188
8.1.1	PERFORMANCE OF CURRENT PARAMETERS FROM LITERATURE	188
8.1.2	NEW MODEL PARAMETERS FOR SPC-SAFT-GV AND SPC-SAFT-JC.....	189
8.1.3	NEW MODEL PARAMETERS FOR CPA-GV AND CPA-JC	191
8.2	NON-POLAR/HYDROGEN BONDING SYSTEMS.....	193
8.2.1	VAPOUR-LIQUID-EQUILIBRIA OF ALCOHOL/ALKANE SYSTEMS	193
8.2.2	EXCESS ENTHALPY	203
8.2.3	EXCESS VOLUME	206
8.3	HYDROGEN BONDING/HYDROGEN BONDING SYSTEMS	207
8.3.1	VAPOUR-LIQUID-EQUILIBRIA.....	207
8.3.2	EXCESS ENTHALPY	218
8.4	POLAR (NON-HB)/HYDROGEN BONDING SYSTEMS.....	222
8.4.1	UNIVERSAL CROSS-ASSOCIATION APPROACH.....	222
8.4.2	VAPOUR-LIQUID EQUILIBRIA	224
8.5	MULTI-COMPONENT VLE	228
8.6	CHAPTER SUMMARY.....	231
8.6.1	SPC-SAFT-GV AND SPC-SAFT-JC	231
8.6.2	CPA-GV AND CPA-JC.....	232
8.6.3	SCIENTIFIC CONTRIBUTION	232
CHAPTER 9	CONCLUSIONS	233
9.1	MAJOR SHORTCOMINGS OF SPC-SAFT	233
9.2	NEW 2C ASSOCIATION SCHEME WITHIN SPC-SAFT	234
9.3	SPC-SAFT-GV AND SPC-SAFT-JC	234

9.3.1	APPLICATION TO POLAR (NON-HB) COMPONENTS.....	235
9.3.2	APPLICATION TO HYDROGEN BONDING COMPONENTS	235
9.4	CPA-JC AND CPA-GV	236
9.4.1	APPLICATION TO POLAR (NON-HB) COMPONENTS.....	236
9.4.2	APPLICATION TO HYDROGEN BONDING COMPONENTS	236
9.5	CONTRIBUTIONS OF THIS WORK.....	237
CHAPTER 10 FUTURE WORK		239
10.1	DEVELOPMENT OF A NEW REFERENCE TERM.....	239
10.2	INCORPORATION OF NEW MODEL PARAMETERS INTO GROUP CONTRIBUTION REGRESSIONS	240
10.3	DETERMINING MODEL PARAMETERS FOR MORE COMPONENTS	240
10.4	IMPROVING THE POLAR TERMS	240
10.5	IMPROVING THE ASSOCIATION TERM.....	240
10.6	REFINING THE NEW UNIVERSAL CROSS-ASSOCIATION APPROACH	241
10.7	DEVELOPMENT OF STANDARDIZED DATA BASE	241
REFERENCES		243
APPENDIX A IMPORTANT ASPECTS, CRITERIA AND SELECTION OF MODELS		267
A.1	INTERMOLECULAR FORCES.....	267
A.1.1	POLAR FORCES	269
A.1.2	INDUCTION FORCES AND POLARIZABILITY	270
A.1.3	ATTRACTION (DISPERSION OR LONDON) AND REPULSION FORCES.....	271
A.1.4	SPECIFIC (CHEMICAL) FORCES.....	272
A.1.5	HYDROPHOBIC EFFECT.....	273
A.1.6	INTERMOLECULAR POTENTIAL FUNCTIONS.....	274
A.2	CLASSIFICATION OF THERMODYNAMIC SYSTEMS INVESTIGATED	277
A.2.1	PURE COMPONENT FLUIDS	278
A.2.2	BINARY MIXTURES	278
A.3	PERFORMANCE CRITERIA FOR EOS MODELS.....	279
A.3.1	PARAMETERS.....	281
A.3.2	CRITICAL POINT	281
A.3.3	TWO PHASE REGION.....	281
A.3.4	SINGLE PHASE PROPERTIES	281
A.3.5	NUMERICAL INTENSITY	282
A.3.6	FURTHER CRITERIA	282
A.3.7	MAIN OBJECTIVE	282
APPENDIX B THERMODYNAMIC FRAMEWORK AND ALGORITHMS		283
B.1	THERMODYNAMIC FRAMEWORK	283
B.1.1	THERMODYNAMIC DERIVATIVE PROPERTIES FROM THE STATE FUNCTION	283

B.1.2	FIRST-ORDER DERIVATIVE PROPERTIES	283
B.1.3	SECOND-ORDER DERIVATIVE PROPERTIES	286
B.2	ALGORITHMS	289
B.2.1	EOS ROOT FINDING STRATEGY	289
B.2.2	PHASE EQUILIBRIUM CALCULATIONS.....	289
B.2.3	REGRESSION	290
B.2.4	SOLUTION TO THE ASSOCIATION TERM.....	290
<u>APPENDIX C CONCEPTUAL REVIEW BEHIND CURRENT STATE-OF-THE-ART SAFT MODELS</u>		<u>295</u>
C.1	SOFT-SAFT (1997) AND CROSS-OVER SOFT SAFT (2004).....	295
C.2	SAFT-CP (MODIFIED SAFT-BACK) (2001)	296
C.3	SAFT-VR Mie (2006)	297
C.4	COMPARISON OF SAFT TYPE MODELS	298
<u>APPENDIX D VALIDATION OF MODEL RELIABILITY & ACCURACY</u>		<u>303</u>
<u>APPENDIX E %AAD VALUES OF ASSOCIATING COMPONENTS AND VLE RESULTS FOR CPA-GV AND CPA-JC WITH THE 2B SCHEME</u>		<u>307</u>
E.1	%AAD VALUES OF ASSOCIATING COMPONENTS.....	307
E.2	VLE RESULTS WITH CPA-GV AND CPA-JC WITH THE 2B SCHEME	309
<u>APPENDIX F WORKING EQUATIONS OF MODELS</u>		<u>311</u>
F.1	SIMPLIFIED HARD-SPHERE TERM WORKING EQUATIONS	311
F.1.1	STATE FUNCTION.....	311
F.1.2	FIRST-ORDER DERIVATIVES.....	312
F.1.3	SECOND-ORDER DERIVATIVES.....	314
F.2	SIMPLIFIED CHAIN TERM WORKING EQUATIONS	318
F.2.1	STATE FUNCTION.....	318
F.2.2	FIRST-ORDER DERIVATIVES.....	319
F.2.3	SECOND-ORDER DERIVATIVES.....	319
F.3	PC-SAFT DISPERSION TERM WORKING EQUATIONS	321
F.3.1	STATE FUNCTION.....	321
F.3.2	FIRST-ORDER DERIVATIVES.....	322
F.3.3	SECOND-ORDER DERIVATIVES	326
F.4	GENERAL ASSOCIATION TERM WORKING EQUATIONS	340
F.4.1	STATE FUNCTION.....	341
F.4.2	FIRST-ORDER DERIVATIVES.....	341
F.4.3	SECOND-ORDER DERIVATIVES.....	341
F.5	CPA- CR1 COMBINING RULES USED IN ASSOCIATION TERM	345
F.5.1	FIRST-ORDER DERIVATIVE	345
F.5.2	SECOND-ORDER DERIVATIVES.....	346

F.6	CPA- ECR COMBINING RULES USED IN ASSOCIATION TERM	347
F.6.1	FIRST-ORDER DERIVATIVES.....	348
F.6.2	SECOND-ORDER DERIVATIVES.....	348
F.7	SAFT-CR1 COMBINING RULE USED IN ASSOCIATION TERM	350
F.7.1	FIRST-ORDER DERIVATIVES.....	350
F.7.2	SECOND-ORDER DERIVATIVES.....	351
F.8	JOG AND CHAPMAN'S POLAR TERM.....	352
F.8.1	STATE FUNCTION.....	352
F.8.2	FIRST-ORDER DERIVATIVES.....	353
F.8.3	SECOND-ORDER DERIVATIVES.....	356
F.9	GROSS AND VRABEC'S DIPOLAR TERM.....	372
F.9.1	STATE FUNCTION.....	372
F.9.2	FIRST-ORDER DERIVATIVES.....	373
F.9.3	SECOND-ORDER DERIVATIVES.....	375
<u>NOMENCLATURE</u>		<u>381</u>

Chapter 1

Introduction

A prerequisite for the design and optimization of separation processes is a reliable knowledge of the phase equilibrium behaviour and other thermodynamic properties of the relevant system (1). Phase behaviour and thermodynamic properties are calculated with thermodynamic models that are used to estimate the physical properties of the system in process simulation packages.

The phase equilibrium property is the most important thermodynamic property in separation processes and accurate representation of this property is often the key objective for developing thermodynamic models (2). However, there are a multitude of other thermodynamic properties (isobaric and isochoric heat capacities, isentropic and isothermal compressibilities, thermal expansivity and speed of sound) also required for the efficient design of chemical process plants (3). For example, the isobaric heat capacity is used in the design of heat exchangers and condenser/reboiler requirements. These properties can either be measured experimentally, or predicted with thermodynamic models. Therefore, it is desirable to have a thermodynamic model that can accurately predict both phase equilibria and other thermodynamic properties for pure components and their mixtures.

1.1 Project relevance and problem statement

Most state-of-the-art models have difficulty in predicting thermodynamic properties of complex mixtures with high accuracy. Therefore, it is difficult to design efficient process units where these complex components are encountered often leading to inefficient process design that raises capital and operating costs. The petrochemical industry, amongst others, suffers severely because of the extreme non-ideal behaviour present in most of the systems (1). Of particular interest is the industrial Fischer-Trops (FT) process where hydrocarbons are produced from synthesis gas (CO and H₂). This process is accompanied by the production of water and oxygenates (4) e.g. alcohols ketones, aldehydes, etc. A large fraction of the polar oxygenates tends to dissolve in the aqueous stream and there is often an economic incentive to recover valuable organic products from it (4). Table 1-1 present the composition of the oxygenates from two industrially FT-based processes. Separating components from these mixtures are often extremely challenging, because complex vapour-liquid-liquid equilibria and numerous azeotropes complicate separation (4).

Table 1-1: Composition of Oxygenates (mass%) in Fischer-Trops (FT) Aqueous Product from Fused Iron-Based High Temperature FT Synthesis with Sasol Synthol and Sasol Advanced Technologies (SAS) (4).

Component	Composition	
	Synthol	SAS
Methanol	1.2	0.5
Ethanol	46.4	28.8
1-Propanol	10.7	7.9
2-Propanol	2.5	3.2
1-Butanol	3.5	2.9
2-butanol	0.7	0.9
2-methylpropanol	3.5	1.0
Other alcohols	1.6	1.4
Ethanal	2.5	3.9
propanal	0.8	1.1
Other aldehydes	0.5	0.4
Acetone	8.9	22.1
Butanone	2.5	9.0
Other ketones	0.8	3.4
Ethanoic acid	9.8	8.5
Propanoic acid	2.2	3.0
Butanoic acid	1.2	1.1
Other carboxylic acids	0.7	0.9

There are several good methods available to describe the thermodynamic behaviour of fluids composed of simple components (*n*-alkanes) in which the most prominent intermolecular forces are long range attractive forces (dispersion and weak polar forces) and repulsion forces (5). However, there are many mixtures composed of complex components (water, alcohols, acids, etc.) that cannot be classified as simple fluids. Of particular interest to this study are components that associate through hydrogen bonding and those that exhibit strong multi-polar interactions. The hydrogen bonding forces are stronger than long range attractive forces (dispersion and/or weak polar interactions), but still weaker than true chemical bonds (5). Figure 1-1 shows a representation of the bond strength distribution between molecules and indicates how bond strength varies over several orders of magnitude ranging from weak dispersive forces between simple molecules to strong chemical bonds.

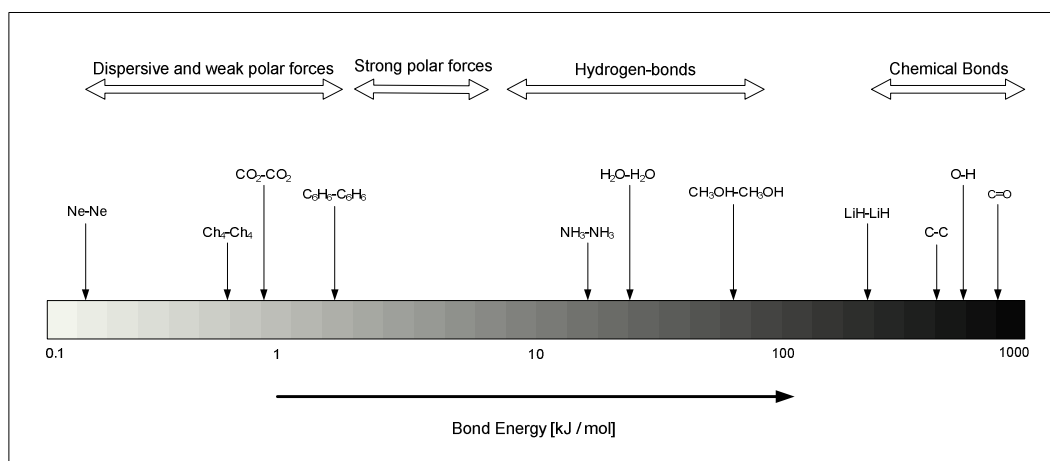


Figure 1-1: Bond strength distribution, indicating the span from dispersion attractions to the formation of chemical bonds. Figure redrawn from ref. (5).

Associating fluids and strongly polar fluids fall between these two extremes. Therefore, they require special attention when modelled thermodynamically (5). A brief review of the main types of intermolecular forces encountered in this study is presented in Appendix A.

For a thermodynamic model to provide an accurate description of the complete thermodynamic behaviour of a system, it has to account for all the intermolecular forces present in the system. In the last two decades several good models have been developed that can account for some of these complex molecular interactions to a certain extent. One such an EOS is the simplified Perturbed Chain – Statistical Associating Fluid Theory (sPC-SAFT) (6). sPC-SAFT generally provides a good representation of the phase equilibrium behaviour, but there are still some errors which cannot be properly explained and large binary interaction parameters (BIPs) are often required. To date, sPC-SAFT has not been extensively applied to thermodynamic properties other than phase equilibria and the boundaries of its full potential have not yet been established. Compared to other SAFT-based models, sPC-SAFT is numerically less intensive and have relatively few pure component parameters compared to other advanced models as discussed in Appendix C.

1.2 Introduction to SAFT

1.2.1 Traditional EOS models

More than a hundred different theoretical EOS models have been published since J.D. van der Waals proposed his well known EOS in 1873 (3). The EOS was the first model that was capable to predict vapour-liquid coexistence (2) i.e. two phase region. The model is given by equation (1-1):

$$P = \frac{RT}{v-b} - \frac{a}{v^2} \quad (1-1)$$

In equation (1-1), P is the pressure, R is the universal gas constant, T is the temperature, v is the specific molar volume, b is the co-volume parameter that characterizes the volume occupied by the molecules and a is the attractive parameter that characterizes the attractive forces between the molecules (2). Therefore, the first term is representative of repulsion interactions between molecules and the second term is representative of all attractive forces between molecules, including dispersion and polar forces. Polar and dispersion forces are often lumped together when treated in EOS models and are known as *Van der Waals* forces. The *Van der Waals* EOS is only able to give qualitative description of the vapour and liquid phases and is rarely sufficiently accurate for critical properties and phase equilibrium calculations, even for simple fluids (2). This led to the development of numerous EOS that improved on *Van der Waals* EOS. Wei and Sadus (2) presented an excellent review article on theoretical EOS models and the reader is referred to it for an in-depth discussions.

In the reference fluid of *Van der Waals*-type EOS, molecules are usually represented as hard-spheres that interact with each other according to an intermolecular potential function that is determined by the expressions used for the repulsive and attractive terms. Consider an alkanol molecule as represented in the framework of most of these simple *Van der Waals*-type models shown Figure 1-2:

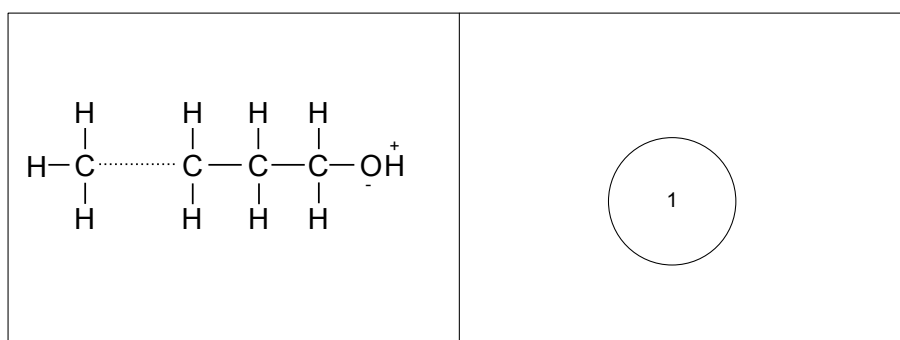


Figure 1-2: Representation of an alkanol molecule as a single sphere in the framework of most *Van der Waals* type EOS models. Hydrogen bonds and strong polar forces that originate from the OH-radical are not explicitly accounted for.

Major sources of non-ideal behaviour are caused by association, solvation and strong polar interactions. A major problem with *Van der Waals* type EOS is that they do not explicitly account for these interactions leading to the development of more advanced theories. Theories accounting for hydrogen bonding (which causes association and solvation) are generally classified into three categories: Chemical, Quasi-chemical and Perturbation theories (7; 8). Perturbation theories were mostly developed to explicitly account for polar interactions (9).

EOS models that result from perturbation theories usually have a sound theoretical foundation and are therefore usually more predictive. There are several perturbation theories, but one in particular, the Statistical Associating Fluids Theory (SAFT), seems to be used extensively in the literature and many of the latest state-of-the-art EOS models are based on SAFT. Both sPC-SAFT and CPA possess strong roots that originated from SAFT.

1.2.2 The SAFT-approach

SAFT is based on the thermodynamic perturbation theory derived by Wertheim (10-15). The key result of Wertheim's theory is a relationship between the residual Helmholtz energy due to association and the monomer density (16). Jackson (17) and Chapman (18) simplified Wertheim's theory by only using the first-order thermodynamic perturbation theory (TPT-1). TPT-1 was then used as the foundation for SAFT (7). SAFT in itself is a general approach to model fluids that exhibit association.

The essence of the original SAFT approach (16) is to use a reference fluid that incorporates both chain length (molecular shape) and molecular association, instead of the much simpler hard-sphere reference fluid used in most *Van der Waals*-type EOS e.g. SRK (19), Peng-Robinson (20), etc. The original SAFT implicitly assumes that there are three major contributions to the total intermolecular potential of a given molecule: the repulsion-dispersion contribution typical of individual segments, the contribution due to chain formation between segments, and the contribution due to association between segments (5). The residual Helmholtz energy is given within the SAFT formalism as the sum of the contributions from these different intermolecular effects, as indicated by equation (1-2):

$$A^r = A^{seg} + A^{chain} + A^{assoc} \quad (1-2)$$

The superscripts *seg*, *chain* and *assoc* refer to the contribution from the "monomeric" segments, from the formation of chains, and from the existence of association sites, respectively (5). The equation is commonly rewritten by separating the segmental term into hard-sphere repulsion and dispersion terms:

$$A^r = A^{hs} + A^{disp} + A^{chain} + A^{assoc} \quad (1-3)$$

The physical basis of the original SAFT model is schematically represented in Figure 1-3:

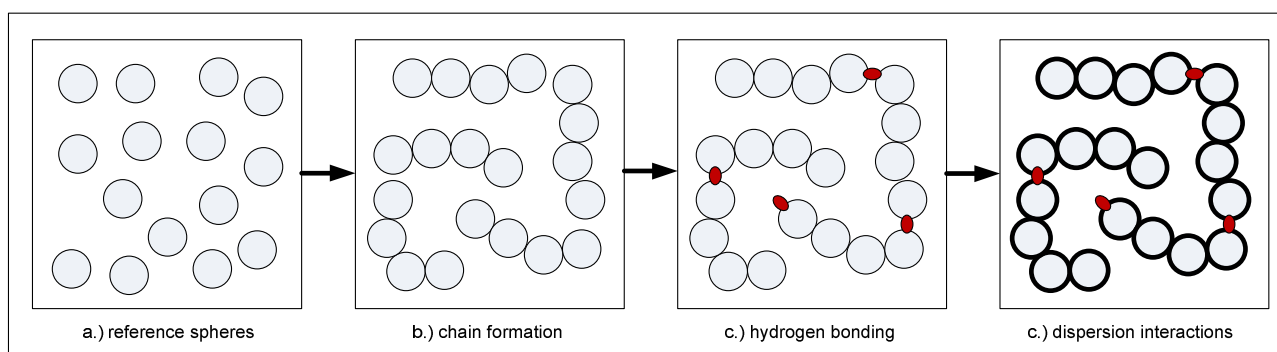


Figure 1-3: Schematic representation of the physical basis of the original SAFT models. a.) The reference fluid consists of hard-spheres. b.) Covalent bonds are imposed on the spheres to account for chain formation. c.) Hydrogen bonds between terminal sites of different chains which result in chain oligomers. d.) Dispersion forces between reference spheres are accounted for through perturbation. Figure redrawn and adapted from ref. (21).

The main strength of SAFT is the expressions that determine the association contribution to the Helmholtz energy. Within SAFT, a given molecule may have any number of association sites. The

association sites are characterized by a non-central potential located near the perimeter of the molecule. Different types of sites can be assigned to a molecule (5). Figure 1-4 illustrates how an alkanol molecule is typically represented in the SAFT framework.

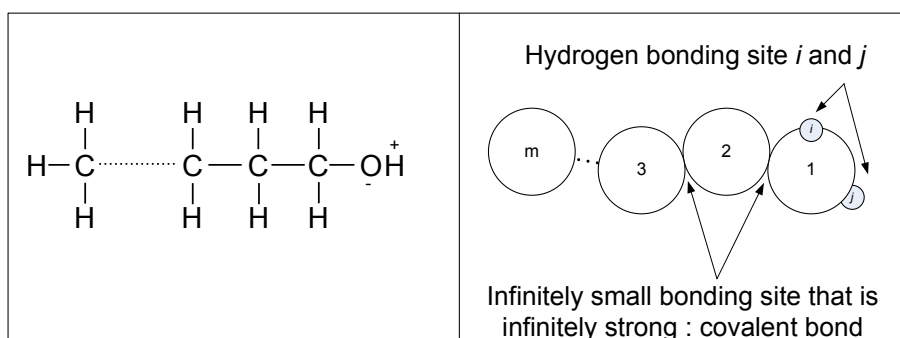


Figure 1-4: Schematic representation of an alkanol in the framework of SAFT. The molecule consists of m segments or spheres and has two bonding sites, i and j , corresponding to a proton and lone electron on the oxygen atom in the OH-radical. Figure redrawn from ref. (5).

From Figure 1-4, it is noticed that the molecular size (chain formations) and molecular association (hydrogen bonds) are accounted for, in contrast to classic cubic EOS models where molecules are only approximated as single spheres (see Figure 1-2).

All SAFT models based on the TPT-1 framework are, however, subject to the following limitations:

- Two molecules can only establish a single bond with each other (5).
- No more than two molecules can be involved in a single bond i.e. three molecules cannot be bonded at a specific point (5).
- A site on one particular molecule cannot bond to more than one site on another molecule (5).
- A molecule cannot bond to another site on the same molecule (5).
- No ring-like structures are allowed to form among the sites. (5).
- Co-operativity and steric hindrances are not accounted for (22).
- Solute aggregation is not explicitly taken into account (23).

Some of these restrictions may be relaxed by modifying the original theory (5). Numerous improvements have also been made to the theory and are discussed in the review articles of Müller & Gubbins (5), Economou (21), Wei & Sadus (2) and Tan *et al.* (9).

1.3 Objectives and aims

The primary aim of this project is to investigate and improve how sPC-SAFT account for complex molecular interactions by examining several thermodynamic properties for selected pure components and binary systems. This investigation considers how molecular interactions influence thermodynamic properties and how sPC-SAFT is able to capture these influences. Improvements were then made to broaden the range of application of the model. The Cubic-Plus-Association

(CPA) (8) EOS was also included in the investigation for comparative purposes, because this model often provides similar performance to sPC-SAFT, yet is mathematically simpler.

In order to achieve these aims, the following objectives can be formulated:

- Apply sPC-SAFT and CPA to a multitude of thermodynamic properties in order to evaluate the performance of these models. Such properties do not include phase equilibria, but rather other properties that have not been investigated thoroughly in previous studies.
- From the above mentioned investigation and from a literature review, weaknesses in the framework of the models are identified.
- Necessary improvements are made to the sPC-SAFT and CPA. Much attention is focused on improving the description of association and strong polar interactions.
- Evaluate the performance of these new improvements made by investigating phase equilibria and other thermodynamic properties.

1.4 Scope and limitations

The field of thermodynamic modelling is extremely broad and it is necessary to define boundaries within which the investigation is conducted.

1.4.1 EOS models considered

The EOS models applied in this research is primarily the sPC-SAFT and CPA EOS models. Other SAFT-based models are not considered.

1.4.2 Components considered

The components of primary interest are those encountered in the petrochemical industry, but this still entails a wide range of components. The components are further narrowed based on the availability of thermodynamic data for several properties and availability of pure component model parameters. The following types of components and their mixtures are thus considered:

- *n*-alkane series
- 1-alcohol series
- ketones and esters, especially acetone
- water

Polymer components are not considered, partly because of the reasons mentioned above, and to limit the scope of the project to manageable size. Polymer components also introduce a new range of molecular interactions that are a study on their own. Therefore, this investigation is limited to small and medium sized components.

Electrolytes, ionic liquids or any metals-containing components are also excluded from the investigation for the same reasons stated above.

1.4.3 Thermodynamic region

If a pure component phase diagram is considered, the main regions of importance are:

- Two-phase vapour liquid region
- Near critical region
- Compressed liquid region
- Superheated vapour region
- Above critical region
- Solid region

The modelling performed in this project is predominantly focussed on the region that encompasses the **two-phase liquid-vapour region** and the **compressed liquid region**. The critical region poses additional complexities that would make it difficult to distinguish whether model performance is poor as a result of molecular interactions that are not properly accounted for, or as a result of critical region complexities, such as density fluctuations.

1.5 Thesis layout and significant contributions

Since sPC-SAFT and CPA have been extensively applied to phase equilibria problems, an initial investigation focussed on applying the models to other thermodynamic properties in order to identify weaknesses in their frameworks from a different point of view. From the conclusions reached in this initial investigation and from problems identified in the literature, improvements were made to sPC-SAFT which were then tested. The major significant novel contributions from this project are summarized below:

- a) The evaluation of the ability of sPC-SAFT and CPA to predict various thermodynamic properties.
- b) The development of the new 2C association scheme for 1-alcohols that results in improved alcohol/water VLE predictions compared to the 2B and 3B association schemes, when incorporated into sPC-SAFT.
- c) The extension of sPC-SAFT and CPA with two dipolar theories to obtain new models. These new models are applied to mixture properties of various non-associating polar components.
- d) Application of new polar sPC-SAFT and CPA-based models to mixture properties of associating components, specifically mixtures containing alcohols are modelled with the new 2C association scheme.
- e) The development of a new ‘universal’ cross-association approach.

The layout presented in Table 1-2 gives an overview of the thesis structure and comments on how the chapters are connected.

Table 1-2: Thesis layout

Chapter	Title	Comments
1	Introduction	Problem statement and scope of work
2	Literature review	Review models and their previous applications. Identify problems with models as reported in the literature.
3	Modelling properties of pure components	Models are applied to various first- and second-order thermodynamic properties in the liquid region in order to evaluate their performance and to identify weaknesses in their frameworks.
4	Modelling properties of binary mixtures	Models are applied to binary mixture properties in the liquid phase to establish if the mixing rules used in the model are adequate.
5	Potential for improvement	From the literature review conducted in Chapter 2 and the findings from Chapter 3 and Chapter 4, potential areas for improvement in sPC-SAFT are identified.
6	A new association scheme for 1-alcohols: the 2C association scheme	A new association scheme is defined that improves the description of 1-alcohols/water phase equilibria with sPC-SAFT.
7	Extending CPA and sPC-SAFT with dipolar terms and application to non-associating components	Dipolar terms are included in the state functions of sPC-SAFT and CPA. The resulting new models are tested and evaluated by considering several properties of non-associating mixtures.
8	Application of polar sPC-SAFT and polar CPA to associating components	The application of the models developed in Chapter 7 are extended to associating components, most notably mixtures containing alcohols and water.
9	Conclusions	
10	Future work	

Chapter 2

Literature review

The primary aim of this chapter is to review sPC-SAFT and CPA according to the following criteria:

- **Concept**
- **Model development**
- **Application** – to determine which type of compounds and mixtures have been modelled and whether only phase equilibria and/or thermodynamic properties were modelled.
- **Shortcomings** – to identify some areas of weaknesses.

In the model development section, only the expressions used for mixtures are given for each EOS. The equations are presented in terms of the reduced residual Helmholtz energy where the independent variables are temperature (T), total molar volume (V) and mole numbers (n). The transformation from the published form is shown in Appendix F. The reason for the transformation is to render all the EOS compatible with the thermodynamic framework presented in Appendix B.

Additional literature related to the significance of the parameter regression routines, utilized by previous workers to determine pure component model parameters, is briefly considered.

2.1 PC-SAFT and simplified PC-SAFT

2.1.1 Concept

i) original

One of the most successful theories that evolved from SAFT is PC-SAFT by Gross and Sadowski (24). PC-SAFT is short for Perturbed Chain-Statistical Associating Fluid Theory. In conventional SAFT models, the influence of chain length is only accounted for in the repulsive contribution of the EOS and not in the dispersive contribution (25), while in PC-SAFT, the influence of chain length is accounted for in both repulsive and dispersive contributions (22). Figure 2-1 illustrates the reference fluid for PC-SAFT and may be compared to the reference fluid of the original SAFT shown in Figure 1-3 d.)

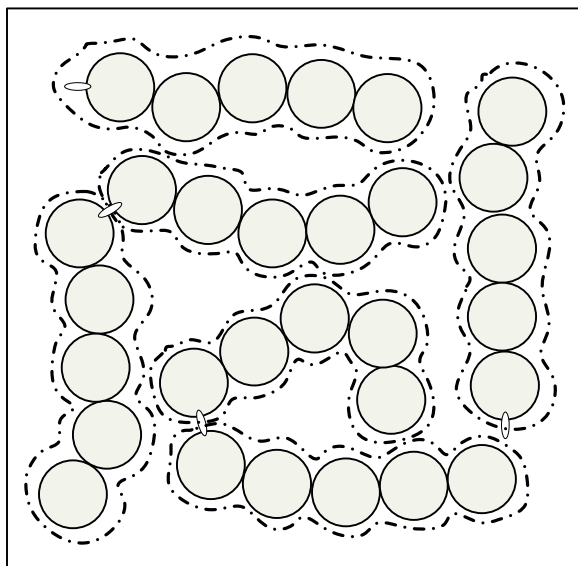


Figure 2-1: Reference fluid for PC-SAFT showing that the influence of chain length on dispersion interactions are accounted for.

A comparison between PC-SAFT and the original SAFT version of Huang and Radosz (26; 27) revealed that the PC-SAFT model is superior in modelling fluid phase equilibria (24) of most systems. Polar forces are treated by lumping them together with the dispersive forces. Therefore, they are not explicitly accounted for, but treated via the *Van der Waals* approach.

ii) simplified

Simplified PC-SAFT was proposed by Von Solms *et al.* (6) in order to markedly reduce computational times for associating components, since the PC-SAFT model is numerically intensive. This simplification was made by assuming that all the segments in the mixture have the same diameter, with the constraint that the volume fraction calculated with this new diameter gives the same volume fraction as the actual mixture (6). The new segment diameter is then used to significantly reduce the mathematical complexity of the radial distribution function, which, in turn, simplifies the hard-chain and associating terms (22). The simplification is justified because it was observed that the values of the segment diameter parameter for different pure components are very similar, as published in the work of Gross and Sadowski (22). For pure components, sPC-SAFT and PC-SAFT are the same; the simplification only affects mixture calculations.

2.1.2 Model description

The reduced residual Helmholtz energy of a system at a certain temperature, volume and mole numbers is defined as follows:

$$\frac{A^r(T, V, \mathbf{n})}{RT} = \frac{A(T, V, \mathbf{n})}{RT} - \frac{A(T, V, \mathbf{n})^{ideal}}{RT} \quad (2-1)$$

In most SAFT based approaches, expressions for the contributions to the residual Helmholtz energy are developed by considering a reference fluid and accounting for other interactions via perturbation expansions:

$$\frac{A^r(T, V, \mathbf{n})}{RT} = \frac{A^{ref}(T, V, \mathbf{n})}{RT} + \frac{A^{pert}(T, V, \mathbf{n})}{RT} \quad (2-2)$$

In PC-SAFT, the reference fluid is a hard-chain (combined hard-sphere and chain term) and the reduced residual Helmholtz energy may be expressed as follows:

$$\frac{A^r(T, V, \mathbf{n})}{RT} = \left(\frac{A^{hs}(T, V, \mathbf{n})}{RT} + \frac{A^{chain}(T, V, \mathbf{n})}{RT} \right)^{ref} + \frac{A^{assoc}(T, V, \mathbf{n})}{RT} + \frac{A^{disp}(T, V, \mathbf{n})}{RT} \quad (2-3)$$

Each of these expressions for the contribution to the reduced residual Helmholtz free energy is individually considered. All the expressions are in terms of the independent variables (T, V, \mathbf{n}) and are not repeated in every term.

i) Hard-sphere contribution

The hard-sphere contribution to the Helmholtz free energy for mixtures is calculated from the theoretical equation developed by Mansoori *et al.* (28) and is given in equation (2-4):

$$\frac{A_{mix}^{hs}}{RT} = \frac{6V}{\pi N_{av}} \left[\frac{\zeta_2^3 + 3\zeta_1\zeta_2\zeta_3 - 3\zeta_1\zeta_2\zeta_3^2}{\zeta_3(1-\zeta_3)^2} + \left(\frac{\zeta_2^3}{\zeta_3^2} - \zeta_0 \right) \ln(1-\zeta_3) \right] \quad (2-4)$$

ζ_n is defined as:

$$\zeta_n = \frac{\pi N_{av}}{6V} \sum_i^{nc} n_i m_i d_i^n \quad n \in \{0, 1, 2, 3\} \quad (2-5)$$

N_{av} is Avogadro's constant, m_i the number of segments per molecule of component i , n_i is the number of moles of component i , V is the total molar volume and d_i is the temperature dependent segment diameter defined as follows:

$$d = \sigma \left[1 - C \exp \left(-3 \frac{\epsilon}{k} \cdot \frac{1}{T} \right) \right] \quad (2-6)$$

In equation (2-6), σ is the temperature independent segment diameter, $\frac{\epsilon}{k}$ is the dispersion energy parameter and C is a constant equal to 0.12, except for hydrogen where it is equal to 0.241. Up to this point, three pure component model parameters have been introduced:

- m (segment number)
- σ (temperature independent segment diameter)
- $\frac{\epsilon}{k}$ (dispersion energy per segment).

These are the characteristic parameters for non-associating pure fluids.

Simplification

Von Solms *et al.* (6) made a simplification to the PC-SAFT model by assuming that all of the segments in the mixture have the same segment diameter, with the constraint that the volume fraction (calculated using this new diameter) gives the same volume fraction as the actual mixture (6). The simplification is expressed as follows:

$$d_{mix} = \left(\frac{\sum_i^{nc} n_i m_i d_i^3}{\sum_i^{nc} n_i m_i} \right)^{1/3} \quad (2-7)$$

One of the implications of the simplification is that the hard-sphere contribution to the Helmholtz free energy for mixtures, as presented in equation (2-4), is significantly simplified and becomes similar to the Carnahan-Starling (29) expression for a pure component:

$$\frac{A_{mix}^{hs}}{RT} = m_{mix} n_{total} \frac{4\eta - 3\eta^2}{(1-\eta)^2} \quad (2-8)$$

The reduced density η in equation (2-8) is calculated with:

$$\eta = n_{total} \frac{N_{av} \pi d_{mix}^3}{6V} m_{mix} \quad (2-9)$$

m_{mix} is defined as follows:

$$m_{mix} = \frac{1}{n_{total}} \sum_i^{nc} n_i m_i \quad (2-10)$$

ii) Chain contribution

The chain contribution to the Helmholtz energy for mixtures is calculated with equation (2-11):

$$\frac{A_{mix}^{chain}}{RT} = \sum_i^{nc} n_i (1 - m_i) \ln(g_{ii}^{hs}) \quad (2-11)$$

The subscript in g_{ii}^{hs} indicates that the function is evaluated between two spheres of molecule i in a mixture of spheres.

The expression was developed by considering hard-spheres with two infinitely small bonding sites that form bonds that are infinitely large. Covalent bonds are therefore effectively formed between the spheres, forming a chain consisting of m -segments (16). The radial distribution function between two spheres in a mixture was also developed by Mansoori *et al.* (28) and is expressed as follows (27):

$$g_{ij}(d_{ij})^{hs} = \frac{1}{1-\zeta_3} + \left(\frac{d_i d_j}{d_i + d_j} \right) \frac{3\zeta_2}{(1-\zeta_3)^2} + \left(\frac{d_i d_j}{d_i + d_j} \right)^2 \frac{2\zeta_2^2}{(1-\zeta_3)^3} \quad (2-12)$$

ζ_n is defined as in equation (2-5). The subscripts ij indicate that the function is evaluated between spheres of two different molecules in the mixtures.

Simplification

Von Solms *et al.* (6) also applied their simplification to the complex radial distribution function. The expression for mixtures then reduces to the pure component expression with the reduced density η evaluated at the mixture properties (d_{mix} and m_{mix}):

$$g_{ij}^{hs} = \frac{1-0.5\eta}{(1-\eta)^3} \quad (2-13)$$

iii) Association contribution

The contribution to the reduced Helmholtz energy, due to association, is calculated as follows (30):

$$\frac{A^{assoc}}{RT} = \sum_i n_i \sum_{A_i} \left(\ln X_{A_i} - \frac{1}{2} X_{A_i} + \frac{1}{2} \right) \quad (2-14)$$

The fraction of molecules i not bonded at site X_{A_i} is as follows (30):

$$X_{A_i} = \frac{1}{1 + \frac{1}{V} \sum_j n_j \sum_{B_j} X_{B_j} \Delta^{A_i B_j}} \quad (2-15)$$

$\Delta^{A_i B_j}$ is the association strength between site A on molecule i and between site B on molecule j . The property is evaluated from equation (2-16):

$$\Delta^{A_i B_j} = \frac{N_{av} \pi}{6} \sigma_{ij}^3 \kappa^{A_i B_j} \left[\exp\left(\frac{\epsilon^{A_i B_j}}{kT}\right) - 1 \right] g_{ij}^{hs} \quad (2-16)$$

$\frac{\epsilon^{A_i B_j}}{k}$ and $\kappa^{A_i B_j}$ is the association energy and the association volume between site A of molecule i and B of molecule j .

The following combining rules are used (25):

$$\sigma_{ij} = \frac{1}{2} (\sigma_i + \sigma_j) \quad (2-17)$$

$$\frac{\epsilon^{A_i B_j}}{k} = 0.5 \left(\frac{\epsilon^{A_i B_i}}{k} + \frac{\epsilon^{A_j B_j}}{k} \right) \quad (2-18)$$

$$\kappa^{A_i B_j} = \sqrt{\kappa^{A_i B_i} \kappa^{A_j B_j}} \left(\frac{\sqrt{\sigma_{ii} \sigma_{jj}}}{\sigma_{ij}} \right)^3 \quad (2-19)$$

Different types of association sites can be assigned to a molecule. The hydrogen bonding is then modelled according to a square-well potential function that has a short well width and a large well

depth to facilitate the short range strong hydrogen bonds (16). The association energy $\frac{\varepsilon^{AB}}{k}$ and the association volume κ^{AB} are two additional pure component parameters used to characterize association in pure fluids. They correspond to the square-well depths and width respectively.

Simplification

The radial distribution function g_{ij}^{hs} is evaluated from equations (2-12) or (2-13), depending on whether the simplification of Von Solms *et al.* (6) is incorporated or not, respectively.

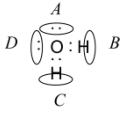
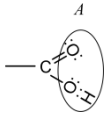
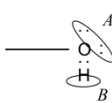
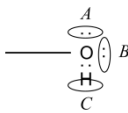
In their simplification, Von Solms *et al.* (6; 31) also used the following combining rule for the association volume:

$$\kappa^{A_i B_j} = \sqrt{\kappa^{A_i B_i} \kappa^{A_j B_j}} \quad (2-20)$$

Association schemes

Before associating components can be modelled within the SAFT-framework, a suitable association scheme has to be selected. The association schemes that are presently used in the literature for associating component within SAFT-based models were originally defined by Huang and Radosz (26; 27). In previous studies, alcohols have been modelled with the 2B (25; 26; 32) or 3B (33; 34) association schemes, water with the 2B (25; 34; 35), 3B (26; 34) and 4C (34; 36) scheme and acids with the 1A (26) scheme. The association schemes may be simplified by realizing that there are essentially three types of association sites *viz*: positive electron acceptor sites, negative electron donor sites and bipolar sites. According to this classification, positive sites will only form a hydrogen bond with negative and bipolar sites, negative sites will only form a hydrogen bond between positive and bipolar sites, and bipolar sites will form hydrogen bonds with all sites. The 2B scheme is equivalent to one negative electron donor site and one positive electron acceptor site, the 3B scheme is equivalent to two negative electron donor sites and one positive electron acceptor site, the 4C scheme is equivalent to two negative electron donor sites and two positive electron acceptor sites and the 1A scheme is equivalent to one bipolar site, as indicated in Table 2-1.

Table 2-1: Selected association schemes within SAFT. Adapted from Kontogeorgis et al. (37).

Species	Formula	Scheme	Equivalent scheme	Site Fractions
water		4C	2 electron donor sites, 2 electron acceptor sites	$X^A = X^B = X^C = X^D$ $X_1 = X^A X^B X^C X^D$
acids		1A	1 bipolar site	$X_1 = X^A$
alcohols		2B	1 electron donor sites, 1 electron acceptor sites	$X^A = X^B$ $X_1 = X^A X^B$
alcohols		3B	2 electron donor sites, 1 electron acceptor sites	$X^A = X^B; X^C = 2X^A - 1$ $X_1 = X^A X^B X^C$

iv) Dispersion contribution

Gross and Sadowski (24) developed a new dispersion term by applying the perturbation theory of Barker and Henderson to a hard-chain reference fluid (24). The new dispersion term is the key improvement of PC-SAFT over other SAFT models because the influence of chain length on dispersion interactions is accounted for. The expression for the dispersion contribution in PC-SAFT is given by equation (2-21) :

$$\begin{aligned} \frac{A_{mix}^{disp}}{RT} = & -2\pi \frac{N_{av} n_{total}^2}{V} I_1(\eta, m_{mix}) \left(m^2 \frac{\epsilon}{kT} \sigma^3 \right)_{mix} \\ & - \pi \frac{N_{av} n_{total}^2}{V} m_{mix} C_1 I_2(\eta, m_{mix}) \left(m^2 \left(\frac{\epsilon}{kT} \right)^2 \sigma^3 \right)_{mix} \end{aligned} \quad (2-21)$$

Where C_1 is the compressibility expression and $I_1(\eta, m)$ and $I_2(\eta, m)$ are integrals from perturbation theory. The expressions $\left(m^2 \frac{\epsilon}{kT} \sigma^3 \right)_{mix}$ and $\left(m^2 \left(\frac{\epsilon}{kT} \right)^2 \sigma^3 \right)_{mix}$ are mixing rules and are defined as follows:

$$\left(m^2 \frac{\epsilon}{kT} \sigma^3 \right)_{mix} = \frac{1}{(n_{total})^2} \sum_i^{nc} \sum_j^{nc} n_i n_j m_i m_j \left(\frac{\epsilon_{ij}}{kT} \right) \sigma_{ij}^3 \quad (2-22)$$

$$\left(m^2 \left(\frac{\epsilon}{kT} \right)^2 \sigma^3 \right)_{mix} = \frac{1}{(n_{total})^2} \sum_i^{nc} \sum_j^{nc} n_i n_j m_i m_j \left(\frac{\epsilon_{ij}}{kT} \right)^2 \sigma_{ij}^3 \quad (2-23)$$

and

$$\frac{\varepsilon_{ij}}{k} = \left(\frac{\varepsilon_i}{k} \frac{\varepsilon_j}{k} \right)^{1/2} (1 - k_{ij}) \quad (2-24)$$

k_{ij} is the binary interaction parameter.

The binary interaction parameter k_{ij} is used to fine tune the fit of the model to experimental data. Ideally this value should be zero.

The compressibility expression C_1 is evaluated from:

$$C_1 = \left[1 + m \frac{8\eta - 2\eta^2}{(1-\eta)^4} + (1-m) \frac{20\eta - 27\eta^2 + 12\eta^3 - 2\eta^4}{[(1-\eta)(2-\eta)]^2} \right]^{-1} \quad (2-25)$$

The original perturbation integrals developed by Gross and Sadowski (24) were lengthy and led to tedious impractical calculations in the engineering environment. For molecules that exhibit soft repulsion, the integrals are functions of temperature, reduced density and segment number (24). The temperature dependency is, however, moderate and Gross and Sadowski (24) assumed that it may be neglected. This assumption enabled them to substitute the lengthy integral by power series functions in reduced density where the coefficients of the power series are functions of the chain length/segment number. The expressions are given in equations (2-26) and (2-27):

$$I_1(\eta, m) = \sum_{i=0}^6 a_i(m) \eta^i \quad (2-26)$$

$$I_2(\eta, m) = \sum_{i=0}^6 b_i(m) \eta^i \quad (2-27)$$

Where $a_i(m)$ and $b_i(m)$ are the power series coefficients of I_1 and I_2 respectively. These are evaluated from:

$$a_i(m) = a_{0i} + \frac{m-1}{m} a_{1i} + \left(\frac{m-1}{m} \right) \left(\frac{m-2}{m} \right) a_{2i} \quad (2-28)$$

$$b_i(m) = b_{0i} + \frac{m-1}{m} b_{1i} + \left(\frac{m-1}{m} \right) \left(\frac{m-2}{m} \right) b_{2i} \quad (2-29)$$

These expressions were derived from perturbation theory and were based on the model developed by Cummings and Stell (38; 39). The influence of nearest-neighbour segments and next-nearest neighbours segments are essentially assumed (24). From equation (2-28) and (2-29) it is noted that the power series coefficients require model constants: a_{0i} , a_{1i} , a_{2i} , b_{0i} , b_{1i} , b_{2i} . Gross and Sadowski (24) determined these universal model constants by fitting the power-series coefficients to pure component data of *n*-alkanes. Vapour pressure and liquid, vapour and supercritical volumes were included in the regression. The constants are presented in Table 2-2.

Table 2-2: Universal model constants for power-series coefficients in dispersion term of PC-SAFT (24).

i	a_{0i}	a_{1i}	a_{2i}	b_{0i}	b_{1i}	b_{2i}
0	0.9105631445	-0.3084016918	-0.0906148351	0.7240946941	-0.5755498075	0.0976883116
1	0.6361281449	0.1860531159	0.4527842806	2.2382791861	0.6995095521	-0.2557574982
2	2.6861347891	-2.5030047259	0.5962700728	-4.0025849485	3.8925673390	-9.1558561530
3	-26.547362491	21.419793629	-1.7241829131	-21.003576815	-17.215471648	20.642075974
4	97.759208784	-65.255885330	-4.1302112531	26.855641363	192.67226447	-38.804430052
5	-159.59154087	83.318680481	13.776631870	206.55133841	-161.82646165	93.626774077
6	91.297774084	-33.746922930	-8.6728470368	-355.60235612	-165.20769346	-29.666905585

The model described thus far is the PC-SAFT EOS and if the simplifications of Von Solms *et al.* (6) are incorporated, the equation is known as the simplified PC-SAFT (sPC-SAFT).

2.1.3 Application of PC-SAFT and sPC-SAFT

i) General phase equilibria

PC-SAFT has been applied to the phase equilibria of many pure components and binary mixtures (24). In the original publication of Gross and Sadowski (24), pure component model parameters for 78 non-associating components (including *n*-alkanes, branched alkanes, cyclo-alkanes, alkenes, benzene derivatives, halogenated hydrocarbons, esters and ethers) were determined and in a subsequent paper (25), the pure component model parameters for associating components were determined (including alkanols, water, amines and acetic acid). The phase equilibria of several binary mixtures were also investigated in these papers. Generally, one binary interaction parameter (BIP) was required to give an accurate representation of the phase equilibria. Gross and Sadowski (24) compared PC-SAFT to the original SAFT model of Huang and Radosz (27) and found that PC-SAFT showed a clear improvement over the original SAFT model. Von Solms *et al.* (6), in turn, compared the performance of the sPC-SAFT model to PC-SAFT and found that there is no noticeable deterioration in the performance of the model as a result of the simplifications made when phase equilibria predictions are considered. For pure components, PC-SAFT and sPC-SAFT use the same working equations and pure component parameters. The simplification only affects properties of mixtures.

A summary of the previous applications of PC-SAFT and sPC-SAFT, that are relevant to the scope of this project, is presented in Table 2-3. In many sources, workers applied the original PC-SAFT to complex mixtures merely to indicate the improvement of additional contribution terms e.g. polar contributions. These applications are not included in this table, but mentioned in section 7.2. Table 2-3 is extended from the summary table presented by Von Solms *et al.* (22) that reviewed the application of PC-SAFT and sPC-SAFT from 2001 to 2005.

Table 2-3: Application summary of original PC-SAFT and sPC-SAFT to phase equilibria applications relevant to this study.

original / simplified	Application	Year	Ref.
original	Model development. Pure component parameters for 78 non-associating substances. VLE for alkane-alkane binaries and CO ₂ -alkane binaries.	2001	(24)
original	Pure components parameters for 18 associating substances including water. All components were, however, modelled with only 2 association sites. VLE and LLE for alcohol-alkane binaries and water-pentanol binary.	2002	(25)
original	VLE for asymmetric alkane binary systems.	2003	(40)
original	Gas solubilities in alkanes.	2003	(41)
simplified	Model development. VLE of gas-alkane and alcohol-alkane binary systems.	2003	(6)
original	Phase equilibria of CO ₂ -benzenes and N ₂ systems.	2003	(42)
original	VLE of ketone-alkane systems. Study shows polar term is needed.	2004	(43)
original	VLE and LLE of methanol- <i>n</i> -alkane systems.	2004	(44)
original	VLE and LLE of methanol-cyclohexane and VLE of polar-cyclohexane binary mixtures. Interaction parameters needed to model systems.	2005	(45)
original	VLE of asymmetric alkane binary systems	2006	(46)
simplified	Phase equilibria (VLE and LLE) of water-alkane systems and water-aniline system.	2006	(36)
original	Critical points on phase diagrams of alkane-alkane binary systems with parameters refitted to match pure component critical data.	2007	(47)
simplified	Phase equilibria of alkanols-alkane systems. Other systems considered include, 1-propanol-water, 1-butanol-water, 1-pentanol-water, ethanol-CO ₂ . Some ternary systems also considered.	2007	(31)
original	Phase equilibria (VLE and LLE) of water/CO ₂ , water/N ₂ and water/ <i>n</i> -alkane binary mixtures. Comparison with CPA showed that PC-SAFT is superior.	2007	(48)
original	VLE and LLE (in some cases) of mixtures of non-polar, polar and associating components. Results compared to CPA and found to be similar for systems considered.	2007	(49)
simplified	VLE of the 104 binary systems of Danner and Gess (50). The binary systems are considered to be a data-base standard for VLE models and are thermodynamically very consistent. Components include non-polar, polar and associating components. Special distinction is made for binary systems that contain acids or water. In most cases, binary interaction parameters were required to correlate the phase behaviour.	2008	(51)
simplified	LLE of selected binary system: water/hydrocarbon, water/1-alkanol, and glycol/hydrocarbon mixtures.	2008	(52)
simplified	Use of monomer fraction data in parameterization of model parameters. Parameters for some alcohols and water determined. Phase equilibria not investigated with new parameters	2010	(33)
simplified	New parameters for methanol determined by including several properties in regression function. New parameters results in good methanol/alkane phase equilibrium predictions, but inaccurate methanol/water VLE predictions.	2010	(32)
simplified	Application to mixtures containing alkanolamines. MEA/ <i>n</i> -heptane LLE and MEA/water VLE studied. Influence of difference association schemes also investigated	2011	(53)

From Table 2-3 it is clear that PC-SAFT and sPC-SAFT have been applied to the phase equilibria of a wide range of pure components and their mixtures. In general, where mixtures with complex components are encountered, large BIPs are often required to model the phase equilibria.

ii) Other thermodynamic derivative properties

PC-SAFT and sPC-SAFT have been applied to only very few thermodynamic properties other than phase equilibria calculations. Usually the applications were only considered at saturated

conditions. A brief description of each relevant application that could be found in the literature is provided in Table 2-4.

Table 2-4: Application summary of original PC-SAFT and simplified PC-SAFT to other thermodynamic properties.

original / simplified	Application	Year	Ref.
original	Excess enthalpy of 1-chlorobutane – <i>n</i> -hexane at $T = 25^{\circ}\text{C}$ and 1 atm. A binary interaction parameter of 0.017 was required to give a fair description of the data.	2001	(24)
original	Isobaric heat capacity of seven non-polar components in the liquid state over a small temperature range and at low pressures. Low %AAD was obtained, however, very few data points were considered.	2001	(24)
original	Excess enthalpy of acetone and <i>n</i> -decane was modelled at $T = 25^{\circ}\text{C}$. With a binary interaction parameter of 0.059, the model was able to give a reasonable representation of the data.	2006	(54)
original	Isothermal compressibility for the binary system of 1-propanol and toluene was considered at $T = 303.15\text{ K}$ and $T = 333.15\text{ K}$ and $P = 5$ to 60 MPa . The model was unable to predict values that were congruent with the data.	2006	(55)
original	Isobaric thermal expansivities of 1-propanol and toluene at $T = 303.15\text{ K}$, 323.15 K and 343.15 K and $P = 0.1$ to 160 MPa . The model was able to give a fairly good description for toluene, but less so for 1-propanol, indicating that the association effects was not properly taken into consideration by the model.	2006	(55)
original	Brief description of the performance of PC-SAFT in predicting some second-order properties, such as speed of sound , isobaric heat capacity and isothermal compressibility of alkanes, but results were not explicitly shown.	2006	(56)

2.1.4 Shortcomings of PC-SAFT and sPC-SAFT

Throughout the literature, several shortcomings specifically to sPC-SAFT and PC-SAFT have been identified. The most prominent shortcomings **in addition to the limitations inherent to the general SAFT approach mentioned in Chapter 1** include:

- Water/hydrocarbon systems where the minimum solubility of the hydrocarbon in the water-rich phase is not captured with respects to temperature (22). The limitation is attributed to the hydrophobic effect that is not accounted for in the models.
- Poor description of polar interactions in molecules such as ketones, esters and aldehydes, especially when modelling polar/alkane phase equilibria.
- Cross-association in polar components where the component does not self-associate, but cross-associates in the presence of other associating molecules e.g. acetone/methanol.
- Description of thermodynamic behaviour in the near critical region (22).
- Modelling of complex mixtures, such as water/alcohol systems, and systems containing strong polar components, large BIPs are often required. The influence of cross-association on water/alcohol phase equilibria is particularly problematic.
- Description of second-order properties. Lafitte *et al.* (56; 57) attempted to refit pure component model parameters of selected *n*-alkanes and 1-alcohols in order to obtain accurate predictions of the speed of sound and isothermal compressibility. They mention that the minimization procedure of this objective function failed. Therefore, they assumed that the PC-SAFT is not capable of correlating these properties. These findings were,

however, only mentioned and no systematic approach was followed to determine the origins of the shortcomings of the.

This section indicates that there are several areas of sPC-SAFT that require further improvement.

2.2 Cubic-plus-association (CPA)

2.2.1 Concept

The original version of CPA EOS was published in 1996 by Kontogeorgis *et al.* (8). The original model is based on a combination of the cubic SRK (19) and the association term from SAFT (37). The model was initially developed to model the phase equilibria of components exhibiting polar interactions and hydrogen bonding (37). The model essentially reduces to the cubic EOS when no hydrogen bonding components are involved (37), but with the difference that model parameters are no longer estimated from critical data but regressed from saturated vapour pressure and saturated liquid density data. The model has proved to be very capable in giving accurate representation of the phase equilibria of a wide variety of complex systems containing alcohols, glycols, water and alkanes (37). However, large BIPs are often required to obtain good results.

Cubic models represent molecules as hard-spheres in their reference fluid, which act according to a defined intermolecular potential function. The association term then effectively adds association sites to these spheres to allow the molecules to form hydrogen bonds. In Figure 1-3, the representation of an alkanol molecule in the framework of SAFT was illustrated. The same molecule can be represented in the framework of CPA, as illustrated in Figure 2-2:

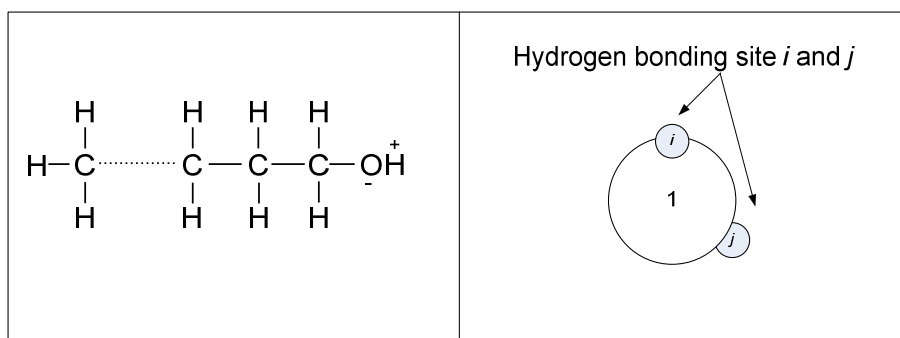


Figure 2-2: Schematic representation of an alkanol molecule in the framework of CPA. The molecule is represented as a single sphere and has 2 association sites: site *i* and *j* corresponding to the proton and lone electron on the oxygen atom in the OH-radical.

From Figure 2-2 it is clear that the framework of CPA makes no provision for the influence of chain length on the thermodynamic behaviour, since a molecule is represented by a single sphere. The current version of the model does not explicitly account for polar forces, but uses the *Van der Waals* approach.

2.2.2 Model description

i) Cubic contribution

The CPA EOS is usually expressed in terms of pressure with individual contributions from the cubic model used to account for physical interactions and the association term from SAFT (8) to account for association. To render CPA compatible with the thermodynamic framework outlined in Appendix B, the pressure equation has to be transformed into an expression for the reduced residual Helmholtz energy. The general expression for the reduced residual Helmholtz energy of the cubic EOS was taken from Michelsen and Møllerup (3):

$$\frac{A^r(T, V, n)}{RT} = F = -n_{total} \ln(1 - B/V) - \frac{D(T)}{RTB(\delta_1 - \delta_2)} \ln\left(\frac{1 + \delta_1 B/V}{1 + \delta_2 B/V}\right) \quad (2-30)$$

The mixture dependent parameters, B and D are defined as follows:

$$D = n_{total}^2 a_{mix} = \sum_i n_i \sum_j n_j a_{ij} \quad (2-31)$$

$$a_{ij} = a_{ji} = \sqrt{a_i a_j} (1 - k_{ij}) \quad (2-32)$$

$$n_{total} B = n_{total}^2 b_{mix} = \sum_i n_i \sum_j n_j b_{ij} \quad (2-33)$$

$$b_{ij} = b_{ji} = \frac{1}{2}(b_i + b_j) \quad (2-34)$$

Where a_i is the energy parameter that characterizes attractive forces, b_i is the co-volume parameter that accounts for repulsive interactions and δ_1 and δ_2 are constants used to determine the volumetric dependence of the attractive contribution (3). When $\delta_1 = 1$ and $\delta_2 = 0$, the expression yields the SRK (19) EOS and when $\delta_1 = 1 + \sqrt{2}$ and $\delta_2 = 1 - \sqrt{2}$, the expression yields the Peng-Robinson (20) EOS. The CPA EOS used in this work is based on the SRK EOS.

The a_i and b_i parameters are calculated with one of two ways:

- The classical method involves estimating the parameters from each component's critical temperature, critical pressure and acentric factor.
- The second method fits the parameters to saturated vapour pressure and saturated liquid density data with regression procedures. CPA uses this second method.

The alpha function energy term for CPA is defined as follows and is not the same as the classical SRK function (8):

$$a(T) = a_0 \left[1 + c_1 (1 - \sqrt{T_r}) \right]^2 \quad (2-35)$$

a_0 and c_1 are pure components parameters in the attractive term and together with the co-volume parameter b , they constitute the three model parameters for non-associating components in the framework of CPA.

ii) Association term

When hydrogen bonding components, such as water and alcohols, are encountered in the system, the association term of CPA becomes active. The association term used is the same as that used by SAFT and is given by equation (2-14). The fraction of non-bonded molecules at site A is also defined by equation (2-15).

In order to render the association term compatible with the model parameters of the cubic function, the association strength $\Delta^{A_i B_j}$ is defined by the following equation (37):

$$\Delta^{A_i B_j} = g(V) \left[\exp\left(\frac{\varepsilon^{A_i B_j}}{RT}\right) - 1 \right] b_{ij} \beta^{A_i B_j} \quad (2-36)$$

$g(V)$ is the radial distribution function and is determined from the Carnahan-Starling expression (29) given by equation (2-37) or in a simplified form proposed by Kontogeorgis *et al.* (58) as shown in equation (2-38):

$$g = \frac{1 - 0.5\eta}{(1 - \eta)^3} \quad (2-37)$$

$$g = \frac{1}{1 - 1.9\eta} \quad (2-38)$$

η is the reduced density, and in CPA is defined as follows:

$$\eta = \frac{B}{4V} \quad (2-39)$$

It is generally accepted to use equation (2-38), because the performance of the model does not deteriorate significantly with the simplification (58). In this work equation (2-38) is used.

Similar to SAFT, $\varepsilon^{A_i B_j}$ and $\beta^{A_i B_j}$ are the association energy and volume between site A on molecule i and site B on molecule j . There are two sets of mixing rules that may be used calculate the association volume and energy: CR1 (37) and ECR (59). CR1 is expressed as follows:

$$\varepsilon^{A_i B_j} = \frac{1}{2} (\varepsilon^{A_i B_i} + \varepsilon^{A_j B_j}) \quad (2-40)$$

$$\beta^{A_i B_j} = \sqrt{\beta^{A_i B_i} \beta^{A_j B_j}} \quad (2-41)$$

And the ECR rule is given (37; 59; 60):

$$\Delta^{A_i B_j} = \sqrt{\Delta^{A_i B_i} \Delta^{A_j B_j}} \quad (2-42)$$

The ECR rule implies that the association strength between two molecule of component i ($\Delta^{A_i B_i}$) and the association strength between two molecule of component j ($\Delta^{A_j B_j}$) are calculated first and from these, the association strength between site A on molecules i and site B on molecule j is calculated.

In some cases the ECR gives better predictions of properties and in other cases, the CR1 yields superior results (61). The CR1 combining rules in this work, unless stated otherwise.

CPA has five pure component parameters ($a_0, c_1, b, \varepsilon^{AB}, \beta^{AB}$) for hydrogen bonding components that are usually fitted to saturated vapour pressure and saturated liquid density data (37).

2.2.3 Application of CPA

Previous applications of CPA are reviewed in this section in a similar fashion presented for PC-SAFT and sPC-SAFT.

i) Phase equilibria

CPA has been applied to the phase equilibria of many different components since the original publication by Kontogeorgis *et al.* (8). In 2005 Kontogeorgis *et al.* (37; 61) published review articles of CPA for the time period of 1996 to 2005. Most of the relevant applications are repeated in Table 2-5 and recent applications are also included. The difference between the *simplified* and *original* forms depends on whether the original radial distribution function was used, or whether the simplified radial distribution function was used.

Table 2-5: Application summary of CPA models to phase equilibria predictions

CPA variant	Application	Year	Ref.
SRK, original	Model description. Pure component parameters for associating components regressed from saturated vapour pressure and saturated liquid density data.	1996	(8)
SRK, original	VLE of alcohol-hydrocarbons.	1997	(62)
SRK, original	LLE alcohol-hydrocarbons.	1997	(63)
SRK, original	LLE of water/ hydrocarbon systems.	1998	(64)
PR, simplified	LLE water/alkanes.	1998	(65)
SRK, original	VLE, LLE of water/alcohols and water/alcohol-hydrocarbons.	1999	(66)
SRK, simplified	VLE, LLE of water/alcohols and water/alcohol-hydrocarbons.	1999	(58)
PR, original	CO ₂ /ethanol/cresols systems.	1999	(67)
SRK, original	LLE of water/alkanes. Comparison with SAFT.	2000	(68)
PR, original	Water/alkanes.	2002	(69)
SRK, simplified	Computing times comparison.	2003	(6)
SRK, simplified	LLE of glycol/alkane systems.	2003	(70)
SRK, simplified	VLE of glycol/water, LLE glycol/water/hydrocarbons.	2003	(71)
SRK, simplified	Methanol/water/oil. Comparison with SRK Huron Vidal mixing rules.	2004	(72)
SRK, simplified	Organic acids.	2004	(73)
SRK, simplified	VLE, LLE and SLE alcohol/alkanes, SLE and VLE of glycol/water.	2005	(74)
SRK, simplified	Amines with alkanes and alcohols.	2005	(75)

CPA variant	Application	Year	Ref.
SRK, simplified	Cross-associating systems (glycol-water, alcohol-water SLE, VLE including hydrate phases), high pressure.	2005	(60)
SRK, simplified	LLE water/aromatics, VLE alcohol/aromatics, LLE water/alcohol/aromatics, LLE glycol/aromatics.	2006	(59)
PR, original	VLE of water/ethanol/CO ₂ system and constituent binaries. CO ₂ had to be treated as an associating component.	2006	(76)
SRK, simplified	Mutual solubilities of hydrocarbons and water. Hydrophobic effect identified as fundamental limitation to the equation.	2007	(77)
SRK, simplified	Phase Equilibria (VLE and LLE) of water/CO ₂ , water/N ₂ and water/ <i>n</i> -alkane binary mixtures. Comparison with PC-SAFT showed that PC-SAFT is superior.	2007	(48)
SRK, simplified	High pressure VLE and LLE in alcohol containing mixtures, mixtures with gas hydrate inhibitors and mixtures with polar and hydrogen bonding components including organic acids.	2007	(78)
PR, original	VLE of water/acetic acid/CO ₂ and constituent binaries.	2007	(79)
PR, original	Evaluation of CPA in binary mixtures of non-polar, polar and associating components. Results compared to PC-SAFT and found to be similar for systems considered.	2007	(49)
SRK, simplified	VLE and LLE of mixtures of acetic acid and various components including non-polar, polar, associating and water.	2008	(80)
SRK, simplified	Phase equilibria for petroleum reservoir fluids containing water aqueous methanol solutions.	2009	(81)
SRK, simplified	Modelling of ternary LLE containing ethyl esters, anhydrous ethanol and water.	2010	(82)
SRK, simplified	Use of monomer fraction data in parameterization of model parameters. Parameters for some alcohols and water determined. Phase equilibria not investigated with new parameters	2010	(33)
SRK, simplified	New parameters for methanol determined by including several properties in regression function. New parameters results in good methanol/alkane phase equilibrium predictions, but inaccurate methanol/water VLE predictions.	2010	(32)
SRK, simplified	Phase equilibria of mixtures containing organic sulphur species (OSS) and water/hydrocarbons.	2010	(83)
SRK, simplified	Wide variety of mixtures containing H ₂ S modelled including water, methanol and alkanes.	2010	(84)
SRK, simplified	Evaluation of the CO ₂ behaviour in binary mixtures with alkanes, alcohols, acids and esters.	2011	(85)
SRK, simplified	Application to mixtures containing alkanolamines. Mixtures of DEA and MEA. MEA/water VLE investigated. Influence of difference association schemes also investigated.	2011	(53)

It is clear from Table 2-5 that CPA has been widely applied to the phase equilibria calculations of various components and mixtures. It should be mentioned that in mixtures of highly polar and hydrogen bonding components, large BIPs are often required to model the phase equilibria of the systems accurately.

ii) Other thermodynamic derivative properties

It appears that CPA has only been applied to a very limited number of other thermodynamic properties. A brief description of each relevant application that could be found in the literature is presented in Table 2-6:

Table 2-6: Application summary of CPA to other thermodynamic properties

CPA variant	Application	Year	Ref.
SRK, simplified	Mass density of water at P = 100 atm, T = 0 to 110 °C. Speed of sound in water at P = 200, 220, 238 atm, T = 0 to 110 °C. Pressure-volume derivative of water at T = 100 °C, P = 0 to 1000 atm. Mass density of methanol at P = 500 atm, T = -100 to 300 °C and at T = 513 K, P = 0 to 500 atm. Speed of sound in water and methanol in the vapour and liquid phase. Mass density of water/methanol binary mixture at T = 25 °C and P = 1 atm. Speed of sound in water/methanol binary mixture at T = 10, 25, 40 °C and P = 1 atm.	2006	(86)

2.2.4 Shortcomings of CPA

The main shortcomings of CPA are that it suffers from the inherent limitations that originate from Wertheim's association term and from limitations associated with the classic cubic EOS, specifically:

- The model does not explicitly account for polar interactions in molecules such as ketones, esters and aldehydes.
- The model cannot properly account for cross-association, specifically in cases when some of the polar components in the mixture do not self-associate, but do cross-associate (61).
- The model deteriorates in the vicinity of the critical region (61).
- The model has difficulty in predicting the minimum solubility of hydrocarbons in water as a result of the hydrophobic effect that is not explicitly accounted for in the association term (77).
- Modelling of water/acids systems are especially problematic (78).

2.3 Accounting for cross-association in SAFT models

The main reason why accounting for cross-association in mixtures (in the presence of a polar component that cross-associates, but does not self-associate) is difficult, is because cross-association parameters cannot be determined from pure component data. There are three main approaches that have been proposed to account for this type of cross-association (solvation):

i) Fitting the association volume

Consider a mixture consisting of a self-associating component and a cross-associating component. Kleiner and Sadowski (87) proposed that the cross-association energy is equal to half the association energy of the associating component and that the cross-association volume is equal to the association volume of the associating component:

$$\varepsilon^{A_i B_j} = \frac{\varepsilon^{A_i B_i}}{2} \quad (2-43)$$

$$\kappa^{A_i B_j} = \kappa^{A_i B_i} \quad (2-44)$$

Kleiner and Sadowski (87) obtained more or less a 10% reduction in %AAD values for the systems they consider by using this approach. The advantage of this approach is that no additional parameters are introduced.

Genner *et al.* (51) attempted to use the approach suggested by Kleiner and Sadowski (87) in the framework of sPC-SAFT, but only obtained marginal improvement to the systems they considered. They then used a modified approach suggested by Folas *et al.* (59) that involves fitting the association volume parameter to VLE data:

$$\varepsilon^{A_i B_j} = \frac{\varepsilon^{A_i B_i}}{2} \quad (2-45)$$

$$\kappa^{A_i B_j} = \text{fitted to binary VLE data} \quad (2-46)$$

This approach has been successfully incorporated into both CPA and PC-SAFT (31; 51; 59; 80). The main disadvantage of this approach is encountered in mixtures with several associating components, because a $\kappa^{A_i B_j}$ needs to be obtained between every binary pair that solvates. In addition, the $\kappa^{A_i B_j}$ obtained is often physically unrealistic e.g. Grenner *et al.* (51) required an association volume between methanol and acetone equal to 3.063.

ii) Fitting the association strength

Instead of fitting the association volume for the cross-association interaction, Perakis *et al.* (76) propose to calculate the cross-associating strength by multiplying the self-associating strength of the self-associating components with a solvating factor:

$$\Delta^{A_i B_j} = \Delta^{A_i B_i} \times s_{ij} \quad (2-47)$$

s_{ij} is an additional BIP and usually fitted to VLE data. The approach has been successfully implemented with the Peng-Robinson based CPA (76; 79). Again, the main disadvantage is that a BIP between each solvating pair of components are required.

iii) Pseudo-association

The third-approach is to treat cross-association molecules, such as acetone and carbon dioxide, as if they were associating molecules, i.e. as pseudo-associating molecules (49). This approach has been successfully implemented with both sPC-SAFT and CPA (49). Although this does not correspond to the physical picture, the approach proves to be very useful in treating polar interactions (49). $\varepsilon^{A_i B_j}$ and $\kappa^{A_i B_j}$ are therefore also fitted to pure component data together with the other pure component parameters.

2.4 Significance of parameter regression and fitting procedures

In CPA and in sPC-SAFT (and most of the new thermodynamic models that are primarily committed to accurate phase equilibrium prediction) parameter regression is performed by tuning the model parameters of each component to fit the saturated vapour pressure and saturated liquid density data. The aim of this section is to explain the influence of the data inclusion on pure component model parameters and the shortcomings thereof.

2.4.1 Relationships between properties and partial derivative of the state function

The mathematical relations of thermodynamic properties in term of the state function are provided in Appendix B. This can be represented schematically as follows:

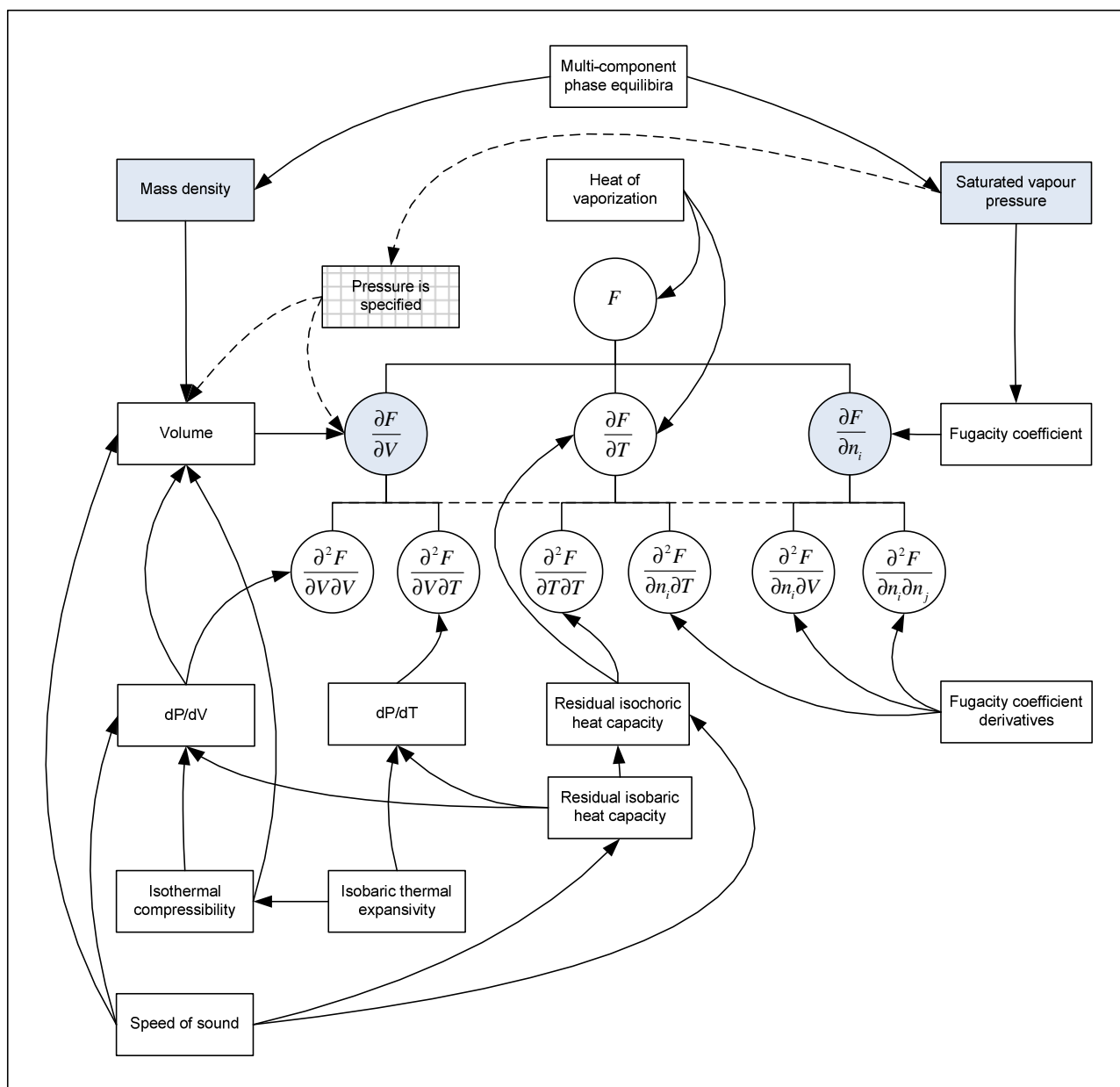


Figure 2-3: Schematic diagram illustrating the relationship between the partial derivatives of the reduced residual Helmholtz energy state function (F) and thermodynamic properties

In Figure 2-3, the circles represent the partial derivatives of the state function and the rectangular blocks the properties. The arrows originating from the block indicate the relationship between properties and the partial derivatives of the state function.

To demonstrate how the diagram works, consider the speed of sound block and equation (2-48):

$$u = \sqrt{-\frac{V^2 \cdot \gamma \cdot \left(\frac{\partial P}{\partial V}\right)_{T,n}}{M_w}} \quad (2-48)$$

Calculation of the speed of sound requires description of the pressure-volume derivative, the volume and the heat capacity ratio. The heat capacity ratio in turn requires description of the isobaric and the isochoric heat capacity which in turn requires their residual counterparts.

Following the diagram, these relationships are shown and the speed of sound can be traced back to be dependent on the following partial derivatives of the state function:

$$\left(\frac{\partial F}{\partial V}\right)_{T,n} \quad \left(\frac{\partial F}{\partial T}\right)_{V,n} \quad \left(\frac{\partial^2 F}{\partial V^2}\right)_{T,n} \quad \left(\frac{\partial^2 F}{\partial T^2}\right)_{V,n} \quad \left(\frac{\partial^2 F}{\partial T \partial V}\right)_n$$

It should be remembered that all these derivative have independent variables: temperature, total volume and mole numbers. For pure components, specifying two *intensive* independent properties completely constrain the state of the system. This implies that if the temperature and pressure are specified in a defined system size, the state of the system is constrained and all properties at that point can be calculated. If the component is in the two-phase vapour-liquid region, it is possible to obtain two volumes that satisfy the pressure equation (equation (B-2) in Appendix B) that corresponds to the volume of each phase.

In the two-phase vapour liquid region, instead of specifying the temperature, pressure and mole numbers; it is also possible to specify the temperature, mole numbers and that the vapour and liquid phases must be in equilibrium with each other: the chemical equilibrium criterion. Specifying that the vapour and liquid phases must be in equilibrium requires that the fugacity of each phase be equal and this is achieved by iterating the pressure until the fugacities are the same. In a pure component, the pressure where the fugacities in each phase are the same is the saturated vapour pressure.

2.4.2 Data in current regression procedures

The model parameters of many new EOS (that are primarily committed to accurate phase equilibrium calculations) are often determined by fitting model parameters to saturated vapour pressure and saturated liquid density data. Considering Figure 2-3, it is seen that the saturated vapour pressure block and mass density block are shaded. This represents the data that is included in the regression procedure when model parameters are estimated. The vapour pressure is determined by adjusting the pressure until the fugacity coefficient in each phase is the same. Accurate description of the fugacity coefficient requires accurate description of the first-order compositional derivative of the state function. Accurate description of the mass density requires accurate description of the volume, which in turn, requires accurate description of the first-order volume derivative at the calculated saturated vapour pressure. The major point that has to be realized is that, by including these properties in the regression procedure, only information regarding the first-order compositional and first-order volume derivatives are included in the regression procedure and no information regarding the first-order temperature derivative or any other derivatives of the state function is included. To amend for the temperature deficiency, typically saturated vapour pressure and saturated liquid density data over an extensive reduced temperature range is included in the parameter estimation, usually between $0.5 < T_r < 0.9$ as this is commonly in the two phase vapour-liquid region. However, this only implies that the temperature dependency of the first-order compositional- and volume derivative will be fairly

adequate and not necessarily the temperature behaviour of the whole model. Usually this is acceptable, because multi-component phase equilibria are primarily dependent on accurate description of the saturated liquid density and saturated vapour pressure, but when other properties are considered, poor predictions are obtained, as will be shown in the subsequent chapters.

In models that have more than three pure component model parameters, the regression procedure often yields multiple sets of pure component parameters that give equally good description of the saturated vapour pressure and saturated liquid density data, but when applied to multi-component phase equilibria and other derivative properties, poor predictions are obtained with some parameter sets.

Some workers (88) argue that if the physical framework of the thermodynamic model is intact, the model parameters should be transferable and accurate predictions of all properties should be obtained, but they neglect to state that the model parameters must be the optimum ones. Another question that arises from these arguments is whether the local minimum of the objective function (from where model parameters are determined) that is formed by only including saturated vapour pressure and liquid density data in the regression is the same as the universal global minimum that would have formed if other data was also included in the fitting procedure. To clarify this point, consider the scenario in Figure 2-4.

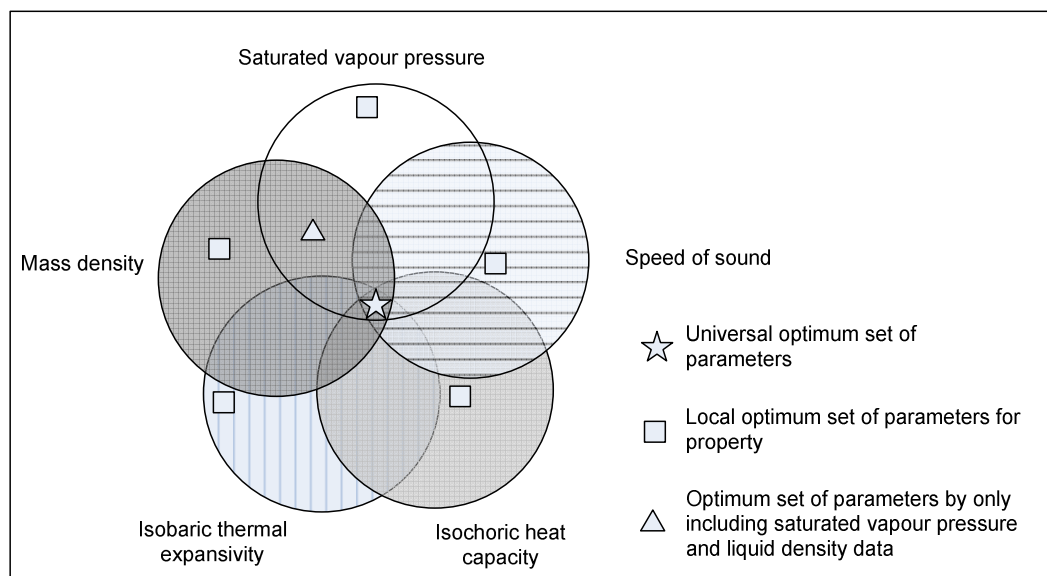


Figure 2-4: Schematic illustration of model parameter sets that can possibly be obtained with regression

In Figure 2-4 it can be seen that if only one type of property is included in the regression, it is likely that there will be a model parameter set that gives a very accurate description of that property, but that this parameter set will not give accurate description of other properties (represented by the squares). Colina *et al.* (89) studied the prediction of Joule-Thomson curves with a SAFT-type model and observed that the prediction of these curves were strongly dependent on the set of parameters used in the calculations for each component and stresses the importance of

fine-tuning the parameters in the fitting procedure. If for instance, saturated vapour pressure and saturated mass density data is included in the fitting procedure, it is likely that a parameter set will be obtained that gives accurate description of both properties and possibly some others (represented by the triangle). Therefore, a study is needed that investigates if universal optimum parameters can be found for sPC-SAFT that will enable accurate description of most properties, as represented by the ‘star’.

There are a few workers that have included additional properties in the regression procedure as discussed below. The following equations are some objective functions currently used:

i) General function

The general function that is commonly used only includes saturated vapour pressure and saturated liquid density (or volume) data and is given by:

$$OF = \sum_{i=1}^{NP} \left[\left(\frac{P_i^{sat,cal} - P_i^{sat,exp}}{P_i^{sat,exp}} \right)^2 + \left(\frac{\rho_i^{sat,cal} - \rho_i^{sat,exp}}{\rho_i^{sat,exp}} \right)^2 \right] \quad (2-49)$$

Most of the published model parameters of sPC-SAFT (24) and CPA (8) used in this project were determined by minimizing this objective function.

ii) SAFT-CP objective function

The objective function of SAFT-CP (90) includes critical properties as well as vapour-liquid equilibria in the regression procedure of the pure component model parameters and is expressed as follows:

$$OF = \left(\frac{T^{crit,cal} - T^{crit,exp}}{T^{crit,exp}} \right)^2 + \left(\frac{P^{crit,cal} - P^{crit,exp}}{P^{crit,exp}} \right)^2 + \left(\frac{\rho^{crit,cal} - \rho^{crit,exp}}{\rho^{crit,exp}} \right)^2 \quad (2-50)$$

$$+ \sum_{i=1}^{NP} \left[\left(\frac{P_i^{sat,cal} - P_i^{sat,exp}}{P_i^{sat,exp}} \right)^2 + \left(\frac{\rho_i^{sat,cal} - \rho_i^{sat,exp}}{\rho_i^{sat,exp}} \right)^2 \right]$$

SAFT-CP (90) performs well in the critical region, however, it requires one additional parameter compared to sPC-SAFT and CPA.

iii) SAFT-VR Mie objective function

Lafitte *et al.* (56) mentioned that some SAFT versions give poor predictions of the isothermal compressibility in the compressed liquid phase when model parameters are determined with the general objective function, at least in the case of *n*-alkanes. They proposed to include compressed liquid density data and speed of sound data in their objective function:

$$\begin{aligned}
 OF = & w_{p^{sat}} \sum_{i=1}^{NP} \left[\left(\frac{P_i^{sat,cal} - P_i^{sat,exp}}{P_i^{sat,exp}} \right)^2 \right] + w_{\rho^{sat}} \sum_{i=1}^{NP} \left[\left(\frac{\rho_i^{sat,cal} - \rho_i^{sat,exp}}{\rho_i^{sat,exp}} \right)^2 \right] \\
 & + w_{\rho^{comp}} \sum_{i=1}^{NP} \left[\left(\frac{\rho_i^{comp,cal} - \rho_i^{comp,exp}}{\rho_i^{comp,exp}} \right)^2 \right] + w_{u^{comp}} \sum_{i=1}^{NP} \left[\left(\frac{u_i^{comp,cal} - u_i^{comp,exp}}{u_i^{comp,exp}} \right)^2 \right]
 \end{aligned} \tag{2-51}$$

$w_{p^{sat}}$, $w_{\rho^{sat}}$, $w_{\rho^{comp}}$ and $w_{u^{comp}}$ are regression weights for each property included in the regression.

In a subsequent paper, Lafitte *et al.* (57) investigated alcohols and extended their objective function by including vapourisation enthalpy data. They mentioned that the main reason for including the data is to ensure that the association parameters of the alcohols have proper physical meaning, since the vapourisation enthalpy is greatly influenced by association. The extended function is presented below:

$$\begin{aligned}
 OF = & w_{p^{sat}} \sum_{i=1}^{NP} \left[\left(\frac{P_i^{sat,cal} - P_i^{sat,exp}}{P_i^{sat,exp}} \right)^2 \right] + w_{\rho^{sat}} \sum_{i=1}^{NP} \left[\left(\frac{\rho_i^{sat,cal} - \rho_i^{sat,exp}}{\rho_i^{sat,exp}} \right)^2 \right] \\
 & + w_{\rho^{comp}} \sum_{i=1}^{NP} \left[\left(\frac{\rho_i^{comp,cal} - \rho_i^{comp,exp}}{\rho_i^{comp,exp}} \right)^2 \right] + w_{u^{comp}} \sum_{i=1}^{NP} \left[\left(\frac{u_i^{comp,cal} - u_i^{comp,exp}}{u_i^{comp,exp}} \right)^2 \right] \\
 & + w_{h^{vap}} \sum_{i=1}^{NP} \left[\left(\frac{h_i^{vap,cal} - h_i^{vap,exp}}{h_i^{vap,exp}} \right)^2 \right]
 \end{aligned} \tag{2-52}$$

Tybjerg *et al.* (32) also used a similar objective function, but included saturated vapour pressure, liquid density, heat of vapourisation and compressibility data into their objective function and obtained good phase equilibrium results for selected systems. Other workers have included monomer fraction data, but the phase equilibria performance of these parameters was not considered (33).

2.5 Chapter summary

Key aspects from this chapter are:

- The simplification made to PC-SAFT by Von Solms *et al.* (6) in order to obtain sPC-SAFT does not deteriorate the performance of the model in phase equilibria applications, but markedly reduces computational requirements.
- PC-SAFT and sPC-SAFT have been extensively applied to phase equilibria of many components and mixtures, but application to other properties appears to be very limited. In the phase equilibria applications reviewed, BIPs are usually required to model complex mixtures accurately.

- PC-SAFT and sPC-SAFT does not explicitly account for strong polar forces, but uses the *Van der Waals* approach. There is multitude of problems associated with this approach, especially when strong polar interactions are present in the system.
- The CPA EOS uses the cubic SRK to account for physical forces and the association term from SAFT to account for association forces. The model has been applied to a wide range of phase equilibria applications, but has only been applied to a very limited number of other thermodynamic properties. In the phase equilibria applications considered, BIPs are usually required to model complex mixtures. The model also does not explicitly account for polar forces, but also uses the *Van der Waals* approach.
- The data included in the regression procedure currently used to determine pure component model parameters in sPC-SAFT and CPA does not include any information regarding temperature partial derivatives of the state function. A systematic study is needed to determine if improved model parameters for sPC-SAFT can be obtained by including various combinations of properties in the regression routine.

Considering the above, a thorough assessment of the model accuracy of sPC-SAFT and CPA on applications other than phase equilibria would prove to be extremely useful. From this assessment, greater insight into the shortcomings of the models is obtained that allows identification of areas that require improvement.

Chapter 3

Modelling properties of pure components

First- and second- order properties of pure components are modelled in this chapter with the following EOS:

- sPC-SAFT (which is the same as PC-SAFT for pure components)
- CPA
- SRK
- Peng-Robinson

SRK and Peng-Robinson are included as suitable references to show the improvements of the more complex CPA and sPC-SAFT models. Special attention is paid to the improvement of CPA from SRK, since the difference in the performance of the models is only a result of parameter regression in the case of non-hydrogen bonding systems where there is no association.

It should be mentioned that experimental data for some of the properties over extensive temperature and pressure ranges are very scarce and was often a deciding factor on which components were selected for thermodynamic modelling. Only data that was available in open literature were considered in this study and was accepted as sufficiently accurate.

The approach followed is to consider different properties of the component groups as classified in appendix A.2.1 and then to compare the performance of the models between the different properties in order to expose some new shortcomings in the models. Specifically, the behaviour of the following components is investigated in this chapter:

- Non-polar group is represented by *n*-hexane and *n*-dodecane.
- Polar (non-HB) group is represented by acetone.
- Hydrogen bonding group is represented by methanol, ethanol and water.

A summary of results for each group is presented in the beginning of each section in tabular format and typical results for each group of components are presented graphically. In the legend of each figure, the names of the models together with the percentage Absolute Average Deviation (%AAD) from the data is given (in brackets after the name of each model). The %AAD is calculated as follows:

$$\%AAD = \frac{1}{np} \sum_i^{np} \frac{|x^{calc} - x^{exp}|}{x^{exp}} \times 100 \quad (3-1)$$

The investigation focuses on the following points for each model, with specific focus on sPC-SAFT and CPA:

- The ability of the model to predict thermodynamic properties. The percentage %AAD is the main value considered. It is desired to have low values for %AAD and to have graphical profiles of experimental data and model predictions that are matching in trends.
- If low %AAD values are not obtained, the ability of the model to capture the trends exhibited by experimental data are investigated. It is desired to have matching trends between experimental data and model predictions.
- To identify shortcomings in the models.
- To consider the influence parameter regression had on the performance of CPA in comparison to SRK.
- To determine if the inclusion of other properties in the parameter regression objective function lead to improve prediction of more properties.

Usually experimental data is published at isothermal conditions and the influence of pressure is observed. Most of the properties in this section are thus presented graphically at two temperatures over wide pressure ranges.

Validation of EOS models

In order to calculate some of the thermodynamic properties that are of interest in this project, the first- and second-order derivatives with respect to the independent variables for each EOS are required. The derivatives were determined analytically and are presented in Appendix F. These derivatives were coded in a computer program and numerically checked to be correct. The reader is referred to Appendix D for more detail regarding model accuracy and validation.

3.1 Pure component parameters used

The pure component parameters used in this chapter were sourced from various published articles and are summarized in the Table 3-1 for sPC-SAFT and in Table 3-2 for CPA. It should be emphasized again that the parameters were fitted to only saturated vapour pressure and saturated liquid density data by the relevant previous researches.

Table 3-1: sPC-SAFT pure component parameters from the literature

Component	Mw g / mol	m	σ [Å]	ε/k [K]	ε^{AB}/k [K]	κ^{AB}	Sch.	Ref.
<i>n</i> -hexane	86.177	3.0576	3.7983	236.77	-	-	-	(24)
<i>n</i> -heptane	100.20	3.4831	3.8049	238.4	-	-	-	(24)
<i>n</i> -dodecane	170.34	5.3060	3.8959	249.21	-	-	-	(24)
acetone	58.079	2.7740	3.2557	253.41	-	-	-	(24)
methanol	32.042	1.5255	3.23	188.9	2899.5	0.06718	2B	(25)
ethanol	46.069	1.2309	4.1057	316.91	2811.02	0.00633	2B	(31)
1-propanol	60.095	1.79963	3.9044	292.11	2811.02	0.00633	2B	(31)
1-hexanol	102.17	2.91583	3.9349	284.91	2811.02	0.00633	2B	(31)
water	18.015	1.5	2.6273	180.3	1804.22	0.18	4C	(36)

Table 3-2: CPA pure component parameters from the literature

Component	T_c [K]	$a0/Rb$ [K]	c_1	b (L / mol)	ε^{AB}/R (L / mol)	$\beta^{AB} \cdot 10^3$	Sch.	Ref.
<i>n</i> -hexane	507.6	2640.030	0.8313	0.10789	-	-	-	(91)
<i>n</i> -heptane	540.2	2799.762	0.9137	0.12535	-	-	-	(91)
<i>n</i> -dodecane	658	3471.038	1.19531	0.21624	-	-	-	(91)
acetone	508.2	2719.569	0.80023	0.0619	-	-	-	(91)
methanol	512.64	1573.707	0.43102	0.030978	2957.782	16.10	2B	(91)
ethanol	513.92	2123.828	0.73690	0.049110	2589.848	8.00	2B	(91)
1-propanol	536.78	2234.515	0.91709	0.064110	2525.860	8.10	2B	(91)
1-hexanol	611.35	2950.202	0.9805	0.1108	2525.860	3.30	2B	(91)
water	647.29	1017.338	0.67359	0.014515	2003.248	69.20	4C	(91)

Using parameters from different sources already introduces some form of biased comparison, since it is doubtful if the regression procedures and quality of data used by the different workers were the same. The robustness of the regression procedures used to determine the pure component parameters influences the performance of the model severely and it is quite possible that some workers used superior procedures compared to others.

3.2 Non-polar components

By investigating non-polar components, the influence of the repulsive and dispersive interactions is effectively isolated. EOS models can then be evaluated on their ability to account for these interactions. The contribution due to association is zero in both CPA and sPC-SAFT for non-polar components. This implies that CPA is the same model as SRK with the only difference being that

the parameters of CPA were fitted to saturated vapour pressure and saturated liquid density data. A summary of the results for the properties investigated are presented in Table 3-3:

Table 3-3: Summary of results for properties investigated for non-polar components with the thermodynamic models

Property, Component and Condition	sPC-SAFT (%AAD)	CPA (%AAD)	SRK (%AAD)	PR (%AAD)	Ref.
Mass density					
• <i>n</i> -hexane at T = 293.15 K (P = 0.1 – 150 MPa)	0.84	0.67	10.3	1.25	(92)
• <i>n</i> -hexane at T = 373.15 K (P = 0.1 – 150 MPa)	1.38	2.65	8.04	1.27	(92)
• <i>n</i> -dodecane at T = 293.15 K (P = 0.1 – 140 MPa)	1.02	5.39	21.2	13.3	(93)
• <i>n</i> -dodecane at T = 353.15 K (P = 0.1 – 140 MPa)	0.94	3.14	19.3	11.3	(93)
Average	1.05	2.96	14.7	6.78	
Isothermal compressibility					
• <i>n</i> -hexane at T = 293.15 K (P = 0.1 – 150 MPa)	19.1	25.7	27.0	28.1	(92)
• <i>n</i> -hexane at T = 373.15 K (P = 0.1 – 150 MPa)	12.8	21.2	25.2	24.4	(92)
• <i>n</i> -dodecane at T = 293.15 K (P = 0.1 – 140 MPa)	40.5	35.2	33.4	36.5	(93)
• <i>n</i> -dodecane at T = 353.15 K (P = 0.1 – 140 MPa)	28.3	29.5	31.8	31.9	(93)
Average	25.2	27.9	29.4	30.2	
Pressure-volume derivative					
• <i>n</i> -hexane at T = 293.15 K (P = 0.1 – 150 MPa)	15.4	37.6	29.0	41.7	(92)
• <i>n</i> -hexane at T = 373.15 K (P = 0.1 – 150 MPa)	10.2	27.9	23.7	29.6	(92)
• <i>n</i> -dodecane at T = 293.15 K (P = 0.1 – 140 MPa)	28.4	57.6	38.5	52.4	(93)
• <i>n</i> -dodecane at T = 353.15 K (P = 0.1 – 140 MPa)	21.6	46.5	33.9	43.3	(93)
Average	18.9	42.4	31.3	41.8	
Isobaric thermal expansivity					
• <i>n</i> -dodecane at T = 293.15 K (P = 0.1 – 140 MPa)	9.91	55.4	57.3	57.7	(93)
• <i>n</i> -dodecane at T = 353.15 K (P = 0.1 – 140 MPa)	3.32	50.7	52.7	52.8	(93)
Average	6.62	53.1	55.0	55.3	
Isochoric heat capacity					
• <i>n</i> -hexane at T = 293.15 K (P = 0.1 – 100 MPa)	7.12	5.34	7.80	4.81	(94)
• <i>n</i> -hexane at T = 373.15 K (P = 0.1 – 100 MPa)	4.77	5.25	7.01	4.84	(94)
• <i>n</i> -dodecane at T = 293.15 K (P = 0.1 – 140 MPa)	4.40	5.52	5.43	2.81	(93)
• <i>n</i> -dodecane at T = 353.15 K (P = 0.1 – 140 MPa)	5.37	5.96	7.53	5.36	(93)
1. <i>n</i> -dodecane at P = 0.1 MPa	3.84	5.83	7.25	5.22	(93)
2. <i>n</i> -dodecane at P = 50 MPa	4.44	5.30	6.85	4.72	(93)
Average	4.99	5.53	6.98	4.63	
Isobaric heat capacity					
• <i>n</i> -hexane at T = 293.15 K (P = 0.1 – 100 MPa)	1.17	5.42	3.1	5.53	(94)
• <i>n</i> -hexane at T = 373.15 K (P = 0.1 – 100 MPa)	0.22	2.63	1.09	2.54	(94)
• <i>n</i> -dodecane at T = 293.15 K (P = 0.1 – 140 MPa)	1.74	6.89	5.20	7.47	(93)
• <i>n</i> -dodecane at T = 353.15 K (P = 0.1 – 140 MPa)	0.91	4.05	2.63	4.51	(93)
Average	1.01	4.75	3.01	5.01	
Pressure-temperature derivative					
• <i>n</i> -hexane at T = 293.15 K (P = 0.1 – 100 MPa)	19.7	23.8	28.7	21.8	(92), (94)
• <i>n</i> -hexane at T = 373.15 K (P = 0.1 – 100 MPa)	16.6	22.5	27.9	21.8	(92), (94)
• <i>n</i> -dodecane at T = 293.15 K (P = 0.1 – 140 MPa)	21.7	29.2	37.2	31.0	(93)
• <i>n</i> -dodecane at T = 353.15 K (P = 0.1 – 140 MPa)	26.6	30.8	38.6	32.8	(93)
Average	21.2	26.6	33.1	26.9	
Heat capacity ratio					
• <i>n</i> -hexane at T = 293.15 K (P = 0.1 – 100 MPa)	5.55	10.2	10.1	9.87	(94)
• <i>n</i> -hexane at T = 373.15 K (P = 0.1 – 100 MPa)	4.33	7.49	7.26	7.02	(94)
• <i>n</i> -dodecane at T = 293.15 K (P = 0.1 – 140 MPa)	2.72	10.1	10.1	10.0	(93)

Property, Component and Condition	sPC-SAFT (%AAD)	CPA (%AAD)	SRK (%AAD)	PR (%AAD)	Ref.
• <i>n</i> -dodecane at T = 353.15 K (P = 0.1 – 140 MPa)	4.39	9.44	9.46	9.38	(93)
Average	4.25	9.31	9.23	9.07	
Speed of sound					
• <i>n</i> -hexane at T = 293.15 K (P = 0.1 – 150 MPa)	11.9	13.01	16.7	15.3	(92)
• <i>n</i> -hexane at T = 373.15 K (P = 0.1 – 150 MPa)	9.01	9.62	12.4	11.1	(92)
• <i>n</i> -dodecane at T = 293.15 K (P = 0.1 – 140 MPa)	17.1	25.1	33.1	32.6	(93)
• <i>n</i> -dodecane at T = 353.15 K (P = 0.1 – 140 MPa)	13.9	19.6	27.1	25.3	(93)
• <i>n</i> -propane	9.17	8.85	8.76	8.86	(94)
Average	12.2	15.2	19.6	18.6	
First-order volume derivative of F					
• <i>n</i> -hexane at T = 293.15 K (P = 0.1 – 150 MPa)	0.39	0.62	7.93	0.51	(92)
• <i>n</i> -hexane at T = 373.15 K (P = 0.1 – 150 MPa)	0.83	3.01	8.31	1.59	(92)
• <i>n</i> -dodecane at T = 293.15 K (P = 0.1 – 140 MPa)	0.37	2.33	10.2	6.21	(93)
• <i>n</i> -dodecane at T = 353.15 K (P = 0.1 – 140 MPa)	0.38	1.39	10.4	5.8	(93)
Average	0.49	1.84	9.21	3.53	
Second-order volume derivative of F					
• <i>n</i> -hexane at T = 293.15 K (P = 0.1 – 150 MPa)	15.7	38.2	29.8	42.4	(92)
• <i>n</i> -hexane at T = 373.15 K (P = 0.1 – 150 MPa)	10.5	27.7	24.1	30.6	(92)
• <i>n</i> -hexane at P = 5 MPa	13.7	22.8	40.7	26.8	(92)
• <i>n</i> -hexane at P = 100 MPa	12.3	42.6	26.8	46.6	(92)
• <i>n</i> -dodecane at T = 293.15 K (P = 0.1 – 140 MPa)	28.6	58.0	38.8	52.7	(93)
• <i>n</i> -dodecane at T = 353.15 K (P = 0.1 – 140 MPa)	21.9	47.0	34.2	43.8	(93)
Average	17.1	39.4	32.4	40.5	
Second-order temperature-volume derivative of F					
• <i>n</i> -hexane at T = 293.15 K (P = 0.1 – 100 MPa)	23.6	27.9	33.8	25.5	(92)
• <i>n</i> -hexane at T = 373.15 K (P = 0.1 – 100 MPa)	20.6	27.2	33.6	26.2	(92)
• <i>n</i> -dodecane at T = 293.15 K (P = 0.1 – 140 MPa)	25.8	34.3	43.8	36.4	(92), (94)
• <i>n</i> -dodecane at T = 353.15 K (P = 0.1 – 140 MPa)	29.9	36.6	46.0	39.0	(92), (94)
Average	25.0	31.5	39.3	31.8	

It follows that sPC-SAFT provides superior predictions of thermodynamic properties compared to the three cubic EOS. This is too expected, considering the models firm fundamental framework. However, Table 3-3 also indicate that large errors are still experienced in the prediction of most second-order properties. In the remainder of this section, representative results are presented graphically to discuss some of the shortcomings in more detail.

3.2.1 Mass density

The mass density is dependent on the first-order volume derivative of the state function, as shown in equations (B-2) to (B-4). It is expected that sPC-SAFT and CPA will give good representation of this property, especially in the low pressure regions, because saturated liquid density data were included in the parameter regression.

i) *n*-hexane

The mass density of *n*-hexane is shown in Figure 3-1 and Figure 3-2:

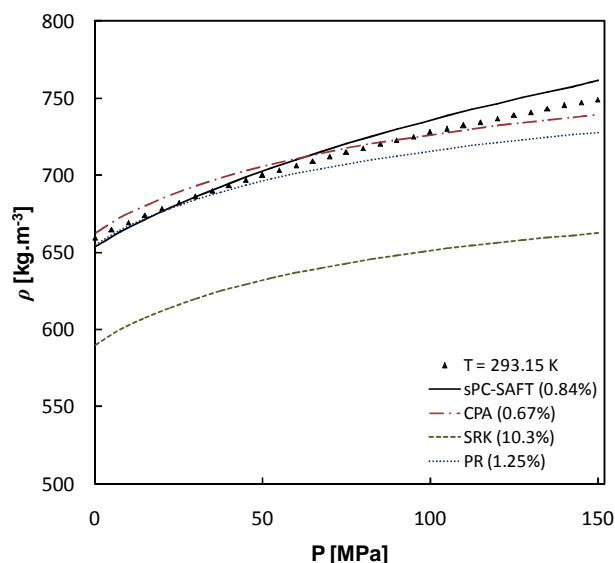


Figure 3-1: Mass density of *n*-hexane at $T = 293.15$ K. Data from ref. (92).

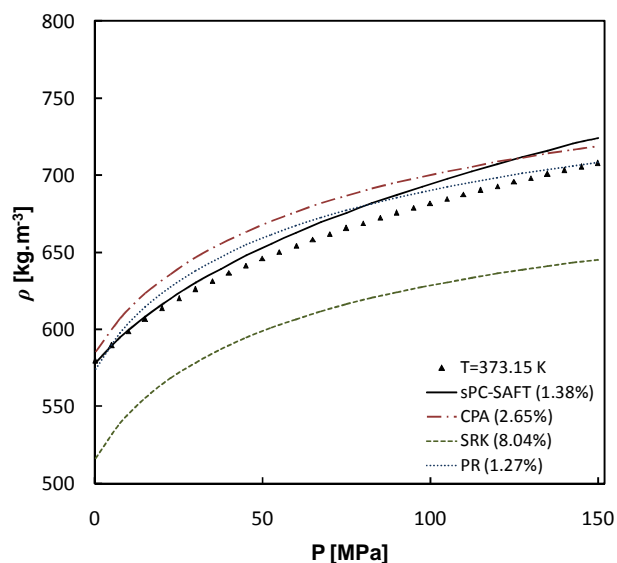


Figure 3-2: Mass density of *n*-hexane at $T = 373.15$ K. Data from ref. (92).

From Figure 3-1, it is observed that sPC-SAFT, CPA and Peng-Robinson provide a good representation of the experimental data and are superior to SRK. It is well known that Peng-Robinson gives slightly better correlation of volumetric properties than SRK (3). At the higher pressures, sPC-SAFT starts to over-predict the mass density slightly.

It is especially interesting to note that the graphical profiles of CPA and SRK are essentially the same; the parameter regression seems to have only shifted the prediction of SRK upwards in vertical position on the graph to provide a better representation of the experimental data.

In Figure 3-2, the correlations of CPA and sPC-SAFT deteriorated slightly, but generally the same comments hold for the higher temperature plot.

ii) *n*-dodecane

n-Dodecane is a twelve-carbon molecule and is regarded as a heavy *n*-alkane and is twice the size of *n*-hexane. sPC-SAFT provides a superior correlation of the mass density of *n*-dodecane compared to the other models (see Figure 3-3). The improvement of CPA compared to SRK as a result of parameter regression is also noticeable, with regression shifting the prediction of CPA towards the experimental data, but not changing the trend.

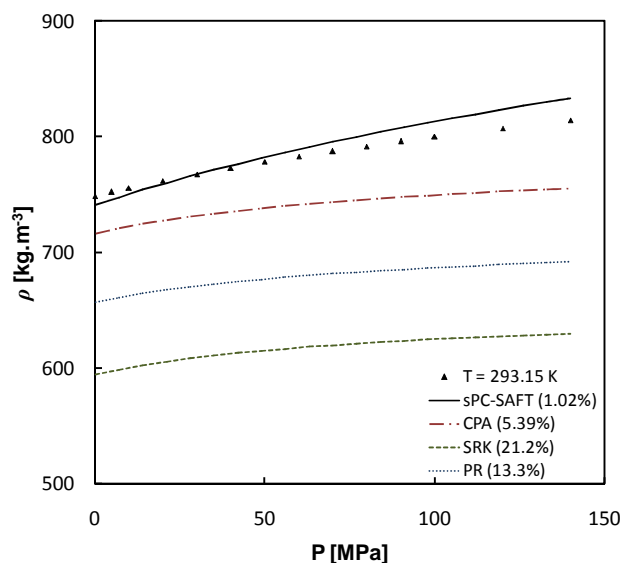


Figure 3-3: Mass density of *n*-dodecane at $T = 293.15$ K. Data from ref. (93).

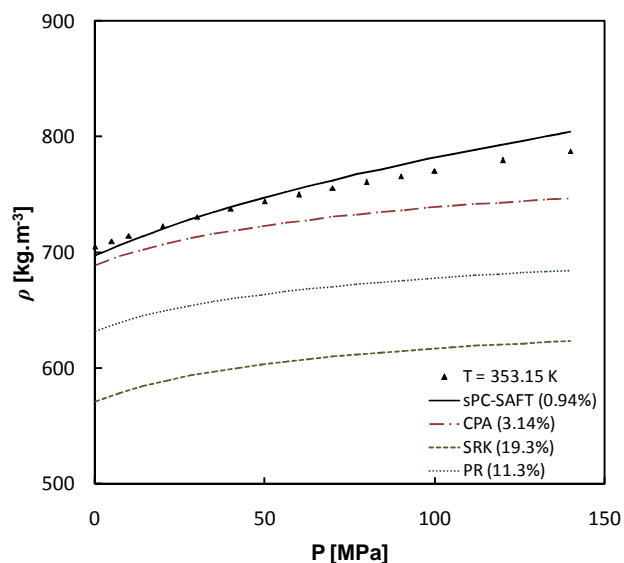


Figure 3-4: Mass density of *n*-dodecane at $T = 353.15$ K. Data from ref. (93).

In Figure 3-4, sPC-SAFT still gives a correlation of the same accuracy, while CPA improved considerably in accuracy. The change in experimental data with the increase in temperature is well followed by sPC-SAFT (the shift in prediction is of the same magnitude), while the shift in CPA is larger than the shift of the experimental data. This possibly indicates some discrepancy in the temperature dependency of CPA.

The influence of increasing chain length on model performance can be investigated if the results are compared with the results of *n*-hexane. Comparing the mass density plots of *n*-dodecane with the mass density plots of *n*-hexane (Figure 3-1 and Figure 3-2), it seems that the chain length is responsible for the difference in the shape of the curvature between sPC-SAFT and the cubic models. Cubic models represent *n*-dodecane molecules as round spheres in its physical framework, while sPC-SAFT represents the molecule as smaller spheres connected in a chainlike manner (the segment number parameter indicated that *n*-dodecane is represented as 5.306 spheres).

3.2.2 Pressure-volume derivative

Experimental data for the isothermal compressibility and volume are used to calculate the pressure-volume derivative as shown in equation (3-2):

$$\left(\frac{\partial P}{\partial V}\right)_{T,n} = -\frac{1}{\beta_T V} \quad (3-2)$$

i) *n*-hexane

From Figure 3-5, only sPC-SAFT is able to follow the correct trend of the pressure-volume derivative for *n*-hexane. The predictions of CPA, SRK and Peng-Robinson do not match the trends

of the experimental data. The strength in the physical framework of sPC-SAFT now clearly becomes evident and the additional mathematical complexity of the model becomes justifiable.

The results for the pressure-volume derivative of *n*-hexane are shown in Figure 3-5 and Figure 3-6:

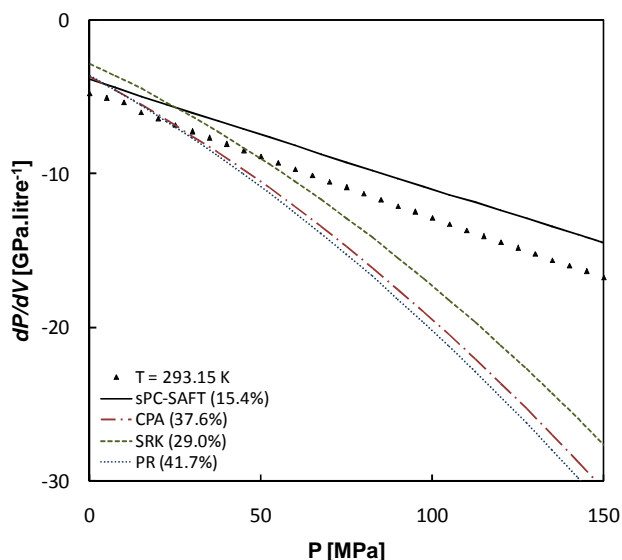


Figure 3-5: Pressure-volume derivative of *n*-hexane at $T = 293.15$ K. Data calculated from ref. (92).

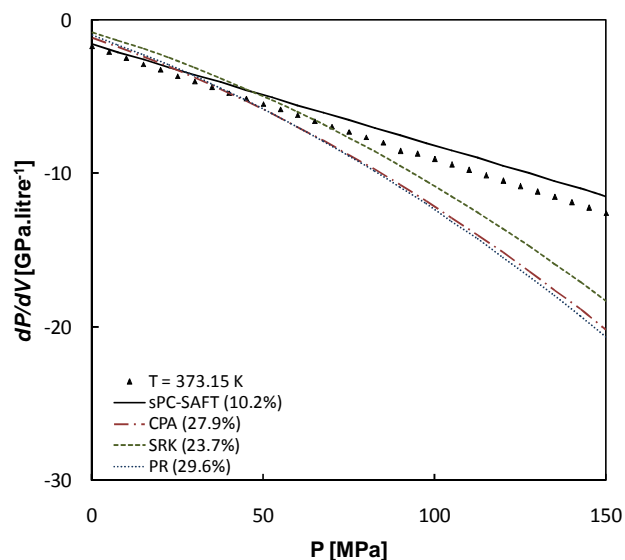


Figure 3-6: Pressure-volume derivative of *n*-hexane at $T = 373.15$ K. Data calculated from ref. (92).

Figure 3-6 shows that the prediction with sPC-SAFT improves considerably at the higher temperature. This indicates that there is some problem with the temperature dependency of sPC-SAFT, especially at low temperatures.

ii) *n*-dodecane

Conducting similar calculations as for *n*-hexane, Figure 3-7 and Figure 3-8 are obtained for the pressure-volume derivative and second-order volume derivative of *n*-dodecane:

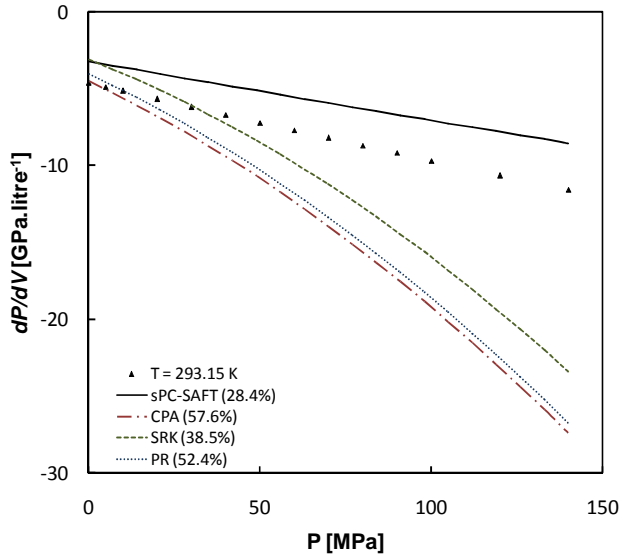


Figure 3-7: Pressure-volume derivative of *n*-dodecane at $T = 293.15$ K. Data from ref. (93).

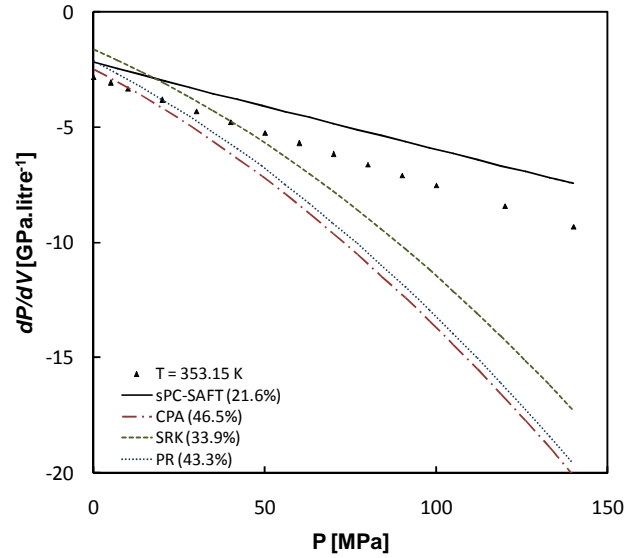


Figure 3-8: Pressure-volume derivative of *n*-dodecane at $T = 353.15$ K. Data from ref. (93).

From Figure 3-7 and Figure 3-8 very similar results are obtained for *n*-dodecane compared to *n*-hexane. Once again sPC-SAFT is the only model that is remotely able to capture the curvature of the data, while the other models give poor predictions. However, for all models the %AAD increased compared to *n*-hexane, indicating the difficulty and necessity to properly account for the influence of chain length. Since the trend of sPC-SAFT is more or less correct, the question arises whether it would be possible to obtain improved predictions of second-order properties with sPC-SAFT, if they are included in the regression routine.

Perakis *et al.* (79) mentioned that in their investigation, which predominantly centred on phase equilibria calculations at low pressures, they found no evidence that the physical term of SAFT-based models is superior to that of CPA. However, these results now indicate that the physical term of sPC-SAFT is indeed superior to CPA, especially at high pressures and when second-order properties are considered.

3.2.3 Isochoric heat capacity

The isochoric heat capacity is a rather special property, since the residual part is only dependent on the first- and second- order temperature derivatives of the reduced residual Helmholtz energy function, as shown in equation (3-4):

$$C_V(T, V, \mathbf{n}) = C_V^{ideal}(T) + C_V^r(T, V, \mathbf{n}) \quad (3-3)$$

$$\frac{C_V^r(T, V, \mathbf{n})}{R} = -T^2 \left(\frac{\partial^2 F}{\partial T^2} \right)_{V, \mathbf{n}} - 2T \left(\frac{\partial F}{\partial T} \right)_{V, \mathbf{n}} \quad (3-4)$$

The ideal part of the property is calculated with the DIPPR correlations (95).

i) *n*-hexane

In Figure 3-9 it is observed that all the models over-predict the isochoric heat capacity of *n*-hexane. Only the prediction by sPC-SAFT matches the trends of the experimental data fairly well, although the prediction is slightly sensitive to changes in pressure. On the other hand, the cubic models show an insensitive pressure dependency. The trends of CPA compared to SRK do not change as a result of the parameter regression, but the prediction only shifts downward on the graph towards the experimental data.

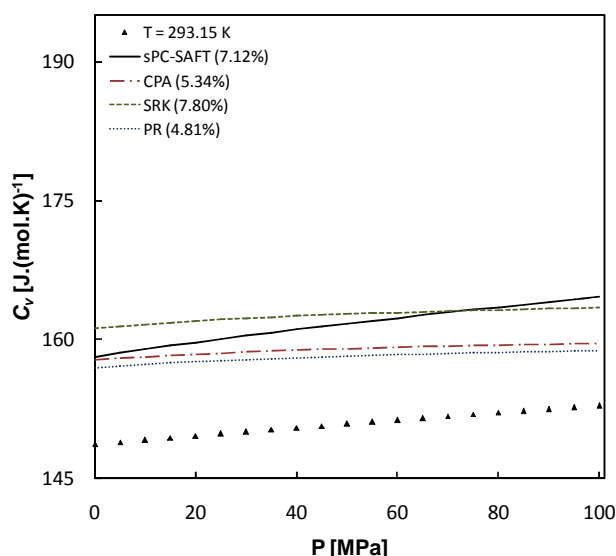


Figure 3-9: Isochoric heat capacity of *n*-hexane at $T = 293.15\text{ K}$. Data from ref. (94).

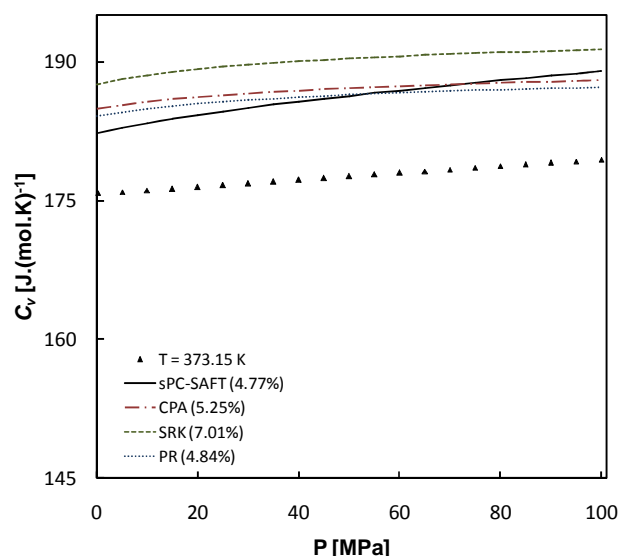


Figure 3-10: Isochoric heat capacity of *n*-hexane at $T = 373.15\text{ K}$. Data from ref. (94).

At $T = 293.15\text{ K}$, the ideal isochoric heat capacity value is $131.57\text{ J.}(\text{mol.K})^{-1}$ and is only a function of temperature. This implies that the error originates from the residual contribution. Consider the experimental point at $T = 293.15\text{ K}$ and $P = 0.1\text{ MPa}$. The experimental isochoric heat capacity value is $148.6\text{ J.}(\text{mol.K})^{-1}$ and sPC-SAFT predicts an isochoric heat capacity value of $158.4\text{ J.}(\text{mol.K})^{-1}$. The ideal contribution accounts for 89% ($131.57/148.6$) of the property which means that the residual part is approximately be equal to $17.0\text{ J.}(\text{mol.K})^{-1}$. sPC-SAFT predicts a value of $26.8\text{ J.}(\text{mol.K})^{-1}$ ($158.4 - 131.57$), implying the residual part is over-predicted by 58 % ($26.8/17.0$). This in turn implies that the temperature dependency of the state function derivatives is incorrect.

In Figure 3-10 at $T = 373.15\text{ K}$ the ideal contribution is equal to $163.8\text{ J.}(\text{mol.K})^{-1}$ and the same argument holds as at the lower temperature.

If it is assumed that a prediction of sPC-SAFT can be shifted upwards or downwards on the graph with parameter regression for some properties, it would be worthwhile to try and shift the prediction of sPC-SAFT to fit isochoric heat capacity experimental data. The chances are good that the temperature dependency of the model will be corrected/improved if the model is able to accurately describe the property. This requires an investigation on the influence of model parameters on properties. It is expected that there would be a trade-off in accuracy between certain properties, but the question is whether the accuracies can be distributed in such a way

that important properties of interest are predicted with good accuracy, while properties of lesser interest are predicted with a poorer accuracy. A preliminary investigation that continues on these arguments is presented in section 3.5 for sPC-SAFT.

ii) *n*-dodecane

From isochoric heat capacity results for *n*-dodecane shown in Figure 3-11 and Figure 3-12, only the prediction of sPC-SAFT moderately matches the trend of experimental data, although the prediction is too sensitive to changes in pressure. The cubic models (CPA, SRK and Peng-Robinson) all show the wrong pressure dependency of the property. The results are very similar to the results of *n*-hexane and the same conclusions may be made.

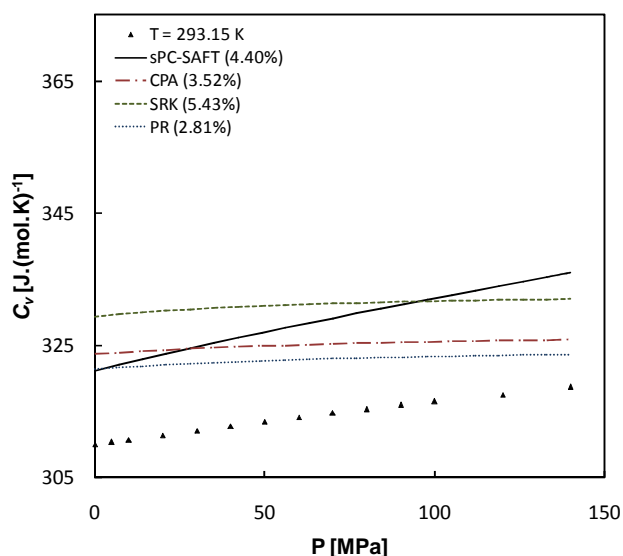


Figure 3-11: Isochoric heat capacity of *n*-dodecane at $T = 293.15$ K. Data from ref. (93).

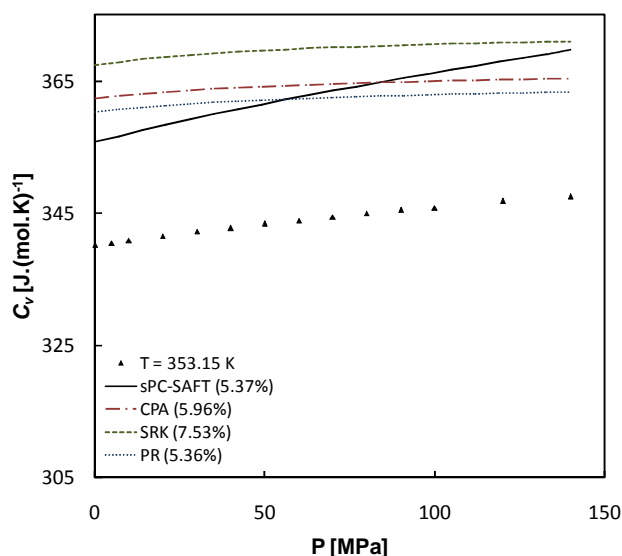


Figure 3-12: Isochoric heat capacity of *n*-dodecane at $T = 353.15$ K. Data from ref. (93).

The temperature dependency of the isochoric heat capacity of *n*-dodecane is also investigated and shown in Figure 3-13 and in Figure 3-14:

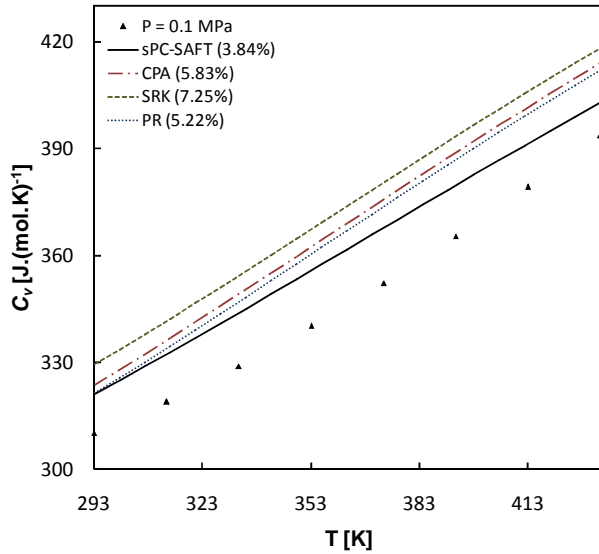


Figure 3-13: Isochoric heat capacity of *n*-dodecane at $P = 0.1$ MPa. Data from ref. (93).

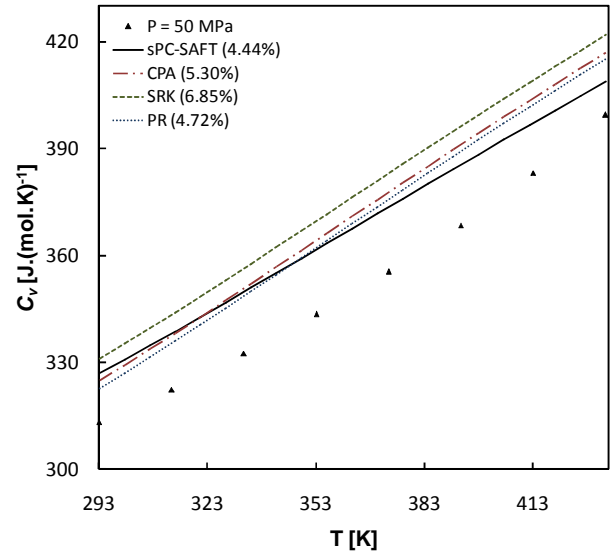


Figure 3-14: Isochoric heat capacity of *n*-dodecane at $P = 50$ MPa. Data from ref. (93).

From Figure 3-13 and Figure 3-14, the cubic models all exhibit the same temperature dependency of the isochoric heat capacity and the trends they predict match the experimental data. sPC-SAFT predicts a trend that is not the same compared to the experimental data. This is quite surprising considering the additional complexity of the EOS compared to the cubic models and the question arises how much of the discrepancies can be remedied with proper parameter regression.

3.2.4 Isobaric heat capacity

The isobaric heat capacity is a more complicated property than the isochoric heat capacity and is expressed as follows:

$$\frac{C_P^r - C_V^r}{R} = -\frac{T \left(\frac{\partial P}{\partial T} \right)_{V,n}^2}{R \left(\frac{\partial P}{\partial V} \right)_{T,n}} - n \quad (3-5)$$

The ideal part of the property is also calculated with DIPPR correlations (95).

i) *n*-hexane

None of the models are able to capture the trend of isobaric heat capacity of *n*-hexane in Figure 3-15. The cubic models all have similar predictions. It is very interesting to notice that SRK has the lowest %AAD of the cubic models and that the parameter regression of CPA actually resulted in a poorer prediction of the property. sPC-SAFT has the lowest %AAD value, but the minimum occurring at about 60 MPa is problematic. At $T = 293.15$ K, the ideal contribution to the property is $139.9 \text{ J.(mol.K)}^{-1}$. At 0.1 MPa, the ideal contribution accounts for 73% ($139.9/192.25$) of the property, the residual part is equal to $52.3 \text{ J.(mol.K)}^{-1}$ and sPC-SAFT predicts a residual value of

53.1 J.(mol.K)⁻¹, only overestimating the property by 1%. However, the deviation at the high pressure end is more severe and needs to be investigated further.

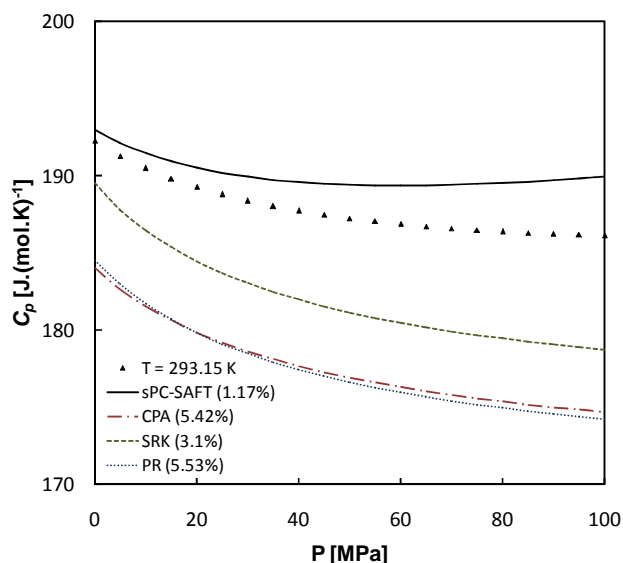


Figure 3-15: Isobaric heat capacity of *n*-hexane at $T = 293.15$ K. Data from ref. (94).

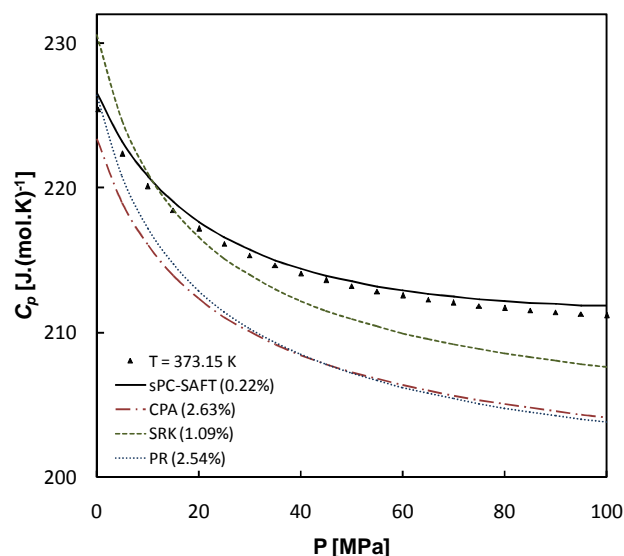


Figure 3-16: Isobaric heat capacity of *n*-hexane at $T = 373.15$ K. Data from ref. (94).

In Figure 3-16, sPC-SAFT provides an accurate description of the property (%AAD = 0.22), while the cubic models are less accurate. The %AAD of all models decrease with an increase in temperature.

ii) *n*-dodecane

The isobaric heat capacity of *n*-dodecane is shown in Figure 3-17 and Figure 3-18:

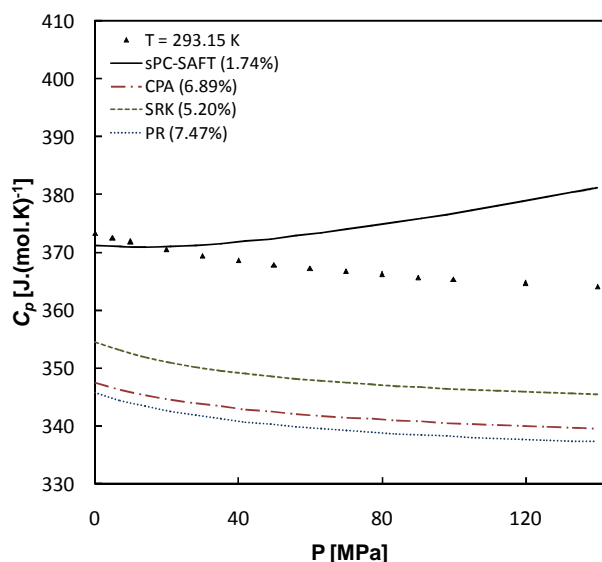


Figure 3-17: Isobaric heat capacity of *n*-dodecane at $T = 293.15$ K. Data from ref. (93).

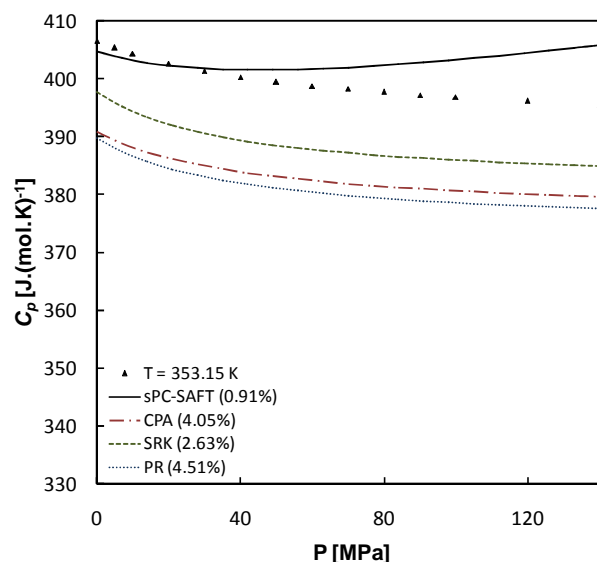


Figure 3-18: Isobaric heat capacity of *n*-dodecane at $T = 353.15$ K. Data from ref. (93).

From Figure 3-17 and Figure 3-18, sPC-SAFT predicts a very peculiar trend compared to the trend of the experimental data. The diverging behaviour of the property as the pressure increases confirms that there is some problem in the pressure dependency in the description of the isobaric

heat capacity. The divergence decreases with an increase in temperature (Figure 3-17 at $T = 293.15$ K and Figure 3-18 at $T = 353.15$ K). The trends of the cubic models are surprisingly consistent with the trend of the experimental data, although the property is under-predicted.

As in the case of the isochoric heat capacity, the contribution of the ideal part remains constant in Figure 3-17 and Figure 3-18, implying that the problem originates from the residual contribution to the isobaric heat capacity.

In order to further investigate why sPC-SAFT predicts diverging behaviour of the isobaric heat capacity at high pressure, consider equation (3-5) re-written as follows:

$$C_p^r = C_v^r - T \frac{\left(\frac{\partial P}{\partial T}\right)_{V,n}^2}{\left(\frac{\partial P}{\partial V}\right)_{T,n}} - Rn \quad (3-6)$$

From equation (3-6), it can be seen that in order to have an accurate description of the residual part of the isobaric heat capacity, it is necessary to have an accurate description of the residual isochoric heat capacity, pressure-volume derivative and pressure-temperature derivative and that the residual isobaric heat capacity is most sensitive for errors in the pressure-temperature derivative (because any errors are squared). The behaviour of the pressure-volume derivative and the isochoric heat capacity has already been investigated and, in order to determine the cause of the peculiar behaviour in sPC-SAFT, it is necessary to investigate the pressure-temperature derivative.

3.2.5 Pressure-temperature derivative

Equation (3-5) may also be rearranged to obtain an expression for the pressure-temperature derivative:

$$\left(\frac{\partial P}{\partial T}\right)_{V,n} = \sqrt{-\left(\frac{C_p^r - C_v^r}{T} + \frac{nR}{T}\right) \cdot \left(\frac{\partial P}{\partial V}\right)_{T,n}} \quad (3-7)$$

This may also be transformed as follows:

$$\left(\frac{\partial P}{\partial T}\right)_{V,n} = \sqrt{-\left(\frac{C_p^{real} - C_v^{real} - R}{T} + \frac{nR}{T}\right) \cdot \left(\frac{\partial P}{\partial V}\right)_{T,n}} \quad (3-8)$$

Equation (3-8) implies that, if experimental values for the isochoric heat capacity, isobaric heat capacity and pressure-volume derivatives are available, it would be possible to calculate an 'experimental value' for the pressure-temperature derivative.

It is also possible to calculate an “experimental value” for the pressure-temperature derivative from experimental values of the isobaric thermal expansivity and isothermal compressibility. The following equation is used:

$$\left(\frac{\partial P}{\partial T}\right)_{V,n} = \frac{\alpha_p}{\beta_T} \quad (3-9)$$

i) *n*-hexane

From Figure 3-19 and Figure 3-20 it is noted that all models under-predict the pressure-temperature derivative of *n*-hexane. The cubic models are more or less able to reproduce the trends of the data, while sPC-SAFT shows diverging behaviour from the data as the pressure increases.

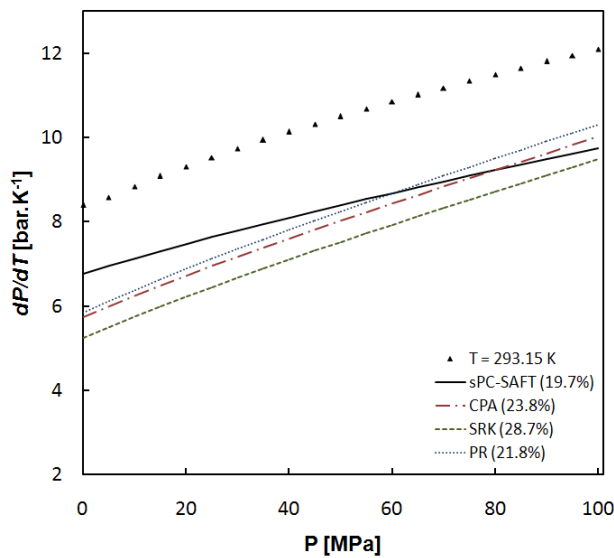


Figure 3-19: Pressure-temperature derivative of *n*-hexane at $T = 293.15$ K. Data calculated from ref. (92) and ref. (94).

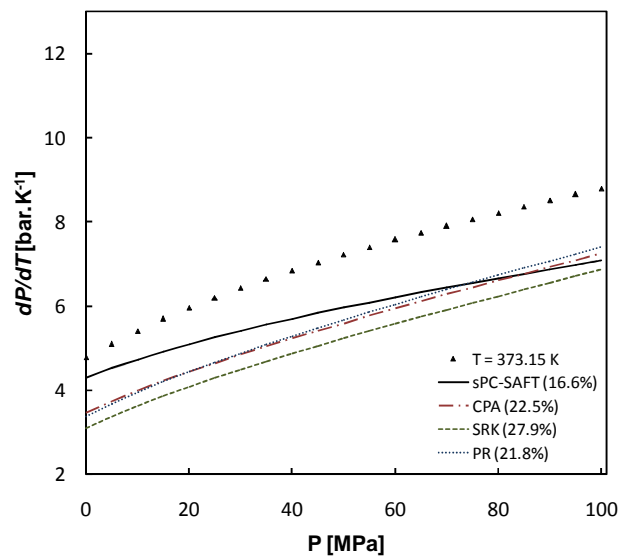


Figure 3-20: Pressure-temperature derivative of *n*-hexane at $T = 373.15$ K. Data calculated from ref. (92) and ref. (94).

The question now still remains why the cubic models were able to remotely capture the trends of the isobaric heat capacity (in Figure 3-17). Consider equation (3-6) again:

$$C_p^r = C_v^r - T \frac{\left(\frac{\partial P}{\partial T}\right)_{V,n}^2}{\left(\frac{\partial P}{\partial V}\right)_{T,n}} - Rn \quad (3-6)$$

Reviewing Figure 3-5 (pressure-volume derivative), Figure 3-9 (isochoric heat capacity) and Figure 3-19 (pressure-temperature derivative) it will be noticed that the squared error in the pressure-temperature derivative is effectively cancelled out by the non-linear error in the pressure-volume derivative. The combination of errors in the first and second terms in equation (3-6) leads to a cancellation of error that enables cubic models to falsely capture the trends of the isobaric heat capacity more or less correctly.

3.2.6 Heat capacity ratio

The heat capacity ratio is calculated from equation (3-7):

$$\gamma = \frac{C_P}{C_V} = \frac{\kappa_T}{\kappa_S} \quad (3-10)$$

The main reason for considering the heat capacity ratio is to investigate how it influences the speed of sound.

i) *n*-hexane

All the models under-predict the heat capacity ratio and the trends of all the models are fairly consistent with the trend exhibited by the experimental data in Figure 3-21. In light of the isobaric and isochoric heat capacity plots, the fact that the trends of the cubic models are in accordance with that of the data is surprising. There seems to be a trade-off in the physical framework of the cubic models between the two heat capacities in such a way that the trend of the heat capacity ratio is maintained (although it is still underestimated). A major part of the trade-off originates from the cancellation of errors between the pressure-temperature and pressure-volume derivatives, as discussed earlier. sPC-SAFT follows the trend of the isochoric heat capacity relatively well, but shows a strange minimum in the isobaric heat capacity. However, the effect is barely noticeable (from 50 MPa the slope slightly changes).

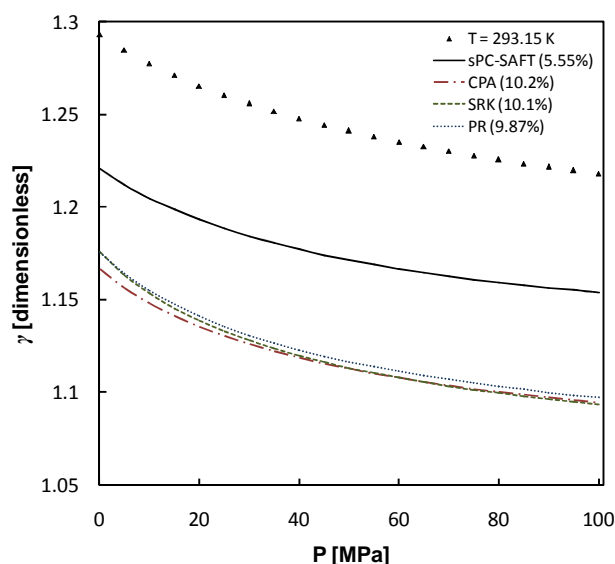


Figure 3-21: Heat capacity ratio of *n*-hexane at $T = 293.15$ K. Data calculated from ref. (94).

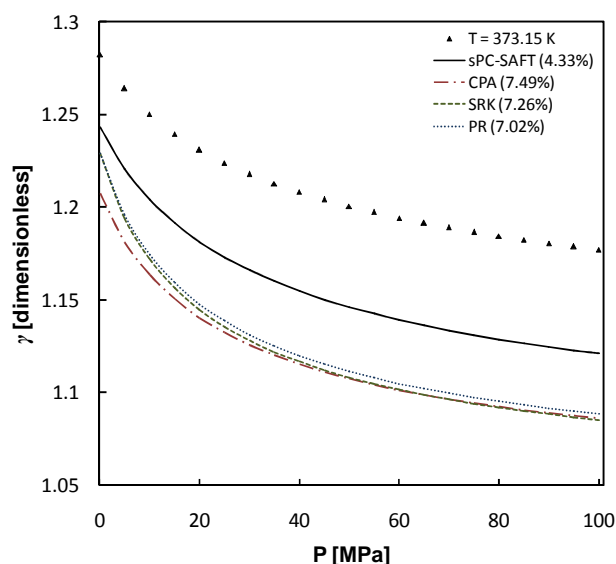


Figure 3-22: Heat capacity ratio of *n*-hexane at $T = 373.15$ K. Data calculated from ref. (94).

In Figure 3-22, there are some inconsistencies in the trends predicted by the models, compared to the data. In the lower pressure end, between 0.1 and 30 MPa, all the models show a pressure dependency that is too large (i.e. a change in pressure resulted in a too large change in the property). At the higher pressure, however, the error in the property remains constant. The

dramatic change in prediction between Figure 3-21 and Figure 3-22 indicates once again that there is some incorrect temperature dependency in all the models, especially sPC-SAFT.

3.2.7 Speed of sound

Accurate description of the speed of sound is regarded as a strict test for any EOS (96), because accurate descriptions of numerous partial derivatives are required as explained in Figure 2-3. The speed of sound may be expressed as follows:

$$u = \sqrt{\frac{V^2 \cdot \gamma \cdot \left(\frac{\partial P}{\partial V} \right)_{T,n}}{M_w}} \quad (3-11)$$

i) *n*-hexane

The speed of sound in *n*-hexane is shown in Figure 3-23 and in Figure 3-24:

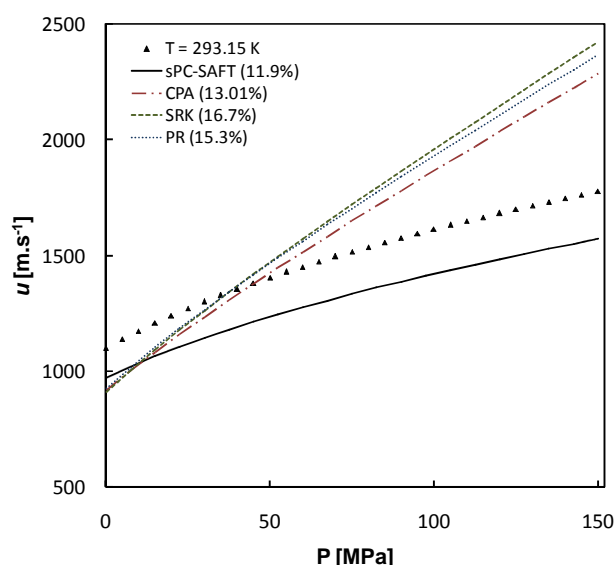


Figure 3-23: Speed of sound in *n*-hexane at $T = 293.15$ K. Data from ref. (92).

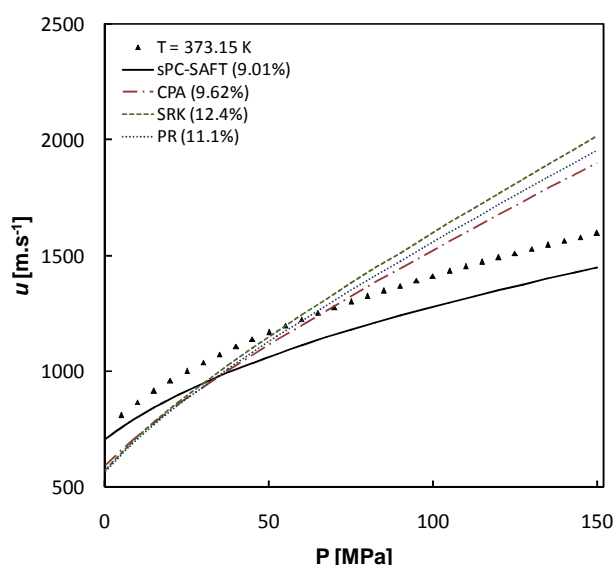


Figure 3-24: Speed of sound in *n*-hexane at $T = 373.15$ K. Data from ref. (92).

According to Figure 3-23 and Figure 3-24, sPC-SAFT is far superior in correlating the speed of sound compared to the other models. The cubic models fail to reproduce the curvature of the experimental data. Since the trends of all the models for the heat capacity ratio are very similar (Figure 3-21 and Figure 3-22), it can be concluded that the improvement of sPC-SAFT is a result of the improved description of the pressure-volume derivative.

ii) *n*-dodecane

From Figure 3-25 and Figure 3-26, similar results are obtained for the speed of sound in *n*-dodecane compared to *n*-hexane.

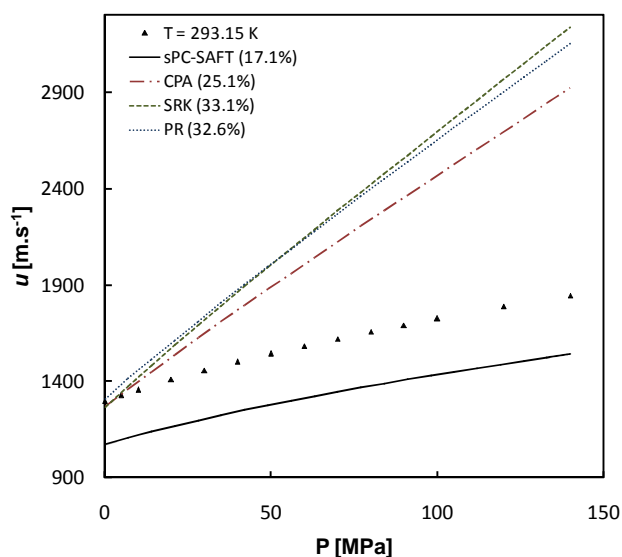


Figure 3-25: Speed of sound in *n*-dodecane at $T = 293.15$ K. Data from ref. (93).

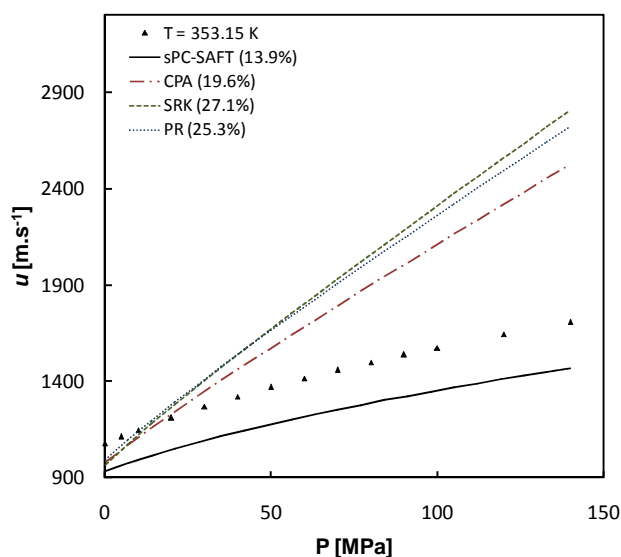


Figure 3-26: Speed of sound in *n*-dodecane at $T = 353.15$ K. Data from ref. (93).

Gregorowicz *et al.* (97) investigated some thermodynamic properties for pure fluids with simple EOS models, amongst others Peng-Robinson. One of the main conclusions from their investigation was that, in order to describe some of the singularities and extrema's associated with second-order derivative properties, the co-volume parameter has to be at least temperature and in some cases, temperature and volume dependent. The results from the non-polar section are in accordance with these findings, since none of the cubic models were able to describe most of the second-order properties considered in this section with great accuracy, especially the pressure-volume derivative.

3.2.8 Section highlights

Prominent findings from this section are:

- sPC-SAFT, Peng-Robinson and CPA are able to correlate the mass density of *n*-hexane with good accuracy, but with an increase in chain length, the cubic models (CPA, SRK, Peng-Robinson) start to predict larger deviations from the data, as shown in the mass density plots of *n*-dodecane.
- An improvement in the physical framework of sPC-SAFT over the framework of cubic models is its ability to describe the pressure-volume derivative with reasonable accuracy at high pressures.
- sPC-SAFT shows a slightly incorrect temperature dependent deficiency for several properties, including the pressure-volume derivative and isochoric heat capacity.
- sPC-SAFT shows some peculiar behaviour in modelling the isobaric heat capacity with diverging behaviour occurring as the pressure increases. The cubic models, in general, have reasonable trends, but under-predict the property. The framework of the cubic model allows errors to cancel out between the residual isochoric heat capacity, pressure-volume derivative and pressure-temperature derivative.

- The errors in the isobaric heat capacity predictions in sPC-SAFT are traced back to predominantly an incorrect description of the pressure-temperature derivative and it is expected that an improved description of the derivative would increase the accuracy of the isobaric heat capacity predictions.
- Accurate description of the speed of sound is mostly dominated by an accurate description of the pressure-volume derivative. Therefore, sPC-SAFT was able to reproduce the values of the experimental data with some degree of accuracy, while the cubic models failed.
- Improving the description of derivative properties with cubic-based models most likely requires modifications to the co-volume parameter.

In general, it seems as if sPC-SAFT possesses the physical framework to correlate the thermodynamic behaviour of non-polar components. However, a major question that arises from this section is whether the performance of sPC-SAFT can be improved by advanced parameter regression. This could possibly be done by including properties in the regression that are directly dependent on temperature partial derivative of the state function e.g. isochoric heat capacity.

The performance of CPA is similar to that of sPC-SAFT when first-order properties are considered, but is significantly inferior when second-order properties are considered, especially those properties that are dominated by the pressure-volume derivative.

In the next section, properties of polar components that do not hydrogen bond are considered.

3.3 Polar (non-HB) components

For polar components, it is expected that the models will predict similar trends to those predicted for non-polar components, because the polar forces are treated in a similar fashion as dispersive forces. The fact that only pure components are considered means that the simplification of lumping the polar and dispersive forces together will not deteriorate the performance of the models significantly, however, when mixtures are considered, it is expected that the performance of the model would deteriorate considerably. Acetone is considered in this section to be a good representation of a polar (non-hydrogen bonding) component. Table 3-4 provides a summary of all properties considered.

Table 3-4: Summary of results for properties investigated for polar (non-HB) components

Property	sPC-SAFT (%AAD)	CPA (%AAD)	SRK (%AAD)	PR (%AAD)	Data ref.
Mass density					
• acetone at T = 248.15 K (P = 0.1 – 100 MPa)	1.59	3.23	22.8	14.8	(98)
• acetone at T = 298.15 K (P = 0.1 – 100 MPa)	1.41	1.67	21.6	13.4	(98)
Average	1.50	2.45	22.2	14.1	
Isothermal compressibility					
• acetone at T = 298.15 K (P = 0.1 – 60 MPa)	9.11	17.0	9.13	10.6	(99)
• acetone at T = 328.06 K (P = 0.1 – 60 MPa)	11.9	11.8	12.2	9.1	(99)

Property	sPC-SAFT (%AAD)	CPA (%AAD)	SRK (%AAD)	PR (%AAD)	Data ref.
Average	10.5	14.4	10.7	9.9	
Pressure-volume derivative					
• acetone at T = 298.15 K (P = 0.1 – 60 MPa)	8.73	19.1	22.1	7.68	(99)
• acetone at T = 328.06 K (P = 0.1 – 60 MPa)	12.7	13.1	26.6	11.2	(99)
Average	10.7	16.1	24.4	9.44	
Isobaric thermal expansivity					
• acetone at T = 298.15 K (P = 0.1 – 60 MPa)	6.41	22.9	21.5	22.5	(99)
• acetone at T = 328.06 K (P = 0.1 – 60 MPa)	14.5	23.8	21.8	22.2	(99)
Average	10.5	23.4	21.7	22.4	
Isobaric heat capacity					
• acetone at T = 248.15 K (P = 0.1 – 100 MPa)	2.27	9.07	3.78	8.25	(98)
• acetone at T = 298.15 K (P = 0.1 – 100 MPa)	0.41	7.11	2.42	6.18	(98)
Average	1.34	8.09	3.10	7.22	
Pressure-temperature derivative					
• acetone at T = 298.15 K (P = 0.1 – 60 MPa)	3.1	7.1	22.7	14.5	(99)
• acetone at T = 328.06 K (P = 0.1 – 60 MPa)	3.58	13.58	28.4	21.2	(99)
Average	3.34	10.3	25.5	17.9	
Speed of sound					
• acetone at T = 248.15 K (P = 0.1 – 100 MPa)	1.21	17.0	21.4	23.3	(98)
• acetone at T = 298.15 K (P = 0.1 – 100 MPa)	3.00	9.00	13.1	13.3	(98)
Average	2.11	13.0	17.3	18.3	
First-order volume derivative of F					
• acetone at T = 248.15 K (P = 0.1 – 100 MPa)	2.22	4.22	31.6	20.4	(98)
• acetone at T = 298.15 K (P = 0.1 – 100 MPa)	2.62	2.87	40.1	24.8	(98)
Average	2.42	3.55	35.9	22.6	
Second-order volume derivative of F					
• acetone at T = 298.15 K (P = 0.1 – 60 MPa)	9.16	19.9	21.5	7.66	(99)
• acetone at T = 328.06 K (P = 0.1 – 60 MPa)	13.5	13.7	26.1	11.0	(99)
Average	11.3	16.8	23.8	9.33	
Second-order temperature-volume derivative of F					
• acetone at T = 298.15 K (P = 0.1 – 60 MPa)	3.24	7.71	24.6	15.7	(99)
• acetone at T = 328.06 K (P = 0.1 – 60 MPa)	3.97	14.4	30.8	23.0	(99)
Average	3.61	11.1	27.7	19.4	

As expected, Table 3-4 indicates that sPC-SAFT provides the best overall predictions for the properties of acetone. Peng-Robinson also performs well. As with the non-polar components, sPC-SAFT does not provide very accurate predictions of most second-order properties considered in this investigation. Representative results are presented graphically in the following sections:

3.3.1 Mass density

i) acetone

According to Figure 3-27, sPC-SAFT correlates the mass density with good accuracy, although there is a slight under-prediction. CPA performs slightly worse showing a deviation that increases with

increasing pressure. Both SRK and Peng-Robinson show reasonable trends, but the mass density is severely under-predicted. The improvement of CPA compared to SRK as a result of the parameter regression is noteworthy.

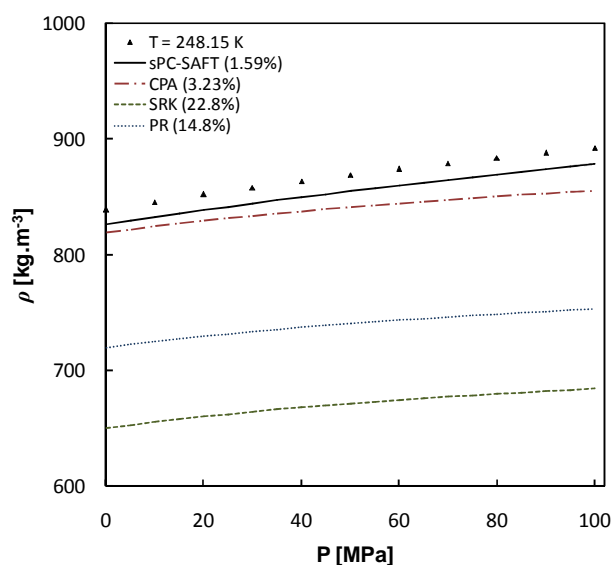


Figure 3-27: Mass density of acetone at $T = 248.15$ K. Data from ref. (98).

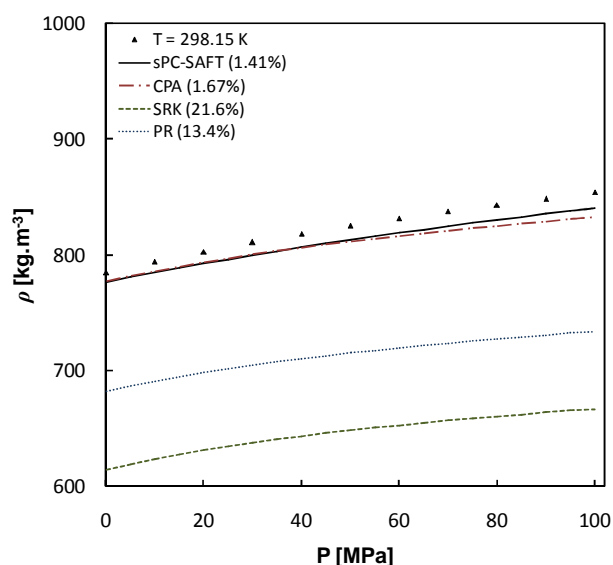


Figure 3-28: Mass density of acetone at $T = 298.15$ K. Data from ref. (98).

Both sPC-SAFT and CPA provide good predictions of the property (Figure 3-28). The fact that CPA provides a better prediction is probably due to the decreased effect of the polar forces at the higher temperature.

Comparing the mass density plots of *n*-hexane (Figure 3-1 and Figure 3-2) with acetone, it is interesting to compare the performance of Peng-Robinson for the two components. Peng-Robinson is able to give a sufficiently accurate description of the property for *n*-hexane but fails for acetone. The poor performance is probably due to the presence of polar forces.

3.3.2 Pressure-volume derivative

From Figure 3-29, the cubic models predict the same inconsistent trends compared to the experimental data. sPC-SAFT also predicts an erroneous trend.

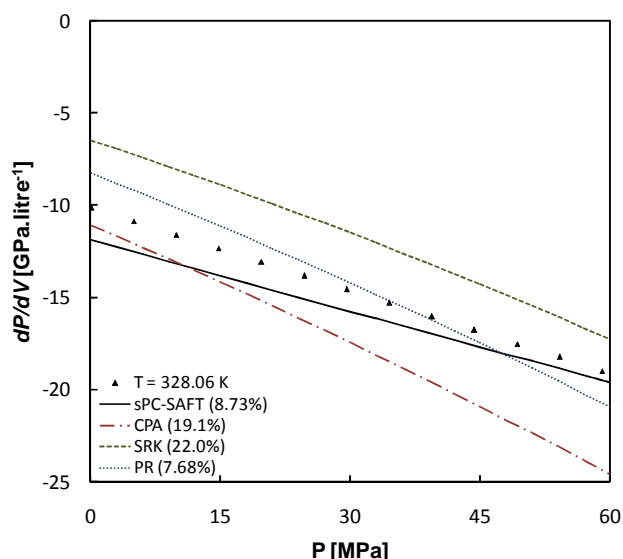


Figure 3-29: Pressure-volume derivative of acetone at $T = 298.15$ K. Data from ref. (99).

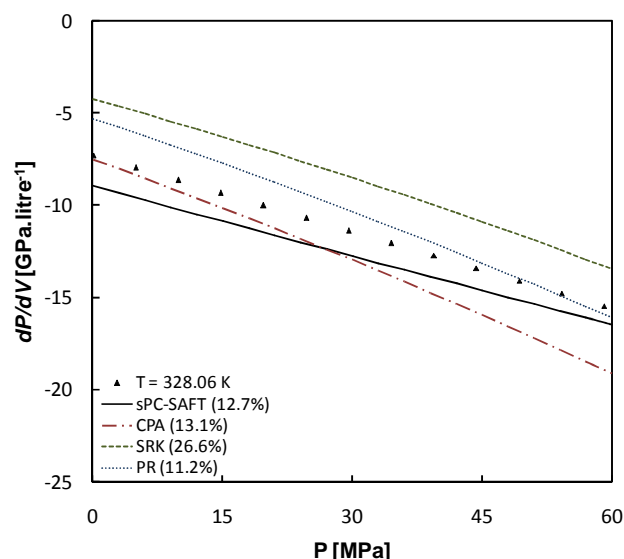


Figure 3-30: Pressure-volume derivative of acetone at $T = 328.06$ K. Data from ref. (99).

The behaviour of sPC-SAFT is rather surprising when compared with the pressure-volume predictions of *n*-hexane (Figure 3-5 and Figure 3-6) and *n*-dodecane (Figure 3-7 and Figure 3-8). In the last mentioned components, the pressure-volume derivative was over-predicted and the error remained constant for *n*-hexane and slightly increased with pressure for *n*-dodecane. For acetone, however, sPC-SAFT under-predicts the property and starts with a large error that decreases as pressure increases. Further investigation is needed to determine the cause, but it is suspected that it might be as a result of the artificially large dispersion energy parameter. Another explanation may be that acetone is a smaller molecule than *n*-hexane. The shape of acetone molecules is therefore closer to that of a sphere compared to *n*-hexane molecules.

In Figure 3-30, the trends stay more or less the same. It was expected that with an increase in temperature the trend of the experimental data would change as a result of the diminished polar forces. However, there is no evidence to suggest such a trend. This possibly indicates that polar forces do not influence the shape of the pressure-volume derivative significantly.

3.3.3 Isobaric heat capacity

i) acetone

The isobaric heat capacity of acetone is shown in Figure 3-31 and Figure 3-32:

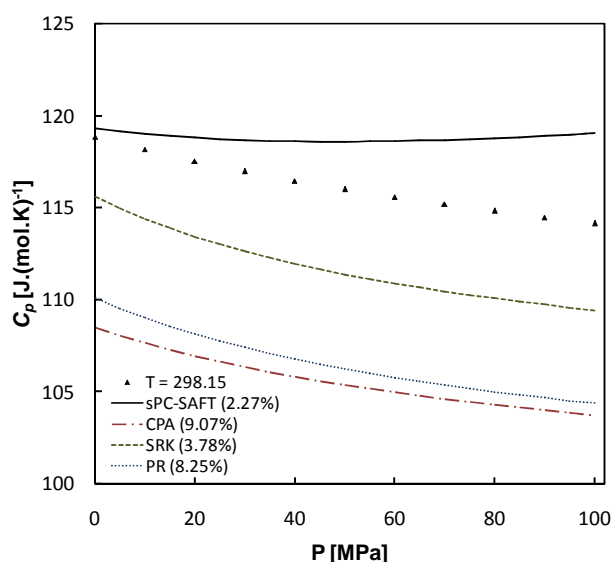


Figure 3-31: Isobaric heat capacity of acetone at $T = 248.15$ K. Data from ref. (98).

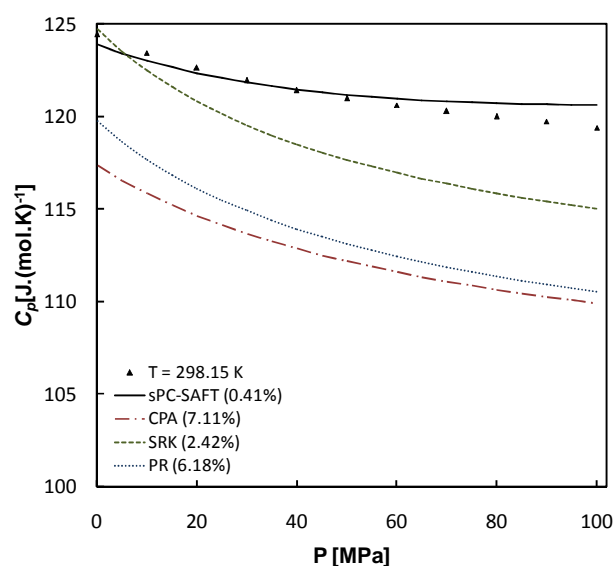


Figure 3-32: Isobaric heat capacity of acetone at $T = 298.15$ K. Data from ref. (98).

According to Figure 3-31, the cubic models predict trends that are most consistent with the experimental data, while sPC-SAFT shows the same incorrect pressure dependency as observed for *n*-hexane and *n*-dodecane (referring to the minimum and diverging behaviour as the pressure increases). sPC-SAFT overestimates the residual contribution by 10% at 100 MPa.

In Figure 3-32 at $T = 298.15$ K, sPC-SAFT is able to predict the property with fair accuracy, while the cubic models show a poor trends compared to the experimental data. In sPC-SAFT, the diverging effect again decreases with an increase in temperature and is consistent with the results found for *n*-hexane and *n*-dodecane. It is suspected that it is the same problem in all three components that are responsible for the peculiar behaviour.

3.3.4 Pressure-temperature derivative

i) acetone

The pressure-temperature derivative of acetone is shown Figure 3-33 and Figure 3-34:

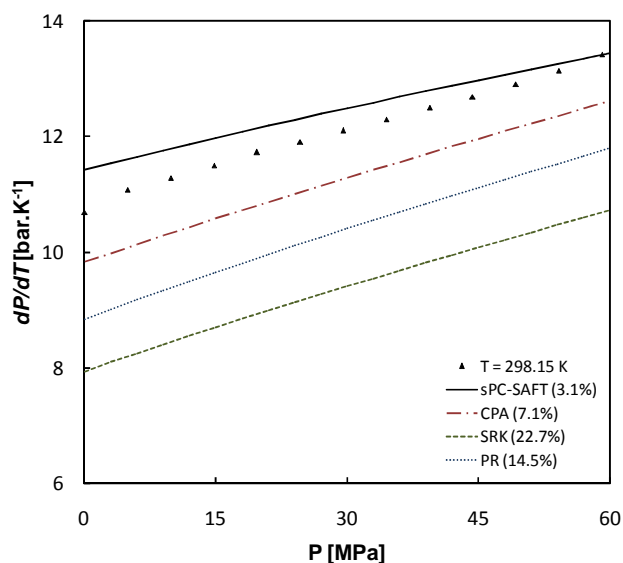


Figure 3-33: Pressure-temperature derivative of acetone at $T = 298.15$ K. Data calculated from ref. (99).

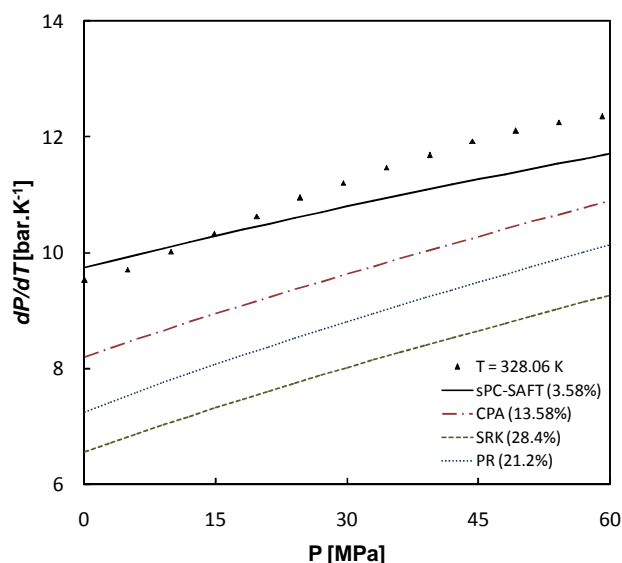


Figure 3-34: Pressure-temperature derivative of acetone at $T = 328.06$ K. Data calculated from ref. (99).

From Figure 3-33, the cubic models predict trends that are fairly consistent with the data and the improvement of CPA compared to SRK is again significant. sPC-SAFT shows an incorrect trend and these results are consistent with those for *n*-hexane and *n*-dodecane. The trends stay more or less the same in Figure 3-34.

3.3.5 Speed of sound

i) acetone

Only sPC-SAFT is able to remotely predict the speed of sound in acetone in both Figure 3-35 and Figure 3-36. The improvement of sPC-SAFT compared to the cubic models is a result of the improved description of the pressure-volume derivative and these results are consistent with those of *n*-hexane and *n*-dodecane. The prediction of sPC-SAFT is still problematic in the low pressure region, but satisfactory predictions are obtained as the pressure increases. The low pressure error is traced back to poor description of the pressure-volume derivative, or ultimately the second-order volume derivative of the state function.

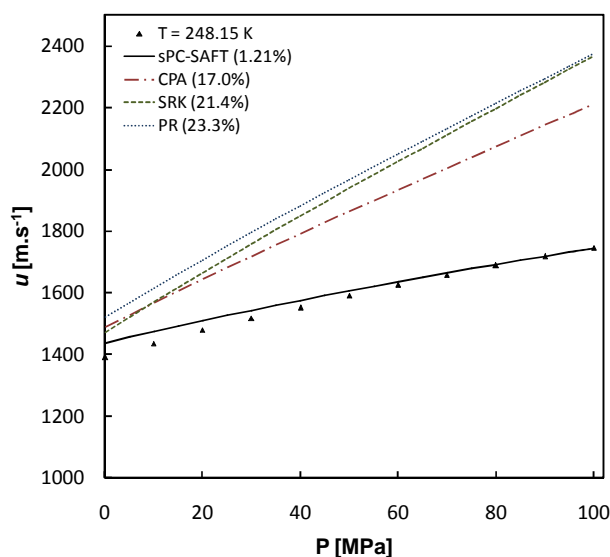


Figure 3-35: Speed of sound in acetone at $T = 248.15$ K. Data from ref. (98).

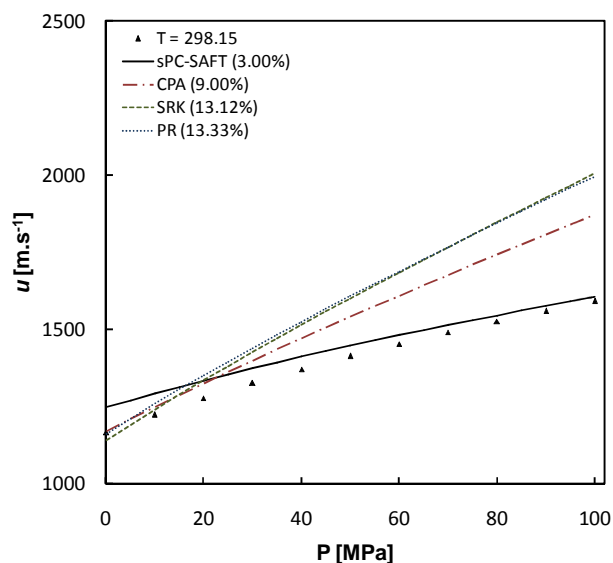


Figure 3-36: Speed of sound in acetone at $T = 298.15$ K. Data from ref. (98).

To investigate this further, the speed of sound in *n*-propane is shown in Figure 3-37. *n*-propane is very similar to acetone as it also has three carbon atoms. If the change in trend is a result of polar forces that are wrongfully accounted for in the dispersion energy parameter, the trend predicted for *n*-propane should be different to acetone and rather similar to *n*-hexane and *n*-dodecane:

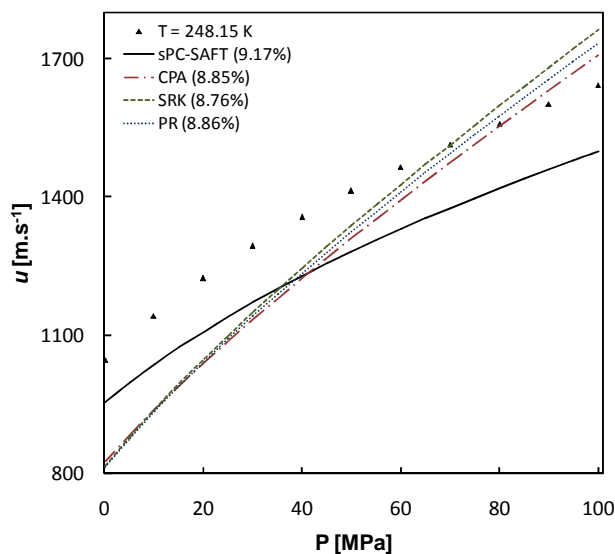


Figure 3-37: Speed of sound in *n*-propane at $T = 248.15$ K. Data from ref. (94).

From Figure 3-37, sPC-SAFT under-predicts the speed of sound in *n*-propane and the behaviour of the model with regards to the data is more similar to the behaviour of *n*-hexane and *n*-dodecane (Figure 3-23 and Figure 3-25) than to acetone (Figure 3-35). This is confirmation that accounting for polar forces by lumping them together with dispersive forces results in erroneous model behaviour. These results make the inclusion of a polar contribution term in sPC-SAFT more justifiable.

It also should be mentioned that the speed of sound description of sPC-SAFT in acetone is more accurate (lower %AAD) compared to the non-polar components, although its trend is not that consistent with the experimental data. This, in turn, indicates that the model parameters used for non-polar components are possibly not optimized and that it may be possible to shift the predictions of the non-polar components to fit the data more accurately. The question arises if this would result in a significant trade off in the properties that determine the accuracy of phase equilibria descriptions.

3.3.6 Section highlights

Continuing on the section highlights of the non-polar components (section 3.2.8), it was found that in general, the behaviour of all models for acetone as representative of the polar (non-hydrogen bonding) group was not very different to that of non-polar components. There seems to be subtle differences in the behaviour of polar (non-HB) components compared to that of non-polar components that become more evident when second-order properties are considered. Preliminary results indicate that improved predictions might be obtained if a polar term is included in the state function.

3.4 Hydrogen bonding components

In the modelling of hydrogen bonding components, it is expected that sPC-SAFT and CPA will be superior in correlating their properties compared to SRK and Peng-Robinson, because of the additional association term. The association term, however, increases the numerical intensity of the models considerably and requires two additional pure component parameters to account for the association in the system. It is important to realize that for these components, CPA is no longer a cubic model.

Properties of methanol, ethanol and water are considered in this section. A summary of the properties investigated in this section is presented in Table 3-5.

Table 3-5: Summary of results for properties investigated for hydrogen bonding components

Property	sPC-SAFT (%AAD)	CPA (%AAD)	SRK (%AAD)	PR (%AAD)	Ref.
Mass density					
• methanol at T = 273.15 K (P = 0.1 – 280 MPa)	1.21	0.63	27.7	20.4	(100)
• methanol at T = 333.15 K (P = 0.1 – 280 MPa)	1.83	0.80	27.3	19.9	(100)
• ethanol at T = 273.15 K (P = 0.1 – 280 MPa)	3.30	3.64	19.7	11.6	(101)
• ethanol at T = 333.15 K (P = 0.1 – 280 MPa)	2.51	2.61	19.1	11.0	(101)
• water at T = 298.15 K (P = 0.1 – 150 MPa)	4.16	0.41	25.6	17.8	(94)
• water at T = 348.15 K (P = 0.1 – 150 MPa)	4.14	0.74	26.5	18.6	(94)
Average	2.86	1.47	24.3	16.6	
Isothermal compressibility					
• methanol at T = 273.15 K (P = 0.1 – 280 MPa)	9.98	20.1	58.1	62.4	(100)

Property	sPC-SAFT (%AAD)	CPA (%AAD)	SRK (%AAD)	PR (%AAD)	Ref.
• methanol at T = 333.15 K (P = 0.1 – 280 MPa)	7.80	16.7	42.2	47.9	(100)
• ethanol at T = 273.15 K (P = 0.1 – 280 MPa)	4.76	40.4	54.0	58.4	(101)
• ethanol at T = 333.15 K (P = 0.1 – 280 MPa)	9.55	30.6	37.2	42.1	(101)
Average	8.02	26.9	47.9	52.7	
Pressure-volume derivative					
• methanol at T = 273.15 K (P = 0.1 – 280 MPa)	7.96	27.3	72.9	112	(100)
• methanol at T = 333.15 K (P = 0.1 – 280 MPa)	5.49	21.6	28.9	54.5	(100)
• ethanol at T = 273.15 K (P = 0.1 – 280 MPa)	4.81	65.2	76.7	114	(101)
• ethanol at T = 333.15 K (P = 0.1 – 280 MPa)	8.43	43.7	32.0	56.6	(101)
Average	6.67	39.5	52.6	84.3	
Isobaric thermal expansivity					
• methanol at T = 273.15 K (P = 0.1 – 280 MPa)	11.6	17.1	20.1	21.7	(100)
• methanol at T = 333.15 K (P = 0.1 – 280 MPa)	14.3	16.1	12.8	11.6	(100)
• ethanol at T = 273.15 K (P = 0.1 – 280 MPa)	16.5	30.5	26.1	26.5	(101)
• ethanol at T = 333.15 K (P = 0.1 – 280 MPa)	18.2	22.6	18.7	17.2	(101)
Average	15.2	21.6	19.4	19.3	
Isochoric heat capacity					
• methanol at T = 273.15 K (P = 0.1 – 280 MPa)	11.8	14.5	37.0	26.1	(94)
• methanol at T = 333.15 K (P = 0.1 – 280 MPa)	13.6	6.46	18.7	9.86	(94)
• water at T = 298.15 K (P = 0.1 – 150 MPa)	23.6	17.3	9.8	17.4	(94)
• water at T = 348.15 K (P = 0.1 – 150 MPa)	18.8	8.66	10.0	18.2	(94)
Average	16.9	11.7	18.9	17.9	
Isobaric heat capacity					
• methanol at T = 273.15 K (P = 0.1 – 280 MPa)	18.2	16.7	45.4	37.7	(94)
• methanol at T = 333.15 K (P = 0.1 – 280 MPa)	16.7	8.53	30.6	23.0	(100)
• ethanol at T = 273.15 K (P = 0.1 – 280 MPa)	2.67	10.1	35.9	27.5	(101)
• ethanol at T = 333.15 K (P = 0.1 – 280 MPa)	0.93	6.69	14.6	8.56	(101)
• water at T = 298.15 K (P = 0.1 – 150 MPa)	20.2	9.21	17.6	9.6	(94)
• water at T = 348.15 K (P = 0.1 – 150 MPa)	17.9	4.0	15.6	8.3	(94)
Average	12.8	9.21	26.6	19.1	
Pressure-temperature derivative					
• methanol at T = 273.15 K (P = 0.1 – 280 MPa)	19.7	10.3	88.9	109	(100)
• methanol at T = 333.15 K (P = 0.1 – 280 MPa)	20.6	5.52	60.5	75.9	(100)
• ethanol at T = 273.15 K (P = 0.1 – 280 MPa)	12.8	17.7	60.8	76.9	(101)
• ethanol at T = 333.15 K (P = 0.1 – 280 MPa)	10.7	12.1	38.8	51.6	(101)
Average	15.9	11.4	62.3	78.4	
Heat capacity ratio					
• methanol at T = 273.15 K (P = 0.1 – 280 MPa)	4.10	1.68	5.31	6.98	(94)
• methanol at T = 333.15 K (P = 0.1 – 280 MPa)	3.61	2.22	10.2	12.1	(94)
• water at T = 298.15 K (P = 0.1 – 150 MPa)	4.54	9.76	30.5	32.7	(94)
• water at T = 348.15 K (P = 0.1 – 150 MPa)	1.1	5.11	29.9	32.7	(94)
Average	3.34	4.69	19.0	21.1	
Speed of sound					
• methanol at T = 274.74 K (P = 0.1 – 280 MPa)	6.51	12.8	87.4	89.8	(100)
• methanol at T = 332.95 K (P = 0.1 – 280 MPa)	6.06	9.20	64.2	64.5	(100)
• ethanol at T = 273.91 K (P = 0.1 – 280 MPa)	2.1	30.5	66.5	67.4	(101)
• ethanol at T = 333.01 K (P = 0.1 – 280 MPa)	4.83	21.3	45.5	44.6	(101)
• water at T = 298.15 K (P = 0.1 – 150 MPa)	24.1	22.2	132	141	(94)
• water at T = 348.15 K (P = 0.1 – 150 MPa)	14.2	7.98	88.5	93.7	(94)
Average	9.63	17.3	80.7	83.5	
First-order volume derivative of F					

Property	sPC-SAFT (%AAD)	CPA (%AAD)	SRK (%AAD)	PR (%AAD)	Ref.
• methanol at T = 273.15 K (P = 0.1 – 280 MPa)	1.02	0.59	29.8	21.5	(100)
• methanol at T = 333.15 K (P = 0.1 – 280 MPa)	3.12	2.22	51.2	36.5	(100)
• ethanol at T = 273.15 K (P = 0.1 – 280 MPa)	2.72	1.93	13.3	7.35	(101)
• ethanol at T = 333.15 K (P = 0.1 – 280 MPa)	2.84	2.02	23.4	12.4	(101)
• water at T = 298.15 K (P = 0.1 – 150 MPa)	12.4	0.98	74.3	52.2	(94)
• water at T = 348.15 K (P = 0.1 – 150 MPa)	10.1	1.91	63.2	44.9	(94)
Average	5.37	1.61	42.5	29.1	
Second-order volume derivative of F					
• methanol at T = 273.15 K (P = 0.1 – 280 MPa)	8.31	28.1	77	117	(100)
• methanol at T = 333.15 K (P = 0.1 – 280 MPa)	5.99	22.5	32.7	59.0	(100)
• ethanol at T = 273.15 K (P = 0.1 – 280 MPa)	4.97	66.6	79.0	117	(101)
• ethanol at T = 333.15 K (P = 0.1 – 280 MPa)	8.98	45.0	33.9	58.8	(101)
Average	7.06	40.6	55.7	87.9	
Second-order temperature-volume derivative of F					
• methanol at T = 273.15 K (P = 0.1 – 280 MPa)	30.7	17.8	140	171	(100)
• methanol at T = 333.15 K (P = 0.1 – 280 MPa)	31.9	7.80	88.2	110	(100)
• ethanol at T = 273.15 K (P = 0.1 – 280 MPa)	19.5	30.6	95.6	120	(101)
• ethanol at T = 333.15 K (P = 0.1 – 280 MPa)	17.1	18.5	56.8	75.5	(101)
Average	24.8	18.7	95.2	119	

Table 3-5 shows that both sPC-SAFT and CPA provide more accurate predictions for properties of hydrogen bonding components, compared to SRK and Peng-Robinson. The association term greatly improves the predictions of both associative models and shows that accounting for hydrogen bonding is absolutely necessary to obtain fair predictions of both first- and second-order properties.

3.4.1 Mass density

i) methanol

In Figure 3-38, it is noted that only sPC-SAFT and CPA are able to correlate the mass density for methanol with sufficient accuracy, while SRK and Peng-Robinson have large errors and show incorrect trends. The correlation of CPA is slightly superior to sPC-SAFT, possibly because the parameter regression procedure and/or data used in determining the model parameters for CPA was superior than those used for sPC-SAFT as it is doubtful that CPA is a superior model than sPC-SAFT. At higher temperatures (Figure 3-39) the prediction of sPC-SAFT seems to be diverging slightly more.

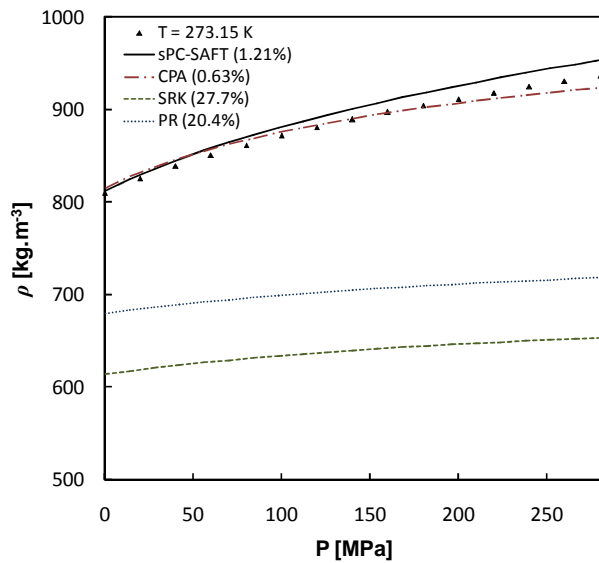


Figure 3-38: Mass density of methanol at $T = 273.15$ K. Data from ref. (100).

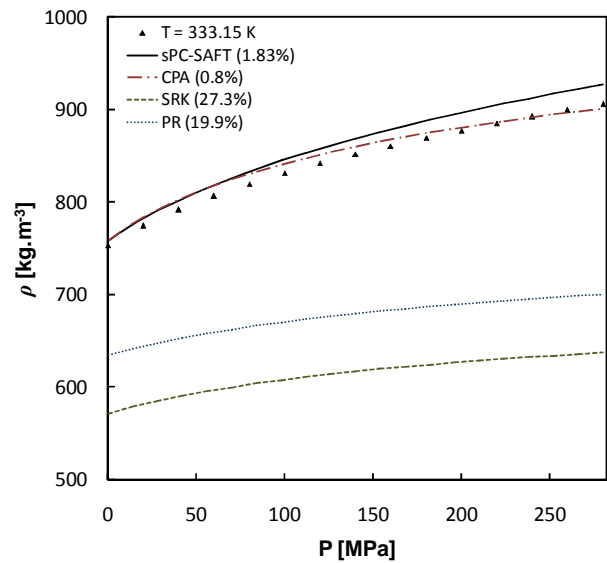


Figure 3-39: Mass density of methanol at $T = 333.15$ K. Data from ref. (100).

Comparing the mass density plots of methanol with that of *n*-hexane (Figure 3-1 and Figure 3-2), it is noticed that the density of *n*-hexane increases more with an increase in pressure. The methanol molecules are already tightly packed as a result of hydrogen bonding between the molecules and subsequently, the effect of pressure increase is smaller. It is noticed that the magnitude of error in the predictions of SRK and Peng-Robinson increases from *n*-hexane (Figure 3-1 and Figure 3-2) to acetone (Figure 3-27 and Figure 3-28) and are largest for methanol. This shows that the classical SRK and Peng-Robinson models yield poor predictions for additional attractive forces, other than dispersion.

ii) ethanol

According to Figure 3-40, none of the models correlate the mass density of ethanol with high accuracy. However, sPC-SAFT follows the trend of the experimental data correctly. CPA manages to correlate the property well in the low pressure region, but deviates substantially as the pressure increases. The prediction of CPA closely resembles that of SRK and Peng-Robinson, especially as the pressure increases. Therefore, it may be possible that the contributions accounting for dispersion and association in CPA are not in the correct balance, i.e. some polar and dispersive forces are overestimated in the dispersion term and the association forces are underestimated or vice versa. The parameters characterizing dispersion (a_o and c_I) and the parameters characterizing association (ε^{AB}/k and β^{AB}) are closely related, since they account for attractive forces and the magnitude of each contribution may not necessarily be correct (in this case it may be that the dispersion parameters in CPA are too large and the association parameters too small, because CPA seems to behave similar to the cubic models). If this is the case, additional data needs to be included in the parameter regression in order to insure that the parameters are more correct.

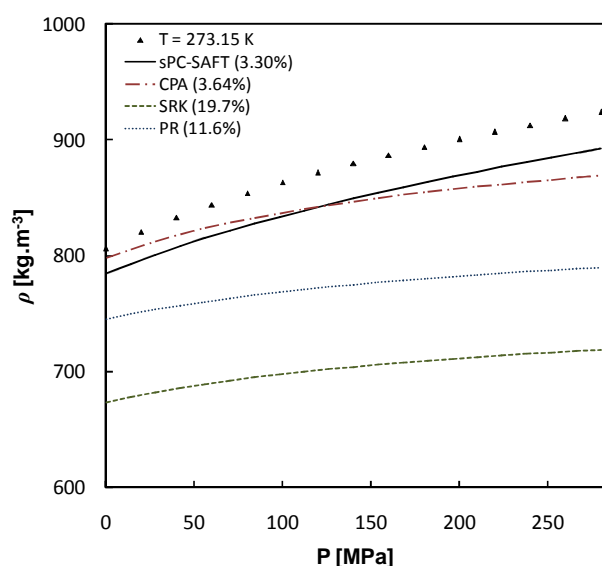


Figure 3-40: Mass density of ethanol at $T = 273.15$ K. Data from ref. (101).

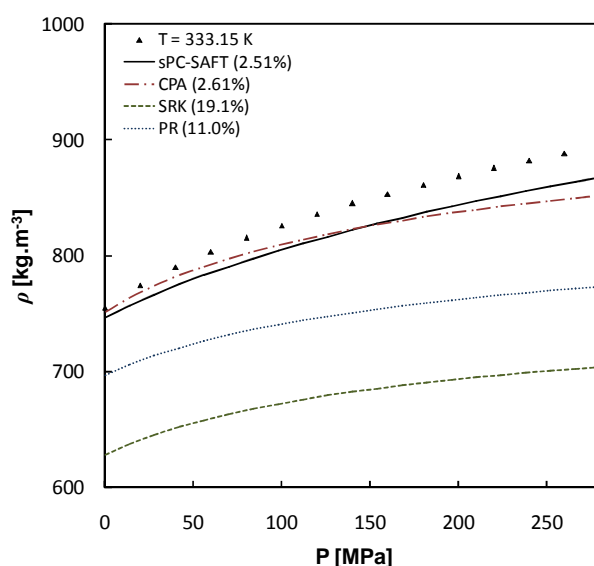


Figure 3-41: Mass density of ethanol at $T = 333.15$ K. Data from ref. (101).

In Figure 3-41, the trends remain the same as in Figure 3-40. The %AAD of CPA and sPC-SAFT, however, decreases by approximately 30%. This may be as a result of temperature dependent forces, like polar and association forces, that diminish and results in the molecules behaving more non-polar.

iii) water

From Figure 3-42 and Figure 3-43, it is observed that only CPA accurately correlates the mass density for water with good accuracy, although the trend is slightly incorrect. sPC-SAFT under-predicts the property, yet has the same trend as CPA. SRK and Peng-Robinson under-predict the property and have incorrect trends. Considering the experimental data, the increase in density as the pressure increases is rather small compared to the other components. The association forces cause the component to be less compressible than non-polar components. Furthermore, the temperature dependency of the property is well covered by both CPA and sPC-SAFT.

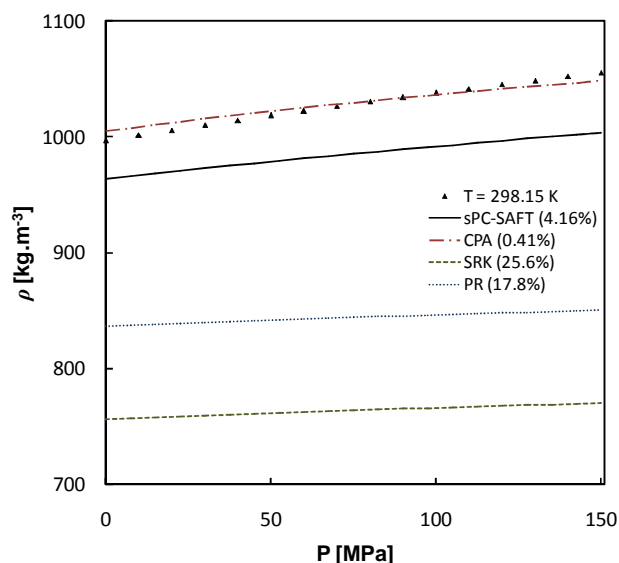


Figure 3-42: Mass density of water at $T = 298.15$ K. Data from ref. (94).

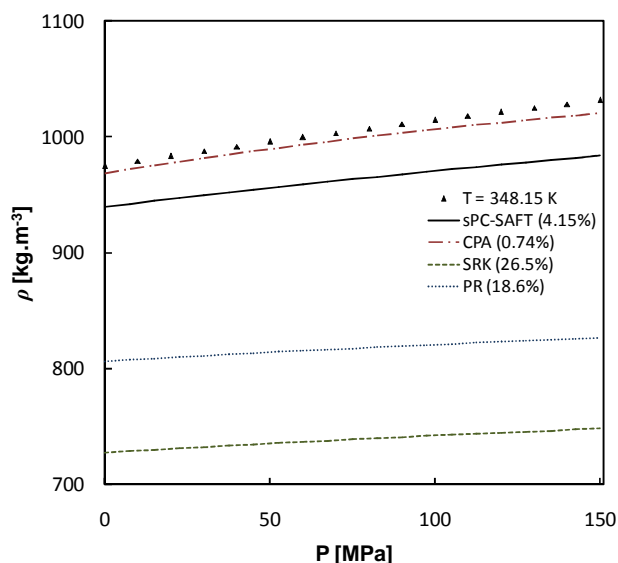


Figure 3-43: Mass density of water at $T = 348.15$ K. Data from ref. (94).

The performance of sPC-SAFT for water is particularly problematic. Several investigations and suggestions surrounding the correct molecular approximation for water in the framework of SAFT have been made in the literature (21). In particular, the discussions were focussed on the correct number of association sites that had to be attributed to water. (Suggestions range from two to four sites (21)). The parameters used in the present study were optimized for phase equilibria calculations, but do not seem to be satisfactory for other properties, especially if the %AAD in the mass density plots is considered. A future investigation on the correct number of association sites by considering, not only phase equilibria properties, but other properties as well, may prove useful.

3.4.2 Pressure-volume derivative

i) methanol

From Figure 3-44 and Figure 3-45, sPC-SAFT over-predicts the pressure-volume derivative slightly, yet its trend is basically consistent with the experimental data. In the low pressure region, CPA predicts the property accurately, but diverges quickly as the pressure increases. Comparing the trends of CPA with SRK and Peng-Robinson, it seems as if the combined effect of the association term and the parameter regression only succeeded in shifting the prediction towards the experimental data. Therefore, it seems as if the property is dominated by the hard-sphere repulsive interactions rather than attractive interactions. This implies that CPA will never be able to accurately describe the pressure-volume derivative, because it uses the cubic model to account for repulsive interactions.

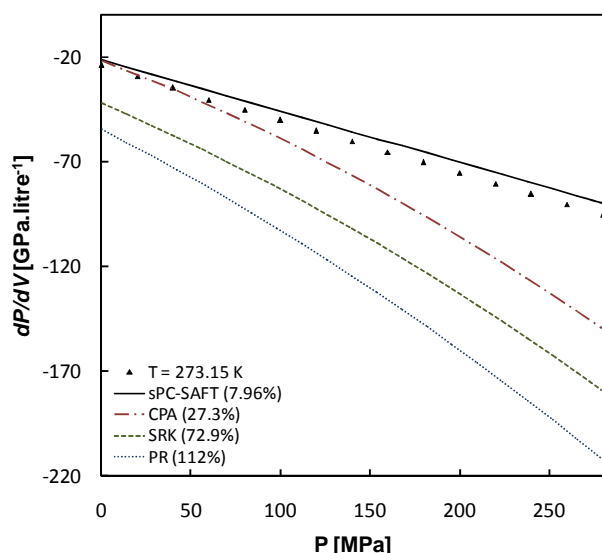


Figure 3-44: Pressure-volume derivative of methanol at $T = 273.15$ K. Data from ref. (100).

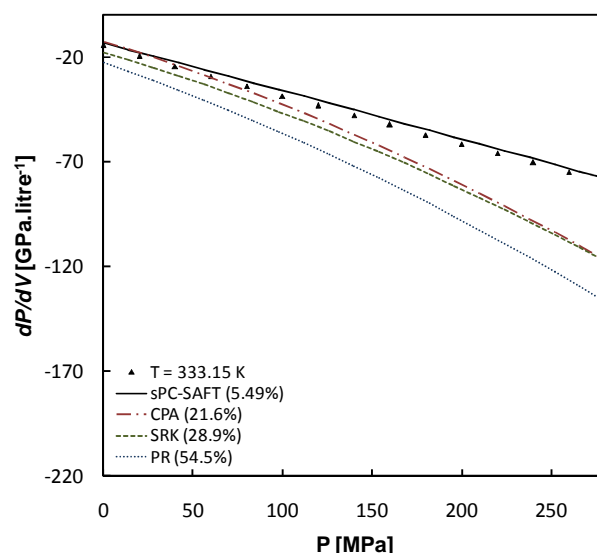


Figure 3-45: Pressure-volume derivative of methanol at $T = 333.15$ K. Data from ref. (100).

Considering how little the experimental data for the pressure-volume derivative changed with a change in temperature and comparing how much the prediction of the cubic models changed, it is clear that the temperature dependency of in the cubic models is incorrect.

ii) ethanol

In Figure 3-46 and Figure 3-47, it is observed that sPC-SAFT provides a reasonable correlation of the pressure-volume derivative for ethanol, although there is a slight under-prediction in the low pressure region. The other models diverge as the pressure increases.

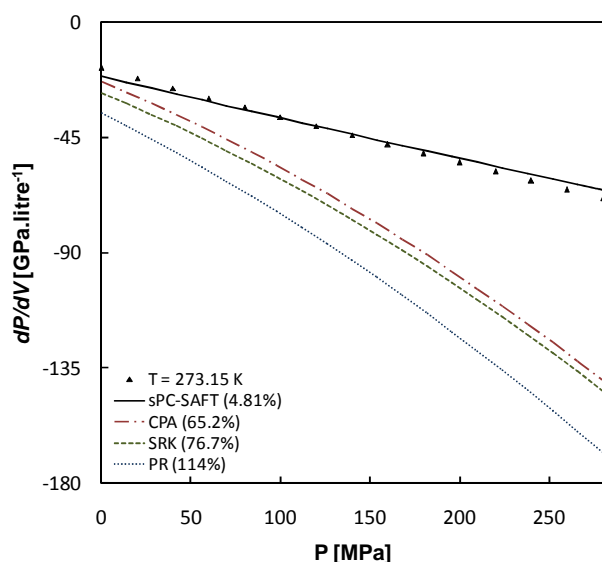


Figure 3-46: Pressure-volume derivative of ethanol at $T = 273.15$ K. Data from ref. (101).

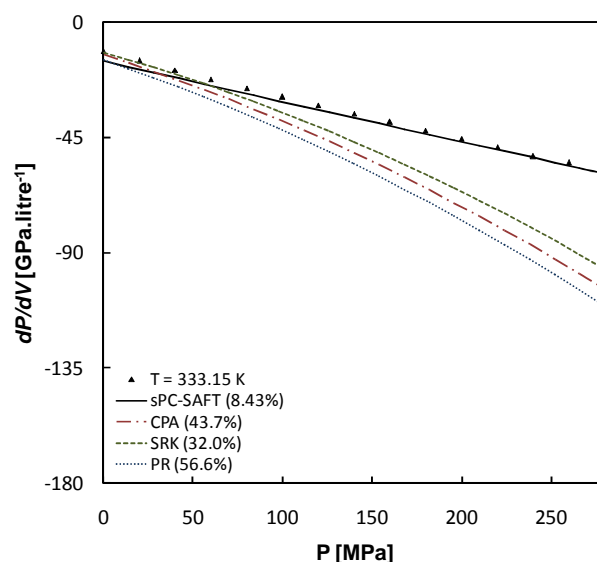


Figure 3-47: Pressure-volume derivative of ethanol at $T = 333.15$ K. Data from ref. (101).

Comparing the pressure-volume derivative of acetone (Figure 3-29) with the pressure-volume derivative of ethanol, it is noticed that at first the property is also under-predicted and then as the pressure increases, the prediction of sPC-SAFT improves (note the pressure scale for acetone only

reaches 60 MPa). It is possible that the cause of this initial under-prediction has the same source in both components and may be as a result of polar forces which are wrongfully accounted for. The low pressure under-prediction is not found with methanol; therefore, it might be possible to correct the error with parameter regression.

3.4.3 Isochoric heat capacity

i) methanol

None of the models are able to correlate the isochoric heat capacity of methanol with great accuracy as shown in Figure 3-48. sPC-SAFT is able to reproduce the trend of the data, the trend of CPA seems to be a slightly inconsistent and the cubic models produce predictions that seem consistent, but the %AAD's are large. The difference in predictions between SRK and CPA may be attributed to the additional influence of the association term on the property. Compared to the isochoric heat capacities of *n*-hexane (Figure 3-9 and Figure 3-10) and *n*-dodecane (Figure 3-11 and Figure 3-12), the influence of pressure on the property is less, since the isochoric heat capacity hardly increases over the pressure range of 280 MPa.

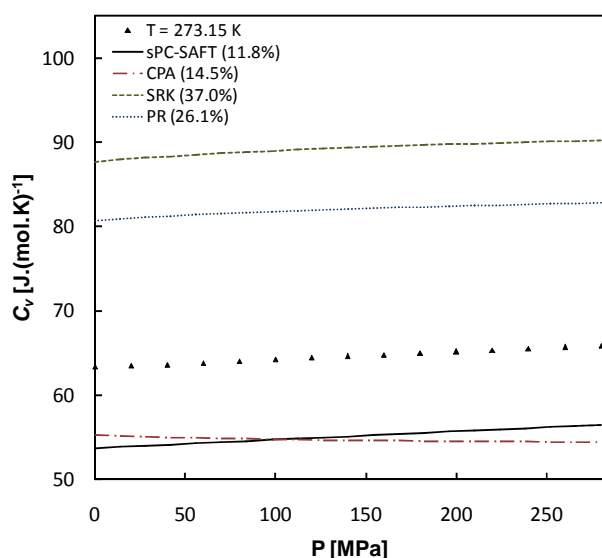


Figure 3-48: Isochoric heat capacity of methanol at $T = 273.15$ K. Data from ref. (94).

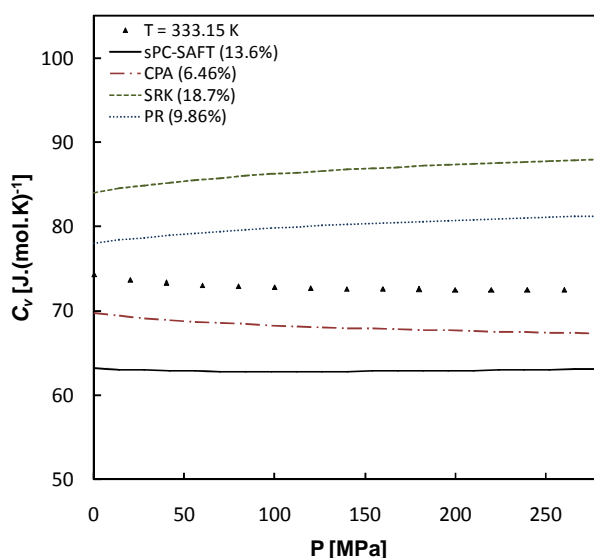


Figure 3-49: Isochoric heat capacity of methanol at $T = 333.15$ K. Data from ref. (94).

The influence of pressure on the isochoric heat capacity is barely noticeable in Figure 3-49. The property slightly decreases with an increase in pressure and then seems to remain constant. In this case, only CPA is able to capture the trend of the data and the difference in predictions between CPA and SRK is once again prominent. Comparing the magnitude of change in experimental data as a result of temperature increase with that of CPA and sPC-SAFT, it is noted that the change in CPA is too large, while the change in sPC-SAFT is of similar magnitude to the data. This possibly indicates that sPC-SAFT captures the influence of temperature on caloric properties more accurately compared to CPA.

ii) water

Contrary to the non-polar components (*n*-hexane and *n*-dodecane) where the isochoric heat capacity increased with an increase in pressure, here the isochoric heat capacity decreases with an increase in pressure (Figure 3-50 and Figure 3-51). It is suspected that hydrogen bonding and polar forces between the water molecules are responsible for the peculiar behaviour.

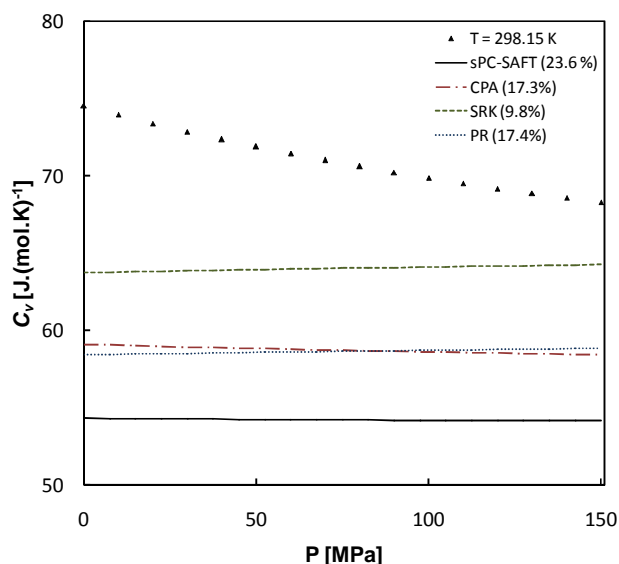


Figure 3-50: Isochoric heat capacity of water at $T = 298.15$ K. Data from ref. (94).

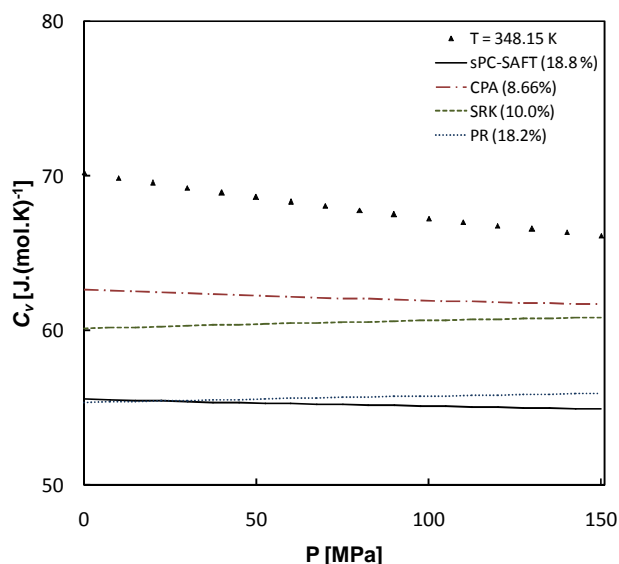


Figure 3-51: Isochoric heat capacity of water at $T = 348.15$ K. Data from ref. (94).

None of the models are able to capture the trend of the data. CPA and sPC-SAFT predict a slight decrease, yet the effect causing the downward slope seems to be underestimated. Comparing CPA and SRK, the association term does seem to decrease the property; this may imply that the degree of association is underestimated by both models, or that the polar forces are wrongfully accounted for in the dispersion term. It may be possible to correct the error by adjusting the parameters e.g. increasing the association energy parameter and decreasing the dispersion energy parameter or by including a polar term in the state function.

3.4.4 Isobaric heat capacity

i) methanol

The isobaric heat capacity is not significantly influenced by pressure in Figure 3-52. The correlations of sPC-SAFT and CPA are similar (%AAD = 18.2% and %AAD = 16.7%), and although the error is larger, the prediction of sPC-SAFT is slightly superior. The predictions of the cubic models are not completely erroneous, but their %AAD values are large compared to the other models. Again the difference in the predictions of CPA and SRK is significant.

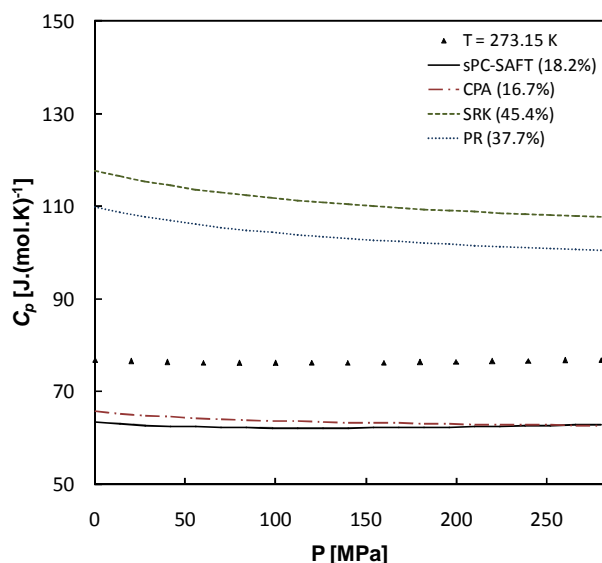


Figure 3-52: Isobaric heat capacity of methanol at $T = 273.15$ K. Data from ref. (94).

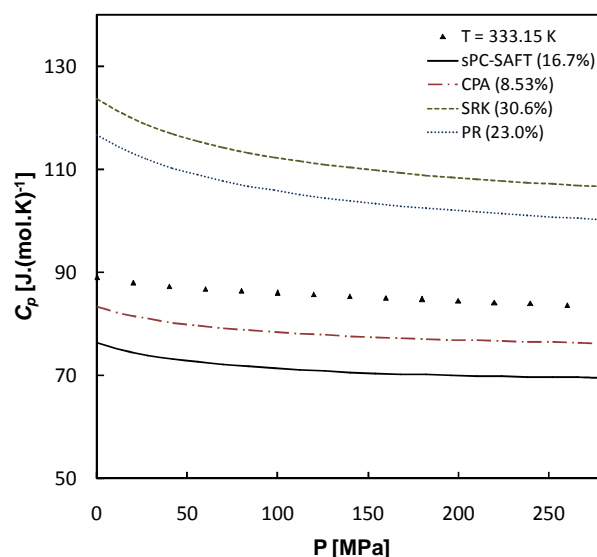


Figure 3-53: Isobaric heat capacity of methanol at $T = 333.15$ K. Data from ref. (100).

In Figure 3-53, CPA and sPC-SAFT have very similar predictions that are consistent with the experimental data. The prediction of CPA, however, shifts closer to the experimental data with the increase in temperature. The influence of temperature, as accounted for in the model, again indicates that certain forces are not adequately accounted for.

ii) ethanol

In Figure 3-54 sPC-SAFT provides the best prediction of the data (lowest %AAD), but CPA seems to predict a more consistent trend with the experimental data. The prediction of sPC-SAFT forms a minimum and then predicts an increase in the property as the pressure increases. Similar results were obtained for *n*-hexane, *n*-dodecane and acetone. This effect is not due to association, but originates from an incorrect description of the repulsive and dispersive forces.

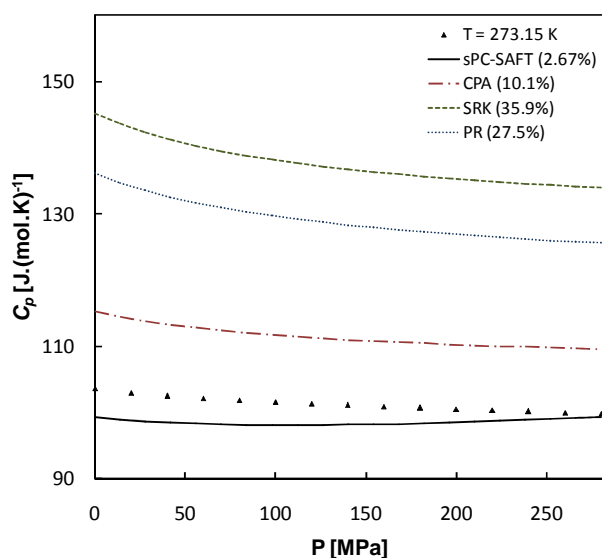


Figure 3-54: Isobaric heat capacity of ethanol at $T = 273.15$ K. Data from ref. (101).

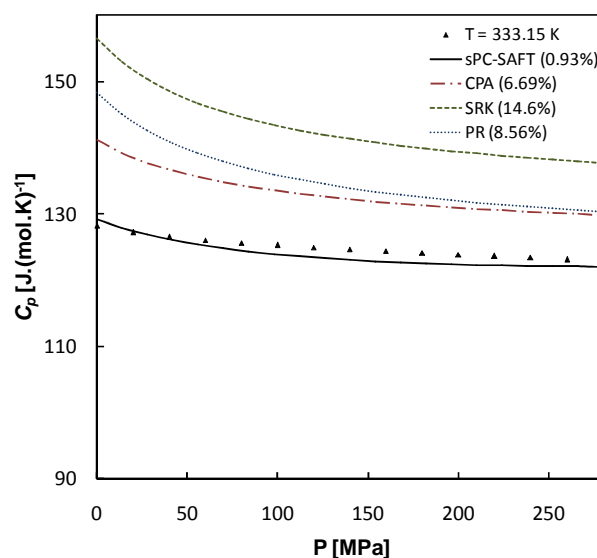


Figure 3-55: Isobaric heat capacity of ethanol at $T = 333.15$ K. Data from ref. (101).

In Figure 3-55, sPC-SAFT gives a good representation of the experimental data and no minimum is predicted. Similar results were obtained for *n*-hexane: the minimum did not form at higher temperature. This once again indicates that the temperature dependency of sPC-SAFT needs further improvement.

iii) water

The isobaric heat capacity for water is given in Figure 3-56 and Figure 3-57:

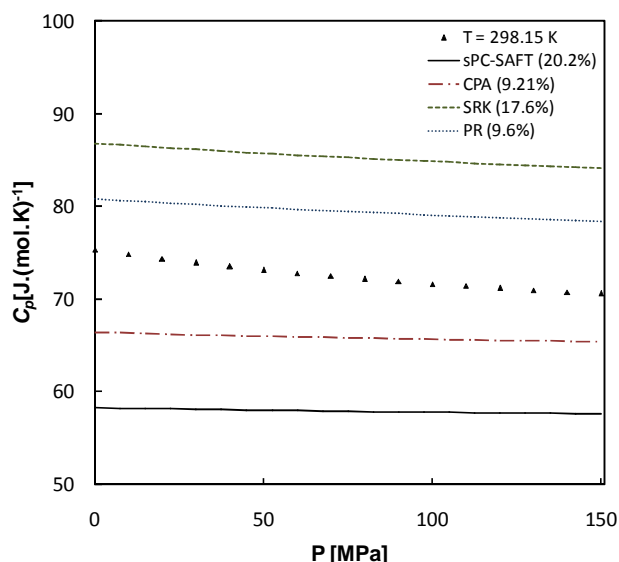


Figure 3-56: Isobaric heat capacity of water at $T = 298.15$ K. Data from ref. (94).

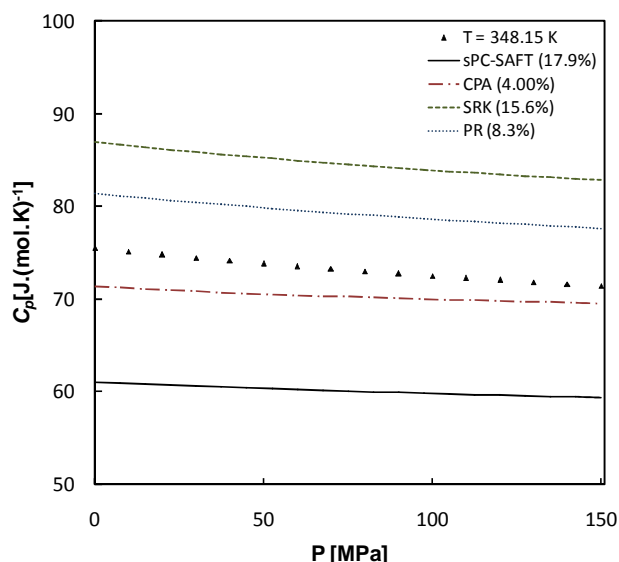


Figure 3-57: Isobaric heat capacity of water at $T = 348.15$ K. Data from ref. (94).

In Figure 3-56, the isobaric heat capacity decreases with an increase in pressure and is probably caused by the isochoric heat capacity which shows a similar downward trend (Figure 3-50). CPA and sPC-SAFT have trends that are very similar and the predictions of both models are insensitive to changes in pressure. The cubic models predict a decrease in the property with an increase in pressure which is surprising, since the models are not able to predict a decrease in the isochoric heat capacity (Figure 3-50). This once again indicates the inconsistency in the framework of the cubic models.

At the increased temperature ($T = 348.15$ K) in Figure 3-57, the change in experimental data is not significant. The prediction of sPC-SAFT also does not change significantly with the temperature increase and the magnitude of the change is of the same size as the data. The prediction of CPA, however, changes considerably and indicates oversensitivity towards changes in temperature.

3.4.5 Pressure-temperature derivative

i) methanol

In Figure 3-58, the pressure-temperature derivative of methanol is not accurately correlated by any of the models. sPC-SAFT under-predicts the property, but its trend is most consistent with the data. Again, the large difference in the predictions of CPA and SRK is prominent, although the association term and regression only succeeded in shifting the prediction and not in changing its shape. The same observations are made for the high temperature plot at $T = 333.15$ K in Figure 3-59.

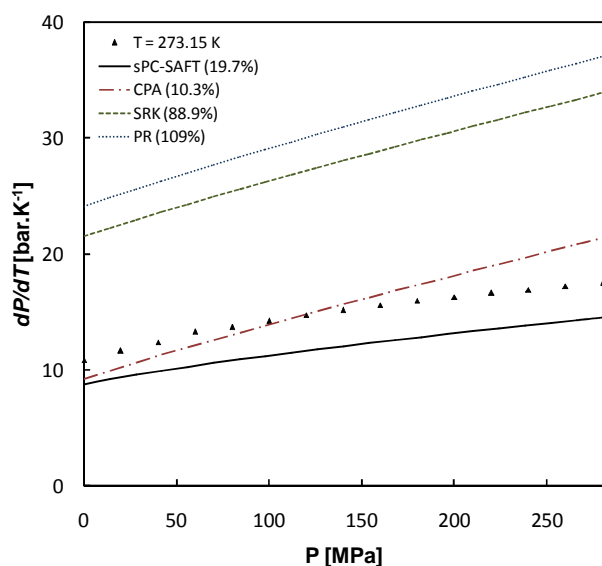


Figure 3-58: Pressure-temperature derivative of methanol at $T = 273.15$ K. Data calculated from ref. (100).

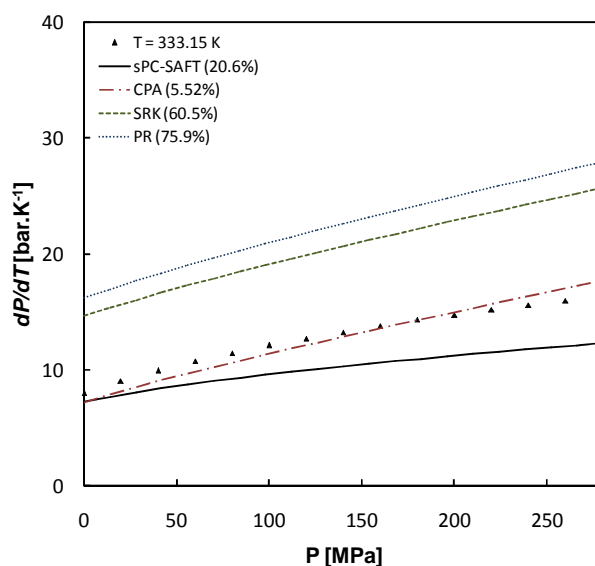


Figure 3-59: Pressure-temperature derivative of methanol at $T = 333.15$ K. Data calculated from ref. (100).

ii) ethanol

Comparing the pressure-temperature graphs of methanol (Figure 3-58 and Figure 3-59) with Figure 3-60 and Figure 3-61, it is noticed that the results are similar. This is expected, since methanol and ethanol are very similar molecules. None of the models accurately capture the trends of the data points with sPC-SAFT being the most consistent.

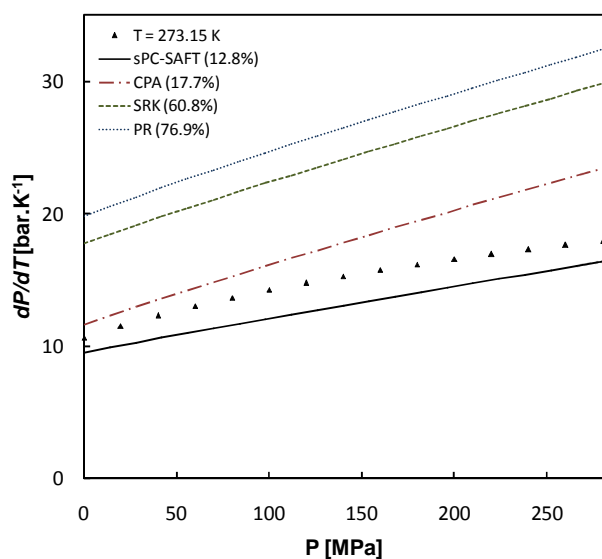


Figure 3-60: Pressure-temperature of ethanol at $T = 273.15$ K. Data from ref. (101).

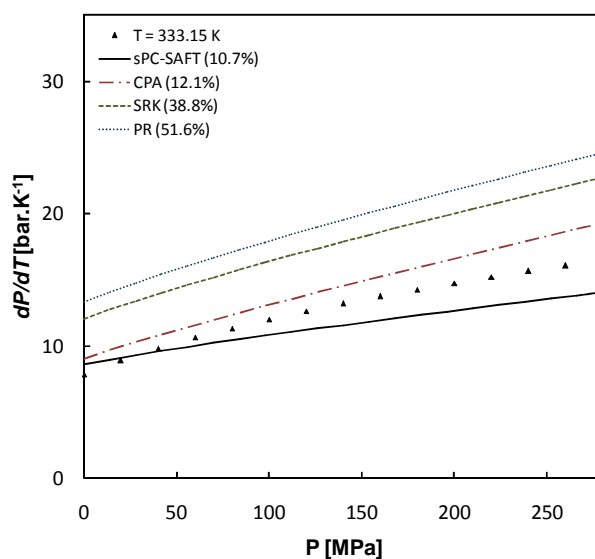


Figure 3-61: Pressure-temperature of ethanol at $T = 333.15$ K. Data from ref. (101).

3.4.6 Heat capacity ratio

i) methanol

The heat capacity ratio of methanol is shown in Figure 3-62 and Figure 3-63:

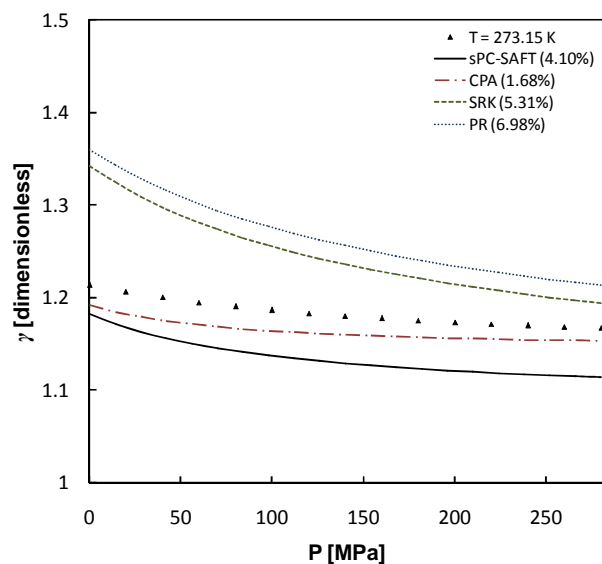


Figure 3-62: Heat capacity ratio of methanol at $T = 293.15$ K. Data calculated from ref. (94).

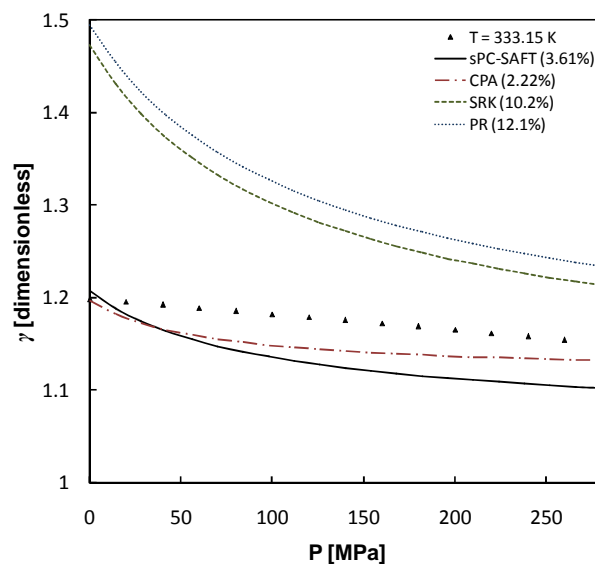


Figure 3-63: Heat capacity ratio of methanol at $T = 373.15$ K. Data calculated from ref. (94).

From Figure 3-62 and Figure 3-63, only CPA is able to give a good correlation of the property, although it slightly under-predicts the heat capacity ratio (%AAD = 1.68%). The trend of sPC-SAFT is reasonable compared to the data, but the initial divergence in the low pressure region is problematic. The association term in CPA greatly influences the prediction, as seen in comparison

with the prediction of SRK. This indicates that attractive forces (dispersive and associative) have a strong influence on caloric properties. Similar results were obtained for ethanol.

3.4.7 Speed of sound

Considering equation (3-11) again:

$$u = \sqrt{-\frac{V^2 \cdot \gamma \cdot \left(\frac{\partial P}{\partial V}\right)_{T,n}}{M_w}} \quad (3-11)$$

Since the mass density, pressure-volume derivative and heat capacity ratio have been investigated, it is now possible to interpret speed of sound results in a more meaningful manner.

i) methanol

In Figure 3-64 and Figure 3-65, only sPC-SAFT is able to correlate the data with reasonable accuracy, while the other models provide less satisfactory results. Following similar arguments as earlier, it is concluded that accurate description of the speed of sound primarily requires an accurate description of the pressure-volume derivative.

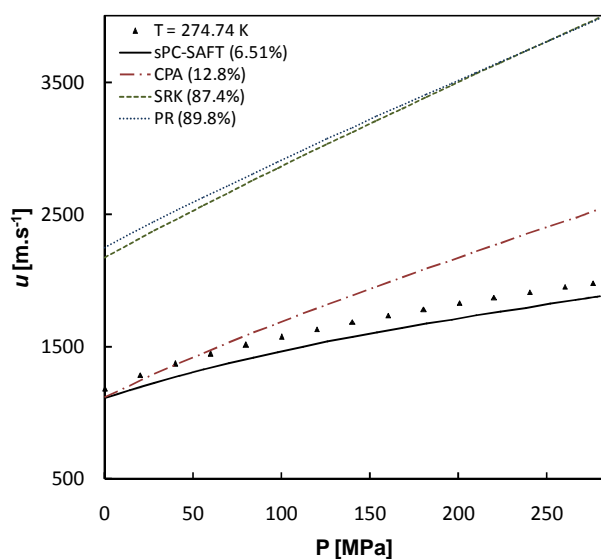


Figure 3-64: Speed of sound in methanol at $T = 274.74$ K. Data from ref. (100).

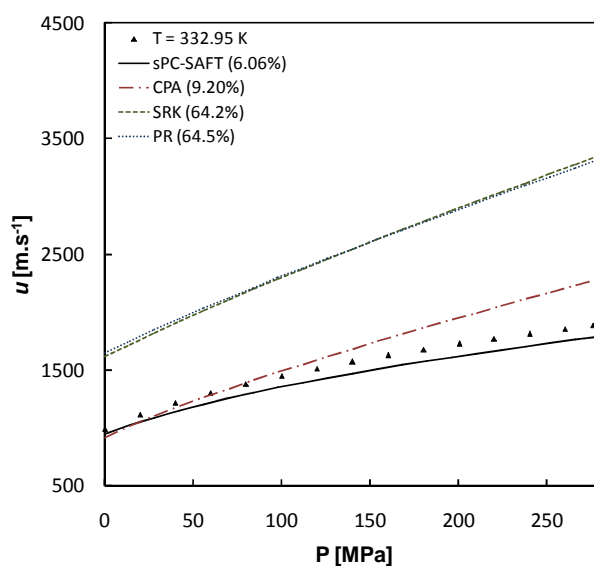


Figure 3-65: Speed of sound in methanol at $T = 332.95$ K. Data from ref. (100).

Knowing that the accuracy of the pressure-volume derivative is mainly dependent on the second-order volume derivative of the reduced residual Helmholtz energy state function, research should be focussed on improving its description in order to accurately correlate the speed of sound.

ii) ethanol

According to Figure 3-66 and Figure 3-67, only sPC-SAFT is able to correlate the speed of sound in ethanol with good accuracy, although there is some error in the description in the low pressure region. In Figure 3-60 and Figure 3-61, it is noticed that sPC-SAFT under-predicts the pressure-volume derivative in the low pressure region and this results in the over-prediction of the speed of sound.

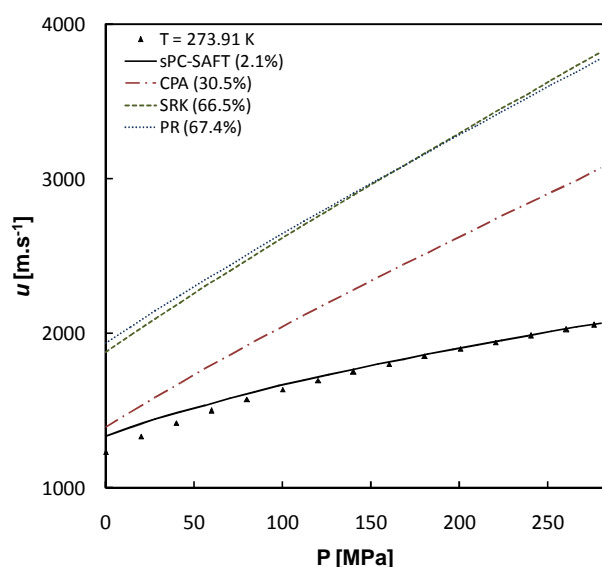


Figure 3-66: Speed of sound in ethanol at $T = 273.91$ K. Data from ref. (101).

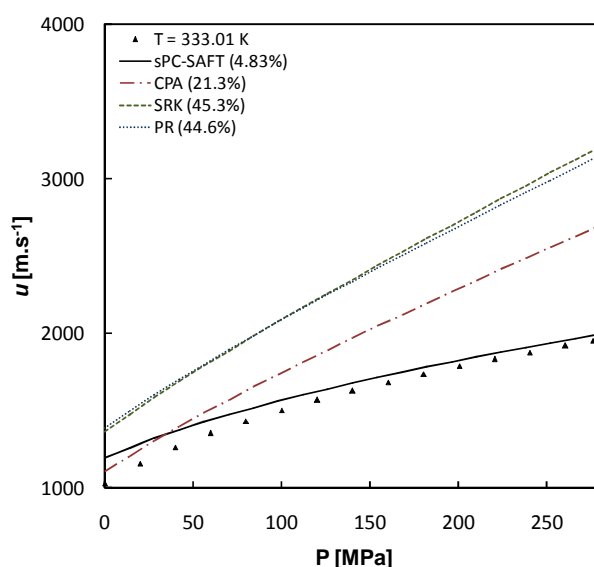


Figure 3-67: Speed of sound in ethanol at $T = 333.01$ K. Data from ref. (101).

iii) water

From Figure 3-68 and Figure 3-69 it follows that the speed of sound is over-predicted by all the models. The trend of sPC-SAFT is most consistent with that of the data.

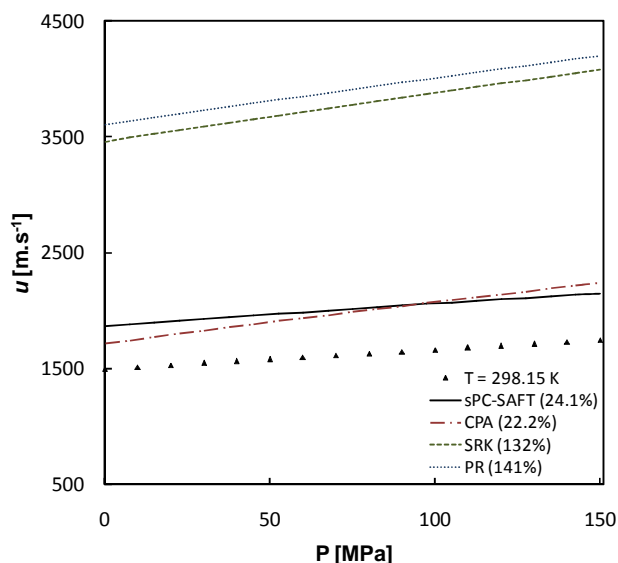


Figure 3-68: Speed of sound in water at $T = 298.15$ K. Data from ref. (94).

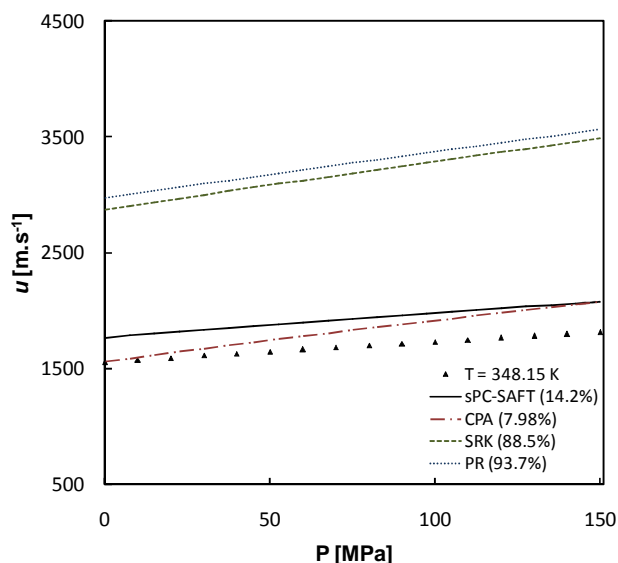


Figure 3-69: Speed of sound in water at $T = 348.15$ K. Data from ref. (94).

3.4.8 Section highlights

It is clear that association forces influence thermodynamic properties considerably. The key aspects are:

- Peng-Robinson and SRK are not able to correlate any of the properties with reasonable accuracies and are not suitable for thermodynamic modelling where hydrogen bonding properties are encountered.
- Only sPC-SAFT is able to give fairly good description of the pressure-volume derivative for both methanol and ethanol. The pressure-volume derivative of ethanol shows the same low pressure underestimation as observed with acetone. Possible reasons for the problem include:
 - The polar forces may be wrongfully accounted for in the dispersion energy parameter.
 - The parameters used for ethanol are not the optimum ones for predicting second-order derivative properties.
- The association term influences caloric properties considerably more than volumetric properties as observed from difference in behaviour between CPA and SRK.
- The correctness of the model parameters of hydrogen bonding components modelled in this section is questionable and possibly need optimization. Accounting for polar forces explicitly in these components also seems to be necessary.
- The speed of sound in methanol and ethanol is reasonably well correlated by sPC-SAFT as a result of the improved description of the pressure-volume derivative. CPA shows much improvement over SRK, but because CPA is not able to give accurate description of the pressure-volume derivative, its prediction failed similarly to that of cubic models.

During the investigation conducted into the ability of sPC-SAFT in predicting properties of non-polar, polar and hydrogen bonding components, a key question that arose was if it would be

possible to improve the performance of sPC-SAFT by including additional properties in the objective function when determining model parameters. This issue is now considered in the next section.

3.5 Limits of parameter regression with sPC-SAFT

In an attempt to establish if model parameters can be optimized to predict several properties simultaneously with a single set of model parameters, regression was conducted by inclusion of several property groupings. The properties under consideration included the saturated vapour pressure (P^{sat}), the saturated liquid density ($\rho^{sat,liq}$), the speed of sound in saturated liquid ($u^{sat,liq}$), the isochoric heat capacity of saturated liquid ($C_v^{sat,liq}$) and the heat of vapourisation (h^{vap}). Saturated properties were selected to ensure that the model correctly predicts a two-phase region. The Levenberg-Marquardt algorithm was used together with a least squares objective function. In all cases, equal regression weights were assigned to the properties and the properties included in the regression were in the temperature range $0.5 < T_r < 0.9$ with 30 data points for each property. Data for P^{sat} , $\rho^{sat,liq}$, h^{vap} were obtained from the DIPPR 801 database (95) and $u^{sat,liq}$ and $C_v^{sat,liq}$ were taken from NIST (94). The parameter sets for *n*-hexane were determined for the groupings as indicated in Table 3-6.

Table 3-6: sPC-SAFT model parameters for *n*-hexane regressed from different properties

set	Data included in regression	Parameters	% AAD				
			P^{sat}	$\rho^{sat,liq}$	h^{vap}	$u^{sat,liq}$	$C_v^{sat,liq}$
1	$P^{sat}; \rho^{sat,liq}$	Published parameters (24) $\varepsilon/k = 236.77$, $\sigma = 3.798$, $m = 3.058$	0.64	0.62	1.99	6.18	4.21
2	$P^{sat}; \rho^{sat,liq}; u^{sat,liq}$	$\varepsilon/k = 234.39$, $\sigma = 3.759$, $m = 3.124$	1.38	0.28	2.63	5.91	4.36
3	$P^{sat}; \rho^{sat,liq}; C_v^{sat,liq}$	$\varepsilon/k = 240.65$, $\sigma = 3.830$, $m = 2.974$	0.71	0.45	1.95	6.30	4.07
4	$P^{sat}; \rho^{sat,liq}; h^{vap}$	$\varepsilon/k = 237.83$, $\sigma = 3.808$, $m = 3.032$	0.60	0.53	1.87	6.23	4.16
5	$P^{sat}; u^{sat,liq}$	$\varepsilon/k = 237.52$, $\sigma = 3.740$, $m = 3.067$	1.46	4.11	3.08	5.85	4.32
6	$P^{sat}; C_v^{sat,liq}$	$\varepsilon/k = 362.97$, $\sigma = 3.579$, $m = 1.698$	1.56	>100	9.76	14.8	1.24
7	$P^{sat}; h^{vap}$	$\varepsilon/k = 224.86$, $\sigma = 3.862$, $m = 3.286$	0.45	13.71	0.37	8.17	4.34
8	$\rho^{sat,liq}; u^{sat,liq}$	$\varepsilon/k = 190.40$, $\sigma = 3.186$, $m = 4.899$	23.1	1.43	15.8	1.11	7.38
9	$\rho^{sat,liq}; C_v^{sat,liq}$	$\varepsilon/k = 299.29$, $\sigma = 4.548$, $m = 1.789$	>100	0.19	17.9	20.2	0.47
10	$\rho^{sat,liq}; h^{vap}$	$\varepsilon/k = 228.38$, $\sigma = 3.716$, $m = 3.196$	14.8	0.31	0.37	7.97	4.20

Table 3-6 provides a good indication of the trade-off in accuracy between properties during parameter regression. In several cases the parameters converged to unrealistic values in order to correlate the properties. Groups 2 – 4 show that only marginal improvements are obtained by including different properties in the regression in addition to P^{sat} and $\rho^{sat,liq}$. The properties of group 4 are all first-order properties and it seems that model parameters of sPC-SAFT can be

marginally optimized for non-associating components by including the heat of vapourisation in the regression, although the improvement is not really significant.

Furthermore, groups 7 and 10 show that in order to decrease the %AAD of h^{vap} below 1%, a significant trade-off in accuracy is required in $\rho^{sat,liq}$ (group 7) or P^{sat} (group 10). Therefore, it seems as if sPC-SAFT is only able to correlate two first-order properties with high accuracy and that the best overall performance of the model for non-polar components is obtained by including P^{sat} , $\rho^{sat,liq}$ and h^{vap} . Group 8 shows that properties that primarily depend on the first-order volume derivative (P^{sat} , $\rho^{sat,liq}$) and second-order volume derivative ($u^{sat,liq}$) cannot be accurately described simultaneously. This was further verified by performing a parameter sensitivity analysis where one parameter was changed and the rest kept constant. When the change of one parameter increased the accuracy of the first-order volume derivative, a decrease in accuracy was observed in the second-order volume derivative and vice versa. Group 9 shows that $\rho^{sat,liq}$ and $C_v^{sat,liq}$ can simultaneously be correlated accurately, but the model parameters seems unrealistic (*n*-hexane is correlated as 1.8 spheres) and the saturated vapour pressure is poorly predicted.

The same regression study was performed on *n*-dodecane and acetone. The behaviour of sPC-SAFT was similar in both components compared to the behaviour of *n*-hexane. Parameters for these components estimated from P^{sat} ; $\rho^{sat,liq}$; h^{vap} are presented in Table 3-7. Again, the improvement of results by including the heat of vapourisation in the regression is negligible for non-associating components.

Table 3-7: sPC-SAFT model parameter regressed for *n*-dodecane and acetone

set	Component	Data included in regression	Parameters	% AAD		
				P^{sat}	$\rho^{sat,liq}$	h^{vap}
1	<i>n</i> -dodecane	P^{sat} ; $\rho^{sat,liq}$	Published parameters (24) $\varepsilon/k = 249.21$, $\sigma = 3.896$, $m = 5.306$	0.95	0.71	1.37
2	<i>n</i> -dodecane	P^{sat} ; $\rho^{sat,liq}$; h^{vap}	$\varepsilon/k = 247.11$, $\sigma = 3.865$, $m = 5.397$	0.63	0.47	1.12
3	acetone	P^{sat} ; $\rho^{sat,liq}$	Published parameters (24) $\varepsilon/k = 253.41$, $\sigma = 3.256$, $m = 2.774$	0.88	1.52	2.28
4	acetone	P^{sat} ; $\rho^{sat,liq}$; h^{vap}	$\varepsilon/k = 253.96$, $\sigma = 3.271$, $m = 2.758$	1.00	1.63	1.98

A number of sets of parameters were determined for methanol using the various property groupings as indicated in Table 3-8. Similar results are found for methanol compared to *n*-hexane. Again, it seems as if sPC-SAFT is only able to correlate first-order properties simultaneously.

Table 3-8: sPC-SAFT model parameters for methanol regressed from different properties

set	Data included in regression	Parameters	% AAD				
			P^{sat}	$\rho^{sat,liq}$	h^{vap}	$u^{sat,liq}$	$C_v^{sat,liq}$
1	$P^{sat}; \rho^{sat,liq}$	Published parameters (25) $\varepsilon/k = 188.9$, $\sigma = 3.230$, $m = 1.525$ $\varepsilon^{AB}/k = 2899.5$, $\beta^{AB} = 0.06718$;	1.89	0.53	6.73	4.04	15.1
2	$P^{sat}; \rho^{sat,liq}; u^{sat,liq}$	$\varepsilon/k = 167.73$, $\sigma = 2.843$, $m = 2.142$ $\varepsilon^{AB}/k = 2712.3$, $\beta^{AB} = 0.1526$;	1.52	1.16	6.37	0.87	14.4
3	$P^{sat}; \rho^{sat,liq}; C_v^{sat,liq}$	$\varepsilon/k = 294.41$, $\sigma = 3.678$, $m = 1.188$ $\varepsilon^{AB}/k = 2536.7$, $\beta^{AB} = 0.02062$;	1.24	3.07	5.66	41.4	2.37
4	$P^{sat}; \rho^{sat,liq}; h^{vap}$	$\varepsilon/k = 176.41$, $\sigma = 2.689$, $m = 2.604$ $\varepsilon^{AB}/k = 2342.1$, $\beta^{AB} = 0.2414$;	0.49	0.32	0.32	21.5	10.1
5	$P^{sat}; u^{sat,liq}$	$\varepsilon/k = 194.1$, $\sigma = 3.799$, $m = 1.632$ $\varepsilon^{AB}/k = 2877.4$, $\beta^{AB} = 0.0314$;	0.82	42.8	6.33	0.46	2.92
6	$P^{sat}; C_v^{sat,liq}$	$\varepsilon/k = 158.85$, $\sigma = 3.607$, $m = 2.390$ $\varepsilon^{AB}/k = 2788.5$, $\beta^{AB} = 0.0572$;	0.73	58.7	12.4	7.42	0.69
7	$P^{sat}; h^{vap}$	$\varepsilon/k = 151.55$, $\sigma = 2.065$, $m = 3.817$ $\varepsilon^{AB}/k = 1979.6$, $\beta^{AB} = 1.538$;	0.29	42.5	0.26	28.1	16.87
8	$\rho^{sat,liq}; u^{sat,liq}$	$\varepsilon/k = 243.86$, $\sigma = 3.756$, $m = 1.027$ $\varepsilon^{AB}/k = 1288.3$, $\beta^{AB} = 0.3454$;	>100	0.38	40.6	0.58	28.9
9	$\rho^{sat,liq}; C_v^{sat,liq}$	$\varepsilon/k = 177.1$, $\sigma = 2.681$, $m = 2.655$ $\varepsilon^{AB}/k = 3154.5$, $\beta^{AB} = 0.0455$;	45.1	0.17	20.0	24.4	0.32
10	$\rho^{sat,liq}; h^{vap}$	$\varepsilon/k = 177.39$, $\sigma = 2.991$, $m = 1.894$ $\varepsilon^{AB}/k = 2991.6$, $\beta^{AB} = 0.0856$;	31.0	0.14	0.21	2.18	14.4

Parameters for ethanol and water that were regressed by inclusion of P^{sat} , $\rho^{sat,liq}$ and h^{vap} in the regression are presented in Table 3-9. Although the parameters for water show a significant decrease in the %AAD of $\rho^{sat,liq}$ and h^{vap} , they are not suitable for VLE calculations. The parameters result in liquid-liquid demixing in the ethanol-water system and it was found that the primary cause for this was the large segment number of water ($m = 2.579$). The demixing did not occur when the segment number was fixed at 1.5, but then the other properties were less accurately correlated. The results are consistent with the work of Tybjerg *et al.*(32), although care should be taken to ensure that the parameters are physical realistic and still provide good VLE predictions.

Table 3-9: sPC-SAFT model parameter regressed for ethanol and water

Component	Data included in regression	Parameters	% AAD		
			P^{sat}	$\rho^{sat,liq}$	h^{vap}
1	ethanol	$P^{sat}; \rho^{sat,liq}$ Published parameters (31) $\varepsilon/k = 205.36$, $\sigma = 3.104$, $m = 2.572$ $\varepsilon^{AB}/k = 2456.0$, $\beta^{AB} = 0.06735$;	1.02	0.55	2.25
2	ethanol	$P^{sat}; \rho^{sat,liq}; h^{vap}$ $\varepsilon/k = 316.91$, $\sigma = 4.106$, $m = 1.231$ $\varepsilon^{AB}/k = 2811.02$, $\beta^{AB} = 0.00633$;	0.28	0.39	0.38
3	water	$P^{sat}; \rho^{sat,liq}$ Published parameters (36) $\varepsilon/k = 180.3$, $\sigma = 2.627$, $m = 1.500$ $\varepsilon^{AB}/k = 1804.22$, $\beta^{AB} = 0.18$;	0.89	2.96	4.17
4	water	$P^{sat}; \rho^{sat,liq}; h^{vap}$ $\varepsilon/k = 133.14$, $\sigma = 2.073$, $m = 2.579$ $\varepsilon^{AB}/k = 1748.4$, $\beta^{AB} = 0.5763$	0.95	1.19	1.57

The results presented in this section unfortunately show that only limited improvement can be obtained by including other properties in the objective function during parameter regression. sPC-SAFT in its current form cannot give simultaneous accurate predictions of the first-order properties needed for good phase equilibrium calculations (saturated vapour pressure and liquid density) and second-order properties such as the speed of sound and the isochoric heat capacity.

3.6 Chapter summary

3.6.1 Overview of comparison between models

The average %AAD values for each property investigated in the non-polar section (see Table 3-3) was used to construct Figure 3-70:

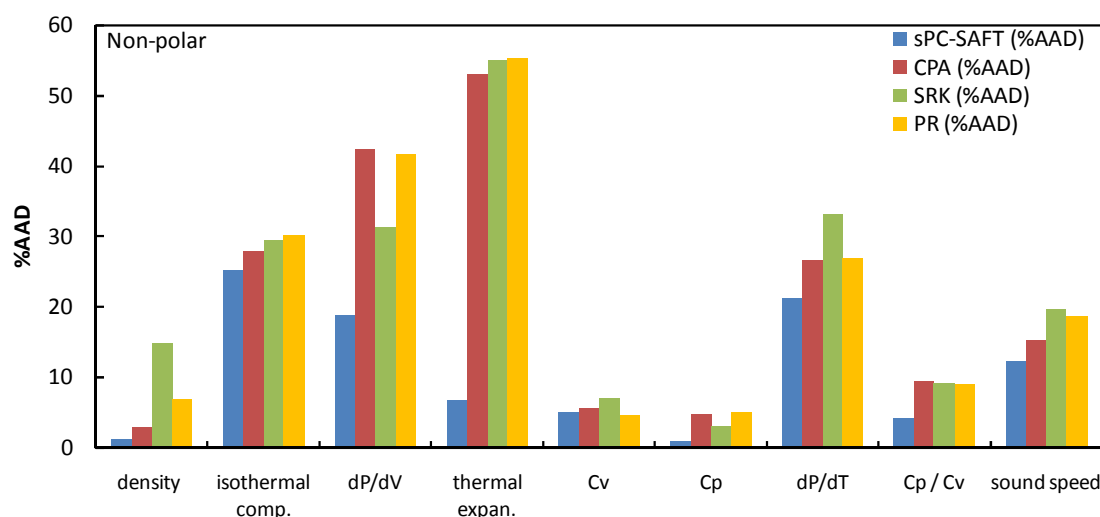


Figure 3-70: Model comparison for thermodynamic properties of **non-polar components**. Figure constructed from the results presented in Table 3-3.

From Figure 3-70, the superior performance of sPC-SAFT can be appreciated. The influence of parameter regression can be observed by comparing the performance of CPA with SRK. For some properties, SRK performs better and in other cases CPA is superior. Therefore, it seems that there is a trade-off in the framework of the cubic models to give improved prediction of some properties, while sacrificing accuracy in others.

The average %AAD for each property investigated in the polar (non-HB) section is presented in Figure 3-71 (see Table 3-4):

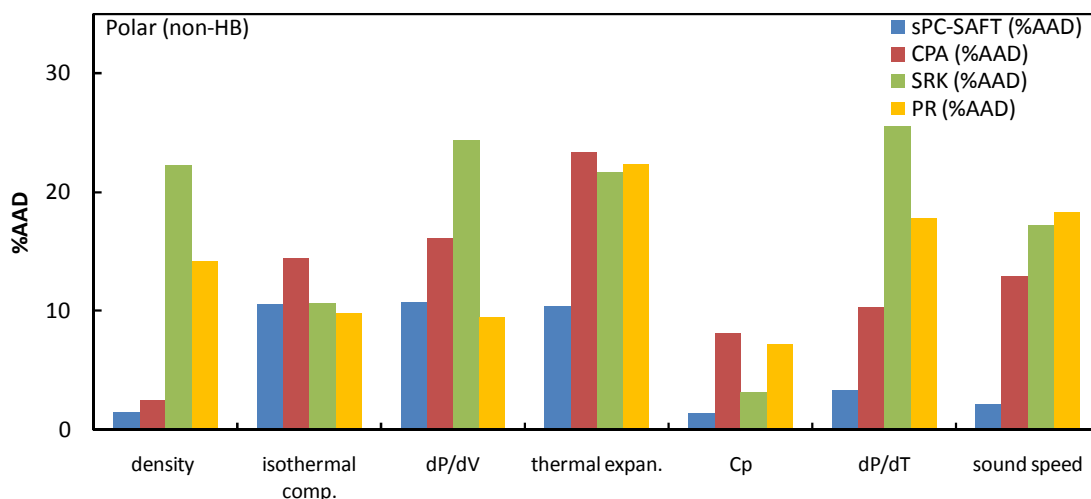


Figure 3-71: Model comparison for thermodynamic properties of **polar (non-HB) components**. Figure constructed from the results presented in Table 3-4.

sPC-SAFT is superior to the other models, except for the pressure-volume derivative as shown in Figure 3-71. The difference in model performance of CPA and SRK is emphasized again. It is suspected that, because the polar forces introduce more complexity that has to be accounted for by the models, the parameter regression results in a more significant trade-off between properties. Thus, accurate description of certain properties are obtained, while sacrificing accurate description of others.

The average %AAD values for the properties considered in the hydrogen bonding section (see Table 3-5) are presented in Figure 3-72:

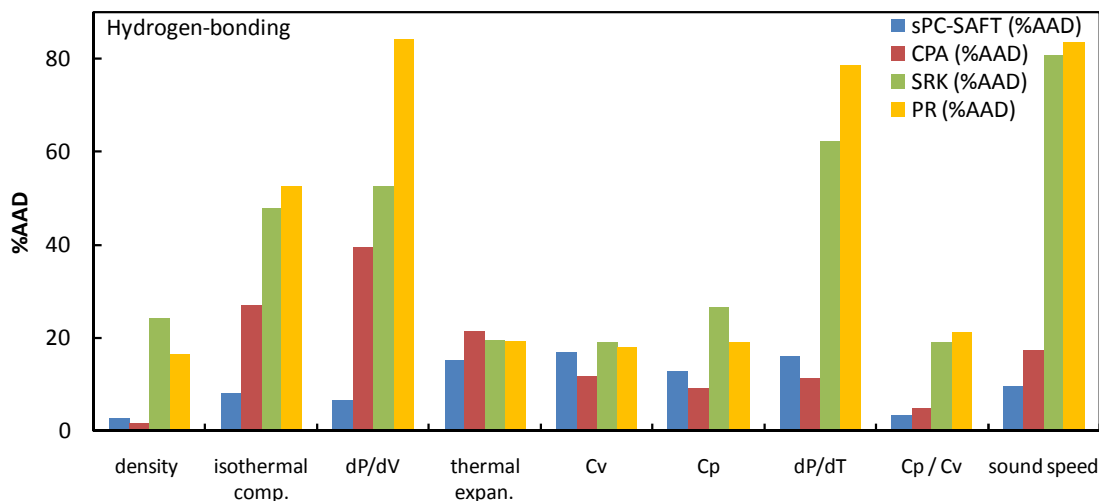


Figure 3-72: Model comparison for thermodynamic properties of **hydrogen bonding components**. Figure constructed from results presented in Table 3-5.

In Figure 3-72, sPC-SAFT and CPA show a significant improvement over the cubic models, primarily because they explicitly account for association. It is peculiar that CPA performs superior than sPC-SAFT in the prediction of some properties, because in the non-polar and polar components sections, it was concluded that sPC-SAFT is superior in accounting for physical forces. Since the

models use the same association term to account for hydrogen bonding, it is suspected that the parameter regression procedure used to determine CPA model parameters was superior than the regression procedure used to determine the sPC-SAFT model parameters.

In order to continue to illustrate the difference in performance between the models, the average deviation over all properties for a class of components (therefore, a summary of Figure 3-70, Figure 3-71 and Figure 3-72) is presented in Figure 3-73:

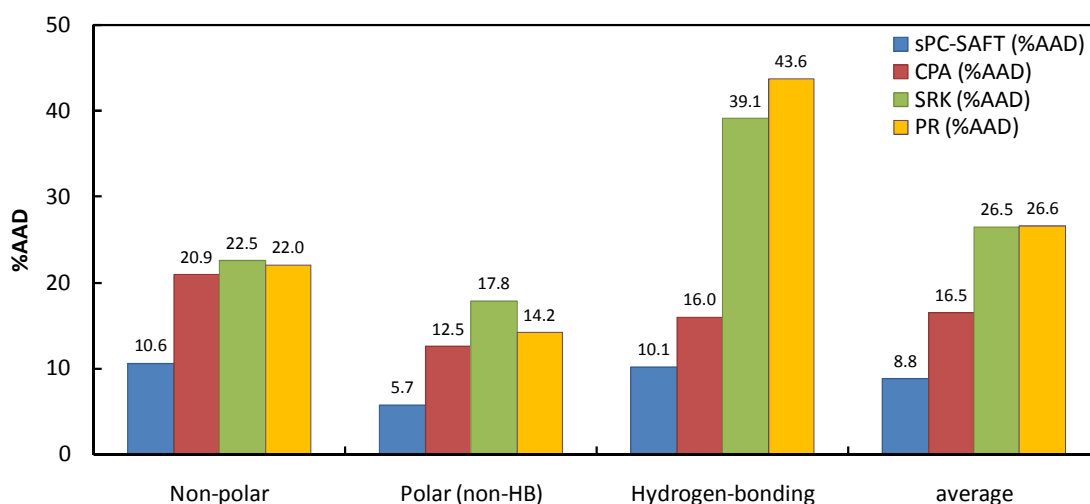


Figure 3-73: Model comparison between non-polar, polar and hydrogen bonding components.

sPC-SAFT generally performs the best in all pure component classes. The strength of the association term and the influence of parameter regression can be clearly observed if the %AAD values of sPC-SAFT and CPA are compared to the values of SRK and Peng-Robinson for hydrogen bonding components. It is also particularly interesting to note the %AAD values for CPA and SRK for the non-polar group of components. It is surprising that a clear cut difference is not observed between the models, giving some indication of the trade-off between properties, as mentioned earlier.

From the average cluster in Figure 3-73, sPC-SAFT performs the best followed by CPA and lastly the cubic models. The fact that the same experimental data was considered for all components makes the comparison between the models less biased.

3.6.2 Chapter highlights

In the modelling of pure components, the following critical aspects have been identified:

- A major improvement of sPC-SAFT compared to cubic based models (in the compressed liquid phase) is its ability to give a fairly good description of the pressure-volume derivative. In CPA, physical forces are accounted for with the cubic part of the model, which implies that CPA will never be able to give a good description of the derivative, especially at high pressures.

- For non-polar components, sPC-SAFT and CPA indicate temperature dependent deficiencies for several properties.
- For polar (non-HB) components, it is justifiable to include a polar contribution term to the state function of sPC-SAFT. Preliminary results indicate that the *Van der Waals* approach results in an artificially large energy parameter that compromises the performance of the model in predicting derivative properties.
- Hydrogen bonding influences caloric properties more than volumetric properties and both CPA and sPC-SAFT provide improved predictions of these properties as a result of the association term.
- The description of the isobaric heat capacity is influenced significantly by the pressure-temperature derivative. In general, sPC-SAFT and CPA under-predict the derivative for most components. sPC-SAFT has some difficulty in predicting trends that are consistent with isobaric heat capacity data at high pressures, while CPA performs slightly better.
- The cubic models have an internal error cancellation when describing the isobaric heat capacity, where errors in the pressure-temperature derivative are cancelled out by errors in the pressure-volume derivative.
- The parameter regression of CPA results in a trade-off between properties. It seems as if volumetric properties are described more accurately at the expense of accuracy in caloric properties.
- A parameter regression study with sPC-SAFT shows that the model cannot simultaneously predict first- and second-order properties.

In this chapter, only the thermodynamic properties of pure component were considered and, as a consequence, only interactions between *like* molecules. EOS models are almost always applied to determine properties of mixtures and this implies that these models must be able to account for additional interactions that originate between molecules of different species. Therefore, in Chapter 4, the properties for selected binaries are modelled in order to investigate how well the EOS models account for *unlike* interactions.

Chapter 4

Modelling properties of binary mixtures

In this chapter thermodynamic properties of binary mixtures are briefly modelled with the same EOS used in Chapter 3. The binary mixtures are classified as explained in section A.2.2. Properties for the following binary systems are investigated:

- Non-polar/Non-polar
- Non-polar/Polar (non-HB)
- Non-polar/Hydrogen bonding
- Hydrogen bonding/Hydrogen bonding

Polar/Polar and Polar/Hydrogen bonding systems are omitted, because cross-association is frequently present and needs to be accounted for explicitly in order to obtain reasonable predictions. Thermodynamic property data, especially second-order properties are scarce and only a limited number of properties could be sourced. In this chapter special attention is paid to excess properties. The predictions of all models are **without any binary interaction parameters (BIPs)**, because it is desired to investigate how well the models are able to predict properties of binary systems. In subsequent chapters, the influence of the BIP is considered in more detail. Specific trends in mixture properties are investigated in order to determine if the models are able to reproduce these trends with pure component model parameters. More attention is paid to molecular interactions between dissimilar molecules and the ability of the models to account for them.

4.1 Non-polar/Non-polar systems

Investigating the performance of the models for these types of systems, tests the ability of the model to account for repulsive and dispersive forces, not only between *like* molecules, but also between *unlike* molecules.

4.1.1 Mass density

i) *n*-hexane/*n*-decane

From Figure 4-1, sPC-SAFT is slightly superior in predicting the experimental data compared to CPA. CPA shows significant deviation at high concentration of *n*-decane (low concentration of *n*-hexane). This is probably because CPA does not have the framework to represent the chain-like structure of the molecule.

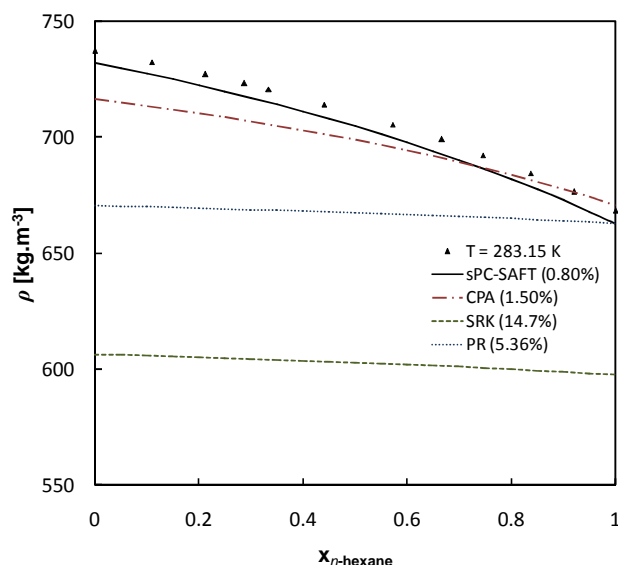


Figure 4-1: Mass density of the *n*-hexane/*n*-decane system at $T = 283.15$ K and $P = 1$ atm. Data from ref. (102).

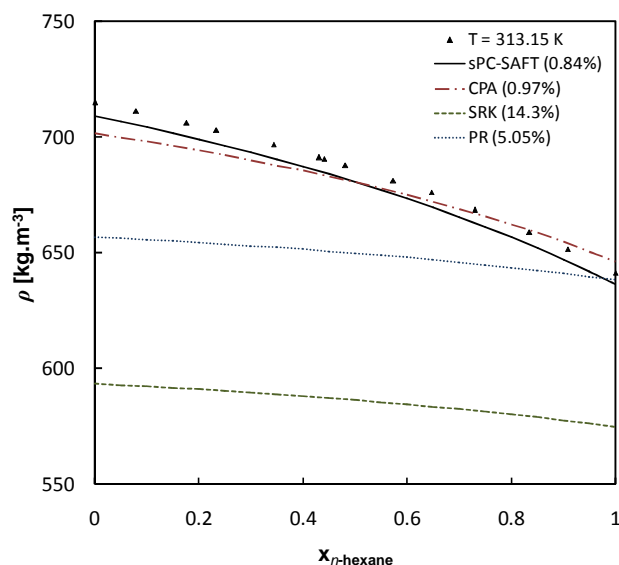


Figure 4-2: Mass density of the *n*-hexane/*n*-decane system at $T = 313.15$ K and $P = 1$ atm. Data from ref. (102).

Very similar results are obtained in Figure 4-2. The deviation of CPA at the *n*-decane rich end is less and it is suspected that the increase in kinetic energy as a result of the temperature increase, results in the molecule behaving more sphere-like.

Again, it is observed that for models such as sPC-SAFT and CPA, if the pure component parameters can be refitted to obtain a more accurate description of the property in the pure component limits, then the mixture property would be described with good accuracy. However, the capabilities of CPA are questionable, because for larger molecules, the “one-sphere” approximation is not sufficient and the regression would probably lead in a trade-off in accuracy in phase equilibria properties.

4.1.2 Excess volume

The excess volume provides information on how the molecules pack together in the mixture and is defined as:

$$V^E = V_{mix}(T, P, \mathbf{n}) - \sum_i^{nc} V_{pure,i}(T, P, n_i) \quad (4-1)$$

Negative excess volumes indicate that the molecules in the mixture pack more tightly together than the pure species counterparts and may arise when the *unlike* interactions are stronger than the *like* interactions, or when the structure that forms in the mixture has cavities into which the molecules can dissolve into each other.

i) *n*-hexane/*n*-heptane

In Figure 4-3, the excess volume is negative and all the models show the correct trend. CPA and sPC-SAFT perform similarly and SRK and Peng-Robinson perform similarly. Although the errors of all the models are quite large, the magnitude at the minimum is approximately $-0.025 \text{ cm}^3 \cdot \text{mol}^{-1}$, which is very small. The improvement of CPA compared to SRK is again noted and attributed to the pure component parameters used.

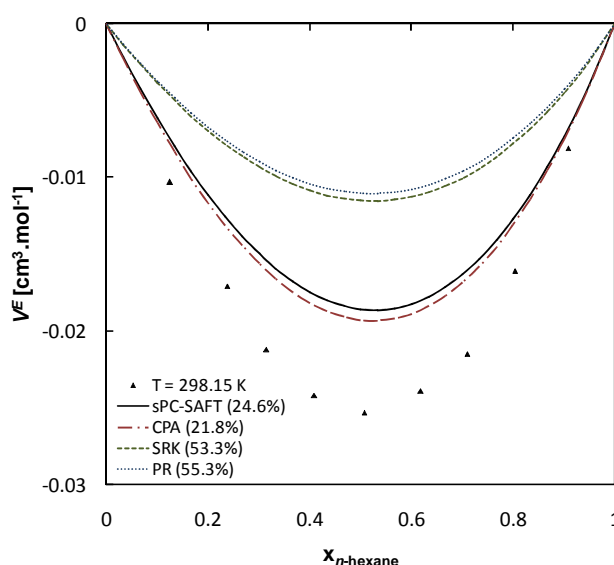


Figure 4-3: Excess volume of the *n*-hexane/*n*-heptane system at $T = 298.15 \text{ K}$ and $P = 1 \text{ atm}$. Data from ref. (103).

ii) *n*-hexane/*n*-decane

In Figure 4-4, the excess volume is negative and only sPC-SAFT and CPA predict the correct trend, while both SRK and Peng-Robinson predict positive excess volumes. It is remarkable how similar the predictions of sPC-SAFT and CPA and it is suspected that the reason for the likeness in prediction is due to the fact that the same type of data was used in the regression procedure (saturated vapour pressure and saturated liquid density data).

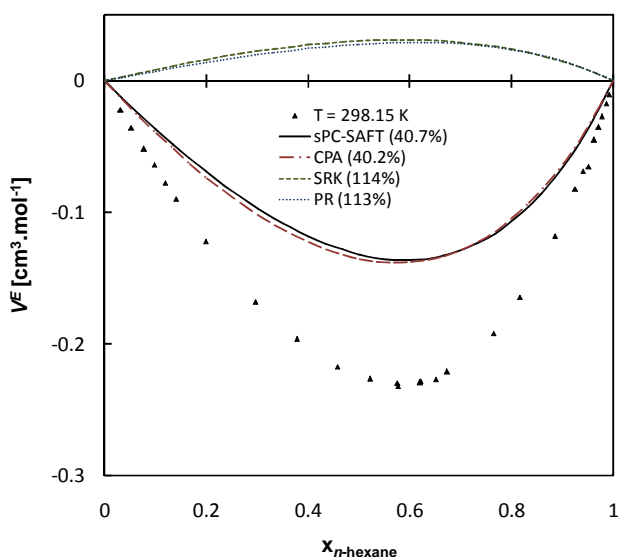


Figure 4-4: Excess volume of the *n*-hexane/*n*-decane system at $T = 298.15$ K and $P = 1$ atm. Data from ref. (104).

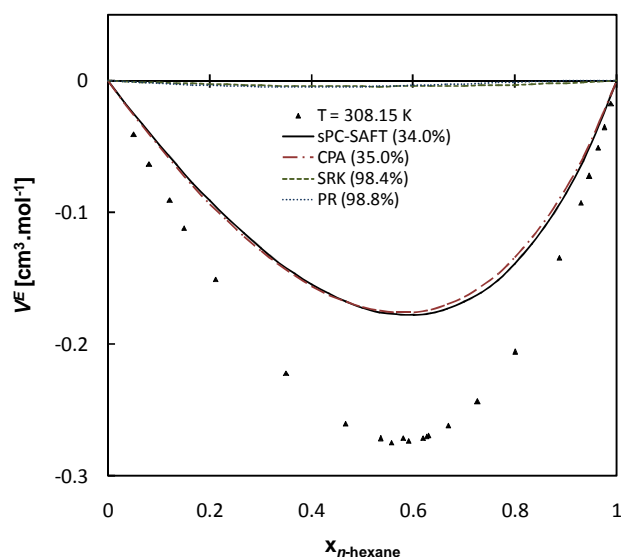


Figure 4-5: Excess volume of the *n*-hexane/*n*-decane system at $T = 308.15$ K and $P = 1$ atm. Data from ref. (104).

In Figure 4-5, the excess volume becomes more negative with an increase in temperature and all the models follow this behaviour.

4.1.3 Excess enthalpy

The excess enthalpy is a good indication of a models temperature dependency and is defined as follows:

$$H^E = H^r(T, P, \mathbf{n}) - \sum_i^{nc} H_i^r(T, P, n_i) \quad (4-2)$$

$$H^r(T, P, \mathbf{n}) = -RT^2 \left(\frac{\partial F}{\partial T} \right)_{V, \mathbf{n}} + PV - nRT \quad (4-3)$$

The excess enthalpy is the difference between the residual enthalpy of the mixture and that of the pure component contributions. The residual enthalpy is strong function of the first-order temperature derivative of the state function. Often the behaviour of the excess enthalpy is understood in terms of the mixing process and the interactions that influence the behaviour. The sign and magnitude of the excess enthalpy (heat of mixing) roughly reflect the differences in the strengths of intermolecular attractions between pairs of *like* species on the one side, and pairs of *unlike* species on the other (105). In a standard mixing process, interactions between *like* molecules are disrupted, and interactions between *unlike* species are promoted (105). If the *unlike* interactions are *weaker* than the average of those between molecules of the same kind, then more energy is required in the mixing process to break *like* attractions than is made available by the formation of *unlike* attractions (105). In this case, the excess enthalpy is positive and corresponds to an endothermic mixing process. If the *unlike* attractions are *stronger*, then the excess enthalpy is negative and the mixing process is correspondingly exothermic (105). Stated differently, if the *unlike* interactions are *stronger* than the *like* interactions they replace, then the

mixture is more stable than the pure species counterparts and the excess enthalpy is negative or exothermic. When the *like* interactions are *stronger*, then the mixture is less stable than the pure species counterparts resulting in an excess enthalpy that is positive or endothermic (106).

Molecular theory suggests that dispersion forces between *unlike* molecules are weaker than the average of dispersion forces between the *like* molecules and are well approximated by the geometric mean of the corresponding *like* interactions and consequently, the excess enthalpy is positive for mixtures of non-polar components (107; 106)

i) *n*-hexane/*n*-decane

The excess enthalpy of the *n*-hexane/*n*-decane system is shown in Figure 4-6:

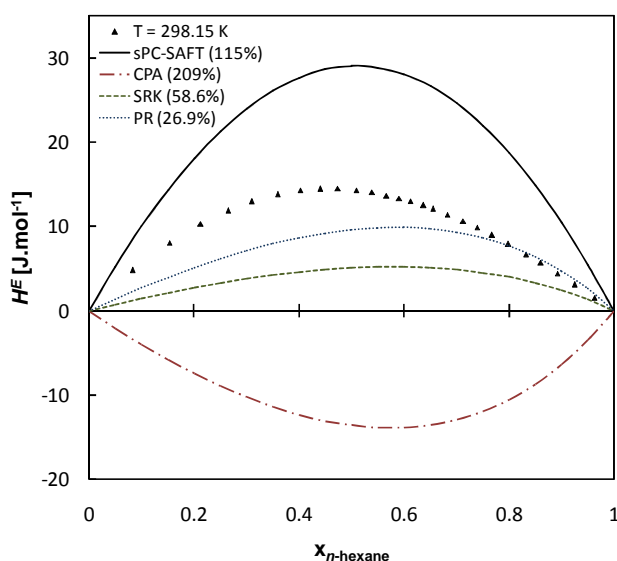


Figure 4-6: Excess enthalpy of the *n*-hexane/*n*-decane system at $T = 298.15 \text{ K}$ and $P = 1 \text{ atm}$. Data from ref. (104).

In Figure 4-6, none of the models are able to predict the excess enthalpy with great accuracy. sPC-SAFT severely over-predicts the property, while the other models under-predict the property. CPA predicts a negative value for the excess enthalpy and this implies that the model depicts the *unlike* interactions to be stronger than the *like* interactions, which is contrary to the real picture. Consider the excess volume plot for the mixture in Figure 4-4 and Figure 4-5. Using the SRK predictions as the reference, it is noticed that the parameter regression improved the description of the excess volume predictions, but this resulted in a worsened prediction for the excess enthalpy (Figure 4-6). Therefore, it seems that in the framework of CPA, a trade-off occurred due to the parameter regression that resulted in an improved description of volumetric properties and an inferior description of caloric properties.

4.1.4 Excess isobaric heat capacity

The excess isobaric heat capacity provides an indication of the level of order present in the mixture (108). A positive excess isobaric heat capacity indicates that order is being created by the mixing process and a negative value for the property indicates that order is being destroyed as a result of the mixing process relative to the pure component counterparts (108). Excess isobaric heat capacity is calculated as follows:

$$C_p^E = C_p^r(T, P, \mathbf{n}) - \sum_i^{nc} C_{p,i}^r(T, P, n_i) \quad (4-4)$$

i) *n*-hexane/*n*-heptane

In Figure 4-7, the excess isobaric heat capacity is negative, indicating that there is less order in the mixture relative to the pure component counterparts. All the models are able to follow the trend of the data with SRK and Peng-Robinson being the most accurate. sPC-SAFT under-predicts the property and CPA over-predicts the property.

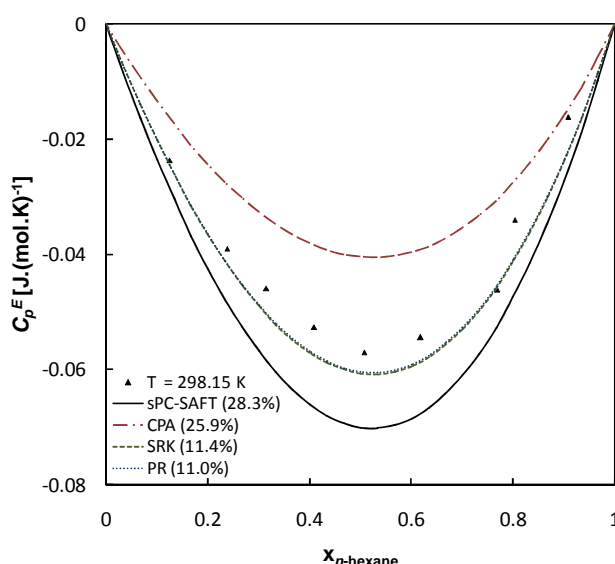


Figure 4-7: Excess isobaric heat capacity of the *n*-hexane/*n*-heptane system at $T = 298.15$ K and $P = 1$ atm. Data from ref. (103).

Recall that the isobaric heat capacity is a strong function of the first- and second-order temperature derivatives. It is again noticed that the temperature dependency of CPA worsened as a result of the parameter regression. The temperature dependency of sPC-SAFT is also not satisfactory.

4.1.5 Section highlights

The results presented in this section show that sPC-SAFT and CPA do not accurately predict the binary properties investigated. The correct trends are usually predicted with sPC-SAFT and CPA

and the performance of both models may be improved by fitting a BIP to the data. However, as will be shown in future chapters, the BIP tends to be property-specific for a given system.

4.2 Non-polar/Polar (non-HB) systems

Mixtures of non-polar and polar (non-HB) systems have repulsive, dispersive and polar forces present in their structures. Investigating the temperature dependency of these mixtures should be useful, since the polar forces are temperature-dependent and the dispersive forces are not.

4.2.1 Mass density

i) acetone/*n*-hexane

In Figure 4-8 and Figure 4-9, both sPC-SAFT and CPA correlate the property well, while both SRK and Peng-Robinson predict less satisfactory results. It is interesting to note that Peng-Robinson is able to predict the correct value for the mass density in the *n*-hexane pure component limit and then systematically fails as the concentration of acetone increases. This clearly demonstrates that the way in which the model parameters are estimated in Peng-Robinson and SRK are not sufficient to account for the polar interactions.

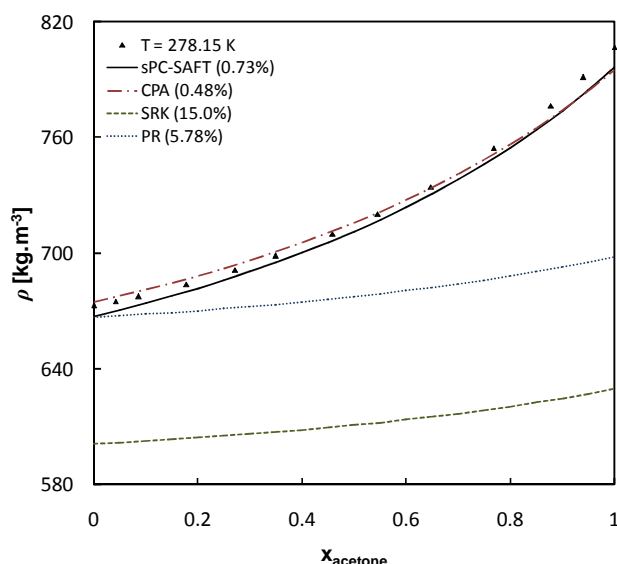


Figure 4-8: Mass density of the acetone/*n*-hexane system at $T = 278.15\text{ K}$ and $P = 1\text{ atm}$. Data from ref. (109).

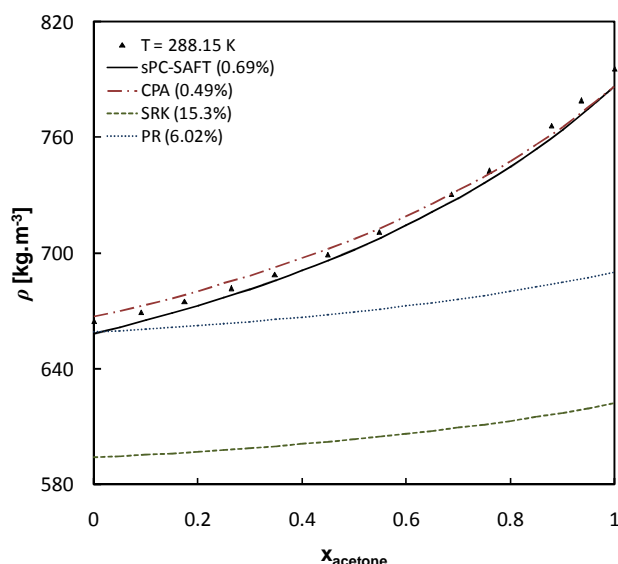


Figure 4-9: Mass density of the acetone/*n*-hexane system at $T = 288.15\text{ K}$ and $P = 1\text{ atm}$. Data from ref. (109).

In the mass density section of the non-polar/non-polar binary mixtures (section 4.1.1), the mass density of the mixture increased as the concentration of the heavy component increased. In addition to this, molecules with longer chains are more dense than shorter molecules. Comparing these results with Figure 4-8 and Figure 4-9, it is observed that the mass density of the mixture increases as the fraction acetone increases. Keeping in mind that acetone is a smaller molecule

than *n*-hexane, the contrasting behaviour of the mixture (compared to section 4.1.1) is attributed to the polar forces of acetone molecules. The fact that CPA and sPC-SAFT are able to follow the trend of the property justifies the generally accepted *Van der Waals* approach to a certain extent; however, the approximation is valid for the first-order volume derivative and most probably not for all partial derivatives of the state function.

4.2.2 Excess volume

i) acetone/*n*-hexane

The excess volume for a mixture of acetone and *n*-hexane is shown in Figure 4-10 and Figure 4-11:

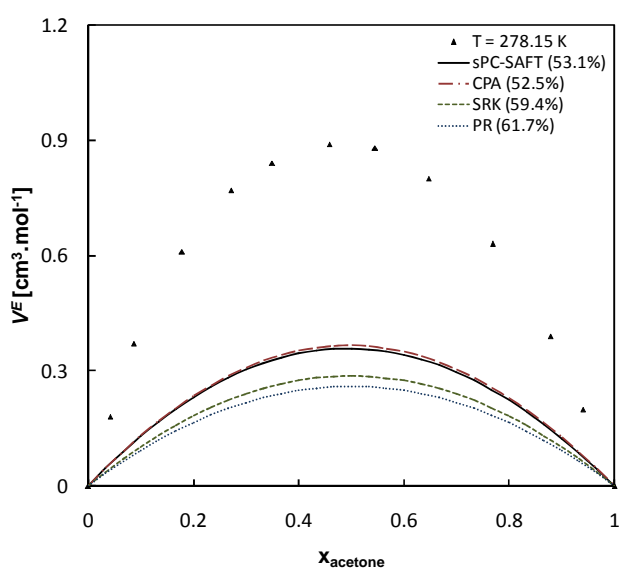


Figure 4-10: Excess volume of the acetone/*n*-hexane system at $T=278.15\text{ K}$ and $P = 1\text{ atm}$. Data from ref. (109).

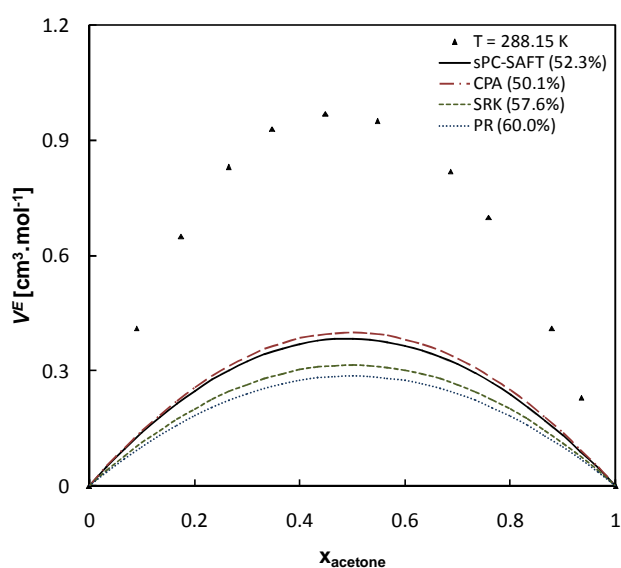


Figure 4-11: Excess volume of the acetone/*n*-hexane system at $T=288.15\text{ K}$ and $P = 1\text{ atm}$. Data from ref. (109).

From Figure 4-10, the excess volume is positive over the whole concentration range and all the models predict the correct trend, although the property is vastly underestimated. The maximum in excess volume is roughly equal to $0.9\text{ cm}^3.\text{mol}^{-1}$ at $x_{\text{acetone}} = 0.5$.

In Figure 4-11, the excess volume becomes more positive with an increase in temperature and the prediction of all the models also increases with increase in temperature, which is encouraging. The maximum in excess volume is roughly equal to $1.0\text{ cm}^3.\text{mol}^{-1}$ at $x_{\text{acetone}} = 0.5$.

In the non-polar/non-polar section, the excess volumes of *n*-hexane/*n*-heptane (Figure 4-3) and *n*-hexane/*n*-decane (Figure 4-4 and Figure 4-5) systems were investigated. The excess volumes for these systems were negative with the value of the minimum for the *n*-hexane/*n*-heptane mixture equal to $-0.025\text{ cm}^3.\text{mol}^{-1}$ at $x_{n\text{-hexane}} = 0.5$ and for *n*-hexane/*n*-decane system, the minimum is equal to $-0.25\text{ cm}^3.\text{mol}^{-1}$ at $x_{n\text{-hexane}} = 0.6$. From the non-polar/non-polar section it can be concluded that the repulsive and dispersive interactions between *unlike* molecules lead to a net negative effect on the excess volume.

Comparing this behaviour to Figure 4-10, where a positive maximum is observed, it is noticed that the presence of the acetone molecules changes the behaviour of the mixture severely. In the acetone/*n*-hexane mixture, the dispersive and repulsive interaction should still contribute to the excess volume in a similar fashion. Therefore, the positive contribution probably originates from the diminishing polar forces between the acetone molecules as a result of the mixing and results in the mixture to pack less tightly compared to the pure species counterparts.

It is encouraging to see that sPC-SAFT and CPA are capable of predicting the maximum and again, the use *Van der Waals* approach to treat polar interaction is partly justified. However, the results show that the behaviour of polar and dispersive forces in the mixture is not the same. The success of the approach is therefore limited. To illustrate the argument, consider the simplified hypothetical case of molecular interactions in a mixture of polar and non-polar molecules:

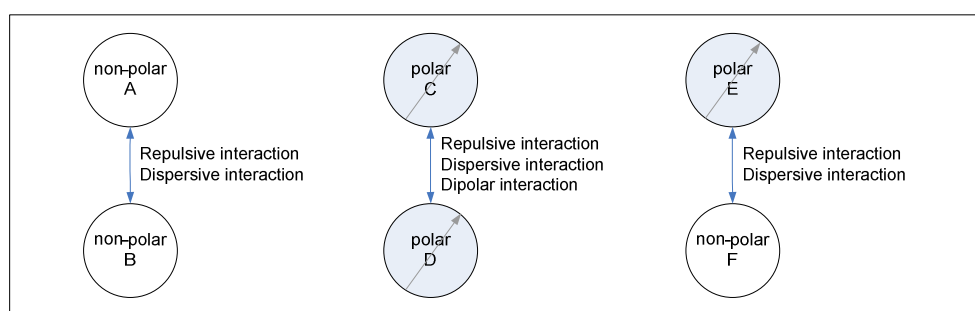


Figure 4-12: Simplified representation of interactions in non-polar/polar (non-HB) mixtures.

In Figure 4-12, non-polar molecules are represented by white spheres and polar molecules by shaded spheres. Three classes of interactions are identified between molecules in the mixture as indicated in Figure 4-12:

- interactions between two non-polar molecules (spheres A and B) - AB (*like*) interactions.
- interactions between two polar molecules (spheres C and D) - CD (*like*) interactions.
- interactions between one non-polar molecule and one polar molecule (sphere E and F) - EF (*unlike*) interactions.

In models such as CPA and sPC-SAFT, where the dispersive and polar forces are lumped together and treated with the *Van der Waals* approach, consider the simplified representation of the molecules and interactions in the framework of these type of models in Figure 4-13:

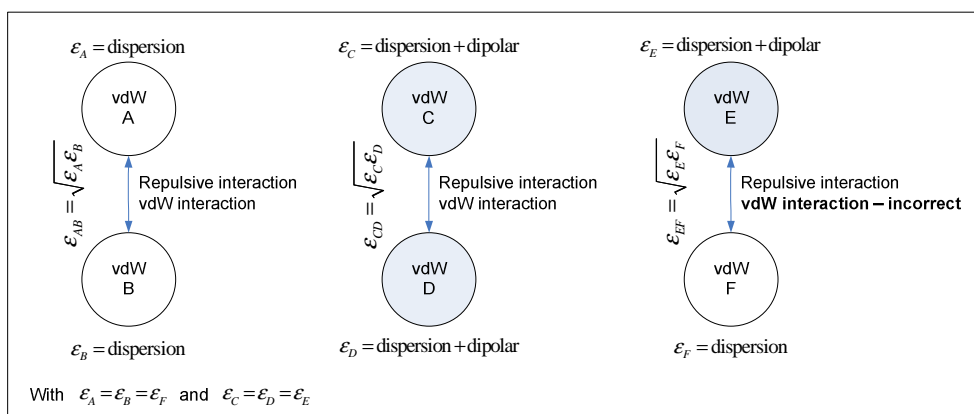


Figure 4-13: Simplified representation of interactions present in non-polar/polar (non-HB) mixtures by models using the Van der Waals approach to account polar forces.

In Figure 4-13, ε_i are energy pure component parameters assigned in models to account for *Van der Waals* (dispersion and polar) forces. The geometric mean rule is commonly used to define the *Van der Waals* interactions between molecules. The three classes of interactions from Figure 4-12 are accounted for in the following way:

- The interactions between two non-polar molecules (A-B interactions) are naturally well accounted for in the *Van der Waals* approach, since there are only dispersive and no polar forces.
- The interactions between two polar molecules (C-D interactions) are also reasonable well accounted for, since the dipolar and dispersive forces do have the same separation distance dependency and treating the combined dispersive and polar interaction as a one *Van der Waals* interaction generally gives acceptable results. The energy parameters characterising the *Van der Waals* interaction between polar molecules is generally larger than those between non-polar molecules as a result of the lumping together of the forces.
- The main problem with the *Van der Waals* approach is encountered in mixtures of non-polar and strongly polar components, because the approach effectively accounts for “half” a dipolar interaction between a polar and a non-polar molecule that is not present. The energy parameter for the polar molecule is artificially large because of the *Van der Waals* (lumping) approach and this results in the mixture parameter ε_{EF} to be artificially large. (Although induction forces may form, depending on the polarizability, the effect thereof is small compared to the other interactions; refer to Appendix A). The problem is not encountered in interactions between two polar molecules, because the dipole interaction is present. The temperature dependency is, however, not completely correct for (C-D) interactions.

These arguments emphasize again the advantage of including a polar term in the framework of models such as sPC-SAFT.

4.2.3 Excess enthalpy

i) acetone/*n*-hexane

From Figure 4-14, the excess enthalpy for the mixture is positive over the entire concentration range and the models follow the correct trend, but severely underestimate the property. Consider the magnitude of the maximum at $x_{\text{acetone}} = 0.5$, which is equal to $1300 \text{ J}\cdot\text{mol}^{-1}$. Comparing this value to the maximum in excess enthalpy for the *n*-hexane/*n*-decane mixture (Figure 4-6) where the maximum is approximately $13 \text{ J}\cdot\text{mol}^{-1}$, it is clear that the polar interactions influence the caloric properties significantly.

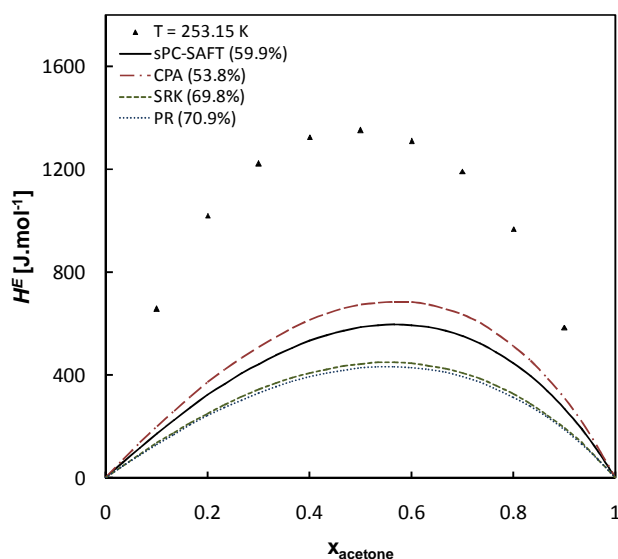


Figure 4-14: Excess enthalpy of the acetone/*n*-hexane system at $T = 253.15 \text{ K}$ and $P = 1 \text{ atm}$. Data from ref. (110).

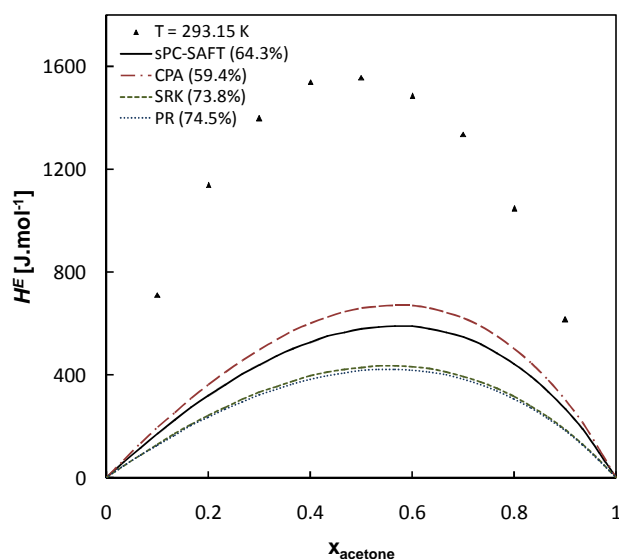


Figure 4-15: Excess enthalpy of the acetone/*n*-hexane system at $T = 293.15 \text{ K}$ and $P = 1 \text{ atm}$. Data from ref. (110).

In Figure 4-15, the excess enthalpy increases with an increase in temperature while the predictions of the models do not really change relative to the change in the experimental data. The results show that the dispersive forces are independent of temperature relative to the polar forces, which diminish at the higher temperature. All the models treat the polar forces via the *Van der Waals* approach and the effect thereof can be observed by the fact that the predictions of the models barely change with an increase in temperature (relative to the experimental data).

These figures again indicate the necessity of including a polar term in the framework of the models such as sPC-SAFT.

4.2.4 Section highlights

This section showed that mixture behaviour for non-polar/non-polar systems compared to non-polar/polar (non-HB) mixtures is totally different as a result of the polar interactions. The main points are:

- Properties are influenced considerably by polar forces (attractive) forces, especially caloric properties, and models that use the *Van der Waals* approach to account for polar forces have shortcomings in their temperature dependency.
- The inclusion of a polar term in the framework of models such as sPC-SAFT may potentially remedy the problem.

4.3 Non-polar/Hydrogen bonding systems

At the pure component limits of non-polar/hydrogen bonding mixtures, on the one side, the thermodynamic behaviour is primarily dominated by repulsive and dispersive interactions (non-polar side) and on the other side, the behaviour is strongly influenced by hydrogen bonding and polar forces (hydrogen bonding side). As the concentration of the non-polar molecule increases, the ability of the models to account for the decreasing level of hydrogen bonding and polar forces is tested.

4.3.1 Mass density

i) *n*-hexane/1-hexanol

The mass density of *n*-hexane/1-hexanol mixture is shown in Figure 4-16 and Figure 4-17:

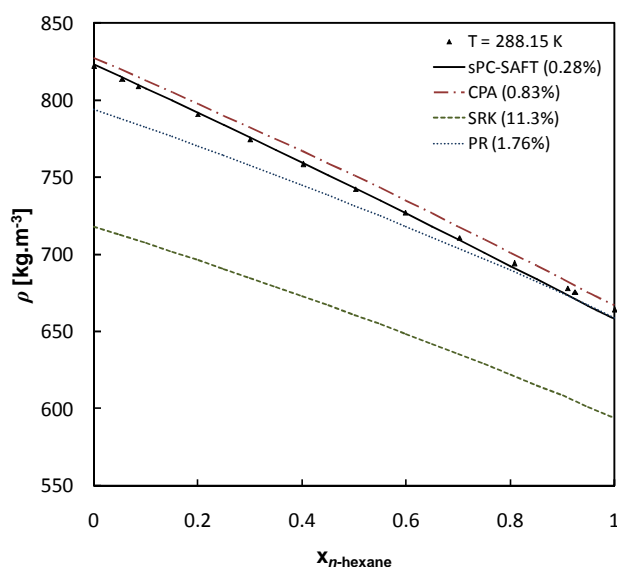


Figure 4-16: Mass density of the *n*-hexane/1-hexanol system at $T=288.15\text{ K}$ and $P = 1\text{ atm}$. Data from ref. (111).

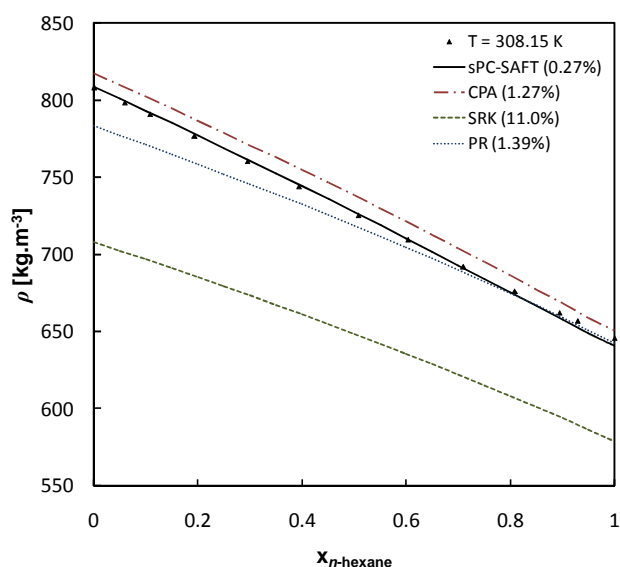


Figure 4-17: Mass density of the *n*-hexane/1-hexanol system at $T=308.15\text{ K}$ and $P = 1\text{ atm}$. Data from ref. (111).

In Figure 4-16, both sPC-SAFT and CPA are able to correlate the property accurately and both SRK and Peng-Robinson have problems in the 1-hexanol-rich end as a result of the hydrogen bonding and polar forces. *n*-hexane and 1-hexanol are very similar molecules with the only difference being that an OH-group substituted an H-atom on the first C-atom of the chain. The density of the

mixture is highest in the 1-hexanol-rich end as a result of the hydrogen bonds and polar forces that allow the molecules to pack more tightly together. Furthermore, both CPA and sPC-SAFT have an adequate temperature dependency for the mass density at low temperatures, as can be seen by examining Figure 4-17.

ii) *n*-decane/1-propanol

In Figure 4-18, sPC-SAFT and CPA predict the property with sufficient accuracy, with sPC-SAFT being slightly superior. It was previously mentioned, in section 4.3.1, that cubic equations fail to accurately describe the thermodynamic behaviour of large molecules such as *n*-decane, because they represent the chain-like molecule as a single sphere. This explains the deviation of CPA in the *n*-decane rich end in Figure 4-18. The same discussion holds for Figure 4-19 and it can also be seen that both CPA and sPC-SAFT have a proper temperature dependency for the mass density.

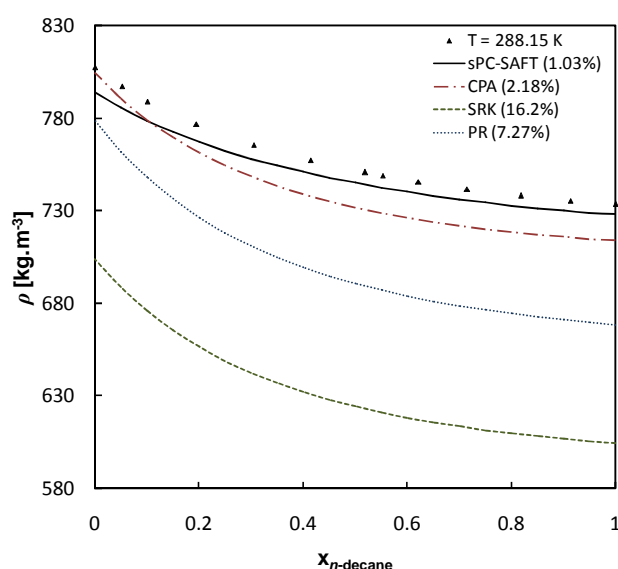


Figure 4-18: Mass density of the *n*-decane/1-propanol system at $T = 288.15\text{ K}$ and $P = 1\text{ atm}$. Data from ref. (112).

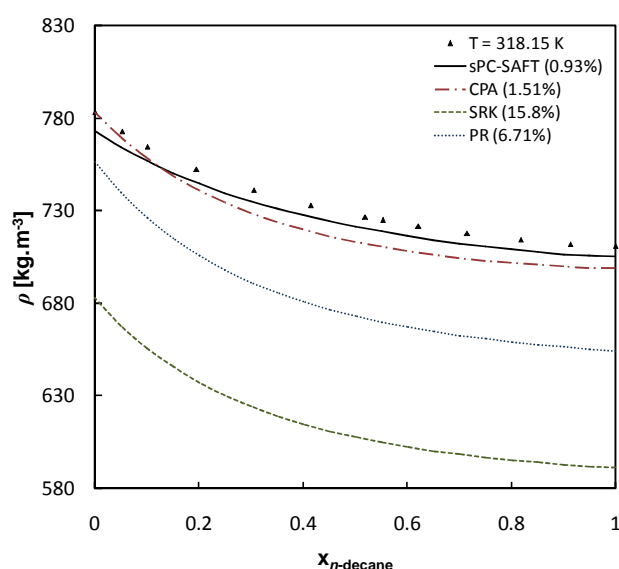


Figure 4-19: Mass density of the *n*-decane/1-propanol system at $T = 318.15\text{ K}$ and $P = 1\text{ atm}$. Data from ref. (112).

The association term in both CPA and sPC-SAFT is able to account for the influence of hydrogen bonding in the mass density of the mixture. It can, however, not be assumed that the association term is able to account for the influence of hydrogen bonding on all other properties, since some properties are more influenced by certain types of forces than others, as will be shown in subsequent sections.

4.3.2 Excess volume

i) *n*-hexane/1-hexanol

In Figure 4-20, the experimental data form a minimum at approximately $x_{n\text{-hexane}} = 0.4$ and then passes through a maximum in the *n*-hexane-rich side (the maximum is more clear in Figure 4-21).

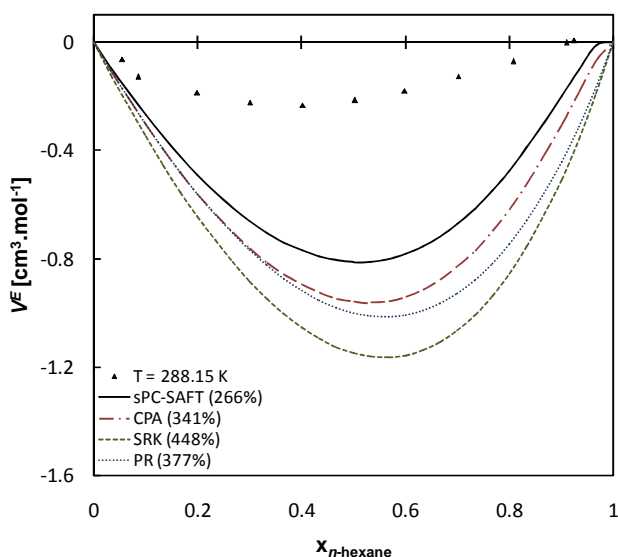


Figure 4-20: Excess volume of the *n*-hexane/1-hexanol system at $T = 288.15\text{ K}$ and $P = 1\text{ atm}$. Data from ref. (111).

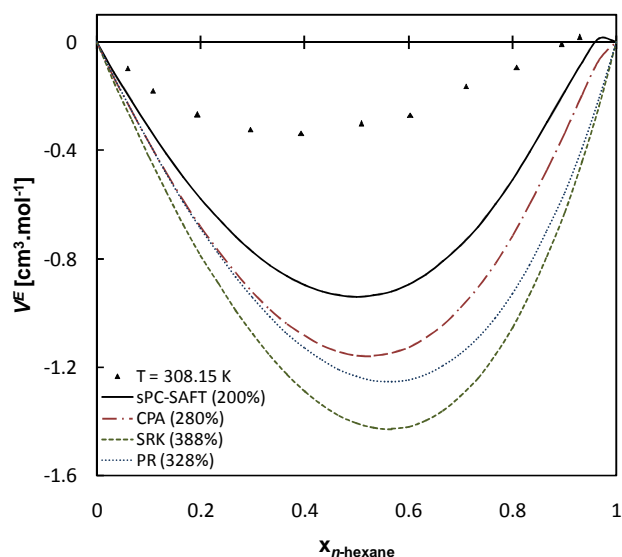


Figure 4-21: Excess volume of the *n*-hexane/1-hexanol system at $T = 308.15\text{ K}$ and $P = 1\text{ atm}$. Data from ref. (111).

In mixtures of non-polar/non-polar components, the excess volumes are negative (see Figure 4-3 to Figure 4-5) and the magnitude is small for mixtures where components have similar sizes (*n*-hexane/*n*-heptane) and becomes more negative as the asymmetry between molecules increases (*n*-hexane/*n*-decane). In mixtures of non-polar/polar (non-HB) components, the excess volumes are positive (Figure 4-10 and Figure 4-11 for acetone/*n*-hexane mixture) and large in magnitude.

These two contributions seem to be present in the mixture of *n*-hexane/1-hexanol, one contributing negatively to the excess volume and the other positively. Part of the positive contribution is a result of the diminishing polar forces and part of the negative contribution is a result of the net effect of repulsive and dispersive interactions. The negative contribution is, however, very small, since the molecules are similar in size. The question now remains how the hydrogen bonding forces affects the property. It is postulated that the hydrogen bonding forces allows the mixture to pack more tightly and consequently, a negative contribution is expected.

All the models predict negative values that are too large in magnitude. Therefore, it seems as if the negative contributions to the property are overestimated and that the positive contributions to the property are underestimated. If it is assumed that polar forces contribute positively to the excess volume, it seems that accounting for the polar forces via the *Van der Waals* approach leads to the incorrect behaviour in the models. In models such as CPA and sPC-SAFT, polar forces can be either incorrectly accounted for in the energy parameters (a_0 and c_1 in CPA and ε/k in sPC-SAFT) or in the association parameters ($\beta^{A_i B_j}$ and $\varepsilon^{A_i B_j}$ in CPA and $\kappa^{A_i B_j}$ and $\varepsilon^{A_i B_j}$ in sPC-SAFT). Since it is assumed that both dispersive and hydrogen bonding forces contribute negatively to the property, it is difficult to pinpoint the error in the models. It appears that not accounting explicitly for polar forces results in problematic description of the excess volume. The association models (CPA and

sPC-SAFT) show encouraging evidence that they are capable of capturing the maximum that forms in the *n*-hexane-rich side which is encouraging.

4.3.3 Excess enthalpy

i) *n*-hexane/1-hexanol

In Figure 4-22, the experimental data shows positive excess enthalpy over the entire concentration range, with a maximum at $x_{n\text{-hexane}} = 0.62$ equal to 500 J.mol⁻¹ and a trend that is skewed to the *n*-hexane-rich side. Both CPA and sPC-SAFT overestimate the excess enthalpy, but are capable in predicting the skewed trend, while SRK and Peng-Robinson provide a more symmetric prediction that is more or less of the correct order of magnitude. Since CPA differs from SRK as a result of the association term (and parameter regression), it is most probable that the skewed trend is caused by the hydrogen bonding between 1-hexanol molecules.

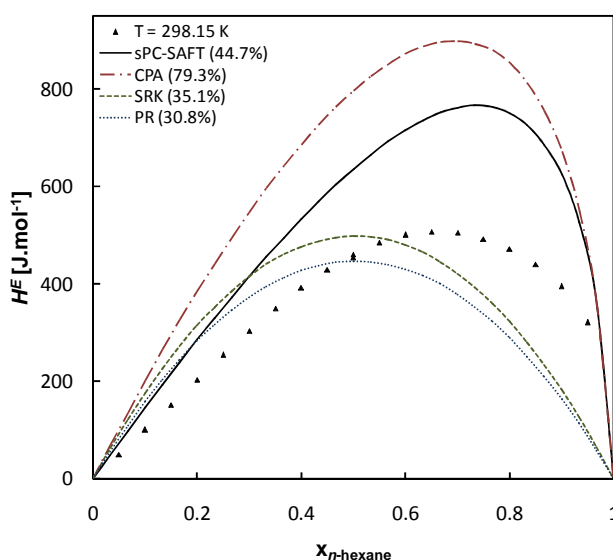


Figure 4-22: Excess enthalpy of the *n*-hexane/1-hexanol system at $T = 298.15$ K and $P = 1$ atm. Data from ref. (110).

In section 4.1, the excess enthalpy of the *n*-hexane/*n*-decane system (Figure 4-6) is positive with a maximum value equal to 15 J.mol⁻¹ at 298.15 K. For systems where the molecules are even more similar in size, the value will be smaller. This implies that the large value of the maximum in Figure 4-22 is not caused by the net effect of repulsive and dispersive interactions as a result of the mixing.

In section 4.2, the excess enthalpy of *n*-hexane/acetone (Figure 4-14 and Figure 4-15) shows a maximum of 1300 J.mol⁻¹ at $T = 253.15$ K and 1600 J.mol⁻¹ at 293.15 K.

In the *n*-hexane/1-hexanol system, the *like* interactions between the 1-hexanol molecules are strong, since dispersive, polar and hydrogen bonding forces contribute and the *like* interactions between *n*-hexane molecules are much weaker, since only dispersive attractive forces are present. The *unlike* interactions between a *n*-hexane and 1-hexanol molecules are also significantly weaker

than the *like* interactions between the 1-hexanol molecules, but probably a little stronger than the *like* interactions between the *n*-hexane molecules as induction is possible. The relative weakness of the *like* interactions to the *unlike* interactions leads to the positive excess enthalpy of the property. It is suspected that the skewed effect is caused by a systematic break down of the hydrogen bonding network between the 1-hexanol molecules as the concentration *n*-hexane increases. For hydrogen bonds to form, the 1-hexanol molecules must be in a certain proximity to each other to form the bonds and from $x_{n\text{-hexane}} = 0$ to 0.62, this hydrogen bonding network seems to exist. At $x_{n\text{-hexane}} = 0.62$, it is believed that this hydrogen bonding network starts to break down rapidly, because the molecules are too dilute to maintain the network.

4.3.4 Isobaric heat capacity

i) *n*-decane/1-propanol

In Figure 4-23, the isobaric heat capacity increases with an increase in *n*-decane concentration and exhibit a maximum at roughly $x_{n\text{-decane}} = 0.95$. This phenomenon was explained by Costas & Patterson (108), using a simple association model for the excess isobaric heat capacity (which is closely related to the isobaric heat capacity). The explanation centred on the level of structure that occurs in the mixture as a result of hydrogen bonding between 1-propanol molecules and can briefly be described as follows: At infinite dilution of 1-propanol molecules, there is no structure in the mixture. As the 1-propanol concentration increases the level of structure in the mixture rises dramatically, because all the 1-propanol monomers come together over long distances to form multimers. The maximum change in level of structure is attributed to the maximum in the data. As the concentration of 1-propanol increases further, the 1-propanol molecules still come together, but now over shorter distances, because there is already a high level of structure in the mixture.

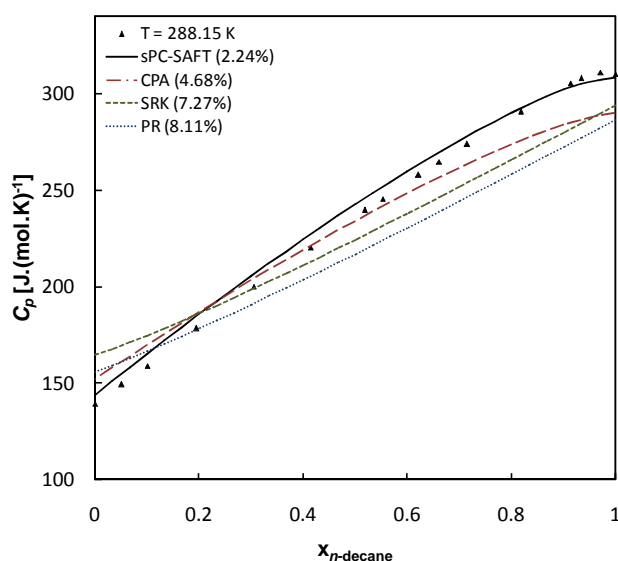


Figure 4-23: Isobaric heat capacity of the *n*-decane/1-propanol system at $T = 288.15\text{ K}$ and $P = 1\text{ atm}$. Data from ref. (112).

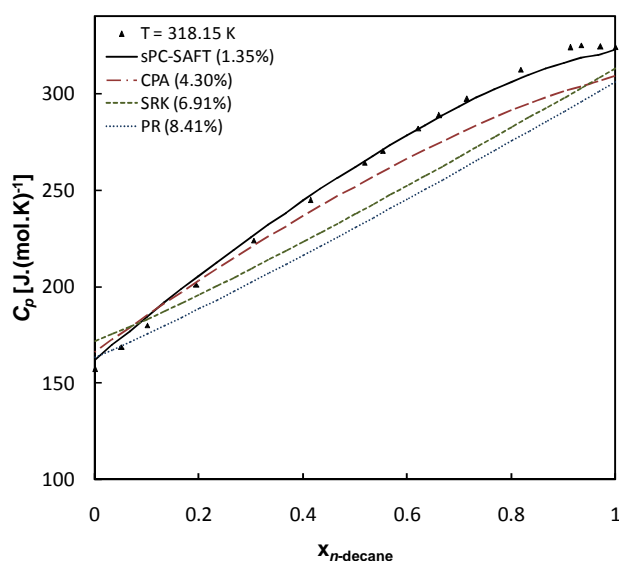


Figure 4-24: Isobaric heat capacity of the *n*-decane/1-propanol system at $T = 318.15\text{ K}$ and $P = 1\text{ atm}$. Data from ref. (112).

Both sPC-SAFT and CPA are able to capture the trends in the experimental data to some extent. This is somewhat expected, since the property is influenced greatly by molecular association and these models both explicitly account for them. It is once again expected that if accurate prediction of the pure component properties can be managed by the association models, both models would be able to represent the property with reasonable accuracy, especially at low pressures.

From Figure 4-23, the maximum peak shifts to a higher 1-propanol concentration (lower *n*-decane concentration) and the association model used by Costas & Patterson (108) is also able to explain the shift in the maximum peak: The hydrogen bonds are more resilient to form at the higher temperature and the maximum change in level of structure in the mixture is reached at higher 1-propanol concentrations. sPC-SAFT and CPA are again able to capture this trend to some extent. It seems as if the maximum at $x_{n\text{-decane}} = 0.9$ is not that well captured, but it is difficult to say whether this is a result of poor pure component parameters or whether the models are not able to capture the effect.

4.3.5 Excess isobaric heat capacity

i) *n*-hexane/1-hexanol

Only CPA and sPC-SAFT are able to predict a positive value for the excess isobaric heat capacity in Figure 4-25. Although the %AAD for each model is still large (13.5% and 32.5% respectively), the results are encouraging and the strength of the association term can be appreciated. The fact that SRK and Peng-Robinson predict negative values is in accordance with the formulation of the model where attractive forces are approximated via the *Van der Waals* approach. Therefore, it is expected that the behaviour of these models will be similar to their behaviour for non-polar/non-polar mixture.

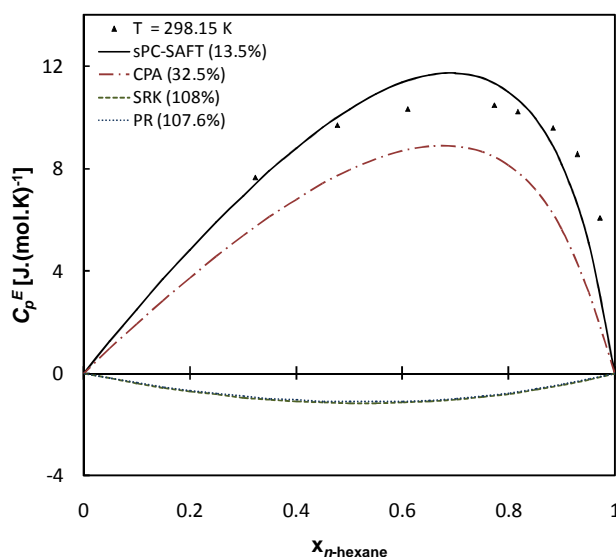


Figure 4-25: Excess isobaric heat capacity of the *n*-hexane/1-hexanol system at $T = 298.15\text{ K}$ and $P = 1\text{ atm}$. Data from ref. (113).

4.3.6 Section highlights

From the discussion presented for selected mixtures of non-polar/hydrogen bonding components, it follows that:

- In mixtures with one associating component, association models such as sPC-SAFT and CPA that is based on Wertheim's association term are able to account for prominent trends in properties caused by hydrogen bonding.
- In some of the properties considered, problems with sPC-SAFT and CPA are still encountered. The shortcomings in the model, however, seem to originate from polar forces that are not explicitly accounted for by models in these type of mixtures.

4.4 Hydrogen bonding / Hydrogen bonding systems

In hydrogen bonding/hydrogen bonding systems, solvation and association usually have a noticeable influence on the thermodynamic behaviour of the system. Repulsion, dispersion, induction, polar and hydrogen bonding interactions all have to be taken into account.

In models such as CPA and sPC-SAFT, cross-association is effectively accounted for, because both components have association parameters that were determined during parameter regression.

4.4.1 Mass density

i) methanol/ethanol

In Figure 4-26, the association models provide good correlation of the mixture mass density, while the cubic models under-predict the mass density. However, closer inspection reveals that sPC-SAFT and CPA have model trends that are not very consistent with the experimental data, especially the prediction of sPC-SAFT.

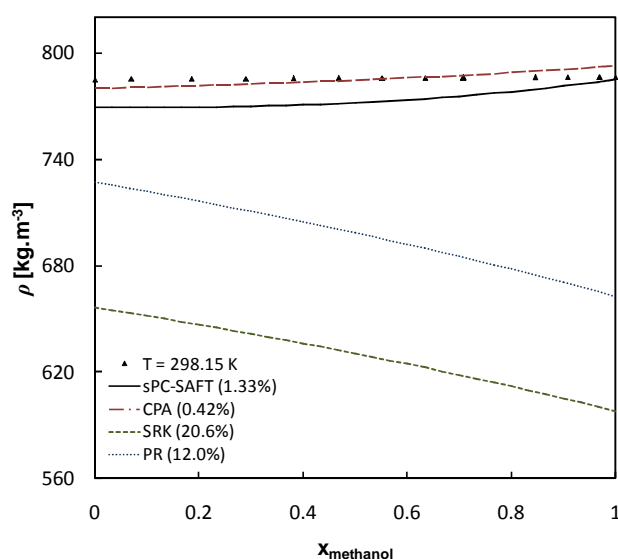


Figure 4-26: Mass density of the methanol/ethanol system at $T = 298.15\text{ K}$ and $P = 1\text{ atm}$. Data from ref. (114).

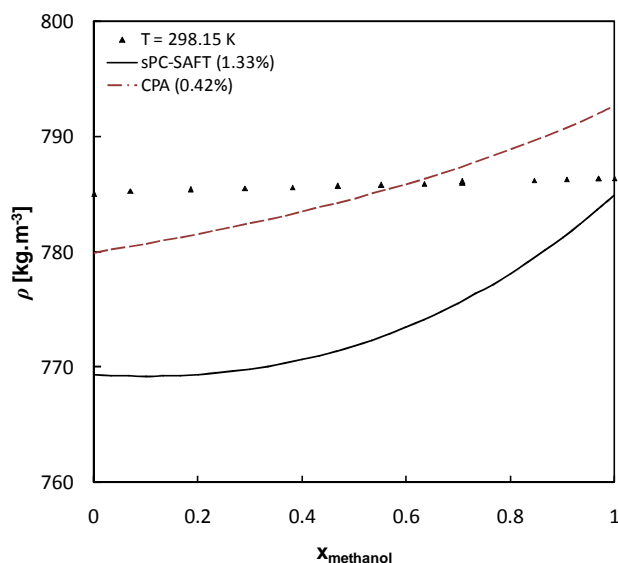


Figure 4-27: Enlargement of the mass density of the methanol/ethanol system at $T = 298.15\text{ K}$ and $P = 1\text{ atm}$ with the predictions of only sPC-SAFT and CPA. Data from ref. (114).

The predictions of CPA and sPC-SAFT are enlarged in Figure 4-27 to emphasize the problem. The experimental data exhibits a slightly convex behaviour and the models show a slight concave behaviour. Since the association term accounts for self-association and cross-association to a certain extent, a possible explanation for the observed difference between the experimental data and model predictions may be that polar forces are incorrectly accounted for via the *Van der Waals* approach. For this system, however, it is expected that the *Van der Waals* approach would give acceptable representation of the polar forces and that the energy parameters would be well-behaved in the mixture, since both components are polar (therefore, *like* interactions are similar). Further reasons for the incorrect trend of sPC-SAFT may now be attributed to limitations inherent to SAFT, such as co-operativity, as mentioned in section 1.2.2.

ii) 1-propanol/1-hexanol

In Figure 4-28, both sPC-SAFT and CPA provide relatively accurate predictions of the mixture mass density (low %AAD = 0.41 for CPA and 0.69 for sPC-SAFT). The trend of the experimental data and association models seems to be slightly convex and, there are no contrasting model predictions as in the case for the methanol/ethanol mixture (Figure 4-27).

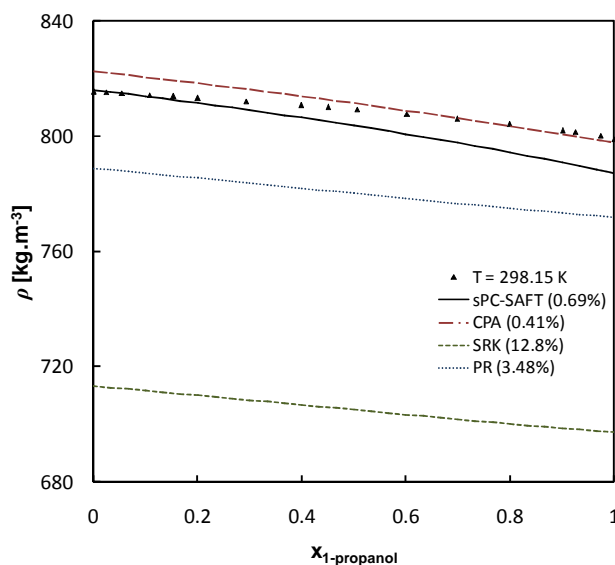


Figure 4-28: Mass density of the 1-propanol/1-hexanol system at $T = 298.15\text{ K}$ and $P = 1\text{ atm}$. Data from ref. (115).

A possible explanation why the model predictions for the 1-propanol/1-hexanol system is more or less consistent with the data, is related to the level of hydrogen bonding and polar forces present in the system. Consider the 1-propanol molecules to consist out of two non-polar segments and one hydrogen bonding polar segment and the 1-hexanol molecule to consist out of five non-polar segments and one hydrogen bonding polar segment. The ratio of non-polar segment to hydrogen bonding polar segment therefore varies between 2:1 in pure 1-propanol and 5:1 in the pure 1-hexanol. In mixtures such as methanol/ethanol, the ratio would vary between 0:1 in the methanol pure component limit and 1:1 in the ethanol pure component limit. The proximity of hydrogen bonding molecules to each other is therefore higher in the methanol/ethanol mixture compared to the 1-propanol/1-hexanol mixture. Additional molecular interactions that influence thermodynamic behaviour such as hydrogen bond co-operativity are more likely to be prominent in mixtures such as methanol/ethanol or any other mixture where a low ratio of non-polar segments to hydrogen bonding polar segment is encountered.

iii) ethanol/water

In Figure 4-29 and Figure 4-30, sPC-SAFT and CPA provides superior predictions of the experimental data compared to the cubic models, but there is a definite inconsistency in the prediction if the trends are considered. Approximately between ethanol fractions of $x_{\text{ethanol}} = 0.1$ and 0.4 , there are molecular interactions causing the density to be unusually high. Although the association models account for cross-association to certain extent in the mixture, there seems to be no evidence that the models are capable of capturing the irregular trend exhibited by the data.

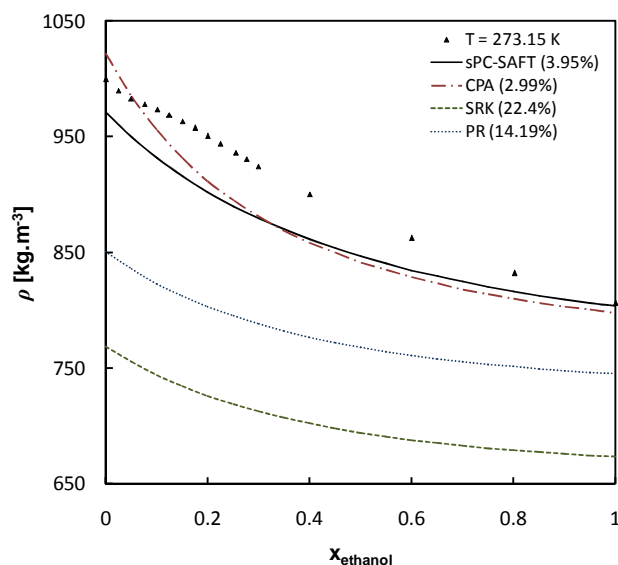


Figure 4-29: Mass density of the ethanol/water system at $T = 273.15\text{ K}$ and $P = 1\text{ atm}$. Data from ref. (116).

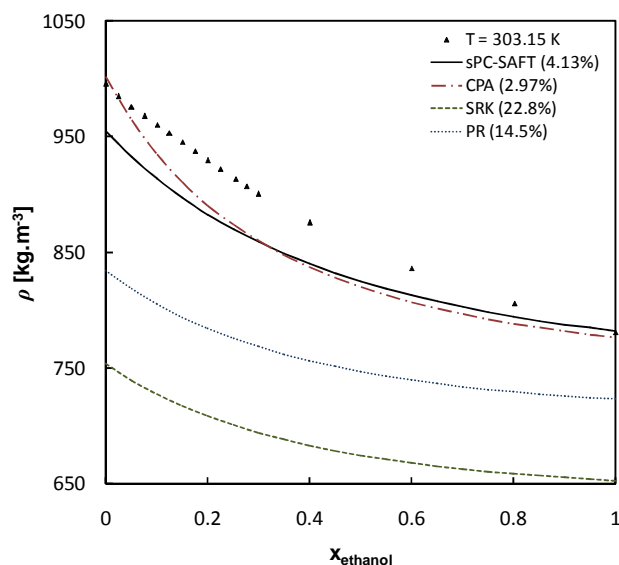


Figure 4-30: Mass density of the ethanol/water system at $T = 303.15\text{ K}$ and $P = 1\text{ atm}$. Data from ref. (116).

Similar to the discussion presented in the previous section regarding the ratio of non-polar segments to hydrogen bonding polar segments, it will be realized that this ratio varies between 0:1 in the water pure component limit and 1:1 in the ethanol pure component limit. Water is considered to have two ‘positive’ sites and two ‘negative’ sites and ethanol two ‘negative’ sites and one ‘positive’ site that can hydrogen bond. This implies that the ratio of ‘positive’ to ‘negative’ sites varies between 1:1 and 1:2. This, combined with the fact that there is a high level of hydrogen bonding polar segments in the mixture, probably gives rise to molecular effects such as co-operativity and other effects associated with hydrogen bonding networks. These effects are not accounted for by the association term and possibly indicate the limitations associated with Wertheim’s term. Naturally, not all possible hydrogen bonds will form, because some hydrogen bonds will sterically hinder the formation of others, this also being the reason why molecules such as ethanol are commonly modelled in the framework of sPC-SAFT and CPA as two-site molecules instead of three. However, it is believed that the manner in which these molecules will behave (as a two or three-site molecule), will be partly dependent on the components they are in mixture with. Similar findings were made by Perakis *et al.* (79).

In Figure 4-31, Figure 4-32, Figure 4-33 and Figure 4-34 additional plots of the mass density for the ethanol/water mixture are given at higher pressures and temperatures:

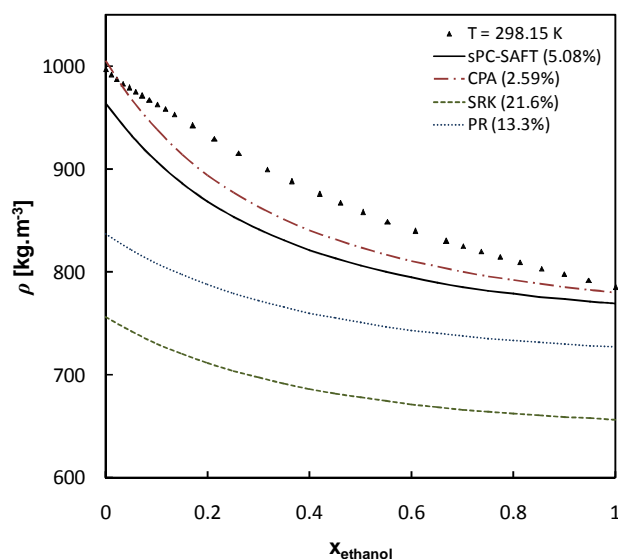


Figure 4-31: Mass density of the ethanol/water system at $T = 298.15$ K and $P = 0.4$ MPa. Data from ref. (117).

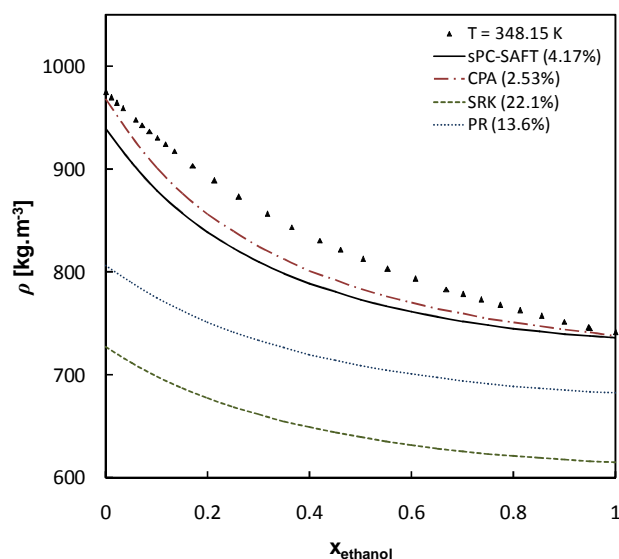


Figure 4-32: Mass density of the ethanol/water system at $T = 348.15$ K and $P = 0.4$ MPa. Data from ref. (117).

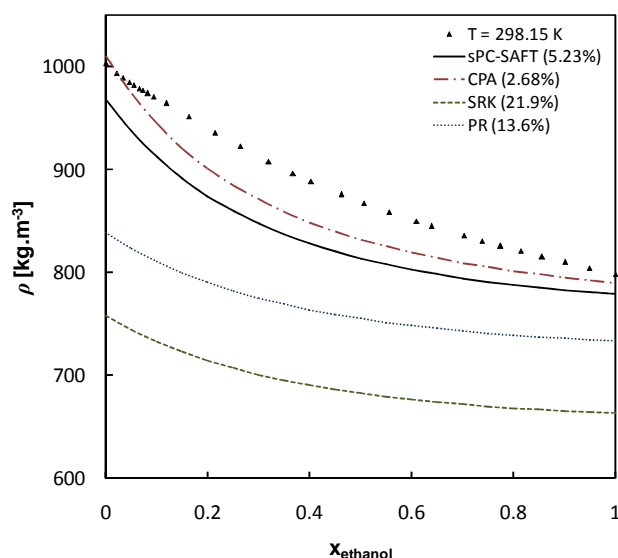


Figure 4-33: Mass density of the ethanol/water system at $T = 298.15$ K and $P = 15$ MPa. Data from ref. (117).

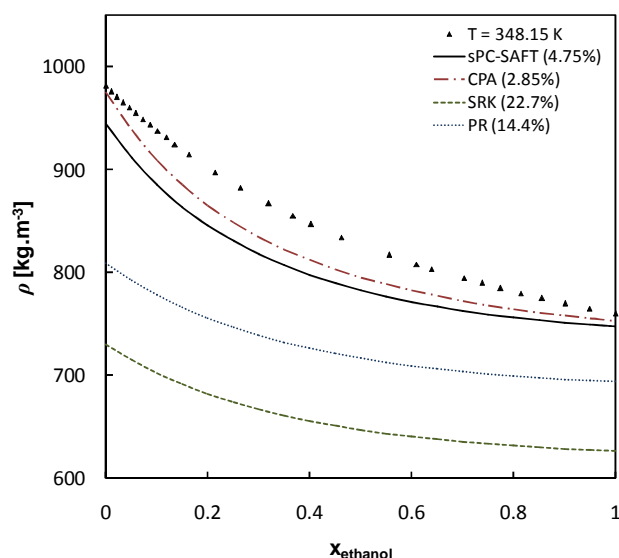


Figure 4-34: Mass density of the ethanol/water system at $T = 348.15$ K and $P = 15$ MPa. Data from ref. (117).

The molecular effects that give rise to the increased density in the water-rich side are insensitive to changes in pressure (compare Figure 4-31 & Figure 4-32 with Figure 4-33 & Figure 4-34 where the increase in pressure is from 0.4 MPa to 15 MPa), but are sensitive to changes in temperature (compare Figure 4-31 & Figure 4-33 with Figure 4-32 & Figure 4-34 where the temperature increases from 298.15 K to 348.15 K). The increase in temperature reduces the high density irregularity in the water-rich side. Therefore, the molecular interactions that cause the mass density to be higher, diminish with increasing temperature. Seeing that neither CPA nor sPC-SAFT are able to predict the increase in density in the water-rich end, this possibly indicates problems with the association term, or it may be as a result of polar forces that are not accounted for correctly. Either way, there are definite shortcomings in the models when complex interactions are considered.

4.4.2 Excess volumes

i) methanol/ethanol

None of the models are able to reproduce the sigmoidal behaviour exhibited by the experimental data in Figure 4-35 (enlargement shown in Figure 4-36). The %AAD of all the models are extremely large (it should be kept in mind that the experimental value is very small so any deviation from the data is considerably amplified in the %AAD calculation). Of particular concern is the poor prediction of sPC-SAFT. The model completely overshoots the experimental data and both sPC-SAFT and CPA show no evidence that they are capable of capturing the negative contribution to the property.

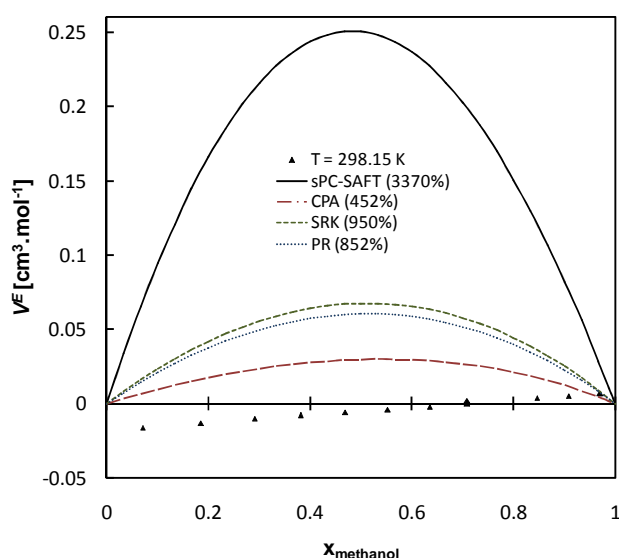


Figure 4-35: Excess volume of the methanol/ethanol system at $T=298.15\text{ K}$ and $P = 1\text{ atm}$. Data from ref. (114).

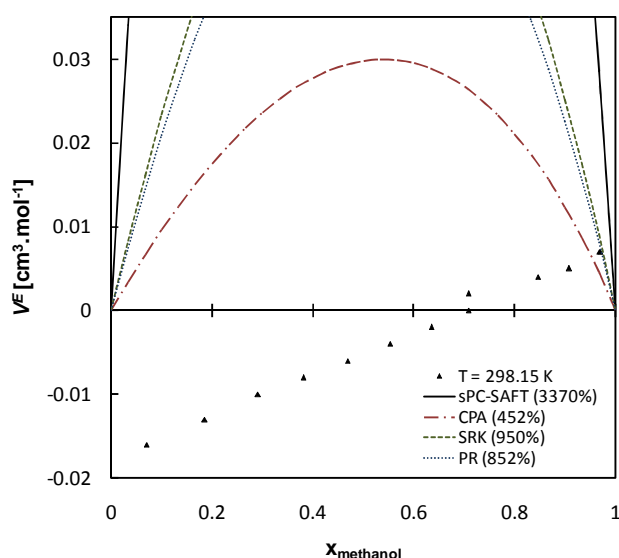


Figure 4-36: Excess volume of the methanol/ethanol system at $T=298.15\text{ K}$ and $P = 1\text{ atm}$. Data from ref. (114).

sPC-SAFT is considered to be superior to CPA. The result from Figure 4-35 therefore possibly indicates that the pure component model parameters used in sPC-SAFT are incorrect. Contradicting results such as these should be re-investigated with model parameter determined using the same data and the same regression procedure.

4.4.3 Excess enthalpy

i) ethanol/water

From Figure 4-37 to Figure 4-40, it is clear that the behaviour of the excess enthalpy for this mixture is extremely complex. Consider the trends of the experimental data in Figure 4-37, the minimum at approximately $x_{\text{ethanol}} = 0.18$ indicates that the structure that forms at this point between the ethanol and water molecules is most stable. As the concentration of ethanol increases from this point, a rapid increase in the excess enthalpy is observed, indicating that the

stability of the mixture is rapidly decreasing. At $x_{\text{ethanol}} = 0.5$, the experimental data shows an inflection point and another inflection point at approximately $x_{\text{ethanol}} = 0.9$. There seems to be a couple of molecular effects contributing to the property and none of the association models are even remotely able to capture the mentioned trends.

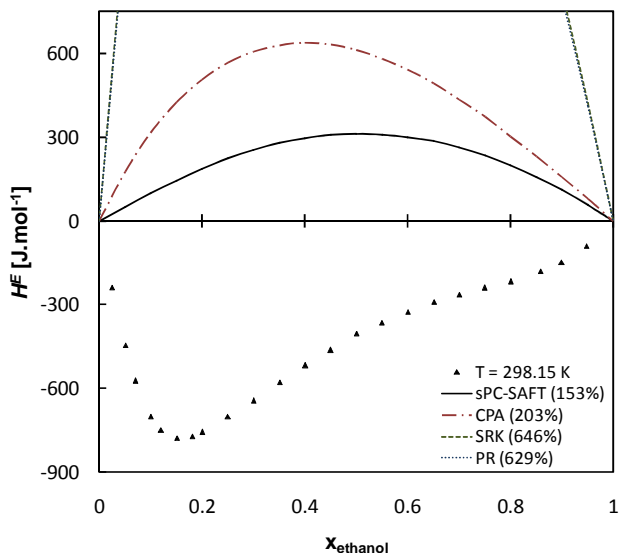


Figure 4-37: Excess enthalpy of the ethanol/water system at $T = 298.15 \text{ K}$ and $P = 0.4 \text{ MPa}$. Data from ref. (118).

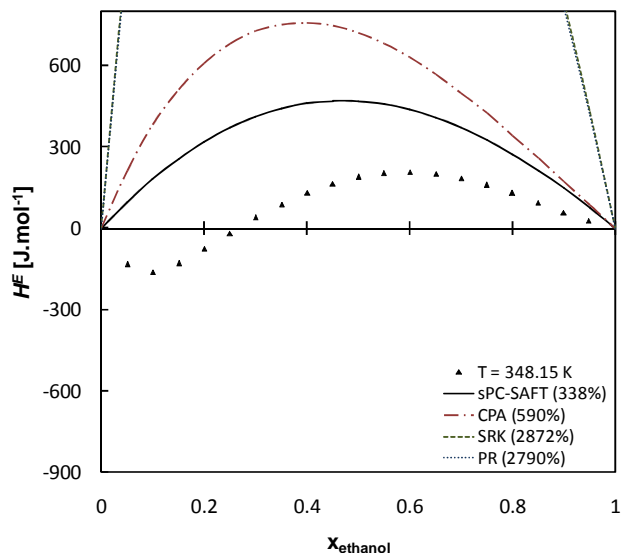


Figure 4-38: Excess enthalpy of the ethanol/water system at $T = 348.15 \text{ K}$ and $P = 0.4 \text{ MPa}$. Data from ref. (119).

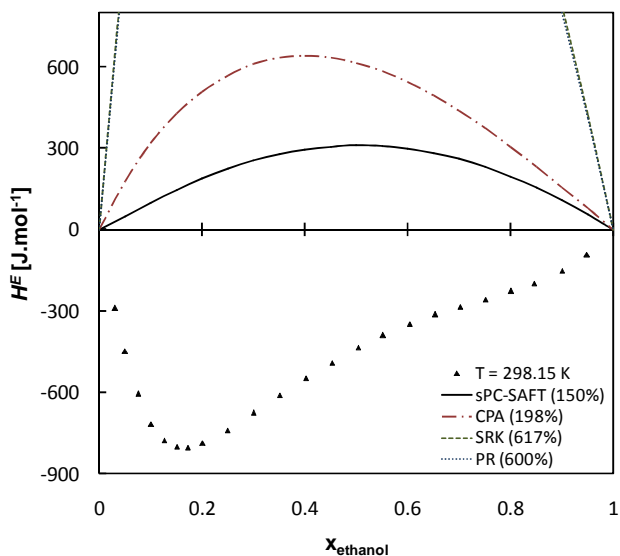


Figure 4-39: Excess enthalpy of the ethanol/water system at $T = 298.15 \text{ K}$ and $P = 15 \text{ MPa}$. Data from ref. (118).

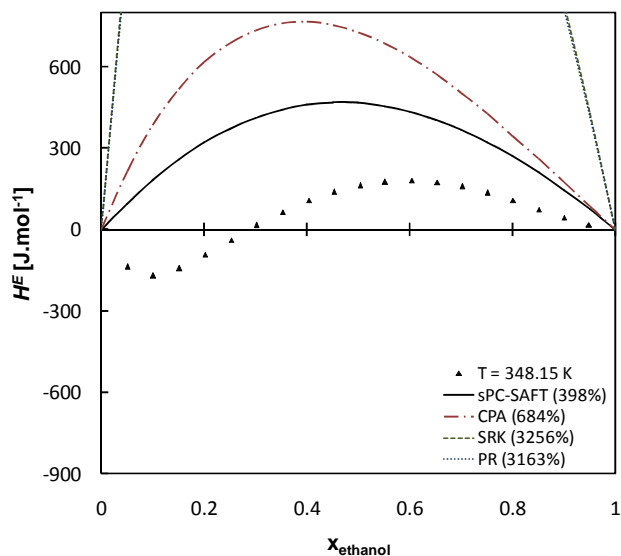


Figure 4-40: Excess enthalpy of the ethanol/water system at $T = 348.15 \text{ K}$ and $P = 15 \text{ MPa}$. Data from ref. (119).

In Figure 4-38, the increase in temperature (from 298.15 K to 348.15 K) causes the excess enthalpy to become positive in the ethanol-rich side and forms a maximum at $x_{\text{ethanol}} = 0.6$. The minimum in the water-rich side is still maintained. The remote change in model predictions of sPC-SAFT and CPA with temperature once again indicates that there are problems with the temperature dependency of the models.

In Figure 4-39 and Figure 4-40, the pressure increases from 0.4 MPa to 15 MPa. Neither the experimental data, nor the predictions of the models change noticeably with the increase in pressure.

Possible factors that could be responsible or at least contributing to the poor predictions of the association models include:

- Polar forces that are incorrectly accounted for.
- Hydrogen bonding networks that form between the water and ethanol molecules that are not accounted for i.e. co-operativity that is not accounted for. The fact that there are multiple inflection points possibly indicates that the networks reach maximums at certain concentrations (corresponding to stable mixtures e.g. in Figure 4-37 at $x_{\text{ethanol}} = 0.18$ and $x_{\text{ethanol}} = 0.8$. Therefore, it seems as if another minimum in the excess enthalpy wants to form here).
- Poor pure component parameters.
- The mixing rules used to account for cross-association are not adequate.

Comparing the mass density plots of the water/ethanol mixture in section 4.4.1 (Figure 4-31 to Figure 4-34), it is noted that complex phenomena manifests in both properties, but that the effects are more prominent in the excess enthalpy.

4.4.4 Speed of sound

i) ethanol/water

In Figure 4-41 the complex thermodynamic behaviour of the ethanol/water system is again observed by the maximum that manifests at $x_{\text{ethanol}} = 0.12$ in the speed of sound experimental data. It is believed that the hydrogen bonding network that forms between the molecules allows the mixture to pack more tightly than in the pure species. This causes the speed of sound to travel faster through the mixture at $x_{\text{ethanol}} = 0.12$.

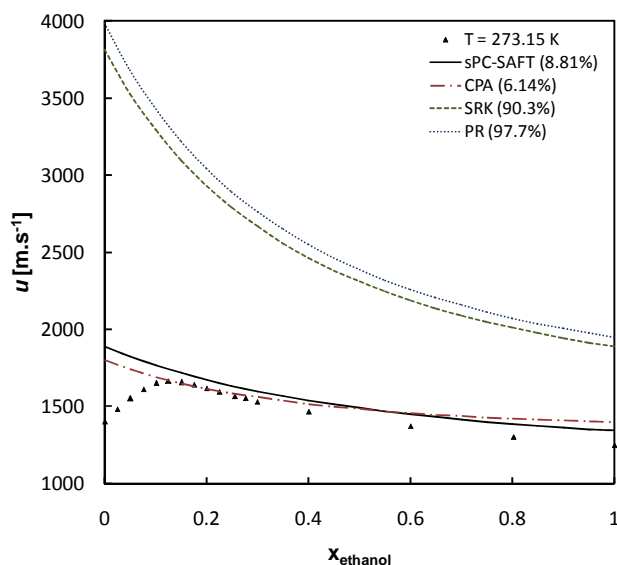


Figure 4-41: Speed of sound in the ethanol/water system at $T = 273.15\text{ K}$ and $P = 1\text{ atm}$. Data from ref. (116).

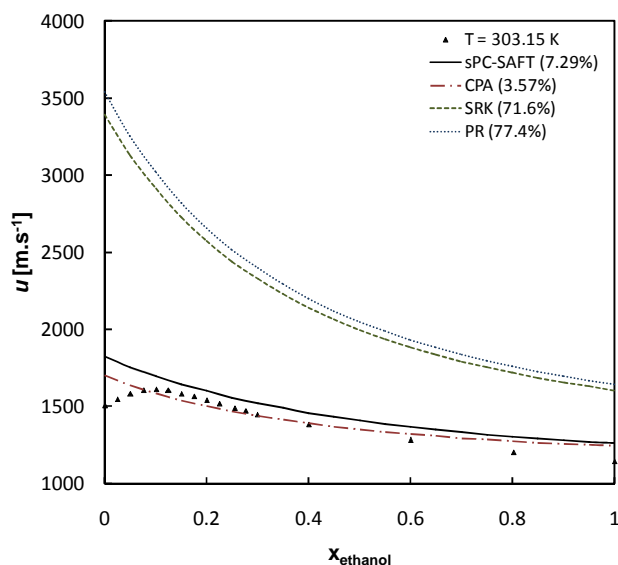


Figure 4-42: Speed of sound in the ethanol/water system at $T = 303.15\text{ K}$ and $P = 1\text{ atm}$. Data from ref. (116).

The maximum is less pronounced in the experimental data at higher temperature (Figure 4-42). This corresponds with the rest of the data for the mixture, where an increase in temperature weakens the influence of the hydrogen bonding network.

4.4.5 Excess isobaric heat capacity

i) methanol/water

In Figure 4-43, the excess isobaric heat capacity experimental data is positive and skewed towards the water-rich end. A maximum forms at approximately $x_{\text{methanol}} = 0.18$ and has a value of roughly $6\text{ J} \cdot (\text{mol} \cdot \text{K})^{-1}$. The positive values indicate that increased order is created in the mixture relative to the order of the pure species counterpart as a result of the mixing process (108). sPC-SAFT and CPA predicts positive values of the excess isobaric heat capacity, but the property is underestimated and the predictions are fairly symmetric. It is interesting to note that the predictions by SRK and Peng-Robinson are essentially zero. This implies that these models predict that there is no change in structure relative to the pure species and is in accordance with the formulation of the models where hydrogen bonding is not accounted for. Since CPA and SRK essentially only differ as a result of the association term, the positive contribution to the isobaric heat capacity in the prediction of CPA is attributed the presence of the association term. Therefore, the association term seems to under-predict the level of structure present in the methanol/water mixture. The shortcoming of the association term can be attributed to the simplifications made in its derivation that resulted in bond co-operativity to be unaccounted for. The finding is further justified by considering the excess isobaric heat capacity of the *n*-hexane/1-hexanol mixture (Figure 4-25). In this mixture, the association term was able to account for the order creation to an acceptable measure. However, it should be kept in mind that the *n*-hexane/1-hexanol mixture is considerably less complex than the methanol/water mixture.

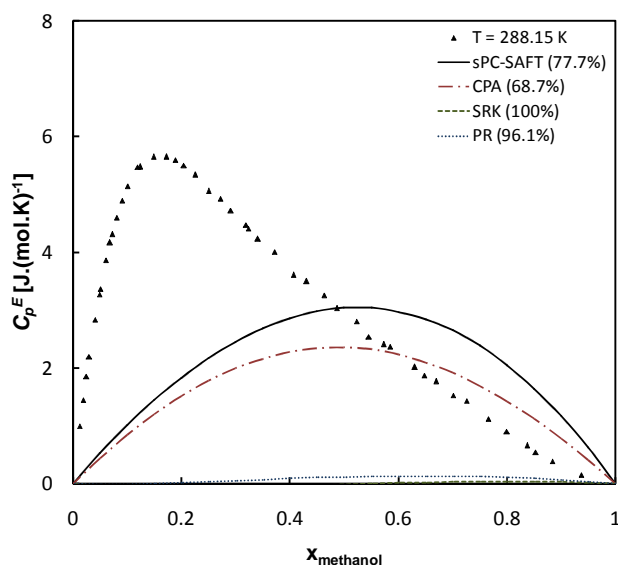


Figure 4-43: Excess isobaric heat capacity of the methanol/water system at $T = 288.15$ K and $P = 1$ atm. Data from ref. (120).

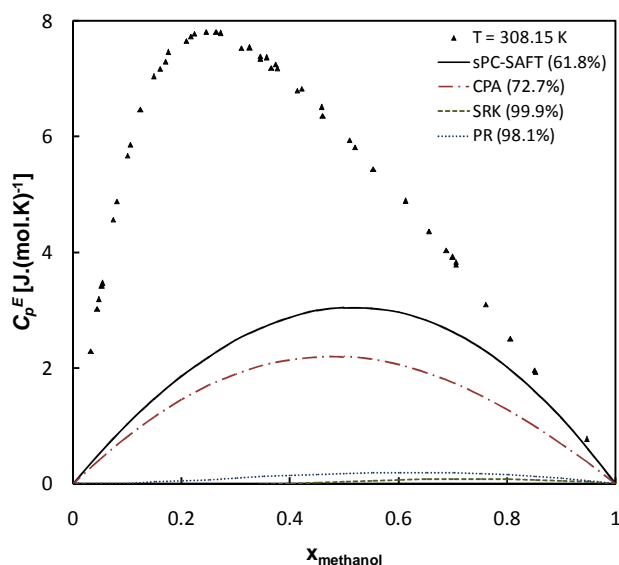


Figure 4-44: Excess isobaric heat capacity of the methanol/water system at $T = 308.15$ K and $P = 1$ atm. Data from ref. (120).

In Figure 4-44, the excess isobaric heat capacity increases with an increase in temperature, while the predictions of the association models remain more or less constant. The trend of the data also changes significantly. A probable explanation why the level of structure increases with an increase in temperature is unknown. It was expected that the level of structure would decrease, since the strength of the hydrogen bonds decreases with an increase in temperature.

Some controversy exists in the literature on whether methanol should be modelled as a molecule with two or three sites in the framework of SAFT. In the early stages of the SAFT approach, it was generally accepted that alcohols are best modelled with two sites. Von Solms *et al.* (121) investigated methanol/*n*-alkane binary mixtures and found that methanol was best represented with three sites ('two' negative and one 'positive'). This possibly indicates that in the presence of certain components, molecules such as methanol act as three-site molecules and, as a two-site molecule in the presence of other components. Problems like these again boil down to limitations in the association term.

ii) ethanol/water

In Figure 4-45, the excess isobaric heat capacity for the ethanol/water mixture is positive over the entire concentration range and forms a maximum at $x_{\text{ethanol}} = 0.18$. There seems to be another order creation contribution at $x_{\text{ethanol}} = 0.65$. Comparing the excess isobaric heat capacity of ethanol/water with the excess enthalpy plot in Figure 4-37 (note that the excess isobaric heat capacity is at 288.15 K and the excess enthalpy at 298.15 K), the most stable mixture occurs at the level of highest order creation and this gives further evidence that the peculiar behaviour of the water/ethanol mixture is largely dominated by hydrogen bonding that forms network-like structures. The property is, however, severely underestimated by the association models.

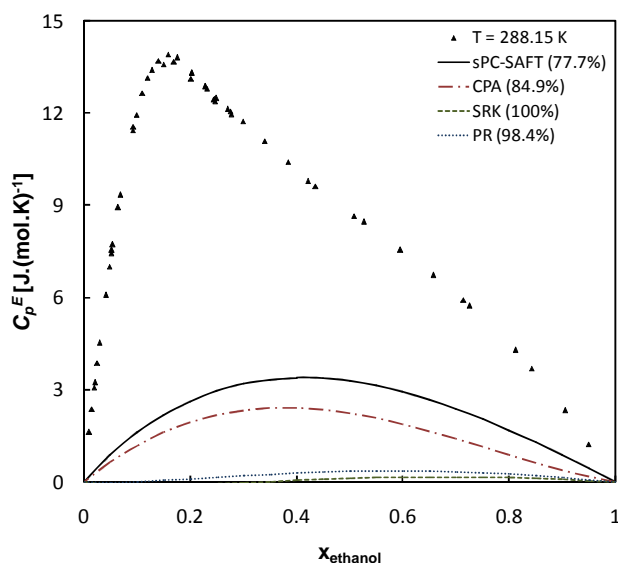


Figure 4-45: Excess isobaric heat capacity of the ethanol/water system at $T = 288.15$ K and $P = 1$ atm. Data from ref. (120).

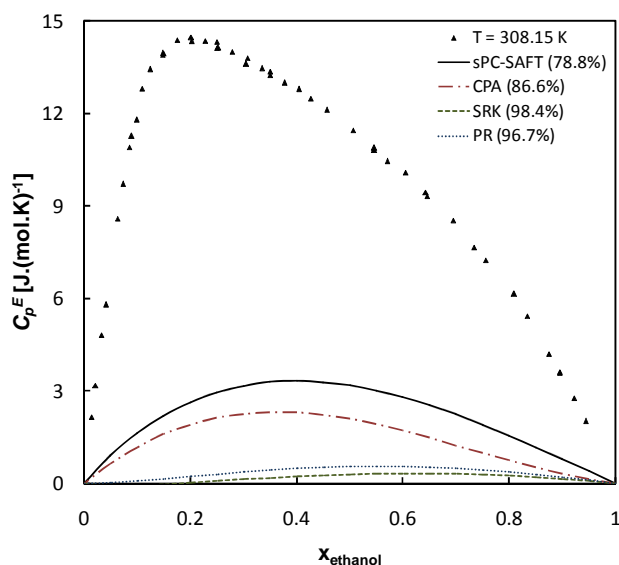


Figure 4-46: Excess isobaric heat capacity of the ethanol/water system at $T = 308.15$ K and $P = 1$ atm. Data from ref. (120).

In Figure 4-46, the magnitude of the maximum still remains more or less the same, but the trend exhibited by the experimental data changed somewhat. Similar to the methanol/water mixture, the prediction of the association models changes very little with increasing temperature.

Von Solms *et al.* (121) studied hydrogen bonding in selected mixtures of 1-alkanols and *n*-alkanes and found that hydrogen bond co-operativity did not have to be explicitly accounted for in those mixtures. The results from the non-polar/hydrogen bonding section (section 4.3) generally confirm this finding. However, the results from this section indicate that co-operativity needs to be accounted for in mixtures of hydrogen bonding/hydrogen bonding components, where the concentration of hydrogen bonding polar segments is high, i.e. in mixtures where polar hydrogen bonding segments are in close proximity to each other, and not diluted by non-polar segments.

4.4.6 Section highlights

The work in this section accentuated a few important points:

- Wertheim's association term is able to correlate the properties for some of the mixtures. Generally, mixtures with dilute hydrogen bonding segments are adequately represented.
- In mixtures where hydrogen bonding segments are in close proximity to each other (such as water/ethanol), hydrogen bond co-operativity seems to form and influence thermodynamic behaviour significantly. The association term of Wertheim does not account for these effects and consequently, poor representation of these mixtures are obtained with models such as sPC-SAFT and CPA.
- Other possible factors that should also be considered in these mixtures are a) cross-association, b) the influence of polar forces, c) steric hindrances in hydrogen bonding and d) the influence of mixture composition with respects to number of bonding-sites on molecules.

4.5 Chapter summary

In this chapter, several thermodynamic properties for binary mixtures were investigated with sPC-SAFT, CPA, Peng-Robinson and SRK. In general, the deviation from the experimental data is considerably higher compared to the deviation from pure component experimental data.

The following points are evident:

- sPC-SAFT seems to have the framework to correlate dispersive and repulsive interactions for most properties considered, but improvement to the theory is likely to be necessary if better predictions of mixture properties are required.
- Additional evidence is presented showing that the regression procedure of CPA results in a sacrifice of accuracy in strongly temperature-dependent properties to obtain an improved description of volumetric properties.
- Properties of mixtures that are dominated by the pressure-volume derivative are poorly predicted by CPA at high pressures, but are reasonably represented at low pressures.
- Wertheim's association term used in models such as CPA and sPC-SAFT, seems to adequately account for the influence of hydrogen bonding in mixture of **non-polar/hydrogen bonding** components where the hydrogen bonding segments are dilute and the influence hydrogen bonding network structures are small.
- Wertheim's association term seems to be able to correlate the properties for **hydrogen bonding/hydrogen bonding** mixtures where hydrogen bonding segments are dilute, as the influence of hydrogen bonding networks seems to be small.
- In mixtures where the concentration of hydrogen bonding segments is high (such as water/ethanol), hydrogen bond co-operativity seems to form and influences the thermodynamic behaviour significantly. The association term of Wertheim does not account for these effects and consequently, poor representations of these mixture properties are obtained with models such as sPC-SAFT and CPA.

From the literature review presented in Chapter 2 and the results and discussions presented in Chapter 3 and Chapter 4, it is now possible to identify possible areas within the framework of sPC-SAFT that could be improved.

Chapter 5

Improvement of sPC-SAFT

By examining several thermodynamic properties of selected pure components and binary systems in Chapter 3 and Chapter 4, it was shown how sPC-SAFT and CPA account for complex molecular interactions. Results for SRK and Peng-Robinson were also presented to illustrate how CPA and sPC-SAFT improve on the predictions of popular cubic EOS.

Based on the literature review presented in Chapter 2 and the findings from Chapter 3 and Chapter 4, specific weaknesses have been identified in sPC-SAFT:

5.1 Possible areas of improvement

5.1.1 Accounting for polar forces

sPC-SAFT and CPA treat strong polar forces via the *Van der Waals* approach and have difficulty in accurately describing most thermodynamic properties of polar components. The consequences of *Van der Waals* approach when predicting pure component properties are less severe than in binary mixtures properties, where significantly larger deviations from experimental data are observed.

This study showed that it is necessary to explicitly account for strong polar interactions in the framework of sPC-SAFT. Literature applications of sPC-SAFT mainly focussed on phase equilibrium calculations also suggested that the performance of sPC-SAFT may be greatly enhanced if a polar term could be included in the state function of sPC-SAFT.

5.1.2 Description of hydrogen bonding between water and alcohols

Wertheim's association term provides a reasonable description of hydrogen bonding in systems where the influence of hydrogen bonding networks is rather small. In mixtures, that contain a high concentration of hydrogen bonding segments (such as water/ethanol), hydrogen bond co-operativity seems to form, which severely influences thermodynamic behaviour. The Wertheim association term does not account for these molecular effects and, consequently, poor

representations of mixture properties are obtained with models such as sPC-SAFT and CPA. Related to this problem, is the choice of association scheme used to model these associating components. Currently, there is no comprehensive study available in the literature on sPC-SAFT that systematically investigates the influence of association schemes on thermodynamic properties. More work is required to improve the description of hydrogen bonding between water and alcohols.

5.1.3 Deficiency in temperature dependency of models

sPC-SAFT and CPA display an incorrect temperature dependency for several properties, especially properties that are strongly influenced by temperature. A parameter regression study with sPC-SAFT showed that the inclusion of second-order properties in the regression function did not lead to parameter sets that were able to describe first- and second-order properties simultaneously. Therefore, second-order properties such as the isochoric heat capacity, which is strongly influenced by temperature, cannot be predicted with good accuracy. The improvement of the temperature dependency of these models should therefore be considered.

5.1.4 Improvement of the reference term

One of the major advantages of sPC-SAFT compared to cubic-based models is the ability of sPC-SAFT to give a reasonably good description of the pressure-volume derivative at high pressures in the liquid phase. Models that use cubic equations to account for physical interactions, such as CPA, diverge rapidly from the experimental data as the pressure increases.

Several important thermodynamic properties such as the speed of sound are dependent on the pressure-volume derivative. This implies that cubic-based models, such as CPA, will only be able to give reasonable representations of these properties in the low pressure region and will be less accurate in the high pressure region.

The pressure-volume derivative is dependent on the second-order volume derivative of the state function. The relative contributions from each term are presented in Figure 5-1:

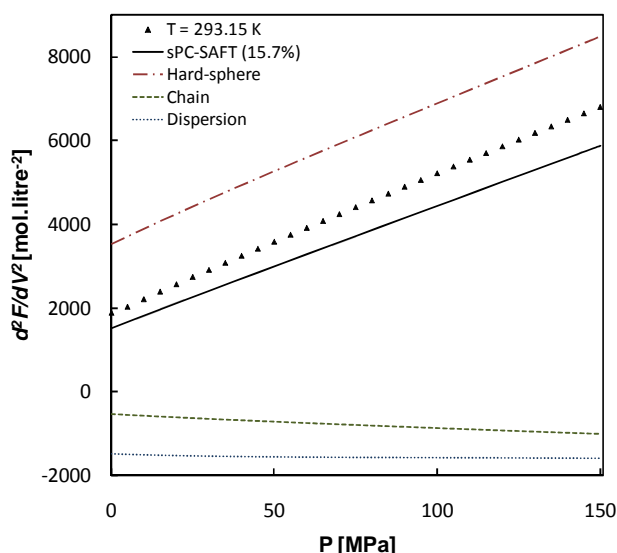


Figure 5-1: sPC-SAFT EOS decomposition of the second-order volume derivative of the state function of *n*-hexane at $T = 293.15$ K. Data calculated from ref. (92).

From Figure 5-1, the derivative is predominantly influenced by the hard-sphere term, but it seems as if the incorrect slope is possibly caused by the chain term. Since the contribution from the chain term is largely influenced by the radial distribution function, and the fact that the hard-sphere term is derived from the radial distribution function, improving the reference term will possibly improve the description of second-order derivative properties.

As briefly discussed in Appendix C.3, Lafitte *et al.* (56) developed SAFT-VR Mie and the main improvement in this version of SAFT is that the description of repulsive interactions are improved compared to other SAFT models, thus resulting in an improved description of second-order properties. They still used the hard-sphere reference term, but developed a new dispersion term and cavity function (used in chain term, instead of radial distribution function) that captures the distance dependency of repulsive forces more accurately. A recent molecular simulation study by Nezbeda (122) showed that structural properties are defined by short-range interactions (both repulsive and attractive e.g. hydrogen bonding), but that long range forces only play a marginal role and may be treated with perturbation. Therefore, it may be useful to develop a new reference term that describes repulsive interactions more accurately, instead of developing perturbation terms rectify the incorrect description of repulsive interactions by the hard-sphere term.

5.2 Scope of project

The major novel contributions from this research project are presented in Chapter 6 to 8, focussing on:

- Improving the description of hydrogen bonding between water and alcohols in the framework of sPC-SAFT.
- Improving the description of polar interactions in the framework of sPC-SAFT.

In Chapter 6, a new association scheme is developed for 1-alcohols that improve the phase equilibrium predictions between 1-alcohols and water in the framework of sPC-SAFT. In Chapter 7, sPC-SAFT is extended with two prominent polar terms that explicitly account for dipolar interactions. The new EOS are applied to the VLE and selected thermodynamic properties for polar (non-HB) mixtures. In Chapter 8, the performance of the new association scheme, developed in Chapter 6, is tested within the framework of the new models developed in Chapter 7. The main property investigated is VLE, the main reason being that only limited improvement could be obtained in the prediction of other thermodynamic properties with the new sPC-SAFT-based models as a result of the inherent shortcomings identified in Chapter 3 and Chapter 4.

Chapter 6

A new association scheme for alcohols

Accurate predictions of vapour-liquid-equilibria (VLE) for alcohol/water mixtures with equation of state (EOS) models remain a major challenge in thermodynamic modelling. Many SAFT-based models, such as sPC-SAFT (6; 31; 32; 51; 52), SAFT-VR (123; 124; 125), SAFT (26; 27; 126), sSAFT (126) and other PC-SAFT-variants (25; 35), to only mention a few, are still not able to accurately predict most of these types of phase equilibria without binary interaction parameters (BIPs). Mixtures of water with alcohols are commonly encountered on petrochemical plants, as well as in fermentation broths, and the alcohols usually have to be separated from the water and possibly from one another. These components cause large deviations from ideal behaviour in mixtures as a result of the presence of various intermolecular forces and molecular effects such as hydrogen bonding, polar forces and bond co-operativity. EOSs have to account for these molecular influences, in one way or another, in order to provide good phase equilibrium predictions.

Several approaches have been followed to improve model performance for alcohol/water systems with SAFT-type EOS, which include: a) adding additional terms to the state function such as polar terms (35; 54; 127), b) estimating pure component parameters by including several properties in the regression function (32; 33), c) using different association schemes (32; 33; 34; 121) and d) predicting phase specific binary interaction parameters (128). However, the success of these approaches seems to be rather limited.

Therefore, the objective of this chapter is to improve the performance of sPC-SAFT in predicting the VLE of 1-alcohol/water mixtures without relying on BIPs to obtain correct phase predictions. To achieve this, a new association, the 2C scheme, is defined for 1-alcohols and the performance of sPC-SAFT with the new association scheme is compared to the original 2B and 3B association schemes proposed by Huang and Radosz (26; 27). This new association scheme is also evaluated and compared by considering phase equilibria for other alcohol/alcohol and *n*-alkane/alcohol systems in order to gain a comprehensive understanding of the performance of the new scheme and identify areas of compromise. Furthermore, the performance of sPC-SAFT with the new association scheme is compared to CPA (8). Lastly, multi-component mixtures are modelled with sPC-SAFT using various association schemes.

6.1 Current status of sPC-SAFT in predicting phase equilibrium of alcohol/water systems

A brief review of the previous application with sPC-SAFT was presented in Chapter 2. As far could be ascertained, the most comprehensive evaluation of the performance of sPC-SAFT in predicting the phase equilibria of 1-alcohol/water systems was published by Grenner *et al.* (31). They modelled alcohols with the 2B association scheme and investigated the phase equilibria of C2 to C5 alcohols in water. Their results showed that the model is capable of predicting the VLE of alcohol/water systems, but requires at least one BIP per system.

Modelling systems with methanol is notoriously difficult. This is evident from the literature by considering the various parameters sets that have been published for methanol, as summarized by Kontogeorgis *et al.* (33) and Tybjerg *et al.* (32). Recently, Grenner *et al.* (51) modelled the water/methanol system with the original 2B parameters determined for PC-SAFT by Gross and Sadowski (25) and required a BIP to obtain good correlation of methanol/water VLE. Tybjerg *et al.* (32) also investigated the methanol/water system with the parameters they determined, but found that none of the PC-SAFT parameter sets showed good predictive performance. In all cases mentioned, the BIPs for these alcohol water systems were reported to be negative, indicating that cross-association is most probably underestimated with the 2B scheme (129). Haslam *et al.* (128) proved from fundamental principles that negative BIPs may also occur when polar interactions are treated with the *Van der Waals* approach i.e. when they are not explicitly treated with a contribution to the state function, but accounted for with the other terms in the state function. In sPC-SAFT, the influence of polar interactions in alcohol/water systems may largely be accounted for with the association term provided that an adequate association scheme is used.

From these discussions, it is clear that there are still shortcomings in the VLE predictions of alcohol/water systems with sPC-SAFT that need to be addressed. Simpler EOS such as CPA, have the ability to describe these systems fairly well without BIPs (60; 37; 61; 66; 76), although system-specific combining rules are required to obtain the best results. It is argued that a physically more realistic EOS, such as sPC-SAFT, should be able to at least provide a predictive performance of the same accuracy or better. The major source of error in the alcohol/water VLE predictions of sPC-SAFT most probably originates from the under-estimation of cross-association, as indicated by the negative BIPs when the 2B scheme is used. Therefore, a more appropriate associative scheme is proposed in this chapter to improve the description of the cross-association between alcohols and water.

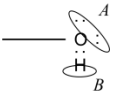
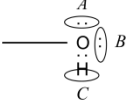
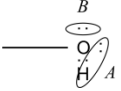
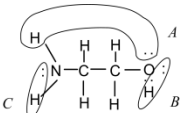
6.2 Development of a new association scheme

Before associating components can be modelled within the SAFT approach, a suitable association scheme has to be assigned to the component under consideration e.g. 2B or 3B for alcohols. One approach in selecting an association scheme is to consider results from molecular simulation studies. Clark *et al.* (34) followed such an approach to determine the most appropriate association scheme for water within the SAFT methodology. As explained by Clark *et al.* (34), the 3B scheme is a counterpart of the TIP4P-type (130) models and the 4C scheme corresponds with the TIP5P (131) model when water is considered. They tested the 2B, 3B and 4C association schemes within the SAFT-VR (123; 124) framework and found the 4C scheme to be most suited for capturing several thermodynamic properties for water. Consequently, water is modelled as a 4C component in this chapter.

In several recent simulation studies (132-138), alcohols have been modelled with OPLS potential functions developed by Jorgensen (138). By simulating small alcohols in pure species with these potential functions, he showed in his original study that between 70% and 80% of the molecules have two hydrogen bonds (chain formation) and 3% to 8% form three hydrogen bonds (branching of chains). Within the framework of SAFT, this indicates that the majority of alcohol molecules show behaviour that may best be described by the 2B scheme and a minority show behaviour that corresponds to the 3B scheme. Therefore, an association scheme exhibiting behaviour representative of both 2B and 3B schemes simultaneously might prove to be beneficial.

As will be shown in Section 6.4, when alcohols are modelled with sPC-SAFT, neither the 2B nor 3B schemes provide satisfactory predictions (with $k_{ij} = 0$) for the VLE of alcohol/water systems. The 2B scheme underestimates cross-association, while the 3B scheme overestimates cross-association. This indicates that, in the framework of sPC-SAFT, an intermediate association scheme is required. To address this shortcoming, it was decided to group a donor and acceptor site together i.e. a bipolar site and add another negative electron donor site to account for the remaining lone pair, as indicated in Table 6-1. This new association scheme for 1-alcohols is denoted 2C.

Table 6-1: Selected association schemes within SAFT. Table adapted from Kontogeorgis et al.23

Species	Formula	Scheme	Equivalent scheme	Site Fractions
alcohols		2B	1 electron donor sites, 1 electron acceptor sites	$X^A = X^B$ $X_1 = X^A X^B$
alcohols		3B	2 electron donor sites, 1 electron acceptor sites	$X^A = X^B; X^C = 2X^A - 1$ $X_1 = X^A X^B X^C$
alcohols (new scheme)		2C	2 electron donor sites, 1 bipolar site	$X^B = \sqrt{X^A}$ $X_1 = X^A X^B$
MEA		3A	3 bipolar sites	$X^A = X^B = X^C$ $X_1 = X^A X^B X^C$

Thus, alcohols are modelled with two association sites, but retain a character similar to the 3B scheme. When using the 2B scheme, the fraction of non-bonded donor and acceptor sites on the alcohol are always equal. This is not entirely physically correct, because there are two lone pairs of electrons that participate in hydrogen bonding i.e. two electron donor sites. In the 3B scheme, there are twice as many donor sites than electron acceptor sites, which is theoretically more correct. The 2C scheme retains this theoretically more correct behaviour to a certain degree, since there will also always be more non-bonded negative donor sites than bipolar sites, according to the following relationship:

$$X^B = \sqrt{X^A} \quad (6-1)$$

As with the other association schemes, the site fraction for the bipolar site can also be analytically calculated, although the expression is more complex compared to other schemes:

$$X^A = \frac{1}{6} \left(-\frac{4}{\Delta\rho} + \frac{2 \cdot 2^{1/3}}{\left(2\Delta^3\rho^3 + 27\Delta^4\rho^4 + 3\sqrt{3}\sqrt{\Delta^7\rho^7(4 + 27\Delta\rho)} \right)^{1/3}} + \frac{2^{2/3} \left(2\Delta^3\rho^3 + 27\Delta^4\rho^4 + 3\sqrt{3}\sqrt{\Delta^7\rho^7(4 + 27\Delta\rho)} \right)^{1/3}}{\Delta^2\rho^2} \right) \quad (6-2)$$

To further support our methodology of grouping an acceptor and donor site together, modelling of MEA (monoethanolamine) for which Kontogeorgis and Folas (129) recommend the 4C scheme, is used as an example. MEA possesses hydroxyl and amine functional groups, which make the VLE description of the MEA and water system difficult to model. Following the above-mentioned

grouping approach, it results in the 3A scheme for MEA, as indicated in Table 6-1. Comparative results shown in Figure 6-1 indicate that improved predictions are indeed obtained for MEA with the 3A scheme when compared to the 2B and 4C schemes.

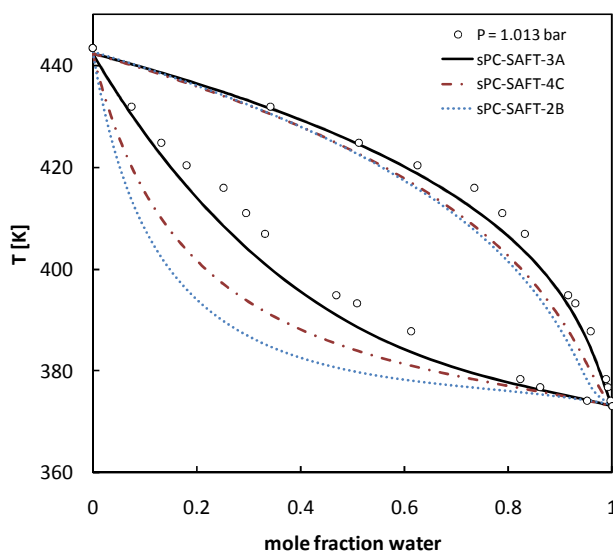


Figure 6-1: VLE predictions of the MEA/water system. MEA is modeled with the 3A, 4C and 2B association schemes and water with the 4C association scheme. Experimental data taken from ref. (139).

The newly defined 2C association scheme changes the association dynamics of the alcohol/water system and can be explained by considering which possible hydrogen bonds will form between the different sites on the molecules, as depicted in Table 6-2. The shaded sections indicate which hydrogen bonds form between the water and alcohol molecules i.e. cross-association. From Table 6-2, it is observed that the 2C scheme provides cross-associative behaviour similar to the 3B scheme, but only from two association sites (consider the similarities between the shaded sections of the 2C and 3B configurations).

Table 6-2: Difference between the association dynamics of alcohol-water systems when alcohols are modelled with the 2C, 2B and 3B association schemes. A±,+- = alcohol association sites, W+,- = water association sites, Y = Yes, hydrogen bond will form and N = No, hydrogen bond will not form. The matrix indicates which hydrogen bonds will take place between respective sites. The shaded sections indicate the cross-association hydrogen bonds that form between alcohol and water molecules for each scheme configuration.

2C-4C association configuration							2B-4C association configuration						
Site	A [±]	A ⁻	W ⁺	W ⁺	W ⁻	W ⁻	Site	A [±]	A ⁻	W ⁺	W ⁺	W ⁻	W ⁻
A [±]	Y	Y	Y	Y	Y	Y	A [±]	N	Y	N	N	Y	Y
A ⁻	Y	N	Y	Y	N	N	A ⁻	Y	N	Y	Y	N	N
W ⁺	Y	Y	N	N	Y	Y	W ⁺	N	Y	N	N	Y	Y
W ⁺	Y	Y	N	N	Y	Y	W ⁺	N	Y	N	N	Y	Y
W ⁻	Y	N	Y	Y	N	N	W ⁻	Y	N	Y	Y	N	N
W ⁻	Y	N	Y	Y	N	N	W ⁻	Y	N	Y	Y	N	N

3B-4C association configuration							
Site	A [±]	A ⁻	A ⁻	W ⁺	W ⁺	W ⁻	W ⁻
A [±]	N	Y	Y	N	N	Y	Y
A ⁻	Y	N	N	Y	Y	N	N
A ⁻	Y	N	N	Y	Y	N	N
W ⁺	N	Y	Y	N	N	Y	Y
W ⁺	N	Y	Y	N	N	Y	Y
W ⁻	Y	N	N	Y	Y	N	N
W ⁻	Y	N	N	Y	Y	N	N

The level of association is effectively increased with the 2C scheme when compared to the 2B scheme, but is not as strong as the level of association with the 3B scheme. The 2C scheme captures the behaviour of 1-alcohols in mixture with water more accurately than the 2B and 3B schemes, as shown in Section 6.4.

6.3 Model parameters

The parameters used in this chapter are presented in Table 6-3 and Table 6-4 for sPC-SAFT and CPA respectively. sPC-SAFT parameters based on the 2C scheme were determined by including saturated vapour pressure, liquid density and heat of vapourisation data in the regression function according to equation (6-3) and parameters based on the 2B scheme were obtained from the literature. sPC-SAFT-3B parameters that could not be found in the literature was also determined with equation (6-3). The %AAD values of the properties used in equation (6-3) are also given in Table 6-3 and Table 6-4.

$$OF = \alpha \sum_{i=1}^{NP} \left(\frac{P_i^{sat,cal} - P_i^{sat,exp}}{P_i^{sat,exp}} \right)^2 + \beta \sum_{i=1}^{NP} \left(\frac{\rho_i^{sat,cal} - \rho_i^{sat,exp}}{\rho_i^{sat,exp}} \right)^2 + \gamma \sum_{i=1}^{NP} \left(\frac{h_i^{vap,calc} - h_i^{vap,exp}}{h_i^{vap,exp}} \right)^2 \quad (6-3)$$

The DIPPR correlations (95) were used to generate the data included in the regression function. Thirty points were generated for each property in the range $0.5 < T_r < 0.9$. In addition to saturated vapour pressure and liquid density data, heat of vapourisation data were included in the regression routine, because the property is sensitive to association effects (32; 140) as discussed in Chapter 2. In equation (6-3), α , β and γ are regression weights and were usually set equal to 4, 2 and 1 respectively. Several sets of regression weights were tested and it was found that the mentioned configuration usually provides good parameters. The main reason for assigning higher regression weights to the saturated vapour pressure and liquid density is, in the event that the model parameters are unable to correlate all three properties simultaneously, an error in heat of vapourisation, followed by an error in saturated liquid density and lastly, an error in saturated vapour pressure is preferred.

With respects to CPA, results based on both 2B and 3B parameters are presented for comparative purposes. Usually, alcohols are modelled with the 2B scheme but, as discussed by Kontogeorgis *et al.* (61), the 3B scheme provides better VLE predictions of alcohol/water systems and is therefore also included in this study. Results for CPA based on the 2C scheme were also investigated. Unfortunately, only improved results for the methanol/water system were obtained.

Table 6-3: sPC-SAFT pure component parameters used in this chapter

Component	M_w [g/mol]	m	σ [Å]	ε/k [K]	ε^{AB}/k [K]	κ^{AB}	ΔP^{sat} [%] ^a	$\Delta \rho^{sat}$ [%] ^a	Δh^{vap} [%] ^a	Sch.	Ref.
<i>n</i> -butane	58.12	2.3316	3.7086	222.88	-	-	0.57	0.44	1.25	-	(24)
<i>n</i> -pentane	72.14	2.6896	3.7729	231.20	-	-	0.25	1.30	1.60	-	(24)
<i>n</i> -hexane	86.10	3.0576	3.7983	236.77	-	-	0.64	0.62	1.99	-	(24)
<i>n</i> -heptane	100.2	3.4831	3.8049	238.40	-	-	0.26	0.87	1.41	-	(24)
<i>n</i> -octane	114.2	3.8176	3.8373	242.78	-	-	0.43	0.76	1.00	-	(24)
<i>n</i> -nonane	170.3	5.3060	3.8959	249.21	-	-	0.53	0.59	0.86	-	(24)
water	18.02	1.5000	2.6273	180.30	1804.22	0.18000	0.78	2.96	4.17	4C	(36)
MEA	61.08	2.3981	3.3722	320.03	1743.41	0.03051	0.72	0.80	4.21	4C	This work
MEA	61.08	2.3033	3.4075	333.48	2122.99	0.01166	0.59	0.81	3.98	3A	This work
MEA	61.08	2.2602	3.4148	349.14	2780.37	0.01137	0.47	0.73	3.47	2B	This work
methanol	32.04	2.8770	2.5763	164.91	2304.11	0.36080	0.95	1.20	1.90	2B	(32)
ethanol	46.07	1.2309	4.1057	316.91	2811.02	0.00633	1.15	2.30	1.20	2B	(31)
1-propanol	60.09	1.7996	3.9044	292.11	2811.02	0.00633	0.70	1.30	1.48	2B	(31)
1-butanol	74.12	2.9832	3.7852	276.90	2811.02	0.00633	2.44	0.92	2.20	2B	(31)
1-pentanol	88.14	2.6048	3.9001	282.31	2811.02	0.00633	3.10	0.33	1.45	2B	(31)
1-octanol	130.2	3.8470	3.8872	373.92	2811.02	0.00633	4.22	0.36	1.48	2B	(31)
methanol	32.04	2.4573	2.8050	198.80	2009.10	0.08880	0.99	1.80	5.86	3B	(33)
ethanol	46.07	3.6829	2.7310	180.17	1831.14	0.14580	0.10	0.06	0.71	3B	This work
1-propanol	60.09	3.3294	3.1243	220.03	1891.02	0.03880	0.20	0.24	1.29	3B	This work
1-butanol	74.12	3.2765	3.3876	242.37	2084.03	0.01506	0.18	0.21	1.19	3B	This work
1-pentanol	88.14	3.3261	3.5707	255.03	2094.72	0.01392	0.10	0.16	0.83	3B	This work
1-octanol	130.2	3.4955	4.0332	283.03	2671.59	0.00430	0.22	0.42	0.84	3B	This work

Component	M_w [g/mol]	m	σ [Å]	ε/k [K]	ε^{AB}/k [K]	κ^{AB}	ΔP^{sat} [%] ^a	$\Delta \rho^{sat}$ [%] ^a	Δh^{vap} [%] ^a	Sch.	Ref.
methanol	32.04	2.1000	2.7998	197.23	2535.00	0.82300	0.52	0.37	0.50	2C	This work
ethanol	46.07	2.3609	3.1895	207.56	2695.69	0.03270	0.18	0.21	3.32	2C	This work
1-propanol	60.09	2.9537	3.2473	226.36	2448.02	0.02280	0.27	0.25	1.17	2C	This work
1-butanol	74.12	2.9614	3.5065	253.29	2601.00	0.00740	0.19	0.33	1.23	2C	This work
1-pentanol	88.14	3.1488	3.6350	261.96	2555.34	0.00750	0.09	0.10	0.83	2C	This work
1-hexanol	102.1	3.1542	3.8188	277.24	2946.10	0.00250	0.09	0.42	0.85	2C	This work
1-heptanol	116.2	3.5340	3.8750	273.90	3134.88	0.00160	0.34	1.13	0.61	2C	This work
1-octanol	130.2	3.4634	4.0391	285.52	3165.66	0.00210	0.20	0.52	0.79	2C	This work
1-nonanol	144.2	3.4386	4.1846	299.43	3456.50	0.00110	0.10	0.16	0.60	2C	This work
1-decanol	158.2	3.7185	4.2237	296.22	3348.48	0.00180	0.13	0.25	0.52	2C	This work

^aThe %Absolute Average Deviation (%AAD) of the properties (saturated vapour pressure (P^{sat}), saturated liquid density (ρ^{sat}), heat of vapourisation (h^{vap}). ^a %AAD = $\sum_i^{np} |X_i^{calc} - X_i^{exp}| / |X_i^{exp}|$ where $X_i = P^{sat}, \rho^{sat}$ and h^{vap} .

Table 6-4: CPA pure component parameters used in this Chapter

Component	T_c [K]	$a_\theta/(Rb)$ [K]	c_1	b [L/mol]	ε^{AB}/R [K]	$\beta^{AB} \cdot 10^3$	ΔP^{sat} [%] ^a	$\Delta \rho^{sat}$ [%] ^a	Δh^{vap} [%] ^a	Sch.	Ref.
<i>n</i> -butane	425.1	2193.08	0.70771	0.07208	-	-	0.55	4.04	2.03	-	(91)
<i>n</i> -pentane	469.7	2405.10	0.79585	0.09100	-	-	0.41	0.89	2.55	-	(91)
<i>n</i> -hexane	507.6	2640.03	0.83130	0.10789	-	-	0.91	0.62	2.72	-	(91)
<i>n</i> -heptane	540.2	2799.76	0.91370	0.12535	-	-	0.97	0.51	2.34	-	(91)
<i>n</i> -octane	568.7	2944.91	0.99415	0.14244	-	-	0.64	0.61	2.20	-	(91)
<i>n</i> -nonane	658.0	3471.04	1.19531	0.21624	-	-	0.50	0.71	2.02	-	(91)
water	647.2	1017.34	0.67359	0.01451	2003.25	69.2	0.89	1.34	1.73	4C	(91)
methanol	512.6	1540.08	0.9249	0.03205	2315.20	57.8	1.56	0.70	2.16	2B	(32)
ethanol	513.9	2123.82	0.73690	0.04911	2589.85	8.00	1.8	0.43	1.60	2B	(91)
1-propanol	536.7	2234.52	0.91709	0.06411	2525.86	8.10	1.06	0.58	0.87	2B	(91)
1-butanol	563.0	2368.59	0.97840	0.07970	2525.86	8.20	2.27	1.29	2.82	2B	(91)
1-pentanol	469.7	2808.75	0.93580	0.09745	2525.86	3.60	0.61	0.63	1.48	2B	(91)
methanol	512.6	1652.74	1.0068	0.0334	1932.76	34.4	0.59	0.63	3.36	3B	(37)
ethanol	513.9	2062.79	1.0564	0.0500	1804.08	17.3	1.50	0.52	1.15	3B	(37)
1-propanol	536.7	2342.63	0.9857	0.0655	2062.55	6.30	0.55	0.62	1.23	3B	(37)
1-butanol	563.0	2536.50	0.8681	0.0814	2428.42	2.90	1.31	0.92	2.16	3B	(37)
1-pentanol	469.7	2792.14	0.9807	0.0979	2166.34	3.40	1.16	0.64	1.75	3B	(37)

^aThe %Absolute Average Deviation (%AAD) of the properties (saturated vapour pressure (P^{sat}), saturated liquid density (ρ^{sat}), heat of vapourisation (h^{vap}). ^a %AAD = $\sum_i^{np} |X_i^{calc} - X_i^{exp}| / |X_i^{exp}|$ where $X_i = P^{sat}, \rho^{sat}$ and h^{vap} .

Generally, sPC-SAFT parameters based on the 2B, 2C and 3B schemes provide similar correlations for the pure component properties, as seen from Table 6-3. Common trends that are general to PC-SAFT parameters for a homologous series are observed for the alcohol parameters based on the 2C scheme: the segment number (m), segment diameter (σ) and dispersion energy parameter (ε/k) generally increase with molecular size. This is consistent with the parameter sets presented by Grenner *et al.* (31) and Gross and Sadowski (25). The m , σ and ε/k parameter values based on

the 2C scheme usually lie between the values of the 2B and 3B schemes. Therefore, the physical meaning of the parameter values is still retained to an acceptable degree. The association energy values based on the 2C scheme also increases with molecular size and are in fair agreement with the spectroscopy data cited by Kontogeorgis *et al.* (33), although the values for the larger alcohols appear to be rather large. Nath and Bender (141) reported an enthalpy of association value equal to 2630 K for methanol. The association energy parameter value based on the 2C scheme (2535 K) corresponds the best with this value when compared to the parameter values obtained with both the 2B (2304 K) and 3B (2009 K) schemes.

The 2B parameters for methanol, for both sPC-SAFT and CPA, were obtained from the recent study published by Tybjerg *et al.* (32). These parameters have been fitted by them to saturated vapour pressure, liquid density, heat of vapourisation and compressibility factor data and provided improved VLE results for some methanol/alkane systems compared to other 2B parameters in the literature (32). The methanol sPC-SAFT-3B parameters have been determined by Kontogeorgis *et al.* (33) by fitting saturated vapour pressure, liquid density and monomer fraction data. The remaining alcohol parameters obtained from the literature had previously been determined by only including saturated vapour pressure and liquid density data in the regression function (sPC-SAFT-2B parameters (31), CPA-2B parameters (91) and CPA-3B parameters (37)).

In this chapter, the mixing rules employed in the association term of sPC-SAFT are the normal CR1 mixing rules (refer to section 2.1.2) and in CPA, the CR1 or ECR (refer to section 2.2.2) combining rule is employed, depending on which mixing rule provides the best result for the system under investigation.

The results are presented in the following sub-sections. The objective is to evaluate the phase equilibria performance of sPC-SAFT coupled with the new 2C association scheme and compare the results with the 2B and 3B association schemes, specifically for alcohol/water systems. Comparisons are also made to CPA, which has proven to be capable of describing most systems under investigation. However, relevant predictions for CPA are only shown in graphically.

Furthermore, the phase equilibria of alcohol/alcohol, alcohol/*n*-alkane and multi-component mixtures are also investigated in order to establish the advantages and disadvantages of the 2C scheme under a variety of conditions.

6.4 VLE and VLLE of alcohol/water mixtures

The phase equilibria of the first five primary alcohols are considered with results for methanol, ethanol and 1-propanol at several temperatures and pressures summarized in Table 6-5. The 2C scheme performs better than both the 2B and 3B schemes with sPC-SAFT in all systems considered. The predictive capability of sPC-SAFT-2C is generally as good as, or better than, the best predictions with CPA for the systems presented here.

Table 6-5: VLE results for alcohol/water systems for sPC-SAFT

Mixture	<i>T</i> or <i>P</i>	Prediction				Correlation			<i>np</i>	ref.
		<i>k_{ij}</i>	Δy (x10 ²) ^a	$\frac{\Delta P(\%)^b}{\Delta T(K)^a}$		<i>k_{ij}</i>	Δy (x10 ²) ^a	$\frac{\Delta P(\%)^b}{\Delta T(K)^a}$		
sPC-SAFT-2C										
methanol/water	318.15 K	0	0.93	2.95		-0.002	0.83	2.44	11	(142)
	323.15 K	0	1.37	3.03		-0.002	1.35	2.54	14	(143)
	333.15 K	0	0.60	2.48		-0.002	0.60	1.93	18	(143)
	1.013 bar	0	0.69	0.21		-0.002	0.75	0.25	21	(144)
	5.066 bar	0	0.83	1.44		-0.002	0.92	1.56	22	(145)
ethanol/water	323.15 K	0	1.33	3.17		-0.001	0.73	0.90	14	(143)
	333.15 K	0	0.99	0.37		-0.001	1.03	0.33	36	(143)
	0.333 bar	0	1.92	0.57		-0.001	1.86	0.49	28	(146)
	1.013 bar	0	0.69	0.45		-0.001	0.75	0.49	13	(50)
	6.669 bar	0	0.91	0.53		-0.001	1.00	0.46	19	(147)
1-propanol/water	333.15 K	0	1.66	1.57		0.007	1.49	1.03	23	(148)
	0.30 bar	0	2.80	0.72		0.007	2.03	0.26	26	(149)
	1.00 bar	0	1.82	1.00		0.007	1.18	0.48	28	(149)
Average			1.27	1.42			1.12	1.01		
sPC-SAFT-2B										
methanol/water	318.15 K	0	4.26	18.0		-0.050	0.75	1.20	11	(142)
	323.15 K	0	2.42	16.5		-0.050	0.61	2.59	14	(143)
	333.15 K	0	3.37	17.4		-0.050	0.48	1.83	18	(143)
	1.013 bar	0	3.15	2.80		-0.050	0.86	0.51	21	(144)
	5.066 bar	0	4.43	2.51		-0.05	1.25	1.27	22	(145)
ethanol/water	323.15 K	0	3.52	10.3		-0.037	0.65	0.77	14	(143)
	333.15 K	0	3.60	9.30		-0.037	0.82	0.57	36	(143)
	0.333 bar	0	7.42	4.07		-0.037	1.45	0.44	28	(146)
	1.013 bar	0	5.47	3.50		-0.037	0.52	0.35	13	(50)
	6.669 bar	0	6.47	5.94		-0.037	1.33	2.09	19	(147)
1-propanol/water	333.15 K	0	VLLE	VLLE		-0.018	1.17	0.78	23	(148)
	0.30 bar	0	VLLE	VLLE		-0.018	2.13	0.40	26	(149)
	1.00 bar	0	VLLE	VLLE		-0.018	1.01	0.36	28	(149)
Average			4.41	9.03			1.00	1.01		
sPC-SAFT-3B										
methanol/water	318.15 K	0	4.51	11.7		0.052	1.42	2.55	11	(142)
	323.15 K	0	2.78	10.9		0.052	1.99	0.94	14	(143)
	333.15 K	0	3.62	11.2		0.052	0.99	1.88	18	(143)
	1.013 bar	0	3.23	2.48		0.052	0.84	0.32	21	(144)
	5.066 bar	0	2.50	3.10		0.052	1.84	0.24	22	(145)
ethanol/water	323.15 K	0	3.71	7.94		0.035	1.43	0.95	14	(143)
	333.15 K	0	3.53	7.43		0.035	1.45	0.99	36	(143)
	0.333 bar	0	6.33	2.56		0.035	3.34	0.93	28	(146)
	1.013 bar	0	4.20	2.43		0.035	1.63	0.81	13	(50)
	6.669 bar	0	2.95	1.26		0.035	1.93	2.29	19	(147)
1-propanol/water	333.15 K	0	3.84	7.58		0.026	1.49	0.76	23	(148)

Mixture	T or P	Prediction			Correlation			np	ref.
		k_{ij}	$\Delta y (\times 10^2)^a$	$\frac{\Delta P(\%)^b}{\Delta T(K)^a}$	k_{ij}	$\Delta y (\times 10^2)^a$	$\frac{\Delta P(\%)^b}{\Delta T(K)^a}$		
	0.30 bar	0	5.97	2.13	0.026	1.96	0.35	26	(149)
	1.00 bar	0	4.14	2.15	0.026	0.69	0.28	28	(149)
Average			3.94	5.60		1.62	1.02		

^a $\Delta z = \sum_i^{np} |z_i^{calc} - z_i^{exp}|$ where z represents y or T and np is the number of data points. ^b Deviations as %AAD.

The VLE model predictions ($k_{ij} = 0$) of the methanol/water system are shown in Figure 6-2 and the corresponding correlation (k_{ij} fitted to the VLE data) in Figure 6-3. sPC-SAFT does not require a BIP to accurately predict the VLE of the methanol/water system with the 2C scheme, while both sPC-SAFT and CPA do require relatively large BIPs with both the 2B and 3B schemes to provide accurate correlation of the experimental data. Clark *et al.* (34) managed to predict the VLE of the methanol/water system with similar accuracy as sPC-SAFT-2C using SAFT VR without a BIP. Fu and Sadler(126) also investigated this system with sSAFT and SAFT, but required relatively large BIPs with both models to represent the system.

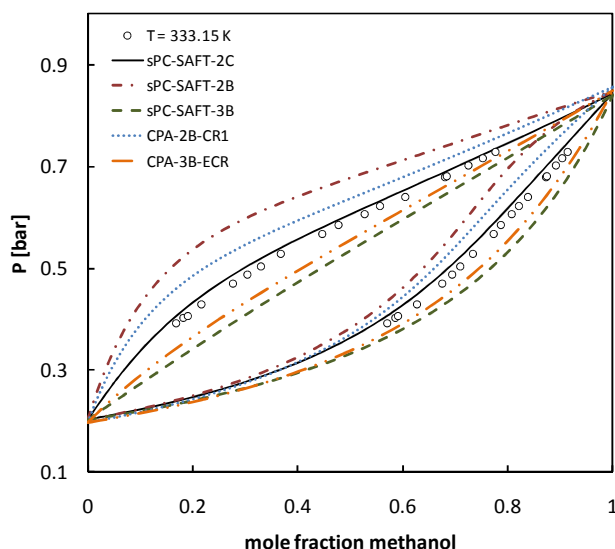


Figure 6-2: VLE predictions of the methanol/water system with sPC-SAFT and CPA using various association schemes. Experimental data taken from ref. (143).

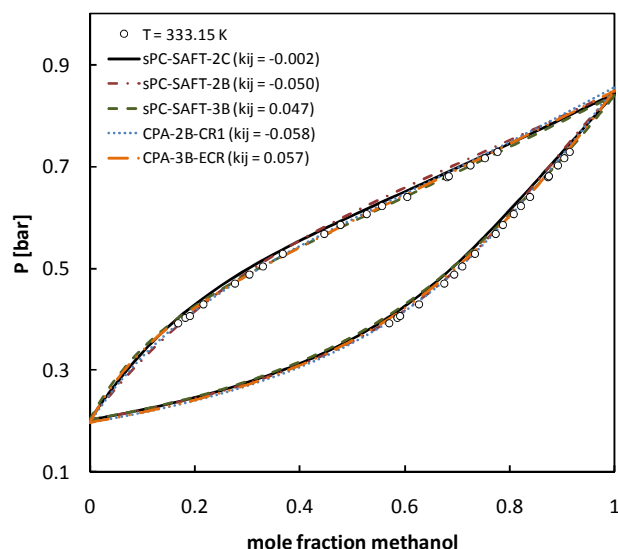


Figure 6-3: VLE correlations of the methanol/water system with sPC-SAFT and CPA using various association schemes. Experimental data taken from ref. (143).

From Figure 6-2, both model predictions of sPC-SAFT and CPA based on the 2B scheme are similar and both model predictions based on the 3B scheme are similar. The BIPs in Figure 6-3 indicate that the cross-association for this particular system is underestimated with the 2B scheme and that the cross-association with the 3B scheme is overestimated. The prediction of sPC SAFT-2C is the only prediction that correctly captures the influence of the interactions on the VLE between the two components.

It is not posed that the actual bonding on molecular level occurs as described by the 2C scheme. From the discussion presented by Guo *et al.* (150) and Dixit *et al.* (151), it is evident that various molecular effects, such as complex ring-like structures and microscopic demixing seem to be present in the mixture. The SAFT association term does not account for these molecular effects. A

solution to the problem is to use an association scheme that can best capture the influences of various molecular interactions present in the system. It is here where the 2C scheme is superior to the 2B and 3B association schemes for alcohol/water systems in the framework of sPC-SAFT.

Very good results are also obtained for the ethanol/water system using sPC-SAFT with the 2C scheme. The phase diagram is accurately predicted, as indicated in Figure 6-4. Similar trends are observed with sPC-SAFT-2B and sPC-SAFT-3B compared to the methanol/water system: the 2B scheme underestimates cross-association and the 3B scheme overestimates cross-association, as indicated by the respective BIPs in Figure 6-5. CPA with the 3B scheme and ECR rule also provides a very good prediction of the ethanol/water VLE, but CPA with the 2B scheme and the CR1 combining rules underestimates cross-association. The ECR combining rule was also tested with sPC-SAFT and it was found that both combining rules provide similar results and in most systems, there is little or no noticeable difference. The performance of CPA, on the other hand, is profoundly affected by the choice of combining rule (60). Recently, Paraghad *et al.* (125) studied the ethanol/water system with a SAFT-VR-Sutherland model and required a BIP of -0.091 to obtain a representative description of the system. The %AAD value in pressure was still rather large (8.74%).

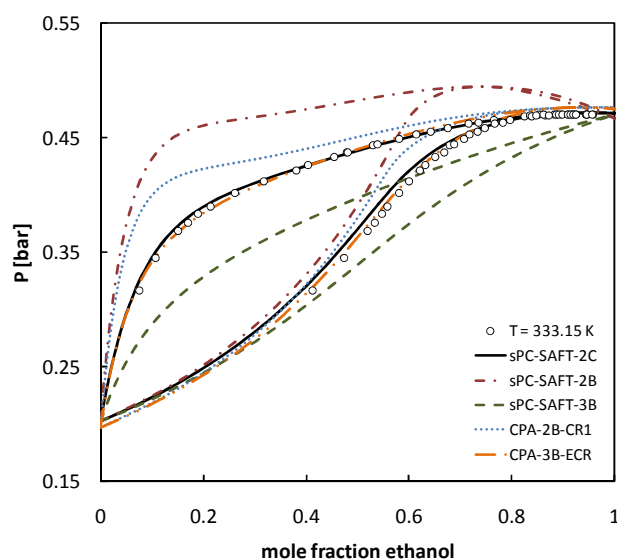


Figure 6-4: VLE predictions of the ethanol/water system with sPC-SAFT and CPA using various association schemes. Experimental data taken from ref. (143)

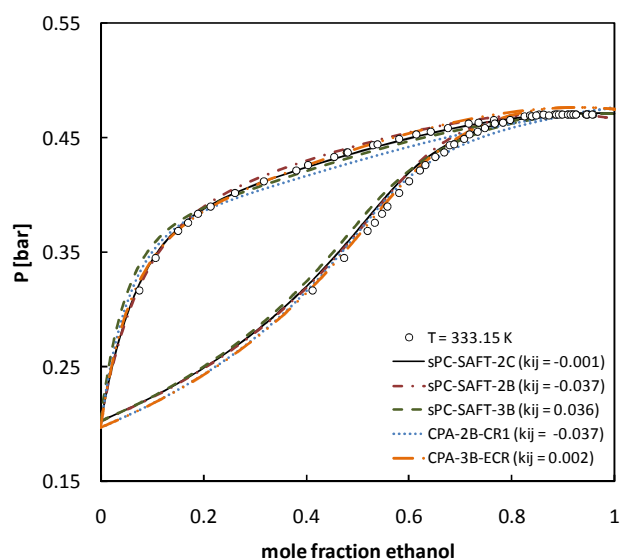


Figure 6-5: VLE correlations of the ethanol/water system with sPC-SAFT and CPA using various association schemes. Experimental data taken from ref. (143)

VLE results of the 1-propanol/water system are shown in Figure 6-6. sPC-SAFT-2C provides a good prediction of the system, which can be somewhat improved with a small BIP. As with methanol and ethanol, sPC-SAFT-2B underestimates cross-association which leads to incorrect VLE predictions. The false phase split may be corrected with a BIP. An advantage of sPC-SAFT-2C over sPC-SAFT-2B, is that false phase splits are only obtained at much lower temperatures. sPC-SAFT-3B overestimates the cross-association and a large positive BIP is required to obtain good correlation of the VLE data. CPA describes the 1-propanol/water system adequately when the ECR rule is used, although a false phase split is obtained if a small BIP is not used. Comparing the values of the

BIP in Figure 6-6, it is evident that sPC-SAFT-2C ($k_{ij} = 0.007$) has the best predictive performance followed by CPA-3B-ECR ($k_{ij} = 0.01$).

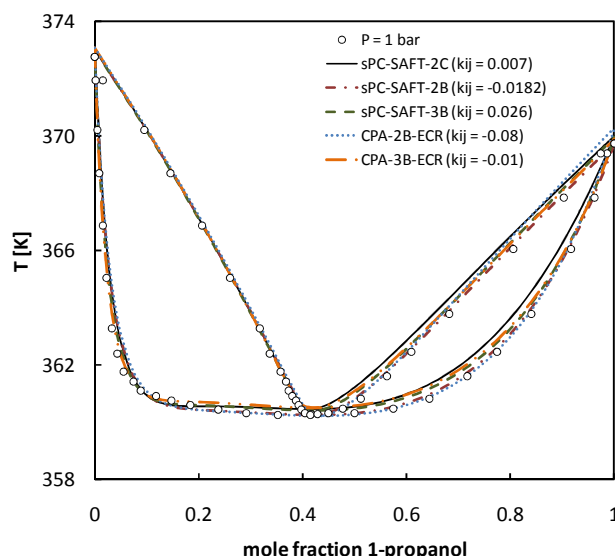


Figure 6-6: VLE correlations of the 1-propanol/water system with sPC-SAFT and CPA using various association schemes.. Experimental data taken from ref. (149).

Figure 6-7 show the VLLE predictions for the systems of 1-butanol/water and Figure 6-8 show an enlargement of the VLE region.

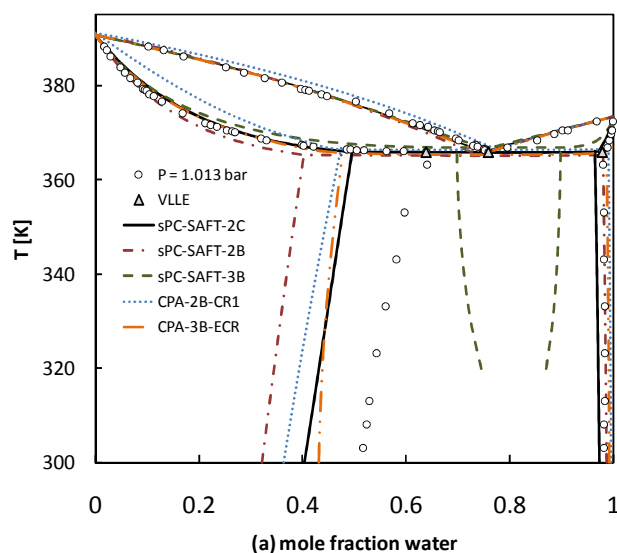


Figure 6-7: VLLE predictions of the water/1-butanol system with sPC-SAFT and CPA using various association schemes. Experimental data taken from ref. (152) and (153).

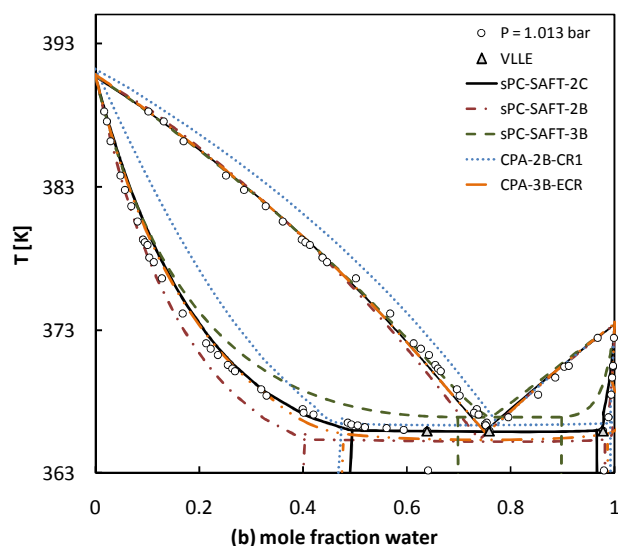


Figure 6-8: VLE predictions of the water/1-butanol system with sPC-SAFT and CPA using various association schemes. Experimental data taken from ref. (152) and (153).

sPC-SAFT-2C accurately predicts the VLE data without requiring any BIPs, but the LLE is not as well predicted. As with the previous alcohol/water systems, sPC-SAFT-2B underestimates the cross-association. Neither the VLE nor the LLE data are as well predicted as by sPC-SAFT-2C. CPA-2B-CR1 provides fair prediction of the phase diagram, although neither the VLE nor the LLE data is

accurately predicted. The VLLE predictions of CPA-2B-CR1 may be improved by fitting a BIP to LLE data as reported by Kontogeorgis *et al.* (61), but this leads to even poorer VLE predictions. CPA 3B-ECR provides improved VLE and LLE predictions compared to CPA-2B-CR1, although sPC-SAFT-2C still seems somewhat superior.

The 1-pentanol/water system was also investigated and representative results are given in Figure 6-9 and Figure 6-10. Similar results are found compared to the 1-butanol/water system. The VLE is extremely well predicted with sPC-SAFT using the 2C association scheme. However, the composition of the alkane-rich liquid is not predicted with sufficient accuracy in the region of the three-phase line. sPC-SAFT-3B provides superior predictions than sPC-SAFT-2C in the three-phase line region, but shows the an incorrect liquid composition predictions at low temperatures of the alkane-rich phase.

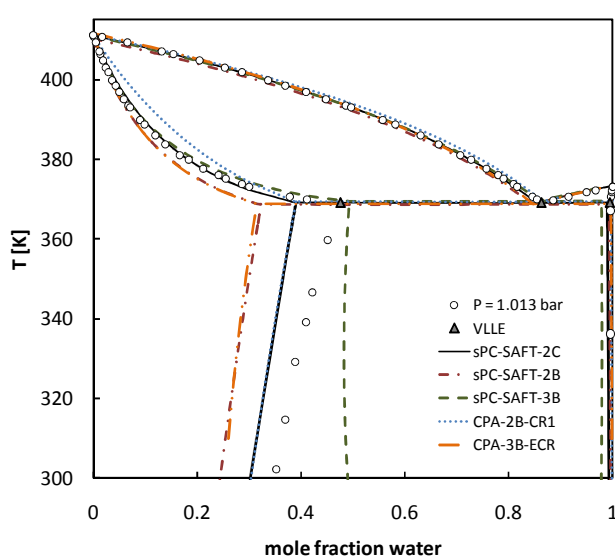


Figure 6-9: VLLE predictions of the water/1-pentanol system with sPC-SAFT and CPA using various association schemes. Experimental data taken from ref. (154) and (153).

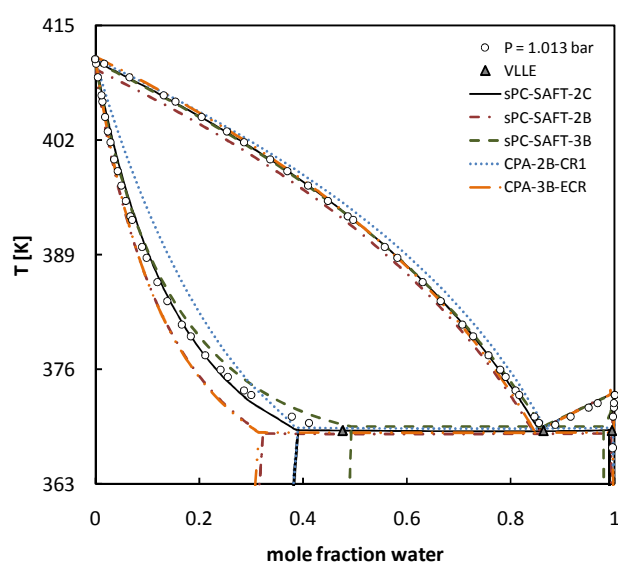


Figure 6-10: VLE predictions of the water/1-pentanol system with sPC-SAFT and CPA using various association schemes. Experimental data taken from ref. (154) and (153).

From this section, it is clear that sPC-SAFT combined with the 2C scheme provides superior phase equilibrium predictions (compared to sPC-SAFT with the 2B and 3B schemes) for 1-alcohol/water systems. A major improvement in especially VLE predictions is obtained, with large reduction in the error in vapour phase composition and pressure (see Table 6-5). The 2C scheme captures the influence of molecular interactions on phase equilibria between water and alcohols molecules more accurately than the other schemes within the framework of sPC-SAFT.

6.5 VLE of alcohol/alcohol mixtures

The VLE of several alcohol/alcohol systems are investigated in order to compare the performance of the 2B, 3B and 2C association schemes with sPC-SAFT, as summarized in Table 6-6. Generally, the performances of these schemes are very similar. This is to be expected, since the interactions

between *like* and *unlike* molecules are similar. The only exception is for methanol-containing systems modelled with sPC-SAFT, where modelling with the 2C scheme provides significantly improved predictions compared to the 2B scheme. Table 6-6 also shows the respective correlations of the VLE systems where BIPs were fitted to the data.

Table 6-6: VLE results for alcohol/alcohol systems for sPC-SAFT

Mixture	<i>T</i> or <i>P</i>	Prediction			Correlation			<i>np</i>	ref.
		<i>k_{ij}</i>	$\Delta y(\text{x10}^2)^{\text{a}}$	$\Delta P(\%)^{\text{b}}/\Delta T(\text{K})^{\text{a}}$	<i>k_{ij}</i>	$\Delta y(\text{x10}^2)^{\text{a}}$	$\Delta P(\%)^{\text{b}}/\Delta T(\text{K})^{\text{a}}$		
sPC-SAFT-2C									
methanol/ethanol	298.15 K	0	0.47	1.00	-0.002	0.42	0.52	11	(155)
methanol/ethanol	373.15 K	0	0.37	0.78	-0.002	0.29	0.53	10	(156)
methanol/1-propanol	333.35 K	0	0.23	0.67	-0.001	0.29	0.59	26	(157)
methanol/1-octanol	1.013 bar	0	2.45	1.69	0.009	1.88	1.50	25	(158)
ethanol/1-propanol	333.15 K	0	1.42	4.04	0.012	0.63	0.37	9	(159)
ethanol/1-butanol	343.15 K	0	0.72	0.86	0.004	0.49	0.61	8	(160)
ethanol/1-octanol	1.013 bar	0	2.04	0.94	0.004	1.70	0.89	25	(158)
1-propanol/1-pentanol	1.013 bar	0	0.59	0.54	-0.006	0.77	0.12	19	(161)
Average			1.04	1.31		0.81	0.64		
sPC-SAFT-2B									
methanol/ethanol	298.15 K	0	5.93	16.6	-0.043	2.76	3.44	11	(155)
methanol/ethanol	373.15 K	0	5.07	14.7	-0.043	2.19	3.43	10	(156)
methanol/1-propanol	333.35 K	0	3.44	10.6	-0.031	0.71	2.10	26	(157)
methanol/1-octanol	1.013 bar	0	0.79	2.73	-0.018	1.00	1.20	25	(158)
ethanol/1-propanol	333.15 K	0	1.12	3.14	0.010	0.63	0.45	9	(159)
ethanol/1-butanol	343.15 K	0	0.42	1.53	-0.003	0.30	1.13	8	(160)
ethanol/1-octanol	1.013 bar	0	2.48	2.11	0.006	1.98	2.18	25	(158)
1-propanol/1-pentanol	1.013 bar	0	0.58	0.79	-0.009	1.17	0.18	19	(161)
Average			2.48	6.53		1.34	1.76		
sPC-SAFT-3B									
methanol/ethanol	298.15 K	0	0.38	0.87	-0.001	0.33	0.60	11	(155)
methanol/ethanol	373.15 K	0	0.48	0.84	-0.001	0.38	0.58	10	(156)
methanol/1-propanol	333.35 K	0	0.11	1.23	-0.003	0.26	0.53	26	(157)
methanol/1-octanol	1.013 bar	0	1.32	1.87	-0.009	1.80	1.33	25	(158)
ethanol/1-propanol	333.15 K	0	1.11	3.00	0.008	0.60	0.40	9	(159)
ethanol/1-butanol	343.15 K	0	0.41	2.51	-0.005	0.42	0.49	8	(160)
ethanol/1-octanol	1.013 bar	0	1.59	4.22	-0.026	1.33	0.89	25	(158)
1-propanol/1-pentanol	1.013 bar	0	0.67	0.73	-0.008	0.80	0.12	19	(161)
Average			0.76	1.91		0.74	0.62		

^a $\Delta z = \sum_i^{np} |z_i^{calc} - z_i^{exp}|$ where *z* represents *y* or *T* and *np* is the number of data points. ^b Deviations as %AAD.

The VLE prediction of the methanol/ethanol system is presented in Figure 6-11 and the corresponding correlation in Figure 6-12. Clearly, sPC-SAFT with the 2B scheme is unable to represent the system accurately, even with a BIP. On the other hand, sPC-SAFT with either the 2C or 3B schemes provides very accurate predictions of the system. CPA also provides very good predictions with both association schemes.

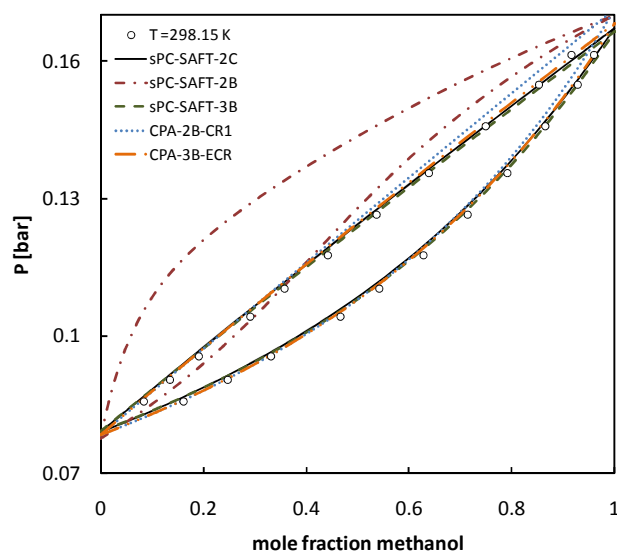


Figure 6-11: VLE predictions of the methanol/ethanol system with sPC-SAFT and CPA using various association schemes. Experimental data taken from ref. (155).

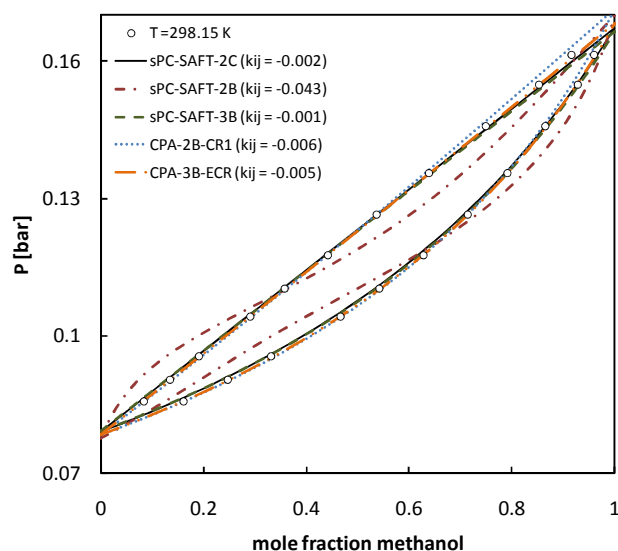


Figure 6-12: VLE correlations of the methanol/ethanol system with sPC-SAFT and CPA using various association schemes. Experimental data taken from ref. (155).

In Figure 6-13, the VLE of methanol/1-propanol is shown and similar results are found compared to the results of the methanol/ethanol VLE. sPC-SAFT with the 2B scheme is once again unable to give an accurate VLE prediction of the system. Therefore, it seems as if the methanol 2B parameters for sPC SAFT from Tybjerg *et al.* (32) are unable to describe the behaviour of methanol in systems where the level of hydrogen bonding is extremely high. The VLE of similar alcohol/alcohol mixtures have also been studied with other SAFT-based models (126; 35). Generally, most SAFT models are able to provide accurate representation al alcohol/alcohol VLE with no, or very small BIPs.

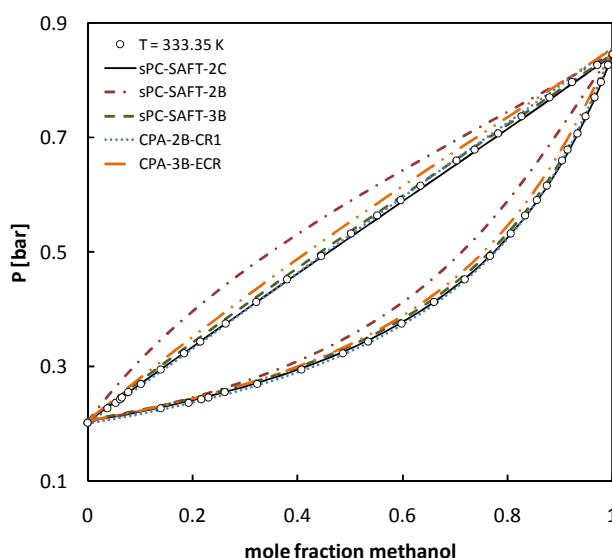


Figure 6-13: VLE predictions of the methanol/1-propanol system with sPC-SAFT and CPA using various association schemes. Experimental data taken from ref. (157).

Form this section, it is evident that the 2C scheme provides good description of alcohol/alcohol and alcohol/water interactions. No compromise in the predictive performance of sPC-SAFT is

therefore experienced when using the 2C association scheme in the modeling of alcohol/alcohol systems.

6.6 VLE and LLE of alcohol/*n*-alkane mixtures

The VLE of 1-alcohols with several *n*-alkanes are also considered, as summarized in Table 6-7. For almost all systems under consideration, the sPC-SAFT-2B provides slightly superior results to sPC-SAFT-2C, especially in the case of methanol-containing systems. sPC-SAFT-3B is prone to predict false phase splits in alcohol/alkane mixtures, especially when the alcohol is short-chained. However, no false phase splits are obtained with sPC-SAFT-2C for the systems investigated. Generally, BIPs can be used to provide good representation of all systems with sPC-SAFT using all three association schemes, as indicated in Table 6-7. However, the BIPs required by sPC-SAFT-2C to represent the data accurately are larger compared to the BIPs required by sPC-SAFT-2B and sPC-SAFT-3B.

Table 6-7 VLE results for alcohol/*n*-alkane systems with sPC-SAFT

Mixture	<i>T</i> or <i>P</i>	Prediction				Correlation			<i>np</i>	ref.
		<i>k_{ij}</i>	$\Delta y(\text{x}10^2)^{\text{a}}$	$\Delta P(\%)^{\text{b}}/\Delta T(\text{K})^{\text{a}}$		<i>k_{ij}</i>	$\Delta y(\text{x}10^2)^{\text{a}}$	$\Delta P(\%)^{\text{b}}/\Delta T(\text{K})^{\text{a}}$		
sPC-SAFT-2C										
methanol/ <i>n</i> -butane	323.15 K	0	0.95	7.31		0.021	0.68	1.29	11	(162)
methanol/ <i>n</i> -pentane	372.70 K	0	4.48	9.34		0.030	1.66	2.62	11	(163)
methanol/ <i>n</i> -hexane	343.15 K	0	4.21	9.91		0.024	1.98	2.34	24	(164)
ethanol/ <i>n</i> -pentane	372.15 K	0	2.77	7.01		0.023	2.08	5.31	10	(165)
ethanol/ <i>n</i> -hexane	323.15 K	0	3.88	8.14		0.021	1.16	1.39	20	(166)
ethanol/ <i>n</i> -heptane	333.15 K	0	3.39	7.55		0.019	0.62	0.85	16	(167)
ethanol/ <i>n</i> -octane	318.15 K	0	2.65	8.28		0.016	0.65	1.64	17	(168)
1-propanol/ <i>n</i> -hexane	323.15 K	0	1.97	7.34		0.009	0.55	1.89	22	(169)
1-propanol/ <i>n</i> -heptane	333.15 K	0	3.10	5.89		0.015	1.57	1.93	33	(169)
1-propanol/ <i>n</i> -octane	363.15 K	0	2.63	6.95		0.017	1.22	1.83	24	(170)
1-propanol/ <i>n</i> -nonane	298.15 K	0	1.43	5.34		0.007	0.81	1.07	17	(171)
1-butanol/ <i>n</i> -hexane	348.15 K	0	2.00	9.57		0.017	0.95	2.27	12	(172)
1-butanol/ <i>n</i> -octane	373.15 K	0	4.35	10.68		0.024	1.74	2.17	22	(173)
Average			2.90	7.95		1.20	2.05			
sPC-SAFT-2B										
methanol/ <i>n</i> -butane	323.15 K	0	0.69	0.41		0.001	0.69	0.46	11	(162)
methanol/ <i>n</i> -pentane	372.70 K	0	1.62	2.28		0.007	1.20	1.45	11	(163)
methanol/ <i>n</i> -hexane	343.15 K	0	1.06	1.00		-0.001	1.05	0.98	24	(164)
ethanol/ <i>n</i> -pentane	372.15 K	0	1.38	4.26		0.007	1.30	3.21	10	(165)
ethanol/ <i>n</i> -hexane	323.15 K	0	1.38	2.89		0.003	1.34	2.30	20	(166)
ethanol/ <i>n</i> -heptane	333.15 K	0	1.58	2.46		0.007	2.10	2.82	16	(167)
ethanol/ <i>n</i> -octane	318.15 K	0	1.56	3.27		0.008	1.85	4.22	17	(168)

Mixture	T or P	Prediction			Correlation			np	ref.
		k_{ij}	$\Delta y(x10^2)^a$	$\Delta P(\%)^b/\Delta T(K)^a$	k_{ij}	$\Delta y(x10^2)^a$	$\Delta P(\%)^b/\Delta T(K)^a$		
1-propanol/n-hexane	323.15 K	0	1.73	6.63	0.009	0.41	1.30	22	(169)
1-propanol/n-heptane	333.15 K	0	2.64	5.12	0.014	1.30	1.58	33	(169)
1-propanol/n-octane	363.15 K	0	2.52	6.17	0.016	1.26	2.07	24	(170)
1-propanol/n-nonane	298.15 K	0	1.61	5.48	0.008	1.09	0.89	17	(171)
1-butanol/n-hexane	348.15 K	0	1.30	8.05	0.015	0.73	1.68	12	(172)
1-butanol/n-octane	373.15 K	0	3.54	9.82	0.023	1.64	1.55	22	(173)
Average			1.74	4.45		1.22	1.89		

sPC-SAFT-3B

methanol/n-butane	323.15 K	0	VLE	VLE	-0.008	0.53	1.58	11	(162)
methanol/n-pentane	372.70 K	0	1.56	2.70	-0.002	1.58	2.71	11	(163)
methanol/n-hexane	343.15 K	0	VLE	VLE	-0.007	1.40	2.31	24	(164)
ethanol/n-pentane	372.15 K	0	1.53	3.98	-0.012	0.60	1.23	10	(165)
ethanol/n-hexane	323.15 K	0	VLE	VLE	-0.011	0.89	1.03	20	(166)
ethanol/n-heptane	333.15 K	0	VLE	VLE	-0.012	0.48	0.72	16	(167)
ethanol/n-octane	318.15 K	0	VLE	VLE	-0.013	0.45	1.29	17	(168)
1-propanol/n-hexane	323.15 K	0	0.99	2.58	-0.003	0.52	1.77	22	(169)
1-propanol/n-heptane	333.15 K	0	1.75	2.42	0.003	1.98	2.47	33	(169)
1-propanol/n-octane	363.15 K	0	1.78	2.93	0.003	1.71	2.11	24	(170)
1-propanol/n-nonane	298.15 K	0	0.93	4.18	-0.004	0.79	0.97	17	(171)
1-butanol/n-hexane	348.15 K	0	1.42	6.56	0.009	1.03	2.65	12	(172)
1-butanol/n-octane	373.15 K	0	3.33	8.36	0.018	2.11	2.60	22	(173)
Average			1.66	4.21		1.08	1.80		

^a $\Delta z = \sum_i^{np} |z_i^{calc} - z_i^{exp}|$ where z represents y or T and np is the number of data points. ^b Deviations as %AAD.

VLE investigations of alcohol/alkane mixtures have been studied by a vast amount of SAFT-models including SAFT (126; 44), LJ-SAFT (174; 175), PC-SAFT-variants (25; 35; 44) and SAFT-VR (125) to mention a few. Generally, most of these SAFT-based models are also able to give similar descriptions of alcohol/alkane VLE with a single BIP. From Table 6-7, the magnitude of the BIPs required by sPC-SAFT-2C is generally larger compared to sPC-SAFT-2B and sPC-SAFT-3B, especially for the smaller alcohols. These BIP values are smaller or of the same magnitude as the other SAFT-based models mentioned. (It is realized that BIP values of different SAFT-based models cannot be directly compared, because the potential function on which different models are based influences the BIP value, as discussed by Haslam *et al.* (128). However, some indication is at least obtained.)

Figure 6-14 and Figure 6-15 show VLE predictions and correlations of the methanol/*n*-hexane system respectively.

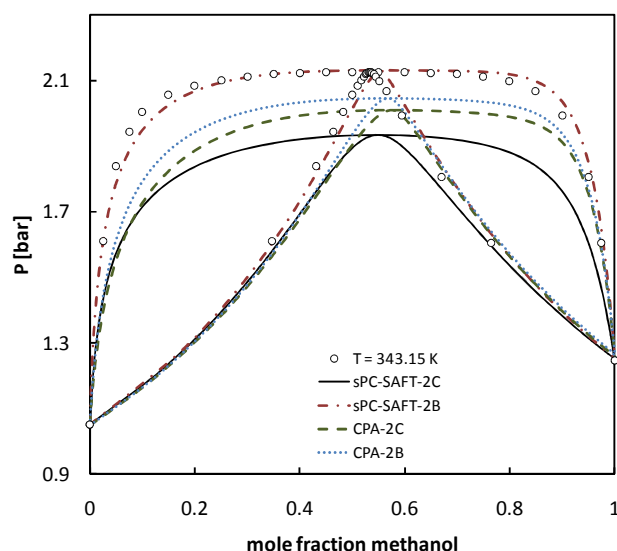


Figure 6-14: VLE correlations of the methanol/*n*-hexane system with sPC-SAFT and CPA using various association schemes. Experimental data taken from ref. (164).

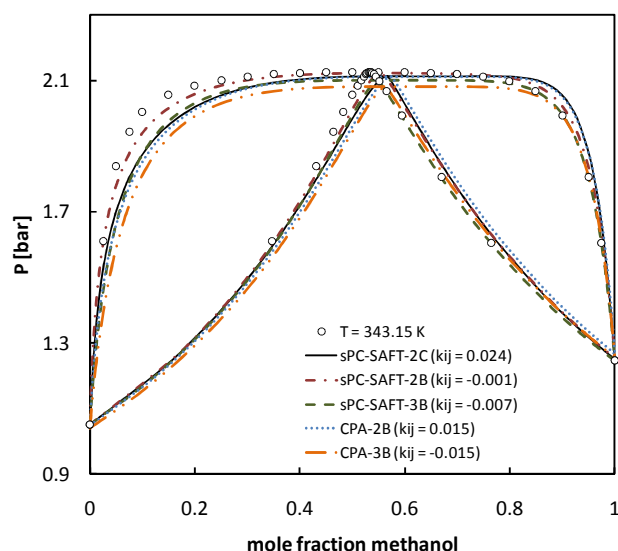


Figure 6-15: VLE correlations of the methanol/*n*-hexane system with sPC-SAFT and CPA using various association schemes. Experimental data taken from ref. (164).

From Figure 6-14, sPC-SAFT with the 2B scheme and parameters of Tybjerg *et al.* (32) provide very accurate prediction of the data that can be marginally improved with a small BIP, as shown in Figure 6-15. sPC-SAFT with the 2C scheme predicts the occurrence of the azeotropic point at a lower pressure than the experimental data, but may be corrected with a BIP. The performance of the 3B scheme is, however, less satisfying. Both sPC SAFT-3B and CPA-3B predicts false VLLE that requires BIPs to obtain the correct phase behaviour.

Figure 6-16 and Figure 6-17 show LLE correlations of the methanol/*n*-hexane and methanol/*n*-octane systems. The BIPs were fitted to the alkane-rich phase and only sPC SAFT-2B with the parameters from Tybjerg *et al.* (32) provides simultaneous good description of both phases. sPC-SAFT-2C provides correlations very similar to CPA-2B and is not as accurate as sPC-SAFT-2B, but an acceptable qualitative description is obtained. Similar results were also obtained when the methanol/*n*-octane system.

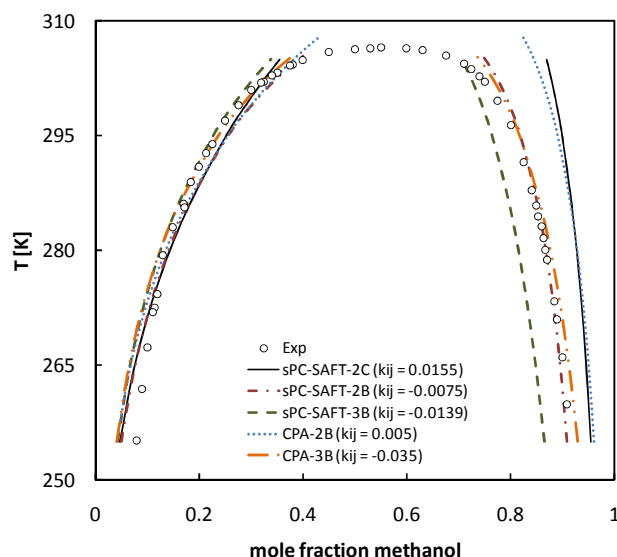


Figure 6-16: LLE correlations of the methanol/*n*-hexane system with sPC-SAFT and CPA using various association schemes. Experimental data taken from ref. (176).

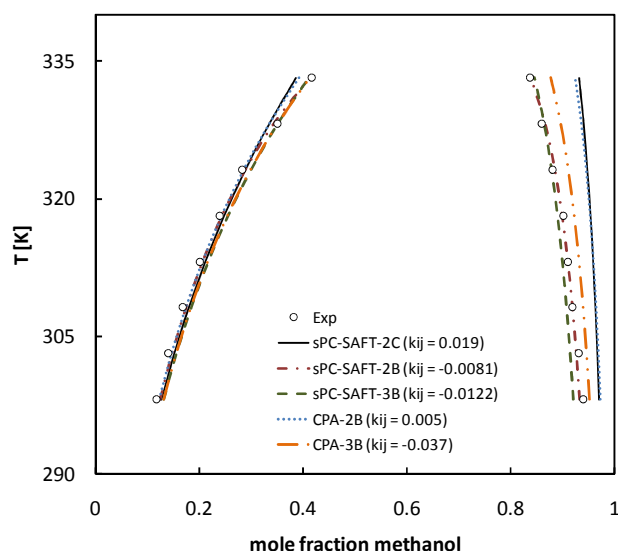


Figure 6-17: LLE correlations of the methanol/*n*-octane system with sPC-SAFT and CPA using various association schemes. Experimental data taken from ref. (177).

Considering the results of sPC-SAFT for methanol with water, alcohols and alkanes, it seems as if self-associative behaviour of methanol is best described by the 2B parameters of Tybjerg *et al.* (32) (methanol/alkane systems) and that the cross-associative behaviour is best described by the 2C parameters presented in this work (methanol/water systems and methanol/alcohol systems). In the case of sPC-SAFT-2B, large BIPs are required to obtain fair description of the methanol/water and methanol/alcohol systems and small or no BIPs are required to obtain accurate description of methanol/alkane systems. On the other hand, in the case of sPC-SAFT-2C, small or no BIPs are required to obtain good description of methanol/water and methanol/alcohol systems, but relatively large BIPs are required to obtain good description of methanol/alkane systems. In essence, neither of the schemes combined with sPC-SAFT performs exceedingly well for all three types of systems and the choice of scheme should therefore be based on the region that the user regards most important to predict accurately.

The VLE of ethanol/*n*-hexane system is also investigated and results are shown in Figure 6-18. Similar results are found compared to the methanol/*n*-hexane system. The correlations of sPC-SAFT-2C and sPC-SAFT-3B were the most accurate and the predictions of sPC-SAFT-2B, CPA-2B and CPA-3B had some difficulty in describing the compositions of the alkane-rich region.

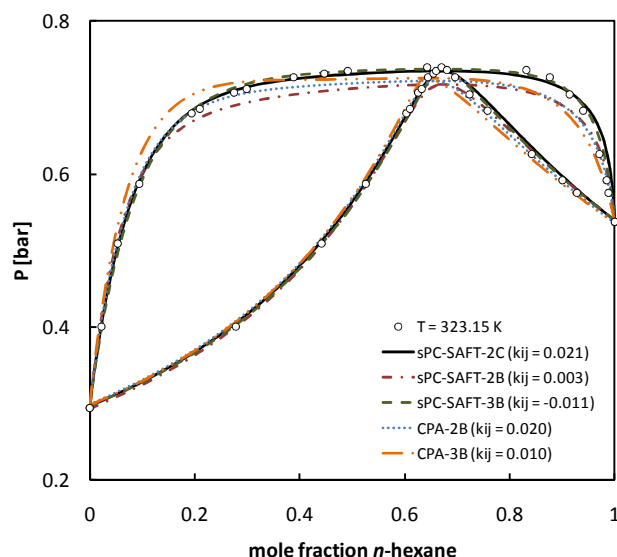


Figure 6-18: VLE correlations of the *n*-hexane/ethanol system at $T = 323.15$ K with sPC-SAFT and CPA using difference association schemes. Experimental data taken from ref. (166).

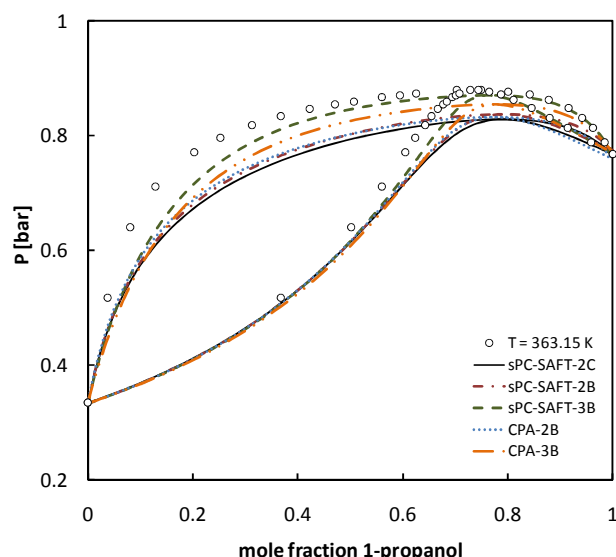


Figure 6-19: VLE predictions of the 1-propanol/*n*-octane system at $T = 363.15$ K with sPC-SAFT and CPA using different association schemes. Experimental data taken from ref. (170).

Figure 6-19 shows the VLE predictions of 1-propanol/*n*-octane. sPC-SAFT-2C, sPC-SAFT-2B and CPA-2B provide VLE predictions that are almost identical. It appears that the difference between the 2C and 2B association schemes becomes smaller as the chain length of the alcohol increases. The predictions of sPC-SAFT-3B and CPA-3B are superior to the predictions based on the 2B and 2C schemes.

From this section it is concluded that sPC-SAFT coupled with the 2C association scheme provides slightly worse predictions of alcohol/alkane mixtures, especially for short chain alcohols. It furthermore appears that the difference between the 2C and the 2B association schemes becomes smaller as the chain length increases. This is due to the fact the contribution of the association term becomes smaller as the chain length increases and that the other interactions become more dominant.

6.7 Multi-component phase equilibria

Multi-component systems consisting of water, alcohols and hydrocarbons are especially difficult to model. Usually, only either the compositions of the water-rich phase or the hydrocarbon-rich phase are predicted with sufficient accuracy. In Figure 6-20, the LLE of the ethanol/water/*n*-hexane system is shown (all $k_{ij} = 0$) and it is clear that sPC-SAFT-2C provides very good composition predictions of both phases. sPC-SAFT-2B is slightly more inaccurate, especially in the plait point region. sPC-SAFT-3B requires a BIP between ethanol and *n*-hexane to prevent a false liquid-liquid split between these two components and is least accurate of the three association schemes considered ($k_{ij} = -0.011$, obtained from fitting VLE).

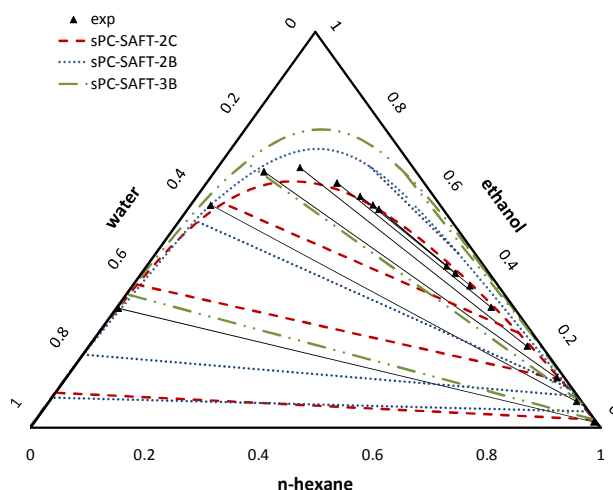


Figure 6-20: LLE predictions of the ethanol/*n*-hexane/water system at $T = 298.15$ K with sPC-SAFT. Experimental data taken from ref. (153).

BIPs may be used to improve the predictions of sPC-SAFT-2B and sPC-SAFT-3B for ethanol/*n*-hexane/water system. However, the k_{ij} values obtained by fitting the corresponding binary VLE data either worsen the correlations or do not lead to significant improvement. Therefore, specific k_{ij} values are necessary to predict the ternary LLE accurately. A possible solution might be to obtain phase specific k_{ij} predictions by following a similar approach as discussed by Haslam *et al.* (128).

Unfortunately, the same good results are not experienced for systems with larger alcohols. The performance of sPC-SAFT in predicting LLE of the 1-propanol/water/*n*-heptane system with all three schemes was investigated. None of the model configurations provide good predictions of the said system. sPC-SAFT-2C still provides predictions that are slightly superior to the other two schemes, but not with the same accuracy as for the ethanol/water/*n*-hexane system. Furthermore, the representation of the 1-propanol/water/*n*-heptane system could be improved with BIPs, but very accurate correlations of the system with sPC-SAFT combined with any of the schemes was not obtained. It may perhaps be that the inability of sPC SAFT to accurately predict multi-component LLE is not as a result of the choice of association scheme, but rather an inherent shortcoming in the SAFT model.

In Figure 6-21, the LLE results for the methanol/water/1-octanol system are presented. Predictions with all three association schemes are with BIPs equal to zero. sPC-SAFT-2C and sPC-SAFT-2B provide predictions which exhibit the correct qualitative trends, although the prediction of sPC-SAFT-2C is slightly more accurate. A BIP between water and 1-octanol may be used to improve the description of the 1-octanol-rich phase, but this leads to a tradeoff in accuracy in the description of the water-rich phase with both sPC-SAFT-2C and sPC-SAFT-2B. The prediction with sPC-SAFT-3B does not exhibit the correct trend (consider the tie-lines). Using a BIP to adjust the solubility of octanol in the water-rich phase in sPC-SAFT-3B, delivers worse results, especially in the plait point region.

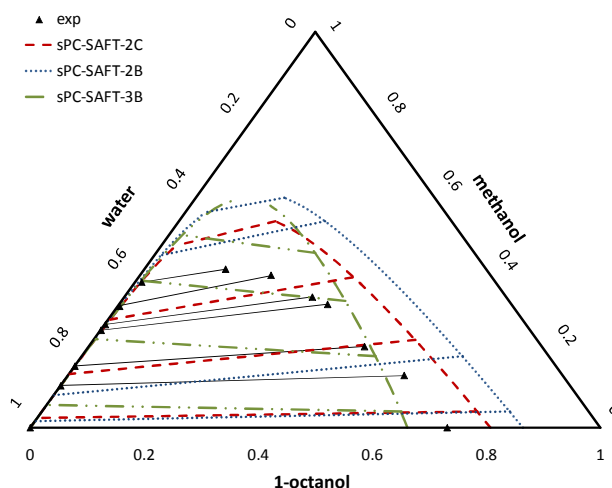


Figure 6-21: LLE predictions of the methanol/water/1-octanol system at $T = 298.15$ K. with sPC-SAFT using various associating schemes. Experimental data taken from ref. (178).

From this section, it follows that there are still major challenges experienced when modelling multi-component phase equilibria with systems that are extremely non-ideal. Further improvement to related theories is still required.

6.8 Chapter Summary

The newly presented 2C association scheme allows sPC-SAFT to predict the phase equilibrium behaviour of 1-alcohols in mixtures with water more accurately compared to when the 2B or 3B schemes are used. This association scheme consists of one bipolar site and one negative acceptor site and is a combination of the 1A and 2B/3B association schemes originally defined by Huang and Radosz (26; 27).

The most notable findings are:

- In the case of sPC-SAFT, the 2C scheme provides significant improvement - for the investigated water/alcohol systems - compared to the 2B and 3B schemes (%AAD in pressure decreasing by up to 15% and the error in vapour phase composition decreasing by up to 4%). For alcohol/water systems, sPC-SAFT-2C provides predictions that are as good as, or better than the best predictions obtained with CPA.
- The VLE of alcohol/alcohol systems are also well predicted with sPC-SAFT-2C. However, the 2C scheme results in slightly worse phase predictions of the VLE of alcohol/alkane mixtures when compared to sPC-SAFT-2B, but this may be corrected with a BIP.
- Furthermore, evidence is provided that sPC-SAFT-2C predicts the LLE of water/alcohol/alkane and water/alcohol/alcohol systems slightly more accurately than sPC-SAFT-2B and sPC-SAFT-3B. However, there seems to be inherent shortcomings in the framework of sPC-SAFT preventing accurate multicomponent VLE predictions.

Since alcohols and water possess permanent dipoles, accounting explicitly for polar forces might yield further improvement. In Chapter 7, sPC-SAFT and CPA are extended with two prominent polar terms and applied to polar (non-HB) components. Chapter 8 subsequently focusses on the application of the new polar models to the hydrogen bonding systems investigated in Chapter 6.

6.8.1 Scientific Contribution

The work presented in this chapter has been published in the following journal:

Title: New Association Scheme for 1-Alcohols in Alcohol/Water Mixtures with sPC-SAFT: The 2C Association Scheme

Authors: Adriaan J. de Villiers, Cara E. Schwarz, and Andries J. Burger

Journal: Industrial & Engineering Chemistry Research **2011**, 50, 8711–8725

Chapter 7

Extending sPC-SAFT and CPA with dipolar terms: Application to non-associating components

In the original formalism of SAFT (16) and CPA (8), the contribution to the Helmholtz free energy as a result of polar interactions was not explicitly considered and was effectively grouped together with dispersion interactions (35; 179) as *Van der Waals* interactions. However, in mixtures where polar interactions are strong and prevalent, they cannot be grouped together with the dispersion interactions, because the resulting parameters that characterize these interactions become artificially large (179). As a result, the predictive capability of the models is severely reduced when properties for mixtures have to be estimated (179). This necessitated the development of polar terms that explicitly accounts for polar interactions. With respect to SAFT-type models, equation (1-3) is extended as follows:

$$A^r = A^{hs} + A^{disp} + A^{chain} + A^{assoc} + A^{polar} \quad (7-1)$$

Several expressions for polar terms have been developed over the years as reviewed by Tan *et al.* (9). Several of these polar terms have been included within the framework of PC-SAFT. However, there are still shortcomings and concerns regarding the capability of these models and the appropriateness of the model parameters e.g. VLE calculations of many simple polar/alkane systems still required BIPs to accurately represent VLE data. The focus of this chapter is to extend the sPC-SAFT EOS with polar theories, and to determine appropriate model parameters for the resulting EOS. As a secondary objective, CPA is also extended with the polar theories. Therefore, the following points are addressed in this chapter:

- Review of most prominent polar terms in the literature that would render sPC-SAFT and CPA able to account for strong polar interactions.
- Modification of polar theories to render them compatible with both sPC-SAFT and CPA.
- Determining appropriate model parameters for non-associating polar components (Parameters for associating polar components are determined in Chapter 8).
- Investigation and evaluation of the ability of models to predict VLE and other thermodynamic properties.

7.1 Perturbation theory for dipolar fluids

As mentioned, several workers have developed polar terms that provide a contribution to the Helmholtz free energy. It is not the aim of this section to review all previously published work regarding polar terms, instead the main concepts involved in the derivation of these theories are only mentioned and the most promising polar terms that are incorporated into this work are reviewed.

Theories that account for polar interactions are usually derived by considering the polar molecule through two approaches: the classical molecular-approach or the improved segment-approach.

7.1.1 Molecular-approach and segment-approach

i) Molecular-approach

The concept behind the ‘molecular-approach’ is to consider a non-spherical dipolar molecule and treat it as if it was a sphere with the same molecular volume and an ideal dipole at the centre of the sphere (179). The major limitation of this approach is that, as the molecule becomes larger, the effect of the dipole weakens excessively, because of the large effective separation distance of the dipoles. The effect of the non-sphericity of the molecule on the dipolar interactions is also not considered (179). Theories based on this approach usually do not agree well with simulation data, especially when complex chainlike molecules are considered (179).

ii) Segment-approach

In contrast to the molecular-approach, the segment-approach explicitly accounts for multiple dipolar functional groups and the non-spherical shape of the molecule in the polar term (179). In Figure 7-1, the difference between the molecular and segment-approach is illustrated by considering a typical alkanone molecule (e.g. di-ethyl ketone):

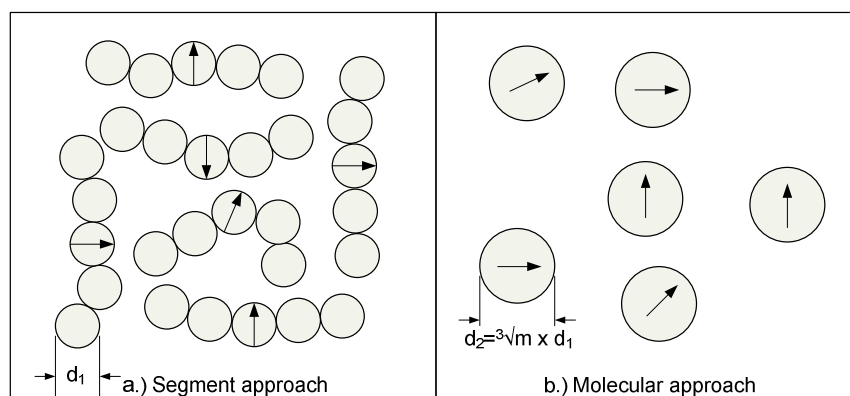


Figure 7-1: Representation of alkanone molecules: a.) Segment approach, b.) Molecular approach. Figure redrawn from Jog et al. (179).

In both approaches, the non-polar segments dilute the polar interactions (179). This is consistent with the idea that polar interactions are less significant in long-chain alkanone molecules than in short-chain alkanone molecules. However, this effect is artificially exaggerated in the molecular approach, because the distance between closest dipolar segments is greater than in the segment approach (179). For molecules with a single polar segment, Jog *et al.* (179) showed that the difference between the molecular and segmental dipolar contributions to the Helmholtz free energy can be expressed as follows:

$$\frac{A_{molecular}^{polar}}{A_{segment}^{polar}} = \frac{1}{m} \quad (7-2)$$

From equation (7-2), for a molecule with a single polar segment, the difference to the contribution of the Helmholtz free energy between the two approaches differs by a factor of the segment number (m), and hence, the difference between the two approaches is more pronounced as the chain length of the molecule increases (179). Therefore, the molecular approach underestimates the effect of the dipolar interactions as the chain length of the molecule increases. This implies, that EOS such as CPA will have to compensate for this limitation within its framework in one way or another. In contrast, EOS such as sPC-SAFT that approximate molecules as a chain of segments connected together, are physically more realistic.

Al-Saifi *et al.* (35) identified three different groups that each developed successful expressions for the contribution of dipolar interaction to the Helmholtz free energy (35) based on the segment-approach. These polar terms also feature in the review article of Tan *et al.* (9) and seem to be the most successful in modelling phase equilibria of polar components. For this investigation, it was decided to incorporate two of these polar into the frameworks of sPC-SAFT and CPA, namely:

- The JC-dipolar term developed by Jog and Chapman (127; 179).
- The GV-dipolar term developed by Gross and Vrabec (54).

The remaining polar term developed by Karakatsani, Spyriouni and Economou (180; 181) was omitted from this investigation, because the work of Al-saif *et al.* (35) indicated that this polar term is inferior to the JC- and GV-dipolar terms.

7.1.2 Jog and Chapman's polar (JC)

i) Concept

The dipolar term of Jog and Chapman was developed from Wertheim's first-order thermodynamic perturbation theory (127) and considers dipoles to be aligned perpendicular to the molecular axis formed between the dipolar segment and the non-polar segment preceding it (127). The dipolar contribution to the Helmholtz free energy is obtained by dissolving all of the bonds in the chain and applying a u -expansion to the resulting mixture of polar and non-polar spherical segments (179). In the u -expansion, the dipolar contribution is an infinite series of second-, third-

and higher-order terms. The second- and third-order terms are calculated explicitly, and the higher order terms are estimated by a Pade approximant of Rushbrook *et al.* (182). The resulting expression was in excellent agreement with molecular simulation data.

ii) Incorporation into PC-SAFT-type models

When the polar term is combined with PC-SAFT, the resulting EOS is generally referred to as **polar PC-SAFT**. However, in this project the notation of Al-Saifi *et al.* (35) is adopted to avoid confusion with other polar terms and consequently, is referred to as PC-SAFT-JC. Therefore, adding this dipolar term to the state-function of sPC-SAFT results in the formation of **sPC-SAFT-JC**.

The dipolar contribution to the Helmholtz free energy in terms of a Pade approximant is written as follows:

$$\frac{A^{\text{dipolar}}}{RT} = \frac{\frac{A_2^{\text{dipolar}}}{RT}}{1 - A_3^{\text{dipolar}} / A_2^{\text{dipolar}}} \quad (7-3)$$

A_2^{dipolar} and A_3^{dipolar} are the second-order and third-order terms in the u -expansion and, for mixtures, are evaluated from the following expressions:

$$\frac{A_{2,\text{mix}}^{\text{dipolar}}}{RT} = -\frac{2\pi}{9} \frac{N_{\text{av}}}{V} \frac{1}{(kT)^2} \sum_i^{nc} \sum_j^{nc} n_i n_j m_i m_j x_{pi} x_{pj} \frac{\mu_i^2 \mu_j^2}{d_{ij}^3} I_{2,ij} \quad (7-4)$$

$$\frac{A_{3,\text{mix}}^{\text{dipolar}}}{RT} = \frac{5}{162} \pi^2 N_{\text{av}}^2 \left(\frac{1}{V}\right)^2 \frac{1}{(kT)^3} \sum_i^{nc} \sum_j^{nc} \sum_k^{nc} n_i n_j n_k m_i m_j m_k x_{pi} x_{pj} x_{pk} \frac{\mu_i^2 \mu_j^2 \mu_k^2}{d_{ij} d_{jk} d_{ik}} I_{3,ijk} \quad (7-5)$$

In equation (7-4) and (7-5), μ_i the functional group dipole moment of molecule i , $I_{2,ii}$ is the angular pair correlation functions, $I_{3,iii}$ is the triplet pair correlation function and x_{pi} is the fraction of dipolar segments on the chain molecule i and considered to be an additional adjustable parameter. For a chain molecule with one dipolar group, the value of x_{pi} should ideally be equal to $1/m_i$, but because a chain molecule is approximated as homonuclear chain of tangentially connected segments in the framework of SAFT, a small difference arises. Therefore, x_{pi} is treated as an extra adjustable parameter (179). The functional group dipole moment may be considered as an adjustable parameter or may be calculated from quantum mechanical calculations. $I_{2,ii}(\rho^*)$ and $I_{3,iii}(\rho^*)$ are complex integrals that were fitted to the following mathematical functions of Rushbrook *et al.* (182):

$$I_{2,ii}(\rho^*) = \frac{1 - 0.3618\rho^* - 0.3205(\rho^*)^2 + 0.1078(\rho^*)^3}{(1 - 0.5236\rho^*)^2} \quad (7-6)$$

$$I_{3,iii}(\rho^*) = \frac{1 + 0.62378\rho^* - 0.11658(\rho^*)^2}{1 - 0.59056\rho^* + 0.20059(\rho^*)^2} \quad (7-7)$$

$$\rho_{mix}^* = \frac{N_{av} n_{total}}{V} d_{x,mix}^3 \quad (7-8)$$

And d_x^3 is defined as:

$$d_{x,mix}^3 = \frac{1}{n_{total}} \sum_i^{nc} m_i n_i d_i^3 \quad (7-9)$$

Combining the two before mentioned equations, ρ_{mix}^* can be expressed as:

$$\rho_{mix}^* = \frac{N_{av}}{V} \sum_i^{nc} m_i n_i d_i^3 \quad (7-10)$$

Therefore, the EOS that emerges by including the JC-dipolar term in the statefunction of sPC-SAFT is termed sPC-SAFT-JC. This EOS has four pure component parameters ($m, \sigma, \varepsilon/k, x_p$) for non-associating components and six pure component parameters for associating components ($m, \sigma, \varepsilon/k, x_p, \varepsilon^{AB}/k, \kappa^{AB}$).

iii) Incorporation into CPA-type models

The original expressions of the JC-dipolar term were developed to be compatible with the framework of SAFT-type models based on a segment approach. Some modifications are necessary in order to render the polar term compatible with the framework of CPA. CPA approximates molecules as single spheres and consequently the advantages gained by using segment based theories as discussed in section 7.1.1 are lost. Therefore, a simplified version of the polar term is used that corresponds to a molecular-based version of the theory. Essentially, the theory is modified to no longer be dependent on the segment number (m) and the SAFT model parameters in the JC-term are related to the model parameters of CPA. The resulting expressions for the second- and third-order terms that are used in this work are:

$$\frac{A_2^{dipolar}}{RT} = -\frac{2\pi}{9} \frac{N_a}{V} \frac{1}{(kT)^2} \sum_i^{nc} \sum_j^{nc} n_i n_j x_{pi} x_{pj} \frac{\mu_i^2 \mu_j^2}{d_{ij}^3} I_{2,ij}(\rho^*) \quad (7-11)$$

$$\frac{A_3^{dipolar}}{RT} = \frac{5}{162} \pi^2 \frac{N_a^2}{V^2} \frac{1}{(kT)^3} \sum_i^{nc} \sum_j^{nc} \sum_k^{nc} n_i n_j n_k x_{pi} x_{pj} x_{pk} \frac{\mu_i^2 \mu_j^2 \mu_k^2}{d_{ij} d_{jk} d_{ik}} I_{3,ijk}(\rho^*) \quad (7-12)$$

The temperature dependent segment diameter (d) of SAFT is easily related to the co-volume parameter (b) of CPA with (129):

$$d_i = \sigma_i = \sqrt[3]{\frac{3b_i}{2\pi N_a}} \quad (7-13)$$

The substitution assumes that the temperature dependent segment diameter is equal to the temperature independent segment diameter and may be calculated from the temperature independent co-volume parameter (b) of CPA. The following combining rule is used to calculate d_{ij} :

$$d_{ij} = 0.5 (d_i + d_j) \quad (7-14)$$

The expressions for the correlation functions, $I_{2,ij}$ and $I_{3,ijk}$, are as presented in equations (7-6)-(7-7) and the specific expression for the reduced density, ρ^* , is defined by:

$$\rho^* = \frac{3B}{2\pi V} \quad (7-15)$$

The polar term is somewhat simplified because the derivatives of ρ^* is only dependent on V and n . This implies that the derivatives of $I_{2,ij}$ and $I_{3,ijk}$ are also only dependent on V and n . The temperature derivatives of equations (7-11) and (7-12) are also simplified because the segment diameters are also no longer temperature dependent. When CPA is combined with the modified polar term of JC, the resulting EOS is termed CPA-JC. For non-associating polar components, this EOS requires four pure component parameters (a_0 , b , c_1 , x_p) and six model parameters for associating fluids (a_0 , b , c_1 , x_p , ε^{AB}/k , β^{AB}).

7.1.3 Gross and Vrabec's dipolar (GV)

i) Concept

The group of Gross not only developed expressions for the contribution to the Helmholtz free energy as a result of dipolar interactions (54), but also contributions for quadrupolar (183), dipole-quadrupole (184) and induced polar interactions (185). Their contribution to the Helmholtz energy as a result of polar interactions is expressed as:

$$\frac{A^{polar}}{RT} = \frac{A^{dipolar}}{RT} + \frac{A^{quadrupolar}}{RT} + \frac{A^{dipole-quadrupole}}{RT} + \frac{A^{ind}}{RT} \quad (7-16)$$

Each contribution was developed separately, but followed the same general approach. All polar terms are based on third-order perturbation theory and are written in terms of Pade approximants. In this work, only the dipolar term is considered.

ii) Incorporation into PC-SAFT-type models

When the polar term is combined with PC-SAFT, the resulting equation is generally referred to as the Perturbed Chain Polar – Statistical Associating Fluid Theory (**PCP-PSAFT**). However, in this work, only the dipolar term is considered and the resulting EOS that emerges when the dipolar term is included in the state function of PC-SAFT is referred to as PC-SAFT-GV. Similar to sPC-SAFT-JC, when the GV-dipolar term is included in the state function of sPC-SAFT, the resulting EOS is referred to as **sPC-SAFT-GV**.

The dipolar term is also written in the form of a Pade approximant (54):

$$\frac{A_{mix}^{dipolar}}{RT} = \frac{A_{2,mix}^{dd} / RT}{1 - A_{3,mix}^{dd} / A_{2,mix}^{dd}} \quad (7-17)$$

$A_{2,mix}^{dd}$ is the second-order perturbation term for a dipolar fluid and $A_{3,mix}^{dd}$ is the third-order term.

For linear symmetric molecules, these terms are evaluated from the following equations (54; 9):

$$\frac{A_2^{dd}}{RT} = -\frac{N_{av}}{V} \frac{\pi}{(kT)^2} \sum_i^{nc} \sum_j^{nc} n_i n_j \frac{n_{pi} n_{pj}}{m_i m_j} \frac{\mu_i^2 \mu_j^2}{\sigma_{ij}^3} J_{2,ij}^{dd} \quad (7-18)$$

$$\frac{A_3^{dd}}{RT} = -\frac{4N_{av}^2 \pi^2}{3} \left(\frac{1}{V}\right)^2 \frac{1}{(kT)^3} \sum_i^{nc} \sum_j^{nc} \sum_k^{nc} n_i n_j n_k \frac{n_{pi} n_{pj} n_{pk}}{m_i m_j m_k} \frac{\mu_i^2 \mu_j^2 \mu_k^2}{\sigma_{ij} \sigma_{jk} \sigma_{ik}} J_{3,ijk}^{dd} \quad (7-19)$$

In equations (7-18) and (7-19), n_{pi} is the number of dipole moments on molecule i , μ_i is the dipole moment, $J_{2,ij}^{dd}$ is the integral over the reference fluid pair correlation function and $J_{3,ijk}^{dd}$ is the integral over the reference fluid three-body correlation function. The other variables are the same as previously defined. The n_{pi} parameter is similar to the x_{pi} parameter in the polar term of Jog and Chapman and effectively allows this dipolar contribution to model molecules with multiple dipolar groups. The integral over the pair correlation function $J_{2,ij}^{dd}$ is a function of temperature, density and segment number. In order to limit the number of adjustable constants, the integral over the three-body correlation function $J_{3,ijk}^{dd}$ was assumed to be independent of temperature and only a function of density and segment number (183; 54). Simple power series functions were then assumed for $J_{2,ij}^{dd}$ and $J_{3,ijk}^{dd}$ in the following form:

$$J_{2,ij}^{dd} = \sum_{n=0}^4 \left(a_{n,ij} + b_{n,ij} \frac{\epsilon_{ij}}{kT} \right) \eta^n \quad (7-20)$$

$$J_{3,ijk}^{dd} = \sum_{n=0}^4 c_{n,ijk} \eta^n \quad (7-21)$$

In the original derivation, another simplification made, was to assume that the third-order pair correlation function is zero, i.e. $J_{3,ijk}^{dd} = 0$ (183; 54). This assumption is valid for molecules of hard repulsion, but is generally only a crude approximation (183; 54). This assumption is regarded as the most severe simplification, because the treatment of mixtures is somewhat compromised. The power series coefficients are represented by the expressions derived by Hu *et al.* (186; 187) and depends only on the chain length (54; 183):

$$a_{n,ij} = a_{0n} + \frac{m_{ij}-1}{m_{ij}} a_{1n} + \left(\frac{m_{ij}-1}{m_{ij}} \right) \left(\frac{m_{ij}-2}{m_{ij}} \right) a_{2n} \quad (7-22)$$

$$b_{n,ij} = b_{0n} + \frac{m_{ij}-1}{m_{ij}} b_{1n} + \left(\frac{m_{ij}-1}{m_{ij}} \right) \left(\frac{m_{ij}-2}{m_{ij}} \right) b_{2n} \quad (7-23)$$

$$c_{n,ijk} = c_{0n} + \frac{m_{ijk}-1}{m_{ijk}} c_{1n} + \left(\frac{m_{ijk}-1}{m_{ijk}} \right) \left(\frac{m_{ijk}-2}{m_{ijk}} \right) c_{2n} \quad (7-24)$$

The combining rules for the chain length are defined as follows:

$$m_{ij} = (m_i m_j)^{1/2} \quad \text{with } m_{ij} \leq 2 \quad (7-25)$$

$$m_{ijk} = (m_i m_j m_k)^{1/3} \quad \text{with } m_{ijk} \leq 2 \quad (7-26)$$

The model constants in equations (7-22)-(7-24) were fitted to molecular simulation data for the two-centre Lennard-Jones plus point dipole fluid that consisted of vapour pressure, saturated liquid and vapour density and virial coefficient data (54; 35). The resulting model constants are given in Table 7-1 (54). An important restriction to the formalism is that the dipole moment is allowed to stretch over only two segments ($m_{ij} \leq 2$ and $m_{ijk} \leq 2$), because only molecules with $m = 2$ were considered in the regression (54). The restriction does not imply that the molecules are restricted to two segments, but that the dipole moment of larger molecules with $m > 2$ are restricted to stretch over two or fewer segments.

Table 7-1: Model constants of the GV-dipolar term (54)

n	a_{0n}	a_{1n}	a_{2n}	b_{0n}	b_{1n}	b_{2n}	c_{0n}	c_{1n}	c_{2n}
0	0.3043504	0.9534641	-1.1610080	0.2187939	-0.5873164	3.4869576	-0.0646774	-0.9520876	-0.6260979
1	-0.1358588	-1.8396383	4.5258607	-1.1896431	1.2489132	-14.915974	0.1975882	2.9924258	1.2924686
2	1.4493329	2.0131180	0.9751222	1.1626889	-0.5085280	15.372022	-0.8087562	-2.3802636	1.6542783
3	0.3556977	-7.3724958	-12.281038	0	0	0	0.6902849	-0.2701261	-3.4396744
4	-2.0653308	8.2374135	5.9397575	0	0	0	0	0	0

In the formalism of the model, the dipole moment is aligned along the molecular axis and this poses as a restriction to the model (54). The physical properties of a fluid are considerably more affected by a dipole moment that is aligned perpendicular to the molecular axis compared to an axial alignment (188; 189). Therefore, it is expected that in components where the dipole moment is aligned perpendicular to the molecular axis, the polar contribution to the Helmholtz free energy will be underestimated by the polar term of Gross and Vrabec (54).

In the original paper of Gross and Vrabec (54), the dipolar term was combined with PC-SAFT. The number of polar segments (n_p) was set equal to 1 by default for polar components with mono-functional groups. In this work, it was decided to consider n_p as an additional pure component parameter, because of the underestimation of polar forces on properties, as discussed above. Therefore, when the GV-dipolar term is included in the state function of sPC-SAFT, the resulting EOS is denoted sPC-SAFT-GV and requires four pure component parameters (m , σ , ε/k , n_p) for non-associating components and six model parameters (m , σ , ε/k , n_p , ε^{AB}/k , κ^{AB}) parameters for associating components.

iii) Incorporation into CPA-type models

Similar simplifications are made to the GV-term, as made to the JC polar term, in order to render it compatible with CPA. The resulting expressions for the second- and third-order terms are presented below:

$$\frac{A_2^{dd}}{RT} = -\frac{N_{av}}{V} \frac{\pi}{(kT)^2} \sum_i^{nc} \sum_j^{nc} n_i n_j \cdot n_{pi} n_{pj} \frac{\mu_i^2 \mu_j^2}{\sigma_{ij}^3} J_{2,ij}^{dd} \quad (7-27)$$

$$\frac{A_3^{dd}}{RT} = -\frac{4N_{av}^2\pi^2}{3V^2} \frac{1}{(kT)^3} \sum_i^{nc} \sum_j^{nc} \sum_k^{nc} n_i n_j n_k \cdot n_{pi} n_{pj} n_{pk} \frac{\mu_i^2 \mu_j^2 \mu_k^2}{\sigma_{ij} \sigma_{jk} \sigma_{ik}} J_{3,ijk}^{dd} \quad (7-28)$$

The temperature independent segment diameter σ is related to the co-volume parameter of CPA as shown in equation (7-13). The correlation functions used are provided below:

$$J_{2,ij}^{dd} = \sum_{w=0}^4 (a_{w,ij} + b_{w,ij} \alpha_{ij}(T)) \eta^w \quad (7-29)$$

$$J_{3,ijk}^{dd} = \sum_{w=0}^4 c_{w,ijk} \eta^w \quad (7-30)$$

In the original publication of Gross and Vrabec (54), the coefficients in equations (7-29) and (7-30) depends on chain length. In the framework of CPA, the coefficients are no longer functions of chain length, because all molecules are approximated as single spheres. Therefore, only 12 universal model constants are required compared to 36 constants of the original expression. The reduced density, η , is calculated with (37):

$$\eta = \frac{B}{4V} \quad (7-31)$$

The function $\alpha_{ij}(T)$ in equation (7-29), is related to the dimensionless segment energy by assuming that the attractive part follows a Lennard-Jones potential from (129; 106):

$$\alpha_{ij}(T) = \sqrt{\alpha_i(T) \alpha_j(T)} \quad (7-32)$$

$$\alpha_i(T) = \left(\frac{a_i(T)}{4b_i RT} \right)$$

When the modified polar term of GV is included in the state function of CPA, the resulting EOS is termed CPA-GV. This EOS requires four pure component parameters (a_0 , b , c_1 , n_p) for non-associating polar components and six pure component parameters (a_0 , b , c_1 , n_p , ϵ^{AB}/k , β^{AB}) for associating polar components.

7.2 Application and shortcomings of polar terms

The applications of the polar terms combined with applicable SAFT-type EOS are presented in the following section.

7.2.1 Phase equilibria

The phase equilibria applications of SAFT-based EOS combined with one of the polar terms discussed in the previous section are presented in Table 7-2. In most cases the results were

compared with the EOS (usually PC-SAFT) without the polar term and generally, improved results were obtained. In some cases, accurate phase equilibria predictions were managed without a BIP and in other cases the required value of the BIP was only slightly smaller.

Table 7-2: Application summary of polar terms to phase equilibria applications

Polar variant	Application	Year	Ref.
SAFT-JC	VLE of acetone-alkane systems. Polar term performed very satisfactorily.	2001	(179)
PC-SAFT-JC CK-SAFT-JC	Pure component parameters for ketone family fitted to saturated vapour pressure and liquid density data. VLE of ketone/alkane systems modelled.	2003	(190)
PC-SAFT-JC	VLE of ketone-alkane systems. BIP still required.	2004	(43)
PC-SAFT-JC	Pure components parameters for monoethers, diethers, polyethers, epoxies and cyclic ethers, esters and ketones by fitting saturated vapour pressure and liquid density data. VLE of polar/alkane systems. BIP still required.	2005	(191)
PC-SAFT-GV (dipolar)	Pure component parameters for dipolar components including ketones, aldehydes, esters, ethers and other miscellaneous components. VLE of acetone/alkane systems.	2006	(54)
PC-SAFT-GV (dipolar and quadrupolar)	Pure component parameters for additional components including refrigerants. VLE of selected alkane / polar and polar / polar systems. The aim of study was to show the improvement of using London's advanced combining rule.	2007	(192)
PC-SAFT-JC PC-SAFT-GV	Pure component parameters for alkanols, water and glycols for PC-SAFT+JC and PC-SAFT+GV. VLE of alkanol / n-alkane binary systems, alkanol / alkanol systems, water / alkanol systems. In general, the polar term of Jog and Chapman performed superior than the other two polar terms.	2008	(35)

Table 7-2 shows that the polar terms have been applied to several systems. In a comparative study by Al-Saifi *et al.* (35), the dipolar terms of each respective group were compared against each other and generally, PC-SAFT-JC performed better than PC-SAFT-GV when the VLE of binary mixtures with alcohols were considered. However, the models were not compared on an equal basis. In PC-SAFT-JC, x_p was included in the regression routine as an adjustable parameter, while in PC-SAFT-GV, n_p was set equal to 1 by default. Therefore, the degrees of freedom granted to each EOS was not the same. Part of the work presented here, is to compare these theories on a more equal basis by granting the respective EOS the same degrees of freedom when model parameters are regressed.

7.2.2 Other thermodynamic derivative properties

The polar terms in combination with SAFT-based equations have been applied to a limited number of thermodynamic properties. The specific cases that could be sourced are mentioned in Table 7-3 below:

Table 7-3: Application summary of polar terms to other thermodynamic properties

Polar variant	Application	Year	Ref.
---------------	-------------	------	------

Polar variant	Application	Year	Ref.
PC-SAFT+GC (dipolar) PC-SAFT+JC	Enthalpy of vapourisation of acetone. The polar term of Gross performed marginally better than that of Jog and Chapman. Excess enthalpy of acetone / <i>n</i> -decane system at T = 298.15 K. The polar term of Gross and Vrabec performed marginally better compared to that of Jog and Chapman.	2006	(54)
PC-SAFT+GC (dipolar and quadrupolar)	Excess enthalpy of ethane/CO ₂ at T = 248.1 K and P = 3 and 10.9 MPa and T = 308.4 K and P = 4 and 11 MPa. Excess enthalpy of cyclohexane/benzene at T = 280.15, 323.15, 393.15 K and 1 bar. Aim of the study was to show the improvement of London's combining rule.	2007	(192)
PC-SAFT+JC PC-SAFT+GC	Excess enthalpy of binary systems composed of ethylene glycol and methanol/ethanol/1-propanol/2-propanol. Only Jog and Chapman's polar term yielded satisfactory results with the errors in the other EOS being very large.	2008	(35)

From Table 7-3 it is again clear that, in comparison to phase equilibria application, the application of polar terms to describe the behaviour of other thermodynamic properties have been neglected. There are, however, still a few problems that can be identified in the literature regarding these terms.

7.2.3 Shortcomings of polar terms

In addition to the limitations of the models, as a result of the simplifications mentioned, there are some shortcomings reported in the literature regarding the polar terms that emerged when the model was applied to the thermodynamic behaviour of some polar systems. The first major difficulty with all polar terms is to find the effective dipole moment. Usually dipole moments are determined under vacuum in the gas-phase. The polarity changes in the liquid phase, making the dipole moment determined in the gas-phase somewhat arbitrary. For example, the dipole moment of water is approximately equal to 1.85 Debye in the gas-phase, but in the bulk liquid phase, it is equal to 2.5-3 Debye (35; 128). Neither polar theory explicitly accounts for this change in dipole moment between mediums. However, most workers use the gas-phase dipole moment and then compensate for the change in polarity with the other parameters. This approach will also be used in this work. Other problems encountered with both PC-SAFT-JC and PC-SAFT-GV are:

- The models erroneously predict liquid-liquid splitting at low temperatures (54; 35).
- Phase equilibria in aqueous systems are still problematic (35).
- For simple systems, such as *n*-heptane/butanone, BIPs are still required to accurately predict the VLE. This possibly indicates that either the models are not as accurate as portrayed in the literature, or that the model parameters presented in the literature are not appropriate.
- Very few applications to other thermodynamic properties than VLE.

7.3 Regression and model parameter determination

The aim of this section is to discuss all aspects surrounding the model parameter determination for the following polar models:

- sPC-SAFT-JC
- sPC-SAFT-GV
- CPA-JC
- CPA-GV

7.3.1 Method and data included

As discussed in Section 2.4.2, there are several objective functions currently being used in the literature to determining model parameters of SAFT-type models. It is important to choose an objective function that would allow the model parameters to behave as orthogonal as possible to each other during the regression procedure, thus determining the most appropriate contributions from each term in the state function. In the literature, problems encountered during parameter determination with similar models have been reported. With regards to PC-SAFT-JC (Polar PC-SAFT), Sauer and Chapman (190) noted that, during the regression routine, a broad minimum exists such that a wide range of parameters will accurately represent the experimental pure component data. Gross and Vrabec (54) reported that x_p commonly tends to zero for some components when fitted to only pure component data. It is believed that this behaviour of the model is experienced because the dispersion and polar forces behave very similar in pure components (both intermolecular potentials have the same separation distance (r) dependency: $r^{1/6}$ (193) as discussed in Appendix A) and this behaviour makes the distinction between the correct contributions from the respective terms rather challenging. Similar problems were experienced in this work during the initial regression procedures when only pure component data was included in the regression routine (saturated vapour pressure, liquid density and heat of vapourisation). To partially resolve this problem, a similar approach was followed as proposed by Dominik *et al.* (191). In their parameter estimation for non-associating polar component with PC-SAFT-JC, they included binary VLE data in the regression function to identify the correct parameters for some esters and ethers. They used binary systems where the polar components were in mixture with n -alkanes. This makes a lot of sense, since the polar and dispersive forces behave differently in these systems: dipolar interactions only occur between polar molecules while dispersion interactions occur between all molecules. Therefore, identifying the model parameters that yield the correct contributions from each term becomes more attainable when binary data is included in the regression routine.

Al-Saifi *et al.* (35) used a simplex method in their regression procedure and was able to obtain good model parameters for alcohols without including binary data in the regression function and noted that it was not necessary to include binary VLE data in order to obtain the optimum set of

parameters for alcohols. However, rather significant errors were still observed in the VLE predictions of some systems.

Thus, for the parameter estimation in this work, the Levenberg-Marquart algorithm with a least squares objective function was used (equation (7-33)) and the following data was included in the regression function: saturated vapour pressure, liquid density, heat of vapourisation (only in sPC-SAFT-GV and sPC-SAFT-JC) and binary VLE data (if available):

$$OF = \sum_{i=1}^{NP} \left[\alpha \left(\frac{P_i^{sat,cal} - P_i^{sat,exp}}{P_i^{sat,exp}} \right)^2 + \beta \left(\frac{\rho_i^{sat,cal} - \rho_i^{sat,exp}}{\rho_i^{sat,exp}} \right)^2 + \gamma \left(\frac{h_i^{vap,cal} - h_i^{vap,exp}}{h_i^{vap,exp}} \right)^2 + \varepsilon (X_i^{VLE,error})^2 \right] \quad (7-33)$$

Where α , β , γ and ε are regression weights. $X_i^{VLE,error}$ is a combination of errors between the experimental vapour phase mole fraction and the calculated value and the error between the experimental saturation P or T and the calculated value, depending on whether an isothermal or isobaric VLE set was included in the regression routine. Pure component data were obtained from the DIPPR correlations (95) in the range $0.5 < T_r < 0.9$ and VLE data from the literature. The dipole moments used were obtained from the DIPPR database (95). Initially, high regression weights were assigned to the pure component data and a low regression weight to the binary data ($P^{sat} = 10$, $\rho^{sat} = 8$, $VLE = 1$). The parameters were then evaluated by comparing the performance of the models against all data included in the regression routine and, if satisfactory results were not obtained, the regression weights were changed.

The newly determined model parameters do not only perform well for the binary system included in the regression function, but also for other systems not included in the regression routine. It is realized that including binary data in the regression function is not the method of preference in determining pure component model parameters, but the significant improvement in the performance of both models justifies the decision.

7.3.2 New model parameters for sPC-SAFT-GV and sPC-SAFT-JC

The model parameters determined in this work are presented in Table 7-4 for sPC-SAFT-GV and in Table 7-5 for sPC-SAFT-JC.

Table 7-4: Model Parameters for non-self-associating components for sPC-SAFT-GV

	<i>MW</i> [g/mol]	σ [Å]	<i>m</i>	ε/k [K]	n_p	μ [D]	VLE data (ref.)	ΔP^{sat} [%] ^a	$\Delta \rho^{sat}$ [%] ^a	Δh^{vap} [%] ^a
acetone	58.08	3.2280	2.7855	210.14	1.4848	2.88	<i>n</i> -hexane (194)	1.15	1.20	0.86
2-butanone	72.11	3.4163	2.9716	227.34	1.7570	2.76	<i>n</i> -heptane (195)	0.12	0.44	0.57
2-pentanone	86.13	3.5069	3.2779	234.31	1.9167	2.77	equation (7-34)	0.23	0.19	1.90
3-pentanone	86.13	3.5121	3.2454	236.32	1.8016	2.82	<i>n</i> -heptane (196)	0.35	0.29	2.25

	<i>MW</i> [g/mol]	σ [Å]	<i>m</i>	ε/k [K]	n_p	μ [D]	VLE data (ref.)	ΔP^{sat} [%] ^a	$\Delta \rho^{sat}$ [%] ^a	Δh^{vap} [%] ^a
2-hexanone	100.1	3.6081	3.5350	243.63	2.2417	2.68	equation (7-34)	0.50	0.14	0.84
3-hexanone	100.1	3.6197	3.4763	242.70	1.9547	2.87	equation (7-34)	0.94	0.16	1.68
2-heptanone	114.1	3.6794	3.8533	248.48	2.5687	2.61	equation (7-34)	0.72	0.57	1.35
3-heptanone	114.1	3.5879	4.0497	240.27	2.2160	2.81	equation (7-34)	1.35	0.25	1.80
4-heptanone	114.1	3.7115	3.7269	247.25	2.7998	2.50	equation (7-34)	0.08	0.56	0.54
MIPK	86.13	3.5401	3.1404	228.46	2.1164	2.76	<i>n</i> -octane (197)	1.06	1.11	1.24
MIBK	100.1	3.6859	3.3174	238.31	2.5270	2.67	<i>n</i> -octane (198)	2.35	0.45	1.68
cyclopentanone	84.11	3.5572	2.7375	284.22	1.2584	3.24	<i>n</i> -cyclohexane (199)	0.70	0.22	1.72
cyclohexanone	98.14	3.7456	2.7827	293.29	1.8196	3.09	<i>n</i> -cyclohexane (200)	0.58	0.34	1.68
propanal	58.08	3.3080	2.5806	224.88	1.4762	2.52	<i>n</i> -pentane (201)	1.12	0.46	0.89
butanal	72.10	3.5082	2.7321	240.55	1.5463	2.72	<i>n</i> -heptane (201)	1.21	0.29	1.48
pentanal	86.13	3.5222	3.2319	238.26	2.1358	2.57	<i>n</i> -heptane (202)	0.36	0.22	0.83
hexanal	100.1	3.6076	3.5107	248.24	2.1670	2.58	equation (7-34)	1.44	0.22	0.99
methyl formate	60.05	3.0300	2.7255	199.43	2.9784	1.77	<i>n</i> -hexane (203)	1.85	2.14	1.32
ethyl formate	74.08	3.2706	2.8895	213.21	3.0255	1.93	<i>n</i> -hexane (203)	1.05	1.49	1.75
propyl formate	88.11	3.3658	3.2404	222.11	3.5158	1.91	<i>n</i> -hexane (203)	1.54	0.97	1.22
butyl formate	102.1	3.4716	3.5899	228.85	3.4977	2.02	<i>n</i> -hexane (203)	0.43	0.44	1.17
methyl acetate	74.08	3.1859	3.1106	208.08	4.0319	1.68	<i>n</i> -pentane (204)	0.98	0.78	0.61
ethyl acetate	88.11	3.2966	3.4967	210.60	4.1937	1.78	<i>n</i> -hexane (205)	0.92	0.61	0.75
propyl acetate	102.1	3.4139	3.7750	219.79	4.5411	1.79	<i>n</i> -heptane (206)	1.19	0.40	1.78
butyl acetate	116.2	3.5083	4.0469	231.92	3.7704	1.84	<i>n</i> -hexane (207)	0.60	0.13	0.70
propyl propionate	116.2	3.5146	4.0268	227.57	4.5048	1.79	<i>n</i> -nonane (206)	1.18	0.70	3.56
diethyl ether	74.12	3.5173	2.9377	215.98	3.7598	1.15	<i>n</i> -pentane (208)	0.61	0.10	1.21
dibutyl ether	130.2	3.7213	4.3492	234.54	2.9182	1.17	<i>n</i> -hexane (209)	0.46	0.12	0.88
Average								0.89	0.53	1.33

^aThe %Absolute Average Deviation (%AAD) of the properties (saturated vapour pressure (P^{sat}), saturated liquid density (ρ^{sat}), heat of vapourisation (h^{vap}). ^a %AAD = $\sum_i^{np} |X_i^{calc} - X_i^{exp}| / |X_i^{exp}|$ where $X_i = P^{sat}, \rho^{sat}$ and h^{vap} .

Table 7-5: Model Parameters for non-self-associating components for sPC-SAFT-JC

	MW [g/mol]	σ [Å]	m	ε/k [K]	x_p	μ [D]	VLE data (ref.)	ΔP^{sat} [%] ^a	$\Delta \rho^{sat}$ [%] ^a	Δh^{vap} [%] ^a
acetone ^b	58.08	3.6028	2.1873	245.49	0.2969	2.72	-	-	-	-
2-butanone	72.11	3.7334	2.3870	259.87	0.2654	2.76	<i>n</i> -heptane (195)	1.26	1.90	2.22
2-pentanone	86.13	3.7500	2.7860	256.87	0.2305	2.77	equation (7-35)	0.85	1.10	3.18
3-pentanone	86.13	3.7468	2.7760	258.75	0.2155	2.82	<i>n</i> -heptane (196)	0.67	1.40	3.21
2-hexanone	100.1	3.7860	3.1491	260.34	0.2153	2.68	equation (7-35)	1.03	1.33	1.36
3-hexanone	100.1	3.7977	3.0975	260.36	0.1877	2.87	equation (7-35)	0.20	0.89	2.07
2-heptanone	114.1	3.8097	3.5428	260.50	0.2016	2.61	equation (7-35)	0.24	1.22	1.68
3-heptanone	114.1	3.7355	3.6881	251.34	0.1739	2.81	equation (7-35)	0.72	0.45	2.00
4-heptanone	114.1	3.8429	3.4347	260.43	0.2197	2.50	equation (7-35)	0.69	1.24	1.11
MIPK	86.13	3.8376	2.6147	253.56	0.2878	2.76	<i>n</i> -octane (197)	2.52	1.04	1.71
MIBK	100.1	3.9338	2.8486	260.11	0.2928	2.67	<i>n</i> -octane (198)	1.22	0.94	2.27
cyclopentanone	84.11	3.8016	2.3203	317.66	0.1926	3.24	<i>n</i> -cyclohexane (199)	0.58	1.50	2.32
cyclohexanone	98.14	4.0195	2.3362	330.74	0.2695	3.09	<i>n</i> -cyclohexane (200)	0.40	1.28	2.44
propanal	58.08	3.6558	2.010	261.77	0.3077	2.52	<i>n</i> -pentane (201)	0.39	1.27	1.62
butanal	72.10	3.7925	2.2513	271.13	0.2626	2.72	<i>n</i> -heptane (201)	0.29	0.99	1.97
pentanal	86.13	3.7403	2.7946	259.52	0.2519	2.57	<i>n</i> -heptane (202)	0.76	0.94	0.57
hexanal	100.1	3.7552	3.188	2.62.37	0.2057	2.58	equation (7-35)	0.77	0.52	1.12
methyl formate	60.05	3.5283	1.8914	241.08	0.7444	1.77	<i>n</i> -hexane (203)	0.53	1.21	2.51
ethyl formate	74.08	3.6570	2.2111	246.49	0.5632	1.93	<i>n</i> -hexane (203)	0.8	0.92	2.64
propyl formate	88.11	3.6829	2.6432	247.24	0.4901	1.91	<i>n</i> -hexane (203)	0.31	0.78	1.94
butyl formate	102.1	3.6728	3.1363	246.62	0.3437	2.02	<i>n</i> -hexane (203)	1.36	0.64	2.12
methyl acetate	74.08	3.5018	2.4676	237.90	0.5862	1.68	<i>n</i> -pentane (204)	0.49	0.95	2.04
ethyl acetate	88.11	3.5418	2.9464	231.15	0.4591	1.78	<i>n</i> -hexane (205)	0.40	0.76	2.11
propyl acetate	102.1	3.6107	3.2966	236.09	0.4131	1.79	<i>n</i> -heptane (206)	0.32	0.72	2.73
butyl acetate	116.2	3.6034	3.8062	239.39	0.2724	1.84	<i>n</i> -hexane (207)	0.23	0.61	0.93
propyl propionate	116.2	3.71744	3.5975	238.51	0.4009	1.79	<i>n</i> -nonane (206)	1.98	2.49	3.74
diethyl ether	74.12	3.58608	2.8041	221.77	0.4874	1.15	<i>n</i> -pentane (208)	0.34	0.34	1.42
dibutyl ether	130.2	3.73823	4.3010	235.68	0.2911	1.17	<i>n</i> -hexane (209)	0.45	0.14	0.94
Average								0.73	1.02	1.99

^aThe %Absolute Average Deviation (%AAD) of the properties (saturated vapour pressure (P^{sat}), saturated liquid density (ρ^{sat}), heat of vapourisation (h^{vap}). ^a %AAD = $\sum_i^{np} |X_i^{calc} - X_i^{exp}| / |X_i^{exp}|$ where $X_i = P^{sat}, \rho^{sat}$ and h^{vap} .

Although the model parameters presented by Dominik *et al.* (191) for Polar PC-SAFT could be used with sPC-SAFT-JC, it was found that most of the parameters did not perform well for the systems investigated in this work and consequently the parameters were re-determined to ensure a fair comparison between the models. The existing ketone parameters for Polar-PC-SAFT have been determined by Sauer and Chapman (190), but they showed that BIPs were required to model

simple ketone/alkane systems with the parameters they determined. Consequently, the newly determined model parameters for the ketones are used, because the author is of the opinion that sPC-SAFT-JC should be able to predict the VLE of simple ketone/alkane systems accurately without relying on BIPs. The acetone parameters determined by Tumakaka and Sadowski (43) provide good VLE predictions and will be used throughout this study for sPC-SAFT-JC. The pure component model parameters used for sPC-SAFT were taken from Gross and Sadowski (24).

With respect to sPC-SAFT-GV, the n_p parameters are significantly larger than 1 for all components, indicating a larger polar contribution in the model. Figure 7-2 shows the respective contributions to the reduced chemical potential of 2-butanone for sPC-SAFT-GV and sPC-SAFT-GV-Lit ($n_p = 1$) (54).

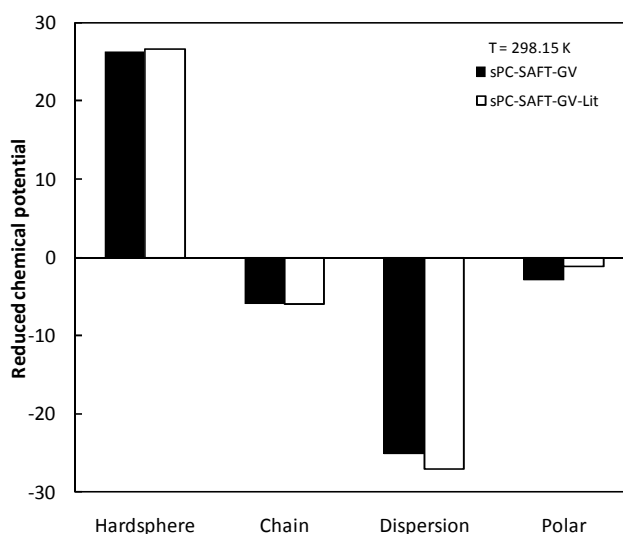


Figure 7-2: Contributions to the reduced chemical potential of 2-butanone at $T = 298.15$ K. The new parameters dramatically increase the polar contribution compared to the contribution of literature parameters.

From Figure 7-2, the polar contribution with the new model parameters is more than double compared to the polar contribution when $n_p = 1$. Furthermore, from Table 1 and Table 2, it is clear that the pure component properties are well correlated with the new model parameters and that no significant trade-off occurs as a result of including binary VLE data in the regression function.

With respects to Polar PC-SAFT, Sauer and Chapman (190) and Dominik *et al.* (191) showed that there is a relationship between the fraction of polar segments and the segment number between the sequential members in a homologous series: the product of x_p and m seems to stay constant. Similar ideas were used here to develop the following relations that provide good estimates of n_p and x_p :

$$n_p = \frac{K \cdot (A \cdot M_w + B)}{\mu^2} \quad (7-34)$$

$$x_p = \frac{K}{(A \cdot M_w + B) \cdot \mu^2} \quad (7-35)$$

Essentially, K is a constant for a homologous series and $A \cdot M_w + B = m$. The constants for the respective molecular groups are given in Table 7-6 for n_p and Table 7-7 for x_p . Since access to good VLE data for only two mono-ethers was possible, no correlation constants are given for the mono ether group.

Table 7-6: n_p (number of polar segments in sPC-SAFT-GV) prediction constants

Group	K	A	B
Aldehydes	4.1041	0.02375	1.1414
Ketones	4.4208	0.02258	1.3821
Cyclic and branched ketones	5.4339	0.01038	2.0859
Esters	3.6697	0.02364	1.2880

Table 7-7: x_p (fraction of polar segments in sPC-SAFT-JC) prediction constants

Group	K	A	B
Aldehydes	4.2199	0.02605	0.47538
Ketones	4.9316	0.02871	0.47537
Cyclic and branched ketones	5.6899	0.00915	1.73750
Esters	4.3399	0.03182	-0.01459

7.3.3 New model parameters for CPA

Similar to the model parameters for sPC-SAFT-JC and sPC-SAFT-GV, model parameters are also presented for CPA-GV in Table 7-8 and for CPA-JC in Table 7-9. In addition to binary VLE data, only saturated vapour pressure and liquid density data were included in the parameter regression of CPA-JC and CPA-GV. Heat of vapourization data was omitted in the regression, because the %AAD values in pressure and density typically exceeded 1% when included.

Table 7-8: Model Parameters for CPA-GV.

	T_C [K]	$a0/Rb$ [K]	b [L/mol]	cI	n_p	μ [D]	VLE data (ref.)	ΔP^{sat} [%] ^a	$\Delta \rho^{sat}$ [%] ^a
acetone	508.2	2342.74	0.0581035	0.69575	0.4541	2.88	<i>n</i> -hexane (194)	0.73	1.63
2-butanone	535.5	2520.05	0.0737249	0.77373	0.5682	2.76	<i>n</i> -heptane (195)	0.42	1.60
3-pentanone	560.9	2701.31	0.0894959	0.85416	0.5750	2.82	<i>n</i> -heptane (196)	0.28	1.02
MIPK	553.4	2513.23	0.0887316	0.82519	0.7325	2.76	<i>n</i> -octane (197)	2.02	1.78
MIBK	574.6	2700.91	0.1052501	0.85113	0.8838	2.67	<i>n</i> -octane (198)	1.87	0.82
propanal	504.4	2312.14	0.0569882	0.69885	0.5256	2.52	<i>n</i> -hexane (203)	0.44	0.98
butanal	537.2	2562.04	0.0732788	0.74094	0.5195	2.72	<i>n</i> -hexane (203)	0.83	0.62
pentanal	566.1	2648.26	0.0890874	0.84755	0.7684	2.57	<i>n</i> -hexane (203)	0.43	0.81
methyl formate	487.2	2151.77	0.0466299	0.68662	0.9500	1.77	<i>n</i> -pentane (204)	0.53	0.91
ethyl formate	508.4	2263.68	0.0630809	0.74903	1.0734	1.93	<i>n</i> -hexane (205)	0.22	1.14
propyl formate	538.0	2455.02	0.0789729	0.83393	1.2883	1.91	<i>n</i> -heptane (206)	1.25	0.74

	T_C [K]	$a0/Rb$ [K]	b [L/mol]	cI	n_p	μ [D]	VLE data (ref.)	ΔP^{sat} [%] ^a	$\Delta \rho^{sat}$ [%] ^a
butyl formate	559.0	2649.21	0.0967047	0.92012	1.2724	2.02	<i>n</i> -hexane (207)	0.52	0.80
methyl acetate	506.6	2291.67	0.0621704	0.79024	1.3785	1.68	<i>n</i> -nonane (206)	0.38	0.96
ethyl acetate	523.3	2404.61	0.0791189	0.88067	1.4856	1.78	<i>n</i> -hexane (203)	0.70	0.86
propyl acetate	549.7	2597.21	0.0964396	0.93973	1.6321	1.79	<i>n</i> -hexane (203)	1.13	0.77
butyl acetate	575.4	2825.61	0.1150490	1.01055	1.4477	1.84	<i>n</i> -hexane (203)	0.96	0.73
propyl propionate	568.6	2776.06	0.1140997	0.99538	1.6563	1.79	<i>n</i> -hexane (203)	0.97	0.75
diethyl ether	466.7	2312.08	0.0815527	0.82466	1.6352	1.15	<i>n</i> -pentane (208)	0.83	0.67
dibutyl ether	584.1	2988.11	0.1508453	1.06679	1.6604	1.17	<i>n</i> -hexane (209)	0.50	0.67
Average								0.79	0.96

^aThe %Absolute Average Deviation (%AAD) of the properties (saturated vapour pressure (P^{sat}), saturated liquid density (ρ^{sat}), heat of vapourisation (h^{vap}). ^a %AAD = $\sum_i^{np} |X_i^{calc} - X_i^{exp}| / |X_i^{exp}|$ where $X_i = P^{sat}, \rho^{sat}$

Table 7-9: Model Parameters for CPA-JC.

	T_C [K]	$a0/Rb$ [K]	b [L/mol]	cI	x_p	μ [D]	VLE data (ref.)	ΔP^{sat} [%] ^a	$\Delta \rho^{sat}$ [%] ^a
acetone	508.2	2176.52	0.0626852	0.73278	0.6700	2.88	<i>n</i> -hexane (194)	0.70	1.64
2-butanone	535.5	2413.61	0.0786549	0.79914	0.8000	2.76	<i>n</i> -heptane (195)	0.47	1.68
3-pentanone	560.9	2632.06	0.0936058	0.86633	0.7851	2.82	<i>n</i> -heptane (196)	0.24	1.17
MIPK	553.4	2451.56	0.0931746	0.85124	0.9500	2.76	<i>n</i> -octane (197)	0.99	0.54
MIBK	574.6	2610.28	0.1141075	0.88449	1.1982	2.67	<i>n</i> -octane (198)	2.35	2.78
propanal	504.4	2188.46	0.0612351	0.72867	0.7547	2.52	<i>n</i> -pentane (201)	0.47	0.97
butanal	537.2	2486.41	0.0771915	0.75545	0.7120	2.72	<i>n</i> -heptane (201)	0.74	0.61
pentanal	566.1	2575.66	0.0940306	0.86640	1.0382	2.57	<i>n</i> -heptane (202)	0.43	0.84
methyl formate	487.2	1953.62	0.0508512	0.73350	1.4500	1.77	<i>n</i> -hexane (203)	0.29	0.77
ethyl formate	508.4	2159.87	0.0676821	0.78554	1.4810	1.93	<i>n</i> -hexane (203)	0.80	0.66
propyl formate	538.0	2365.26	0.0840005	0.85905	1.7773	1.91	<i>n</i> -hexane (203)	1.16	0.61
butyl formate	559.0	2588.32	0.1022199	0.93402	1.7107	2.02	<i>n</i> -hexane (203)	0.68	1.54
methyl acetate	506.6	2169.62	0.0671809	0.83190	1.9551	1.68	<i>n</i> -pentane (204)	0.39	0.88
ethyl acetate	523.3	2313.77	0.0843720	0.91598	2.0261	1.78	<i>n</i> -hexane (205)	0.82	0.84
propyl acetate	549.7	2530.92	0.1013952	0.96305	2.1700	1.79	<i>n</i> -heptane (206)	1.14	0.79
butyl acetate	575.4	2803.26	0.1184371	1.01500	1.8354	1.84	<i>n</i> -hexane (207)	0.84	0.78
propyl propionate	568.6	2740.90	0.1179603	1.00274	2.1425	1.79	<i>n</i> -nonane (206)	1.10	0.85
diethyl ether	466.7	2299.72	0.0831251	0.82606	2.0660	1.15	<i>n</i> -pentane (208)	0.74	0.56
dibutyl ether	584.1	2976.50	0.1514936	1.064805	2.4182	1.17	<i>n</i> -hexane (209)	0.46	0.66
Average								0.78	1.0

^aThe %Absolute Average Deviation (%AAD) of the properties (saturated vapour pressure (P^{sat}), saturated liquid density (ρ^{sat}), heat of vapourisation (h^{vap}). ^a %AAD = $\sum_i^{np} |X_i^{calc} - X_i^{exp}| / |X_i^{exp}|$ where $X_i = P^{sat}, \rho^{sat}$

Predictive correlations for the n_p parameter of CPA-GV and the x_p parameters of CPA-JC, similar to equations (2-33) and (2-34), could not be developed with the same accuracy as for sPC-SAFT-GV and sPC-SAFT-JC. Common trends between components in a homologous series is observed: the co-volume parameter (b) and energy parameters (a_0) increase with molecular size and is consistent with trends observed in previous CPA parameter studies (8; 37).

7.4 Non-polar/Polar (non-HB) systems

In this section, the polar CPA- and sPC-SAFT-based models are mainly applied to VLE calculations of alkane/polar mixtures. Excess enthalpies and excess volumes are also investigated with the models to a limited extent. Generally, second-order properties are not predicted with good accuracy, because the shortcomings identified in Chapter 3 and Chapter 4 regarding the description of physical interactions (repulsive and dispersive) have not been improved. Therefore, only a few representative examples are shown with sPC-SAFT-based models to illustrate the influence of the polar terms on some second-order properties.

7.4.1 Vapour-liquid equilibria

The VLE of several polar/alkane systems have been investigated. A summary of the results are presented in Table 7-10 for sPC-SAFT, sPC-SAFT-GV and sPC-SAFT-JC. Results for the CPA-based models are shown in Table 7-11:

Table 7-10: VLE predictions of polar-*n*-alkane mixtures with sPC-SAFT, sPC-SAFT-GV and sPC-SAFT-JC

Mixture	T or P	sPC-SAFT		sPC-SAFT-GV		sPC-SAFT-JC		n_p	ref.
		Δy ($\times 10^2$) ^a	$\frac{\Delta P(\%)^b}{\Delta T(K)^a}$	Δy ($\times 10^2$) ^a	$\frac{\Delta P(\%)^b}{\Delta T(K)^a}$	Δy ($\times 10^2$) ^a	$\frac{\Delta P(\%)^b}{\Delta T(K)^a}$		
acetone/ <i>n</i> -pentane	298.15 K	8.13	19.5	1.11	2.47	0.97	1.39	14	(210)
acetone/ <i>n</i> -hexane	313.15 K	10.5	22.6	0.90	1.30	1.22	1.31	27	(194)
acetone/ <i>n</i> -heptane	313.15 K	7.05	22.3	0.68	1.55	0.75	1.67	16	(194)
acetone/ <i>n</i> -octane	313.15 K	4.77	20.9	0.26	1.58	0.41	2.49	21	(194)
2-butanone/ <i>n</i> -hexane	333.15 K	7.83	15.6	0.40	0.69	1.09	1.11	12	(211)
2-butanone/ <i>n</i> -heptane	318.15 K	7.86	14.2	0.47	0.60	0.78	1.69	18	(195)
3-pentanone/ <i>n</i> -heptane	353.15 K	4.60	9.08	0.44	0.45	1.06	0.56	17	(196)
MIPK/ <i>n</i> -octane	1.013 bar	4.48	4.00	0.33	0.15	0.61	0.55	31	(197)
MIPK/ <i>n</i> -cyclohexane	1.013 bar	6.18	4.44	0.44	0.14	0.60	0.33	31	(197)
MIBK/ <i>n</i> -heptane	343.15 K	4.52	10.63	0.47	0.82	0.94	1.32	15	(195)
MIBK/ <i>n</i> -octane	0.94 bar	5.30	4.40	0.66	0.25	0.51	0.10	21	(198)
MIBK/cyclohexane	0.8 bar	4.56	4.36	1.58	0.31	1.90	0.43	14	(212)
cyclopentanone/cyclohexane	313.15 K	3.32	16.9	0.74	3.64	0.70	4.50	21	(199)
cyclohexanone/cyclohexane	323.15 K	3.58	21.7	0.69	2.42	0.26	1.31	13	(200)
propanal/ <i>n</i> -pentane	313.15 K	8.70	15.0	2.60	1.31	3.31	1.72	26	(201)

Mixture	<i>T</i> or <i>P</i>	sPC-SAFT		sPC-SAFT-GV		sPC-SAFT-JC		<i>np</i>	ref.
		Δy ($\times 10^2$) ^a	$\frac{\Delta P(\%)^b}{\Delta T(K)^a}$	Δy ($\times 10^2$) ^a	$\frac{\Delta P(\%)^b}{\Delta T(K)^a}$	Δy ($\times 10^2$) ^a	$\frac{\Delta P(\%)^b}{\Delta T(K)^a}$		
butanal/ <i>n</i> -heptane	318.15 K	4.92	13.1	0.44	1.54	0.80	0.67	19	(201)
pentanal/ <i>n</i> -heptane	348.15 K	4.42	12.0	0.53	2.02	0.97	1.73	11	(202)
methyl formate/ <i>n</i> -hexane	1.013 bar	9.63	7.11	2.04	0.73	2.75	0.44	25	(203)
methyl formate/ <i>n</i> -heptane	1.013 bar	10.3	10.1	1.65	2.17	1.70	1.78	36	(213)
ethyl formate/ <i>n</i> -hexane	1.013 bar	8.07	5.26	0.74	0.43	0.44	0.14	32	(203)
ethyl formate/ <i>n</i> -heptane	1.013 bar	8.68	7.22	1.14	0.77	0.94	0.33	34	(214)
ethyl formate/ <i>n</i> -octane	1.013 bar	4.82	8.31	1.16	1.63	0.72	0.83	38	(214)
ethyl formate/ <i>n</i> -nonane	1.013 bar	6.98	10.3	0.34	0.95	1.10	1.10	31	(214)
ethyl formate/ <i>n</i> -decane	1.013 bar	4.51	11.6	2.46	2.98	1.27	0.86	27	(214)
propyl formate/ <i>n</i> -hexane	1.013 bar	5.69	4.37	0.51	0.31	0.35	0.11	26	(203)
propyl formate/ <i>n</i> -heptane	1.013 bar	4.13	4.94	0.98	0.56	0.30	0.37	26	(215)
propyl formate/ <i>n</i> -nonane	1.013 bar	5.20	7.71	1.09	1.63	0.36	0.93	27	(215)
butyl formate/ <i>n</i> -hexane	1.013 bar	4.77	3.19	1.13	0.15	1.24	0.26	25	(203)
methyl acetate/ <i>n</i> -pentane	298.15 K	7.63	16.2	0.93	1.50	0.26	1.04	19	(204)
methyl acetate/ <i>n</i> -heptane	1.013 bar	5.84	6.13	1.5	1.17	0.59	0.54	25	(213)
ethyl acetate/ <i>n</i> -hexane	1.013 bar	5.36	4.38	0.59	0.22	0.24	0.10	22	(205)
ethyl acetate/ <i>n</i> -heptane	323.15 K	4.85	12.8	0.86	1.32	0.47	0.75	19	(216)
ethyl acetate/ <i>n</i> -heptane	343.15 K	4.33	11.9	0.79	1.07	0.35	0.33	19	(216)
ethyl acetate/ <i>n</i> -octane	1.013 bar	5.37	5.07	0.82	0.97	0.55	0.59	18	(217)
propyl acetate/ <i>n</i> -heptane	1.013 bar	3.57	3.20	0.54	0.15	0.63	0.15	32	(206)
propyl acetate/ <i>n</i> -nonane	1.013 bar	2.99	3.65	1.03	0.82	1.06	0.71	31	(206)
butyl acetate/ <i>n</i> -hexane	1.013 bar	1.77	2.51	0.36	0.15	0.32	0.15	25	(207)
propyl propionate/ <i>n</i> -heptane	1.013 bar	2.29	2.08	0.76	0.30	1.20	0.48	34	(206)
propyl propionate/ <i>n</i> -nonane	1.013 bar	2.40	2.43	1.01	0.22	1.08	0.30	42	(206)
diethyl ether/ <i>n</i> -pentane	1.013 bar	0.87	0.69	0.39	0.07	0.40	0.072	14	(208)
diethyl ether/ <i>n</i> -hexane	1.013 bar	1.33	1.22	0.53	0.34	0.56	0.36	16	(208)
Average		5.29	9.15	0.86	1.00	0.86	0.87		

^a $\Delta z = \sum_i^{np} |z_i^{calc} - z_i^{exp}|$ where *z* represents *y* or *T* and *np* is the number of data points. ^b Deviations as %AAD.

Clearly, from Table 7-10, very good predictions are obtained without BIPs by both sPC-SAFT-GV and sPC-SAFT-JC. The pure component parameters of the polar species were fitted to pure component data and one binary VLE set, where the second component was non-polar. These parameters do not only provide good predictions for the binary system included in the regression routine, but also for all other VLE systems investigated. This indicates that the parameters correctly capture the influence of the respective forces and are not system-specific. It will be shown in subsequent sections that sPC-SAFT-GV and sPC-SAFT-JC perform similarly in predicting VLE.

Table 7-11 shows results for VLE systems investigated with the CPA-type models.

Table 7-11: VLE predictions of polar-*n*-alkane mixtures with CPA, CPA-GV and CPA-JC

Mixture	<i>T</i> or <i>P</i>	CPA		CPA-GV		CPA-JC		<i>np</i>	ref.
		Δy ($\times 10^2$) ^a	$\frac{\Delta P(\%)^b}{\Delta T(K)^a}$	Δy ($\times 10^2$) ^a	$\frac{\Delta P(\%)^b}{\Delta T(K)^a}$	Δy ($\times 10^2$) ^a	$\frac{\Delta P(\%)^b}{\Delta T(K)^a}$		
acetone/ <i>n</i> -pentane	298.15 K	8.38	20.5	1.25	2.27	0.70	1.02	14	(210)
acetone/ <i>n</i> -hexane	313.15 K	10.4	22.9	2.26	2.80	1.28	1.45	27	(194)
acetone/ <i>n</i> -heptane	313.15 K	6.85	22.1	1.57	4.17	0.76	2.61	16	(194)
acetone/ <i>n</i> -octane	313.15 K	4.50	20.6	0.91	5.91	0.39	3.00	21	(194)
2-butanone/ <i>n</i> -hexane	333.15 K	6.59	14.2	1.06	1.69	0.75	1.30	12	(211)
2-butanone/ <i>n</i> -heptane	318.15 K	7.63	14.4	1.13	2.04	0.52	1.08	18	(195)
3-pentanone/ <i>n</i> -heptane	353.15 K	6.37	13.5	0.58	0.52	0.30	0.36	17	(196)
MIPK/ <i>n</i> -octane	1.013 bar	4.40	3.91	0.79	0.52	0.53	0.67	31	(197)
MIPK/ <i>n</i> -cyclohexane	1.013 bar	6.38	4.74	0.47	0.33	0.65	0.25	31	(197)
MIBK/ <i>n</i> -heptane	343.15 K	4.47	10.8	0.92	1.16	0.47	0.71	15	(195)
MIBK/ <i>n</i> -octane	0.94 bar	5.19	5.30	0.64	0.16	0.56	0.10	21	(198)
MIBK/cyclohexane	0.8 bar	4.55	4.52	1.79	0.24	1.90	0.43	14	(212)
propanal/ <i>n</i> -pentane	313.15 K	7.99	16.9	1.75	1.18	1.37	0.67	26	(201)
butanal/ <i>n</i> -heptane	318.15 K	4.61	12.4	0.92	1.17	0.58	0.64	19	(201)
pentanal/ <i>n</i> -heptane	348.15 K	4.40	12.2	1.11	0.93	0.82	1.07	11	(202)
methyl formate/ <i>n</i> -hexane	1.013 bar	9.50	7.06	4.05	0.91	2.85	0.51	25	(203)
methyl formate/ <i>n</i> -heptane ^b	1.013 bar	9.86	9.72	2.21	1.34	1.65	1.77	36	(213)
ethyl formate/ <i>n</i> -hexane	1.013 bar	8.17	5.48	0.81	0.30	0.37	0.14	32	(203)
ethyl formate/ <i>n</i> -heptane	1.013 bar	8.57	7.26	1.33	0.60	1.09	0.51	34	(214)
ethyl formate/ <i>n</i> -octane	1.013 bar	4.65	8.12	1.07	1.11	1.01	1.00	38	(214)
ethyl formate/ <i>n</i> -nonane	1.013 bar	6.50	9.79	0.98	1.39	0.65	0.85	31	(214)
ethyl formate/ <i>n</i> -decane	1.013 bar	3.77	10.3	1.93	2.77	2.21	2.78	27	(214)
propyl formate/ <i>n</i> -hexane	1.013 bar	5.77	4.63	0.47	0.17	0.29	0.15	26	(203)
propyl formate/ <i>n</i> -heptane	1.013 bar	4.10	5.07	0.68	0.27	0.58	0.34	26	(215)
propyl formate/ <i>n</i> -nonane	1.013 bar	4.77	7.34	0.59	0.64	0.73	0.95	27	(215)
butyl formate/ <i>n</i> -hexane	1.013 bar	5.03	3.57	1.03	0.26	1.03	0.22	25	(203)
methyl acetate/ <i>n</i> -pentane	298.15 K	7.57	17.2	0.39	1.05	0.47	1.25	19	(204)
methyl acetate/ <i>n</i> -heptane	1.013 bar	5.45	5.95	1.02	0.82	1.12	0.87	25	(213)
ethyl acetate/ <i>n</i> -hexane	1.013 bar	5.75	4.83	0.49	0.16	0.35	0.12	22	(205)
ethyl acetate/ <i>n</i> -heptane	323.15 K	5.05	13.8	0.88	1.62	0.80	1.27	19	(216)
ethyl acetate/ <i>n</i> -heptane	343.15 K	4.55	12.8	0.64	0.90	0.65	0.73	19	(216)
ethyl acetate/ <i>n</i> -octane	1.013 bar	5.55	5.22	0.39	0.52	0.47	0.65	18	(217)
propyl acetate/ <i>n</i> -heptane	1.013 bar	3.81	3.48	0.63	0.22	0.51	0.15	32	(206)
propyl acetate/ <i>n</i> -nonane	1.013 bar	3.01	3.69	1.27	0.96	1.16	0.86	31	(206)
butyl acetate/ <i>n</i> -hexane	1.013 bar	1.85	2.80	0.45	0.19	0.44	0.18	25	(207)
propyl propionate/ <i>n</i> -heptane	1.013 bar	2.43	2.55	0.84	0.30	0.82	0.32	34	(206)
propyl propionate/ <i>n</i> -nonane	1.013 bar	2.60	2.71	1.12	0.22	1.10	0.21	42	(206)
diethyl ether/ <i>n</i> -pentane	1.013 bar	0.94	0.88	0.41	0.13	0.41	0.13	14	(208)
diethyl ether/ <i>n</i> -hexane	1.013 bar	1.34	1.37	0.49	0.30	0.49	0.32	16	(208)

Mixture	<i>T</i> or <i>P</i>	CPA		CPA-GV		CPA-JC		<i>np</i>	ref.
		Δy (x10 ²) ^a	$\frac{\Delta P(\%)}{\Delta T(K)}$ ^b	Δy (x10 ²) ^a	$\frac{\Delta P(\%)}{\Delta T(K)}$ ^b	Δy (x10 ²) ^a	$\frac{\Delta P(\%)}{\Delta T(K)}$ ^b		
dibutyl ether/ <i>n</i> -hexane	308.15 K	0.19	1.80	0.16	0.17	0.27	1.04	14	(209)
Average		5.33	8.91	1.04	1.06	0.83	0.82		

^a $\Delta z = \sum_i^{np} |z_i^{calc} - z_i^{exp}|$ where *z* represents *y* or *T* and *np* is the number of data points. ^b Deviations as %AAD.

Similar results are obtained with the polar CPA-type models compared to the sPC-SAFT-type models: major improvement is obtained with CPA-GV and CPA-JC compared to CPA. Unfortunately, similar liquid-liquid-demixing problems were encountered with CPA-GV as reported by Al-Saifi *et al.* (35) for PC-SAFT-GV. CPA-GV predicted false liquid-liquid-demixing for the methyl formate/*n*-heptane system at *P* = 1.013 bar. The error is easily corrected with a small BIP (CPA-GV k_{ij} = -0.009). False liquid-liquid demixing was not observed for any of the other systems with either CPA-JC or CPA-GV, but it is suspected that at lower temperatures, both models may predict false liquid-liquid splits. These problems seem to be common to the JC and GV theories, even when incorporated into PC-SAFT. The CPA-JC and CPA-GV models do, however, provide very good VLE predictions for a wide range of system over extensive conditions and therefore, are still very useful.

In the following subsection, graphical results are presented for some of the different polar groups with alkanes. In most instances, graphical results of the sPC-SAFT-based models and the CPA-based models are presented on separate figures. Furthermore, the predictions of sPC-SAFT-GV-Lit are also presented on some figures to indicate model predictions with $n_p = 1$. These parameters were taken from Gross and Vrabec (54).

i) alkane/ketone systems

Figure 7-3 and Figure 7-4 show VLE predictions of the acetone/*n*-hexane system at *T* = 313.15 K for the sPC-SAFT-based and CPA-based models respectively.

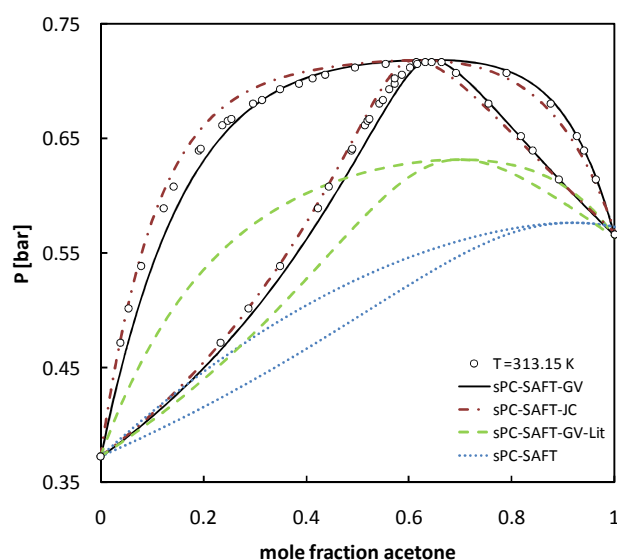


Figure 7-3: Isothermal VLE predictions of the acetone/n-hexane system at $T = 313.15$ K sPC-SAFT-GV, sPC-SAFT-JC, sPC-SAFT-GV-Lit and sPC-SAFT. Experimental data taken from ref.(194).

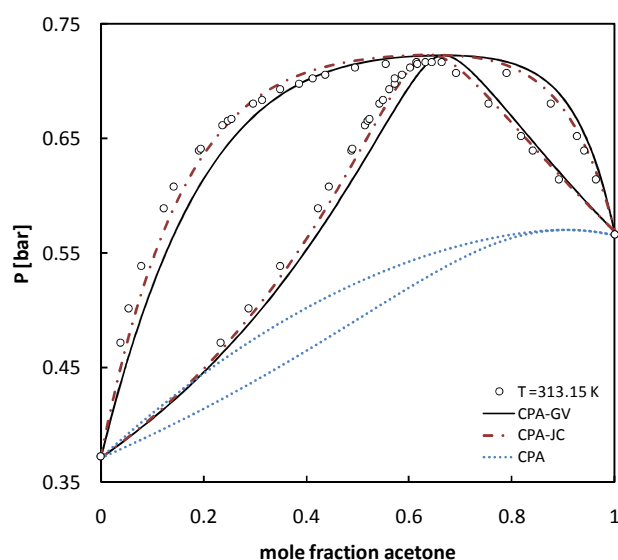


Figure 7-4: Isothermal VLE predictions of the acetone/n-hexane system at $T = 313.15$ K with CPA-GV, CPA-JC and CPA. Experimental data taken from ref. (194).

From Figure 7-3, both sPC-SAFT-GV and sPC-SAFT-JC provide similar VLE predictions that are accurate without BIPs. The VLE prediction of sPC-SAFT-GV-Lit, where $n_p = 1$, clearly does not have the correct contributions of each term in the state function. The *unlike* interactions are overestimated by sPC-SAFT-GV-Lit, because the dispersive contribution is too large and the polar contribution is too small. Large improvements are obtained compared to the original sPC-SAFT EOS.

Similar observations are made for CPA-GV and CPA-JC in Figure 7-4. Both models yield accurate predictions that are superior to the original CPA EOS. Furthermore, the predictions of sPC-SAFT-GV and CPA-GV are similar and the predictions of sPC-SAFT-JC and CPA-JC are similar.

VLE predictions for the MIPK/*n*-octane system with sPC-SAFT-based models are presented Figure 7-5, and in Figure 7-6, predictions with the CPA-based models are shown. The model parameters for both sPC-SAFT-GV and sPC-SAFT-JC were fitted by including MIPK/*n*-octane data in the regression procedure. These parameters also provide good VLE predictions for the MIPK/cyclohexane system, as shown in Figure 7-7. Similarly, in Figure 7-8, CPA-GV and CPA-JC also predict the VLE of the MIPK/cyclohexane system accurately. This indicates that the parameters for the various polar models are not system specific, but capture the behaviour of the polar components more accurately than the original versions of the models.

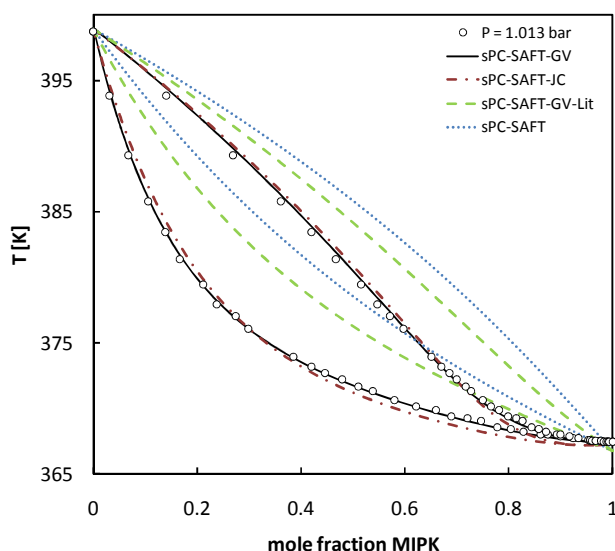


Figure 7-5: Isobaric VLE predictions of the MIPK (methyl isopropyl ketone)/n-octane system at $P = 1.013$ bar with *sPC-SAFT-GV*, *sPC-SAFT-JC*, *sPC-SAFT-GV-Lit* and *sPC-SAFT*. Experimental data taken from ref. (197).

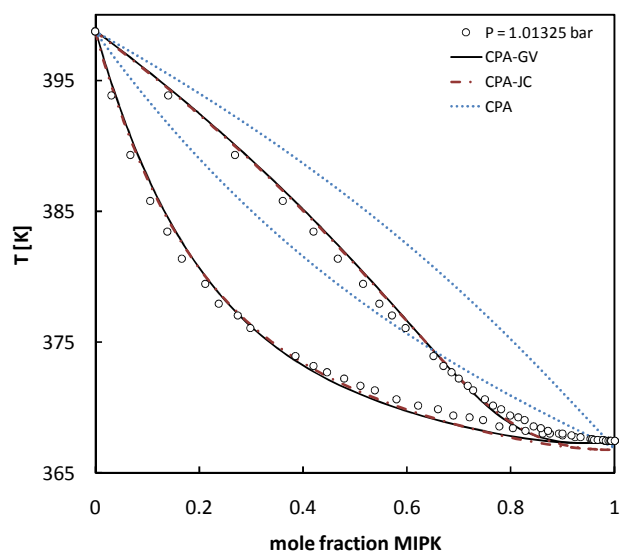


Figure 7-6: Isobaric VLE predictions of the MIPK (methyl isopropyl ketone)/n-octane system at $P = 1.01325$ bar with *CPA-GV*, *CPA-JC* and *CPA*. Experimental data taken from ref. (197).

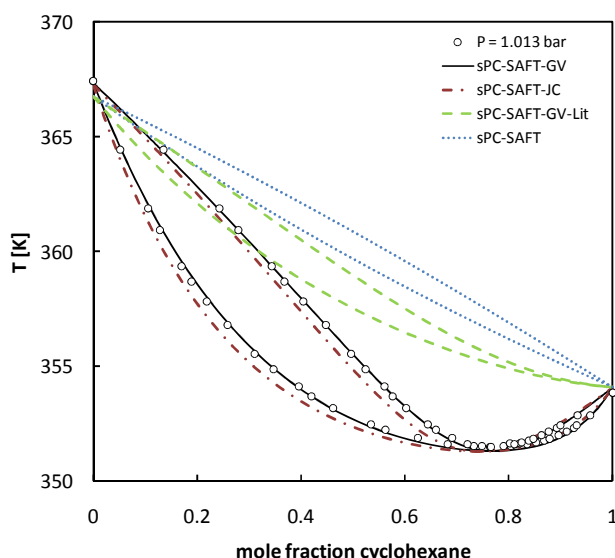


Figure 7-7: Isobaric VLE predictions of the cyclohexane/MIPK (methyl isopropyl ketone) system at $P = 1.013$ bar with *sPC-SAFT-GV*, *sPC-SAFT-JC*, *sPC-SAFT-GV-Lit* and *sPC-SAFT*. Experimental data taken from ref. (197).

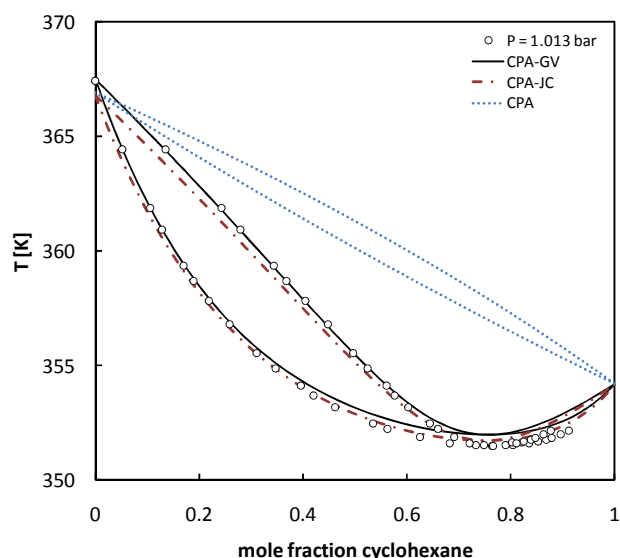


Figure 7-8: Isobaric VLE predictions of the cyclohexane/MIPK (methyl isopropyl ketone) system at $P = 1.013$ bar with *CPA-GV*, *CPA-JC*, *CPA-GV-Lit* and *CPA*. Experimental data taken from ref. (197).

Unfortunately, in some systems, very small BIPs are still required to obtain very accurate VLE representation of the data. The VLE predictions (Figure 7-9 and Figure 7-10) and corresponding correlations (Figure 7-11 and Figure 7-12) of the 2-butanone/cyclohexane system at $T = 323.15$ K are shown below:

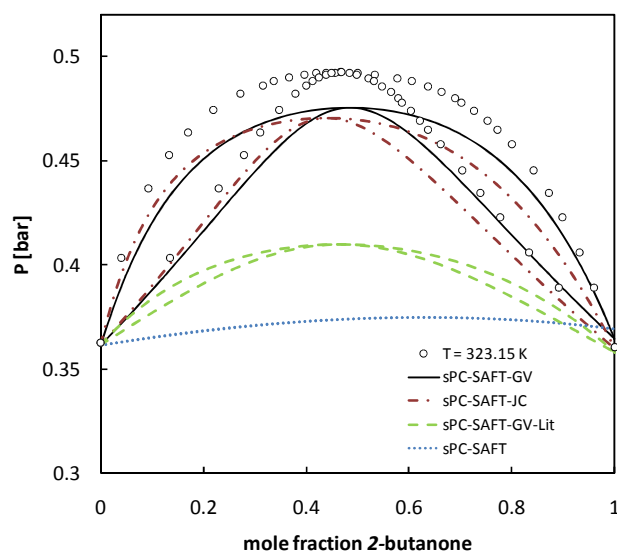


Figure 7-9: Isothermal VLE predictions of the 2-butanone/cyclohexane system at $T = 323.15$ K with sPC-SAFT-GV, sPC-SAFT-JC, sPC-SAFT-GV-Lit and sPC-SAFT. Experimental data taken from ref. (218).

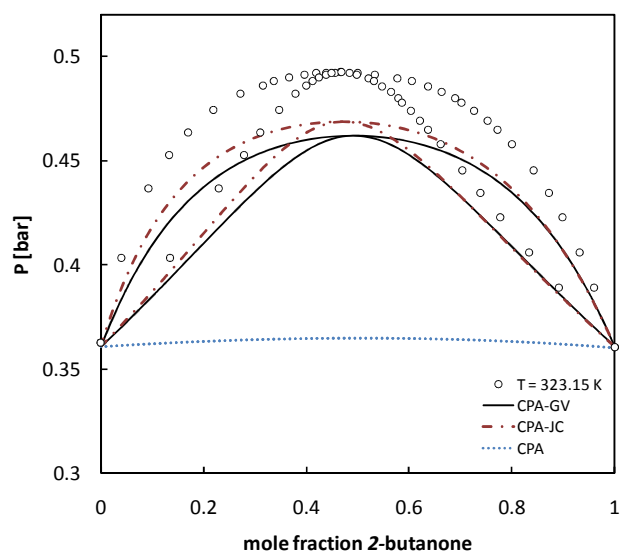


Figure 7-10: Isothermal VLE predictions of the 2-butanone/cyclohexane system at $T = 323.15$ K with CPA-GV, CPA-JC and CPA. Experimental data taken from ref. (218).

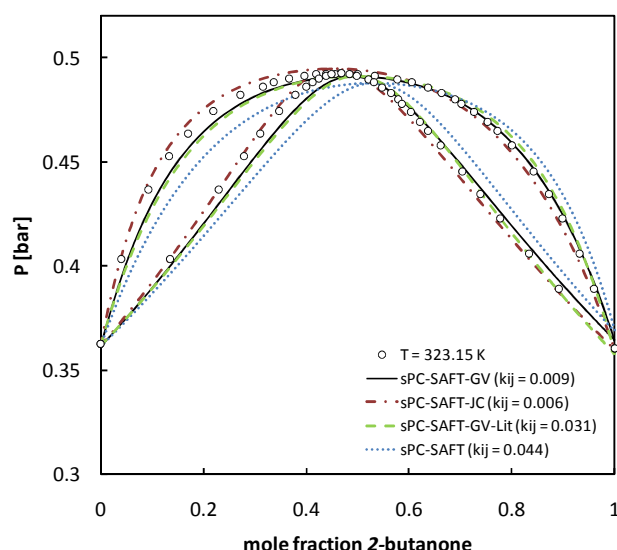


Figure 7-11: Isothermal VLE correlations of the 2-butanone/cyclohexane system at $T = 323.15$ K with sPC-SAFT-GV, sPC-SAFT-JC, sPC-SAFT-GV-Lit and sPC-SAFT. Experimental data taken from ref. (218).

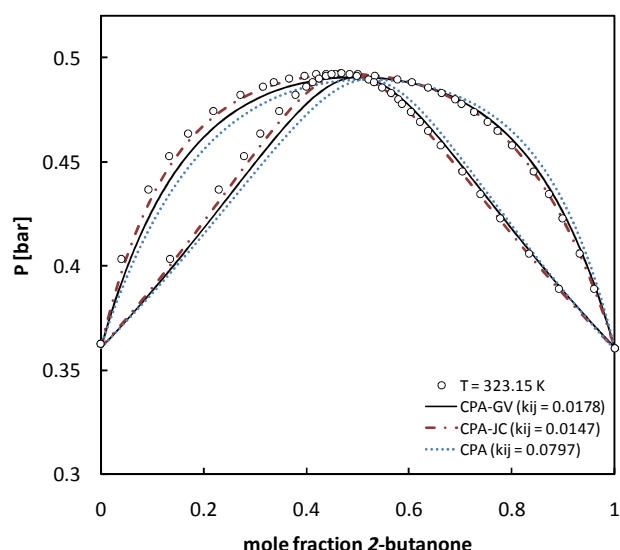


Figure 7-12: Isothermal VLE correlations of the 2-butanone/cyclohexane system at $T = 323.15$ K with CPA-GV, CPA-JC and CPA. Experimental data taken from ref. (218).

From Figure 7-9 and Figure 7-10, it is clear that the polar versions of both sPC-SAFT and CPA perform similarly and provide improved VLE predictions compared to the original sPC-SAFT and CPA models. However, the predictions with sPC-SAFT-GV, sPC-SAFT-JC, CPA-GV and CPA-JC still require small BIPs to obtain accurate representation of the data, as shown in Figure 7-11 and Figure 7-12. These BIPs are, however, very small (sPC-SAFT-JC = 0.006, sPC-SAFT-GV = 0.009, CPA-JC = 0.0147, CPA-GV = 0.0178, sPC-SAFT = 0.044, CPA = 0.0797).

Figure 7-13 shows the VLE results for the 2-hexanone/*n*-nonane system for the sPC-SAFT-based models. It should be mentioned that only the liquid phase mole fraction and the saturation

temperature were measured experimentally by Siimer *et al.* (219), while the vapour phase mole fraction were determined with the Margules model. Both sPC-SAFT-GV and sPC-SAFT-JC provide good representations of the experimental data. The model parameters of 2-hexanone were determined by calculating n_p and x_p from equations (7-34) and (7-35), respectively. The other parameters (σ , m and ε/k) were regressed from pure component data. This shows that equations (7-34) and (7-35) provide fairly good estimates for n_p and x_p .

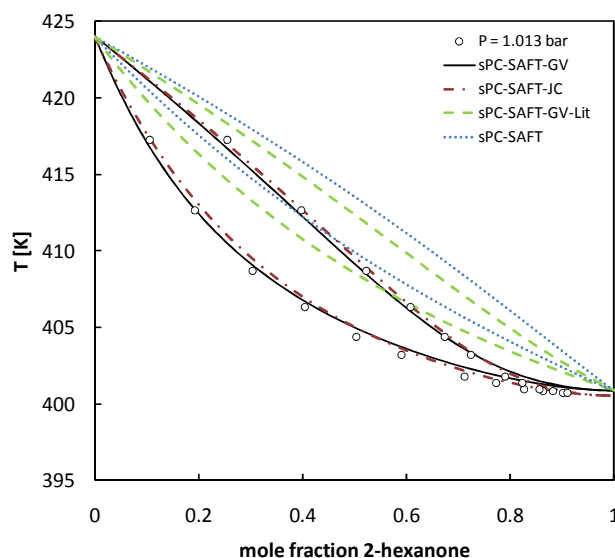


Figure 7-13: Isobaric VLE predictions of the 2-hexanone/*n*-nonane system at $P = 1.013$ bar with sPC-SAFT-GV, sPC-SAFT-JC, sPC-SAFT-GV-Lit and sPC-SAFT. Experimental data taken from ref. (219).

ii) alkane/aldehyde systems

The VLE of butanal and *n*-heptane is well predicted by both sPC-SAFT-GV and sPC-SAFT-JC, as shown in Figure 7-14, while the performance of sPC-SAFT-GV-Lit and sPC-SAFT is rather poor. Figure 7-15 shows that CPA-GV and CPA-JC also provides good predictions of the system. Generally, the performance of sPC-SAFT-GV, sPC-SAFT-JC, CPA-GV and CPA-JC are similar for all non-polar/polar systems when VLE is considered.

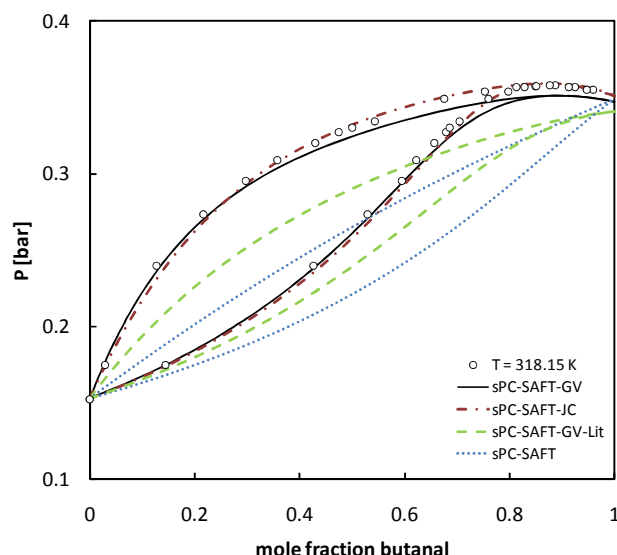


Figure 7-14: Isothermal VLE predictions of the butanal/n-heptane system at $T = 318.15$ K with sPC-SAFT-GV, sPC-SAFT-JC, sPC-SAFT-GV-Lit and sPC-SAFT. Experimental data taken from ref. (203).

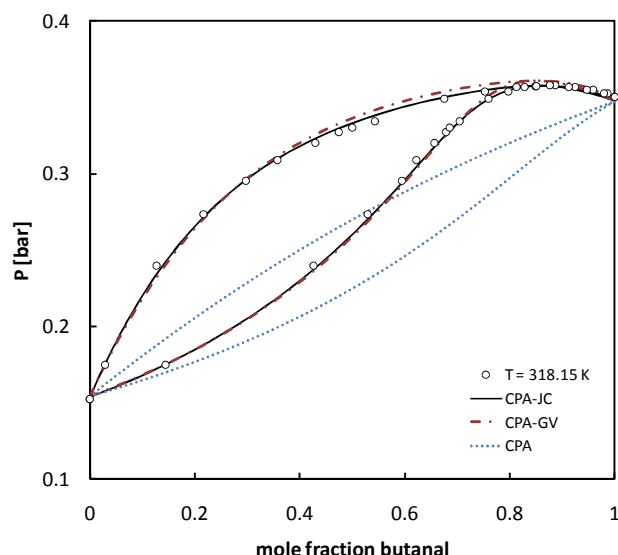


Figure 7-15: Isothermal VLE predictions of the butanal/n-heptane system at $T = 318.15$ K with CPA-GV, CPA-JC and CPA. Experimental data taken from ref. (203).

iii) alkane/ester systems

The VLE results for the propyl formate/n-nonane system are shown in Figure 7-16 for sPC-SAFT-based models and in Figure 7-17 for CPA-based models. Similar to the other results presented thus far, both polar versions of both sPC-SAFT and CPA provide accurate predictions that coincide well with the experimental data.

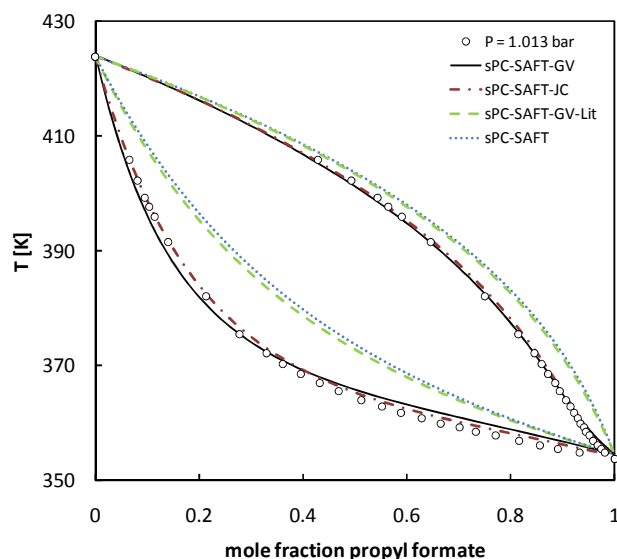


Figure 7-16: Isobaric VLE predictions of the propyl formate/n-nonane system at $P = 1.013$ bar with sPC-SAFT-GV, sPC-SAFT-JC, sPC-SAFT-GV-Lit and sPC-SAFT. Experimental data taken from ref. (215).

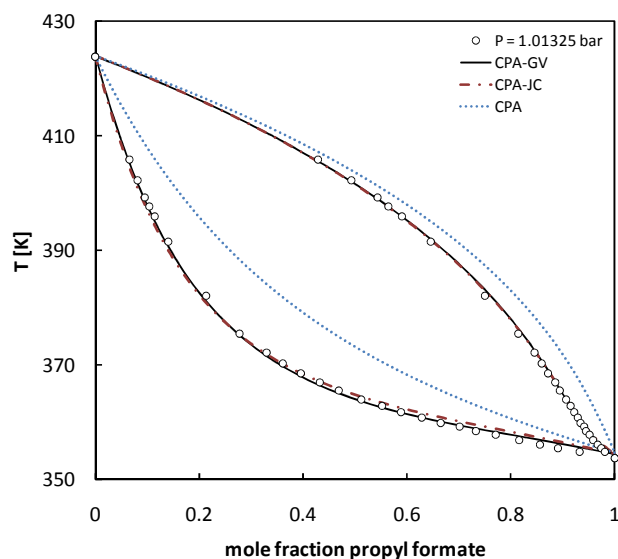


Figure 7-17: Isobaric VLE predictions of the propyl formate/n-nonane system at $P = 1.013$ bar with CPA-GV, CPA-JC and CPA. Experimental data taken from ref. (215).

Similar results are also found for other ester/alkane systems. Figure 7-18 and Figure 7-19 show VLE predictions for the methyl acetate/*n*-pentane system with sPC-SAFT-based models and CPA-based models respectively. Good prediction of the data is obtained by all four polar models, which is superior to the original sPC-SAFT and CPA models. Several mixtures containing different esters were investigated (see Table 7-10 and Table 7-11) and, sPC-SAFT-JC, sPC-SAFT-GV, CPA-JC and CPA-GV seem to be able to account for the position of the ester functional group on the molecule.

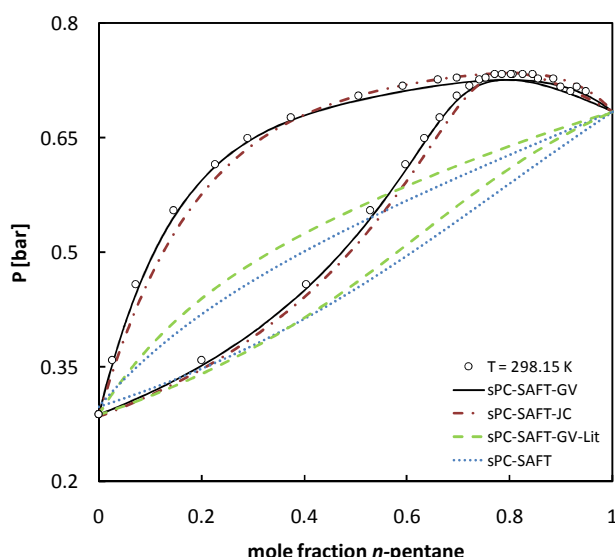


Figure 7-18: Isothermal VLE predictions of the methyl acetate/*n*-pentane system at $T = 298.15$ K with sPC-SAFT-GV, sPC-SAFT-JC, sPC-SAFT-GV-Lit and sPC-SAFT. Experimental data taken from ref. (204).

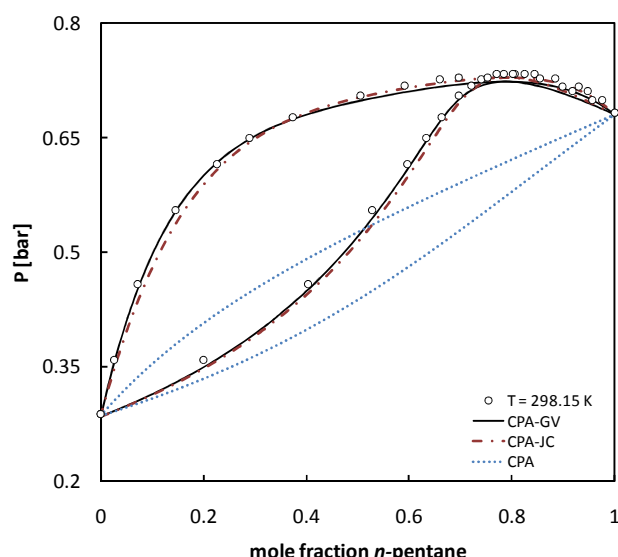


Figure 7-19: Isothermal VLE predictions of the methyl acetate/*n*-pentane system at $T = 298.15$ K with CPA-GV, CPA-JC and CPA. Experimental data taken from ref. (204).

iv) alkane/ether systems

The small dipole moments of ethers implies that the influence of polar forces are very small, but not negligible, especially in systems like diethyl ether and *n*-pentane as shown in Figure 7-20 for sPC-SAFT-based models, and in Figure 7-21 for the CPA counterparts.

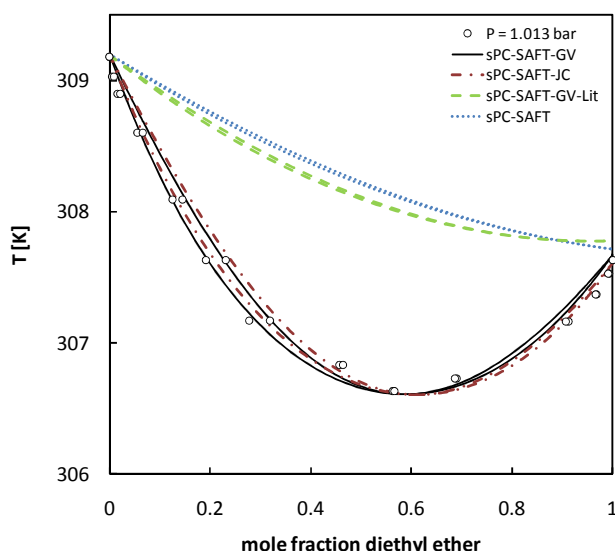


Figure 7-20: Isobaric VLE predictions of the diethyl ether/*n*-pentane system at $P = 1.013$ bar with sPC-SAFT-GV, sPC-SAFT-JC, sPC-SAFT-GV-Lit and sPC-SAFT. Experimental data taken from ref. (208).

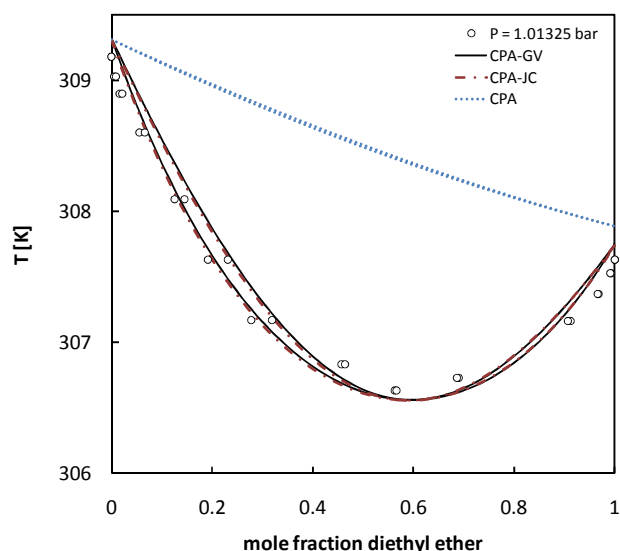


Figure 7-21: Isobaric VLE predictions of the diethyl ether/*n*-pentane system at $P = 1.01325$ bar with CPA-GV, CPA-JC and CPA. Experimental data taken from ref. (208).

In Figure 7-20, notice how little difference there is between the model predictions of sPC-SAFT and sPC-SAFT-GV-Lit, which clearly shows that the GV-polar term provides very little improvement for components with small dipole moments when $n_p = 1$. Great improvement is achieved when $n_p = 3.7598$ for diethyl ether, as shown by the prediction of sPC-SAFT-GV.

7.4.2 Excess enthalpy

The model parameters presented in section 7.3.2 (sPC-SAFT-GV and sPC-SAFT-JC) and section 7.3.3 (CPA-JC and CPA-GV) provide good VLE predictions for most systems investigated in the previous section. This is to be expected, since VLE data was included in the regression procedure. Therefore, the model parameters have been optimized for VLE calculations.

However, it is desirable to have models that can predict both VLE and other thermodynamic properties, such as excess enthalpy data, accurately with the same set of model parameters. Therefore, the excess enthalpies of several systems were also investigated as shown in Table 7-12:

Table 7-12: Excess enthalpy predictions with sPC-SAFT, sPC-SAFT-GV, sPC-SAFT-JC, CPA, CPA-GV and CPA-JC

Mixture	T [K]	%AAD			%AAD			n_p	ref.
		sPC-SAFT	sPC-SAFT-GV	sPC-SAFT-JC	CPA	CPA-GV	CPA-JC		
acetone/ <i>n</i> -pentane	293.2 K	40.1	13.8	27.9	64.2	25.5	14.9	13	(110)
acetone/ <i>n</i> -hexane	293.2 K	64.2	13.4	30.6	59.3	32.9	20.9	16	(110)
acetone/ <i>n</i> -heptane	298.15 K	65.2	12.5	28.8	58.3	33.0	21.0	19	(220)
2-butanone/ <i>n</i> -hexane	298.15 K	72.8	18.3	26.2	69.2	22.5	12.8	19	(221)
2-butanone/ <i>n</i> -heptane	298.15 K	73.2	17.6	27.2	67.0	26.5	15.6	20	(222)
3-pentanone/ <i>n</i> -hexane	298.15 K	73.8	15.8	31.7	74.8	10.8	7.32	20	(222)
3-pentanone/ <i>n</i> -heptane	298.15 K	74.8	16.2	31.4	72.2	15.0	9.81	20	(222)
3-pentanone/ <i>n</i> -octane	298.15 K	75.0	15.7	32.3	71.2	17.6	11.5	20	(222)

Mixture	T [K]	%AAD				%AAD			np	ref.
		sPC-SAFT	sPC-SAFT-GV	sPC-SAFT-JC		CPA	CPA-GV	CPA-JC		
2-hexanone/ n -nonane	298.15 K	82.2	28.8	16.3		-	-	-	20	(223)
butanal/ n -heptane	298.15 K	68.0	10.4	49.6		60.3	47.2	40.3	10	(110)
pentanal/cyclohexane	298.15 K	95.8	40.4	11.5		96.5	8.26	2.54	9	(224)
methyl formate/ n -hexane	291.15 K	62.0	24.8	15.3		53.0	28.6	10.7	14	(203)
ethyl formate/ n -hexane	291.15 K	70.3	24.1	24.8		64.7	32.7	14.2	14	(203)
propyl formate/ n -hexane	291.15 K	75.2	17.8	33.9		72.2	31.8	17.5	15	(203)
propyl formate/ n -nonane	298.15 K	78.8	25.9	19.3		70.3	26.1	9.61	18	(225)
butyl formate/ n -hexane	291.15 K	76.5	23.1	23.0		76.6	10.7	7.90	15	(203)
methyl acetate/ n -nonane	298.15 K	75.4	28.1	8.80		61.1	24.8	7.35	17	(226)
propyl acetate/ n -heptane	298.15 K	83.4	28.3	12.4		81.6	4.37	6.31	17	(227)
Average		72.6	20.8	25.1		69.0	23.4	13.1		

From Table 7-12, it is clear that the polar versions of both sPC-SAFT and CPA provide large improvements to the original versions, but are still not accurate enough. sPC-SAFT-GV and CPA-JC performed the best in each model-based category with the lowest %AAD (20.8% and 13.1% respectively). It was observed that sPC-SAFT-GV provided superior excess enthalpy predictions for components with large dipole moments (ketones), but that sPC-SAFT-JC provided superior excess enthalpy predictions for components with smaller dipole moments (esters).

A few graphical results are presented below that show the representative results of the models.

i) alkane/ketone systems

Excess enthalpy predictions of the acetone/*n*-hexane system are shown in Figure 7-22 and Figure 7-23 for the sPC-SAFT-based and CPA-based models respectively. sPC-SAFT-GV provides the best predictions of this property with the new model parameters, while sPC-SAFT-GV-Lit with $n_p = 1$ underestimates the property. sPC-SAFT and CPA provide similar predictions that underestimate the excess enthalpy of the system (similar results were obtained in Chapter 4, see Figure 4-14 and Figure 4-15). This indicates that the attractive interactions between the *unlike* molecules are overestimated. sPC-SAFT-JC, CPA-GV and CPA-JC over-estimate the excess enthalpy and indicate that the polar contributions to the property in these models are probably too large. A possible solution may be to use different dipole moments for the vapour and liquid phases, as recommended by Haslam *et al.* (128).

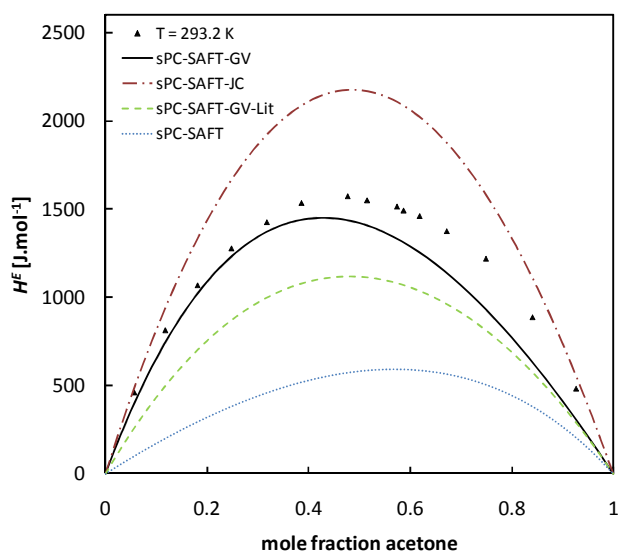


Figure 7-22: Excess enthalpy predictions of the acetone/*n*-hexane system at $T = 293.2$ K with sPC-SAFT-GV, sPC-SAFT-JC, sPC-SAFT-GV-Lit and sPC-SAFT. Experimental data taken from ref. (110).

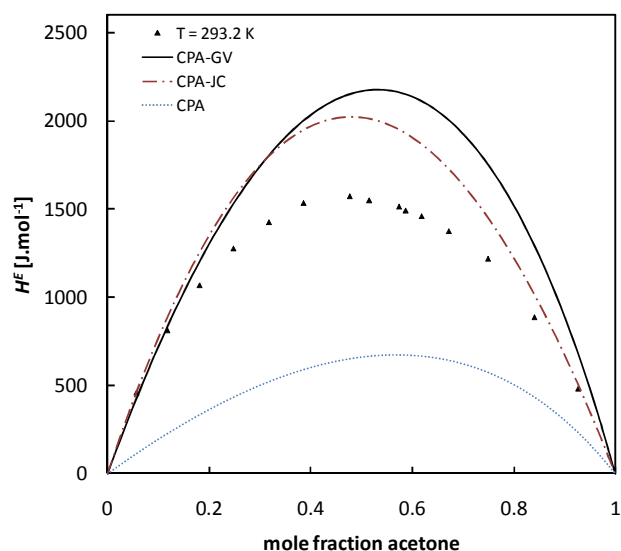


Figure 7-23: Excess enthalpy predictions of the acetone/*n*-hexane system at $T = 293.2$ K with CPA-GV, CPA-JC and CPA. Experimental data taken from ref. (110).

ii) alkane/aldehyde systems

Excess enthalpy predictions for the butanal/*n*-heptane is shown in Figure 7-24 and Figure 7-25 for the sPC-SAFT-based and CPA-based models respectively.

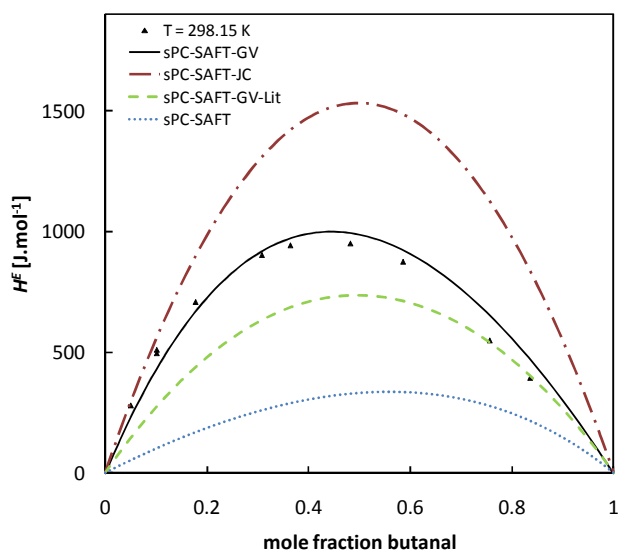


Figure 7-24: Excess enthalpy predictions of the butanal/*n*-heptane system at $T = 298.15$ K with sPC-SAFT-GV, sPC-SAFT-JC, sPC-SAFT-GV-Lit and sPC-SAFT. Experimental data taken from ref. (110).

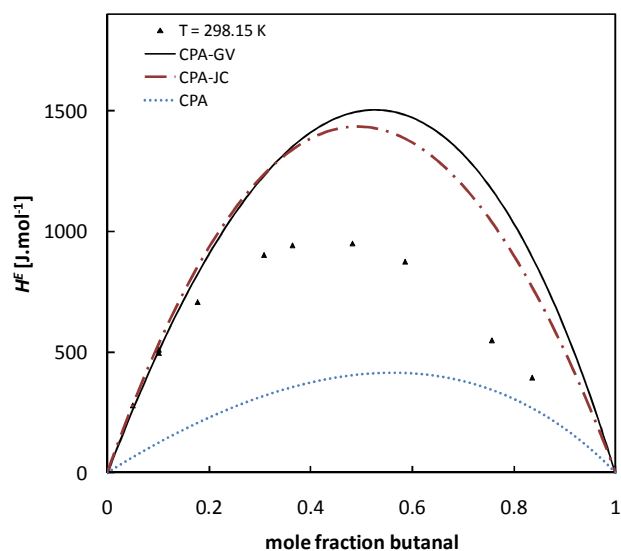


Figure 7-25: Excess enthalpy predictions of the butanal/*n*-heptane system at $T = 298.15$ K with CPA-GV, CPA-JC and CPA. Experimental data taken from ref. (110).

Similar results are observed compared to the acetone/*n*-hexane system (Figure 7-22 and Figure 7-23): sPC-SAFT-GV provides the best predictions of the excess enthalpy. Attempts were made with sPC-SAFT-GV, sPC-SAFT-JC, CPA-GV and CPA-JC to fit model parameters to pure component data and excess enthalpy data, rather than to pure component data and VLE data. This was

motivated by the fact that sPC-SAFT-GV predicts the excess enthalpies of the butanal/*n*-heptane and acetone/*n*-hexane systems fairly well with model parameters determined when including VLE data in the regression function. Also, excess enthalpy data is often available for a system when VLE data is not available. For the majority of systems investigated in this study, it was found that both sPC-SAFT-GV and sPC-SAFT-JC were still not able to simultaneously predict both the VLE and excess enthalpy accurately with the same set of pure component parameters. The good results of sPC-SAFT-GV for the butanal/*n*-heptane and acetone/*n*-hexane systems, as presented, are rather coincidental.

It should be mentioned that the excess enthalpy predictions for all models may be improved by fitting a BIP to the data. However, this BIP obtained cannot then be used in VLE calculations. Therefore, property specific BIPs are still required.

7.4.3 Excess volume

Investigating the excess volume is also important as discussed in appendix B.1.2.

i) alkane/ketone system

Excess volume predictions for the acetone/*n*-hexane system at $T = 298.15$ K are shown in Figure 7-26 for sPC-SAFT-type models and in Figure 7-27 for CPA-type models.

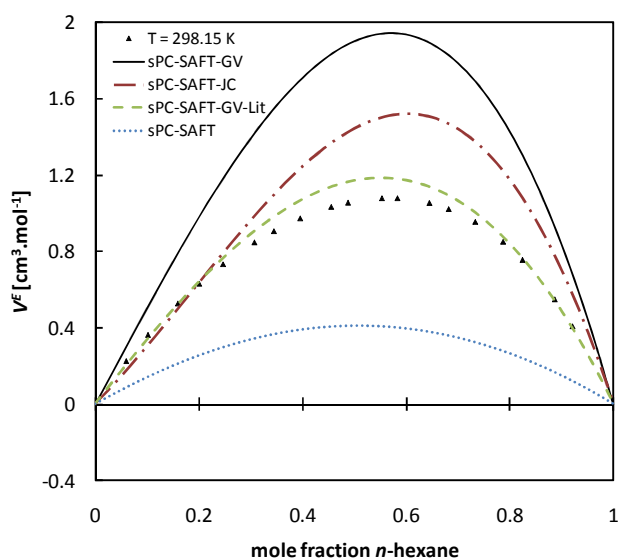


Figure 7-26: Excess volume predictions of the acetone/*n*-hexane system at $T = 298.15$ K with sPC-SAFT-GV, sPC-SAFT-JC, sPC-SAFT-GV-Lit and sPC-SAFT. Experimental data taken from ref. (228).

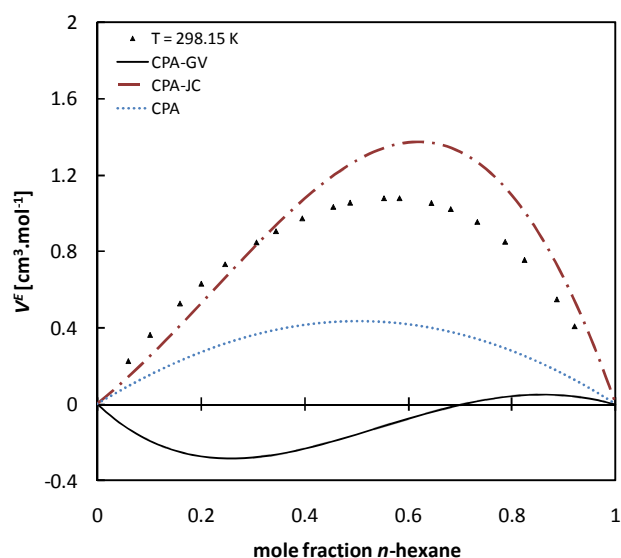


Figure 7-27: Excess volume predictions of the acetone/*n*-hexane system at $T = 298.15$ K with CPA-GV, CPA-JC and CPA. Experimental data taken from ref. (228).

From Figure 7-26, sPC-SAFT-GV-Lit provides an accurate prediction of the excess volume, while sPC-SAFT-GV and sPC-SAFT-JC overpredict the property. The excess volumes of several other systems were also investigated and it was found that the good result of sPC-SAFT-GV-Lit was merely coincidental for the acetone/*n*-hexane system.

In Figure 7-27, CPA-JC predicts the excess volume with fair accuracy, while CPA-GV provides poor results.

ii) alkane/ester system

From Figure 7-28, both sPC-SAFT-GV and sPC-SAFT-JC provide reasonable excess volume predictions of the ethyl acetate/*n*-hexane system. sPC-SAFT-GV-Lit severely underestimates the property and provides little improvement compared to original sPC-SAFT EOS. Figure 7-29 show that only CPA-JC predicts the excess volume reasonably.

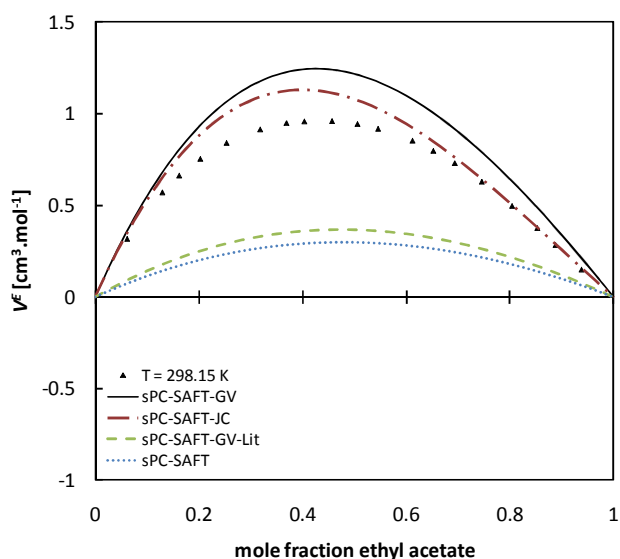


Figure 7-28: Excess volume predictions of the ethyl acetate/*n*-hexane system at $T = 298.15$ K with sPC-SAFT-GV, sPC-SAFT-JC, sPC-SAFT-GV-Lit and sPC-SAFT. Experimental data taken from ref. (228).

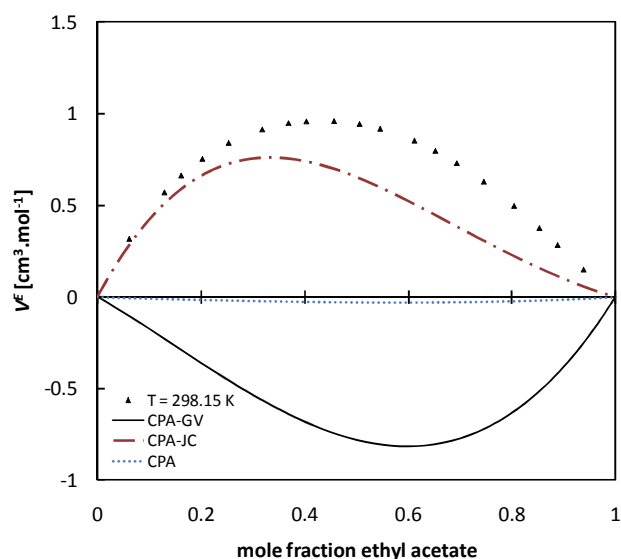


Figure 7-29: Excess volume predictions of the ethyl acetate/*n*-hexane system at $T = 298.15$ K with CPA-GV, CPA-JC and CPA. Experimental data taken from ref. (228).

7.4.4 Second-order properties

Several second-order properties were also modelled, but generally little or no improvement was obtained compared to the performance of the original models, as evaluated in Chapter 3 and Chapter 4. The main reason is that the description of the repulsive and dispersive interactions has not been improved by adding polar terms to the state function. The speed of sound in the acetone/*n*-hexane system is shown in Figure 7-30 and the speed of sound in the ethyl acetate/*n*-hexane system is shown in Figure 7-31.

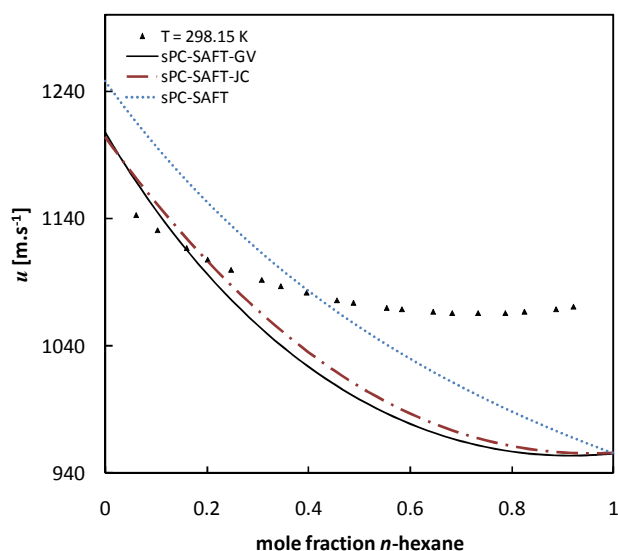


Figure 7-30: Speed of sound predictions in the acetone/*n*-hexane system at $T = 298.15$ K with *sPC-SAFT-GV*, *sPC-SAFT-JC*, and *sPC-SAFT*. Experimental data taken from ref. (228).

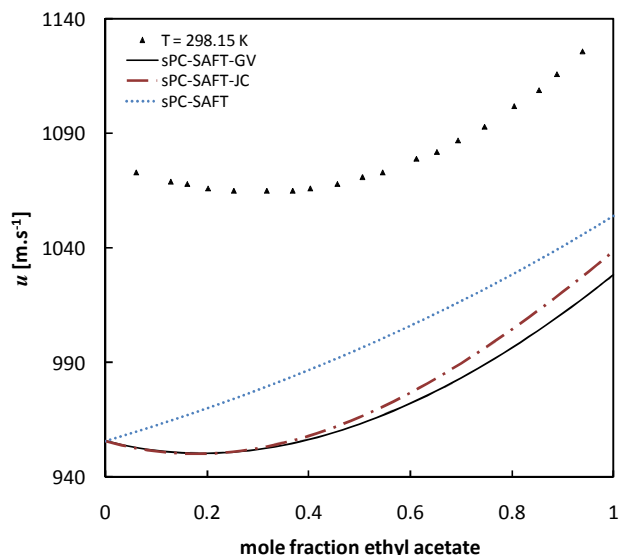


Figure 7-31: Speed of sound predictions in the ethyl acetate/*n*-hexane system at $T = 298.15$ K with *sPC-SAFT-GV*, *sPC-SAFT-JC*, and *sPC-SAFT*. Experimental data taken from ref. (228).

From Figure 7-30 and Figure 7-31, it is clear that the trends in the model predictions of the *sPC-SAFT-GV* and *sPC-SAFT-JC* more closely coincide with the trend exhibited by the data points. It does seem that the influence of polar interactions on the speed of sound is captured more accurately, but the improvement is small compared to the original *sPC-SAFT* model. Therefore, improvement in the description of the repulsive and dispersive interactions is necessary before accurate predictions of second-order properties such as the speed of sound can be obtained.

7.5 Polar (non-HB)/Polar (non-HB)

In this section, models are applied to properties of polar/polar mixtures. Generally, the polar variants and the original version of both *sPC-SAFT* and CPA perform similarly when VLE is considered, because the *like* and *unlike* interactions are of the same magnitude. Little or no improvement is obtained in the prediction of other properties.

7.5.1 Vapour-liquid equilibria

VLE results for several polar/polar systems are presented in Table 7-13 for *sPC-SAFT* based models and in Table 7-14 for the CPA-based models.

Table 7-13: VLE predictions of polar-polar mixtures with sPC-SAFT, sPC-SAFT-GV and sPC-SAFT-JC

Mixture	T or P	sPC-SAFT		sPC-SAFT-GV		sPC-SAFT-JC		np	ref.
		Δy (x10 ²) ^a	$\frac{\Delta P(\%)^b}{\Delta T(K)^a}$	Δy (x10 ²) ^a	$\frac{\Delta P(\%)^b}{\Delta T(K)^a}$	Δy (x10 ²) ^a	$\frac{\Delta P(\%)^b}{\Delta T(K)^a}$		
ethyl formate/2-butanone	313.15 K	1.48	0.76	0.97	0.92	0.94	0.41	9	(229)
methyl acetate/butanol	323.15 K	0.31	0.67	0.46	1.18	0.36	0.26	17	(230)
propyl acetate/butanol	323.15 K	0.53	0.73	0.53	1.01	0.66	0.58	14	(230)
methyl acetate/ethyl acetate	353.15 K	0.51	2.43	0.43	2.03	0.39	0.83	11	(231)
diethyl ether/acetone	303.15 K	2.48	5.51	0.33	0.79	0.40	0.77	13	(232)
dibutyl ether/acetone	1.013 bar	3.81	6.01	0.68	0.69	1.31	1.22	17	(233)
acetone/2-butanone	3.447 bar	1.65	0.51	1.56	0.47	1.48	0.47	14	(234)
acetone/3-pentanone	1.013 bar	0.41	0.50	0.58	0.68	0.55	0.62	12	(235)
Average		1.40	2.14	0.69	0.97	0.76	0.65		

^a $\Delta z = \sum_i^{np} |z_i^{calc} - z_i^{exp}|$ where z represents y or T and np is the number of data points. ^b Deviations as %AAD.

Table 7-14: VLE predictions of polar-polar mixtures with CPA, CPA-GV and CPA-JC.

Mixture	T or P	CPA		CPA-GV		CPA-JC		np	ref.
		Δy (x10 ²) ^a	$\frac{\Delta P(\%)^b}{\Delta T(K)^a}$	Δy (x10 ²) ^a	$\frac{\Delta P(\%)^b}{\Delta T(K)^a}$	Δy (x10 ²) ^a	$\frac{\Delta P(\%)^b}{\Delta T(K)^a}$		
ethyl formate/2-butanone	313.15 K	1.07	1.35	1.04	0.95	0.81	0.53	9	(229)
methyl acetate/butanol	323.15 K	0.44	1.74	0.40	0.98	0.40	0.99	17	(230)
propyl acetate/butanol	323.15 K	0.71	1.01	0.71	0.91	0.66	0.76	14	(230)
methyl acetate/ethyl acetate	353.15 K	0.34	1.10	0.30	1.60	0.33	1.15	11	(231)
diethyl ether/acetone	303.15 K	2.34	5.88	0.86	2.14	0.58	1.52	13	(232)
dibutyl ether/acetone	1.013 bar	3.23	5.21	1.17	1.45	0.99	1.02	17	(233)
acetone/2-butanone	3.447 bar	1.65	0.52	1.64	0.49	1.54	0.44	14	(234)
acetone/3-pentanone	1.013 bar	0.47	0.64	0.57	0.72	0.71	0.76	12	(235)
Average		1.28	2.18	0.84	1.16	0.75	0.90		

^a $\Delta z = \sum_i^{np} |z_i^{calc} - z_i^{exp}|$ where z represents y or T and np is the number of data points. ^b Deviations as %AAD.

From Table 7-13 and Table 7-14, it is noted that all the models provide acceptable VLE predictions. However, the predictions of the original sPC-SAFT and CPA are less accurate for ketone/ether systems. In these systems the differences between the *like* and *unlike* interactions are significant and are brought about by the large difference in dipole moment between the ketone and ether molecules. The polar versions of both models are able to account for the difference between dipole moments when VLE is considered.

Some graphical results are presented in the following subsection to emphasize some of the findings mentioned.

i) ether/ketone systems

VLE predictions of the diethyl ether/acetone system with sPC-SAFT and CPA are shown in Figure 7-32 and Figure 7-33 respectively. The polar variants of both sPC-SAFT and CPA provide accurate

predictions of the data, while the original versions are less accurate. The dipole moment of diethyl ether is 1.15 D and the dipole moment of acetone is 2.88 D. The *unlike* and *like* interactions are therefore markedly different and is the reason why the original CPA and sPC-SAFT models are less accurate.

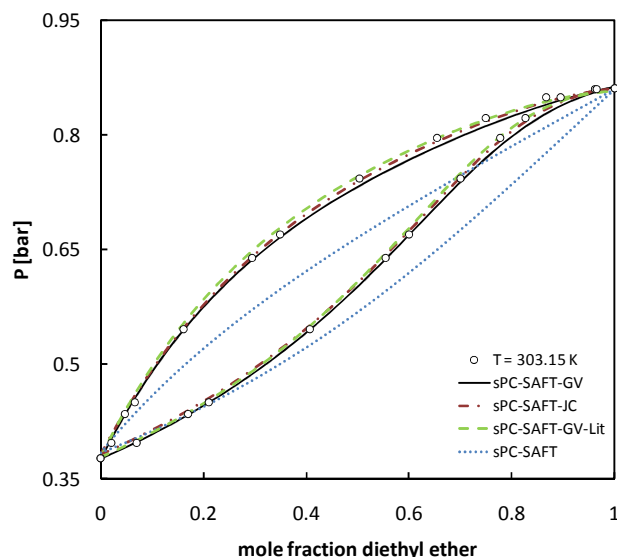


Figure 7-32: Isothermal VLE predictions of the diethyl ether/acetone system at $T = 303.15\text{ K}$ with sPC-SAFT-GV, sPC-SAFT-JC, sPC-SAFT-GV-Lit and sPC-SAFT. Experimental data taken from ref. (232).

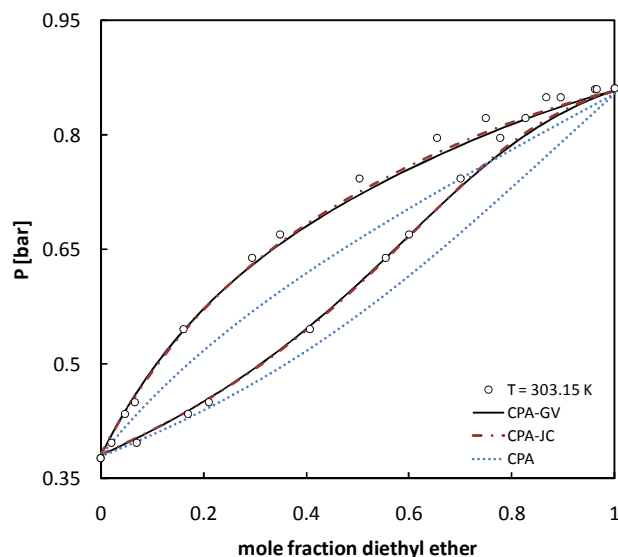


Figure 7-33: Isothermal VLE predictions of the diethyl ether/acetone system at $T = 303.15\text{ K}$ with CPA-GV, CPA-JC and CPA. Experimental data taken from ref. (232).

7.5.2 Excess enthalpy

The results in Figure 7-34 and Figure 7-35 indicate that some improvement is obtained with the polar models compared to the original versions for the acetone/ethyl acetate system. For this particular system, CPA-GV and CPA-JC provide good predictions of the excess enthalpy. sPC-SAFT-GV-Lit completely overestimates the property, while sPC-SAFT-GV and sPC-SAFT-JC slightly underestimated the property.

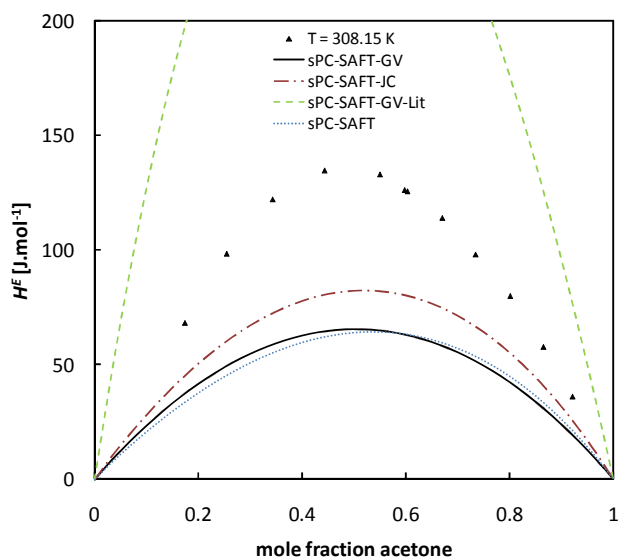


Figure 7-34: Excess enthalpy predictions of the acetone/ethyl acetate system at $T = 308.15$ K with sPC-SAFT-GV, sPC-SAFT-JC, sPC-SAFT-GV-Lit and sPC-SAFT. Experimental data taken from ref.(236).

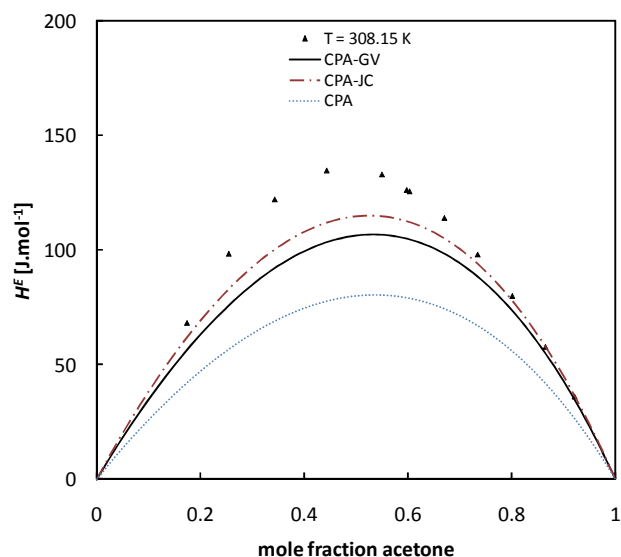


Figure 7-35: Excess enthalpy predictions of the acetone/ethyl acetate system at $T = 308.15$ K with CPA-GV, CPA-JC and CPA. Experimental data taken from ref.(236).

7.5.3 Excess volume

Excess volume predictions of the ethyl acetate/acetone system with sPC-SAFT-based models are presented in Figure 7-36 and results with CPA-based models are shown in Figure 7-37. Not one of the models manages to capture the irregular characteristics displayed by the data points. The sPC-SAFT-based models are generally more accurate compared to the CPA-based models, except for the prediction of sPC-SAFT-GV-Lit.

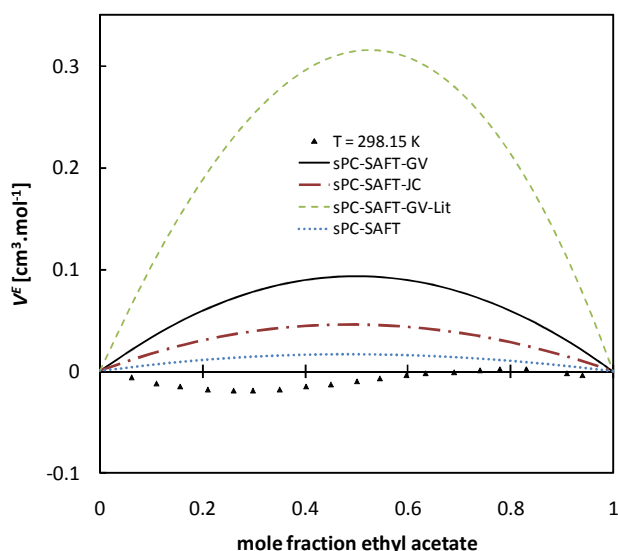


Figure 7-36: Excess volume predictions of the ethyl acetate/acetone system at $T = 298.15$ K with sPC-SAFT-GV, sPC-SAFT-JC, sPC-SAFT-GV-Lit and sPC-SAFT. Experimental data taken from ref. (228).

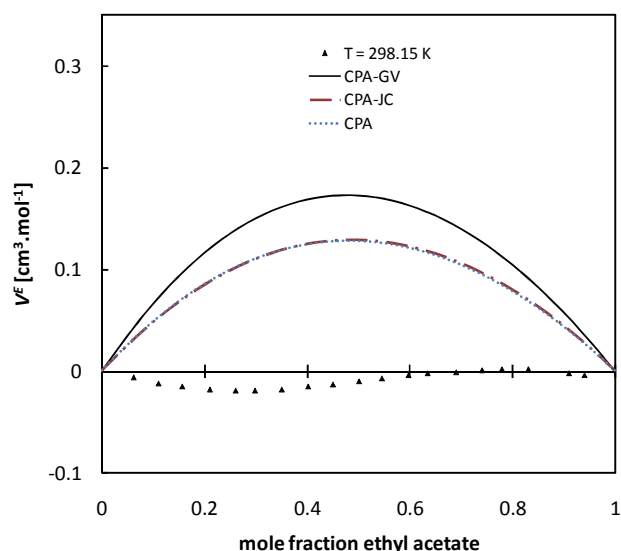


Figure 7-37: Excess volume predictions of the ethyl acetate/acetone system at $T = 298.15$ K with CPA-GV, CPA-JC and CPA. Experimental data taken from ref. (228).

7.6 Multi-component VLE

The VLE of ternary systems are also investigated with the polar sPC-SAFT and CPA models. Representative results for selected systems are presented in the Table 7-15 and Table 7-16 respectively:

Table 7-15: VLE predictions of ternary mixtures with sPC-SAFT-GV, sPC-SAFT-JC and sPC-SAFT at $P = 1.013$ bar.

Mixture/Model	$\Delta x_2(\times 10^2)^a$	$\Delta x_3(\times 10^2)^a$	$\Delta y_1(\times 10^2)^a$	$\Delta y_2(\times 10^2)^a$	$\Delta y_3(\times 10^2)^a$	np	ref
acetone(1)/diethylether(2)/n-hexane(3) ($P = 1.013$ bar)							15 (237)
sPC-SAFT-GV(all $k_{ij} = 0$)	2.12	2.12	2.63	1.55	2.70		
sPC-SAFT-JC (all $k_{ij} = 0$)	1.98	1.98	1.89	1.47	1.58		
sPC-SAFT ($k_{12} = 0.015$, $k_{13} = 0.05$, $k_{23} = 0.013$)	1.93	1.93	1.99	2.34	1.13		
ethyl acetate(1)/n-hexane(2)/acetone(3) ($P = 1.013$ bar)							106 (205)
sPC-SAFT-GV(all $k_{ij} = 0$)	2.14	2.14	2.03	1.40	2.21		
sPC-SAFT-JC (all $k_{ij} = 0$)	1.93	1.93	1.71	1.09	2.48		
sPC-SAFT ($k_{12} = 0.035$, $k_{13} = 0.006$, $k_{23} = 0.05$)	3.72	3.54	1.60	4.50	4.60		
cyclohexane (1)/MIPK (2)/n-octane(3) ($P = 1.013$ bar)							77 (197)
sPC-SAFT-GV(all $k_{ij} = 0$)	1.55	1.55	0.44	0.82	0.86		
sPC-SAFT -JC (all $k_{ij} = 0$)	1.70	1.70	0.78	0.71	0.82		
sPC-SAFT ($k_{12} = 0.037$, $k_{13} = 0$, $k_{23} = 0.036$)	1.42	1.42	1.08	1.03	0.48		

^a $\Delta z = \sum_i^{np} |z_i^{calc} - z_i^{exp}|$ where z represents y or x and np is the number of data points.

Table 7-15 shows that sPC-SAFT-GV and sPC-SAFT-JC provide good VLE predictions of non-associating polar multi-component systems. sPC-SAFT also provides good predictions when BIPs are used (BIPs determined from binary VLE data). Similarly, Table 7-16 shows that both CPA-GV and CPA-JC provide good VLE predictions of multi-components systems.

Table 7-16: VLE predictions of ternary mixtures with CPA-GV, CPA-JC and CPA at $P = 1.013$ bar.

Mixture/Model	$\Delta x_2(\times 10^2)^a$	$\Delta x_3(\times 10^2)^a$	$\Delta y_1(\times 10^2)^a$	$\Delta y_2(\times 10^2)^a$	$\Delta y_3(\times 10^2)^a$	np	ref
acetone(1)/ diethyl ether(2)/n-hexane(3) (P = 1.013 bar)						15	(237)
CPA-GV(all $k_{ij} = 0$)	3.36	3.36	2.60	2.19	1.66		
CPA-JC (all $k_{ij} = 0$)	2.68	2.68	2.18	1.79	1.57		
CPA ($k_{12} = 0.025$, $k_{13} = 0.08$, $k_{23} = 0.025$)	2.30	2.25	1.95	2.32	1.28		
ethyl acetate(1)/n-hexane(2)/acetone(3) (P = 1.013 bar)						106	(205)
CPA-GV(all $k_{ij} = 0$)	3.10	3.10	1.36	3.24	3.95		
CPA-JC (all $k_{ij} = 0$)	3.07	3.07	1.23	2.86	3.58		
CPA ($k_{12} = 0.069$, $k_{13} = 0.011$, $k_{23} = 0.08$)	4.35	4.11	1.67	5.03	4.84		
cyclohexane (1)/MIPK (2)/n-octane(3) (P = 1.013 bar)						77	(197)
CPA-GV(all $k_{ij} = 0$)	1.37	1.37	0.95	1.08	0.74		
CPA-JC (all $k_{ij} = 0$)	1.46	1.46	0.92	1.12	0.82		
CPA ($k_{12} = 0.067$, $k_{13} = 0$, $k_{23} = 0.064$)	1.54	1.52	1.26	1.25	0.62		

^a $\Delta z = \sum_i^{np} |z_i^{calc} - z_i^{exp}|$ where z represents y or x and np is the number of data points.

This section provides convincing evidence that good VLE predictions can be obtained with both polar variants of sPC-SAFT and CPA. With respects to sPC-SAFT-GV, the results indicate that improvement in multi-component VLE is also obtained when n_p is included as an adjustable parameter for polar components.

7.7 Chapter Summary

The JC and GV polar theories have been modified and incorporated into the sPC-SAFT and CPA EOS. The resulting new EOS, sPC-SAFT-JC, sPC-SAFT-GV, CPA-JC and CPA-GV, each require four pure component model parameters to model non-hydrogen bonding polar components. Pure component parameters are regressed for several polar components by including pure component data and binary VLE data in the objective function. A summary of the performance of the polar sPC-SAFT and CPA-based models are presented in following subsections:

7.7.1 sPC-SAFT-GV and sPC-SAFT-JC

For sPC-SAFT modified by polar terms, it follows that:

- Considerable improvement in VLE prediction is obtained with both sPC-SAFT-JC and sPC-SAFT-GV (compared to the original sPC-SAFT) model for ketone/alkane,

aldehyde/alkane, ester/alkane, ether/alkane and polar/polar binary mixtures. The VLEs of multi-component systems are also predicted with good accuracy.

- In sPC-SAFT-GV, n_p is treated as an adjustable pure component parameter, which enables the model to capture the contribution of the polar term more correctly. The results show that the GV-term significantly underestimates the influence of polar forces when $n_p = 1$.
- sPC-SAFT-GV and sPC-SAFT-JC perform equally well in predicting the VLE of all the systems investigated, with neither model being superior to the other.
- Both sPC-SAFT-GV and sPC-SAFT-JC still have difficulty in accurately predicting excess enthalpies and other properties of polar/alkane and polar/polar systems. The results may be improved by fitting BIPs, however, these BIPs appear to be property-specific.
- The simplification made to the original PC-SAFT model to obtain sPC-SAFT does not seem to deteriorate the performance of the model when extended with a polar term. Therefore, sPC-SAFT-JC and sPC-SAFT-GV provide very feasible alternatives to Polar PC-SAFT (PC-SAFT-JC) and PCP-SAFT (PC-SAFT-GV), because excellent performance is obtained at a lower numerical cost.

7.7.2 CPA-GV and CPA-JC

The performances of the CPA-based models are quite similar to their sPC-SAFT counterparts. The main findings regarding CPA-JC and CPA-GV are summarized below:

- Both CPA-JC and CPA-GV provide improved VLE predictions for polar/alkane and polar/polar systems compared to the original CPA EOS. Small BIPs are occasionally required to obtain accurate VLE predictions.
- When VLE is considered, the models perform similarly, with neither model being superior to the other.
- Both CPA-GV and CPA-JC provide good VLE predictions of multicomponent systems.
- Excess enthalpies are most accurately described with CPA-JC, although BIPs are still required.

The EOS (sPC-SAFT-GV, sPC-SAFT-JC, CPA-GV, CPA-JC) developed in this chapter provide good VLE description of polar non-associating components and are mathematically simpler compared to Polar PC-SAFT and PCP-SAFT. These newly developed EOS are applied to associating components in Chapter 8.

7.7.3 Scientific Contribution

The results related to the polar sPC-SAFT and CPA models, as presented in this chapter, have been published in the following journal:

Title: Improving vapour–liquid-equilibria predictions for mixtures with non-associating polar components using sPC-SAFT extended with two dipolar terms.

Authors: A.J. de Villiers, C.E. Schwarz, A.J. Burger

Journal: Fluid Phase Equilibria **2011**, 305, 174-184

Title: Extension of the CPA equation of state with dipolar theories to improve vapour-liquid-equilibria predictions

Authors: A.J. de Villiers, C.E. Schwarz, A.J. Burger

Journal: Fluid Phase Equilibria **2011** 312, 66-78

Chapter 8

Application of Polar sPC-SAFT and Polar CPA to associating components

In this chapter, the polar models (sPC-SAFT-GV, sPC-SAFT-JC, CPA-GV and CPA-JC) developed in Chapter 7 are applied to associating components, most notably, mixtures containing alcohols and water. PC-SAFT-JC based models have previously been applied to mixtures containing alcohols, but so far, only limited success has been achieved. Al-Saifi *et al.* (35) applied PC-SAFT-JC (127), PC-SAFT-GV (54) and PC-SAFT-KSE (180) to the VLE of alcohol/alkane, alcohol/alcohol and alcohol/water mixtures. Improved results have been obtained compared to the original PC-SAFT model, but significant errors (generally, 10% AAD in pressure) in binary VLE predictions were still present in alcohol/alkane mixtures and the VLE predictions of alcohol/water mixtures were rather poorly correlated with PC-SAFT-GV and PC-SAFT-KSE. Only PC-SAFT-JC provided reasonable alcohol/water representations, but only short-chained alcohols were considered. Furthermore, Al-Saifi *et al.* (35) modelled both water and alcohols as 2B molecules and did not consider any other association scheme configurations. They mention that improved results might be obtained if other configurations are investigated. They also set the n_p parameter in PC-SAFT-GV (by default) equal to 1 for water and alcohols and did not consider it as an adjustable parameter in their regression procedure. Kleiner and Sadowski (87) investigated mixtures with water using PC-SAFT-GV and found that, when dipolar interactions are explicitly accounted for in the model, worse results are obtained compared to when water was modelled without polar interactions.

From these discussions, it is clear that the application and ability of polar PC-SAFT models have not yet been fully considered and a more thorough investigation is needed. Therefore, the objectives of this chapter are:

- To determine if the 2B parameters of Al-Saifi *et al.* (35) for PC-SAFT-JC and PC-SAFT-GV may be used for sPC-SAFT-GV and sPC-SAFT-JC.
- To determine the most appropriate association scheme for alcohols and water within the framework of the sPC-SAFT-JC, sPC-SAFT-GV, CPA-JC and CPA-GV EOS.
- To investigate the ability of the polar models in predicting VLE and LLE of mixtures containing associating components, specifically mixtures containing either alcohols or water.
- To investigate the performance of the polar models when other thermodynamic properties are considered (focus on excess enthalpies and excess volumes).

It is shown that the best overall predictions of alcohol/alkane and alcohol/water VLE are obtained when alcohols are modelled with the 2C scheme in sPC-SAFT-GV and sPC-SAFT-JC.

8.1 Association schemes and model parameters

In this section, the major problems encountered with the alcohol and water model parameters currently available in the literature for sPC-SAFT-GV and sPC-SAFT-JC, are demonstrated and new model parameters based on different association schemes are determined.

8.1.1 Performance of current parameters from literature

i) sPC-SAFT-GV and sPC-SAFT-JC

For hydrogen bonding components, the choice of association scheme profoundly affects the behaviour of the respective model. In Figure 8-1 and Figure 8-2, the VLE predictions of the ethanol/*n*-heptane and ethanol/water systems are shown for sPC-SAFT-JC-L and sPC-SAFT-GV-L (L that indicates literature parameters from Al-Saifi *et al.* (35) are used):

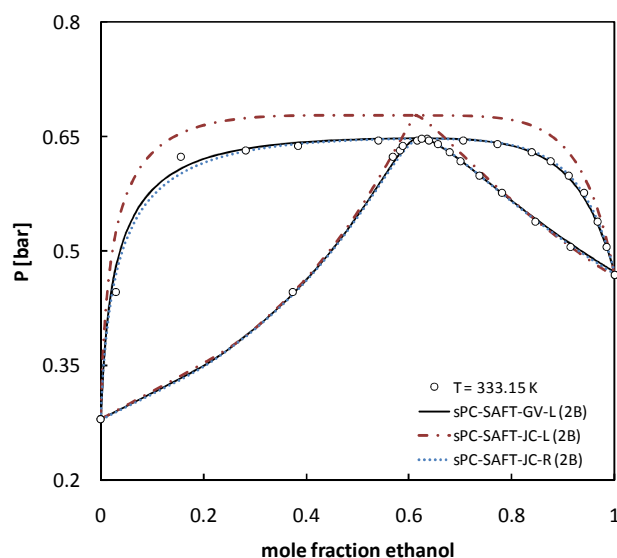


Figure 8-1: VLE predictions of the ethanol/*n*-heptane system with sPC-SAFT-GV-L, sPC-SAFT-JC-L (literature parameters from Al-Saifi *et al.* (35) and sPC-SAFT-JC-R (re-fitted parameters). Experimental data from ref. (167).

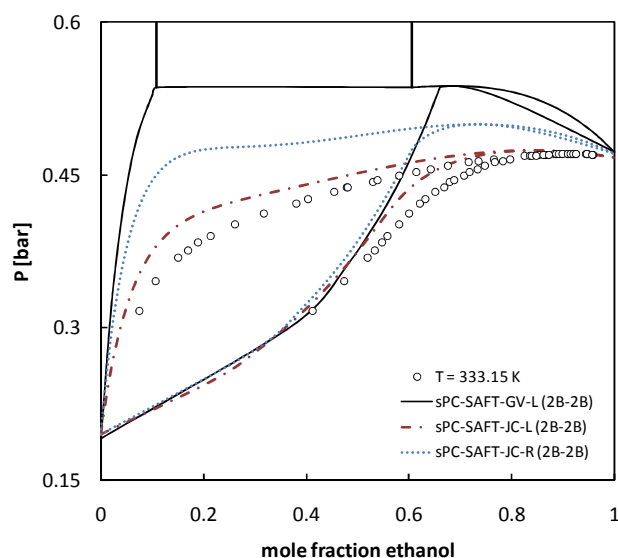


Figure 8-2: VLE predictions of the ethanol/water system with sPC-SAFT-GV-L, sPC-SAFT-JC-L (ethanol and water parameters from Al-Saifi *et al.* (35)) and sPC-SAFT-JC-R (water parameters from Al-Saifi *et al.* (35) and refitted ethanol parameters).

From Figure 8-1, sPC-SAFT-GV-L provides a good representation of the experimental data, while the prediction of sPC-SAFT-JC-L is less accurate. The performance of sPC-SAFT-JC may be improved by refitting the ethanol parameters (sPC-SAFT-JC-R).

The ethanol parameters applied in Figure 8-1 are used in conjunction with the 2B literature parameters from Al-Saifi *et al.* (35) for water to generate the results in Figure 8-2. sPC-SAFT-GV-L

and sPC-SAFT-JC-R (the models that accurately predicted ethanol/*n*-heptane VLE), are now least accurate for the water/ethanol VLE (sPC-SAFT-GV-L predicts false VLLE). sPC-SAFT-JC-L, the model that provided the least accurate prediction of ethanol/*n*-heptane VLE, is now most accurate. This dilemma is encountered for most alcohol/alkane and alcohol/water systems: both sPC-SAFT-JC and sPC-SAFT-GV are unable to describe both types of systems accurately with model parameters currently available in the literature. Therefore, new parameters were developed here based on different association schemes for alcohols and water. The model predictions, based on the different association schemes, are compared and evaluated in subsequent sections.

8.1.2 New model parameters for sPC-SAFT-GV and sPC-SAFT-JC

Model parameters for sPC-SAFT-GV are presented in Table 8-1 and for sPC-SAFT-JC in Table 8-2. New model parameters for alcohols based on all three association schemes (2B, 2C and 3B) were determined with the same regression function used in Chapter 7 (saturated vapour pressure, saturated liquid density, heat of vapourisation and binary VLE data were included in the objective function, see equation (7-33)). This enabled a fair and unbiased evaluation of the models and between the different association schemes. Graphical results with the 2B parameters determined by Al-Saifi *et al.* (35) are nonetheless presented in subsequent sections in order to compare the performance of the models with literature. The model parameters for water were determined by following a similar strategy as proposed by Grenner *et al.* (36) for sPC-SAFT and were based on the same physical arguments proposed by them, namely: a) the segment number, *m*, should be small, b) the dispersion energy parameter should be between 47 and 160 K (238) and, c) the association energy value should be close to 1813 K (239).

Table 8-1: New sPC-SAFT-GV model parameters for associating components

	Sch	<i>M_w</i> [g/mol]	σ [Å]	<i>m</i>	ε/k [K]	<i>n_p</i>	μ [D]	ε^{AB}/k [K]	κ^{AB}	VLE data (ref.)
methanol	2B	32.042	2.7164	2.5541	177.84	0.4534	1.70	2296.3	0.23514	<i>n</i> -hexane (164)
ethanol	2B	46.068	3.0954	2.5766	194.85	0.9684	1.70	2474.3	0.07586	<i>n</i> -heptane(167)
1-propanol	2B	60.095	3.3093	2.8182	225.43	1.6270	1.68	2342.9	0.03578	<i>n</i> -heptane (169)
1-butanol	2B	74.122	3.4799	3.0286	244.82	2.1267	1.67	2413.7	0.01595	<i>n</i> -nonane (171)
1-pentanol	2B	88.148	3.6846	3.0395	258.33	2.8120	1.70	2443.4	0.01390	<i>n</i> -heptane (240)
1-hexanol	2B	102.17	3.7951	3.2100	269.07	3.2378	1.65	2750.9	0.00551	<i>n</i> -hexane (241)
1-heptanol	2B	116.20	3.9324	3.3700	273.10	3.5211	1.74	2899.9	0.00474	<i>n</i> -decane (242)
1-octanol	2B	130.23	4.0346	3.4766	280.68	3.8898	1.65	2985.2	0.00451	<i>n</i> -decane (243)
methanol	2C	32.042	3.1616	1.7023	197.42	0.8712	1.70	2627.8	0.05194	<i>n</i> -hexane (164)
ethanol	2C	46.068	3.2558	2.2361	202.27	1.1933	1.70	2695.1	0.03035	<i>n</i> -heptane(167)
1-propanol	2C	60.095	3.3108	2.8017	223.67	1.7900	1.68	2466.7	0.02063	<i>n</i> -heptane (169)
1-butanol	2C	74.122	3.5584	2.8439	249.85	2.4012	1.67	2609.8	0.00702	<i>n</i> -nonane (171)
1-pentanol	2C	88.148	3.7464	2.9049	261.98	3.0290	1.70	2622.1	0.00661	<i>n</i> -heptane (240)
1-hexanol	2C	102.17	3.8609	3.0600	274.08	3.4930	1.65	2945.8	0.00244	<i>n</i> -hexane (241)

	Sch	M_w [g/mol]	σ [Å]	m	ε/k [K]	n_p	μ [D]	ε^{AB}/k [K]	κ^{AB}	VLE data (ref.)
1-heptanol	2C	116.20	3.9627	3.3250	274.25	3.9540	1.74	3159.9	0.00164	<i>n</i> -decane (242)
1-octanol	2C	130.23	4.0233	3.4971	279.31	4.4152	1.65	3112.8	0.00230	<i>n</i> -decane (243)
methanol	3B	32.042	2.7169	2.6253	184.07	0.0994	1.70	2073.1	0.11135	<i>n</i> -hexane (164)
ethanol	3B	46.068	2.9519	3.0099	198.77	1.5453	1.70	2002.0	0.06557	<i>n</i> -heptane(167)
propanol	3B	60.095	3.2899	2.9001	230.11	1.1578	1.68	2039.7	0.02419	<i>n</i> -heptane (169)
1-butanol	3B	74.122	3.4585	3.0982	244.97	1.4524	1.67	2132.9	0.01346	<i>n</i> -nonane (171)
1-pentanol	3B	88.148	3.6411	3.1551	256.69	2.0850	1.70	2134.1	0.01268	<i>n</i> -heptane (240)
1-hexanol	3B	102.17	3.8058	3.2001	271.54	2.1001	1.65	2460.4	0.00507	<i>n</i> -hexane (241)
1-heptanol	3B	116.20	3.9387	3.3990	275.19	2.1001	1.74	2685.2	0.00322	<i>n</i> -decane (242)
1-octanol	3B	130.23	4.0188	3.5284	280.45	2.1141	1.65	2639.6	0.00465	<i>n</i> -decane (243)
water	4C	18.015	2.6204	1.50518	149.96	0.3161	1.85	1816.0	0.20245	-

Table 8-2: New sPC-SAFT-JC model parameters for associating components

	Sch	M_w [g/mol]	σ [Å]	m	ε/k [K]	x_p	μ [D]	ε^{AB}/k [K]	κ^{AB}	VLE data (ref.)
methanol	2B	32.042	2.7721	2.5391	176.67	0.06951	1.70	2318.3	0.23930	<i>n</i> -hexane (164)
ethanol	2B	46.068	3.1053	2.5570	192.25	0.16095	1.70	2483.8	0.08310	<i>n</i> -heptane(167)
1-propanol	2B	60.095	3.2424	2.9841	219.17	0.17079	1.68	2263.7	0.05209	<i>n</i> -heptane (169)
1-butanol	2B	74.122	3.4648	3.0771	243.92	0.21892	1.67	2340.6	0.01971	<i>n</i> -nonane (171)
1-pentanol	2B	88.148	3.7011	3.0186	260.36	0.300023	1.70	2381.3	0.01619	<i>n</i> -heptane (240)
1-hexanol	2B	102.17	3.8144	3.1800	271.36	0.31273	1.65	2701.8	0.00614	<i>n</i> -hexane (241)
1-heptanol	2B	116.20	3.9465	3.3101	275.01	0.31001	1.74	2857.7	0.00574	<i>n</i> -decane (242)
1-octanol	2B	130.23	4.0510	3.4483	283.14	0.29186	1.65	2964.7	0.00472	<i>n</i> -decane (243)
methanol	2C	32.042	3.1718	1.6887	192.36	0.2960	1.70	2621.3	0.06390	<i>n</i> -hexane (164)
ethanol	2C	46.068	3.2876	2.1752	198.25	0.2525	1.70	2734.2	0.03440	<i>n</i> -heptane(167)
1-propanol	2C	60.095	3.2777	2.8852	218.69	0.2030	1.68	2416.1	0.02910	<i>n</i> -heptane (169)
1-butanol	2C	74.122	3.4803	3.0345	244.09	0.2507	1.67	2452.0	0.01090	<i>n</i> -nonane (171)
1-pentanol	2C	88.148	3.7261	2.9606	262.16	0.3343	1.70	2508.9	0.00828	<i>n</i> -heptane (240)
1-hexanol	2C	102.17	3.8261	3.1511	272.08	0.3470	1.65	2828.6	0.00310	<i>n</i> -hexane (241)
1-heptanol	2C	116.20	3.9788	3.2864	277.01	0.3814	1.74	3054.3	0.00198	<i>n</i> -decane (242)
1-octanol	2C	130.23	4.0488	3.4503	282.74	0.3347	1.65	3089.0	0.00224	<i>n</i> -decane (243)
methanol	3B	32.042	2.6231	2.7184	183.94	0.0238	1.70	2072.6	0.11125	<i>n</i> -hexane (164)
ethanol	3B	46.068	2.9784	2.9434	199.29	0.0483	1.70	2023.4	0.06206	<i>n</i> -heptane(167)
1-propanol	3B	60.095	3.1338	3.3026	218.64	0.0713	1.68	1891.3	0.04085	<i>n</i> -heptane (169)
1-butanol	3B	74.122	3.4512	3.1233	244.23	0.1513	1.67	2099.5	0.01497	<i>n</i> -nonane (171)
1-pentanol	3B	88.148	3.6366	3.1754	256.37	0.2145	1.70	2085.3	0.01432	<i>n</i> -heptane (240)
1-hexanol	3B	102.17	3.8065	3.2068	271.58	0.2161	1.65	2430.9	0.00538	<i>n</i> -hexane (241)
1-heptanol	3B	116.20	3.9500	3.3826	275.04	0.2501	1.74	2647.6	0.00345	<i>n</i> -decane (242)

	Sch	M_w [g/mol]	σ [Å]	m	ε/k [K]	x_p	μ [D]	ε^{AB}/k [K]	κ^{AB}	VLE data (ref.)
1-octanol	3B	130.23	4.028	3.5081	281.64	0.1659	1.65	2641.7	0.00457	<i>n</i> -decane (243)
water	4C	18.015	2.6179	1.500	144.82	0.1250	1.85	1838.9	0.20936	-

The averages of the %AAD values of the 1-alcohol pure component properties included in the regression function for sPC-SAFT-GV and sPC-SAFT-JC, based on the different association schemes, are presented in Table 8-3. The %AAD values for individual components are presented in Appendix E:

Table 8-3: Averages of the %AAD values of 1-alcohols pure component properties included in the parameter regression with sPC-SAFT-GV and sPC-SAFT-JC.

Model	ΔP^{sat}	$\Delta \rho^{sat}$	Δh^{vap}
sPC-SAFT-GV-2B	0.31	0.43	1.00
sPC-SAFT-GV-2C	0.22	0.39	0.96
sPC-SAFT-GV-3B	0.28	0.61	1.55
sPC-SAFT-JC-2B	0.36	0.54	1.13
sPC-SAFT-JC-2C	0.28	0.44	1.40
sPC-SAFT-JC-3B	0.29	0.59	1.61

Table 8-3 shows that accurate correlations of the saturated vapour pressure, liquid density and heat of vapourisation are obtained with both sPC-SAFT-GV and sPC-SAFT-JC based on all three association schemes.

The most important observations regarding these new model parameters are summarized below:

- Generally, the segment number (m), segment diameter (σ) and the dispersion energy parameters increase with an increase in carbon number for all parameter sets.
- The association energy parameter is of the same magnitude for smaller alcohols between 1-propanol and 1-pentanol, but then increases drastically (20%) for larger alcohols. This is especially evident in the parameters based on the 3B scheme. Similar trends are observed in the association parameter values determined by Al-Saifi *et al.* (35).
- The 4C water parameters determined for sPC-SAFT-GV and sPC-SAFT-JC correspond well with the targeted values mentioned above.

8.1.3 New model parameters for CPA-GV and CPA-JC

Parameters for alcohols based on both the 2B and 3B schemes have been determined. Similar results are obtained with the 2B and 3B association schemes when the VLE of alcohol/alkane mixtures are considered, but the 3B scheme provides superior VLE predictions of alcohol/water mixtures. Consequently, only results based on the 3B scheme are discussed in this chapter. Comparative results based on the 2B scheme are presented in Appendix E for alcohol/alkane mixtures and alcohol/alcohol mixtures.

Table 8-4: New CPA-GV model parameters for associating components.

	Sch	T_C [K]	$a0/(Rb)$ [K]	b [L/mol]	cI	n_p	μ [D]	ε^{AB}/R [K]	β^{AB}	VLE data (ref.)
methanol	2B	512.5	1582.66	0.031573	0.46917	0.29751	1.70	2819.72	0.018111	<i>n</i> -hexane (164)
ethanol	2B	514.0	1785.72	0.047423	0.73778	0.36551	1.70	2751.72	0.011050	<i>n</i> -heptane(167)
1-propanol	2B	536.8	2164.90	0.063837	0.85852	0.61257	1.68	2587.13	0.007230	<i>n</i> -heptane (169)
1-butanol	2B	563.1	2568.84	0.080979	0.86404	0.75787	1.67	2665.97	0.002911	<i>n</i> -nonane (171)
1-pentanol	2B	588.1	2732.84	0.096374	0.88379	1.17228	1.70	2625.77	0.002680	<i>n</i> -heptane (240)
1-hexanol	2B	611.3	2967.17	0.112193	0.83702	1.38283	1.65	3099.88	0.000830	<i>n</i> -hexane (241)
1-heptanol	2B	632.3	2976.05	0.132213	1.02715	2.07848	1.74	3029.08	0.000581	<i>n</i> -decane (242)
1-octanol	2B	652.3	3229.32	0.147919	0.94591	1.57983	1.65	3231.03	0.000640	<i>n</i> -decane (243)
methanol	3B	512.5	1496.03	0.032856	1.12620	0.09999	1.70	1950.34	0.042419	<i>n</i> -hexane (164)
ethanol	3B	514.0	1768.97	0.048762	1.09446	0.14629	1.70	2060.03	0.017937	<i>n</i> -heptane(167)
1-propanol	3B	536.8	2250.34	0.064968	0.94326	0.44109	1.68	2152.93	0.006236	<i>n</i> -heptane (169)
1-butanol	3B	563.1	2597.82	0.081782	0.93178	0.51925	1.67	2275.45	0.002739	<i>n</i> -nonane (171)
1-pentanol	3B	588.1	2751.77	0.097151	0.90479	0.95894	1.70	2333.74	0.002303	<i>n</i> -heptane (240)
1-hexanol	3B	611.3	2957.17	0.112730	0.87378	1.30033	1.65	2722.91	0.000823	<i>n</i> -hexane (241)
1-heptanol	3B	632.3	2981.49	0.133052	1.03263	1.88802	1.74	2703.22	0.000622	<i>n</i> -decane (242)
1-octanol	3B	652.3	3191.68	0.148252	1.01929	1.82277	1.65	2805.76	0.000559	<i>n</i> -decane (243)
water	4C	647.1	754.006	0.885072	0.0141937	0.15042	1.85	1945.22	0.088380	-

Table 8-5: New CPA-JC model parameters for associating components.

	Sch	T_C [K]	$a0/(Rb)$ [K]	b [L/mol]	cI	x_p	μ [D]	ε^{AB}/R [K]	β^{AB}	VLE data (ref.)
methanol	2B	512.5	1573.83	0.031822	0.400240	0.34201	1.70	2897.05	0.015420	<i>n</i> -hexane (164)
ethanol	2B	514.0	1735.14	0.047843	0.826921	0.46941	1.70	2643.03	0.014590	<i>n</i> -heptane(167)
1-propanol	2B	536.8	2140.71	0.064501	0.876540	0.75990	1.68	2561.17	0.007771	<i>n</i> -heptane (169)
1-butanol	2B	563.1	2551.28	0.081741	0.087011	0.95011	1.67	2650.10	0.003050	<i>n</i> -nonane (171)
1-pentanol	2B	588.1	2714.60	0.097893	0.907020	1.46910	1.70	2565.59	0.002921	<i>n</i> -heptane (240)
1-hexanol	2B	611.3	2957.67	0.113694	0.853871	1.67761	1.65	3058.02	0.000860	<i>n</i> -hexane (241)
1-heptanol	2B	632.3	2960.60	0.135274	1.022450	2.59420	1.74	3034.38	0.000561	<i>n</i> -decane (242)
1-octanol	2B	652.3	3244.51	0.149121	0.942717	1.61552	1.65	3237.25	0.000640	<i>n</i> -decane (243)
methanol	3B	512.5	1365.97	0.032559	1.35802	0.08001	1.70	1826.17	0.067878	<i>n</i> -hexane (164)
ethanol	3B	514.0	1746.84	0.048794	1.12221	0.19429	1.70	2037.20	0.019403	<i>n</i> -heptane(167)
1-propanol	3B	536.8	2238.93	0.065276	0.93793	0.54910	1.68	2167.25	0.006138	<i>n</i> -heptane (169)
1-butanol	3B	563.1	2338.02	0.082922	1.03900	0.78679	1.67	2156.94	0.006170	<i>n</i> -nonane (171)
1-pentanol	3B	588.1	2485.35	0.098272	0.99169	1.00216	1.70	2245.91	0.005727	<i>n</i> -heptane (240)
1-hexanol	3B	611.3	2948.57	0.114094	0.85127	1.50762	1.65	2749.75	0.000856	<i>n</i> -hexane (241)

	Sch	T_C [K]	$a0/(Rb)$ [K]	b [L/mol]	cI	x_p	μ [D]	ε^{AB}/R [K]	β^{AB}	VLE data (ref.)
1-heptanol	3B	632.3	3065.18	0.130616	0.90413	1.46012	1.74	2862.31	0.000731	<i>n</i> -decane (242)
1-octanol	3B	652.3	3240.83	0.149424	0.94659	1.28113	1.65	2906.85	0.000639	<i>n</i> -decane (243)
water	4C	647.1	644.239	1.362483	0.01426461	0.17244	1.85	1843.84	0.112535	-

Both the co-volume (b) and energy parameter ($a0/Rb$) increase more or less linearly with an increase in molecular mass. The parameters trends are consistent with other CPA parameters (37). The averages of the %AAD values for the pure component properties included in the regression function are presented in Table 8-6. The %AAD values for the individual components are also presented in Appendix E.

Table 8-6: Averages of the %AAD values of 1-alcohols pure component properties included in the parameter regression with CPA-GV and CPA-JC

Model	ΔP^{sat}	$\Delta \rho^{sat}$	Δh^{vap}
CPA-GV-2B	0.30	0.74	1.59
CPA-GV-3B	0.29	0.73	2.88
CPA-JC-2B	0.29	0.79	1.75
CPA-JC-3B	0.17	0.67	3.22

8.2 Non-polar/Hydrogen bonding systems

The non-polar/hydrogen bonding systems investigated in this section comprise binary mixtures of alkanes with alcohols. These mixtures are industrially very important, especially in the petrochemical industry, as discussed in Chapter 1. Modelling these type of systems is difficult, because of the large difference between *like* and *unlike* interactions. This section focuses predominantly on alkane/alcohol VLE, but some excess enthalpies and other properties are also briefly investigated. Comparisons are made with sPC-SAFT-JC and sPC-SAFT-GV combined with the 2C, 2B and 3B association schemes for alcohols. The results with the different association schemes are indicated as sPC-SAFT-GV-XX and sPC-SAFT-JC-XX where the XX refers to the association scheme used to model the alcohol. Results with the 2B parameters determined by Al-Saifi *et al.* (35) (for PC-SAFT-GV and PC-SAFT-JC) are also presented in some figures in order to compare the performance of the models with the new model parameters with literature (sPC-SAFT-GV-2B-Lit and sPC-SAFT-JC-2B-Lit). For CPA-GV and CPA-JC, only results based on the 3B scheme are presented (CPA-GV-3B and CPA-JC-3B).

8.2.1 Vapour-liquid-equilibria of alcohol/alkane systems

A summary of results for the alcohol/alkane systems considered are presented in tabular format.

Table 8-7: VLE predictions of *n*-alkane/alcohol mixtures with sPC-SAFT-GV-2C, sPC-SAFT-GV-2B and sPC-SAFT-GV-3B.

Mixture	<i>T</i> or <i>P</i>	sPC-SAFT-GV-2C		sPC-SAFT-GV-2B		sPC-SAFT-GV-3B		<i>np</i>	ref.
		Δy (x10 ²) ^a	$\frac{\Delta P(\%)^b}{\Delta T(K)^a}$	Δy (x10 ²) ^a	$\frac{\Delta P(\%)^b}{\Delta T(K)^a}$	Δy (x10 ²) ^a	$\frac{\Delta P(\%)^b}{\Delta T(K)^a}$		
methanol/ <i>n</i> -butane	323.15 K	0.50*	1.53*	0.60*	0.61*	0.40*	1.30*	11	(162)
methanol/ <i>n</i> -pentane	372.70 K	2.02	3.67	1.61	2.68	1.22	2.11	11	(163)
methanol/ <i>n</i> -hexane	343.15 K	1.33*	2.35*	1.38	1.61	0.72*	1.40*	24	(164)
methanol/ <i>n</i> -hexane	348.15 K	1.97	1.72	2.03	1.95	1.39*	1.54*	24	(241)
methanol/ <i>n</i> -octane	1.013 bar	1.02*	1.94*	0.70*	1.34*	0.88*	1.38*	13	(244)
ethanol/ <i>n</i> -pentane	372.70 K	0.78	1.94	0.62	1.63	0.68	1.58	10	(165)
ethanol/ <i>n</i> -hexane	298.15 K	0.60	2.68	0.45	2.21	0.76	2.75	9	(245)
ethanol/ <i>n</i> -hexane	323.15 K	1.66	1.92	1.53	1.77	0.90	1.03	20	(166)
ethanol/ <i>n</i> -heptane	333.15 K	0.76	0.81	0.63	0.66	0.74	1.12	16	(167)
ethanol/ <i>n</i> -octane	318.15 K	0.81	2.19	0.72	2.10	0.82	2.37	17	(168)
ethanol/isooctane	1.013 bar	1.92	1.18	2.36	1.54	3.28	2.13	21	(246)
1-propanol/ <i>n</i> -hexane	323.15 K	1.03	2.79	1.11	3.05	1.34	3.77	22	(169)
1-propanol/ <i>n</i> -heptane	333.15 K	1.02	1.16	1.06	1.23	1.54	1.82	33	(169)
1-propanol/ <i>n</i> -octane	358.15 K	0.90	2.85	0.94	2.82	1.33	3.12	25	(170)
1-propanol/ <i>n</i> -octane	363.15 K	0.75	1.160	0.85	1.17	1.40	1.70	24	(247)
1-propanol/ <i>n</i> -nonane	298.15 K	1.11*	1.15*	1.12*	1.18*	1.07*	1.30*	17	(171)
1-butanol/ <i>n</i> -hexane	323.15 K	0.60	3.48	0.64	3.73	0.67	3.98	10	(248)
1-butanol/ <i>n</i> -hexane	348.15 K	0.83	3.66	0.93	4.03	0.92	4.01	14	(171)
1-butanol/ <i>n</i> -heptane	333.15 K	0.62	1.66	0.75	2.06	0.81	2.24	19	(249)
1-butanol/ <i>n</i> -heptane	363.15 K	1.22	4.95	1.46	5.30	1.56	5.63	22	(249)
1-butanol/ <i>n</i> -octane	373.15 K	1.88	5.25	2.14	5.74	2.30	6.09	22	(173)
1-butanol/ <i>n</i> -nonane	323.15 K	0.79	0.88	0.78	0.78	0.88	0.82	15	(171)
1-butanol/ <i>n</i> -decane	373.15 K	1.80	3.53	1.57	3.22	1.31	2.85	22	(241)
1-butanol/ <i>n</i> -decane	383.15 K	1.52	3.18	1.33	2.93	1.09	2.66	22	(241)
1-pentanol/ <i>n</i> -heptane	348.15 K	0.92	1.09	1.00	1.39	1.07	1.74	19	(240)
1-hexanol/ <i>n</i> -hexane	342.82 K	0.15	0.73	0.15	0.99	0.15	1.08	22	(241)
1-heptanol/ <i>n</i> -decane	0.1359 bar	2.28	0.61	2.15	0.69	3.00	1.00	15	(242)
1-octanol/ <i>n</i> -decane	383.15 K	0.66	0.84	0.70	0.86	0.69	1.01	14	(243)
Average		1.12	2.18	1.12	2.16	1.18	2.27		

^a $\Delta z = \sum_i^{np} |z_i^{calc} - z_i^{exp}|$ where *z* represents *y* or *T* and *np* is the number of data points. ^b Deviations as %AAD.

* VLLE predicted at these conditions. *k_{ij}* values presented in Table 8-8 used to obtain correct phase behaviour.

From Table 8-7, it is clear that when alcohols are modelled in the framework of sPC-SAFT-GV with either the 2C, 2B or 3B association scheme, similar alcohol/alkane VLE representations are obtained. In Chapter 6, it was found that when alcohols are modelled with sPC-SAFT and the 2C scheme, worse alcohol/alkane VLE representations are obtained compared to the 2B and 3B schemes. This is no longer the case when the GV-polar term is also included in the state function of sPC-SAFT. A point of concern, however, is that in some systems with small-chained alcohols at lower temperatures, false liquid-liquid demixing is predicted with all three association schemes. The problem is most severe with the 3B scheme, least severe with the 2B scheme and somewhere

in between with the 2C scheme, as indicated by the magnitude of the k_{ij} -values reported in Table 8-8 (k_{ij} -values used to obtain correct phase behaviour). This possibly indicates that the 2B scheme is the most suited association scheme to model alcohols, but since the results for all three association schemes are very similar, more evidence is required before a universal association scheme can be assigned.

Table 8-8: k_{ij} values used in alcohol/alkane VLE calculations to obtain correct phase behaviour with sPC-SAFT-GV

Mixture	T or P	sPC-SAFT-GV-2C	sPC-SAFT-GV-2B	sPC-SAFT-GV-3B
methanol/ <i>n</i> -butane	323.15 K	-0.0075	-0.0033	-0.0100
methanol/ <i>n</i> -hexane	343.15 K	-0.0040	-0.0010	-0.0080
methanol/ <i>n</i> -hexane	348.15 K	-0.0020	-	-0.0070
methanol/ <i>n</i> -octane	1.013 bar	-0.0175	-0.0120	-0.0160
1-propanol/ <i>n</i> -nonane	298.15 K	-0.0068	-0.0069	-0.00716

Similar to the results presented for sPC-SAFT-GV, Table 8-9 shows VLE results with sPC-SAFT-JC combined with the 2C, 2B and 3B association:

Table 8-9: VLE results of *n*-alkane/alcohol mixtures with sPC-SAFT-JC-2B, sPC-SAFT-JC-2C and sPC-SAFT-JC-3B.

Mixture	T or P	sPC-SAFT-JC-2C		sPC-SAFT-JC-2B		sPC-SAFT-JC-3B		np	ref.
		Δy ($\times 10^2$) ^a	$\frac{\Delta P(\%)^b}{\Delta T(K)^a}$	Δy ($\times 10^2$) ^a	$\frac{\Delta P(\%)^b}{\Delta T(K)^a}$	Δy ($\times 10^2$) ^a	$\frac{\Delta P(\%)^b}{\Delta T(K)^a}$		
methanol/ <i>n</i> -butane	323.15 K	0.59 [*]	0.74 [*]	0.60	0.59	0.40 [*]	1.26 [*]	11	(162)
methanol/ <i>n</i> -pentane	372.7 K	2.29	4.02	1.94	3.41	1.23	2.14	11	(163)
methanol/ <i>n</i> -hexane	343.15 K	1.37	1.37	1.28	1.81	0.74	1.30	24	(164)
methanol/ <i>n</i> -hexane	348.15 K	2.20	2.01	1.80	2.38	1.44	1.48	24	(241)
methanol/ <i>n</i> -octane	1.013 bar	0.70 [*]	1.54 [*]	0.58 [*]	1.15 [*]	0.85 [*]	1.34 [*]	13	(244)
ethanol/ <i>n</i> -pentane	372.7 K	0.96	2.10	0.67	1.58	0.64	1.48	10	(165)
ethanol/ <i>n</i> -hexane	298.15 K	0.58	2.92	0.51	2.67	0.88	3.25	9	(245)
ethanol/ <i>n</i> -hexane	323.15 K	1.65	1.98	1.52	1.73	0.95	1.21	20	(166)
ethanol/ <i>n</i> -heptane	333.15 K	0.75	0.87	0.62	0.71	0.83	1.18	16	(167)
ethanol/ <i>n</i> -octane	318.15 K	0.83	2.46	0.77	2.46	0.92	2.64	17	(168)
ethanol/isooctane	1.0132 bar	1.72	1.05	2.32	1.53	3.31	2.15	21	(246)
1-propanol/ <i>n</i> -hexane	323.15 K	1.06	2.81	1.07	2.81	1.37	3.68	22	(169)
1-propanol/ <i>n</i> -heptane	333.15 K	1.08	1.24	1.11	1.33	1.79	2.20	33	(169)
1-propanol/ <i>n</i> -octane	358.15 K	1.02	3.18	1.12	3.32	1.54	3.50	25	(170)
1-propanol/ <i>n</i> -octane	363.15 K	0.77	1.43	0.92	1.58	1.56	1.96	24	(247)
1-propanol/ <i>n</i> -nonane	298.15 K	1.01 [*]	0.90 [*]	0.99 [*]	0.89 [*]	0.85 [*]	0.95 [*]	17	(171)
1-butanol/ <i>n</i> -hexane	323.15 K	0.70	3.96	0.69	3.95	0.68	4.04	10	(248)
1-butanol/ <i>n</i> -hexane	348.15 K	0.98	4.30	1.03	4.49	0.95	4.19	14	(171)
1-butanol/ <i>n</i> -heptane	333.15 K	0.88	2.47	0.89	2.56	0.85	2.34	19	(249)
1-butanol/ <i>n</i> -heptane	363.15 K	1.56	5.51	1.67	5.65	1.62	5.74	22	(249)
1-butanol/ <i>n</i> -octane	373.15 K	2.30	6.02	2.42	6.28	2.39	6.30	22	(173)
1-butanol/ <i>n</i> -nonane	323.15 K	0.81	0.79	0.77	0.69	0.85	0.74	15	(171)
1-butanol/ <i>n</i> -decane	373.15 K	1.59	3.48	1.51	3.40	1.33	2.97	22	(241)

Mixture	T or P	sPC-SAFT-JC-2C		sPC-SAFT-JC-2B		sPC-SAFT-JC-3B		np	ref.
		Δy (x10 ²) ^a	$\frac{\Delta P(\%)}{\Delta T(K)}^b$	Δy (x10 ²) ^a	$\frac{\Delta P(\%)}{\Delta T(K)}^b$	Δy (x10 ²) ^a	$\frac{\Delta P(\%)}{\Delta T(K)}^b$		
1-butanol/n-decane	383.15 K	1.38	3.22	1.28	3.16	1.10	2.79	22	(241)
1-pentanol/n-heptane	348.15 K	0.99	1.55	1.07	1.81	1.09	2.01	19	(240)
1-hexanol/n-hexane	342.82 K	0.14	1.52	0.14	1.48	0.14	1.28	22	(241)
1-heptanol/n-decane	0.1359 bar	2.10	0.55	2.03	0.46	2.47	0.75	15	(242)
1-octanol/n-decane	383.15 K	0.74	1.18	0.72	1.15	0.71	1.11	14	(243)
Average		1.17	2.33	1.14	2.35	1.20	2.36		

^a $\Delta z = \sum_i^{np} |z_i^{calc} - z_i^{exp}|$ where z represents y or T and np is the number of data points. ^b Deviations as %AAD.

* VLLE predicted at these conditions. k_{ij} values presented in Table 8-10 used to obtain correct phase behaviour.

Table 8-9 shows that similar VLE results are obtained with sPC-SAFT-JC when alcohols are modelled with the 2C, 2B or 3B schemes. Similar to the results for sPC-SAFT-GV, modelling alcohols with the 2C association scheme in the framework of sPC-SAFT-JC do not result in significantly worse VLE results compared to the 2B and 3B association schemes. False phase splits are also obtained with sPC-SAFT-JC at lower temperatures, but this is easily corrected with small BIPs, as indicated in Table 8-10. Al-Saifi *et al.* (35) also reported that PC-SAFT-JC and PC-SAFT-GV are prone to predict false phase splits at lower temperatures. This possibly indicates that the temperature dependencies of these models are not completely correct and should be improved in future studies.

Table 8-10: k_{ij} values used in alcohol/alkane VLE calculations to obtain correct phase behaviour with sPC-SAFT-JC

Mixture	T or P	sPC-SAFT-JC-2C	sPC-SAFT-JC-2B	sPC-SAFT-JC-3B
methanol/n-butane	323.15 K	-0.0030	-	-0.0100
methanol/n-hexane	343.15 K	-	-	-0.0080
methanol/n-hexane	348.15 K	-	-	-0.0070
methanol/n-octane	1.013 bar	-0.0140	-0.0080	-0.0160
1-propanol/n-nonane	298.15 K	-0.0066	-0.0061	-0.0064

Lastly, Table 8-11 shows VLE results for CPA, CPA-GV and CPA-JC. CPA predictions for systems containing 1-hexanol and 1-heptanol could not be calculated, because model parameters based on the 3B scheme are not available in the literature and could not be determined via regression.

Table 8-11: VLE predictions of n-alkane/alcohol mixtures with CPA-3B, CPA-GV-3B and CPA-JC-3B

Mixture	T or P	CPA-3B		CPA-GV-3B		CPA-JC-3B		np	ref.
		Δy (x10 ²) ^a	$\frac{\Delta P(\%)}{\Delta T(K)}^b$	Δy (x10 ²) ^a	$\frac{\Delta P(\%)}{\Delta T(K)}^b$	Δy (x10 ²) ^a	$\frac{\Delta P(\%)}{\Delta T(K)}^b$		
methanol/n-butane	323.15 K	0.71*	2.10*	0.59*	1.38*	0.60	1.36	11	(162)
methanol/n-pentane	372.7 K	2.13	3.71	1.83	3.31	1.90	3.59	11	(163)
methanol/n-hexane	343.15 K	2.39*	3.66*	1.71*	2.74*	1.56*	2.23*	24	(164)
methanol/n-hexane	348.15 K	2.63*	4.01*	2.06*	2.99*	1.98*	2.45*	24	(241)
methanol/n-octane	1.013 bar	1.38*	2.19*	1.03*	1.89*	0.90*	1.65*	13	(244)
ethanol/n-pentane	372.7 K	2.10	6.09	1.19	3.66	1.15	3.54	10	(165)

Mixture	<i>T</i> or <i>P</i>	CPA-3B		CPA-GV-3B		CPA-JC-3B		<i>np</i>	ref.
		Δy (x10 ²) ^a	$\frac{\Delta P(\%)}{\Delta T(K)}^b$	Δy (x10 ²) ^a	$\frac{\Delta P(\%)}{\Delta T(K)}^b$	Δy (x10 ²) ^a	$\frac{\Delta P(\%)}{\Delta T(K)}^b$		
ethanol/ <i>n</i> -hexane	298.15 K	1.09*	1.90*	0.42	1.70	0.48	1.95	9	(245)
ethanol/ <i>n</i> -hexane	323.15 K	1.62	3.01	1.07	2.08	1.04	1.95	20	(166)
ethanol/ <i>n</i> -heptane	333.15 K	1.87	2.54	0.53	0.64	0.53	0.69	16	(167)
ethanol/ <i>n</i> -octane	318.15 K	2.31*	5.24*	0.67*	1.82*	0.65*	1.76*	17	(168)
ethanol/isooctane	1.0132 bar	3.49	1.74	2.00	1.10	2.04	1.25	21	(246)
1-propanol/ <i>n</i> -hexane	323.15 K	0.78	4.15	0.72	1.68	0.75	1.72	22	(169)
1-propanol/ <i>n</i> -heptane	333.15 K	2.21	4.01	1.42	1.68	1.35	1.58	33	(169)
1-propanol/ <i>n</i> -octane	358.15 K	2.57	6.75	1.28	3.14	1.20	2.99	25	(170)
1-propanol/ <i>n</i> -octane	363.15 K	2.34	4.79	1.35	1.63	1.28	1.50	24	(247)
1-propanol/ <i>n</i> -nonane	298.15 K	0.93*	1.25*	1.06*	1.12*	1.11*	1.21*	17	(171)
1-butanol/ <i>n</i> -hexane	323.15 K	0.29	3.20	0.48	3.86	0.41	2.53	10	(248)
1-butanol/ <i>n</i> -hexane	348.15 K	1.29	7.01	1.36	7.10	0.72	4.88	14	(171)
1-butanol/ <i>n</i> -heptane	333.15 K	0.92	3.60	0.91	3.25	0.33	0.91	19	(249)
1-butanol/ <i>n</i> -heptane	363.15 K	1.63	5.01	1.98	6.13	0.55	4.38	22	(249)
1-butanol/ <i>n</i> -octane	373.15 K	2.06	6.09	2.58	6.78	0.97	4.60	22	(173)
1-butanol/ <i>n</i> -nonane	323.15 K	0.52	0.55	1.11	1.30	1.40	2.58	15	(171)
1-butanol/ <i>n</i> -decane	373.15 K	1.99	3.93	1.20	2.49	2.52	5.72	22	(241)
1-butanol/ <i>n</i> -decane	383.15 K	1.71	3.45	1.01	2.10	2.27	4.95	22	(241)
1-pentanol/ <i>n</i> -heptane	348.15 K	2.27	5.91	1.02	1.66	0.67	0.62	19	(240)
1-hexanol/ <i>n</i> -hexane	342.82 K	-	-	0.14	1.01	0.18	0.94	22	(241)
1-heptanol/ <i>n</i> -decane	0.1359 bar	-	-	1.15	0.21	1.03	0.26	15	(242)
Average		1.73	3.83	1.18	2.54	1.10	2.36		

^a $\Delta z = \sum_i^{np} |z_i^{calc} - z_i^{exp}|$ where *z* represents *y* or *T* and *np* is the number of data points. ^b Deviations as %AAD.

* VLLE predicted at these conditions. *k_{ij}* values presented in Table 8-12 used to obtain correct phase behaviour.

Comparing the average values for the different models in Table 8-11 with each other, it appears that CPA-JC and CPA-GV provides slightly improved VLE predictions compared to normal CPA. The improvement, however, is small. False VLLE is predicted for several mixtures, but as with sPC-SAFT-GV and sPC-SAFT-JC, is easily corrected with a small BIP (see Table 8-12). Comparative results based on the 2B scheme are presented in Appendix E.

Table 8-12: *k_{ij}* values used in alcohol/alkane VLE calculations to obtain correct phase behaviour with CPA, CPA-GV and CPA-JC

Mixture	<i>T</i> or <i>P</i>	CPA-3B	CPA-GV-3B	CPA-JC-3B
methanol/ <i>n</i> -butane	323.15 K	-0.005	-0.002	-
methanol/ <i>n</i> -hexane	343.15 K	-0.015	-0.012	-0.009
methanol/ <i>n</i> -hexane	348.15 K	-0.012	-0.009	-0.005
methanol/ <i>n</i> -octane	1.013 bar	-0.042	-0.042	-0.039
ethanol/ <i>n</i> -hexane	298.15 K	-0.004	-	-
ethanol/ <i>n</i> -octane	318.15 K	-0.010	-0.005	-0.006
1-propanol/ <i>n</i> -nonane	298.15 K	-0.008	-0.019	-0.019

In the remainder of this section, representative phase equilibria results for some alcohol/alkane systems are presented graphically. Results with the 2B model parameters from Al-Saifi *et al.* (35) are also included for comparative purposes and are denoted as sPC-SAFT-GV-2B-Lit and sPC-SAFT-JC-2B-Lit.

VLE predictions of the methanol/*n*-hexane system are shown in Figure 8-7 for the GV-based models and Figure 8-8 shows predictions for the JC-based models.

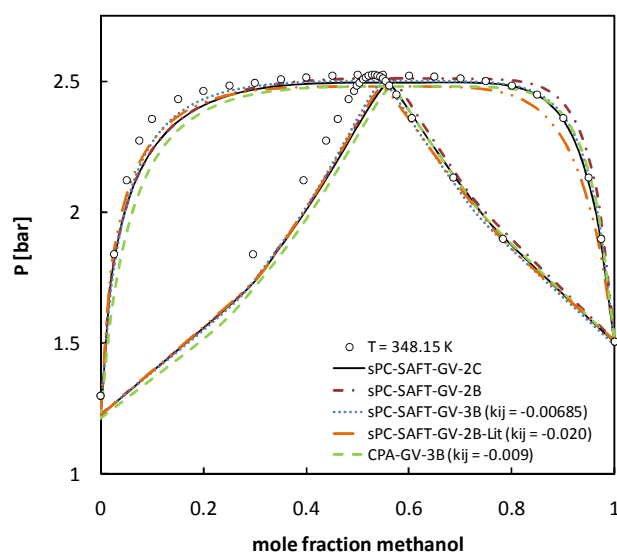


Figure 8-3: VLE results for the methanol/*n*-hexane system with sPC-SAFT-GV-2C, sPC-SAFT-GV-2B, sPC-SAFT-GV-3B, sPC-SAFT-GV-2B-Lit and CPA-GV-3B. Experimental data from ref. (241).

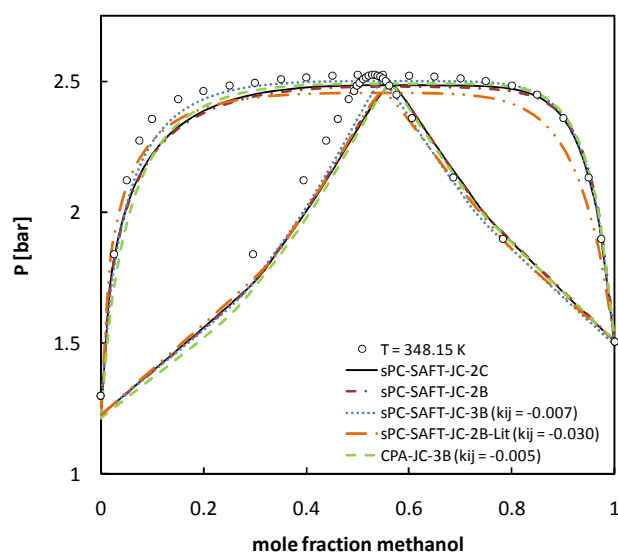


Figure 8-4: VLE results for the methanol/*n*-hexane system with sPC-SAFT-JC-2C, sPC-SAFT-JC-2B, sPC-SAFT-JC-3B, sPC-SAFT-JC-2B-Lit and CPA-JC-3B. Experimental data from ref. (241).

From Figure 8-3 and Figure 8-4, a few important observations can be made: a) the performance of the respective GV- and JC-based models are very similar, indicating that the two polar theories are more or less equivalent, b) when methanol is modelled as a 3B molecule, false phase splits are obtained with the polar sPC-SAFT and CPA models, but it is easily corrected with a small BIP, c) the 2B literature parameters from Al-Saifi *et al.* (35) are slightly inferior to the 2B parameters determined in this work, as indicated by the magnitude of the BIPs, and d) all the models only provide a fair prediction of the azeotrope.

In Figure 8-5 and Figure 8-6, LLE correlations of the methanol/*n*-hexane system with the GV and JC models are shown respectively. From these figures, it is noticed that the correlations based on the 2B parameters from Al-Saifi *et al.* (35) provide the least accurate representation of the LLE data (sPC-SAFT-GV-2B-Lit and sPC-SAFT-JC-2B-Lit). sPC-SAFT-GV-2B, sPC-SAFT-JC-2B, CPA-GV-3B and CPA-JC-3B provide very reasonable correlations, while sPC-SAFT-GV-3B and sPC-SAFT-JC-3B are less accurate. The best correlation of the LLE data is achieved with sPC-SAFT-JC-2C. Unfortunately, sPC-SAFT-GV-2C only manages to provide a correlation that is slightly more accurate than sPC-SAFT-GV-3B. Attempts were made to re-determine methanol sPC-SAFT-GV-2C model parameters, but no parameter sets were found that could provide improved LLE correlations

without sacrificing accuracy in the VLE representation of other types of systems e.g. methanol/ethanol and methanol/water.

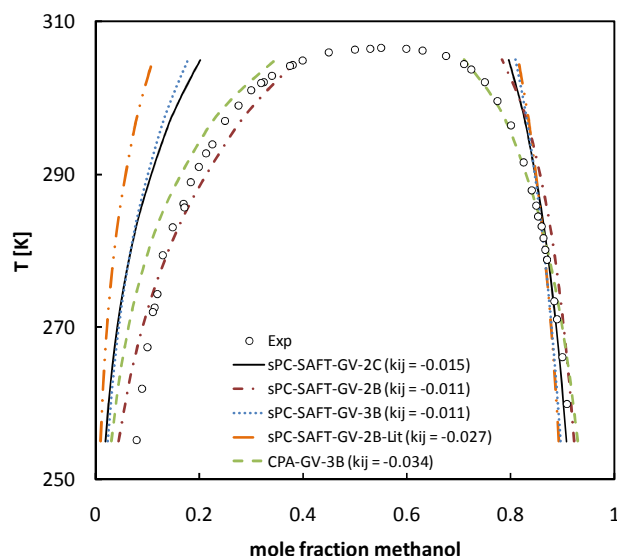


Figure 8-5: LLE correlations of the methanol/*n*-hexane system with sPC-SAFT-GV-2C, sPC-SAFT-GV-2B, sPC-SAFT-GV-3B, sPC-SAFT-GV-2B-Lit, CPA-GV-3B. Experimental data from ref. (176).

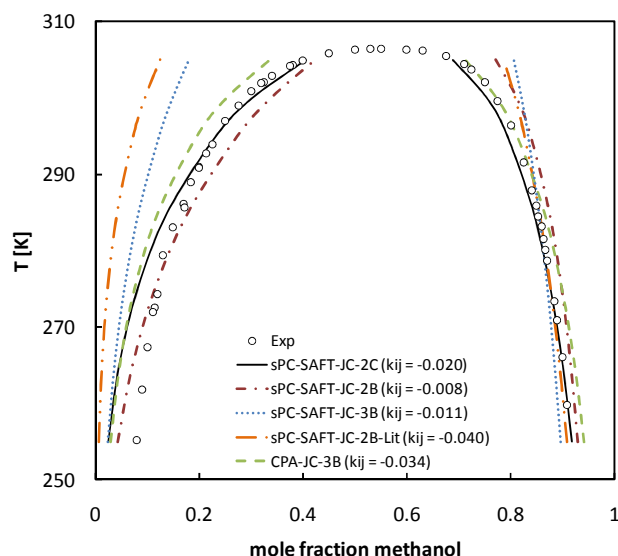


Figure 8-6: LLE correlations of the methanol/*n*-hexane system with sPC-SAFT-JC-2C, sPC-SAFT-JC-2B, sPC-SAFT-JC-3B, sPC-SAFT-JC-2B-Lit, CPA-JC-3B. Experimental data from ref. (176).

From Figure 8-7 and Figure 8-8, it is apparent that the predictions of all models for ethanol/*n*-heptane system are similar. The only prediction that is less accurate compared to the other predictions is sPC-SAFT-JC-2B-Lit with parameters from Al-Saifi *et al.* (35). At this point, there is no major difference between the performance of sPC-SAFT-GV or sPC-SAFT-JC in predicting phase equilibria of alcohol/alkane mixtures. The influence of the association scheme is also negligible in both sPC-SAFT-GV and sPC-SAFT-JC. The influence of the association scheme also becomes smaller with an increase in alcohol chain length, as established in Chapter 6.

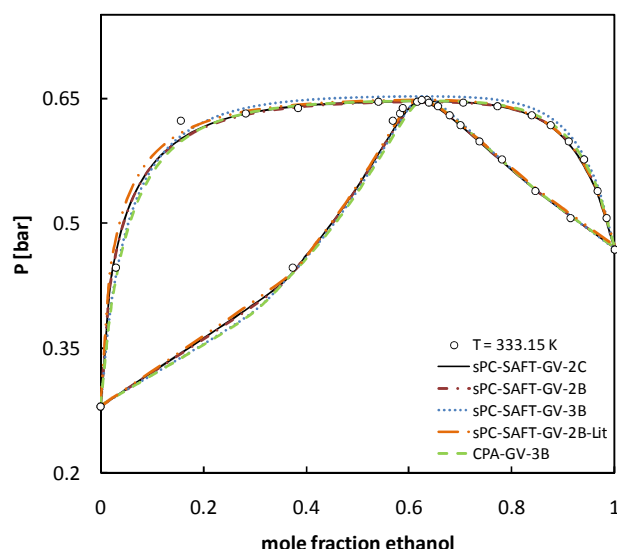


Figure 8-7: VLE predictions of the ethanol/n-heptane system with sPC-SAFT-GV-2C, sPC-SAFT-GV-2B, sPC-SAFT-GV-3B, sPC-SAFT-GV-2B-Lit, CPA-GV-3B. Experimental data from ref. (167).

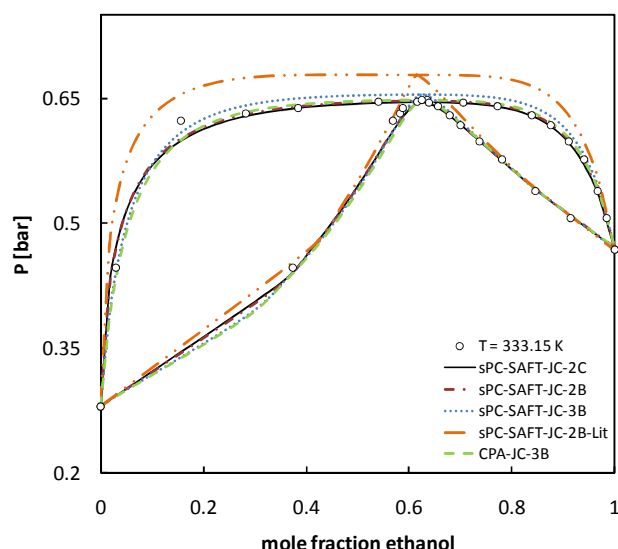


Figure 8-8: VLE predictions of the ethanol/n-heptane system with sPC-SAFT-JC-2C, sPC-SAFT-JC-2B, sPC-SAFT-JC-3B, sPC-SAFT-JC-2B-Lit, CPA-JC-3B. Experimental data from ref. (167).

This is further supported by considering the LLE of ethanol with *n*-tetradecane as presented in Figure 8-9 (GV-based models) and Figure 8-10 (JC-based models). From these figures, the same level of accuracy is obtained with all three association schemes. The BIP values of the predictions based on the 3B scheme is, however, marginally smaller. (The main reason why poor LLE predictions are obtained for the ethanol/*n*-tetradecane system is probably a result of the large asymmetry between the two components).

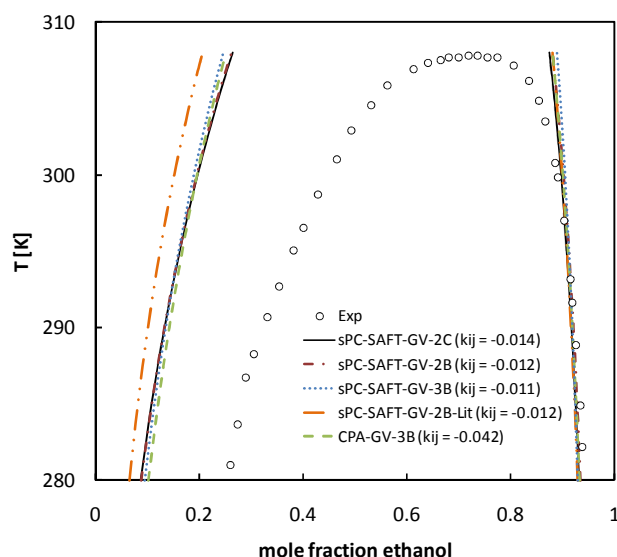


Figure 8-9: LLE correlations of the ethanol/*n*-tetradecane system with sPC-SAFT-GV-2C, sPC-SAFT-GV-2B, sPC-SAFT-GV-3B, sPC-SAFT-GV-2B-Lit, CPA-GV-3B. Experimental data from ref. (250).

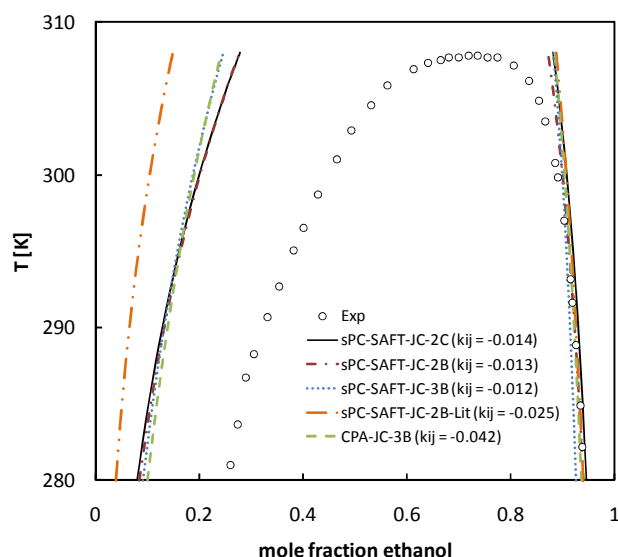


Figure 8-10: LLE correlations of the ethanol/*n*-tetradecane system with sPC-SAFT-JC-2C, sPC-SAFT-JC-2B, sPC-SAFT-JC-3B, sPC-SAFT-JC-2B-Lit, CPA-JC-3B. Experimental data from ref. (250).

Moderate errors in the VLE predictions of some systems were routinely encountered. An example of such a system is the 1-butanol/*n*-octane system as presented in Figure 8-11 and Figure 8-12 for

the GV and JC-based models respectively. From these figures, it follows that the predictions of sPC-SAFT-JC and sPC-SAFT-GV, regardless of the association scheme used, are very similar and display more or less the same magnitude of error. There are a few probable explanations for the error. Some of these include:

- Temperature dependency of the models – the error probably originates from either the polar or dispersion terms.
- The VLE data is not completely accurate.

The predictions of all models may be improved by fitting a BIP as shown in Figure 8-13 (GV-based models) and Figure 8-14 (JC-based models). The correlations obtained are nearly identical for all models considered in this investigation.

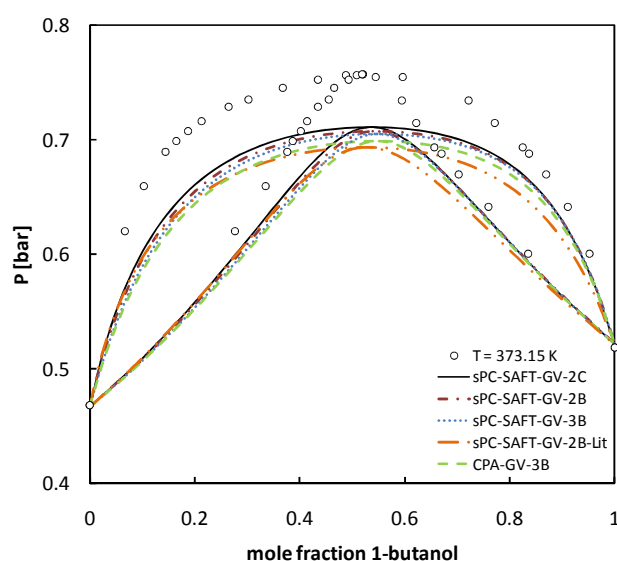


Figure 8-11: VLE predictions of the 1-butanol/n-octane system with sPC-SAFT-GV-2C, sPC-SAFT-GV-2B, sPC-SAFT-GV-3B, sPC-SAFT-GV-2B-Lit, CPA-GV-3B. Experimental data from ref. (173).

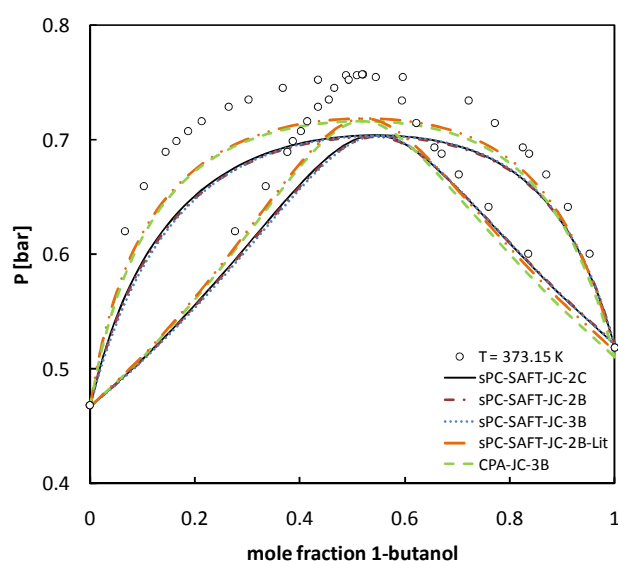


Figure 8-12: VLE predictions of the 1-butanol/n-octane system with sPC-SAFT-JC-2C, sPC-SAFT-JC-2B, sPC-SAFT-JC-3B, sPC-SAFT-JC-2B-Lit, CPA-JC-3B. Experimental data from ref. (173).

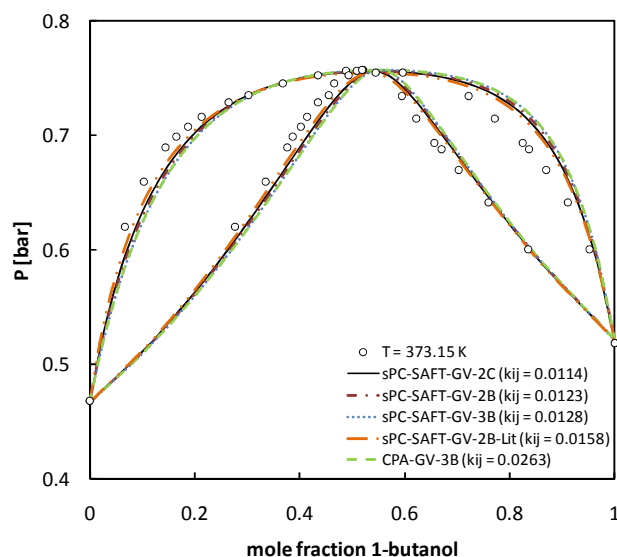


Figure 8-13: VLE correlations of the 1-butanol/n-octane system with sPC-SAFT-GV-2C, sPC-SAFT-GV-2B, sPC-SAFT-GV-3B, sPC-SAFT-GV-2B-Lit, CPA-GV-3B. Experimental data from ref. (173).

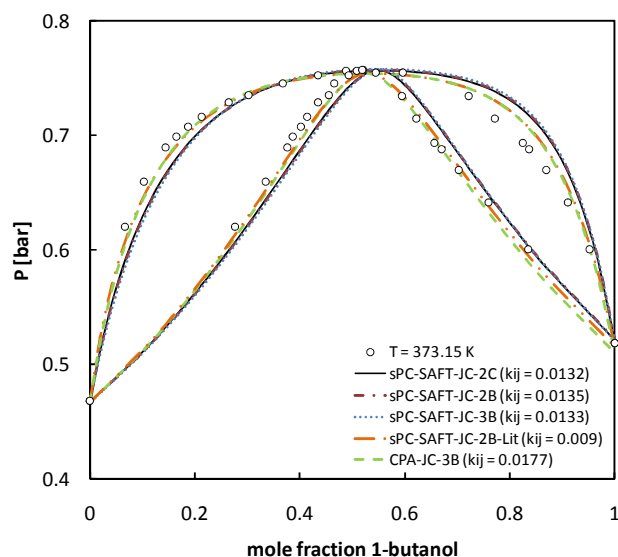


Figure 8-14: VLE correlations of the 1-butanol/n-octane system with sPC-SAFT-GV-2C, sPC-SAFT-GV-2B, sPC-SAFT-GV-3B, sPC-SAFT-GV-2B-Lit, CPA-GV-3B. Experimental data from ref. (173).

Finally, VLE predictions for the *n*-hexane/1-hexanol system with the GV and JC based models are presented in Figure 8-15 and Figure 8-16. Good VLE results appear to be obtained by both polar sPC-SAFT and both polar CPA models for binary systems with components that have a large difference in vapour pressure.

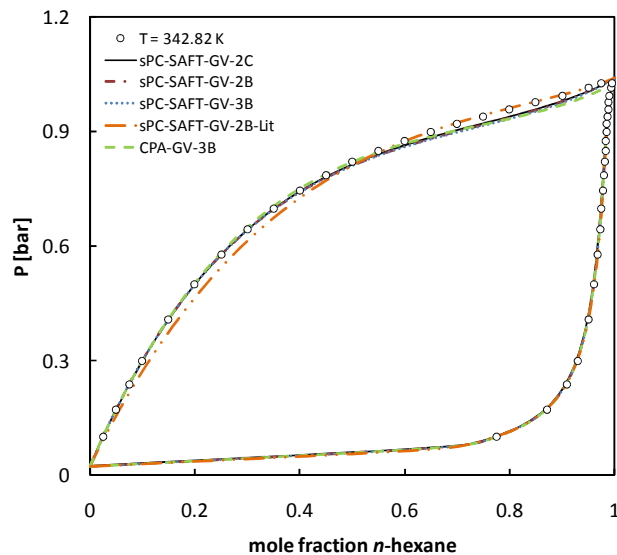


Figure 8-15: VLE predictions of the *n*-hexane/1-hexanol system with sPC-SAFT-GV-2C, sPC-SAFT-GV-2B, sPC-SAFT-GV-3B, sPC-SAFT-GV-2B-Lit, CPA-GV-3B. Experimental data from ref. (241).

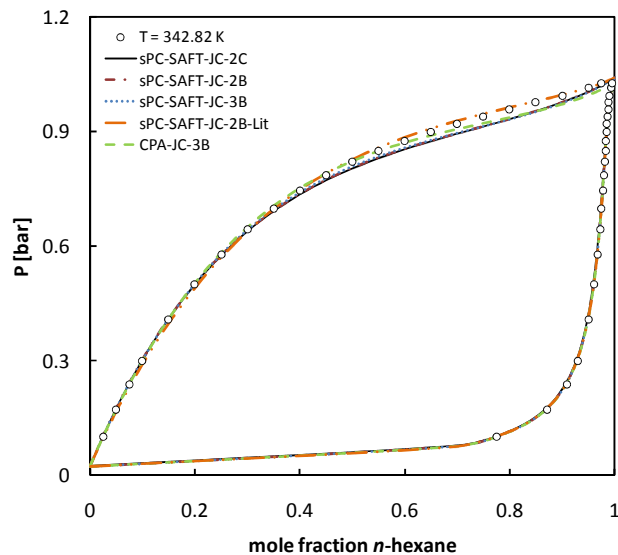


Figure 8-16: VLE predictions of the *n*-hexane/1-hexanol system with sPC-SAFT-JC-2C, sPC-SAFT-JC-2B, sPC-SAFT-JC-3B, sPC-SAFT-JC-2B-Lit, CPA-JC-3B. Experimental data from ref. (241).

From the alcohol/alkane VLE results presented in this section, the main findings are:

- The performance of sPC-SAFT-GV and sPC-SAFT-JC is very similar for the systems investigated.

- The influence of the different association schemes (2B, 2C and 3B) with respect to model predictions is negligible. The major exception seems to be in mixtures containing methanol, where the 2C and 2B schemes are more suited.
- The 2B parameters determined in this work provide slightly improved VLE predictions compared to the parameters of Al-Saifi *et al.* (35). However, it should be mentioned that binary VLE data was included in the regression function in this work, while Al-Saifi *et al.* (35) only included pure component properties.
- CPA-JC and CPA-GV are able to represent alkane/alcohol systems satisfactorily when alcohols are modelled with the 3B scheme.

8.2.2 Excess enthalpy

Excess enthalpies of several alcohol/alkane systems are also investigated with sPC-SAFT-GV, sPC-SAFT-JC, CPA-GV and CPA-JC.

Table 8-13: Excess enthalpy predictions of alcohol/alkane systems with sPC-SAFT-2C, sPC-SAFT-GV-2B, sPC-SAFT-JC-3. Data at 1.013 bar unless otherwise stated.

Mixture	T	%AAD			np	ref.
		sPC-SAFT-GV-2C	sPC-SAFT-GV-2B	sPC-SAFT-GV-3B		
methanol/ <i>n</i> -pentane (P = 5 MPa)	298.15 K	109	93.6	50.1	27	(251)
ethanol/ <i>n</i> -butane (P = 5 MPa)	298.15 K	111	102	83.4	26	(252)
ethanol/ <i>n</i> -butane (P = 5 MPa)	348.15 K	44.0	42.8	49.4	26	(252)
ethanol/ <i>n</i> -hexane	298.15 K	99.2	86.2	70.1	17	(253)
ethanol/ <i>n</i> -heptane	333.15 K	30.9	26.7	29.3	22	(254)
ethanol/ <i>n</i> -nonane	318.15 K	55.1	47.8	43.6	23	(255)
1-propanol/ <i>n</i> -butane (P = 5 MPa)	298.15 K	207	204	186	26	(256)
1-propanol/ <i>n</i> -butane (P = 5 MPa)	348.15 K	40.5	43.2	54.7	26	(256)
1-propanol/ <i>n</i> -heptane	318.15 K	72.6	73.9	77.7	21	(255)
1-butanol/ <i>n</i> -hexane	298.15 K	170	178	158	23	(253)
1-butanol/ <i>n</i> -heptane	288.15 K	215	222	185	10	(110)
1-butanol/ <i>n</i> -heptane	328.15 K	76.9	82.0	82.4	10	(110)
1-butanol/ <i>n</i> -decane	288.15 K	185	189	161	10	(257)
1-pentanol/ <i>n</i> -heptane	298.15 K	113	121	109	25	(258)
1-pentanol/ <i>n</i> -decane	288.15 K	162	170	145	10	(257)
1-hexanol/ <i>n</i> -heptane	288.15 K	183	192	125	10	(257)
1-heptanol/ <i>n</i> -octane	298.15 K	103	97	55	19	(259)
1-octanol/ <i>n</i> -hexane	288.15 K	135	114	28.3	10	(257)
Average		117	116	94.2		

The results in Table 8-13 indicate that sPC-SAFT-GV provides poor predictions of excess enthalpies for alcohol/alkane systems. The predictions based on the 2C and 2B schemes are fairly similar and the predictions based on the 3B scheme are slightly superior. It should be noted that most of the excess enthalpy experimental data modelled were at low temperatures. The predictions of sPC-SAFT-GV (with all three association schemes) improve dramatically at higher temperatures

e.g. consider the results for the 1-propanol/*n*-butane systems at 298.15 K and 348.15 K. The results give a clear indication that the temperature dependency of the model is not very accurate.

Similarly, the results presented for sPC-SAFT-JC in Table 8-14 indicate that the temperature dependency of sPC-SAFT-JC is not correct. The average %AADs for sPC-SAFT-JC are slightly higher compared to sPC-SAFT-GV for all three association schemes. Attempts were made to fit alcohol model parameters to pure component data and excess enthalpy data, instead of pure component data and VLE data. Unfortunately, the resulting model parameters provided poor VLE predictions.

Table 8-14: Excess enthalpy predictions with sPC-SAFT-3B, sPC-SAFT-GV-3B, sPC-SAFT-JC-3B. Data at 1.013 bar unless otherwise stated.

Mixture	<i>T</i>	%AAD			<i>np</i>	ref.
		sPC-SAFT-JC-2C	sPC-SAFT-JC-2B	sPC-SAFT-JC-3B		
methanol/ <i>n</i> -pentane (P = 5 MPa)	298.15 K	140	89.3	52.6	27	(251)
ethanol/ <i>n</i> -butane (P = 5 MPa)	298.15 K	136	121	88.2	26	(252)
ethanol/ <i>n</i> -butane (P = 5 MPa)	348.15 K	46.7	45.4	50.0	26	(252)
ethanol/ <i>n</i> -hexane	298.15 K	116	99.6	74.6	17	(253)
ethanol/ <i>n</i> -heptane	333.15 K	32.5	28.7	30.1	22	(254)
ethanol/ <i>n</i> -nonane	318.15 K	63.2	53.8	46.1	23	(255)
1-propanol/ <i>n</i> -butane (P = 5 MPa)	298.15 K	237	228	207	26	(256)
1-propanol/ <i>n</i> -butane (P = 5 MPa)	348.15 K	41.6	43.6	55.1	26	(256)
1-propanol/ <i>n</i> -heptane	318.15 K	78.21	77.1	77.7	21	(255)
1-butanol/ <i>n</i> -hexane	298.15 K	210	204	170	23	(253)
1-butanol/ <i>n</i> -heptane	288.15 K	273	260	203	10	(110)
1-butanol/ <i>n</i> -heptane	328.15 K	90.5	90.2	85	10	(110)
1-butanol/ <i>n</i> -decane	288.15 K	229	219	175	10	(257)
1-pentanol/ <i>n</i> -heptane	298.15 K	143	149	130	25	(258)
1-pentanol/ <i>n</i> -decane	288.15 K	208	214	176	10	(257)
1-hexanol/ <i>n</i> -heptane	288.15 K	258	241	156	10	(257)
1-heptanol/ <i>n</i> -octane	298.15 K	156	122	91.0	19	(259)
1-octanol/ <i>n</i> -hexane	288.15 K	168	137	35.5	10	(257)
Average		146	135	106		

Table 8-15 shows that the polar CPA-models are also unable to provide accurate excess enthalpy predictions. Similar to sPC-SAFT-GV and sPC-SAFT, the predictions at higher temperature are more accurate than the predictions at low temperature. (CPA predictions for 1-hexanol and 1-heptanol could not be calculated.)

Table 8-15: Excess enthalpy predictions with CPA-3B, CPA-GV-3B, CPA-JC-3B. Data at 1.013 bar unless otherwise stated.

Mixture	<i>T</i>	%AAD			<i>np</i>	ref.
		CPA-3B	CPA-GV-3B	CPA-JC-3B		
methanol/ <i>n</i> -pentane (P = 5 MPa)	298.15 K	152	143.5	154	27	(251)
ethanol/ <i>n</i> -butane (P = 5 MPa)	298.15 K	187	90.6	94.7	26	(252)
ethanol/ <i>n</i> -butane (P = 5 MPa)	348.15 K	76.2	37.9	38.2	26	(252)
ethanol/ <i>n</i> -hexane	298.15 K	205	116	118	17	(253)
ethanol/ <i>n</i> -heptane	333.15 K	69.6	40.3	40.5	22	(254)

Mixture	T	%AAD			np	ref.
		CPA-3B	CPA-GV-3B	CPA-JC-3B		
ethanol/ <i>n</i> -nonane	318.15 K	128	77.4	78.2	23	(255)
1-propanol/ <i>n</i> -butane ($P = 5$ MPa)	298.15 K	154	151	152	26	(256)
1-propanol/ <i>n</i> -butane ($P = 5$ MPa)	348.15 K	31.6	31.7	31.9	26	(256)
1-propanol/ <i>n</i> -heptane	318.15 K	89.9	89.5	88.4	21	(255)
1-butanol/ <i>n</i> -hexane	298.15 K	74.9	168	127	23	(253)
1-butanol/ <i>n</i> -heptane	288.15 K	94.1	216	170	10	(110)
1-butanol/ <i>n</i> -heptane	328.15 K	38.8	87.0	58.1	10	(110)
1-butanol/ <i>n</i> -decane	288.15 K	99.3	206	162	10	(257)
1-pentanol/ <i>n</i> -heptane	298.15 K	90.5	130	66.5	25	(258)
1-pentanol/ <i>n</i> -decane	288.15 K	144	200	113	10	(257)
1-hexanol/ <i>n</i> -heptane	288.15 K	-	172	152	10	(257)
1-heptanol/ <i>n</i> -octane	298.15 K	-	178	75.6	19	(259)
1-octanol/ <i>n</i> -hexane	288.15 K	27.1	127	28.6	10	(257)
Average		-	126	97.4		

From Figure 8-17 and Figure 8-18, it follows that accurate excess enthalpy correlations of the *n*-butane/1-propanol system cannot be obtained at lower temperatures with sPC-SAFT-GV or sPC-SAFT-JC. If larger BIPs are used, all correlations show incorrect spinodal trends. The correlations based on the 3B scheme are least accurate. The %AADs in both figures range more or less between 17% and 43%.

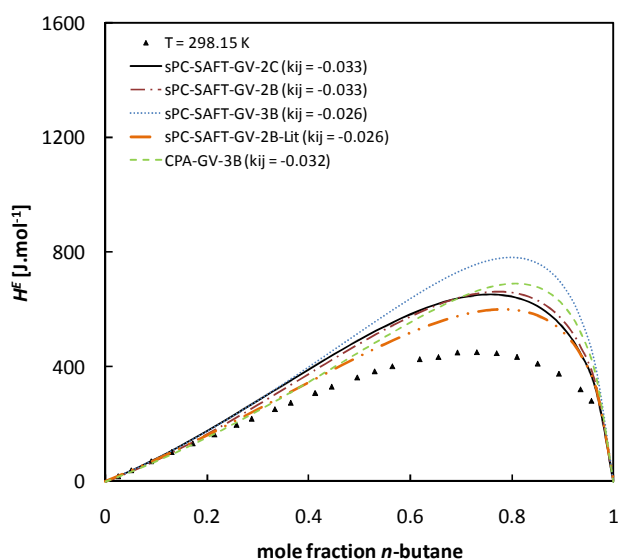


Figure 8-17: Excess enthalpy correlations of the *n*-butane/1-propanol system at $T = 298.15$ K with sPC-SAFT-GV-XX and CPA-GV-XX where the XX represents the association scheme used for 1-propanol. Experimental data taken from ref. (256).

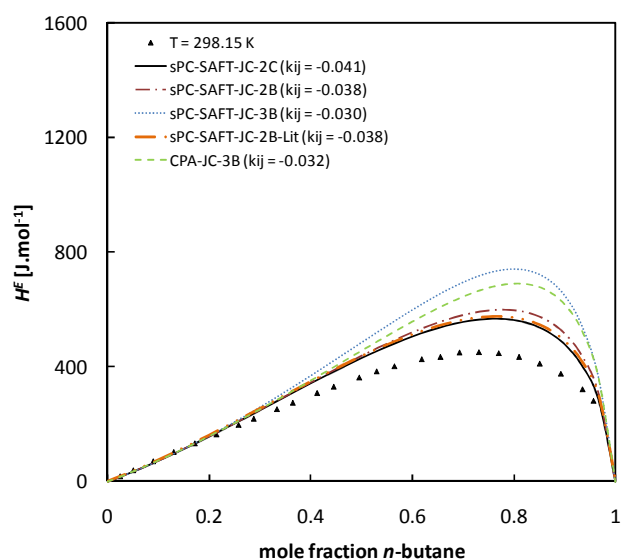


Figure 8-18: Excess enthalpy correlations of the *n*-butane/1-propanol system at $T = 298.15$ K with sPC-SAFT-JC-XX and CPA-JC-XX where the XX represents the association scheme used for 1-propanol. Experimental data taken from ref. (256).

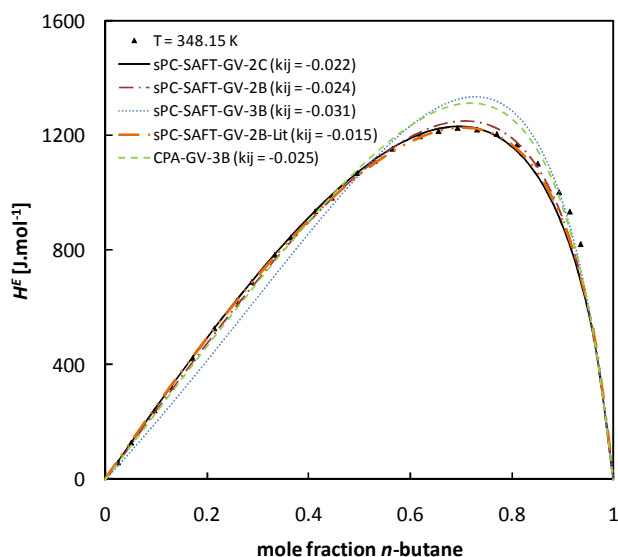


Figure 8-19: Excess enthalpy correlations of the *n*-butane/1-propanol system at $T = 348.15$ K with sPC-SAFT-GV-XX and CPA-GV-XX where the XX represents the association scheme used for 1-propanol. Experimental data taken from ref. (256).

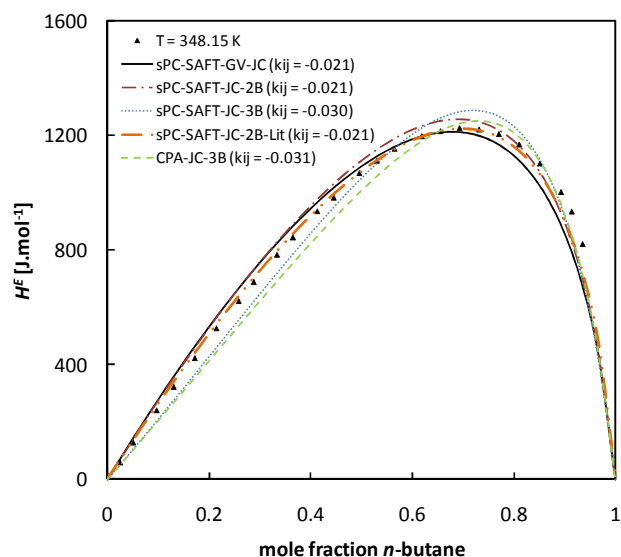


Figure 8-20: Excess enthalpy correlations of the *n*-butane/1-propanol system at $T = 348.15$ K with sPC-SAFT-JC-XX and CPA-JC-XX where the XX represents the association scheme used for 1-propanol. Experimental data taken from ref. (256).

The correlations at $T = 348.15$ K (Figure 8-19 and Figure 8-20) are markedly more accurate compared to the correlations at $T = 298.15$ K (%AADs between 3% and 7% at 348.15 K). Moreover, smaller BIPs are required to obtain the more accurate correlations. The most accurate correlations are obtained with the 2B and 2C schemes for this particular system. However, from Table 8-13 and Table 8-14, the 3B association scheme provides better predictions for other systems.

The fact that more accurate correlations are obtained with smaller BIPs at higher temperatures provides more evidence that the temperature dependency of the models are not correct. This is also supported by the false phase splits obtained at lower temperatures.

8.2.3 Excess volume

The excess volume of several mixtures were also investigated with the polar sPC-SAFT and CPA models. Generally, poor predictions are obtained by all the models. In Figure 8-21 and Figure 8-22, excess volume correlations of the *n*-butane/1-propanol system with the GV and JC models are shown (note that these are at the same conditions as the excess enthalpy correlations shown in Figure 8-19 and Figure 8-20). The BIPs required to obtain improved excess volume correlations are positive, while the BIPs required to obtain good excess enthalpy correlations are negative. This indicates that the models (sPC-SAFT-GV, sPC-SAFT-JC, CPA-GV and CPA-JC) show an internal trade-off in the description of caloric and volumetric properties.

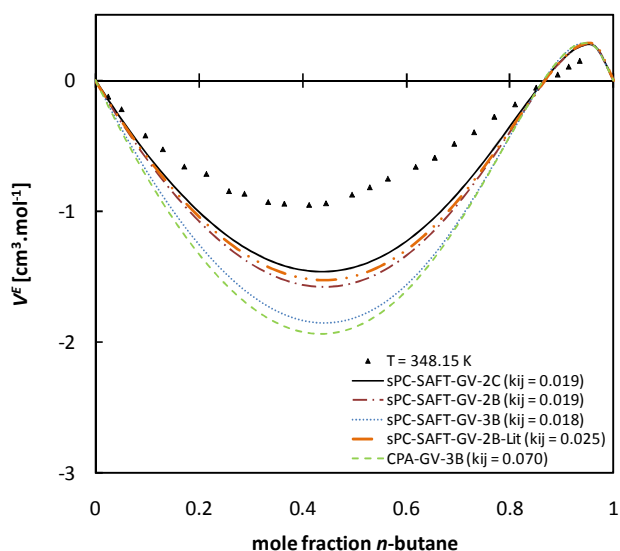


Figure 8-21: Excess volume correlations of the n -butane/1-propanol system at $T = 348.15$ K and 5 MPa with sPC-SAFT-GV-XX and CPA-GV-XX where the XX represents the association scheme used for 1-propanol. Experimental data taken from ref. (256).

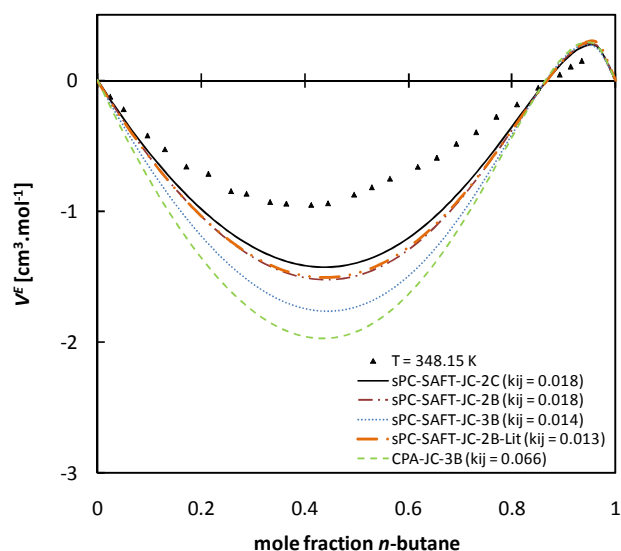


Figure 8-22: Excess volume correlations of the n -butane/1-propanol system at $T = 348.15$ K and 5 MPa with sPC-SAFT-JC-XX and CPA-JC-XX where the XX represents the association scheme used for 1-propanol. Experimental data taken from ref. (256).

The results in this section indicate that the polar sPC-SAFT and CPA models require further refinement before thermodynamic properties, other than VLE can be predicted accurately. For excess enthalpies and excess volumes of alcohol/alkane systems, the models are able to provide qualitative descriptions of the properties when BIPs are used. The BIPs, however, are property-specific: the same BIP cannot be used to obtain good description of both excess enthalpy and excess volume for a particular system. Furthermore, using these BIPs determined from the excess enthalpy or excess volume, result in worse VLE representations.

8.3 Hydrogen bonding/Hydrogen bonding systems

This section investigates the performance of the polar sPC-SAFT and polar CPA models in predicting important thermodynamic properties of hydrogen bonding/hydrogen bonding systems. The VLE and excess enthalpy of alcohol/alcohol and alcohol/water systems are mainly considered. The main reason why other properties are not included is that little or no improvement is obtained with the new polar models, especially in the prediction of second-order properties. This is to be expected, because the models are still subject to the fundamental shortcomings identified in Chapter 3 and Chapter 4.

8.3.1 Vapour-liquid-equilibria

With respects to sPC-SAFT, the main advantage of the 2C scheme (developed in Chapter 6) is that improved VLE predictions of water/alcohol systems are obtained compared to the 2B and 3B association schemes, especially for short-chained alcohols. However, the main disadvantage of the

2C scheme is that slightly worse VLE predictions of alcohol/alkane systems are obtained. In section 8.2, it was found that both sPC-SAFT-JC and sPC-SAFT-GV provide similar predictions of alcohol/alkane VLE, regardless of the association scheme used to model the alcohol. Therefore, this section aims to clarify the following:

- Whether sPC-SAFT-GV and sPC-SAFT-JC suffer from the same shortcomings as sPC-SAFT when alcohols are modelled with the 2B and 3B schemes in VLE predictions of alcohol/water systems.
- If the advantages gained by modelling alcohols with the 2C scheme with sPC-SAFT are also applicable to sPC-SAFT-GV and sPC-SAFT-JC.

i) alcohol/alcohol systems

In alcohol/alcohol systems, the *like* and *unlike* interactions are similar and therefore, it is expected that accurate predictions of these systems will be obtained with sPC-SAFT-GV and sPC-SAFT-JC, regardless of the association scheme used to model the alcohols. This is indeed the case, as verified by the results presented in Table 8-16 for sPC-SAFT-GV and in Table 8-17 for sPC-SAFT-JC.

Table 8-16: VLE predictions of alcohol/alcohol mixtures with sPC-SAFT-GV-2B, sPC-SAFT-GV-2C and sPC-SAFT-GV-3B.

Mixture	<i>T</i> or <i>P</i>	sPC-SAFT-GV-2C		sPC-SAFT-GV-2B		sPC-SAFT-GV-3B		<i>np</i>	ref.
		$\Delta y(\times 10^2)^a$	$\frac{\Delta P(\%)^b}{\Delta T(K)^a}$	$\Delta y(\times 10^2)^a$	$\frac{\Delta P(\%)^b}{\Delta T(K)^a}$	$\Delta y(\times 10^2)^a$	$\frac{\Delta P(\%)^b}{\Delta T(K)^a}$		
methanol/ethanol	298.15 K	0.50	0.85	0.80	2.13	0.39	0.82	11	(155)
methanol/ethanol	373.15 K	0.32	0.49	0.66	1.55	0.44	0.54	10	(156)
methanol/1-propanol	333.35 K	0.13	0.99	0.69	2.98	0.73	2.76	26	(157)
methanol/1-octanol	1.013 bar	2.64	1.94	1.02	1.88	0.71	2.16	25	(158)
ethanol/1-propanol	323.15 K	1.36	3.94	1.33	3.95	0.67	1.26	9	(159)
ethanol/1-propanol	333.15 K	1.39	4.01	1.36	3.99	0.74	1.38	9	(159)
ethanol/1-butanol	343.15 K	0.66	0.71	0.56	0.26	0.32	2.23	8	(160)
ethanol/1-octanol	1.013 bar	1.93	0.82	1.32	1.06	1.08	2.03	25	(158)
1-propanol/1-pentanol	1.013 bar	0.61	0.55	0.58	0.53	0.58	0.57	19	(161)
Average		1.06	1.58	0.92	2.03	0.62	1.53		

^a $\Delta z = \sum_i^{np} |z_i^{calc} - z_i^{exp}|$ where *z* represents *y* or *T* and *np* is the number of data points. ^b Deviations as %AAD.

Table 8-17: VLE predictions of alcohol/alcohol mixtures with sPC-SAFT-JC-2B, sPC-SAFT-JC-2C and sPC-SAFT-JC-3B.

Mixture	<i>T</i> or <i>P</i>	sPC-SAFT-JC-2C		sPC-SAFT-JC-2B		sPC-SAFT-JC-3B		<i>np</i>	ref.
		$\Delta y(\times 10^2)^a$	$\frac{\Delta P(\%)^b}{\Delta T(K)^a}$	$\Delta y(\times 10^2)^a$	$\frac{\Delta P(\%)^b}{\Delta T(K)^a}$	$\Delta y(\times 10^2)^a$	$\frac{\Delta P(\%)^b}{\Delta T(K)^a}$		
methanol/ethanol	298.15 K	0.53	0.96	0.88	2.46	0.42	0.86	11	(155)
methanol/ethanol	373.15 K	0.34	0.60	0.71	1.71	0.47	0.58	10	(156)
methanol/1-propanol	333.35 K	0.22	1.47	0.47	2.36	0.11	0.99	26	(157)
methanol/1-octanol	1.013 bar	2.49	1.74	1.00	1.79	0.71	2.16	25	(158)
ethanol/1-propanol	323.15 K	1.29	3.59	1.33	3.80	1.46	4.52	9	(159)
ethanol/1-propanol	333.15 K	1.32	3.73	1.35	3.89	1.47	4.50	9	(159)

Mixture	<i>T</i> or <i>P</i>	sPC-SAFT-JC-2C		sPC-SAFT-JC-2B		sPC-SAFT-JC-3B		<i>np</i>	ref.
		$\Delta y(\times 10^2)^a$	$\frac{\Delta P(\%)^b}{\Delta T(K)^a}$	$\Delta y(\times 10^2)^a$	$\frac{\Delta P(\%)^b}{\Delta T(K)^a}$	$\Delta y(\times 10^2)^a$	$\frac{\Delta P(\%)^b}{\Delta T(K)^a}$		
ethanol/1-butanol	343.15 K	0.59	0.29	0.54	0.24	0.44	0.23	8	(160)
ethanol/1-octanol	1.013 bar	1.75	0.78	1.20	1.11	1.13	1.62	25	(158)
1-propanol/1-pentanol	1.013 bar	0.69	0.66	0.68	0.66	0.91	0.92	19	(161)
Average		1.02	1.53	0.91	2.00	0.79	1.82		

^a $\Delta z = \sum_i^{np} |z_i^{calc} - z_i^{exp}|$ where *z* represents *y* or *T* and *np* is the number of data points. ^b Deviations as %AAD.

Table 8-18 shows VLE results of alcohol/alcohol systems with CPA-GV, CPA-JC and CPA. As mentioned previously, alcohols are modelled with the 3B scheme. Surprisingly, CPA without the polar terms provides slightly superior predictions of alcohol/alcohol VLE compared to CPA-GV and CPA-JC. It was also found that the CR1 combining rule provided slightly improved predictions compared to the ECR combining rule. Comparative results based on the 2B scheme are presented in Appendix E. (The results presented in Table 8-18 were determined with the CR1 combining rule.)

Table 8-18: VLE predictions of alcohol/alcohol mixtures with CPA-GV-3B, CPA-JC-3B, CPA-3B (using the CR1 combining rule).

Mixture	<i>T</i> or <i>P</i>	CPA-GV-3B		CPA-JC-3B		CPA-3B		<i>np</i>	ref.
		$\Delta y(\times 10^2)^a$	$\frac{\Delta P(\%)^b}{\Delta T(K)^a}$	$\Delta y(\times 10^2)^a$	$\frac{\Delta P(\%)^b}{\Delta T(K)^a}$	$\Delta y(\times 10^2)^a$	$\frac{\Delta P(\%)^b}{\Delta T(K)^a}$		
methanol/ethanol	298.15 K	0.42	1.03	0.43	1.22	0.21	0.27	11	(155)
methanol/ethanol	373.15 K	0.32	0.50	0.27	0.42	0.35	1.28	10	(156)
methanol/1-propanol	333.35 K	0.19	0.76	0.16	1.22	0.17	1.43	26	(157)
methanol/1-octanol	1.013 bar	3.71	3.39	4.46	4.25	0.96	3.30	25	(158)
ethanol/1-propanol	323.15 K	1.32	4.14	1.30	4.12	1.24	3.89	9	(159)
ethanol/1-propanol	333.15 K	1.36	4.16	1.34	4.16	1.28	3.67	9	(159)
ethanol/1-butanol	343.15 K	0.81	1.26	0.60	1.37	0.73	1.17	8	(160)
ethanol/1-octanol	1.013 bar	2.64	1.57	3.27	2.27	1.27	2.42	25	(158)
1-propanol/1-pentanol	1.013 bar	0.56	0.39	0.54	0.31	0.69	0.33	19	(161)
Average		1.26	1.91	1.38	2.15	0.76	1.97		

^a $\Delta z = \sum_i^{np} |z_i^{calc} - z_i^{exp}|$ where *z* represents *y* or *T* and *np* is the number of data points. ^b Deviations as %AAD.

A few representative alcohol/alcohol VLE results are presented in the figures below.

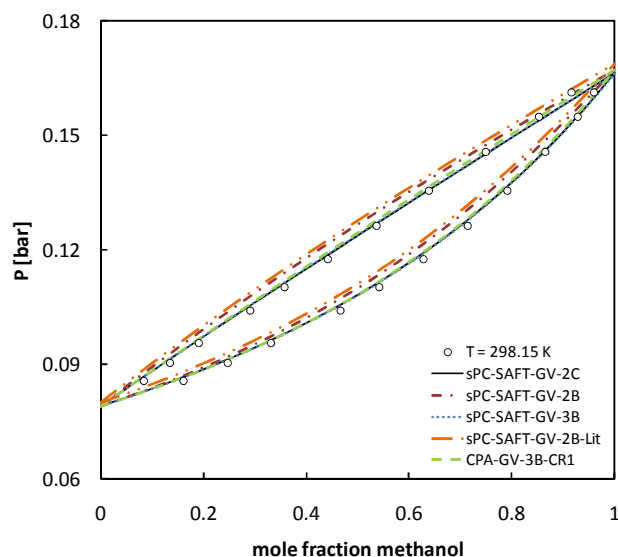


Figure 8-23: VLE predictions of the methanol/ethanol system with sPC-SAFT-GV-XX and CPA-GV-XX-CR1 where the XX represents the association scheme used for the alcohols. Experimental data from ref. (155).

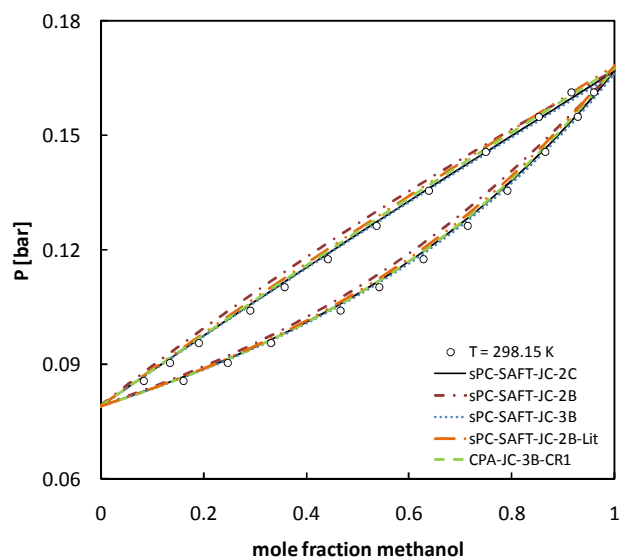


Figure 8-24: VLE predictions of the methanol/ethanol system with sPC-SAFT-JC-XX and CPA-JC-XX-CR1 where the XX represents the association scheme used for the alcohols. Experimental data from ref. (155).

From Figure 8-23 and Figure 8-24, the least accurate predictions are obtained for the methanol/ethanol system with the sPC-SAFT-GV-2B and sPC-SAFT-JC-2B (the 2B parameters determined in this work and the 2B parameters from Al-Saifi *et al.* (35)). The predictions based on the 2C and 3B parameters are slightly more accurate (see Table 8-16 and Table 8-17 for %AAD values). More or less the same discussion applies to the results presented in Figure 8-25 and Figure 8-26 for the ethanol/1-octanol system, the predictions based on the 2C scheme are, however, marginally more accurate compared to the predictions based on the 3B scheme.

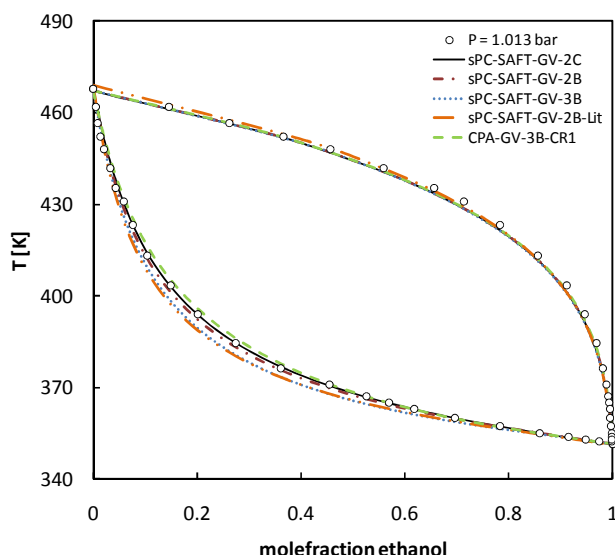


Figure 8-25: VLE predictions of the ethanol/1-octanol system with sPC-SAFT-GV-XX and CPA-GV-XX-CR1 where the XX represents the association scheme used for the alcohols. Experimental data from ref. (158).

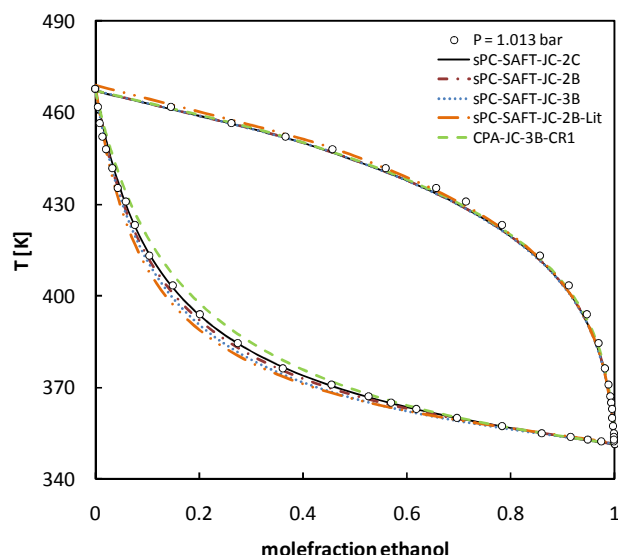


Figure 8-26: VLE predictions of the ethanol/1-octanol system with sPC-SAFT-GV-XX and CPA-GV-XX-CR1 where the XX represents the association scheme used for the alcohols. Experimental data from ref. (158).

The predictions of alcohol/alcohol VLE with sPC-SAFT-GV and sPC-SAFT-JC are very similar regardless of the association scheme selected to model alcohols. However, the predictions based on the 2C and 3B schemes are slightly superior. Furthermore, CPA-GV and CPA-JC are able to predict the VLE of these systems with good accuracy, although the predictions with normal CPA are marginally more accurate.

ii) alcohol/water systems

The results presented in this section are regarded as crucial to this study. As mentioned in the beginning of this section, the key issue that needs to be investigated is whether the 2C scheme still provides improved VLE predictions of alcohol/water systems compared to the 2B and 3B schemes when alcohols are modelled in the framework of sPC-SAFT-GV and sPC-SAFT-JC. Table 8-19, Table 8-20 and Table 8-21 show VLE results for alcohol/water systems with sPC-SAFT-GV, sPC-SAFT-JC and CPA-based models respectively.

Table 8-19: VLE predictions of selected alcohol/water mixtures with sPC-SAFT-GV and the 2C, 2B and 3B schemes. Water modelled with 4C scheme.

Mixture	T or P	sPC-SAFT-GV-2C		sPC-SAFT-GV-2B		sPC-SAFT-GV-3B		np	ref.
		$\Delta y(x10^2)^a$	$\frac{\Delta P(\%)^b}{\Delta T(K)^a}$	$\Delta y(x10^2)^a$	$\frac{\Delta P(\%)^b}{\Delta T(K)^a}$	$\Delta y(x10^2)^a$	$\frac{\Delta P(\%)^b}{\Delta T(K)^a}$		
methanol/water	318.15 K	0.99	2.50	4.61	19.06	2.61	6.78	11	(142)
	323.15 K	1.51	2.07	2.63	17.54	1.86	6.01	14	(143)
	333.15 K	0.72	1.57	3.68	18.71	1.98	6.33	18	(143)
	1.013 bar	0.80	0.28	3.46	3.02	1.82	1.55	21	(144)
	5.066 bar	0.82	1.55	4.72	2.82	1.37	2.02	22	(145)
ethanol/water	323.15 K	0.72	1.42	3.30	10.9	0.63	0.22	14	(143)
	333.15 K	0.87	0.48	3.24	9.42	0.80	0.30	36	(143)

Mixture	<i>T</i> or <i>P</i>	sPC-SAFT-GV-2C		sPC-SAFT-GV-2B		sPC-SAFT-GV-3B		<i>np</i>	ref.
		$\Delta y(\times 10^2)^a$	$\frac{\Delta P(\%)^b}{\Delta T(K)^a}$	$\Delta y(\times 10^2)^a$	$\frac{\Delta P(\%)^b}{\Delta T(K)^a}$	$\Delta y(\times 10^2)^a$	$\frac{\Delta P(\%)^b}{\Delta T(K)^a}$		
1-propanol/water	0.333 bar	1.91	0.63	6.53	3.72	1.73	0.38	28	(146)
	1.013 bar	0.55	0.41	4.41	2.89	0.44	0.38	13	(50)
	6.669 bar	0.71	0.65	4.18	4.28	1.00	1.75	19	(147)
	333.15 K	1.30	0.89	1.64*	0.88*	3.27	6.32	23	(148)
	0.300 bar	2.25	0.52	2.53*	0.39*	4.93	1.79	26	(149)
	1.000 bar	1.33	0.81	1.94*	0.64*	3.10	1.74	28	(149)
Average		1.11	1.06	3.61	7.25	1.96	2.73		

^a $\Delta z = \sum_i^{np} |z_i^{calc} - z_i^{exp}|$ where *z* represents *y* or *T* and *np* is the number of data points. ^b Deviations as %AAD.

* VLLE predicted at these conditions. *k_{ij}* values presented in Table 8-22 used to obtain correct phase behaviour.

The results in Table 8-19 clearly indicate that the best VLE predictions are obtained when short-chained alcohols are modelled with the 2C scheme in the framework of sPC-SAFT-GV. Major improvements are especially obtained for the methanol/water system. Similar to the results found for sPC-SAFT in Chapter 6, the difference between the choice of association scheme seems to become smaller as the chain length increases.

Similar results are found for sPC-SAFT-JC as shown in Table 8-20. When alcohols are modelled with the 2C scheme, improved VLE predictions for water/alcohol systems are obtained. Both sPC-SAFT-GV-2B and sPC-SAFT-JC-2B predict false VLLE phase behaviour for the 1-propanol/water system. As with other systems, the problem can be corrected with a BIP, as given in Table 8-22.

Table 8-20: VLE predictions of selected alcohol/water mixtures with sPC-SAFT-JC and the 2C, 2B and 3B schemes. Water modelled with 4C scheme.

Mixture	<i>T</i> or <i>P</i>	sPC-SAFT-GV-2C		sPC-SAFT-GV-2B		sPC-SAFT-GV-3B		<i>np</i>	ref.
		$\Delta y(\times 10^2)^a$	$\frac{\Delta P(\%)^b}{\Delta T(K)^a}$	$\Delta y(\times 10^2)^a$	$\frac{\Delta P(\%)^b}{\Delta T(K)^a}$	$\Delta y(\times 10^2)^a$	$\frac{\Delta P(\%)^b}{\Delta T(K)^a}$		
methanol/water	318.15 K	1.02	2.47	4.67	19.5	2.99	7.52	11	(142)
	323.15 K	1.64	2.16	2.70	17.9	2.13	7.01	14	(143)
	333.15 K	0.85	1.61	3.70	19.1	2.35	7.26	18	(143)
	1.013 bar	0.94	0.28	3.48	3.08	2.14	1.74	21	(144)
	5.066 bar	0.89	1.62	4.75	2.91	1.58	2.29	22	(145)
ethanol/water	323.15 K	0.81	1.05	3.13	10.70	2.28	4.60	14	(143)
	333.15 K	1.07	0.34	3.10	9.17	2.23	4.42	36	(143)
	0.333 bar	1.96	0.55	6.07	3.58	3.84	1.35	28	(146)
	1.013 bar	0.77	0.48	4.11	2.79	2.38	1.33	13	(50)
	6.669 bar	1.03	0.50	3.94	4.17	1.23	0.51	19	(147)
1-propanol/water	333.15 K	1.28	0.91	1.33*	1.09*	2.08	3.08	23	(148)
	0.300 bar	2.38	0.48	2.90*	0.47*	3.55	1.12	26	(149)
	1.000 bar	1.42	0.79	2.30*	0.77*	2.06	1.13	28	(149)
Average		1.24	1.02	3.55	7.85	2.37	3.34		

^a $\Delta z = \sum_i^{np} |z_i^{calc} - z_i^{exp}|$ where *z* represents *y* or *T* and *np* is the number of data points. ^b Deviations as %AAD.

* VLLE predicted at these conditions. *k_{ij}* values presented in Table 8-22 used to obtain correct phase behaviour.

Table 8-21 shows VLE predictions with CPA, CPA-GV and CPA-JC. The results indicate that CPA-GV and CPA-JC provide improved predictions compared to normal CPA only for the methanol/water system. For the ethanol/water and 1-propanol/water systems, normal CPA provides predictions that are slightly superior to CPA-JC and CPA-GV.

Table 8-21: VLE predictions of selected alcohol/water mixtures with CPA, CPA-GV and CPA-JC. Water modelled with 4C scheme.

Mixture	T or P	CPA-3B		CPA-GV-3B		CPA-JC-3B		np	ref.
		$\Delta y(\times 10^2)^a$	$\frac{\Delta P(\%)^b}{\Delta T(K)^a}$	$\Delta y(\times 10^2)^a$	$\frac{\Delta P(\%)^b}{\Delta T(K)^a}$	$\Delta y(\times 10^2)^a$	$\frac{\Delta P(\%)^b}{\Delta T(K)^a}$		
methanol/water	318.15 K	2.70	7.98	1.76	4.52	1.69	4.33	11	(142)
	323.15 K	1.91	7.13	1.81	4.33	1.88	4.40	14	(143)
	333.15 K	2.33	7.40	1.66	4.32	1.72	4.43	18	(143)
	1.013 bar	2.33	1.67	1.67	1.10	1.79	1.15	21	(144)
	5.066 bar	2.00	2.36	1.43	1.78	1.68	2.06	22	(145)
ethanol/water	323.15 K	0.44	0.72	1.42	1.21	1.55	1.41	14	(143)
	333.15 K	0.53	0.75	1.47	1.16	1.58	1.38	36	(143)
	0.333 bar	2.13	0.53	3.56	1.01	3.77	1.08	28	(146)
	1.013 bar	0.87	0.45	1.75	0.84	1.87	0.89	13	(50)
	6.669 bar	0.82	2.22	1.23	2.16	1.14	2.03	19	(147)
1-propanol/water	333.15 K	1.37*	1.43*	1.78*	1.52*	2.05*	2.17*	23	(148)
	0.300 bar	1.75*	0.48*	2.02*	0.47*	2.23*	0.58*	26	(149)
	1.000 bar	0.52*	0.23*	0.73*	0.27*	0.98*	0.39*	28	(149)
Average		1.52	2.57	1.71	1.90	1.84	2.02		

^a $\Delta z = \sum_i^{np} |z_i^{calc} - z_i^{exp}|$ where z represents y or T and np is the number of data points. ^b Deviations as %AAD.

* VLLE predicted at these conditions. k_{ij} values presented in Table 8-22 used to obtain correct phase behaviour.

Table 8-22: k_{ij} values used in alcohol/water VLE calculations with sPC-SAFT-GV, sPC-SAFT-JC, CPA-GV, CPA-JC

Mixture	T or P	sPC-SAFT-GV-2B	sPC-SAFT-JC-2B	CPA-3B	CPA-GV-3B	CPA-JC-3B
1-propanol/water	333.15	-0.030	-0.033	-0.006	-0.033	-0.039
1-propanol/water	0.3 bar	-0.022	-0.026	-0.006	-0.033	-0.039
1-propanol/water	1 bar	-0.025	-0.029	-0.006	-0.033	-0.039

In the remainder of this section, graphical results are presented to discuss the performance of sPC-SAFT-GV, sPC-SAFT-JC in predicting alcohol/water phase equilibria in more detail.

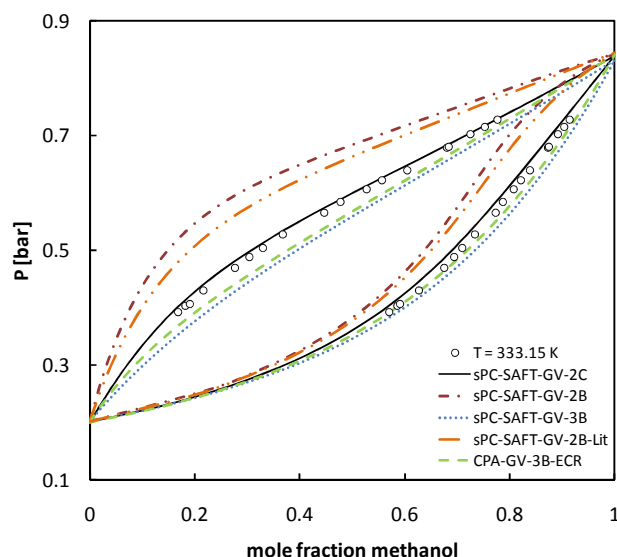


Figure 8-27: VLE predictions of the methanol/water system with sPC-SAFT-GV-XX and CPA-GV-XX where the XX represents the association scheme used for methanol. Experimental data taken from ref. (143).

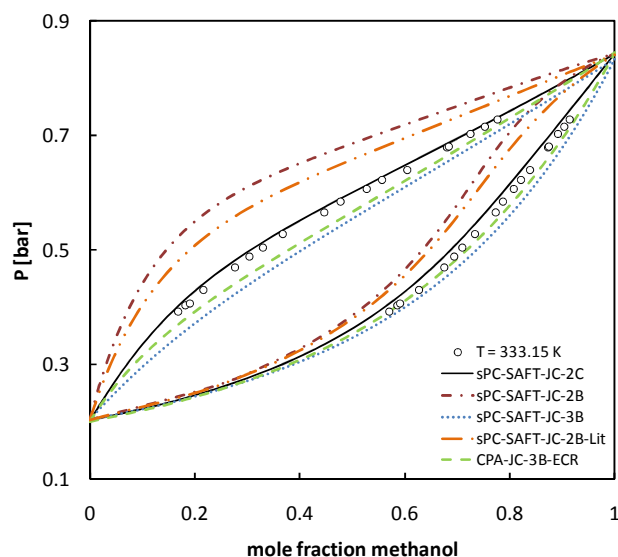


Figure 8-28: VLE predictions of the methanol/water system with sPC-SAFT-JC-XX and CPA-JC-XX where the XX represents the association scheme used for methanol. Experimental data taken from ref. (143).

From Figure 8-27 it follows that the best prediction for the methanol/water VLE is obtained with sPC-SAFT-GV-2C. Similar to the results obtained with normal sPC-SAFT (in Chapter 6), when methanol is modelled with the 2B scheme, it appears that the cross-association of the system is underestimated (with both the 2B parameters determined in this work and the parameters from Al-Saifi *et al.* (35)). Using the 3B scheme to model methanol results in an overestimation of the cross-association by both sPC-SAFT-GV and CPA-GV. Both the ECR and CR1 combining rule were tested with CPA-GV; the best results were obtained with the ECR combining rule.

Similar results are obtained with sPC-SAFT-JC and CPA-JC in Figure 8-28. The sPC-SAFT-JC prediction based on the 2C scheme is again most accurate. The same trends discussed for Figure 8-27 are observed for the JC predictions based on the 2B and 3B association schemes.

In Figure 8-29, sPC-SAFT-GV-2B and sPC-SAFT-2B-Lit provide near-identical VLE predictions of the ethanol/water system. The trends of these models are consistent with an underestimation of the cross-association present in the system, as discussed in Chapter 6 for sPC-SAFT. sPC-SAFT-GV-2C, sPC-SAFT-GV-3B and CPA-GV-3B-ECR predict the VLE with good accuracy. In Figure 8-30, the only accurate sPC-SAFT-JC-based prediction is obtained when ethanol is modelled with the 2C scheme. sPC-SAFT-JC-2B and sPC-SAFT-JC-2B-Lit underestimate cross-association and sPC-SAFT-JC-3B overestimate cross-association. Since the same trends were observed with the model predictions of sPC-SAFT based on the different association schemes (in Chapter 6), it indicates that the phase behaviour is predominantly dictated by the hydrogen bonding in these systems. CPA-JC-3B also gives fairly accurate representation of the VLE data.

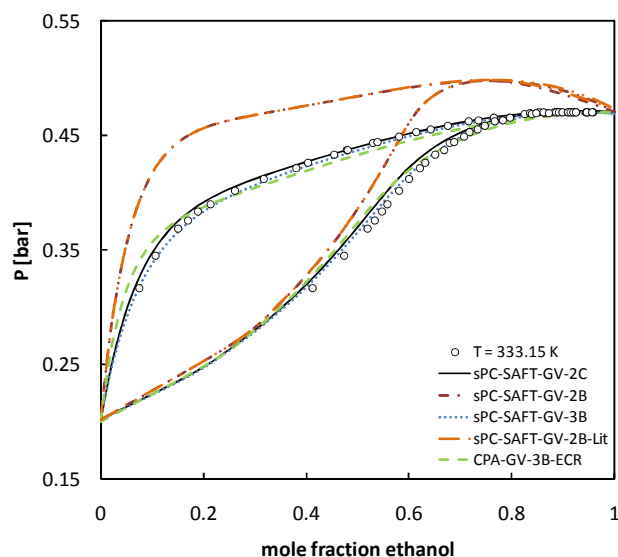


Figure 8-29: VLE predictions of the ethanol/water system with *sPC-SAFT-GV-XX* and *CPA-GV-XX* where the *XX* represents the association scheme used for ethanol. Experimental data taken from ref. (143).

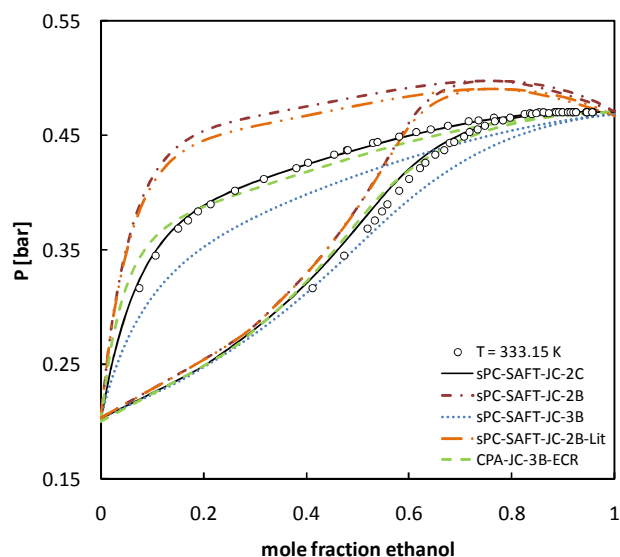


Figure 8-30: VLE predictions of the ethanol/water system with *sPC-SAFT-JC-XX* and *CPA-JC-XX* where the *XX* represents the association scheme used for ethanol. Experimental data taken from ref. (143).

Similar comments apply to the 1-propanol/water system (Figure 8-31 and Figure 8-32) as discussed for the methanol/water and ethanol/water systems. Importantly, the predictions based on the 2B scheme result in false VLE predictions, although a BIP may be used to rectify the error, as indicated. Both *sPC-SAFT-JC* and *sPC-SAFT-GV* predict false phase splits with all three association schemes at some point. The difference, however, is that both *sPC-SAFT-GV* and *sPC-SAFT-JC* can be applied at lower temperatures without obtaining incorrect phase behaviour when the 2C and 3B association schemes are used.

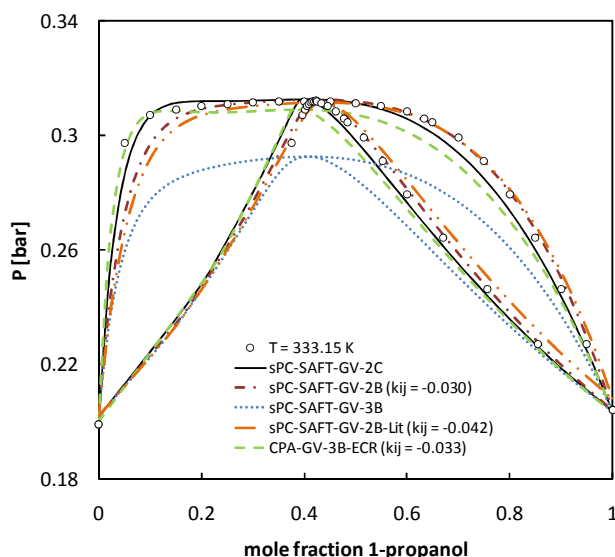


Figure 8-31: VLE predictions and correlations of the 1-propanol/water system with sPC-SAFT-GV-XX and CPA-GV-XX where the XX represents the association scheme used for 1-propanol. Experimental data taken from ref. (148).

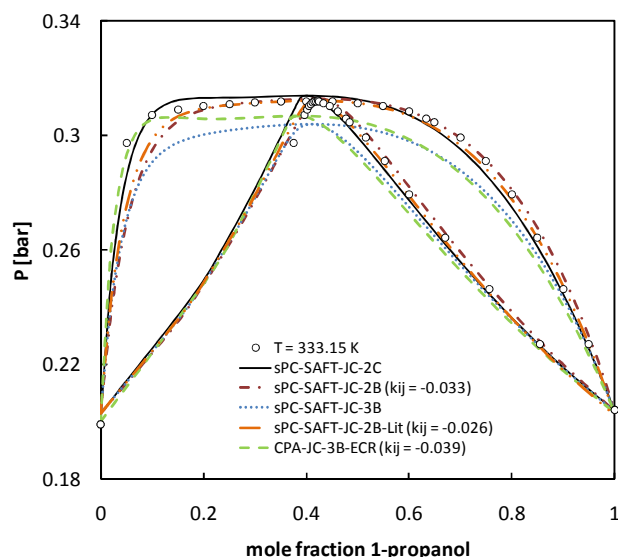


Figure 8-32: VLE predictions and correlations of the 1-propanol/water system with sPC-SAFT-JC-XX and CPA-JC-XX where the XX represents the association scheme used for 1-propanol. Experimental data taken from ref. (148).

Figure 8-33 (a) show VLLE predictions of the 1-butanol/water system with sPC-SAFT-GV and CPA-GV. An enlargement of the VLE section is shown Figure 8-33 (b).

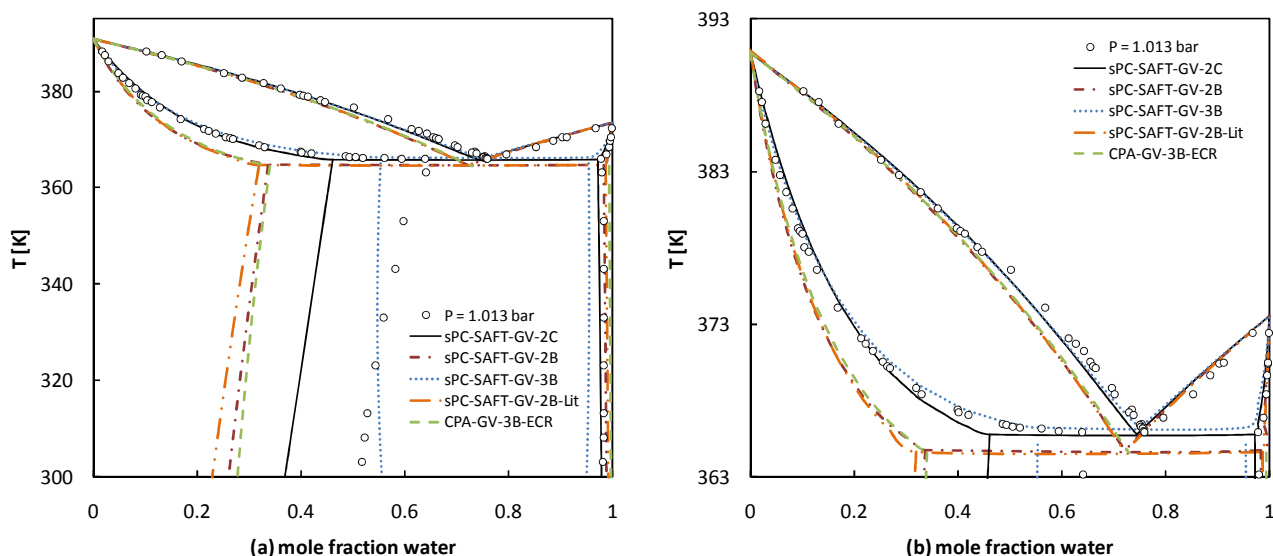


Figure 8-33: (a) VLLE and (b) VLE predictions of the 1-butanol/water system with sPC-SAFT-GV-XX and CPA-GV-XX where the XX represents the association scheme used for 1-butanol. Experimental data taken from ref. (152) and (153).

From Figure 8-33, it follows that sPC-SAFT-GV-2B, sPC-SAFT-GV-2B-Lit and CPA-GV-3B-ECR provide VLLE predictions of similar accuracy. As with the results for the other alcohol/water systems presented thus far, the cross-association seems to be underestimated, resulting in poor VLE and LLE predictions. The composition of the butanol-rich liquid phase is particularly predicted poorly, although the temperature dependency seems appropriate. The solubility of 1-butanol in the water-rich liquid phase is predicted with fair accuracy by these models. sPC-SAFT-GV-3B provides a very accurate VLE representation of the system. The VLLE line is also predicted with fair accuracy.

However, the temperature dependency of the butanol-rich liquid phase composition is poor compared to the trends shown by the 2B and 2C predictions. The solubility of butanol in the water-rich phase is also overestimated. sPC-SAFT-GV-2C provides VLE predictions that are considerably more accurate compared to the predictions based on the 2B scheme. Improvement is also obtained in the LLE representation if compared to the 2B scheme. The solubility of 1-butanol in the water-rich phase is slightly overestimated, but not to the same degree as sPC-SAFT-GV-3B.

Comparing the results in Figure 8-34 with the results shown in Figure 8-33, it is clear that the performances of sPC-SAFT-GV and sPC-SAFT-JC are very similar and that the association schemes influence the performances of both models in a similar manner.

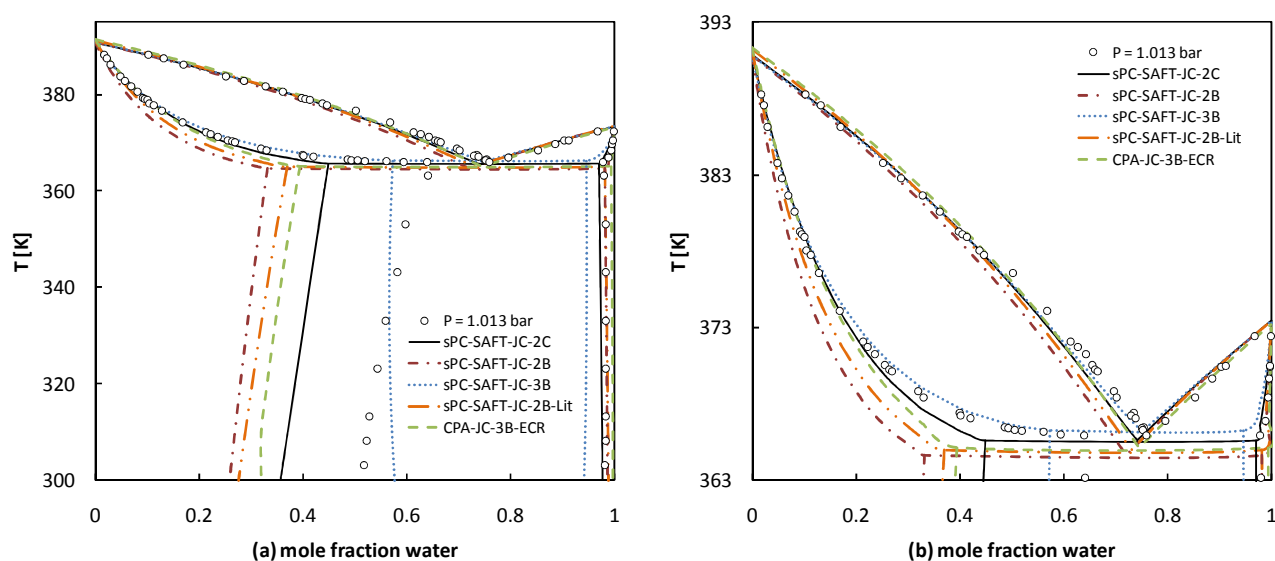


Figure 8-34: (a) VLLE and (b) VLE predictions of the 1-butanol/water system with sPC-SAFT-JC-XX and CPA-JC-XX where the XX represents the association scheme used for 1-butanol. Experimental data taken from ref. (152) and (153).

Figure 8-35 shows VLLE correlations of the 1-pentanol/water system with sPC-SAFT-GV and sPC-SAFT-JC based on different association schemes for 1-pentanol. It is noted that the different correlations of sPC-SAFT-GV and sPC-SAFT-JC that are based on the same association scheme for 1-pentanol are similar. This indicates that the influence of the two polar theories is fairly equal when VLE is considered and coincides with results presented thus far. Furthermore, it is noticed that the best overall representation of the phase behaviour is obtained with sPC-SAFT-GV-2C and sPC-SAFT-JC-2C. The correlations based on the 3B scheme provide very accurate VLE representation, but the LLE representations are only moderate and cannot be corrected with a BIP. The correlations based on the 2B scheme also result in very accurate VLE correlations, but the solubility of 1-butanol in the water-rich phase is too high.

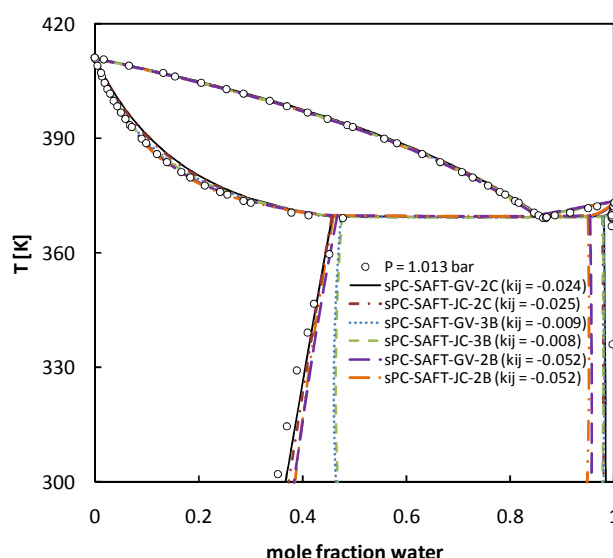


Figure 8-35: VLE correlations of the water/1-pentanol system with sPC-SAFT-GV-XX and sPC-SAFT-JC-XX where the XX represents the association scheme used for 1-pentanol. Experimental data taken from ref. (152) and (153).

The phase equilibria investigation of alcohol/water systems with sPC-SAFT-GV and sPC-SAFT-JC resulted in the following main findings:

- sPC-SAFT-GV and sPC-SAFT-JC provide similar VLE predictions of alcohol/water systems with neither model being notably superior to the other. This coincides with the findings in Chapter 7: the JC and GV polar theories are fairly equal when phase equilibria is considered.
- The 2C association scheme offers improved VLE predictions compared to the 2B and 3B association schemes, especially for short-chained alcohols.
- For larger alcohols that exhibit VLLE behaviour with water, the 2C and 3B association schemes provide accurate VLE representation, however the prediction of LLE is still problematic.
- The correlations based on the 2C association scheme result in the best overall VLLE representation of alcohol (1-butanol or 1-pentanol)/water systems with both sPC-SAFT-GV and sPC-SAFT-JC.

8.3.2 Excess enthalpy

Representative results for a few hydrogen bonding systems are presented in the following sub sections.

i) alcohol/alcohol systems

From Figure 8-36 and Figure 8-37, the best excess enthalpy predictions of the 1-butanol/methanol system are obtained with sPC-SAFT-GV-2C and sPC-SAFT-JC-2C.

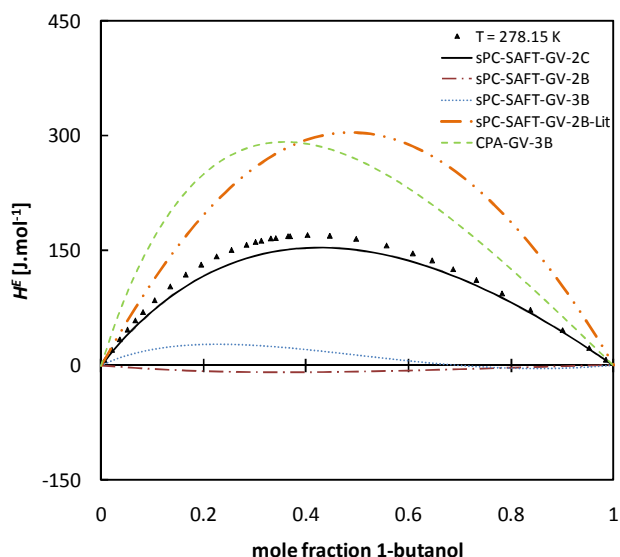


Figure 8-36: Excess enthalpy predictions of the 1-butanol/methanol system at $T = 278.15\text{ K}$ with sPC-SAFT-GV-XX and CPA-GV-XX where the XX represents the association scheme used for 1-butanol and methanol. Experimental data taken from ref. (260).

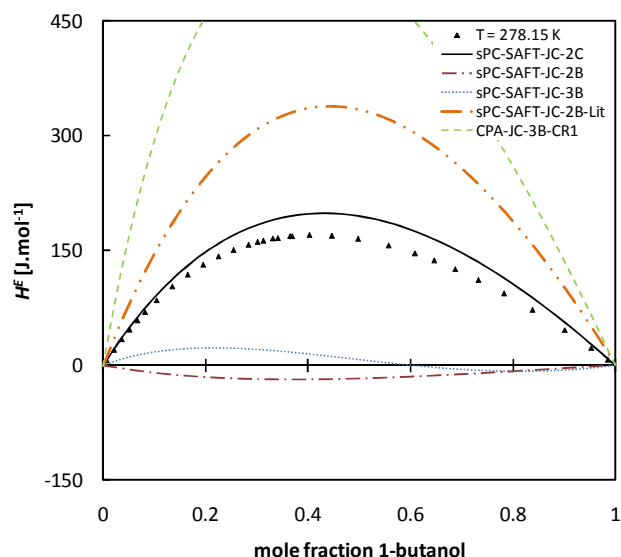


Figure 8-37: Excess enthalpy predictions of the 1-butanol/methanol system at $T = 278.15\text{ K}$ with sPC-SAFT-JC-XX and CPA-JC-XX where the XX represents the association scheme used for 1-butanol and methanol. Experimental data taken from ref. (260).

Figure 8-38 and Figure 8-39 show excess enthalpy predictions of the 1-butanol/methanol system at a higher temperature ($T = 318.15\text{ K}$). The best results are still obtained with the predictions based on the 2C scheme. However, the results also indicate that the temperature dependency of the models is not correct. This can be concluded by comparing how much the experimental data changes with the change in model predictions as a result of the temperature increase. All the models seem to be more sensitive to changes in temperature than what is exhibited by the data.

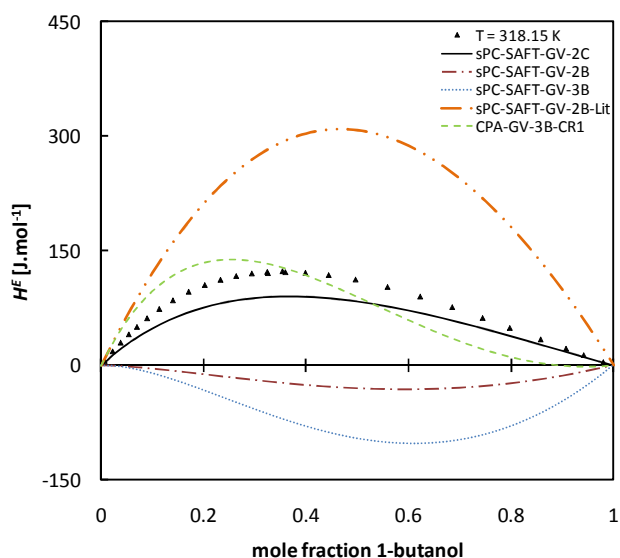


Figure 8-38: Excess enthalpy predictions of the 1-butanol/methanol system at $T = 318.15\text{ K}$ with sPC-SAFT-GV-XX and CPA-GV-XX where the XX represents the association scheme used for 1-butanol and methanol. Experimental data taken from ref. (260).

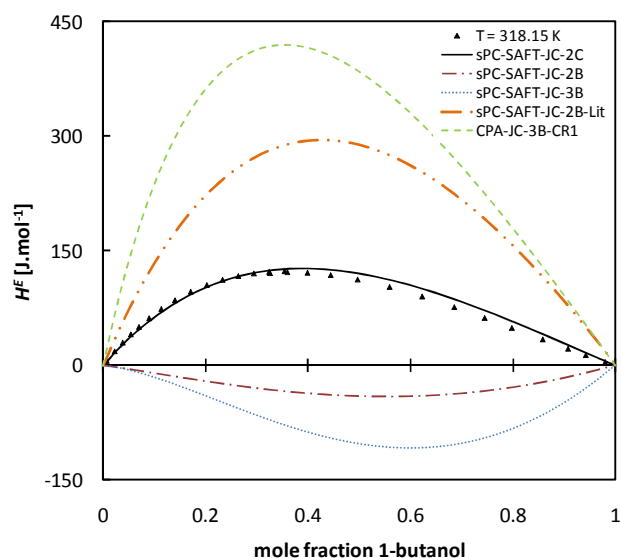


Figure 8-39: Excess enthalpy predictions of the 1-butanol/methanol system at $T = 318.15\text{ K}$ with sPC-SAFT-JC-XX and CPA-JC-XX where the XX represents the association scheme used for 1-butanol and methanol. Experimental data taken from ref. (260).

Figure 8-40 and Figure 8-41 show excess enthalpy correlations of the 1-propanol/1-pentanol with the GV- and JC-based models. The figures show that the same accuracy is obtained with all the models and that the BIPs used are small and very similar. This indicates that, for larger alcohols, similar excess enthalpy predictions are obtained, irrespective of the association scheme and corresponds with findings mentioned earlier (the difference between association schemes becomes smaller as the chain-length of the alcohols increase).

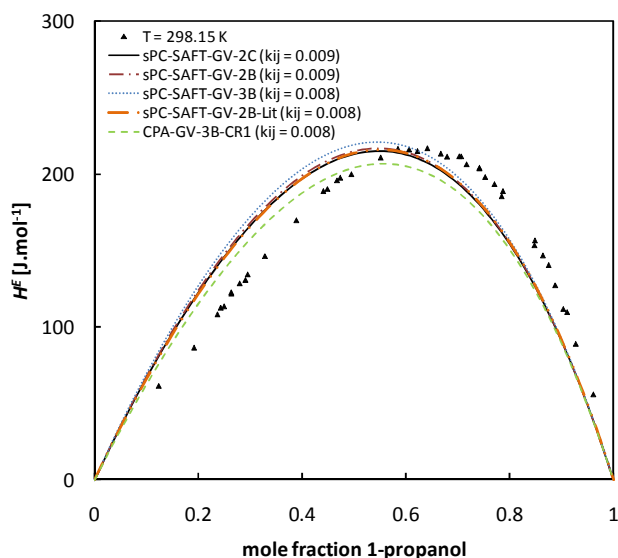


Figure 8-40: Excess enthalpy predictions of the 1-propanol/1-pentanol system at $T = 298.15\text{ K}$ with sPC-SAFT-GV-XX and CPA-GV-XX where the XX represents the association scheme used for 1-butanol and methanol. Experimental data taken from ref. (261).

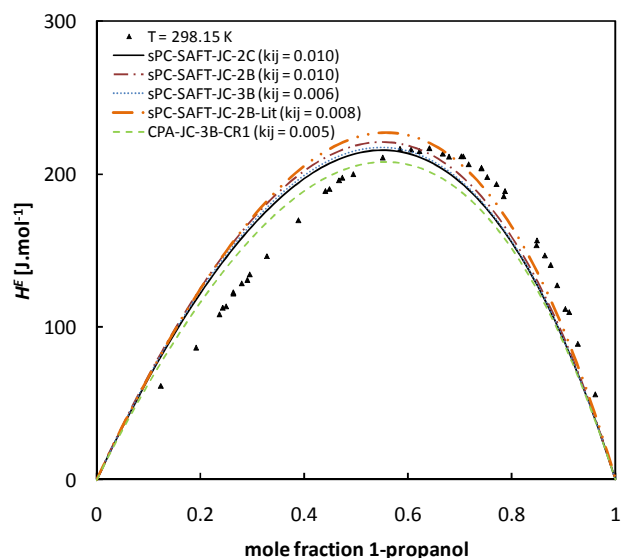


Figure 8-41: Excess enthalpy predictions of the 1-propanol/1-pentanol system at $T = 298.15\text{ K}$ with sPC-SAFT-JC-XX and CPA-JC-XX where the XX represents the association scheme used for 1-butanol and methanol. Experimental data taken from ref. (261).

ii) alcohol/water systems

During the literature review conducted for this project, no publications were encountered that investigated the excess enthalpy of water/alcohol systems with SAFT-based models. Figure 8-42 and Figure 8-43 show excess enthalpy predictions of the ethanol/water system at $T = 298.15\text{ K}$ with the GV- and JC-based models and in Figure 8-44 (GV) and Figure 8-45 (JC), the excess enthalpy is shown at $T = 363.15\text{ K}$.

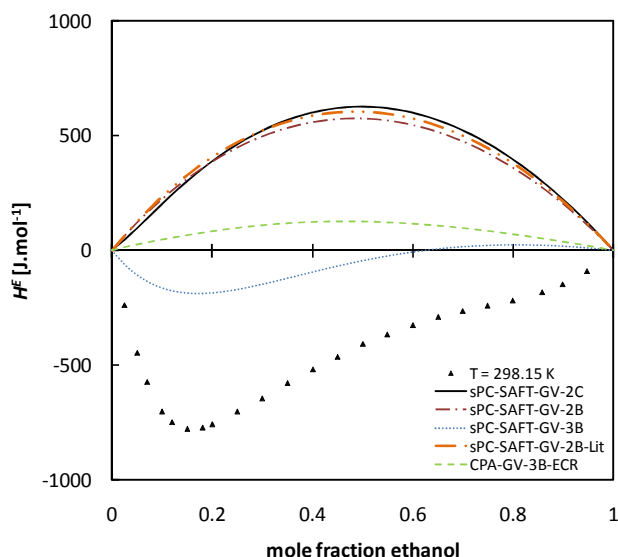


Figure 8-42: Excess enthalpy predictions of the ethanol/water system at $T = 298.15$ K (0.4 MPa) with sPC-SAFT-GV-XX and CPA-GV-XX where the XX represents the association scheme used for ethanol. Experimental data taken from ref. (118).

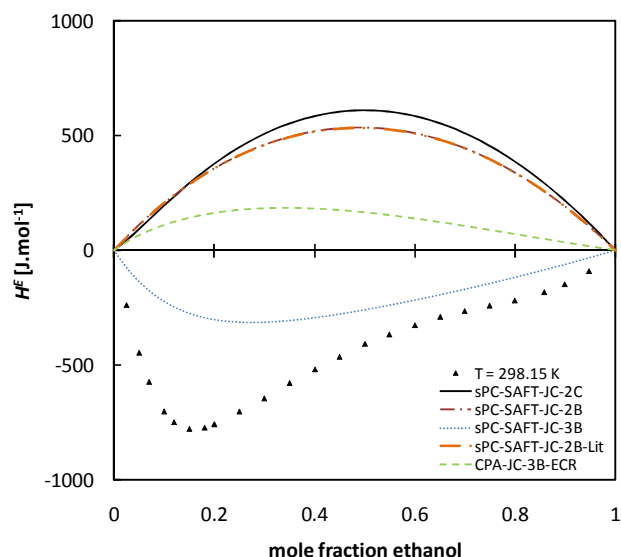


Figure 8-43: Excess enthalpy predictions of the ethanol/water system at $T = 298.15$ K (0.4 MPa) with sPC-SAFT-JC-XX and CPA-JC-XX where the XX represents the association scheme used for ethanol. Experimental data taken from ref. (118).

The complexities exhibited by the experimental data are vast (Figure 8-42 and Figure 8-43). None of the models are able to predict the excess enthalpy accurately, but the predictions based on the 3B scheme (sPC-SAFT-GV-3B and sPC-SAFT-JC-3B) seems to capture some of the important molecular effects, in particular, the minimum exhibited at more or less $x_{\text{ethanol}} = 0.19$. The predictions based on the 2B and 2C schemes are similar and do not correspond well with the data. The CPA-GV-3B and CPA-JC-3B predictions are also not accurate.

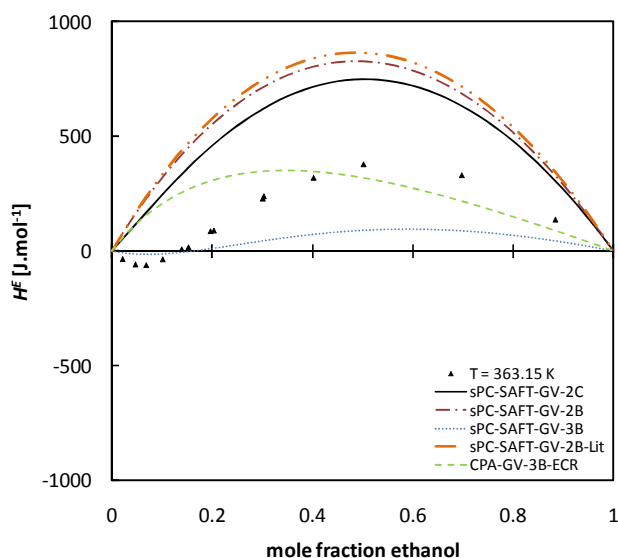


Figure 8-44: Excess enthalpy predictions of the ethanol/water system at $T = 363.15$ K with sPC-SAFT-GV-XX and CPA-GV-XX where the XX represents the association scheme used for ethanol. Experimental data taken from ref. (262).

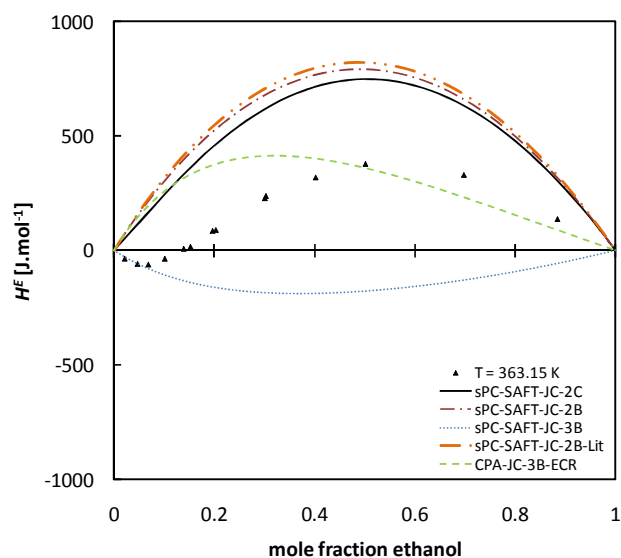


Figure 8-45: Excess enthalpy predictions of the ethanol/water system at $T = 363.15$ K with sPC-SAFT-JC-XX and CPA-JC-XX where the XX represents the association scheme used for ethanol. Experimental data taken from ref. (262).

Figure 8-44 and Figure 8-45 show how the excess enthalpy changes with an increase in temperature. Only sPC-SAFT-GV-3B seems to be able to qualitatively follow this trend. The other predictions are not accurate and do not even show qualitative trends in accordance with the experimental data. Similar results were found for the 1-propanol/water system.

This section showed that improvements to sPC-SAFT-GV and sPC-SAFT-JC are necessary before the excess enthalpy of alcohol/water systems can be predicted accurately. In these systems, molecular effects, such as bond co-operativity, probably influence the property significantly. Therefore, improvement to the association term is required before more accurate excess enthalpy predictions can be obtained with SAFT-based models. Another option is to modify the association theory so that the number of association sites on a molecule becomes dependent on the components in the mixture.

8.4 Polar (non-HB)/Hydrogen bonding systems

The current approaches used in the literature to account for hydrogen bonding in cross-associating systems (with non self-associating components) involve fitting the association volume or a factor of the association strength between the cross- and self-associating components e.g. acetone and methanol, as discussed in section 2.3. Although these approaches do provide reasonable results, the fact that an additional BIP per cross-associating binary system is introduced makes them less useful. Also, the normal approach where the k_{ij} values are fitted to VLE data often does not provide good results for these systems (51). Therefore, an attempt was made to develop a more useful approach.

8.4.1 Universal cross-association approach

The concept is to determine universal values for the association energy and association volume of the cross-associating component. For example, in the case of acetone, this is achieved by assigning one negative electron donor site to acetone and regressing universal association energy and association volume values from binary VLE data. By assigning one negative site, no self-association is induced. This approach suffers from a few weaknesses, the most significant being that the values obtained for the associating energy and volume of the cross-associating component are largely dependent on the association parameters and association scheme used to model the self-associating component. During the regression, it was also found that a broad minimum exists: several combinations of association energy and association volume values are obtained. However, many of these combinations are physically unrealistic (this is also encountered with the other approaches e.g. the association volume between methanol and acetone were reported to be 3.063 by Grenner *et al.* (51)).

To simplify the task, the value for the association volume of the cross-associating components was set equal to the association volume of the 1-alcohol that corresponds best in molecular size, and then to fit the association energy value to binary VLE data. This approach, denoted the ‘universal’ cross-association approach, is illustrated for the acetone/1-propanol system in Figure 8-46.

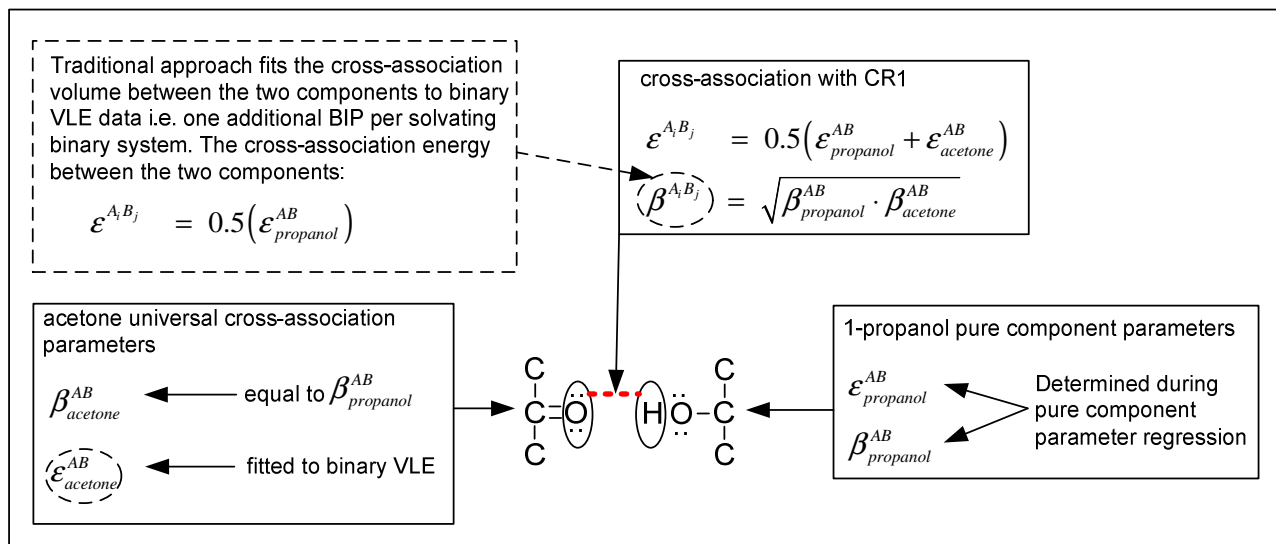


Figure 8-46: Schematic diagram illustrating the new ‘universal’ cross-association approach for the acetone/1-propanol system. The cross-association volume of the solvating component is set equal to the cross-association volume of the 1-alcohol that corresponds best in molecular size. The cross-association energy is fitted to binary VLE data.

Therefore, it was effectively assumed that molecules of similar size will have similar association volumes. The parameters obtained in this manner are physically more realistic. Sample illustrations with the ‘universal’ cross-association approach, are performed with acetone and propyl formate. The parameters used to demonstrate the performance of the new approach are presented in Table 8-23 for sPC-SAFT-GV and in Table 8-24 for sPC-SAFT-JC.

Table 8-23: Universal cross-association values for sPC-SAFT-GV based on different association schemes

Component	Assoc scheme of associating component	ϵ^{AB}/k [K]	β^{AB}	VLE included in the regression
acetone	2C	2160.54	0.0200	methanol (263), ethanol (264), 1-propanol (247)
	2B	1957.79	0.0350	methanol (263), ethanol (264), 1-propanol (247)
	3B	2929.19	0.0240	methanol (263), ethanol (264), 1-propanol (247)
propyl formate	2C	2081.46	0.00661	ethanol (265), 1-propanol (265), 1-butanol (265)
	2B	1639.47	0.01390	ethanol (265), 1-propanol (265), 1-butanol (265)
	3B	2533.62	0.01268	ethanol (265), 1-propanol (265), 1-butanol (265)

Table 8-24: Universal cross-association values for sPC-SAFT-JC based on different association schemes

Component	Assoc scheme of associating component	ϵ^{AB}/k [K]	β^{AB}	VLE included in the regression
acetone	2C	1990.91	0.0290	methanol (263), ethanol (264), 1-propanol (247)
	2B	1884.45	0.0520	methanol (263), ethanol (264), 1-propanol (247)
	3B	2770.73	0.0410	methanol (263), ethanol (264), 1-propanol (247)
propyl formate	2C	1962.63	0.00828	ethanol (265), 1-propanol (265), 1-butanol (265)
	2B	1585.96	0.01619	ethanol (265), 1-propanol (265), 1-butanol (265)
	3B	2459.45	0.01432	ethanol (265), 1-propanol (265), 1-butanol (265)

8.4.2 Vapour-liquid equilibria

A few VLE results are presented to illustrate the new concept. Figure 8-47 and Figure 8-48 show VLE results for the acetone/methanol system with sPC-SAFT-GV-XX and sPC-SAFT-JC-XX respectively. Note that the XX represents the association scheme used for methanol and the ϵ^{AB}/k and β^{AB} values in brackets indicate the cross-association parameters used for acetone. Model predictions (based on the different association schemes) that do not explicitly account for cross-association are also included for comparative purposes.

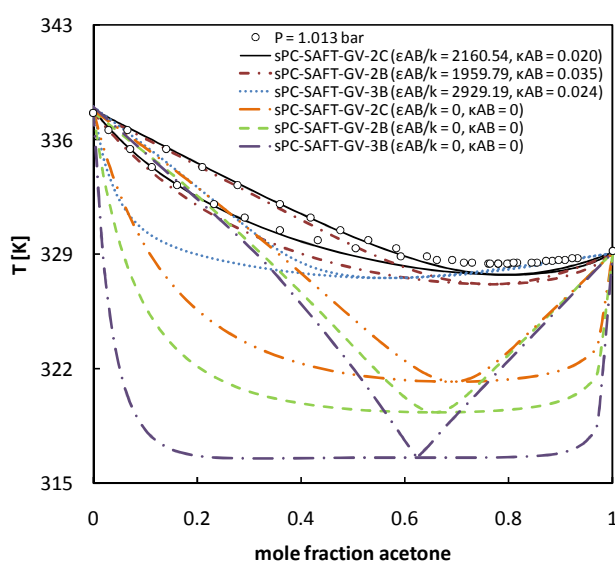


Figure 8-47: VLE predictions of the acetone/methanol system with sPC-SAFT-GV-XX. The XX represents the association scheme used for methanol and the values in brackets indicate the cross-association energy and volume used for acetone. Experimental data from ref. (263).

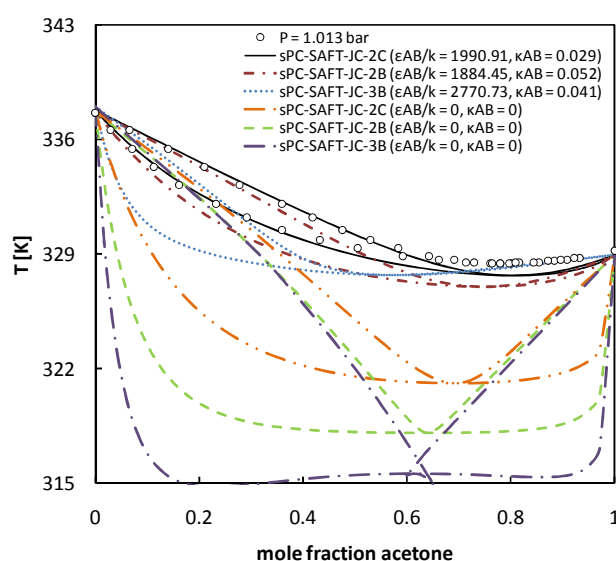


Figure 8-48: VLE predictions of the acetone/methanol system with sPC-SAFT-JC-XX. The XX represents the association scheme used for methanol and the values in brackets indicate the cross-association energy and volume used for acetone. Experimental data from ref. (263).

Figure 8-47 and Figure 8-48 show that large improvements are obtained with the new cross-association approach. The predictions based on the 2C and 2B schemes are most accurate with the predictions based on the 2C scheme being slightly superior to the 2B predictions. The predictions based on the 3B scheme for both sPC-SAFT-GV and sPC-SAFT-JC are not accurate and do not show

the correct phase behaviour when cross-association is explicitly accounted for. As mentioned, the new approach uses the same cross-association energy and volume values to characterize the solvating behaviour of the cross-associating component in other systems. In Figure 8-49 and Figure 8-50, VLE predictions of the acetone/1-propanol system are presented with the same cross-association parameters for acetone:

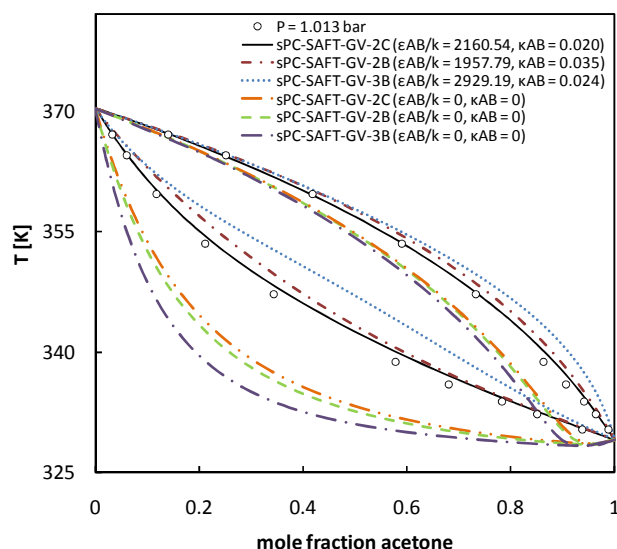


Figure 8-49: VLE predictions of the acetone/1-propanol system with sPC-SAFT-GV-XX. The XX represents the association scheme used for methanol and the values in brackets indicate the cross-association energy and volume used for acetone. Experimental data from ref. (247).

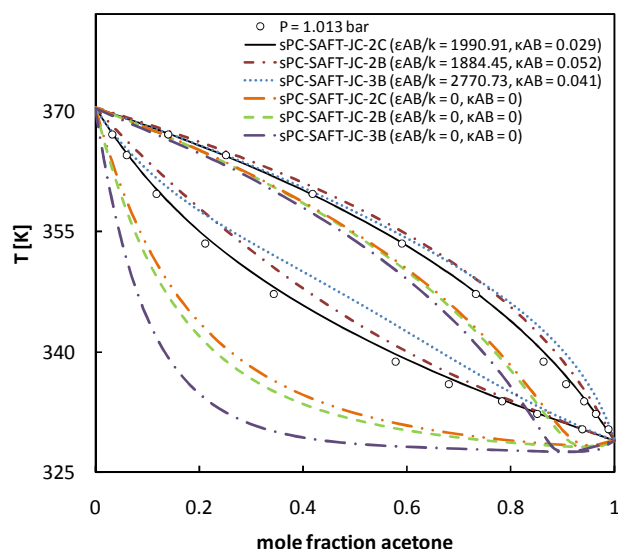


Figure 8-50: VLE predictions of the acetone/1-propanol system with sPC-SAFT-JC-XX. The XX represents the association scheme used for methanol and the values in brackets indicate the cross-association energy and volume used for acetone. Experimental data from ref. (247).

From Figure 8-49 and Figure 8-50, it follows that good VLE representations are obtained with the predictions based on the 2C and 2B association schemes for both sPC-SAFT-GV and sPC-SAFT-JC. Furthermore, it seems as if the cross-associative behaviour of acetone (at least in systems containing alcohols) may be characterized with ‘universal’ association energy and volume parameters.

The same results are observed for propyl formate/alcohol systems. Figure 8-51 and Figure 8-52 confirm that large improvements are obtained with the new approach for the propyl formate/ethanol system, but it also shows that some errors are still present in the VLE description. Admittedly, more refinement to the new approach may be required, but the advantage gained by using universal cross-associating parameters is definitely appealing.

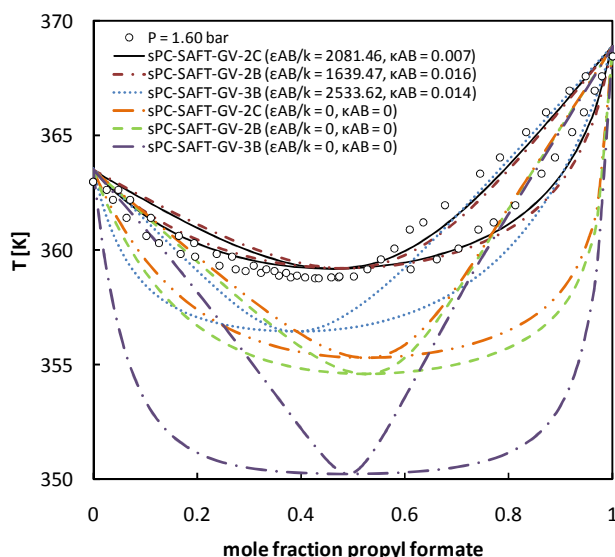


Figure 8-51: VLE predictions of the propyl formate/ethanol system with sPC-SAFT-GV-XX. The XX represents the association scheme used for ethanol and the values in brackets indicate the cross-association energy and volume used for propyl formate. Experimental data from ref. (265).

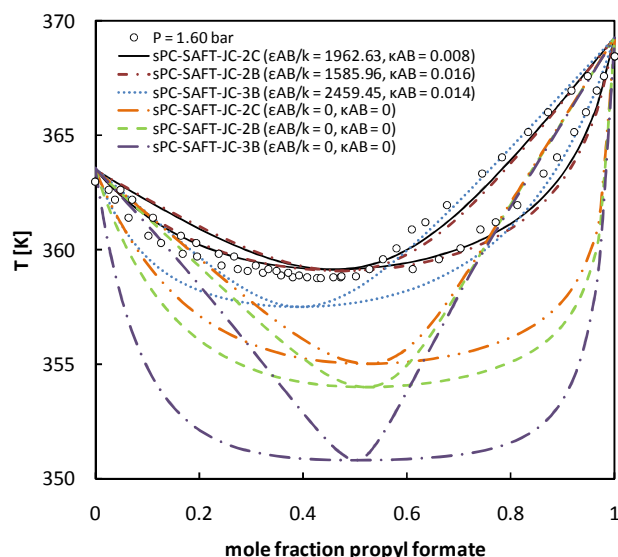


Figure 8-52: VLE predictions of the propyl formate/ethanol system with sPC-SAFT-JC-XX. The XX represents the association scheme used for ethanol and the values in brackets indicate the cross-association energy and volume used for propyl formate. Experimental data from ref. (265).

The same propyl formate cross-association parameters are used to predict the VLE of the propyl formate/1-butanol system, as shown in Figure 8-53 (GV) and Figure 8-54 (JC). Clearly very good VLE representations are obtained with both sPC-SAFT-GV and sPC-SAFT-JC based on both the 2C and 2B association schemes.

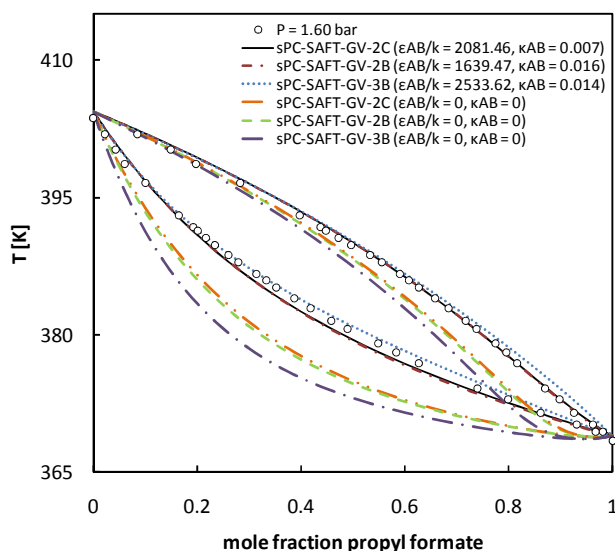


Figure 8-53: VLE predictions of the propyl formate/1-butanol system with sPC-SAFT-GV-XX. The XX represents the association scheme used for 1-butanol and the values in brackets indicate the cross-association energy and volume used for propyl formate. Experimental data from ref. (265).

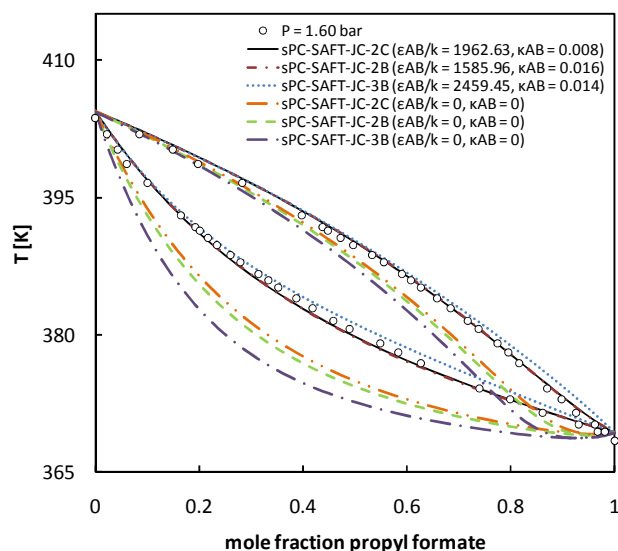


Figure 8-54: VLE predictions of the propyl formate/1-butanol system with sPC-SAFT-JC-XX. The XX represents the association scheme used for 1-butanol and the values in brackets indicate the cross-association energy and volume used for propyl formate. Experimental data from ref. (265).

The transferability of the cross-association parameters was tested by investigating whether the parameters determined for propyl formate may be used for ethyl acetate. Since the molecules of

both components have the same molecular weight and are similar in structure (the functional group only moves by one carbon), it is expected that the parameters should be somewhat transferable. Presented in Figure 8-55 (GV) and Figure 8-56 (JC), are VLE predictions of the methanol/ethyl acetate system:

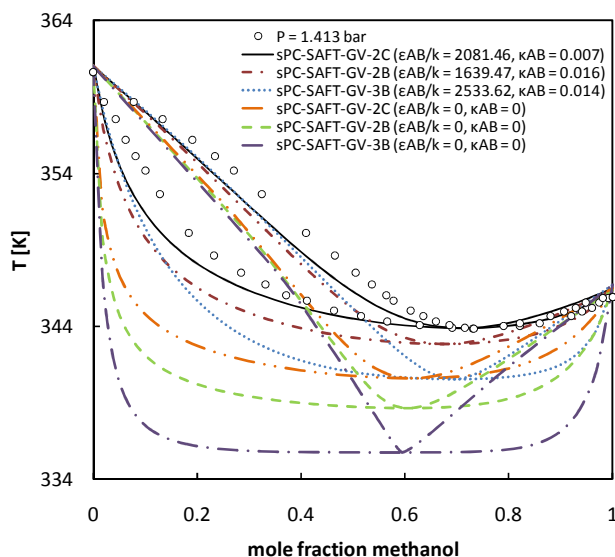


Figure 8-55: VLE predictions of the methanol/ethyl acetate system with sPC-SAFT-GV-XX. The XX represents the association scheme used for methanol and the values in brackets indicate the cross-association energy and volume used for ethyl acetate. Experimental data from ref. (266).

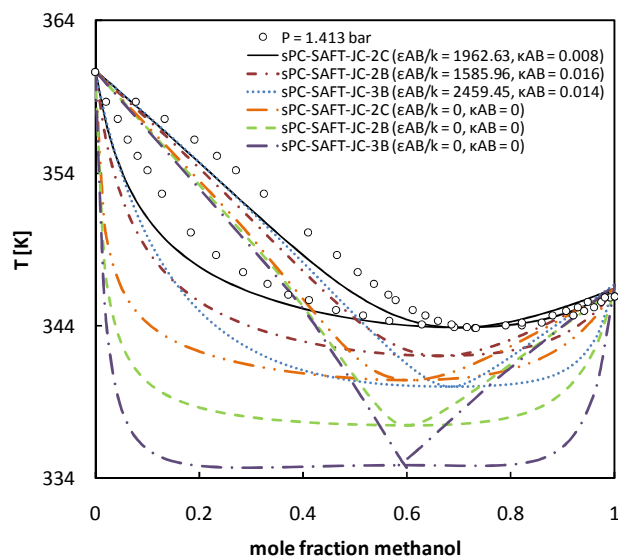


Figure 8-56: VLE predictions of the methanol/ethyl acetate system with sPC-SAFT-JC-XX. The XX represents the association scheme used for methanol and the values in brackets indicate the cross-association energy and volume used for ethyl acetate. Experimental data from ref. (266).

From Figure 8-55 and Figure 8-56, the best predictions are obtained with sPC-SAFT-GV-2C and sPC-SAFT-JC-2C when cross-association is explicitly taken into account. The cross-association parameters for propyl formate seem to be transferable to ethyl acetate. Very good VLE predictions are also obtained for systems with larger alcohols. The VLE of 1-pentanol/ethyl acetate is presented in Figure 8-57 and in Figure 8-58 for the GV and JC models respectively.

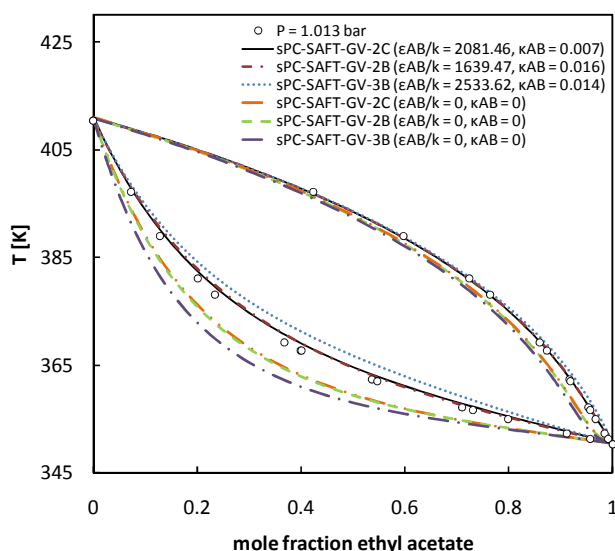


Figure 8-57: VLE predictions of the ethyl acetate/1-pentanol system with sPC-SAFT-GV-XX. The XX represents the association scheme used for 1-pentanol and the values in brackets indicate the cross-association energy and volume used for ethyl acetate. Experimental data from ref. (267).

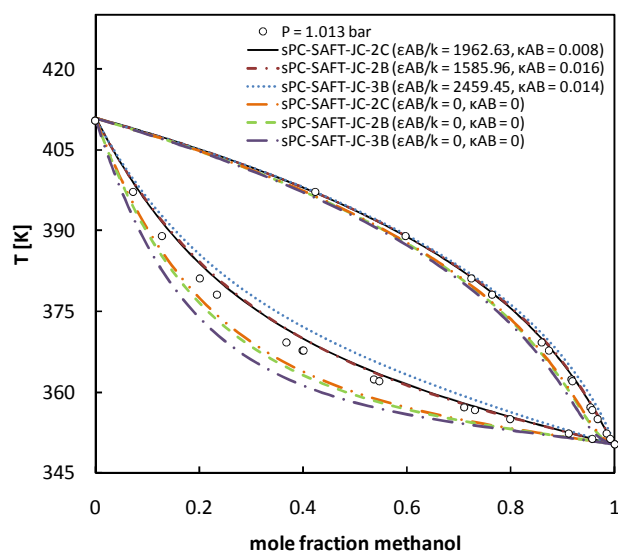


Figure 8-58: VLE predictions of the ethyl acetate/1-pentanol system with sPC-SAFT-JC-XX. The XX represents the association scheme used for 1-pentanol and the values in brackets indicate the cross-association energy and volume used for ethyl acetate. Experimental data from ref. (267).

The new cross-association approach proposed in this section results in improved VLE predictions of binary systems containing an alcohol and a cross-associating component, such as a ketone or ester. The concept behind the new approach is to find ‘universal’ association energy and association volume parameters for the cross-associating component. The advantage of this approach is that it reduces the number of interactions parameters needed to model VLE of multi-component systems that consist of several self- and cross-associating components.

Other properties such as excess enthalpy were briefly investigated. Generally, poor predictions are obtained with both sPC-SAFT-JC and sPC-SAFT-GV that do not drastically improve with the new cross-association approach. Given the large errors experienced with the models in the prediction of other thermodynamic properties for simpler systems as discussed earlier in this chapter and in Chapter 4, this is to be expected. Therefore, other thermodynamic properties of hydrogen bonding/polar (non-HB) systems are not considered here.

8.5 Multi-component VLE

VLE results of some representative ternary systems are presented below for sPC-SAFT-GV (Table 8-25) and sPC-SAFT-JC (Table 8-26) with predictions based on different alcohol association schemes. The cross-association parameters determined for acetone and ethyl acetate in the previous section are also used to compute ternary VLE, and example cases where cross-association is not accounted for are also presented to demonstrate the improvement obtained with the new ‘universal’ approach.

Table 8-25: VLE predictions of ternary mixtures with sPC-SAFT-GV and various association schemes for alcohols

Mixture/Model	<i>T</i> or <i>P</i>	$\Delta x_2(\times 10^2)^a$	$\Delta x_3(\times 10^2)^a$	$\Delta y_1(\times 10^2)^a$	$\Delta y_2(\times 10^2)^a$	$\Delta y_3(\times 10^2)^a$	<i>np</i>	Ref.
water(1)/methanol(2)/ethanol(3)	298.15 K						37	(268)
sPC-SAFT-GV-2C		4.24	4.24	4.02	6.02	1.99		
sPC-SAFT-GV-2B		14.8	14.8	10.3	19.8	9.46		
sPC-SAFT-GV-3B		1.11	1.11	0.72	1.16	0.89		
methanol (1)/ethanol(2)/1-butanol(3)	1.013 bar						14	(269)
sPC-SAFT-GV-2C		3.35	3.35	6.13	2.70	6.13		
sPC-SAFT-GV-2B		4.79	4.79	6.58	2.64	2.75		
sPC-SAFT-GV-3B		4.71	4.71	7.62	2.70	6.95		
water(1)/ethanol(2)/<i>n</i>-hexane (3)	1.013 bar						49	(270)
sPC-SAFT-GV-2C		6.26	6.26	1.58	3.30	3.42		
sPC-SAFT-GV-2B		7.41	7.43	4.27	4.77	6.89		
sPC-SAFT-GV-3B		8.01	8.01	2.36	4.09	4.20		
ethyl acetate(1)/ethanol(2)/1-butanol(3)	0.967 bar						35	(269)
sPC-SAFT-GV-2C		7.89	7.89	2.70	6.47	5.58		
sPC-SAFT-GV-2B		7.85	7.85	3.21	6.56	5.56		
sPC-SAFT-GV-3B		4.06	4.06	2.10	5.72	4.55		
acetone(1)/methanol(2)/1-propanol(3)	1.013 bar						15	(271)
sPC-SAFT-GV-2C		2.33	2.33	1.12	1.66	1.05		
sPC-SAFT-GV-2B		3.20	3.21	2.08	2.20	1.08		
sPC-SAFT-GV-3B		7.32	7.32	3.33	3.91	2.17		
sPC-SAFT-GV-2C (no cross-association)		16.2	16.2	4.95	1.37	4.33		
sPC-SAFT-GV-3B (no cross-association)		23.4	23.4	7.96	2.38	5.80		
acetone(1)/ethyl acetate (2)/ethanol(3)	1.013 bar						59	(272)
sPC-SAFT-GV-2C		5.30	5.21	3.77	1.44	3.90		
sPC-SAFT-GV-2B		3.31	3.29	3.78	1.53	4.37		
sPC-SAFT-GV-3B		11.5	11.9	12.0	4.70	9.40		
sPC-SAFT-GV-2C (no cross-association)		22.1	23.2	20.2	7.97	14.4		
sPC-SAFT-GV-3B (no cross-association)		16.0	15.4	4.83	9.40	7.00		

^a $\Delta z = \sum_i^{np} |z_i^{calc} - z_i^{exp}|$ where *z* represents *y* or *x* and *np* is the number of data points.

Table 8-25 indicates that the best VLE predictions are obtained when alcohols are modelled with the 2C and 3B association schemes. For some systems, better results are obtained with the 2C scheme and for other systems, the predictions based on the 3B scheme are superior. Accounting for cross-association with the new approach leads to improved VLE predictions, as indicated for the acetone/methanol/1-propanol system and in the acetone/ethyl acetate/ethanol system. Similar comments hold for the sPC-SAFT-JC results presented in Table 8-26.

Table 8-26: VLE predictions of ternary mixtures with sPC-SAFT-JC and various association schemes for alcohols

Mixture/Model	<i>T or P</i>	$\Delta x_2(\times 10^2)^a$	$\Delta x_3(\times 10^2)^a$	$\Delta y_1(\times 10^2)^a$	$\Delta y_2(\times 10^2)^a$	$\Delta y_3(\times 10^2)^a$	<i>np</i>	Ref.
water(1)/ methanol(2)/ethanol(3)	298.15 K						37	(268)
sPC-SAFT-JC-2C		4.34	4.34	4.11	5.97	1.85		
sPC-SAFT-JC-2B		14.8	14.8	10.5	19.2	8.66		
sPC-SAFT-JC-3B		5.97	5.97	2.23	2.32	4..08		
methanol(1)/ethanol(2)/1-butanol(3)	1.013 bar						14	(269)
sPC-SAFT-JC-2C		3.52	3.52	6.25	2.67	6.23		
sPC-SAFT-JC-2B		4.76	4.76	6.64	2.65	6.73		
sPC-SAFT-JC-3B		4.36	4.36	6.66	2.59	6.67		
water(1)/ethanol(2)/n-hexane(3)	1.013 bar						49	(270)
sPC-SAFT-JC-2C		6.12	6.12	1.53	3.27	3.48		
sPC-SAFT-JC-2B		7.45	7.46	4.03	4.86	6.75		
sPC-SAFT-JC-3B		8.41	8.41	2.21	4.13	3.48		
ethyl acetate(1)/ethanol(2)/1-butanol(3)	0.967 bar						35	(269)
sPC-SAFT-JC-2C		7.47	7.47	3.03	6.49	5.52		
sPC-SAFT-JC-2B		7.67	7.67	3.50	6.69	5.57		
sPC-SAFT-JC-3B		5.27	5.27	2.08	6.23	5.08		
acetone (1)/methanol(2)/1-propanol(3)	1.013 bar						15	(271)
sPC-SAFT-JC-2C		2.31	2.31	1.19	1.67	1.10		
sPC-SAFT-JC-2B		3.29	3.29	2.31	2.41	0.90		
sPC-SAFT-JC-3B		7.00	7.00	2.84	4.23	2.06		
sPC-SAFT-JC-2C (no cross-association)		17.0	17.0	5.25	1.46	4.57		
sPC-SAFT-JC-3B (no cross-association)		25.2	25.2	6.08	1.96	6.00		
acetone(1)/ethyl acetate (2)/ethanol(3)	1.013 bar						59	(272)
sPC-SAFT-JC-2C		4.22	5.31	2.74	2.27	3.62		
sPC-SAFT-JC-2B		3.74	5.48	4.72	2.60	6.13		
sPC-SAFT-JC-3B		9.52	9.85	9.90	340	7.78		
sPC-SAFT-JC-2C (no cross-association)		21.3	22.3	19.3	8.12	13.2		
sPC-SAFT-JC-3B (no cross-association)		19.9	18.9	3.36	12.3	10.6		

^a $\Delta z = \sum_i^{np} |z_i^{calc} - z_i^{exp}|$ where *z* represents *y* or *x* and *np* is the number of data points.

Both sPC-SAFT-GV and sPC-SAFT-JC are able to provide reasonable predictions of complex VLE. Further refinement to model parameters may lead to improved results, but it is more likely that theoretical improvement to both sPC-SAFT-GV and sPC-SAFT-JC is necessary before very accurate VLE predictions of complex multi-components systems will be achieved. Description of hydrogen bond co-operativity and accounting for the fact that the dipole moment changes in the liquid phase are focus areas that should be researched further.

8.6 Chapter Summary

New model parameters for associating components (alcohols and water) have been determined for sPC-SAFT-GV, sPC-SAFT-JC, CPA-GV and CPA-JC by including pure component and binary VLE data in the regression function. Alcohol parameters based on the 2C, 2B and 3B association schemes have been determined for sPC-SAFT-GV and sPC-SAFT-JC and alcohol parameters based on the 2B and 3B scheme have been determined for CPA-GV and CPA-JC. Model parameters for water are based on the 4C association scheme for all EOS. Furthermore, a new ‘universal’ cross-association approach is proposed that explicitly accounts for cross-association in mixtures where some components cross-associate (solvate), but do not self-associate. The concept behind the new approach is to determine universal association energy and volume values for the cross-associating component that characterizes the solvating behaviour of the component in associating mixtures. The new approach was implemented with sPC-SAFT-GV and sPC-SAFT-JC. The models are applied to the VLE and other thermodynamic properties of several complex binary mixtures. The VLE of a few representative ternary systems were also investigated with sPC-SAFT-GV and sPC-SAFT-GV. The performance of the polar sPC-SAFT and polar CPA models are summarized in the following sections:

8.6.1 sPC-SAFT-GV and sPC-SAFT-JC

When applied to associating components, sPC-SAFT-GV and sPC-SAFT-JC, perform as follows:

- sPC-SAFT-GV and sPC-SAFT-JC perform virtually the same in predicting alcohol/alkane VLE. Generally, very accurate VLE predictions are obtained, and in most cases, no BIPs are required. The difference between the VLE predictions based on the 2C, 2B, 3B association schemes are negligible.
- Other thermodynamic properties, such as excess enthalpies and excess volumes, cannot be predicted with good accuracy, but BIPs may be used to obtain improved correlations. Unfortunately, the BIPs are property-specific.
- Both sPC-SAFT-GV and sPC-SAFT-JC have inappropriate temperature. Large errors are especially observed at low temperatures.
- The VLE of alcohol/alcohol systems are predicted well by both models, but good correlations of other properties still require BIPs in most cases. The influence of the different association schemes on the properties of other alcohol/alcohol systems appears to be small.
- The influence of the association schemes on the VLE predictions of alcohol/water systems is, however, not negligible. The predictions of both sPC-SAFT-JC and sPC-SAFT-GV, based on the 2C association scheme, proved to be superior to the predictions based on the 2B and 3B schemes, especially for small-alcohols that do not exhibit VLLE. Accurate predictions of other alcohol/water thermodynamic properties are still problematic. Only limited success is managed with BIPs.

- The new ‘universal’ approach developed to describe cross-association improves the VLE predictions of both sPC-SAFT-GV and sPC-SAFT-JC significantly.
- Multi-component VLEs of a few ternary systems are predicted with good accuracy, but more improvement to both theories are likely to be necessary before very accurate VLE representations will be obtained. The cross-association approach improves the VLE predictions of both models considerably in relevant ternary systems.

8.6.2 CPA-GV and CPA-JC

The main findings regarding the performance of CPA-JC and CPA-GV are highlighted below:

- The VLE of alkane/alcohols systems are predicted with good accuracy by both CPA-JC and CPA-GV. The predictions of these polar models are slightly more accurate compared to the original CPA model.
- Similar to their sPC-SAFT counterparts, both CPA-JC and CPA-GV have difficulty in predicting other thermodynamic properties accurately. BIPs may be used to improve representations, although these BIPs are also property-specific.
- Both CPA-JC and CPA-GV provide good predictions of alcohol/alcohol VLE, but the original CPA model seems to be slightly superior. Other properties are not predicted satisfactorily.
- In alcohol/water VLE, both CPA-GV and CPA-JC provide acceptable representation of these systems. Compared to normal CPA, the predictions of the polar models are only superior for the methanol/water system. The VLE of other systems are predicted marginally better with normal CPA.
- A major disadvantage of normal CPA, CPA-GV and CPA-JC, is that system specific combining rules for the association term are required. Alcohol/alcohol systems are best described with the CR1 while only the ECR provides acceptable alcohol/water predictions.

8.6.3 Scientific Contribution

The work presented in this chapter shows that, by modelling alcohols with the 2C scheme in sPC-SAFT-GV and sPC-SAFT-JC, notable improvement in the VLE predictions of alcohol/alkane, polar/alcohol and alcohol/water systems are obtained compared to the original sPC-SAFT EOS.

An article reporting the findings presented in this chapter is in preparation.

Chapter 9

Conclusions

The aim of this research was to evaluate and improve how sPC-SAFT accounts for complex molecular interactions. A preliminary investigation (Chapter 3 and Chapter 4) was conducted in which sPC-SAFT, in its original published form, was applied to several thermodynamic properties of pure components and binary mixtures. CPA was also included in this investigation for comparative purposes. Major weaknesses and shortcomings have been identified in the framework of the aforementioned models, as presented in Chapter 5. The work and contributions are now summarized below:

9.1 Major shortcomings of sPC-SAFT

sPC-SAFT suffers from the following limitations:

- sPC-SAFT has an incorrect temperature dependency for thermodynamic several properties, especially properties that are strongly influenced by temperature, such as heat capacities and excess enthalpy.
- Although sPC-SAFT show a significant improvement in the description of the pressure-volume derivative compared to cubic EOS, it is still not sufficiently accurate to provide good descriptions of second-order properties that are largely influenced by this derivative, such as the speed of sound.
- The parameter regression study with sPC-SAFT showed that the inclusion of second-order properties in the regression function does not lead to parameter sets that are able to describe first- and second-order properties simultaneously.
- sPC-SAFT and CPA treat strong polar forces via the *Van der Waals* approach and have difficulty in accurately describing most thermodynamic properties of polar components. This study showed that it is necessary to explicitly account for polar forces in order to obtain improved representation of thermodynamic properties of polar systems.
- The association term does not account for complex molecular effects such as bond co-operativity. Consequently, in mixtures where these effects influence properties severely (such as water/alcohol systems) poor property predictions are obtained with both sPC-SAFT and CPA.

Following the identification of shortcomings in sPC-SAFT, the description of hydrogen bonding interactions in water/alcohol mixtures and the description of polar interactions were selected as the two focus areas for improvement. This resulted in the development of the new 2C association scheme for 1-alcohols (Chapter 6) and new simplified polar PC-SAFT models (Chapter 7 and Chapter 8), denoted sPC-SAFT-GV and sPC-SAFT-JC. Polar variants of CPA were also subsequently developed (CPA-GV and CPA-JC).

The following main conclusions can be drawn regarding the performance of the new 2C association scheme and the new polar sPC-SAFT and CPA models.

9.2 New 2C association scheme within sPC-SAFT

The new 2C scheme for 1-alcohols consist of one bipolar and one negative electron donor site and provides a level of association that is stronger than the 2B scheme, but weaker than the 3B scheme. The performance of the 2C scheme compared to the 2B and 3B association schemes is summarized below:

- The 2C scheme results in improved VLE predictions of alcohol/water systems compared to the 2B and 3B schemes. Large improvements are especially obtained in the VLE prediction of short-chained alcohol/water systems.
- For larger alcohols that exhibit VLLE with water, such as 1-butanol and 1-pentanol, good VLE predictions are obtained with the 2C scheme, but only moderate LLE predictions are obtained that are slightly superior compared to the 2B scheme.
- A disadvantage of the 2C scheme is that slightly worse VLE predictions of alcohol/alkane mixtures are obtained.

9.3 sPC-SAFT-GV and sPC-SAFT-JC

The polar terms of *Gross & Vrabec* (GV) and *Jog & Chapman* (JC) have been incorporated into sPC-SAFT to form sPC-SAFT-JC and sPC-SAFT-GV. New model parameters were regressed for several polar components by including pure component data and binary VLE data in the regression function. In sPC-SAFT-GV, the n_p parameter was not by default set equal to 1 as commonly done in the literature, but rather treated as an adjustable parameter in the regression function. Parameter sets for 1-alcohols based on the 2B, 2C and 3B association schemes were determined to investigate which association scheme is most suited to model alcohols with. New water parameters based on the 4C scheme were also determined. Furthermore, a new 'universal' cross-association approach was proposed that enhances the performance of the models for relevant systems.

9.3.1 Application to polar (non-HB) components

The performance of sPC-SAFT-GV and sPC-SAFT-JC when applied to mixtures containing polar (non-HB) components can be summarized as follows:

- The VLE of simple polar/alkane systems and polar/polar systems can be predicted accurately with both sPC-SAFT-GV and sPC-SAFT-JC. Generally, the performance of the models is similar, with neither model being superior to the other.
- The new model parameters provide more accurate VLE predictions compared to the model parameters currently available in the literature.
- With respects to polar/alkane systems, neither model is able to accurately predict other thermodynamic properties, such as excess enthalpy and excess volume, although some improvement is obtained with the polar sPC-SAFT models compare to normal sPC-SAFT.
- Ternary VLE is also predicted with fairly good accuracy by both sPC-SAFT-GV and sPC-SAFT-JC.

9.3.2 Application to hydrogen bonding components

The ability of sPC-SAFT-GV and sPC-SAFT-JC to predict properties of hydrogen bonding systems can be concluded as follows:

- Alcohol/alkane VLE is predicted with more or less the same accuracy for both sPC-SAFT-GV and sPC-SAFT-JC when alcohols are modelled with any of the 2C, 2B or 3B association schemes.
- The alcohol parameters determined in this study generally result in superior phase equilibria representations compared to the 2B parameters currently available in the literature. Other properties of alcohol/alkane mixtures, such as excess enthalpy and volume, are not predicted with good accuracy, although property specific BIPs can be used to improve results.
- The performance of both sPC-SAFT-GV and sPC-SAFT-JC deteriorate slightly at low temperatures. False phase splits are routinely encountered in VLE calculations and other properties, such as excess enthalpy, require large BIPs to obtain acceptable correlations.
- Alcohol/alcohol VLE is predicted with good accuracy by both models. The predictions based on the 2C and 3B association schemes generally result in marginally superior VLE representations compared to the 2B scheme. Other properties require one BIP per binary system to obtain accurate correlations.
- The major difference between the different association schemes is observed when alcohol/water systems are modelled. The best VLE representations are obtained when alcohols are modelled with the 2C association scheme, especially in short-chained alcohol/water systems.
- In alcohol/water systems that show VLLE behaviour, good VLE predictions are obtained with both 2C and 3B association schemes. Unfortunately, accurate predictions of LLE are

still problematic. When BIPs are used to obtain improved VLE representations, the best overall correlation of both sPC-SAFT-GV and sPC-SAFT-JC are obtained when the alcohols are modelled with the 2C scheme.

- Large improvements are obtained in the VLE prediction of binary mixtures with components that cross-associate, but not self-associate. The improvements are credited to the new ‘universal’ cross-association approach proposed.
- Ternary VLE of representative systems are also predicted with fair accuracy, however, future improvement to both sPC-SAFT-GV and sPC-SAFT-JC seems to be necessary.
- sPC-SAFT-JC and sPC-SAFT-GV are feasible alternatives to PC-SAFT-JC and PC-SAFT-GV, because the developed models provide good performance at a lower numerical cost.

9.4 CPA-JC and CPA-GV

The polar terms of *Gross & Vrabec* (GV) and *Jog & Chapman* (JC) were modified to be compatible within the framework of CPA. Model parameters for several polar (non-associating) and associating components were determined. Pure component data and binary VLE data were also included in the regression function. Parameters for alcohols based on both the 2B and 3B association scheme were determined and water was modelled with the 4C scheme.

9.4.1 Application to polar (non-HB) components

The capabilities of CPA-GV and CPA-JC with respect to polar (non-HB) mixtures are:

- Both CPA-JC and CPA-GV provide very good VLE predictions of polar/alkane systems that are significantly superior to normal CPA.
- The predictions are of similar accuracy compared to their sPC-SAFT counterparts, with neither model being superior to the other.
- Improvements in the prediction of other thermodynamic properties are also obtained compared to normal CPA, such as excess enthalpy, although property-specific BIPs are still required.
- Good predictions of ternary VLE are also obtained.

9.4.2 Application to hydrogen bonding components

The main findings related to the modelling of hydrogen bonding systems with CPA-GV and CPA-JC are:

- Both CPA-GV and CPA-JC provide accurate VLE predictions of alcohol/alkane systems that are slightly more accurate compared to normal CPA.
- Both models required BIPs to provide reasonable predictions of other thermodynamic properties of alcohol/alkane systems.

- The VLE of alcohol/alcohol systems are represented well, but BIP are required to model other properties.
- The modelling of alcohol/water VLE, however, is less satisfying. Compared to normal CPA, both CPA-JC and CPA-GV only show improved VLE predictions for the methanol/water system and are marginally less accurate for other alcohol/water systems investigated.
- Furthermore, a major drawback of all CPA-type models is that system specific combining rules need to be used in the association term to obtain the best results.

9.5 Contributions of this work

From an overall perspective, the work in this thesis enables improved performance of sPC-SAFT (and CPA).

Publication list

Part of the work has already been accepted by the scientific community through publications in peer reviewed journals:

Title: New Association Scheme for 1-Alcohols in Alcohol/Water Mixtures with sPC-SAFT: The 2C Association Scheme

Authors: Adriaan J. de Villiers, Cara E. Schwarz, and Andries J. Burger

Journal: Industrial & Engineering Chemistry Research **2011**, 50, 8711–8725

Title: Improving vapour–liquid-equilibria predictions for mixtures with non-associating polar components using sPC-SAFT extended with two dipolar terms.

Authors: A.J. de Villiers, C.E. Schwarz, A.J. Burger

Journal: Fluid Phase Equilibria **2011**, 305, 174–184

Title: Extension of the CPA equation of state with dipolar theories to improve vapour-liquid-equilibria predictions

Authors: A.J. de Villiers, C.E. Schwarz, A.J. Burger

Journal: Fluid Phase Equilibria **2011**, 312, 66–78

An additional publication reporting the performance of sPC-SAFT-GV and sPC-SAFT-JC when applied to associating components is currently being prepared.

Chapter 10

Future work

10.1 Development of a new reference term

As discussed in Chapter 5, the development of a new reference term is likely required to obtain improved description of second-order properties. This implies that the constants of the PC-SAFT dispersion term will have to be re-determined and that the current potential function will have to be modified. Initially, it was thought that replacing the hard-sphere term with the hard-convex-body (hcb) term would result in improved prediction of second-order properties, because good predictions of second-order properties are obtained with SAFT-CP (90) (which uses the hcb term). This unfortunately is not the case, as shown in Figure 10-1, where predictions of the speed of sound in *n*-hexane are presented with sPC-SAFT and hcb-PC-SAFT.

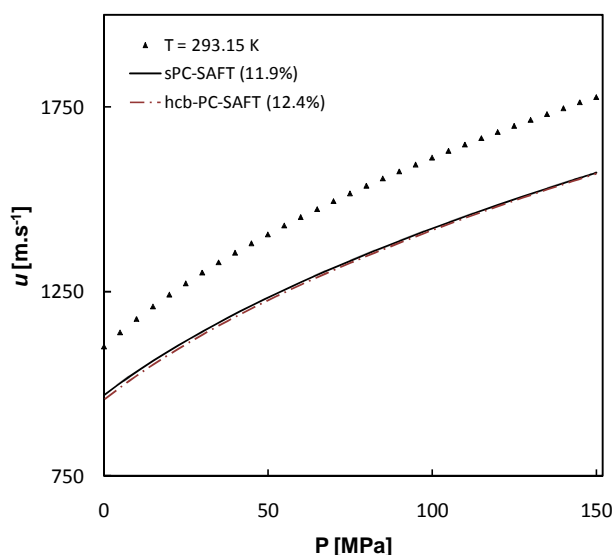


Figure 10-1: Speed of sound in *n*-hexane at $T = 293.15$ K. Data from ref. (92).

Essentially, the only advantage the hcb reference term provides when incorporated into PC-SAFT, is that the description of the critical region is slightly improved. Since both reference terms are hard-body based, it does indicate that the description of the distance dependency of the repulsive

interactions are crucial in predicting second-order properties and that this should be incorporated into the development of a new reference term.

10.2 Incorporation of new model parameters into group contribution regressions

The new model parameters determined for sPC-SAFT-GV and sPC-SAFT-JC can be used to improve the group contribution version of sPC-SAFT (developed by Tihic *et al.* (273; 274)). By including the newly presented parameters in the regression of the polar functional groups, the influence of polar forces may be described more accurately with the group contribution version.

10.3 Determining model parameters for more components

This study was limited to only a few commonly encountered components in the industry. In order to incorporate the newly presented models into simulation packages, parameters for more components need to be determined. The most appropriate parameters seem to be determined when binary VLE data is included in the regression function. Inevitably, VLE data is not always available. To circumvent this problem, more work needs to be done to develop correlations that can predict some of the model parameters with fair accuracy for data-scarce components. The remaining parameters may then be regressed from pure component data.

10.4 Improving the polar terms

Both polar terms greatly enhance the performance of sPC-SAFT and CPA. There are, however, a few shortcomings. The most severe problem is the incorrect temperature dependency of the models, especially in the low temperature region. A possible improvement to both the GV and JC theories are to explicitly account for the change in dipole moment in the liquid phase.

10.5 Improving the association term

The association term needs to be modified in order to explicitly account for hydrogen bond cooperativity in order to predict properties of systems that are severely influenced by hydrogen bonding networks. A possible starting point may be to use the ideas of Sear and Jackson (275), although their approach is more intuitive than rigorous.

10.6 Refining the new universal cross-association approach

The usefulness of the new cross-association approach was only demonstrated for selected systems. More work is needed to refine the approach and to determine the most appropriate model parameters. The transferability of model parameters should also be evaluated and whether generalized parameters for a homologous series of cross-associating components can be determined e.g. universal parameters for ketones, esters, ether, etc.

10.7 Development of standardized data base

Throughout this project, the unavailability of high quality data was frequently encountered. The development of a database standard is required that is similar to the VLE database of Danner and Gess (50), but with various thermodynamic properties. Evaluating these properties should test the ability of a model to account for the influence of several types of molecular interactions in various types of properties at several conditions.

References

1. **Letcher, T. M.** *Chemical Thermodynamics: A 'Chemistry for the 21st Century' monograph*. s.l. : Blackwell Science Ltd, 1999. ISBN 0-632-05127-2.
2. **Wei, Y.; Sadus, R. J.** Equations of State for the Calculation of Fluid-Phase Equilibria. *AIChE Journal*. 2000, Vol. 46, pp. 169-196.
3. **Michelsen, M. L.; Mollerup, J. M.** *Thermodynamic Models: Fundamentals & Computational Aspects*. Denmark : Tie-Line Publications, 2007. ISBN-89-989961-3-4.
4. **Nel, R. J. J.; De Klerk, A.** Fischer-Trops Aqueous Phase Refining by Catalytic Alcohol Dehydration. *Ind. Eng. Chem. Res.* 2007, Vol. 46, pp. 3558-3565.
5. **Muller, E. A.; Gubbins, K. E.** Molecular-Based Equations of State for Associating Fluids: A Review of SAFT and Related Approaches. *Ind. Eng. Chem. Res.* 2001, Vol. 40, pp. 2193-2211.
6. **Von Solms, N.; Michelsen, M. L.; Kontogeorgis, G. M.** Computational and Physical Performance of a Modified PC-SAFT Equation of State for Highly Asymmetric Systems and Associating Mixtures. *Ind. Eng. Chem. Res.* 2003, Vol. 42, pp. 1098-1105.
7. **Economou, I. G.; Donohue, M. D.** Chemical, Quasi-Chemical and Perturbation Theories for Associating Fluids. *AIChE Journal*. 1991, Vol. 37, 12, pp. 1875-1894.
8. **Kontogeorgis, G. M.; Voutsas, E. C.; Yakoumis, I. V.; Tassios, D. P.** An Equation of State for Associating Fluids. *Ind. Eng. Chem. Res.* 1996, Vol. 35, pp. 4310-4318.
9. **Tan, S.P.; Adidharma, H.; Radosz, M.** Recent Advances and Applications of Statistical Associating Fluid Theory. *Ind. Eng. Chem. Res.* 2008, Vol. 47, pp. 8063-8082.
10. **Wertheim, M. S.** Fluids with Highly Directional Attractive Forces. I. Statistical Thermodynamics. *J. Stat. Phys.* 1984, Vol. 35, pp. 19-34.
11. **Wertheim, M. S.** Fluids with Highly Directional Attractive Forces. II. Thermodynamic Perturbation Theory and Integral Equations. *J. Stat. Phys.* 1984, Vol. 35, pp. 35-47.
12. **Wertheim, M. S.** Fluids with Highly Directional Attractive Forces. III. Multiple Attraction Sites. *J. Stat. Phys.* 1986, Vol. 42, pp. 459-467.

13. **Wertheim, M. S.** Fluids with Highly Directional Attractive Forces. IV. Equilibrium Polymerization. *J. Stat. Phys.* 1986, Vol. 42, pp. 477-492.
14. **Wertheim, M. S.** Fluids of Dimerizing Hard Spheres, and Fluid Mixtures of Hard Spheres and Dispheres. *J. Chem. Phys.* 1986, Vol. 85, pp. 2929-2936.
15. **Wertheim, M. S.** Thermodynamic Perturbation Theory of Polymerization. *J. Chem. Phys.* 1987, Vol. 87, pp. 7323-7331.
16. **Chapman, W. G.; Gubbins, K. E.; Jackson, G.; Radosz, M.** New Reference Equation of State for Associating Liquids. *Ind. Eng. Chem. Res.* 1990, Vol. 29, pp. 1709-1721.
17. **Jackson, G.; Chapman, W. G.; Gubbins, K. E.** Phase Equilibria of Associating Fluids: Spherical Molecules with Multiple Bonding Sites. *Molec. Phys.* 1988, Vol. 65, p. 1.
18. **Chapman, W. G.; Jackson, G.; Gubbins, K. E.** Phase Equilibria of Associating Fluids: Chain Molecules with Multiple Sites. *Mol. Phys.* 1988, Vol. 65, pp. 1057-1079.
19. **Soave, G.** Equilibrium constant from a modified Redlich-Kwong equation of state. *Chem. Eng. Sci.* 1972, Vol. 27, pp. 1197-1203.
20. **Peng, D. Y.; Robinson, D. B.** A New Two-Constant Equation of State. *Ind. Eng. Chem. Fundam.* 1976, Vol. 15, 1, pp. 59-65.
21. **Economou, I. G.** Statistical Associating Fluids Theory: A Successful Model for the Calculation of Thermodynamic and Phase Equilibrium Properties of Complex Fluid Mixtures. *Ind. Eng. Chem. Res.* 2002, Vol. 41, pp. 953-962.
22. **Von Solms, N.; Kouskoumvekaki, I. A.; Michelsen, M. L.; Kontogeorgis, G. M.** Capabilities, limitations and challenges of a simplified PC-SAFT equation of State. *Fluid Phase Equilib.* 2006, Vol. 241, pp. 344-353.
23. **Karakatsani, E. K.; Kontogeorgis, G. M.; Economou, I. G.** Evaluation of the Truncated Perturbed Chain-Polar Statistical Associating Fluids Theory for Complex Mixture Phase Equilibria. *Ind. Eng. Chem. Res.* 2006, Vol. 45, pp. 6063-6074.
24. **Gross, J.; Sadowski, G.** Perturbed-Chain SAFT: An Equation of State Based on a Perturbation Theory for Chain Molecules. *J. Phys. Chem. B.* 2001, Vol. 40, pp. 1244-1260.
25. **Gross, J.; Sadowski, G.** Application of the Perturbed-Chain SAFT Equation of State to Associating Systems. *Ind. Eng. Chem. Res.* 2002, Vol. 41, pp. 5510-5515.
26. **Huang, S. H.; Radosz, M.** Equation of State for Small, Large, Polydisperse, and Associating Molecules. *Ind. Eng. Chem. Res.* 1990, Vol. 29, pp. 2284-2294.
27. **Huang, S. H.; Radosz, M.** Equation of State for Small, Large Polydisperse, and Associating Molecules: Extension to Fluid Mixtures. *Ind. Eng. Chem. Res.* 1991, Vol. 30, pp. 1994-2005.

28. **Mansoori, G. A.; Carnahan, N. F.; Starling, K. E; Leland, T. W.** Equilibrium Thermodynamic Properties of the Mixtirure of Hard Spheres. *J. Chem. Phys.* 1971, Vol. 54, pp. 1523-1525.
29. **Carnahan, N. F.; Starling, K. E.** Equation of State for nonattracting rigid spheres. *J. Chem. Phys.* 1969, Vol. 51, pp. 635-636.
30. **Michelsen, M. L.; Hendriks, E. M.** Physical properties from association models. *Fluid Phase Equilib.* 2001, Vol. 180, pp. 165-174.
31. **Grenner, A.; Kontogeorgis, G. M.; Von Solms, N.; Michelsen, M. L.** Modeling phase equilibria of alkanols with the simplified PC-SAFT equation of state and generalized pure compound parameters. *Fluid Phase Equilib.* 2007, Vol. 258, pp. 83-94.
32. **Tybjerg, P. C. V.; Kontogeorgis, G. M.; Michelsen, M. L.; Stenby, E. H.** Phase equilibria modeling of methanol-containing systems with the CPA and sPC-SAFT equations of state. *Fluid Phase Equilib.* 2010, Vol. 288, pp. 128-138.
33. **Kontogeorgis, G. M.; Tsvintzelis, I.; Von Solms, N.; Grenner, A.; Bøgh, D.; Frost, M.; Knage-Rasmussen, A.; Economou, I.G.** Use of monomer fraction data in the parametrization of association theories. *Fluid Phase Equilib.* 2010, Vols. 219-229.
34. **Clark, G. N. I.; Haslam, A.J.; Galindo, A.; Jackson, G.** Developing optimal Wertheim-like models of water for Statistical Associating Fluid Theory (SAFT) and related approaches. *Mol. Phys.* 2006, Vol. 104, pp. 3561-3581.
35. **Al-Saifi, N.M; Hamad, E.Z; Englezos, P.** Prediction of vapor-liquid equilibrium in water-alcohol-hydrocarbon systems with the dipolar perturbed-chain SAFT equation of state. *Fluid Phase Equilib.* 2008, Vol. 271, pp. 82-93.
36. **Grenner, A.; Schmelzer, J.; Von Solms, N.; Kontogeorgis, G. M.** Comparison of Two Association Models (Elliott-Suresh-Donohue and Simplified PC-SAFT) for Complex Phase Equilibria of Hydrocarbon-Water and Amine Containing Mixtures. *Ind. Eng. Chem. Res.* 2006, Vol. 45, pp. 8170-8179.
37. **Kontogeorgis, G. M.; Michelsen, M. L.; Folas, G. K.; Derawi, S.; Von Solms, N.; Stenby, E. H.** Ten Years with the CPA (Cubic-Plus-Association) Equation of State. Part 1. Pure Compounds and Self-Associating Systems. *Ind. Eng. Chem. Res.* 2006, Vol. 45, pp. 4855-4868.
38. **Cummings, P. T.; Stell, G.** Statistical Mechanical Models of Chemical Reactions: Analytical Solution of Models of $A+B \rightleftharpoons AB$ in Percus-Yevick Approximation. *Mol. Phys.* 1984, Vol. 51, pp. 253-287.
39. **Cummings, P. T.; Stell, G.** Statistical mechanical models of chemical reactions. II. Analytic solutions of the Percus-Yevick approximation for a model of homogeneous association. *Mol. Phys.* 1985, Vol. 55, pp. 33-48.

40. **Ting, P. D.; Joyce, P. C.; Jog, P. S.; Chapman, W. G.; Thies, M. C.** Phase equilibrium modeling of mixtures of long-chain and short-chain alkanes using Peng-Robinson and SAFT. *Fluid Phase Equilib.* 2003, Vol. 206, pp. 267-286.
41. **Ghosh, A.; Chapman, W. G.; French, R. N.** Gas solubility in hydrocarbons - a SAFT based approach. *Fluid Phase Equilib.* 2003, Vol. 209, pp. 229-243.
42. **Garcia, J.; Paredes, X.; Fernandez, J.** Analysis of the phase equilibria of CO₂ - alkylbenzene systems with PC-SAFT model. *20th European Symposium on Applied Thermodynamics*. [Poster presentation]. Lahnstein, Germany : s.n., 2003. pp. 121-126.
43. **Tumakaka, F.; Sadowski, G.** Application of the Perturbed-Chain SAFT equation of state to polar systems. *Fluid Phase Equilib.* 2004, Vol. 217, pp. 233-239.
44. **Yarrison, M.; Chapman, W. G.** A systematic study of methanol+n-alkane vapor-liquid and liquid-liquid equilibria using CK-SAFT and PC-SAFT equations of state. *Fluid Phase Equilib.* 2004, Vol. 226, pp. 195-205.
45. **Tumakaka, F.; Gross, J.; Sadowski, G.** Thermodynamic modelling of complex systems using PC-SAFT. *Fluid Phase Equilib.* 2005, Vol. 228, pp. 89-98.
46. **Voutsas, E. C.; Pappa, G. D.; Magoulas, K.; Tassios, D. P.** Vapor liquid equilibrium modeling of alkane systems with Equations of state: "Simplicity versus complexity". *Fluid Phase Equilib.* 2006, Vol. 240, pp. 127-139.
47. **Alfradique, M. F.; Castier, M.** Critical points of hydrocarbon mixtures with Peng-Robinson, SAFT, and PC-SAFT equation of state. *Fluid Phase Equilib.* 2007, Vol. 257, pp. 78-101.
48. **Aparicio-Martinez, S.; Hall, K. R.** Phase equilibria in water containing binary systems from molecular based equation of state. *Fluid Phase Equilib.* 2007, Vol. 254, pp. 112-125.
49. **Voutsas, E.; Perakis, C.; Pappa, G.; Tassios, D.** An evaluation of the Performance of the Cubic-Plus-Association equation of State in mixtures of non-polar, polar and associating compounds: Towards a single model for non-polymeric systems. *Fluid Phase Equilib.* 2007, Vol. 261, pp. 343-350.
50. **Danner, R. P.; Gess, M. A.** A Data-Base Standard for the Evaluation of Vapor-Liquid-Equilibrium Models. *Fluid Phase Equilib.* 1990, Vol. 56, pp. 285-301.
51. **Grenner, A.; Tsivintzelis, I.; Economou, I.; Panayiotou, C.; Kontogeorgis, G. M.** Evaluation of the Nonrandom Hydrogen Bonding (NRHB) Theory and the Simplified Perturbed-Chain-Statistical Associating Fluid Theory (sPC-SAFT). 1. Vapor Liquid Equilibria. *Ind. Eng. Chem. Res.* 2008, Vol. 47, pp. 5636-5650.
52. **Tsivintzelis, I.; Grenner, A.; Economou, I. G.; Kontogeorgis, G. M.** Evaluation of the Nonrandom Hydrogen Bonding (NRHB) Theory and the Simplified Perturbed-Chain-Statistical

Associating Fluid Theory (sPC-SAFT). 2. Liquid-Liquid Equilibria and Prediction of Monomer Fraction in Hydrogen Bonding Systems. *Ind. Eng. Chem. Res.* 2008, Vol. 47, pp. 5651-5659.

53. **Avlund, A. S.; Eriksen, D. K.; Kontogeorgis, G. M.; Michelsen, M. L.** Application of association models to mixtures containing alkanolamines. *Fluid Phase Equilib.* 2011, Vol. 306, pp. 31-37.

54. **Gross, J.; Vrabec, J.** An Equation-of-State Contribution for Polar Components: Dipolar Molecules. *AIChE Journal*. 2006, Vol. 52, pp. 1194-1204.

55. **Watson, G.; Lafitte, T.; Zeberg-Mikkelsen, C. K.; Baylaucq, A.; Bessieres, D.; Boned, C.** Volumetric and derivative properties under pressure for the system 1-propanol + toluene: A discussion of PC-SAFT and SAFT-VR. *Fluid Phase Equilib.* 2006, Vol. 247, pp. 121-134.

56. **Lafitte, T.; Bessieres, D.; Pineiro, M. M.; Daridon, J. L.** Simultaneous estimation of phase behaviour and second-derivative properties using statistical associating fluid theory with variable range approach. *J. Chem. Phys.* 2006, Vol. 124, pp. 024509/1-16.

57. **Lafitte, T.; Pineiro, M. M.; Daridon, J. L.; Bessieres, D.** A Comprehensive Description of Chemical Association Effects on Second Derivative Properties of Alcohols through a SAFT-VR approach. *J. Phys. Chem. B*. 2007, Vol. 111, pp. 3447-3461.

58. **Kontogeorgis, G. M.; Yakoumis, I. V.; Meijer, H.; Hendriks, E. M.; Moorwood, T.** Multicomponent phase equilibrium calculations for water-methanol-alkane mixtures. *Fluid Phase Equilib.* 1999, Vols. 158-160, pp. 201-209.

59. **Folas, G. K.; Kontogeorgis, G. M.; Michelsen, M. L.; Stenby, E. H.** Application of the Cubic-Plus-Association (CPA) Equation of State to Complex Mixtures with Aromatic Hydrocarbons. *Ind. Eng. Chem. Res.* 2006, Vol. 45, pp. 1527-1538.

60. **Folas, G. K.; Gabrielsen, J.; Michelsen, M. L.; Stenby, E. H.; Kontogeorgis, G. M.** Application of the cubic-plus-association (CPA) Equation of State to cross-associating systems. *Ind. Eng. Chem. Res.* 2005, Vol. 44, pp. 3823-3833.

61. **Kontogeorgis, G. M.; Michelsen, M. L.; Folas, G. K.; Derawi, S.; Von Solms, N.; Stenby, E. H.** Ten Years with the CPA (Cubic-Plus-Association) Equation of State. Part 2. Cross-Associating and Multicomponent Systems. *Ind. Eng. Chem. Res.* 2006, Vol. 45, pp. 4869-4878.

62. **Yakoumis, I. V.; Kontogeorgis, G. M.; Voutsas, E. C.; Tassios, D. P.** Vapor-liquid equilibria for alcohol/hydrocarbon systems using CPA Equation of State. *Fluid Phase Equilib.* 1997, Vol. 130, pp. 31-47.

63. **Voutsas, E. C.; Kontogeorgis, G. M.; Yakoumis, I. V.; Tassios, D. P.** Correlation of liquid-liquid equilibria for alcohol/hydrocarbon mixtures using the CPA equation of state. *Fluid Phase Equilib.* 1997, Vol. 132, pp. 61-75.

64. **Yakoumis, I. V.; Kontogeorgis, G. M.; Voutsas, E. C.; Hendriks, E. M.; Tassios, D. P.** Prediction of phase equilibria in binary aqueous systems containing alkanes, cycloalkanes, and alkenes with Cubic-Plus-Association equation of state. *Ind. Eng. Chem. Res.* 1998, Vol. 37, pp. 4175-4182.
65. **Wu, J.; Prausnitz, J. M.** Phase equilibria for systems containing hydrocarbons, water, and salt: An extended Peng-Robinson equation of state. *Ind. Eng. Chem. Res.* 1998, Vol. 37, pp. 1634-1643.
66. **Voutsas, E. C.; Yakoumis, I. V.; Tassios, D. P.** Prediction of phase equilibria in water/alcohol/alkane systems. *Fluid Phase Equilib.* 1999, Vols. 158-160, pp. 151-163.
67. **Pfohl, O.; Pagel, A.; Brunner, G.** Phase equilibria in systems containing o-cresol, p-cresol, carbon dioxide, and ethanol at 323.15-473.15 K and 10-25 MPa. *Fluid Phase Equilib.* 1999, Vol. 157, pp. 53-79.
68. **Voutsas, E. C.; Boulougouris, G. C.; Economidou, I. G.; Tassios, D. P.** Water/hydrocarbon phase equilibria using the thermodynamic perturbation theory. *Ind. Eng. Chem. Res.* 2000, Vol. 39, p. 397.
69. **Peeters, P.** *Nucleation and condensation in gas-vapor mixtures of alkanes and water.* Eindhoven : Technical University of Eindhoven (available from <http://alexandria.tue.nl/extra2/2002/200213383.pdf>), 2002.
70. **Derawi, S. O.; Michelsen, M. L.; Kontogeorgis, G. M.; Stenby, E. H.** Application of the CPA equation of state to glycol/hydrocarbon liquid-liquid equilibria. *Fluid Phase Equilib.* 2003, Vol. 209, pp. 163-184.
71. **Derawi, S. O.; Kontogeorgis, G. M.; Michelsen, M. L.; Stenby, E.** Extension of the Cubic-Plus-Association Equation of State to Glycol-Water Cross-Associating Systems. *Ind. Eng. Chem. Res.* 2003, Vol. 42, pp. 1470-1477.
72. **Bruinsma, D. F. M.; Desens, J. T.; Notz, P. K.; Sloan, E. D.** A novel experimental technique for measuring methanol partitioning between aqueous and hydrocarbon phases at pressures up to 69 MPa. *Fluid Phase Equilib.* 2004, Vols. 222-223, pp. 311-315.
73. **Derawi, S. O.; Zeuthen, J.; Michelsen, M. L.; Stenby, E. H.; Kontogeorgis, G. M.** Extension of the CPA equation of state to organic acids. *Fluid Phase Equilib.* 2004, Vol. 225, pp. 107-113.
74. **Folas, G. K.; Derawi, S. O.; Michelsen, M. L.; Stenby, E. H.; Kontogeorgis, G. M.** Recent applications of the Cubic-Plus-Association (CPA) equation of state to industrially important systems. *Fluid Phase Equilib.* 2005, Vols. 228-229, pp. 121-126.
75. **Kaarsholm, M.; Derawi, S. O.; Michelsen, M. L.; Kontogeorgis, G. M.** Extension of the Cubic-Plus-Association (CPA) Equation of State to Amines. *Ind. Eng. Chem. Res.* 2005, Vol. 44, pp. 4406-4413.

76. **Perakis, C.; Voutsas, E.; Magoulas, K.; Tassios, D.** Thermodynamic modeling of the vapor-liquid equilibrium of the water/ethanol/CO₂ system. *Fluid Phase Equilib.* 2006, Vol. 243, pp. 142-150.
77. **Oliveira, M. B.; Coutinho, J. A. P.; Queimada, A. J.** Mutual solubilities of hydrocarbons and water with the CPA EoS. *Fluid Phase Equilib.* 2007, Vol. 258, pp. 58-66.
78. **Kontogeorgis, G. M.; Folas, G. K.; Muro-Sune, N.; Von Solms, N.; Michelsen, M. L.; Stenby, E. H.** Modelling of associating mixtures for applications in the oil & gas and chemical industries. *Fluid Phase Equilib.* 2007, Vol. 261, pp. 205-211.
79. **Perakis, C. A.; Voutsas, E. C.; Magoulas, K. G.; Tassios, D. P.** Thermodynamic modeling of the Water+Acetic Acid+ CO₂ System: The importance of the Number of Association Sites of Water and of the Nonassociation Contribution for the CPA and SAFT type models. *Ind. Eng. Chem. Res.* 2007, Vol. 46, pp. 932-938.
80. **Muro-Sune, N.; Kontogeorgis, G. M.; Von Solms, N.; Michelsen, M. L.** Phase Equilibrium Modelling for Mixtures with Acetic Acid Using an Association Equation of State. *Ind. Eng. Chem. Res.* 2008, Vol. 47, pp. 5660-5668.
81. **Haghighi, H.; Chapoy, A.; Burgess, R.; Mazloun, S.; Tohidi, B.,** Phase equilibria for petroleum fluids containing water and aqueous methanol solutions: Experimental measurements and modelling using the CPA equation of state. *Fluid Phase Equilib.* 2009, Vol. 278, pp. 109-116.
82. **Follegatti-Romero, L. A.; Lanza, M.; Batista, F. R. M.; Batista, E. A. C.; Oliveira, M. B.; Coutinho, J. A. P.; Meirelles, A. J. A.** Liquid-Liquid Equilibrium for Ternary Systems Containing Ethyl Esters, Anhydrous Ethanol and Water at 298.15, 313.15, and 333.15 K. *Ind. Eng. Chem. Res.* 2010, Vol. 49, pp. 12613-12619.
83. **Awan, J. A.; Tsvintzelis, I.; Breil, M. P.; Coquelet, C.; Richon, D.; Kontogeorgis, G. M.** Phase Equilibria of Mixtures Containing Organic Sulfur Species (OSS) and Water/Hydrocarbons: VLE Measurements and Modeling Using the Cubic-Plus-Association Equation of State. *Ind. Eng. Chem. Res.* 2010, Vol. 49, pp. 12718-12725.
84. **Tsvintzelis, I.; Kontogeorgis, G. M.; Michelsen, M. L.; Stenby, E. H.,** Modeling Phase Equilibria for Acid Gas Mixtures Using the CPA Equation of State. I. Mixtures with H₂S. *AIChE Journal*. 2010, Vol. 56, pp. 2965-2982.
85. **Oliveira, M. B.; Queimada, A. J.; Kontogeorgis, G. M.; Coutinho, J. A. P.** Evaluation of the CO₂ behavior in binary mixtures with alkanes, alcohols, acids and esters using the Cubic-Plus-Association Equation of State. *J. of Supercritical Fluids*. 2011, Vol. 55, pp. 876-892.
86. **Lundstrøm, C.; Michelsen, M. L.; Kontogeorgis, G. M.; Pedersen, K. S.; Sørensen, H.** Comparison of the SRK and CPA equations of state for physical properties of water and methanol. *Fluid Phase Equilib.* 2006, Vol. 247, pp. 149-157.

87. **Kleiner, M.; Sadowski, G.** Modeling of Polar Systems Using PCP-SAFT: An Approach to Account for Induced-Association Interactions. *J. Phys. Chem. C*. 2007, Vol. 111, pp. 15544-15553.
88. **Llovel, F.; Peters, C. J.; Vega, L. F.** Second-Order thermodynamic derivative properties of selected mixtures by soft-SAFT equation of state. *Fluid Phase Equilib.* 2006, Vol. 248, pp. 115-122.
89. **Colina, C. M.; Turens, L. F.; Gubbins, K. E.; Olivera-Fuentes, C.; Vega, L. F.** Predictions of the Joule-Thomson Inversion Curve for the n-Alkane Series and Carbon Dioxide from the Soft-SAFT Equation of State. *Ind. Eng. Chem. Res.* 2002, Vol. 41, pp. 1069-1075.
90. **Chen, J.; Mi, J.** Equation of state extended from SAFT with improved results for non-polar fluids across the critical point. *Fluid Phase Equilib.* 2001, Vol. 186, pp. 165-184.
91. **Breil, M. P.** *The Cubic-Plus-Association EoS : Parameters for pure compounds and interaction parameters*. Department of Chemical and Biochemical Engineering, Technical University of Denmark, IVC-SEP, Centre for Phase Equilibria and Separation Processes. 2009. pp. 1-33.
92. **Daridon, J. L.; Lagourette, B.; Grolier, J. -P. E.** Experimental Measurements of the Speed of Sound in n-Hexane from 293 - 373 K and up to 150 MPa. *Int. J. Thermophys.* 1998, Vol. 19, 1, pp. 145-159.
93. **Khansanshin, T. S.; Shchamialiou, A. P.; Poddubskij, O. G.** Thermodynamic Properties of Heavy n-alkanes in the liquid state: n-Dodecane. *Int. J. Thermophys.* 2003, Vol. 24, pp. 1277-1289.
94. **Lemmon, E.W.; McLinden, M.O.; Friend, D.G.** "Thermophysical Properties of Fluid Systems" in *NIST Chemistry WebBook, NIST Standard Reference Database Number 69*, <http://webbook.nist.gov>. [ed.] P.J. Linstrom and W.G. Mallard. Gaithersburg MD, 20899 : s.n.
95. DIPPR 801 database, Design Institute for Physical Properties. *Sponsored by AIChE*.
96. **Deiters, U. K.; De Reuck, K. M.** Remarks on publications dealing with Equations of State. *Fluid Phase Equilib.* 1999, Vol. 161, pp. 205-219.
97. **Gregorowicz, J.; O'Connell, J. P.; Peters, C. J.** Some characteristics of pure fluid properties that challenge equation-of-state models. *Fluid Phase Equilib.* 1996, Vol. 116, pp. 94-101.
98. **Lago, S.; Giuliano Albo, P.A.** Thermodynamic properties of acetone calculated from accurate experimental speed of sound measurements at low temperatures and high pressures. *J. Chem. Thermodynamics*. 2009, Vol. 41, pp. 506-512.
99. **De Azevedo, G. R.; Szydlowski, J.; Pires, P. F.; Esperanca, H. J. R.; Rebelo, L. P. N.** A novel non-intrusive microcell for sound-speed measurements in liquids. Speed of sound and thermodynamic properties of 2-propanone at pressures up to 160 MPa. *J. Chem. Thermodyn.* 2004, Vol. 36, pp. 211-222.

100. **Sun, T. F.; Biswas, S. N.; Trappeniers, N. J.; Ten Seldam, C. A.** Acoustic and Thermodynamic Properties of Methanol from 273 to 333 K and at Pressures to 280 MPa. *J. Chem. Eng. Data*. 1988, Vol. 33, pp. 395-398.
101. **Sun, T. F.; Ten Seldam, C. A.; Kortbeek, P. J.; Trappeniers, N. J.; Biswas, S. N.** Acoustic and Thermodynamic Properties of Ethanol from 273.15 to 333.15 K and up to 280 MPa. *Phys. Chem. Liq.* 1988, Vol. 18, pp. 107-119.
102. **Goates, J. R.; Ott, J. B.; Grigg, R. B.** Excess volumes of n-hexane + n-heptane, + n-octane, + n-nonane, + n-decane at 283.15K, 298.15K and 313.15K. *J. Chem. Thermodyn.* 1981, Vol. 13, pp. 907-913.
103. **Saito, A.; Tanaka, R.** Excess volumes and heat capacities of binary mixtures formed from cyclohexane, hexane, and heptane at 298.15 K. *J. Chem. Thermodyn.* 1988, Vol. 20, pp. 859-865.
104. **Marsh, K. N.; Ott, J. B.; Costigan, M. J.** Excess enthalpies, excess volumes, and Gibbs free energie for (n-hexane+n-decane) at 298.15 K and 308.15 K. *J. Chem. Thermodyn.* 1980, Vol. 12, pp. 343-348.
105. **Smith, J. M.; Van Ness, H. C.; Abbott, M. M.** *Introduction to Chemical Engineering Thermodynamics*. 7th Edition. New York : McGraw-Hill, 2005. ISBN-13: 978-0-07-310445-4.
106. **Koretsky, M. D.** *Engineering and Chemical Thermodynamics*. Oregon, USA : John Wiley & Sons, 2004. ISBN 0-471-38586-7.
107. **Prausnitz, J. M.; Abrams, D. S.** Statistical thermodynamics of liquid mixtures- New expression for excess Gibbs energy of partly miscible systems. *AIChE Journal*. 1975, Vol. 21, pp. 116-128.
108. **Costas, M.; Patterson, D.** Order destruction and order creation in binary mixtures of non-electrolytes. *Thermochim. Acta*. 1987, Vol. 120, pp. 161-181.
109. **Marino, G.; Pineiro, M. M.; Iglesias, M.; Orge, B.; Tojo, J.** Temperature Dependence of Binary Mixing Properties for Acetone, Methanol, and Linear Aliphatic Alkanes (C6-C8). *J. Chem. Eng. Data*. 2001, Vol. 46, pp. 728-734.
110. **Christensen, C.; Gmehling, J.; Rasmussen, P.; Wedlich, U.** *Heats of mixing data collection - Binary Systems*. Frankfurt : DECHEMA, 1984. ISBN: 3-921 567-49-1.
111. **De Cominges, B. E.; Pineiro, M. M.; Mosteiro, L.; Iglesias, T. P.; Legido, J. L.; Paz Andrade, M. I.** Temperature Dependence of Thermophysical Properties of Hexane-1-Hexanol. *J. Chem. Eng. Data*. 2001, Vol. 46, pp. 1206-1210.
112. **Peleteiro, J.; Gonzalez-Salgado, D.; Cerdeirina, C. A.; Romani, L.** Isobaric heat capacities, densities. isentropic compressibilities and second-order excess derivatives for (1-propanol + n-decane). *J. Chem. Thermodyn.* 2002, Vol. 34, pp. 485-497.

113. **Bravo, R.; Pintos, M.; Baluja, M. C.; Paz Andrade, M. I.** Excess volumes and excess heat capacities of some mixtures: (an isomer of hexanol + an n-alkane) at 298.15 K. *J. Chem. Thermodyn.* 1984, Vol. 16, pp. 73-79.
114. **Iglesias, M.; Orge, B.; Dominguez, M.; Tojo, J.** Mixing properties of the binary mixtures of acetone, methanol, ethanol, and 2-butanone at T = 298.15 K. *Phys. Chem. Liq.* 1998, Vol. 37, pp. 9-29.
115. **Gepert, M.; Stachowska, B.** Experimental and Theoretical Description of Binary Mixtures Containing Monohydric Alcohols. *J. Solution. Chem.* 2006, Vol. 35, pp. 425-453.
116. **D'Arrigo, G.; Paparelli, A.** Sound propagation in water-ethanol mixtures at low temperatures. I. Ultrasonic velocity. *J. Chem. Phys.* 1988, Vol. 88, pp. 405-415.
117. **Ott, J. B.; Sipowska, J. T.; Gruszkiewics, M. S.; Woolley, A. T.** Excess volumes for (ethanol+water) at the temperature (298.15 and 348.15) K and at temperatures 323.15 K and pressures (5 and 15) MPa. *J. Chem. Thermodyn.* 1993, Vol. 25, pp. 307-318.
118. **Ott, J. B.; Stouffer, C. E.; Cornett, G. V.; Woodfield, B. F.; Wirthlin, R. C.; Christensen, J. J.** Excess enthalpies for (ethanol+water) at 298.15 K and pressures of 0.4, 5, 10 and 15 MPa. *J. Chem. Thermodyn.* 1986, Vol. 18, pp. 1-12.
119. **Ott, J. B.; Cornett, G. V.; Stouffer, C. E.; Woodfield, B. F.; Guanquan, C.; Christensen, J. J.** Excess enthalpies of (ethanol+water) at 323.15, 333.15, 348.15 K and from 0.4 to 15 MPa. *J. Chem. Thermodyn.* 1986, Vol. 18, pp. 867-875.
120. **Benson, G. C.; D'Arcy, P. J.** Excess Isobaric heat capacities of Water-n-Alcohol Mixtures. *J. Chem. Eng. Data.* 1982, Vol. 27, pp. 439-442.
121. **Von Solms, N.; Jensen, L.; Kofod, J. L.; Michelsen, M. L.; Kontogeorgis, G. M.** Measurement and modelling of hydrogen bonding in 1-alkanol + n-alkane binary mixtures. *Fluid Phase Equilib.* 2007, Vol. 261, pp. 272-280.
122. **Nezbeda, I.** Towards a unified view of fluids. *Mol. Phys.* 2005, Vol. 103, pp. 59-76.
123. **Gil-Villegas, A.; Galindo, A.; Whitehead, P. J.; Mills, S. J.; Jackson, G.** Statistical associating fluid theory for chain molecules with attractive potentials of variable range. *J. Chem. Phys.* 1997, Vol. 106, p. 4168.
124. **Galindo, A.; Davies, L. A.; Gil-Villegas, A.; Jackson, G.** The thermodynamics of mixtures and the corresponding mixing rules in the SAFT-VR approach for potentials of variable range. *Mol. Phys.* 1998, Vol. 93, pp. 241-252.
125. **Paragand, F.; Feyzi, B.; Behzadi, B.** Application of the SAFT-VR equation of state to vapor-liquid equilibrium calculations for pure components and binary mixtures using the Sutherland potential. *Fluid Phase Equilib.* 2010, Vol. 290, pp. 181-194.

126. **Fu, Y.-H.; Sandler, S. I.** A Simplified SAFT Equation of State for Associating Compounds and Mixtures. *Ind. Eng. Chem. Res.* 1995, Vol. 34, pp. 1897-1909.
127. **Jog, P. K; Chapman, W. G.** Application of Wertheim's thermodynamic perturbation theory to dipolar hard sphere chains. *Mol. Phys.* 1999, Vol. 97, pp. 307-319.
128. **Haslam, A.J.; Galindo, A.; Jackson, G.** Prediction of binary intermolecular potential parameters for use in modeling fluid mixtures. *Fluid Phase Equilib.* 2008, Vol. 266, pp. 105-128.
129. **Kontogeorgis, G.M; Folas, G.K.** *Thermodynamic models for industrial applications - from classical and advanced mixing rules to association theories*. 1st Edition. s.l. : John Wiley & Sons Ltd, 2010. ISBN 978-0-470-69726-9.
130. **Jorgensen, W. L.; Chandrasekhar, J.; Madura, J. D.; Impey, R. W.; Klein, M. L.** Comparison of simple potential functions for simulating liquid water. *J. Chem. Phys.* 1983, Vol. 79, pp. 926-935.
131. **Mahoney, M. W.; Jorgensen, W. L.** A five-site model for liquid water and the reproduction of the density anomaly by rigid, nonpolarizable potential functions. *J. Chem. Phys.* 2000, Vol. 112, pp. 8910-8922.
132. **Moucka, F.; Nezbeda. I.** Water–methanol mixtures with non-Lorentz–Berthelot combining rules: A feasibility study. *J. Mol. Liq.* 2011, Vol. 159, pp. 47-51.
133. **Dopazo-Paz, A.; Gomez-Alvarez, G.; Gonzalez-Salgado, D.** Thermodynamics and structure of the {water + methanol} system viewed from three simple additive pair-wise intermolecular potentials based on the rigid molecule approximation. *Collect. Czech. Chem. Commun.* 2010, Vol. 75, p. 617.
134. **Wensink, E. J. W.; Hoffmann, A. C.; Van Maaren, P. J.; Van der Spoel, D.** Dynamic properties of water/alcohol mixtures studied by computer simulation. *J. Chem. Phys.* 2003, Vol. 119, pp. 7308-7319.
135. **Venables, D. S.; Schmuttenmaer, C. A.** Spectroscopy and dynamics of mixtures of water with acetone, acetonitrile, and methanol. *J. Chem. Phys.* 2000, Vol. 113, pp. 11222-11236.
136. **Saiz, L.; Padro, J. A.; Guardia, E.** Structure and Dynamics of Liquid Ethanol. *J. Phys. Chem. B.* 1997, Vol. 101, pp. 78-86.
137. **Jorgensen, W. L.; Maxwell, D. S.; Tirado-Rives, J.** Development and Testing of the OPLS All-Atom Force Field on Conformational Energetics and Properties of Organic Liquids. *J. Am. Chem. Soc.* 1996, Vol. 118, pp. 11225-11236.
138. **Jorgensen, W. L.** Optimized Intermolecular Potential Functions for Liquid Alcohols. *J. Chem. Phys.* 1986, Vol. 90, pp. 1276-1284.

139. **Cai, Z.; Xie, R.; Wu, Z.** Binary Isobaric Vapor-Liquid Equilibria of Ethanolamines + Water. *J. Chem. Eng. Data.* 1996, Vol. 41, pp. 1101-1103.
140. **Lafitte, T.; Plantier, F.; Pineiro, M. M.; Daridon, J. L.; Bessieres, D.** Accurate Global Thermophysical Characterization of Hydrofluoroethers through a Statistical Associating Fluid Theory Variable Range Approach, Based on New Experimental High-Pressure Volumetric and Acoustic Data. *Ind. Eng. Chem. Res.* 2007, Vol. 46, pp. 6998-7007.
141. **Nath, A.; Bender, E.** On the thermodynamics of associated solutions. I. An analytical method for determining the enthalpy and entropy of association and equilibrium constant or pure liquid substances. *Fluid Phase Equilib.* 1981, Vol. 7, pp. 275-287.
142. **Yao, J.; Li, H.; Han, S.** Vapor-liquid equilibrium data for methanol-water-NaCl at 45°C. *Fluid Phase Equilib.* 1999, Vol. 162, pp. 253-260.
143. **Kurihara, K.; Minoura, T.; Takeda, K.; Kojima, K.** Isothermal Vapor-Liquid Equilibria for Methanol+Ethanol+Water, Methanol + Water, Ethanol + Water. *J. Chem. Eng. Data.* 1995, Vol. 40, pp. 679-684.
144. **Kojima, K.; Tochigi, K.; Seki, H.; Watase, K.** Determination of vapor-liquid equilibria from boiling point curves. *Kagaku Kogaku Robunshu.* 1968, Vol. 32, pp. 149-153.
145. **Hirata, M.; Ohe, S.; Nagahama, K.** *Computer Aided Data Book of Vapor-Liquid Equilibria.* Amsterdam : Elsevier, 1975. ISBN 10-0444-9985-51.
146. **Kirschbaum, E.; Gerstner, F.** Equilibrium curves and boiling and condensation lines of ethyl alcohol-water mixtures under reduced pressures. *Z. Ver. Deut. Ing. Verfahrenstech.* 1939, pp. 10-15.
147. **Otsuki, H.; Williams, F.C.** Effect of pressure on vapor-liquid equilibria for the system ethyl alcohol-water. *Chem. Eng. Data. Series.* 1953, Vol. 49, pp. 55-67.
148. **Woerpel, U.; Vohland, P.; Schuberth, H.** The effect of urea on the vapor-liquid equilibrium behavior of n-propanol/water at 60°C. *Z. Phys. Chem. (Leipzig).* 1977, Vol. 258, pp. 906-912.
149. **Gabaldon, C.; Marzal, P.; Monton, J. B.; Rodrigo, M. A.** Isobaric Vapor-Liquid Equilibria of the Water + 1-Propanol System at 30, 60, and 100 kPa. *J. Chem. Eng. Data.* 1996, Vol. 41, pp. 1176-1180.
150. **Guo, J.-H.; Luo, Y.; Augustsson, A.; Kashtanov, S.; Rubensson, J. -E.; Shuh, D. K.; Agren, H.; Nordgren, J.** Molecular Structure of Alcohol-Water Mixtures. *Phys. Rev. Lett.* 2003, Vol. 91, pp. 1574011-1574014.
151. **Dixit, S.; Crain, J.; Poon, W. C. K.; Finney, J. L.; Soper, A. K.** Molecular segregation observed in a concentrated alcohol-water solution. *Letters to Nature.* 2002, Vol. 416, pp. 829-832.

152. **Iwakabe, K.; Kosuge, H.** Isobaric vapor-liquid-liquid equilibria with a newly developed still. *Fluid Phase Equilib.* 2001, Vol. 192, pp. 171-186.
153. **Sorensen, J. M.; Arlt, W.** *Dechema Chemistry Data Series: Liquid-Liquid Equilibrium Data*. Frankfurt : Dechema, 1979. Vols. V, Part 2. ISBN 39-21-567-173.
154. **Cho, T-H.; Ocho, L.; Kojima, K.** Isobaric vapor-liquid equilibria for binary systems with limited miscibility, water-n-amyl alcohol and water-isoamyl alcohol. *Kagaku Kogaku Robunshu*. 1984, Vol. 10, pp. 181-183.
155. **Hall, D. J.; Mash, C. J.; Pemberton, R. C.** Vapor-liquid equilibrium for the systems water + methanol, water + ethanol, methanol + ethanol and water + methanol + ethanol. *NPL Report*. 1979, Vol. 95, p. 32.
156. **Butcher, K. L.; Robinson, W. I.** Apparatus for determining high-pressure liquid-vaporequilibrium data. I. Methanol-ethanol system. *J. Appl. Chem.* 1966, Vol. 16, pp. 289-292.
157. **Berro, C. H.; Deyrieux, R.; Peneloux, A.** An ebulliometer for rapid and precise measurements of vapor-liquid equilibrium for solutions solutions. The methanol-1-propanol binary system at 60.02.deg. *J. Chim. Phys. Phys.-Chim.Biol.* 1975, Vol. 72, pp. 1118-1123.
158. **Arce, A.; Blanco, A.; Soto, A.; Tojo, J.** Isobaric Vapor-Liquid Equilibria of Methanol + 1-Octanol and Ethanol + 1-Octanol Mixtures. *J.Chem. Eng. Data*. 1995, Vol. 40, pp. 1011-1014.
159. **Udovenko, V. V.; Frid, T. B.** Heats of vaporization of binary mixtures. II. *Zh. Fiz. Khim.* 1948, Vol. 22, pp. 1135-1145.
160. **Kharin, S. E.; Pereygin, V. M.; Remizov, G. P.** Liquid-vapor phase equilibrium in ethanol-n-butanol and water-n-butanol systems. *Izv. Vyssh. Ucheb. Zaved., Khim. Khim. Tekhnol.* 1969, Vol. 12, pp. 424-428.
161. **Asensi, J. C.; Molto, J.; Del Mar Olaya, M.; Ruiz, F.** Isobaric vapour-liquid equilibria data for the binary system 1-propanol + 1-pentanol and isobaric vapour-liquid-liquid equilibria data for the ternary sustem water + 1-propanol + 1-pentanol at 101.3 kPa. *Fluid Phase Equilib.* 2002, Vol. 200, pp. 287-293.
162. **Churkin, V. N.; Gorshkov, V. A.; Pavlov, S. Yu.; Levicheva, E. N.; Karpacheva, L. L.** Liquid-vapor equilibrium in C4 hydrocarbon-methanol binary systems. *Zh. Fiz. Khim.* 1978, Vol. 52, pp. 488-489.
163. **Wilsak, R. A.; Campbell, S. W.; Thodos, G.** Vapor-liquid equilibrium measurements for the n-pentane–methanol system at 372.7, 397.7, 422.6 K. *Fluid Phase Equilib.* 1987, Vol. 33, pp. 157-171.
164. **Wolff, H.; Hoeppel, H. E.** Determination of hydrogen bond association of methanol in n-hexane by vapor pressure measurements. *Ber. Bunsen-Ges. Phys. Chem.* 1968, Vol. 72, pp. 710-721.

165. **Campbell, S. W.; Wilsak, R. A; Thodos, G.** (Vapor + Liquid) equilibrium behavior of (n-pentane + ethanol) at 372.7, 397.7 and 422.6 K. *J. Chem. Thermodyn.* 1987, Vol. 19, pp. 449-460.
166. **Pena, M. D.; Cheda, D. R.** Liquid-vapor equilibrium. I. Systems benzene-cyclohexane at 70.deg. and methanol-n-hexane at 50.deg. *An. Quim.* 1970, Vol. 66, pp. 721-735.
167. **Pena, M. D.; Cheda, D. R.** Liquid-vapor equilibrium. II. Ethanol-n-heptane system at 40 and 60.deg. *An. Quim.* 1970, Vol. 66, pp. 737-745.
168. **Boublikova, L.; Lu, B. C. Y.** Isothermal vapor-liquid equilibriums for the ethanol-n-octane system. *J. Appl. Chem.* 1969, Vol. 19, pp. 89-92.
169. **Pena, M. D.; Cheda, D. R.** Liquid-vapor equilibrium. III. Systems of n-propanol-n-hexane at 50.deg. and n-propanol-n-heptane at 60.deg. *An. Quim.* 1970, Vol. 66, pp. 747-755.
170. **Hiaki, T.; Takahashi, K.; Tsuji, T.; Hongo, M.; Kojima, K.** Vapor-Liquid Equilibria of 1-Propanol or 2-propanol with Octane at 101.3 kPa. *J. Chem. Eng. Data.* 1995, Vol. 40, pp. 274-276.
171. **Heintz, A.; Dolch, E.; Lichtenthaler, R. N.** New Experimental VLE-Data for alkanol/alkane mixtures and their description by an extended real association (ERAS) Model. *Fluid Phase Equilib.* 1986, Vol. 27, pp. 61-79.
172. **Maciel, M. R. W.; Francesconi, A. Z.** Vapor-liquid phase equilibrium measurements for the n-hexane-1-butanol system at 323.15,338.15 and 348.15 K. *Fluid Phase Equilib.* 1989, Vol. 50, pp. 201-208.
173. **Hiaki, T.; Taniguchi, A.; Tsujo, T.; Hongo, M.** Isothermal vapor–liquid equilibria of octane with 1-butanol, 2-butanol, or 2-methyl-2-propanol. *Fluid Phase Equilib.* 1998, Vol. 144, pp. 145-156.
174. **Kraska, T.; Gubbins, K. E.** Phase Equilibria Calculations with a Modified SAFT Equation of State. 1. Pure Alkanes, Alkanols, and Water. *Ind. Eng. Chem. Res.* 1996, Vol. 35, pp. 4727-4737.
175. **Kraska, T.; Gubbins, K. E.** Phase Equilibria Calculations with a Modified SAFT Equation of State. 2. Binary Mixtures of n-Alkanes, 1-Alkanols, and Water. *Ind. Eng. Chem. Res.* 1996,, Vol. 35, pp. 4738-4746.
176. **Hradetzky, G.; Lempe, D. A.** Phase equilibria in binary and higher systems methanol + hydrocarbon (s). Part I. Experimental determination of liquid-liquid equilibrium data and their representation using NRTL equation. *Fluid Phase Equilib.* 1991, Vol. 69, pp. 285-301.
177. **Higashiuchi, H.; Sakuragi, Y.** Measurement and correlation of liquid-liquid equilibria of binary and ternary systems containing methanol and hydrocarbons. *Fluid Phase Equilib.* 1987, Vol. 36, pp. 35-47.

178. **Arce, A.; Antonio, B.; Souza, P.; Vidal, I.** Liquid-Liquid Equilibria of Water + Methanol + 1-Octanol and Water + Ethanol + 1-Octanol at Various Temperatures. *J. Chem. Eng. Data.* 1994, Vol. 39, pp. 378-380.
179. **Jog, P. K.; Sauer, S. G.; Blaesing, J.; Chapman, W. G.** Application of Dipolar Chain Theory to the Phase Behavior of Polar Fluids and Mixtures. *Ind. Eng. Chem. Res.* 2001, Vol. 40, pp. 4641-4648.
180. **Karakatsani, E. K.; Spyriouni, T.; Economou, I. G.** Extended Statistical Associating Fluid Theory (SAFT) Equation of State for Dipolar Fluids. *AIChE Journal.* 2005, Vol. 51, pp. 2328-2342.
181. **Karakatsani, E. K.; Economou, I. G.** Perturbed Chain-Statistical Associating Fluid Theory Extended to Dipolar and Quadrapolar Molecular Fluids. *J. Phys. Chem. B.* 2006, Vol. 110, pp. 9252-9261.
182. **Rushbrook, G. S.; Stell, G.; Hoyer, J. S.** Theory of polar liquids I: Dipolar hard spheres. *Mol. Phys.* 1973, Vol. 26, pp. 1199-1215.
183. **Gross, J.** An Equation-of-State Contribution for Polar Components: Quadrupolar Molecules. *AIChE Journal.* 2005, Vol. 51, pp. 2556-2568.
184. **Vrabec, J.; Gross, J.** Vapor-Liquid Equilibria Simulation and an Equation of State Contribution for Dipole-Quadrupole Interactions. *J. Phys. Chem. B.* 2008, Vol. 112, pp. 51-60.
185. **Kleiner, M.; Gross, J.** An Equation of State Contribution for Polar Components: Polarizable Dipoles. *AIChE Journal.* 2006, Vol. 52, pp. 1951-1961.
186. **Hu, Y.; Liu, H.; Prausnitz, J. M.** Equation of State for fluids containing chainlike molecules. *J. Chem. Phys.* 1996, Vol. 104, pp. 396-404.
187. **Liu, H.; Hu, Y.** Molecular thermodynamic theory for polymer systems II. Equation of state for chain fluids. *Fluid Phase Equilib.* 1996, Vol. 122, pp. 75-97.
188. **Vega, C.; Saager, B.; Fischer, J.** Molecular dynamics studies for the new refrigerant R152a with simple potentials. *Mol. Phys.* 1989, Vol. 68, pp. 1079-1093.
189. **Vega, C.; McBride, C.; Menduina, C.** The second virial coefficient of the dipolar two center Lennard-Jones model. *Phys. Chem.* 2002, Vol. 4, pp. 3000-3007.
190. **Sauer, S. G.; Chapman, W. G.** A Parametric Study of Dipolar Chain Theory with Applications to Ketone Mixtures. *Ind. Eng. Chem. Res.* 2003, Vol. 42, pp. 5684-5696.
191. **Dominik, A.; Chapman, W. G.; Kleiner, M.; Sadowski, G.** Modeling of Polar Systems with the Perturbed-Chain SAFT Equation of State. Investigation of the Performance of Two Polar Terms. *Ind. Eng. Chem. Res.* 2005, Vol. 44, pp. 6928-6938.

192. **Leonhard, K.; Van Nhu, N.; Lucas, K.** Making Equations of state predictive Part 2: An improved PCP-SAFT equation of state. *Fluid Phase Equilib.* 2007, Vol. 258, pp. 40-50.
193. **Prausnitz, J. M.; Lichtenthaler, R. N.; De Azevedo, E. G.** *Molecular Thermodynamics of Fluid Phase Equilibria*. Third. Berkeley : Prentice Hall, 1999. ISBN 0-13-977745-8.
194. **Kolasinska, G.; Goral, M.; Giza, J.** Vapor-liquid equilibriums and excess Gibbs free energy in binary systems of acetone with aliphatic and aromatic hydrocarbons at 313.15 K. *Z. Phys. Chem. (Leipzig)* . 1982, Vol. 263, pp. 151-160.
195. **Takeo, M.; Nishii, K.; Nitta, T.; Katayama, T.** Isothermal vapor-liquid equilibriums for two binary mixtures of heptane with 2-butanone and 4-methyl-2-pentanone measured by a dynamic still with a pressure regulation. *Fluid Phase Equilib.* 1979, Vol. 3, pp. 123-131.
196. **Geiseler, G.; Koehler, H.** Thermodynamic behavior of the binary systems methyl ethyl ketoxime/n-heptane, diethyl ketone/n-heptane, and methyl ethyl ketoxime/diethyl ketone. *Ber. Bun-Senges. Phys. Chem.* 1968, Vol. 72, pp. 697-706.
197. **Chen, C.; Tang, M.; Chen, Y.** Vapor-Liquid Equilibria of Binary and Ternary Mixtures of Cyclohexane, 3-Methyl-2-Butanone, and Octane at 101.3 kPa. *J. Chem. Eng. Data.* 1996, Vol. 41, pp. 557-561.
198. **Wisniak, J.** Phase equilibria in the systems 4-methyl-2-pentanone + octane and hexane + 1,3-dioxolane. *Phys. Chem. Liq.* 1999, Vol. 37, pp. 493-503.
199. **Vandoni, R.** Measurements of partial vapor pressure of cyclopentanone solutions. *Mem. Poudres.* 1938, Vol. 28, pp. 236-251.
200. **Boublik, T.; Lu, B. C. Y.** Vapor-liquid equilibriums of the cyclohexane-cyclohexanone system at 323.15 and 348.15 K. *J. Chem. Eng. Data.* 1977, Vol. 22, pp. 331-333.
201. **Eng, R.; Sandler, S. I.** Vapor-liquid equilibria for three aldehyde/hydrocarbon mixtures. *J. Chem. Eng. Data.* 1984, Vol. 29, pp. 156-161.
202. **Tarakad, R. R.; Scheller, W. A.** Isothermal vapor-liquid equilibrium data for the system n-heptane-n-valeraldehyde at 75 and 90°C. *J. Chem. Eng. Data.* 1979, Vol. 24, pp. 119-120.
203. **Ortega, J.; Sabater, G.; de la Nuez, I.; Quintana, J. J.; Wisniak, J.** Isobaric Vapor-Liquid Equilibrium Data and Excess Properties of Binary Systems Comprised of Alkyl Methanoates + Hexane. *J. Chem. Eng. Data.* 2007, Vol. 52, pp. 215-225.
204. **Lu, B. C. Y.; Ishikawa, T.; Benson, G. C.** Isothermal vapor-liquid equilibria for n-hexane-methyl methacrylate, methyl n-propyl ketone-acetic acid, n-pentane-methyl acetate, and ethyl acetate-acetic anhydride. *J. Chem. Eng. Data.* 1990, Vol. 35, pp. 331-334.

205. **Acosta, J.; Arce, A.; Martinez-Ageitos, J.; Rodil, E.; Soto, A.** Vapor-Liquid Equilibrium of the Ternary System Ethyl Acetate + Hexane + Acetone at 101.32 kPa. *J. Chem. Eng. Data.* 2002, Vol. 47, pp. 849-854.
206. **Ortega, J.; Gonzalez, C.; Galvan, S.** Vapor-Liquid Equilibria for Binary Systems Composed of a Propyl Ester (Ethanoate, Propanoate, Butanoate) + an n-Alkane (C7, C9). *J. Chem. Eng. Data.* 2001, Vol. 46, pp. 904-912.
207. **Feng, L.-C.; Chou, C.-H.; Tang, M.; Chen, Y.-P.** Vapor-Liquid Equilibria of Binary Mixtures 2-Butanol + Butyl Acetate, Hexane + Butyl Acetate, and Cyclohexane + 2-Butanol at 101.3 kPa. *J. Chem. Eng. Data.* 1998, Vol. 43, pp. 658-661.
208. **Klon-Palczewska, M.; Cholinski, J.; Wyrzykowska-Stankiewicz, D.** Isobaric vapor-liquid equilibrium in binary organic solvent mixtures. *Chem. Stosow.* 1980, Vol. 24, pp. 197-209.
209. **Marsh, K. N.; Ott, J. B.; Costigan, M. J.** Excess enthalpies, excess volumes, and excess Gibbs free energies for n-hexane + di-n-butyl ether at 298.15 and 308.15 K. *J. Chem. Thermodyn.* 1980, Vol. 12, pp. 857-862.
210. **Gmehling, J.; Onken, U.; Arlt, A.** *Vapor-Liquid Equilibrium Data Collection: Aldehydes, Ketones and Ethers.* Frankfurt : Dechema, 1979. Vols. I, Part 3+4. ISBN 3-921 567-14-9.
211. **Hanson, D. O.; Van Winkle, M.** Alteration of the relative volatility of hexane-1-hexene by oxygenated and chlorinated solvents. *J. Chem. Eng. Data.* 1967, Vol. 12, pp. 319-325.
212. **Dakshinamurty, P.; Rao, G. J.; Raghavacharya, M. V.; Rao, C. V.** Vapor-liquid equilibria: cyclohexane-methyl isobutyl ketone and benzene-methyl isobutyl ketone systems. *J. Sci. Ind. Research.* 1957, Vol. 16B, pp. 340-344.
213. **Ortega, J.; Espiau, F.; Tojo, J.; Canosa, J.; Rodriguez, A.** Isobaric Vapor-Liquid Equilibria and Excess Properties for the Binary Systems of Methyl Esters + Heptane. *J. Chem. Eng. Data.* 2003, Vol. 48, pp. 1183-1190.
214. **Ortega, J.; Espiau, F.; Dieppa, R.** Measurement and correlation of isobaric vapour-liquid equilibrium data and excess properties of ethyl methanoate with alkanes (hexane to decane). *Fluid Phase Equilib.* 2004, Vol. 215, pp. 175-186.
215. **Galvan, S.; Ortega, J.; Susial, P.; Pena, J. A.** Isobaric vapor-liquid equilibria for propyl methanoate + (n-alkanes, C7, C8, C9) or n-alkanols (C2, C3, C4). *J. Chem. Eng. Jpa.* 1994, Vol. 27, pp. 529-534.
216. **Shealy, G. S.; Sandler, S. I.** Vapor-liquid equilibria of {x isobutyraldehyde + (1-x) heptane}(l) and {x ethyl acetate + (1-x) heptane}(l). *J. Chem. Thermodyn.* 1985, Vol. 17, pp. 143-150.
217. **Chen, Z.; Hu, W.** Isobaric vapor-liquid equilibria of octane-ethyl acetate and octane-isopropyl acetate systems. *Chinese J. Chem. Eng.* 1995, Vol. 3, pp. 180-186.

218. **Crespo Colin, A.; Compostizo, A.; Diaz Pena, M.** Excess Gibbs energy and excess volume of cyclohexane + 2-propanone and of cyclohexane + 2-butanone. *J. Chem. Thermodyn.* 1984, Vol. 16, pp. 497-502.
219. **Siimer, E.; Kirss, H.; Kuus, M. I.; Kudryavtseva, L.** Isobaric vapour-liquid equilibria of the ternary system hexan-2-one + o-xylene + nonane. *Proc. Estonian Acad. Sci. Chem.* 2002, Vol. 51, pp. 19-28.
220. **Akamatsu, Y.; Ogawa, H.; Murakami, S.** Molar excess enthalpies, molar excess volumes and molar isentropic compressions of mixtures of 2-propanone with heptane, benzene and trichloromethane at 298.15 K. *Thermochim. Acta.* 1987, Vol. 113, pp. 141-150.
221. **Kiyohara, O.; Benson, G. C.; Grolier, J.- P.** Thermodynamic properties of binary mixtures containing ketones. I. Excess enthalpies of some aliphatic ketones + n-hexane, + benzene, and + tetrachloromethane. *J. Chem. Thermodyn.* 1977, Vol. 9, pp. 315-323.
222. **Kiyohara, O.; Handa, Y. P.; Benson, G. C.** Thermodynamic properties of binary mixtures containing ketones. III. Excess enthalpies of n-alkanes + some aliphatic ketones. *J. Chem. Thermodyn.* 1979, Vol. 11, pp. 453-460.
223. **Legido, J. L.; Bravo, R.; Paz Andrade, M. I.; Romani, L.; Sarmiento, F.; Ortega, J.** Excess enthalpies of five examples of (2-hexanone + an n-alkane) and five of (2-hexanone + an n-alkanol) at 298.15 K. *J. Chem. Thermodyn.* 1986, Vol. 18, pp. 21-26.
224. **Marongiu, B.** Excess enthalpy. Pentanal-cyclohexane system. *Int. Data Series, Sel. Data Mixtures.* 1984, Vol. 3, p. 211.
225. **Ortega, J.** Excess enthalpies of alkyl formates + (n-alkanes of 1-chloroalkanes). Experimental data and their analysis in terms of the UNIFAC model. *Ber. Bun-senges. Phys. Chem.* 1989, Vol. 93, pp. 730-735.
226. **Ortega, J.; Matos, J. S.; Pena, J. A.** Excess molar enthalpies of methyl alkanoates + n-nonane at 298.15 K. *Thermochim. Acta.* 1990, Vol. 160, pp. 337-342.
227. **Paz Andrade, M. I.; Pintos, M.; Bravo, R.** Excess enthalpy. Propyl ethanoate-hexane system. *Int. Data. Series, Sel. Data Mixtures Ser. A.* 1983, Vol. 3, p. 232.
228. **Acosta, J.; Arce, A.; Rodil, E.; Soto, A.** Densities, Speeds of Sound, Refractive Indices, and the Corresponding Changes of Mixing at 25 °C and Atmospheric Pressure for Systems Composed by Ethyl Acetate, Hexane, and Acetone. *J. Chem. Eng. Data.* 2001, Vol. 46, pp. 1176-1180.
229. **Macedo, E. A.; Mendonca, J. M.; Medina, A. G.** Vapor-liquid equilibrium for the systems ethyl formate-methyl ethyl ketone, ethyl formate-toluene and ethyl formate-methyl ethyl ketone-toluene: new UNIFAC parameters for interactions between the groups ACH/HCOO, ACCH₂/HCOO and CH₂CO/HCOO. *Fluid Phase Equilib.* 1984, Vol. 18, pp. 197-210.

230. **Radnai, G.; Rasmussen, P.; Fredenslund, A.** Vapor-liquid equilibrium data for binary mixtures containing aldehydes and esters and for the mixture 1,1,2-trichloro-1,2,2-trifluoroethane plus n-hexane. *AIChE Symposium Series*. 1984, Vol. 256, pp. 70-79.
231. **Lee, M. -J.; Hsiao, C. -C.; Lin, H. -M.** Isothermal vapor-liquid equilibria for mixtures of methyl tert-butyl ether, methyl acetate, and ethyl acetate. *Fluid Phase Equilib.* 1997, Vol. 137, pp. 231-241.
232. **Sameshima, J.** System: acetone-ethyl ether. *J. Amer. Chem. Soc.* 1918, Vol. 40, pp. 1482-1503.
233. **Resa, J. M.; Gonzalez, C.; Betolaza, M. A.; Ruiz, A.** Behavior of butyl ether as entrainer for the extractive distillation of the azeotropic mixture propanone + diisopropyl ether. Isobaric VLE data of the azeotropic components with the entrainer. *Fluid Phase Equilib.* 1999, Vol. 156, pp. 89-99.
234. **Othmer, D. F.; Chudgar, M. M.; Levy, S. L.** Composition of vapors from boiling solutions. Binary and ternary systems of acetone, methyl ethyl ketone, and water. *Ind. Eng. Chem.* 1952, Vol. 44, pp. 1872-1881.
235. **Glukhareva, M. I.; Taravkova, E. N.; Chashchin, A. M.; Kushner, T. M.; Serafimov, L. A.** Liquid-vapor phase equilibriums in the acetone-diethyl ketone, methyl ethyl ketone-diethyl ketone, and diethyl ketone-acetic acid systems at 760 torr. *Tr. Mosk. in-ta tonkoi khim. tekhnol.* 1974, Vol. 4, pp. 86-89.
236. **Shen, S.; Wang, Y.; Shi, J.; Benson, G. C.; Lu, B. C. -Y.** Excess Enthalpies of the Systems Acetone + Ethyl Acetate and Cyclohexane + Cyclohexanone. *J. Chem. Eng. Data.* 1992, Vol. 37, pp. 400-402.
237. **Goloborodkina, R. V.; Beregovykh, V. V.; Goloborodkin, S. I.; Timofeev, V. S.; L'vov, S. V.** Vapor-liquid equilibrium in three-component solvent systems. *Chim. Farm. Zh.* 1982, Vol. 16, pp. 341-345.
238. **Errington, J. R.; Boulougouris, G. C.; Economou, I. G.; Panagiotopoulos, A. Z.; Theodorou, D. N.** Molecular Simulation of Phase Equilibria for Water-Methane and Water-Ethane Mixtures. *J. Phys. Chem. B.* 1998, Vol. 102, p. 8865.
239. **Koh, C. A.; Tanaka, H.; Walsh, J. M.; Gubbins, K. E.; Zollweg, J. A.** Thermodynamic and structural properties of methanol-water mixtures: experiment, theory, and molecular simulation. *Fluid Phase Equilib.* 1993, Vol. 83, pp. 51-58.
240. **Machova, I.; Linek, J.; Wichterle, I.** Vapor-liquid equilibria in the heptane - 1-pentanol and heptane -3-methyl-1-butanol systems at 75, 85 and 95°C. *Fluid Phase Equilib.* 1988, Vol. 41, pp. 257-267.
241. **Oracz, P.** Recommendations for VLE data on binary 1-alkanol + n-alkane systems. *Fluid Phase Equilib.* 1993, Vol. 89, pp. 103-172.

242. **Cova, D. R.; Rains, R. K.** Vapor-Liquid Equilibria in Hydrocarbon-Alcohol Systems n-Decane-1 - Heptanol and n-Decane-2-Methyl-1 -hexanol. *J. Chem. Eng. Data*. 1974, Vol. 19, pp. 251-253.
243. **Plesnar, Z.; Gierycz, P.; Gregorowicz, J.; Bylicki, A.** Vapor-liquid equilibrium and solid-solid equilibrium in the system formed by octan-1-ol and n-decane. Measurement and calculation. *Thermochim. Acta*. 1989, Vol. 150, pp. 101-109.
244. **Budantseva, L. S.; Lesteva, T. M.; Nemtsov, M. S.** Liquid-vapor equilibrium in systems methanol-C7-8 hydrocarbons of different classes. *Zhurnal Fizicheskoi Khimii*. 1975, Vol. 49, p. 1844.
245. **Iguchi, A.** Vapor-liquid equilibriums at 25°C for binary systems between alcohols and hydrocarbons. *Kagaku Sochi*. 1978, Vol. 20, pp. 66-68.
246. **Ku, H. -C; Tu, C. -H.** Isobaric vapor-liquid equilibria for mixtures of acetone, ethanol, and 2,2,4-trimethylpentane at 101.3kPa. *Fluid Phase Equilib*. 2005, Vol. 231, pp. 99-108.
247. **Gmehling, J.; Onken, U.;** *Vapor-Liquid Equilibrium Data Collection (Supplement 7)*. Frankfurt : Dechema, 2007. Vols. I, Part 2i. ISBN-13: 978-9-89746-089-8.
248. **Rudakovskaya, T. S.; Yunitskii, I. N.; Timofeev, V. S.** Liquid-vapor phase equilibrium and mutual solubility of the components in the ternary 2-butanone-butanol-water mixture. *Sb. Nauch. Tr., Ivanov. Energ. Inst.* 1972, Vol. 14, pp. 216-221.
249. **Berro, C.; Peneloux, A.** Excess Gibbs energies and excess volumes of 1-butanol-n-heptane and 2-methyl-1-propanol-n-heptane binary systems. *J. Chem. Eng. Data*. 1984, Vol. 29, pp. 206-210.
250. **Matsuda, H.; Ochi, K.** Liquid-liquid equilibrium data for binary alcohol + n-alkane (C10-C16) systems: methanol + decane, ethanol + tetradecane, and ethanol + hexadecane. *Fluid Phase Equilib*. 2004, Vol. 224, pp. 31-37.
251. **Ott, J. B.; Sipowska, J. T.; Marchant, B. G.** Excess enthalpies for (pentane + methanol) at the temperatures (283.15, 298.15 and 363.15) K and the pressures (0.4, 5, and 15) MPa. *J. Chem. Thermodyn*. 1994, Vol. 26, pp. 717-725.
252. **Sipowska, J. T.; Ott, J. B.; Lemon, L. R.; Marchant, B. G.; Brown, P. R.** Excess enthalpies and excess volumes for (butane + ethanol) at temperatures (298.15, 323.15 and 348.15) K and the pressures (5, 10 and 15) MPa. *J. Chem. Thermodyn*. 1995, Vol. 27, pp. 1355-1364.
253. **Kwaterski, M.; Rezanova, E. N.; Lichtenthaler, R. N.** Excess molar volumes and excess molar enthalpies of binary and ternary mixtures of (ethanol or 1-butanol), triethylamine and n-hexane. *Fluid Phase Equilib*. 2005, Vol. 237, pp. 170-185.
254. **Van Ness, H. C.; Soczek, C. A.; Kochar, N. K.** Thermodynamic Excess Properties for Ethanol-n-Heptane. *J. Chem. Eng. Data*. 1967, Vol. 12, pp. 346-351.

255. **Christensen, C.; Gmehling, J.; Rasmussen, P.; Wedlich, U.** *Heats of Mixing Data Collection, Binary and Multicomponent Systems (Supplement 2)*. Frankfurt : Dechema, 1984. Vols. III, Part 4. ISBN 39-2156-75-05.
256. **Lemon, L. R.; Moore, J. D.; Brown, P. R.; Ott, J. B.** Excess molar enthalpies and excess molar volumes for (butane + propan-1-ol) at temperatures of (298.15, 323.15, and 348.15) K and pressures of (5, 10, and 15) MPa. *J. Chem. Thermodyn.* 1996, Vol. 28, pp. 187-200.
257. **Nguyen, T. H.; Ratcliff, A.** Heats of Mixing of n-Alcohol-n-Alkane Systems at 15 and 55C. *J. Chem. Eng. Data.* 1975, Vol. 20, pp. 252-255.
258. **Hamam, S. E. M.; Kumaran, M. K.; Benson, G. C.** Excess enthalpies of some binary mixtures: (a C5-alkanol + n-heptane) at 298.15 K. *J. Chem. Thermodyn.* 1984, Vol. 16, pp. 1013-1017.
259. **Sarmiento, F.; Paz Andrade, M. I.; Fernandez, J.; Bravo, R.; Pintos, M.** Excess Enthalpies of 1-Heptanol + n-Alkane and Di-n-propylamine + Normal Alcohol Mixtures at 298.15 K. *J. Chem. Eng. Data.* 1985, Vol. 30, pp. 321-323.
260. **Stokes, R. H.** Excess enthalpies of (butan-1-ol + methanol) at 278.15, 298.15, 318.15 K. *J. Chem. Thermodyn.* 1988, Vol. 20, pp. 1349-1352.
261. **Sun, H. H.; Christensen, J. J.; Izatt, R. M.; Hanks, R. W.** The excess enthalpies of six n-pentanol + alcohol mixtures at 298.15 K. *J. Chem. Thermodyn.* 1980, Vol. 12, pp. 95-99.
262. **Larkin, J. A.** Thermodynamic properties of aqueous non-electrolyte mixtures. I. Excess enthalpy for water + ethanol at 298.15 to 383.15 K. *J. Chem. Thermodyn.* 1975, Vol. 7, pp. 137-148.
263. **Ochi, K.; Lu, B. C. -Y.** Determination and correlation of binary vapor-liquid equilibrium data. *Fluid Phase Equilib.* 1977, Vol. 1, pp. 185-200.
264. **Gmehling, J.; Onken, U.** *Vapor-Liquid Equilibrium Data Collection. Organic Hydroxy Compounds: Alcohols*. s.l. : Dechema, 1977. Vol. I. Part 2a. ISBN 3-921567-09-2.
265. **Falcon, J.; Ortega, J.; Gonzalez, E.** Densities and Vapor-Liquid Equilibria in Binary Mixtures Formed by Propyl Methanoate + Ethanol, +Propan-1-ol, and + Butan-1-ol at 160.0 kPa. *J. Chem. Eng. Data.* 1996, Vol. 41, pp. 859-864.
266. **Blanco, A. M.; Ortega, J.** Densities and Vapor-Liquid Equilibrium Values for Binary Mixtures Composed of Methanol + an Ethyl Ester at 141.3 kPa with Application of an Extended Correlation Equation for Isobaric VLE Data. *J. Chem. Eng. Data.* 1998, Vol. 43, pp. 638-645.
267. **Gmehling, J.; Onken, U.** *Vapor-Liquid Equilibrium Data Collection. Organic Hydroxy Compounds: C5+-Alcohols and Phenols (Supplement 10)*. Frankfurt : Dechema, 2010. Vols. Vol. I, Part 2I. ISBN-13: 978-3-89746-124-6.

268. **Gmehling, J.; Onken, U.; Arlt, W.** *Vapor-Liquid Equilibrium Data Collection: Aqueous-Organic Systems (Supplement 1)*. Frankfurt : Dechema, 1981. Vols. I, Part 1a. ISBN 3-921 567-33-5.
269. **Gmehling, J.; Onken, U.; Arlt, W.** *Vapor-Liquid Equilibrium Data Collection. Organic Hydroxy Compounds: Alcohols (Supplement 1)*. Frankfurt : Dechema, 1982. Vols. Vol. I, Part 2c. ISBN 3-921 567-29-7.
270. **Gomis, V.; Front, A.; Pedraza, R.; Saquete, M. D.** Isobaric vapor–liquid and vapor–liquid–liquid equilibrium data for the water–ethanol–hexane system. *Fluid Phase Equilib.* 2007, Vol. 259, pp. 66-70.
271. **Gultekin, N.** Vapor-Liquid Equilibria at 1 atm for Ternary and Quarternary Systems Composed of Acetone, Methanol, 2-Propanol, and I-Propanol. *J. Chem. Eng. Data.* 1990, Vol. 35, pp. 132-136.
272. **Carta, R.; Dernini, S.; Sanna, P.** Isobaric Vapor-Liquid Equilibria for the Ternary System Acetone-Ethyl Acetate-Ethanol. *J. Chem. Eng. Data.* 1984, Vol. 29, pp. 463-466.
273. **Tihic, A.; Kontogeorgis, G. M.; Von Solms, N.; Michelsen, M. L.** A Predictive Group-Contribution Simplified PC-SAFT Equation of State: Application to Polymer Systems. *Ind. Eng. Chem. Res.* 2008, Vol. 47, pp. 5092-5101.
274. **Tihic, A.; Von Solms, N.; Michelsen, M. L.; Kontogeorgis, G. M.; Constantinou, L.** Application of sPC-SAFT and group contribution sPC-SAFT to polymer systems—Capabilities and limitations. *Fluid Phase Equilib.* 2009, Vol. 281, pp. 70-77.
275. **Sear, R.P.; Jackson, G.** Thermodynamic perturbation theory for association with bond cooperativity. *J. Chem. Phys.* 1996, Vol. 105, pp. 1113-1120.
276. **Du Rand, M.** *Practical Equation of State for Non-Spherical and Asymmetric Systems*. Stellenbosch : Department of Chemical Engineering, University of Stellenbosch, 2004.
277. **Smith, J. M.; Van Ness, H. C.; Abbott, M. M.** *Introduction to Chemical Engineering Thermodynamics*. 5th Edition. s.l. : McGraw-Hill, 1996. ISBN 0-07-059239-X.
278. **Llovel, F.; Pamies, J. C.; Vega, L. F.** Thermodynamic properties of Lennard-Jones chain molecules: Renormalization-group correlations to a modified statistical associating fluid theory. *J. Chem. Phys.* 2004, Vol. 121, pp. 10715-10724.
279. **Kirss, H.; Kuus, M.; Siimer, E.; Kudryavtseva, K.** Excess enthalpies of 1-butanol-2-butanol-n-heptane, 1-hexanol-cyclohexanol-n-nonane, 2-butanol-n-heptane, 1-hexanol-cyclohexanol and cyclohexanol-n-nonane at 298.15 K. *Thermochim. Acta.* 1995, Vol. 255, pp. 63-69.
280. **Tan, S. P.; Adidharma, H.; Radosz, M.** Generalized Procedure for Estimating the functions of Nonbonded Associating Molecules and Their Derivatives in Thermodynamic Perturbation Theory. *Ind. Eng. Chem. Res.* 2004, Vol. 43, pp. 203-208.

281. **Kiselev, S. B.; Ely, J. F.; Tan, S. P.; Adidharma, H.; Radosz, M.** HRX-SAFT Equation of State for Fluid Mixtures: Application to binary Mixtures of Carbon Dioxide, Water and Methanol. *Ind. Eng. Chem. Res.* 2006, Vol. 45, pp. 3981-3990.
282. **Michelsen, M. L.** Robust and Efficient Solution Procedures for Association Models. *Ind. Eng. Chem. Res.* 2006, Vol. 45, pp. 8449-8453.
283. **Michelsen, M. L.** Comments on "Generalized Procedure for Estimating the Fractions of Nonbonded Associating Molecules and Their Derivatives in Thermodynamic Perturbation Theory". *Ind. Eng. Chem. Res.* 2004, Vol. 43, p. 6262.
284. **Blas, F. J.; Vega, L. F.** Thermodynamic Behaviour of Homonuclear and Heteronuclear Lennard-Jones Chains with Association Sites from Simulation and Theory. *Mol. Phys.* 1997, Vol. 92, pp. 135-150.
285. **Blas, F. J.; Vega, L. F.** Prediction of Binary and Ternary Diagrams Using the Statistical Associating Fluid Theory (SAFT) Equation of State. *Ind. Eng. Chem. Res.* 1998, Vol. 37, pp. 660-674.
286. **Johnson, J.; Zollweg, J. A.; Gubbins, K. E.** The Lennard-Jones Equation of State Revisited. *Mol. Phys.* 1993, Vol. 78, pp. 591-615.
287. **Pamies, J. C.; Vega, L. F.** Vapor-Liquid Equilibria and Critical Behavior of Heavy n-Alkanes Using Transferable Parameters from the soft-SAFT Equation of State. *Ind. Eng. Chem. Res.* 2001, Vol. 40, pp. 2532-2543.
288. **Blas, F. J.; Vega, L. F.** Critical Behavior and Partially Miscibility Phenomena in Binary Mixtures of Hydrocarbons by the Statistical Associating Fluid Theory. *Mol. Phys.* 1998, Vol. 109, pp. 7405-7413.
289. **Llovel, F.; Vega, L.** Prediction of Thermodynamic Derivative Properties of Pure Fluids through the Soft-SAFT Equation of State. *J. Phys. Chem.* 2006, Vol. 110, pp. 11427-11437.
290. **Lovell, F.; Pamies, J. C.; Vega, L. F.** Thermodynamic properties of Lennard-Jones chain molecules: Renormalization-group corrections to a modified statistical associating fluids theory. *J. Chem. Phys.* 2004, Vol. 121, pp. 10715-10724.
291. **Lovell, F.; Vega, L. F.** Global Fluid Phase Equilibria and Critical Phenomena of Selected Mixtures Using the Crossover Soft-SAFT Equation. *J. Phys. Chem. B.* 2006, Vol. 110, pp. 1350-1362.
292. **Lovell, F.; Vega, L. F.** Phase equilibria, critical behavior and derivative properties of selected n-alkane/n-alkane and n-alkane/1-alkanol mixtures by crossover soft-SAFT equation of state. *J. of Supercritical Fluids.* 2007, Vol. 41, pp. 204-216.
293. **Maghari, A.; Sadeghi, M. S.** Prediction of sound velocity and the heat capacities of n-alkanes from the modified SAFT-BACK equation of state. *Fluid Phase Equilib.* 2007, Vol. 252, pp. 152-161.

294. **Maghari, A.; Safaei, Z.** Thermodynamic regularities for non-polar fluids from the modified SAFT-BACK equation of state. *Journal of Molecular Liquids*. 2008, Vol. 142, pp. 95-102.
295. **Boublik, T.** Hard convex body equation of state. *J. Chem. Phys.* 1975, Vol. 63, pp. 4084-4085.
296. **Chen, S. S.; Kreglewski, A.** Application of the augmented van der Waals theory of fluids. I. Pure fluids. *Ber. Bunsen-Ges. Phys. Chem.* 1977, Vol. 81, pp. 1048-1052.
297. **Alder, B. J.; Young, D. A.; Mark, M. A.** Studies in molecular dynamics. X. Corrections to the augmented van der Waals theory for the square well fluid. *J. Chem. Phys.* 1972, Vol. 56, pp. 3013-3029.
298. **Pfohl, O.; Brunner, G.** Use of BACK to modify SAFT in order to enable density and phase equilibrium calculations connected to gas-extraction processes. *Ind. Eng. Chem. Res.* 1998, Vol. 37, pp. 2966-2976.
299. **Mi, J.; Chen, J.; Gao, G.; Fei, W. -Y.** Equation of state extended from SAFT with improved results for polar fluids across the critical point. *Fluid Phase Equilib.* 2002, Vol. 201, pp. 295-307.
300. **Chen, J.; Mi, J.; Yu, Y.; Luo, G.** An analytical equation of state for water and alkanols. *Chem. Eng. Sci.* 2004, Vol. 59, pp. 5831-5838.
301. **Maghari, A.; Safaei, Z.; Sarhangian, S.** Prediction of Joule-Thomson inversion curves for polar and non-polar fluids from the SAFT-CP equation of state. *Cryogenics*. 2008, Vol. 48, pp. 48-55.

Appendix A

Important aspects, criteria and selection of models

The aim of this appendix is to provide background information on important subjects considered during this project. In this Appendix, intermolecular forces that need to be accounted for by EOS models are briefly mentioned and the complex phenomena's they cause are discussed. Real pure components and binary mixture systems that were investigated are identified. These systems are selected in such a way to show the influence of certain intermolecular forces. EOS models may then be applied to properties of these identified systems in order to test how well they account for the different types of forces.

Some of the performance criteria used to evaluate EOS models are also presented. These criteria are used to identify the primary models for this investigation.

A.1 Intermolecular forces

Interpretation of observed thermodynamic behaviour in thermodynamic properties is easier to predict and understand on a macroscopic level when there is some understanding of molecular behaviour on a microscopic level. The current understanding of intermolecular forces is far from complete (193) and that the analytical relations that link intermolecular forces to macroscopic properties (i.e. statistical mechanics) are still limited to fairly simple cases.

In Figure A-1, the relative contributions to the *long range attractive forces* (dispersion, polar, induction) for some components are shown:

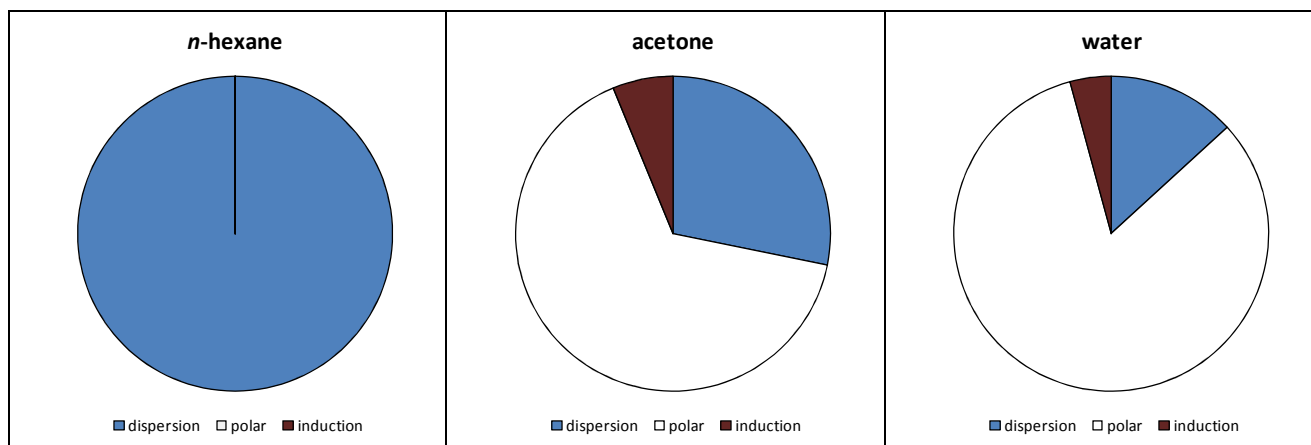


Figure A-1: Long range attractive forces present in *n*-hexane, acetone and water at $T = 298\text{ K}$. Data taken from ref. (105).

From Figure A-1, the only long-range attractive forces in *n*-hexane are dispersion forces. In acetone the contribution from dispersion forces is 28%, from polar forces is 66% and from induction forces is 6%. In water the contributions are 13% from dispersion forces, 83% from polar forces and 4% from induction forces. In addition to this, water can also form hydrogen bonds that severely influence the thermodynamic behaviour of the fluid as already mentioned. Repulsive forces are present in all molecules.

There are many types of intermolecular forces, but the most important forces encountered in complex components and mixtures studied in this project include the following (106; 193):

- *Polar forces* between permanent dipoles, quadrupoles, and higher multi-poles.
- *Induction forces* between a permanent dipole (or quadrupole) and an induced dipole.
- *Dispersion forces* (or London) that is present between all molecules.
- *Repulsion forces* that is present between all molecules.
- *Specific (chemical) forces* leading to association and solvation. These include hydrogen bonds.

Intermolecular forces are usually expressed in terms of potential-energy functions. The intermolecular potential energy function describes the attractive and repulsive forces between two molecules. If two simple spherical molecules are considered that are separated by distance r , the force F between them are related to the intermolecular potential Γ as follows:

$$F = -\frac{d\Gamma}{dr} \quad (\text{A-1})$$

The negative of the potential energy is the work that must be done to separate two molecules from the intermolecular distance r to infinite separation. By convention, a positive potential energy represents a repulsive force and a negative potential energy represents an attractive force. In section A.1.6, some of the most common types of intermolecular potential functions are discussed. The above-mentioned intermolecular forces are briefly reviewed in the following sections.

A.1.1 Polar forces

Consider a molecule with two charges of the same magnitude e , but of opposite sign that is a distance d apart. Such a particle has a dipole moment defined by:

$$\mu = e d \quad (\text{A-2})$$

Asymmetric polar molecules possess permanent dipoles that results from an uneven spatial distribution of electronic charges about the positively charged nuclei (193). The dipoles exhibit an electric field between the positive and negative charges. When one dipole is in the presence of the electric field of another dipole, an interaction takes place that is termed a dipole-dipole interaction. Such an interaction can lead to deviations from ideal behaviour (106) and influence the thermodynamic behaviour of the system. The potential energy $\bar{\Gamma}_{ij}$ between two dipoles i and j in vacuum at a fixed separation r , is found by averaging over all orientations with each orientation weighted according to its Boltzmann factor (193). When the Boltzmann factors are expanded in powers of $1/kT$, $\bar{\Gamma}_{ij}$ is proportional to the dipole moments and the separation distance in the following way:

$$\bar{\Gamma}_{ij} = -C \frac{\mu_i^2 \mu_j^2}{Tr^6} + \dots \quad (\text{A-3})$$

From equation (A-3), it is noted that for a pure polar substance ($i = j$), the potential energy varies as the fourth power of the dipole moment. A small change in the dipole moment can therefore produce large effects on the potential energy. Equation (A-3) also indicates that the potential energy, as a result of dipole moments, is dependent of the inverse separation distance to the sixth power and inversely dependent on temperature. Therefore, these forces decrease considerably as the distance between the molecules increases and influence the thermodynamic behaviour the most at low temperatures. C is a constant that is determined by other factors such as permittivity.

In addition to dipole moments, it is possible for molecules to have quadrupole moments due to the concentration of electric charges at four separate points in a molecule. For the simplest case of a linear molecule, the quadrupole moment is defined as the sum of the second moments of charges (193):

$$Q = \sum_i e_i d_i^2 \quad (\text{A-4})$$

The influence of quadrupole moments on the intermolecular potential energy may be derived in a similar way as that of equation (A-3). For a dipole i -quadrupole j interaction the influence on the potential energy is expressed in equation (A-5):

$$\bar{\Gamma}_{ij} = -C \frac{\mu_i^2 Q_j^2}{Tr^8} + \dots \quad (\text{A-5})$$

For a quadrupole i -quadrupole j interaction, the influence on the potential energy is expressed in equation (A-6):

$$\bar{\Gamma}_{ij} = -C \frac{Q_i^2 Q_j^2}{Tr^{10}} + \dots \quad (A-6)$$

Molecules may also have multi-poles such as octapoles and hexadecapoles. Since the effect of quadrupoles on thermodynamic properties is much less than the effect of dipoles, it is generally agreed that the effect of these higher order multi-poles is usually negligible (106; 193), however, in some cases this is not a good assumption. This relative rank of importance follows because intermolecular forces due to multi-poles higher than dipoles are extremely short range; for dipoles the average potential energy is proportional to the sixth power of the inverse distance of separation and for quadrupoles the average potential energy depends on the tenth power of the reciprocal distance. For higher multi-poles, the exponent is larger (193).

Molecules with these types of polar interactions are alcohols, water, ketones, esters, ethers and aldehydes (127).

A.1.2 Induction forces and polarizability

When a non-polar molecule, that has no permanent dipole moment, is subjected to the electric field of a dipolar molecule, the electrons of the non-polar molecule are displaced from their ordinary positions and a dipole is induced (193). In fields of moderate strength, the induced dipole moment is proportional to the field strength E and is defined as follows:

$$\mu^{\text{induced}} = \alpha E \quad (A-7)$$

The proportionality factor α is a fundamental property of the component and is called the polarizability. Polarizability characterizes how easy a molecule's electron cloud can be displaced by the presence of an electric field (106). The resultant force between the permanent dipole and the induced dipole is always attractive (106). Generally larger molecules have higher polarizabilities, because their valence electrons are farther away from the nuclei and therefore less rigidly held. Also, molecules with a permanent dipole may also have an induced dipole, however, the potential energy from the induced dipole is usually small compared to the permanent dipole (193). The potential energy due to induced dipoles is also dependent on the sixth power of the inverse separation distance, and for a non-polar molecule i and a dipolar molecule j , may be expressed as follows (193):

$$\Gamma_{ij} = -C \frac{(\alpha_i \mu_j^2)}{r^6} \quad (A-8)$$

Polar as well as non-polar molecules can have dipoles induced by an electric field. The mean potential energy due to induction between permanent dipolar molecules is expressed as follows (193):

$$\Gamma_{ij} = -C \frac{(\alpha_i \mu_j^2 + \alpha_j \mu_i^2)}{r^6} \quad (A-9)$$

An electric field may also be caused by permanent quadrupole moments, and if both molecules i and j have quadrupole moments, the influence on the potential energy due to induction may be expressed as (193):

$$\Gamma_{ij} = -C \frac{(\alpha_i Q_j^2 + \alpha_j Q_i^2)}{r^8} \quad (A-10)$$

A.1.3 Attraction (dispersion or London) and repulsion forces

i) Dispersion / London forces

Non-polar molecules such as argon show serious deviation from ideal behaviour at moderate pressures that indicate that there are forces of attraction operating between the molecules, yet argon does not have a dipole-moment and can therefore also not be subject to induction forces (106; 193). In 1930, London showed that these forces are inherently a quantum-mechanical phenomenon (106). He showed that the so-called non-polar molecules are, in fact, non-polar only viewed over a period of time. In a given time instant, the oscillations of the electrons about the nucleus resulted in distortion of the electron arrangement to such a degree as to cause a temporary dipole moment. This dipole moment rapidly changes its magnitude and direction and averages zero over a short period of time, however, these quickly varying dipoles produce electric fields which then induces dipoles in the surrounding molecules. The result of this induction is an attractive force that is commonly referred to as dispersion forces. Further results from London's work showed that the potential energy resulting from these forces is independent of temperature and varies inversely as the sixth power of the separation distance, and between two molecules of a pure substance may be expressed as (193):

$$\Gamma_{ij} = -C \frac{(\alpha_i^2 I_i)}{r^6} \quad (A-11)$$

I_i is the ionization potential. For molecules i and j of dissimilar species, the potential energy is expressed as:

$$\Gamma_{ij} = -C \frac{(\alpha_i \alpha_j)}{r^6} \left(\frac{I_i I_j}{I_i + I_j} \right) \quad (A-12)$$

Dispersion forces are present between all molecules and are surprisingly large (106). The potential energy from dipole-dipole interactions, induced dipole interactions and dispersion forces are all attractive and dependent of the inverse of the separation distance to the sixth power. They are commonly grouped together as *Van Der Waals forces*. For this reason (and in many EOS models) no distinction is made between them.

ii) Repulsion forces

At very small separations between molecules, their electron clouds overlap and the forces between the molecules are strongly repulsive rather than attractive (193). When the electron clouds overlap, columbic repulsion occurs to ensure that no violation of the Pauli exclusion principle takes place (106). These repulsive forces are not yet well at small distances understood as the attractive forces at larger distances. Theoretical considerations suggest that the repulsive potential should be an exponential function of intermolecular separation, but it is more convenient to represent the repulsive potential by an inverse power law type as follows (193):

$$\Gamma_{ij} = \frac{C}{r^n} \quad (A-13)$$

C is a positive constant and n is a number usually taken between 8 and 16.

All the forces mentioned this far are termed physical forces. Usually intermolecular potential functions are developed to approximate these physical forces in real fluid behaviour. In section A.1.6, the most common models encountered in this project are briefly discussed.

A.1.4 Specific (chemical) forces

The physical forces described so far account for most molecular interactions in the gas phase. Solids and liquids form when the net attractive intermolecular forces are stronger than the kinetic energy in the system and, consequently, hold the molecules together (106). In some cases, the forces of attraction can be attributed to *Van der Waals interactions* e.g. *n*-alkanes, but frequently chemical forces play a large role in condensed phases (106) e.g. water and alcohols. It should, however, also be mentioned that chemical forces may also occur in some unique gas systems. The main difference between physical and chemical forces is that chemical forces are saturated, while physical forces are not (193). Chemical forces are responsible for association and solvation, two complex phenomena's that leads to non-ideal behaviour. The most prevalent chemical forces are hydrogen bonding and charge transfer complexes (or acid-base complexes). In this project, hydrogen bonding will be encountered frequently and will only be discuss in the following section.

i) Hydrogen bonding

Hydrogen bonding is the 'chemical bond' that results between an electronegative atom and a hydrogen atom bonded to another electronegative atom in a second molecule (106). Although the normal valence of a hydrogen atom is unity, many hydrogen-containing compounds behave as if the hydrogen atom is bivalent (193); therefore, there is a sharing of a lone pair of electrons that forms the hydrogen bonds between the hydrogen atom and the electronegative atom as illustrated in Figure A-2:

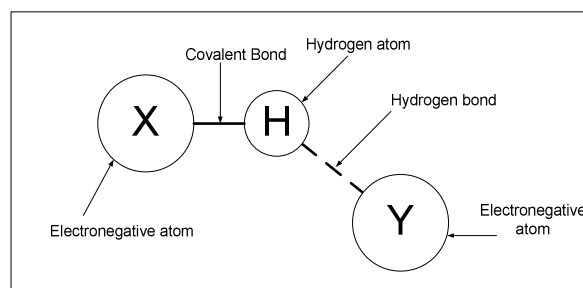


Figure A-2: Schematic diagram of hydrogen bond

The hydrogen bond is similar to a covalent bond with the major difference being that the hydrogen bond strength is much weaker than that of the covalent bond strength (hydrogen bonds are typically between 8 and 40 kJ.mol⁻¹ compared to normal covalent bonds that range between 200 and 400 kJ.mol⁻¹). As a result of this relative strength, the hydrogen bonds are rather broken easily compared to covalent bonds and the effect of hydrogen bonding decreases with an increase in temperature (193). The hydrogen bond is also very directional and occurs only at short separations. The hydrogen bonds are, however, an order of magnitude stronger than all the *Van der Waals forces* (106). Most of the complex behaviour investigated in this project results from solvation and association as already mentioned in Chapter 1. The hydrogen bond is the main intermolecular force responsible for these complex phenomena.

ii) Association and solvation

Association (Self-association) is the phenomenon where two or more of the same type of molecules tends to form clusters via hydrogen bonding. Examples of such molecules are water, alcohols and amines.

Solvation or cross-association is the tendency of dissimilar molecules to form clusters with different types of molecules (193). Mixtures of alcohols and water exhibit strong self-association and solvation (cross-association) (60). Modelling of mixtures with strong polar molecules that do not self associate, but solvates with other molecules is a major challenge in thermodynamic modelling.

Association and solvation profoundly affects phase behaviour and other properties. This is because the effective molecular properties of the clusters (size, energy, and shape), are very different from the monomeric molecules, resulting in the bulk fluid properties to be very different (16) from the monomeric fluid. If accurate physically realistic thermodynamic modelling is desired, association usually has to be accounted for explicitly in systems where hydrogen bonding is encountered.

A.1.5 Hydrophobic Effect

The hydrophobic effect is an entropic phenomenon (193). It arises mainly from the strong hydrogen bonds between water molecules in highly structured liquid water. These attractive forces are disrupted or distorted when a solute is dissolved in water. Upon solubilization of the

solute, hydrogen bonds in water are often not broken, but they are maintained in a distorted form. The water molecules then rearrange themselves such that they can still participate in hydrogen bond formation, more or less as in the bulk pure liquid phase. In doing so, a higher degree of local order is created when compared to pure liquid water, thereby producing a decrease in entropy that leads to an unfavourable Gibbs energy change for solubilization for non-polar solutes in water (193). Hydrocarbons in solution are an example of the hydrophobic effect.

A.1.6 Intermolecular potential functions

As mentioned earlier, intermolecular forces between molecules are usually expressed as intermolecular potential functions that approximate real fluid behaviour. These potential functions are then used in conjunction with fluid theories to develop thermodynamic models. In this project some of the models investigated are built on a few commonly used potential functions and it is the purpose of this section to provide a brief introduction to them. The models include both attractive and repulsive interactions and for net neutral species, the attractive forces are usually described by the *Van der Waals* forces. There is no explicit potential function for the chemical forces. The following functions are discussed:

- Hard-sphere potential
- Sutherland potential
- Square-well potential
- Lennard-Jones potential
- Mie-potentials

i) Hard-sphere potential

The hard sphere potential function is the simplest model of a real fluid. It has no attractive contribution, and treats the molecules as hard spheres. The potential is therefore zero until the diameters of two molecules overlap, where it then increases to infinity. The potential function is mathematically described as:

$$\Gamma = \begin{cases} 0 & \text{for } r > \sigma \\ \infty & \text{for } r \leq \sigma \end{cases} \quad (A-14)$$

A plot of the potential function is represented in Figure A-3:

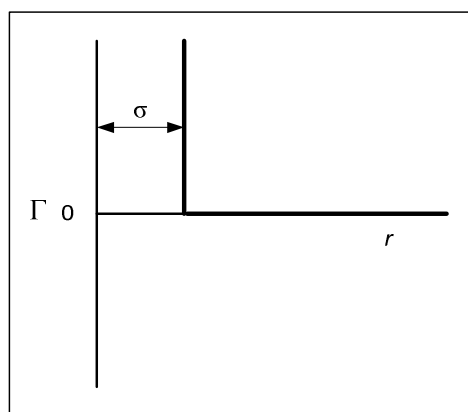


Figure A-3: Hard-sphere potential function

σ is the hard sphere molecular diameter.

ii) Sutherland potential

The Sutherland potential model adds the *Van der Waals* attractive term proportional to the sixth power of the inverse separation distance. The model is given by:

$$\Gamma = \begin{cases} \frac{-A}{r^6} & \text{for } r > \sigma \\ \infty & \text{for } r \leq \sigma \end{cases} \quad (\text{A-15})$$

A is a constant specific to a molecule. The function is plotted in the figure below:

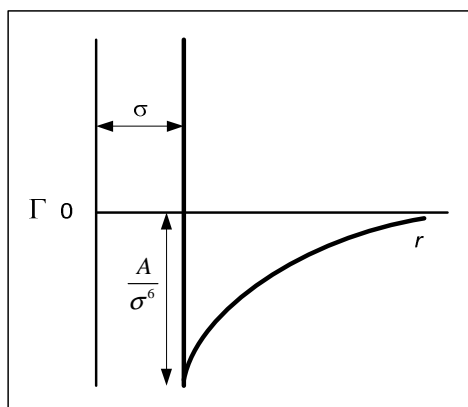


Figure A-4: Sutherland potential function

iii) Square-well potential

The square-well potential is an expansion of the hard-sphere potential, and incorporates an attractive contribution in the form of a square-well, in order to simulate a more realistic potential energy, while still maintaining its simplicity. The model can be mathematically expressed as follows:

$$\Gamma = \begin{cases} 0 & \text{for } r > \lambda\sigma \\ -\epsilon & \text{for } \sigma < r < \lambda\sigma \\ \infty & \text{for } r \leq \sigma \end{cases} \quad (\text{A-16})$$

ε represents the well depth in the model, and λ controls the width of the well. λ usually varies between 1.5 and 2 (276).

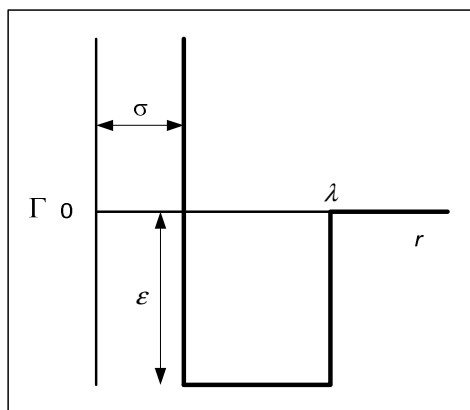


Figure A-5: Square-well potential function

iv) Lennard-Jones potential

The Lennard-Jones potential is a much more realistic approximation of the real molecular interaction energy compared to the models discussed thus far. It approximates the attractive potential energy correctly by having the attractive potential dependent to the sixth power of the inverse separation distance. The dependency of the repulsive potential was set equal to the 12th power of the inverse separation distance. This enables the function to model the steep decline in the short-range repulsive forces with increased distance between the molecules. The potential function is expressed as:

$$\Gamma = 4\varepsilon \left[\left(\frac{\sigma}{r} \right)^{12} - \left(\frac{\sigma}{r} \right)^6 \right] \quad (A-17)$$

The term ε indicates the maximum well depth and lowest intermolecular potential, and is found at the point where the intermolecular attractive and repulsive forces are equal. In equation (A-17), σ is the collision diameter, or the intermolecular distance, and indicates the distance at which the potential function is equal to zero. It is important to note that the Lennard-Jones potential model does not approximate the molecules as hard spheres and allows the particles to be in closer proximity than what the hard-sphere type models would dictate at sufficiently high system energies (276). This simulates the phenomena of overlapping outer electron orbitals at high energy levels. The Lennard-Jones model allows molecules, providing they have enough energy, to interpenetrate completely, effectively treating a particle as consisting out of a point centre surrounded by a completely soft or penetrable cloud (276). The function is plotted in Figure A-6:

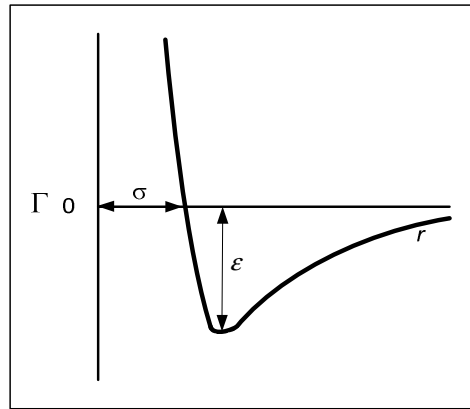


Figure A-6: Lennard Jones potential function

v) Mie potential

The Lennard-Jones potential is actually a modified simplified Mie potential. The Mie potential are given by the following equation:

$$\Gamma = \frac{\varepsilon \left(n^n / m^m \right)^{\frac{1}{(n-m)}}}{n-m} \left[\left(\frac{\sigma}{r} \right)^n - \left(\frac{\sigma}{r} \right)^m \right] \quad (A-18)$$

In the case of the Lennard-Jones potential $n = 12$ and $m = 6$. London showed that that $m = 6$ is the correct separation distance dependency for the *Van der Waals* forces. However, there is no theoretical justification for setting $n = 12$, it was a matter of convenience (193). In some thermodynamic models n is treated as an adjustable parameter.

A.2 Classification of thermodynamic systems investigated

It is necessary to identify real fluids and mixtures that are representative of the intermolecular forces and effects mentioned in section A.1 so that the influence of the different types of molecular forces may be investigated. The fluids and mixtures should be selected in such a way that the individual effects can be isolated and that a model's ability to account for the interactions can be thoroughly tested.

Voutsas *et al.* (49) classified pure components into three classes: non-polar, polar (non-hydrogen bonding) and hydrogen bonding fluids. Similar systems were also defined by Abbott (277) who studied molecular interactions on excess properties and Danner & Gess (50) classified systems according to polarity. The classification of Voutsas *et al.* (49) is used in this study.

A.2.1 Pure component fluids

i) Non-polar fluids

Fluids in this class have no dipole moment and only repulsive and dispersive forces are present between molecules of the fluid. By investigating properties of these components, the dispersion and repulsion interactions are effectively isolated. A model's ability to account for these forces can then be adequately tested. The most common series of real fluids that fall into this category is the *n*-alkane series. Fluids from this series are often encountered in the petroleum industry.

ii) Polar fluids that do not hydrogen bond/self-associate

Some fluids are strongly polar, but do not self-associate, however, they may cross-associate (solvate) in the presence of other molecules such as water. Ketones, ethers and esters fall into this group. By investigating the properties of these fluids, the intermolecular forces present are repulsive, dispersive, induction and polar forces.

One challenge that arises from polar molecules is that in most modelling approaches, the contribution of polar interactions to the system is often lumped together with the dispersion interactions, resulting in dispersion energy parameters that are unrealistically large. This is commonly known as the *Van der Waals* approach. When these components are encountered in mixtures, the predictive ability of the models is often poor because the mixing rules applied to the dispersion energy parameter do not necessarily hold for polar interactions.

Another problem that originates from the *Van der Waals* approach is that polar forces are temperature dependent while dispersion forces are not. Therefore, a model that is based on this approach would have some problems in the description of strongly temperature dependent properties, because at low temperatures the forces will be underestimated and at high temperatures the forces will be overestimated.

iii) Hydrogen bonding fluids that do self-associate

Components such as water and alcohols are strongly polar and they self-associate. Association is arguably the biggest contributor to non-ideal behaviour as already mentioned. Intermolecular forces present in these components are repulsive, dispersive, polar and hydrogen bonding forces.

A.2.2 Binary mixtures

The focus of this project is not only on the thermodynamic modelling of pure components properties, but on the thermodynamic properties of some binary mixture as well. By investigating properties of binary mixtures, the mixing rules used to extend a model's applicability to mixtures are tested. The following systems of binary mixtures are investigated in this project:

i) Non-polar/non-polar systems

A model's ability to account for repulsive and dispersive interactions in the mixture is effectively tested. An example of this type of mixture is *n*-hexane/*n*-heptane.

ii) Non-polar/polar (non-HB) systems

By investigating these types of mixtures, the consequences of the *Van der Waals approach* are exposed. An example of such a mixture is acetone/*n*-hexane.

iii) Non-polar/hydrogen bonding systems

Mixtures such as methanol/*n*-hexane or ethanol/*n*-octane are examples of this group. The self-association between molecules of the hydrogen bonding component, repulsive, dispersive and polar interactions all have to be accounted for in these types of mixtures.

iv) Polar (non-HB)/polar (non-HB) systems

In these type of systems, a model's ability to account for dispersive and repulsive interactions between molecules in the mixture, polar effects including induced polar effects and in some extreme cases, the solvation phenomenon are tested. An example of such a mixture may be acetone/chloroform.

v) Polar (non-HB)/hydrogen bonding systems

Mixtures such as acetone/water exhibit strong non-ideal behaviour, because in this case, the acetone molecule solvates. There is also a large degree of self-association taking place between the water molecules and both components are strongly polar. Modelling the properties of these systems provide a good test for any model.

vi) Hydrogen bonding/hydrogen bonding systems

In these types of mixtures extreme non-ideal behaviour is commonly observed, because there is a strong presence of repulsive, dispersive, polar and hydrogen bonding forces. The hydrogen bonding occurs between *like* and *unlike* molecules i.e. self-association and cross-association (solvation) and accounting for all these types of interactions is usually very challenging for any thermodynamic model. Water/ethanol is an example of such a system.

A.3 Performance criteria for EOS models

It is necessary to define a set of criteria from which the performance of EOS models can be evaluated when investigating some of the thermodynamic properties (as defined in Appendix B) of pure components and binary mixtures (as defined in section A.2).

Deiters and De Reuck (96) started to develop such a set of criteria. Their main objective for developing the criteria was to aid in publications of new EOS models. Frequently it happens that authors of new EOS models, or variations of existing ones, report significant improvements with regard to properties and components they are interested in, but fail to comment on the applicability and application to other properties at different conditions beyond their own immediate field of research (96). This results in numerous EOS models being published that are only evaluated and tested on certain properties at certain conditions. The aim of this section will be to review the criteria and formulate it to be applicable to this project.

It should be noted that generally there are two types of EOS models (96):

- *Empirical EOS* models that usually contain a large number of component-specific parameters. These parameters have little physical meaning, but are fitted to experimental data. The equations are typically designed for one fluid and are very accurate within the thermodynamic range in which the parameters were fitted.
- *Theoretically based EOS* models are based on statistical thermodynamic insight. These equations have fewer component-specific parameters, which usually have proper physical meaning. These equations tend to be less accurate due to limitations in current theories, but can usually represent property trends correctly even far away from the fitted range. These equations have a great predictive ability and can usually be extended to mixtures with simple combining rules. They usually have some empirical feature that enhances the accuracy of the equations in real fluid behaviour, but the physical framework is based on statistical thermodynamics.

The EOS models considered in this project are of the second type. The *general criteria* of EOS models for pure components are presented below as given by Deiters and De Reuck (96):

- Parameters
- The critical point
- The two-phase region
- Single-phase properties
 - Volumetric properties
 - Caloric properties

Further criteria for pure components as mentioned by Deiters and De Reuck (96) are prediction of the following curves:

- The Joule inversion curve.
- The Joule-Thomson inversion curve.
- The Boyle curve
- The isochor inflection curve
- The isobar infection curve

The application of each point in the *general criteria* is briefly discussed below:

A.3.1 Parameters

It is desired to have theoretical EOS with as few as possible meaningful parameters that characterize the component within the framework of the model. Pure component parameters are usually either estimated from relationships between critical properties (T_c , P_c , v_c) or are regressed by fitting the parameters to certain thermodynamic properties in a specified temperature and pressure range. The fitted parameters should preferably be able to calculate all other thermodynamic properties with good accuracy. Some workers argue that, if the physical framework of a model is correct, that one set of pure components parameters should be capable to give a complete description of the whole thermodynamic behaviour (56; 57). Property specific parameters are therefore undesirable.

When these pure component parameters are used in conjunction with mixing rules to extend the applicability of the EOS models to mixtures, accurate prediction of the mixture property should still be maintained.

A.3.2 Critical point

It is well known that analytical EOS's become inaccurate in the vicinity of the critical point (96). Various approaches for treating critical behaviour have been developed, but as stated in section 1.4, modelling in the critical region is not considered in this project. Usually more adjustable pure component parameters are introduced and additional equations have to be developed to account for the complex phenomena's in the critical region, e.g. cross-over soft SAFT (278).

A.3.3 Two phase region

This criterion evaluates the model's ability to predict phase equilibria. It involves the calculation of the saturated vapour pressure and saturated liquid densities at the specified conditions. The pressure in the vapour phase and the density of the liquid phase at the equilibrium point is known as the saturated vapour pressure and saturated liquid density, and accurate prediction of these properties are required in order to describe the phase equilibria of mixture properties.

Most models considered in this project have been extensively applied to the phase equilibria of a multitude of components and mixtures. They have, however, not been extensively applied to the prediction of other thermodynamic properties.

A.3.4 Single phase properties

Single phase properties may refer to properties in the solid, liquid, vapour or supercritical phases. Non-idealities caused by complex molecular interactions are usually more pronounced in the

liquid phase compared to the vapour phase, because of the close proximity of molecules to each other. Consequently, properties in the liquid phase are modelled in this project.

i) Volumetric properties

The ability of an EOS to predict P-V-T data should be demonstrated (96). Other volumetric properties include the isothermal compressibility.

ii) Caloric properties

The estimation of caloric data, such as residual isochoric and isobaric heat capacities is of academic and industrial importance (96). Deiters and De Reuck (96) classify speed of sound as a caloric property and emphasize its importance as a good test for the physical framework of an EOS model.

A.3.5 Numerical intensity

If an EOS model is mathematically too complex, it would not be used in the industry and simulation packages. With the current computer power, this constraint is being relaxed and more complex models are being implemented. However, it is more favourable to work with a simple model than with a complex one, especially if the improvement in model performance is negligible. Therefore, a trade off between accuracy and model complexity exists that have to be considered.

A.3.6 Further criteria

The curves mentioned in the further criteria are beyond the scope of this project. Accurate data for many of the mentioned curves is not available. Some of these curves involve extreme conditions of temperatures and pressures that are difficult to measure experimentally (96).

A.3.7 Main objective

The main objective of a realistic thermodynamic model can be summarized as a model that is able to predict phase behaviour and other thermodynamic derivative properties for complex systems simultaneously with one set of physically meaningful parameters that is easily obtainable and numerically manageable.

Appendix B

Thermodynamic Framework and Algorithms

The definition of the first- and second-order properties are taken and extended from Michelsen and Mollerup (3).

B.1 Thermodynamic Framework

B.1.1 Thermodynamic derivative properties from the state function

It was decided to use the reduced residual Helmholtz energy as the state function, because many of the current state-of-the-art EOS models investigated in this project have been developed in terms thereof and is consequently, widely used in literature. The independent variables of the function are temperature, total volume and mole numbers. All thermodynamic properties are defined in terms of its partial derivatives. The function is defined by as follows:

$$F = \frac{A^r(T, V, \mathbf{n})}{RT} \quad (B-1)$$

The definitions of all the properties investigated in this project are provided in Appendix B.

B.1.2 First-order derivative properties

The following properties are regarded as first-order derivative properties from the state function.

i) Pressure

The pressure of the system is defined by equation (B-2):

$$P = -RT \left(\frac{\partial F}{\partial V} \right)_{T, \mathbf{n}} + \frac{nRT}{V} \quad (B-2)$$

Typically, pressure is specified and equation (B-2) is iteratively solved for the total volume of the system.

ii) Molar and mass density

The molar density of the system is defined as:

$$\rho = \frac{n_{total}}{V} \quad (B-3)$$

Since the volume is solved from equation (B-2), it implies that the mass density is dependent on the first-order volume derivative of the state function and is therefore considered as a first-order property. The mass density is obtained from:

$$\rho_{mass} = \rho \times M_w \quad (B-4)$$

M_w is the molecular weight.

iii) Compressibility factor

The compressibility factor is defines as:

$$Z = \frac{PV}{RT} \quad (B-5)$$

iv) Fugacity coefficient

The fugacity coefficient is the main property used in phase equilibrium calculations and is undoubtedly the most important property of interest. It is dependent on the first-order compositional derivative of the state function and is defined by equation (B-6):

$$\ln \hat{\phi}_i = \left(\frac{\partial F}{\partial n_i} \right)_{T,V} - \ln Z \quad (B-6)$$

v) Saturated vapour pressure and saturated liquid density

It is important to mention at this point the significance of the saturated vapour pressure and liquid density data. The saturated vapour pressure of a pure component is the equilibrium pressure exerted by the liquid phase or differently stated, where the fugacity of the liquid and vapour phases are the same:

$$f^v = f^l \quad (B-7)$$

The fugacity in phase α is defined as:

$$f^\alpha = \hat{\phi}_i^\alpha P \quad (B-8)$$

The saturated liquid density is the density in the liquid phase where the fugacities of the vapour and liquid phases are the same.

vi) Excess properties

Excess properties are defined as the property of the mixture minus that of the equivalent ideal mixture at constant temperature and pressure. The definition is equivalent to the difference between the residual property of the mixture and the corresponding pure component contributions as defined by equation (B-9):

$$M^E = M^r(T, P, \mathbf{n}) - \sum_i^{nc} M_i^r(T, P, n_i) \quad (B-9)$$

Excess properties are considered to arise as a result of a few possible contributions (108):

- A combinatorial or positional entropy of mixing, whose value is not affected by the chemical nature of components, but only by their relative sizes.
- An interactional contribution due to an energetic weakness of *unlike a-b* interactions relative to *like a-a* and *b-b* interactions. This is attributed to the dissimilarity of the chemical nature between two component molecules, which are thus surrounded by force fields of different strength.
- A contribution from volume changes during the mixing process when the pure components are of different free volumes.
- A contribution associated with the effect of structure or order, which may be decreased or enhanced in passing from the pure to the solution state – structural effects of hydrogen bonded networks fall in this category.

vii) Excess enthalpy

This results in the following definition for excess enthalpy:

$$H^E = H^r(T, P, \mathbf{n}) - \sum_i^{nc} H_i^r(T, P, n_i) \quad (B-10)$$

$H^r(T, P, \mathbf{n})$ and $H_i^r(T, P, n_i)$ are the mixture and pure component residual enthalpies and defined as follows:

$$H^r(T, P, \mathbf{n}) = -RT^2 \left(\frac{\partial F}{\partial T} \right)_{V, \mathbf{n}} + PV - nRT \quad (B-11)$$

The excess enthalpy is a first-order property. The excess enthalpy is also equal to the heat of mixing which is a common property used in process design. Theoretically this property also holds some significance and systems composed of alcohols and other organic compounds provide reliable data for testing the following (279):

- model theories of mixtures
- improving group contribution methods
- promoting the understanding of the states, structure and interactions of components in solution

viii) Heat of vapourisation

The heat of vapourisation is defined as the difference in enthalpy between the liquid and vapour phases at saturated conditions:

$$H^{vaporization} = H^{liq}(T, P^{sat}, \mathbf{n}) - H^{vap}(T, P^{sat}, \mathbf{n}) \quad (B-12)$$

This simplifies to:

$$H^{vaporization} = H^{r,liq}(T, P^{sat}, \mathbf{n}) - H^{r,vap}(T, P^{sat}, \mathbf{n}) \quad (B-13)$$

ix) Excess volume

Excess volume is defined by equation (B-14) at constant pressure:

$$V^E = V_{mix}(T, P, \mathbf{n}) - \sum_i^{nc} V_{pure,i}(T, P, n_i) \quad (B-14)$$

The excess volume is therefore also strongly dependent on the first-order volume derivative of the state function. Accurate description of the property requires that the pure component first-order volume derivative and the mixture volume derivative be accurately described by the models.

B.1.3 Second-order derivative properties

The following properties are classified as second-order properties, because they are defined in terms of second-order partial derivatives of the state function:

i) Pressure-volume derivative

The pressure-volume derivative is often encountered in the definition of other properties and is dependent on the second-order volume derivative of the state function:

$$\left(\frac{\partial P}{\partial V}\right)_{T,\mathbf{n}} = -RT \left(\frac{\partial^2 F}{\partial V^2}\right)_{T,\mathbf{n}} - \frac{nRT}{V^2} \quad (B-15)$$

ii) Isochoric heat capacity

The isochoric heat capacity is an important property, because the residual part is only dependent of temperature partial derivatives of the state function:

$$C_V(T, V, \mathbf{n}) = C_V^{ideal}(T) + C_V^r(T, V, \mathbf{n}) \quad (B-16)$$

$$\frac{C_V^r(T, V, \mathbf{n})}{R} = -T^2 \left(\frac{\partial^2 F}{\partial T^2}\right)_{V,\mathbf{n}} - 2T \left(\frac{\partial F}{\partial T}\right)_{V,\mathbf{n}} \quad (B-17)$$

$$C_V^{ideal} = C_P^{ideal} - R \quad (B-18)$$

The ideal isobaric heat capacity part is estimated with DIPPR correlations (95).

iii) Isobaric heat capacity

The isobaric heat capacity is a commonly used property in industry, it is also extremely complex mathematically, and description of the property adequately tests the physical framework of any EOS. The residual part of the property is defined by equation (B-19):

$$\frac{C_P^r - C_V^r}{R} = -\frac{T \left(\frac{\partial P}{\partial T} \right)_{V,n}^2}{R \left(\frac{\partial P}{\partial V} \right)_{T,n}} - n \quad (B-19)$$

iv) Pressure-temperature derivative

The pressure-temperature derivative in the definition of the isobaric heat capacity is defined by:

$$\left(\frac{\partial P}{\partial T} \right)_{V,n} = -RT \left(\frac{\partial^2 F}{\partial T \partial V} \right)_n + \frac{P}{T} \quad (B-20)$$

The derivative adequately tests both the temperature and volume dependency of any model.

v) Isothermal compressibility

The isothermal compressibility is defined as follows:

$$\beta_T = -\frac{1}{V} \left(\frac{\partial V}{\partial P} \right)_{T,n} = -\frac{1}{V} \left/ \left(\frac{\partial P}{\partial V} \right)_{T,n} \right. \quad (B-21)$$

vi) Isentropic compressibility

The isentropic compressibility is very similar to the isothermal compressibility. The heat capacity ratio acts as an additional scaling factor. The isentropic compressibility is the main term used in the speed of sound calculations.

$$\beta_s = -\frac{1}{V} \left(\frac{\partial V}{\partial P} \right)_s = -\frac{1}{V} \frac{C_V}{C_P} \left/ \left(\frac{\partial P}{\partial V} \right)_{T,n} \right. \quad (B-22)$$

vii) Heat capacity ratio / adiabatic index

This ratio of heat capacities is also known as the adiabatic index (99):

$$\gamma = \frac{C_P}{C_V} = \frac{\beta_T}{\beta_s} \quad (B-23)$$

viii) Isobaric thermal expansivity

The isobaric thermal expansivity is calculated as follows:

$$\alpha_P = \beta_T \left(\frac{\partial P}{\partial T} \right)_{V,n} \quad (B-24)$$

ix) Speed of sound

The speed of sound is calculated from equation (B-25):

$$u = \sqrt{\frac{V}{\beta_s M_w}} \quad (B-25)$$

It may also be expressed as:

$$u = \sqrt{-\frac{V^2 \cdot \gamma \cdot \left(\frac{\partial P}{\partial V}\right)_{T,n}}{M_w}} \quad (B-26)$$

$$M_w = \sum_i^{nc} n_i M_{wi} \quad (B-27)$$

Usually speed of sound is measured and then the compressibilities are calculated from the data by using thermodynamic relations. The speed of sound requires accurate description of the following partial derivatives of the state function:

$$\left(\frac{\partial F}{\partial V}\right)_{T,n}, \left(\frac{\partial F}{\partial T}\right)_{V,n}, \left(\frac{\partial^2 F}{\partial V^2}\right)_{T,n}, \left(\frac{\partial^2 F}{\partial T^2}\right)_{V,n}, \left(\frac{\partial^2 F}{\partial T \partial V}\right)_n$$

The speed of sound therefore is sound test for physical framework behind any thermodynamic model.

x) Joule-Thomson coefficient

The Joule-Thomson coefficient is crucial to the design of throttling processes. From the definition in equation (B-28), the property also serves as a sound test for any EOS model:

$$\eta = \left(\frac{\partial T}{\partial P}\right)_{H,n} = -\frac{1}{C_p} \left(V + T \frac{\left(\frac{\partial P}{\partial T}\right)_{V,n}}{\left(\frac{\partial P}{\partial V}\right)_{T,n}} \right) \quad (B-28)$$

xi) Fugacity coefficient derivatives

The fugacity coefficient derivatives are extensively used to make phase equilibrium calculation more efficient. The properties are naturally second-order properties:

Pressure

$$\left(\frac{\partial \ln \hat{\phi}_i}{\partial P}\right)_{T,n} = \frac{\bar{V}_i}{RT} - \frac{1}{P} \quad (B-29)$$

With the partial molar volume defined as:

$$\left(\frac{\partial V}{\partial n_i}\right)_{T,P} = \bar{V}_i = -\left(\frac{\partial P}{\partial n_i}\right)_{T,V} / \left(\frac{\partial P}{\partial V}\right)_{T,n} \quad (B-30)$$

Temperature

$$\left(\frac{\partial \ln \hat{\phi}_i}{\partial T}\right)_{P,n} = \left(\frac{\partial^2 F}{\partial T \partial n_i}\right)_V + \frac{1}{T} - \frac{\bar{V}_i}{RT} \left(\frac{\partial P}{\partial T}\right)_{V,n} \quad (B-31)$$

Composition

$$n \left(\frac{\partial \ln \hat{\phi}_i}{\partial n_j}\right)_{T,P} = n \left(\frac{\partial \ln \hat{\phi}_j}{\partial n_i}\right)_{T,P} = n \left(\frac{\partial^2 F}{\partial n_i \partial n_j}\right)_{T,V} + 1 + \frac{n}{RT} \frac{\left(\frac{\partial P}{\partial n_j}\right)_{T,V} \left(\frac{\partial P}{\partial n_i}\right)_{T,V}}{\left(\frac{\partial P}{\partial V}\right)_{T,n}} \quad (B-32)$$

xii) Excess isobaric heat capacity

The excess isobaric heat capacity is defines as:

$$C_p^E = C_p^r(T, P, \mathbf{n}) - \sum_i^{nc} C_{p,i}^r(T, P, n_i) \quad (B-33)$$

B.2 Algorithms

B.2.1 EOS root finding strategy

In this project, the temperature and pressure are usually specified and it is necessary to calculate the volume at these conditions. A general Newton-Raphson method is used to solve for the required vapour or liquid volume as discussed by Michelsen and Mollerup (3). The working equations are set up in terms of new variable, β , which is defined as “total hard-sphere volume”/“total volume”. This implies that the solution is always between 0 and 1, making it easier to perform Newton-Raphson iterations. It also ensures that un-realistic liquid volumes are not obtained in high-order EOS.

B.2.2 Phase equilibrium calculations

The binary two-phase algorithm employed is based on the strategy proposed by Michelsen and Mollerup (3). Essentially, a set of nonlinear equations are set up that are based on the equifugacity criterion and the conservation of mass. The independent variables solved for are K-factors, mole fractions and P or T , depending on whether an isothermal or isobaric flash is required. A

combination of Successive Substitution iterations and Second-order Newton iterations are used to solve the equations.

The algorithm also performs stability checks with the tangent-plane-distance method as discussed in Michelsen and Mollerup (3). Similar strategies are followed in binary three-phase and ternary two-phase calculations.

B.2.3 Regression

A Levenberg-Marquart regression algorithm is used to determine model parameters for the newly developed EOS.

B.2.4 Solution to the association term

The association term in models such as sPC-SAFT and CPA increases the numerical intensity of the models considerably. The expression for the association term in a mixture is:

$$\frac{A^{assoc}}{RT} = \sum_i n_i \sum_{A_i} \left(\ln X_{A_i} - \frac{1}{2} X_{A_i} + \frac{1}{2} \right) \quad (B-34)$$

n_i refers to the number of moles of component i and the X_{A_i} refers to the fraction of un-bonded monomers at site A on molecule i . These fractions of un-bonded monomers are in turn calculated from a solution of the set of nonlinear equations in the following form (30):

$$X_{A_i} = \frac{1}{1 + \frac{1}{V} \sum_j n_j \sum_{B_j}^{M_j} X_{B_j} \Delta^{A_i B_j}} \quad (B-35)$$

V is the total volume and $\Delta^{A_i B_j}$ is the association strength between site A on molecule i and site B on molecule j . It is here that the additional complexity is evident as the fraction of un-bonded molecules is dependent on itself.

Although equation (B-35) can be analytically solved for specific bonding types as tabulated in the original SAFT-HR paper (26), the problem now becomes that the form of the analytical equations are bonding-type dependent and this makes the coding system specific. So each time the different molecules are used with different bonding schemes, the computer code has to be changed (9). Problems and complexities like these established the need to develop solution procedures that can handle the calculations involved in equation (B-35) and its derivatives.

There are two main solution procedures to the association term: Tan's method (280; 281) and Michelsen's method (30; 282; 283). In this work the solution procedure of Michelsen is used and is briefly described below:

i) Michelsen's method

Michelsen and Hendriks (30) introducing a mathematical Q -function that is equivalent to the association term exporession presented in equation (B-34) when the function is at a maximum and is given below:

$$Q(T, V, \mathbf{X}, \mathbf{n}) = \sum_i^{nc} n_i \sum_{A_i} \left(\ln X_{A_i} - X_{A_i} + 1 \right) - \frac{1}{2} \sum_i^{nc} \sum_j^{nc} n_i n_j \sum_{A_i} \sum_{B_j} X_{A_i} X_{B_j} \Delta^{A_i B_j} \quad (B-36)$$

In a subsequent paper, Michelsen further simplified equation (B-36), by simplifying the notation used for indicating a site on a molecule. Effectively each site is considered separately and a new vector m is defined, which is the number of moles that host a given site. Furthermore, equilibrium-like constants are defined as follows:

$$K_{lk} = K_{kl} = \frac{m_l m_k \Delta^{lk}}{V} \quad (B-37)$$

m_l and m_k are the number of moles that host sites l and k and Δ^{lk} is the association strength between the two sites. The working equation therefore becomes:

$$Q(T, V, \mathbf{X}, \mathbf{n}) = \sum_k^S m_k (\ln X_k - X_k + 1) - \frac{1}{2} \sum_k^S \sum_l^S K_{kl} X_k X_l \quad (B-38)$$

Then the gradient vector is equal to:

$$g_k = \frac{\partial Q}{\partial X_k} = m_k \left(\frac{1}{X_k} - 1 \right) - \sum_l^S K_{kl} X_l \quad (B-39)$$

At a maximum of Q and a solution to the Helmholtz energy contribution due to association, the gradient vector should be zero. When the gradient is zero, a solution to \mathbf{X} is obtained. The Hessian of the Q -function is:

$$H_{kl} = - \left(\frac{m_k}{X_k^2} \right) \delta_{kl} - K_{kl} \quad (B-40)$$

Michelsen proposes a *Successive Substitution* Procedure combined with *Second-Order* Method to solve the equations.

Successive substitution

The form of equation (B-39) suggests that *Successive Substitution* is a simple solution to use in solving the equations (282). In terms of the new variables the procedure becomes:

$$X_k^{(n+1)} = f_k(\mathbf{X}^{(n)}) = \frac{m_k}{m_k + \sum_l^S K_{kl} X_l^{(n)}} \quad (B-41)$$

Successive Substitution will be rapidly convergent if \bar{f} is only weakly dependent on \mathbf{X} (282). Convergence will be linear with a rate determined by the numerically largest eigen value of the Jacobian matrix of \bar{f} . Michelsen (282) analysed the convergence behaviour further by examining a series of common association schemes (as defined by Huang and Radosz (26; 27)). In some cases it is more advantages to use *damped Successive Substitution* as follows:

$$X_k^{(n+1)} = (1 - \omega) \frac{m_k}{m_k + \sum_l K_{kl} X_l^{(n)}} + \omega X_l^{(n)} \quad (B-42)$$

ω is the damping factor between 0 and 1. The main conclusions from the convergence analysis are presented in Table B-1:

Table B-1: Convergence behaviour of Successive Substitution

Scheme	Eigen values λ	Convergence
1A	<ul style="list-style-type: none"> Always negative Vapour like phase, λ close to zero Liquid like phase, λ close to -1 	<ul style="list-style-type: none"> Oscillatory Vapour phase rapid convergence Liquid phase slow convergence – better when damped
2B	<ul style="list-style-type: none"> Two λ with same magnitude but opposite sign 	<ul style="list-style-type: none"> Will depend on how the molecules interact with other molecules in mixture
3B	<ul style="list-style-type: none"> Two λ of equal magnitude with opposite sign and one λ equal to zero 	<ul style="list-style-type: none"> Rapid convergence in the un-damped case compared to the other schemes

Second-order methods

A key strength of Michelsen's method is that the problem can be formulated as an unconstrained maximization problem where global convergence is guaranteed (282). This makes second-order methods very attractive with this problem. Michelsen (282) proposes to use the following Newtonian iteration scheme:

$$\hat{\mathbf{H}}\Delta\mathbf{X} + \mathbf{g} = 0 \quad (B-43)$$

$\hat{\mathbf{H}}$ is a modified Hessian matrix with the following properties (282):

- It is negative definite for all \mathbf{X}
- At the solution $\hat{\mathbf{H}} = \mathbf{H}$

This implies that the direction of $\Delta\mathbf{X}$ will always be an *ascent* direction leading to an increase in the objective function. Should the iteration fail when the full step is taken, a simple line search can be used as remedy (282). The modified Hessian is expressed in equation (B-44) and the proof that it is equal to the original Hessian at the solution is given by Michelsen in ref. (282):

$$\hat{H}_{kl} = - \left(\frac{1}{X_k} \left(m_k + \sum_j K_{kj} X_j \right) \right) \delta_{kl} - K_{kl} \quad (B-44)$$

Michelsen's general algorithm

Michelsen (282) outlines a general algorithm that utilizes the equations above. The main steps as implemented in this work are outlined below (282):

1. Perform 5 steps of *Successive Substitution* with $\omega = 0.2$ and proceed to second-order Newton iterations.
2. Calculate the step $\Delta \mathbf{X}$ from equation (B-43) for the Newton iteration and save a copy of the values $\Delta \mathbf{X}^{copy}$.
3. Set $X_m^{new} = \max(X_m^{old} + \Delta X_m, 0.2 X_m^{old})$. This ensures that all X_m^{new} is positive and that X_m^{old} is not reduced by more than a factor of 5. (The elements of \mathbf{X}^{new} can be tested to ensure they are all positive, if not raise a violation flag).
4. Evaluate the Q -function with \mathbf{X}^{new} and test whether an increase of the objective function were managed, if not raise a violation flag.
5. If the violation flag was raised, set $\Delta \mathbf{X} = \frac{1}{2} \Delta \mathbf{X}$ and return to step 3.
6. If violation flag was not raised, check for convergence. This is done by evaluating the step values in $\Delta \mathbf{X}^{copy}$. If all elements in $\Delta \mathbf{X}^{copy}$ is essentially zero, convergence has been reached. If not set $\mathbf{X}^{old} = \mathbf{X}^{new}$ and repeat from step 2.

Appendix C

Conceptual review behind current state-of-the-art SAFT models

The aim of this appendix is to conceptually review some versions of SAFT that have been successfully applied, to not only phase equilibria properties, but also to some other thermodynamic derivative properties. It was considered to use some of these models for the investigation, but as will be shown, sPC-SAFT and CPA are the appropriate starting point.

C.1 Soft-SAFT (1997) and cross-over soft SAFT (2004)

Soft-SAFT was developed by Blas and Vega (284; 285) in 1997. The main difference between soft-SAFT and the original version of SAFT is that soft-SAFT uses spheres that act according to a Lennard-Jones intermolecular potential for the reference fluid and thereby effectively accounts for repulsive and dispersive interactions simultaneously, instead of the perturbation scheme based on a hard-sphere reference fluid plus dispersive contributions to it (285). They used the Lennard-Jones reference term developed by Johnson *et al.* (286) to account for the repulsive and dispersive interactions. In the original SAFT, the hard-sphere radial distribution function is used in the calculations of the chain and association terms, while in soft-SAFT, the radial distribution function of a Lennard-Jones fluid is used (287). Soft-SAFT has been successfully applied to the phase equilibria of pure long chain *n*-alkanes (287), the phase equilibria of multi-component *n*-alkane mixtures (285) and the critical properties of *n*-alkane binary mixtures (288). Soft-SAFT has also been applied to predict Joule-Thomson inversion curves for some members of the *n*-alkane series and carbon dioxide (89). Colina *et al.* (89) observed that the prediction of these Joule-Thomson curves are strongly dependent on the set of parameters used in the calculations for each component and stresses the importance of fine-tuning the parameters in the fitting procedure. Furthermore, the EOS has been used to predict isochoric & isobaric heat capacities, Joule-Thomson inversion curves and speed of sound for selected *n*-alkane and 1-alkanols (289). Applications also extend to selected binary mixtures of *n*-alkane/*n*-alkane and *n*-alkane/1-alkanol mixtures (88) in which some second-order derivative properties are also modelled, however, the success was limited.

The EOS requires three pure component parameters for non-associating fluids and five parameters for associating fluids. The model also does not explicitly account for polar forces.

Cross-over soft SAFT is an extension of soft-SAFT that accounts for long range density fluctuations in the critical region, but reduces to soft-SAFT far from the critical region (278). The cross-over treatment is based on renormalization group theory (278) and introduces two additional parameters, making the EOS a five parameter model for non-associating components and a seven parameter model for associating components. The cross-over soft-SAFT has been applied to the global phase equilibria of selected components and mixtures (290; 291) and to derivative properties of selected *n*-alkane/*n*-alkane and *n*-alkane/1-alkanol mixtures (292).

The group, however, estimated their model parameters by only including saturated vapour pressure and liquid density data in the regression procedure and argues that including other properties in the fit would reduce the predictive power of the model.

C.2 SAFT-CP (modified SAFT-BACK) (2001)

SAFT-CP where the CP stands for ‘across critical points’ was developed by Chen and Mi (90) and is also referred to in the literature as modified SAFT-BACK (293; 294). The model differs from the original SAFT of Huang and Radosz (26; 27) in two ways.

The first major difference is that a hard convex body fluid is used as the reference fluid, instead of the usual hard-sphere fluid (90). This modification gives consideration to the segment shape in chain molecules by using the hard convex body EOS of Boublik (295) as the reference term and the related expression for chain formation with the radial distribution function of the hard convex body fluid (90). The main idea is to take into account the non-sphericity of the molecules. The degree of non-sphericity is characterized by an additional pure component parameter, α .

Originally Chen and Kreglewski (296) combined the hard convex body EOS with an equation developed by Alder *et al.* (297) to form the (Boublik-Alder-Chen-Kreglewski) BACK EOS, which is successful in calculating thermodynamic properties for small non-spherical molecules like argon and nitrogen, but cannot be used for chain molecules (90). The dispersion term of Alder *et al.* (297) is the same term used by the original SAFT models. Pfohl and Brunner (298) then used BACK to modify SAFT by replacing the hard-sphere reference fluid with the hard convex body reference fluid and obtained improved results for small non-spherical molecules, but there were still some shortcomings for larger molecules in the near critical region. This led to the second modification made by Chen and Mi.

Chen and Mi (90) were able to derive a new dispersion term from perturbation theory that excludes dispersion energy between intramolecular segments, in other words, the effect of chain formation on the dispersion term (similar to PC-SAFT(24)). Chen and Mi (90) showed that chain

formation on dispersion can be incorporated by taking only a fraction of the original dispersion term of Alder *et al.* (297) and is expressed by the following equation:

$$A^{chain,disp} = \lambda \left(\frac{A^{chain,hcb}}{A^{hcb}} \right) A^{disp} \quad (C-1)$$

λ is a constant as a result of conformational characteristics of the interaction potentials and can be kept constant for fluids with the same interaction potential (90). The equation with these two modifications was then applied to calculate phase diagrams (saturation lines and P-V-T behaviour) and vapourisation enthalpies for some *n*-alkanes (90). No binary mixture properties were considered.

The EOS was later extended with an additional term to account for polar interactions explicitly (299) and required one more additional parameter denoted, *c*. Mi *et al.* (299) only applied this extended equation to polar fluids that doesn't self-associate and calculated phase diagrams for a few components (*P-V-T* and saturation lines). In a subsequent paper, Chen *et al.* (300) applied this EOS to water and alkanols. They obtained improved results by only including the polar term and excluding the association term (300). However, they included the dipole moment and *c* as adjustable parameters in the regression. This means that six parameters were used to model a component. The equation in this form was used to calculate phase diagrams (saturation lines and *P-V-T* behaviour) for some 1-alkanol as well (300).

Maghari and co-workers (293; 294; 301) applied SAFT-CP to calculate speed of sound in *n*-alkanes, common bulk modulus, zero-countours and isothermal bulk modulus and Joule-inversion curves of polar (non-HB) and non-polar fluids.

C.3 SAFT-VR Mie (2006)

In SAFT-VR Mie, the VR part of the model characterizes the equation by a variable potential function and the Mie part of the equation indicates that an *n-m* Mie potential function is used to describe the repulsive and dispersion interactions (56). Lafitte *et al.* (56) conducted an investigation in which they compared the prediction of several SAFT-type models (PC-SAFT, SAFT-VR SW, SAFT-VR LJ) for thermodynamic derivative properties including speed of sound, isobaric heat capacity and isothermal compressibility in either saturated or in compressed fluid conditions. They found that the models are unable to predict these properties. However, it seems as if a systematic approach was not followed and the results were not clearly published as to why the above-mentioned models were unable to correlate second-order properties.

Lafitte *et al.* (56) then assumed that SAFT contains the correct physics to model derivative properties and proposed that the deficiency in the model is due to an incorrect description of the intermolecular potential function. They then proposed to use the *n-m* Mie potential function where the *n* and *m* are the respective repulsive and attractive exponents that characterize the

distance dependency of these forces. The repulsive exponent is considered as an extra pure component parameter. The justification for the additional parameter came from the observation of the well known Lennard-Jones potential function where the attractive exponent was set equal to a value of six, because it matches the trend of the dispersion and dipole-dipole interactions (57). The repulsive exponent was set equal to a twelve, because it was mathematically convenient (57). Lafitte *et al.* (57) then argued that this value was not physically supported and had no formal background and mentioned that the influence of a non-conformal intermolecular potential function on thermodynamic derivative properties is a purposeful investigation (57). Their work further showed that the influence of the repulsive exponent in the potential function had a decisive influence on second-derivative properties. The model was applied to phase equilibria and other properties of pure *n*-alkanes (56) and pure 1-alkanols (57). Properties of selected *n*-alkane/1-alkanol binary mixtures were also modelled (57). The model was also applied to the properties of hydrofluoroethers (140).

The model was more successful than the other SAFT-type models in correlating second-order derivative properties, however, a disadvantage of the model is that it requires an additional pure component parameter.

C.4 Comparison of SAFT type models

In the previous section a multitude of models that originated from the SAFT theory is presented. The main concept behind each model and a few applications were briefly mentioned. The aim of this section is to present a short comparison between the models in order to highlight the main differences between the models. This comparison is presented in Table C-1 where the different types of interactions that are explicitly accounted for by models are indicated. The Helmholtz energy contribution term that accounts for these interactions are also indicated and the amount of pure component model parameters required for each model is also shown.

In Table C-1 comments surrounding the application of the models are mentioned. The aim is to give comments on the thermodynamic modelling that has been done on phase equilibria and derivative properties with these SAFT-type equations mentioned. It is not the idea to mention every single application, but more to give a qualitative description of the models' performance.

Table C-1: Comparison between major types of interactions accounted for in certain SAFT type models and the amount of pure component parameters they require

Model	Repulsive interactions	Chain formation	Dispersion interactions	Influence of chain formation on dispersion	Association interactions	Dipolar interactions	Parameters		
							NP	P	HB
PC-SAFT	Yes , via hard-sphere reference term.	Yes , via chain term from Wertheim with hard-sphere RDF.	Yes , via dispersion term from Gross and Sadowski.	Yes , via dispersion term from Gross and Sadowski.	Yes , via association term from Wertheim with hard-sphere RDF.	No , but accounted for via <i>Van der Waals</i> approach.	3	3	5
sPC-SAFT	Yes , via hard-sphere reference term.	Yes , via chain term from Wertheim with hard-sphere RDF.	Yes , via dispersion term from Gross and Sadowski.	Yes , via dispersion term from Gross and Sadowski.	Yes , via association term from Wertheim with hard-sphere RDF.	No , but accounted for via <i>Van der Waals</i> approach.	3	3	5
Soft-SAFT	Yes , via Lennard-Jones reference term.	Yes , via chain term from Wertheim with Lennard-Jones RDF.	Yes , via Lennard-Jones reference term.	No.	Yes , via association term from Wertheim with Lennard-Jones RDF.	No , but accounted for via <i>Van der Waals</i> approach.	3	3	5
Cross over soft-SAFT	Yes , via Lennard-Jones reference term.	Yes , via chain term from Wertheim with Lennard-Jones RDF.	Yes , via Lennard-Jones reference term.	No.	Yes , via association term from Wertheim with Lennard-Jones RDF.	No , but accounted for via <i>Van der Waals</i> approach.	5	5	7
SAFT-CP + polar	Yes , via hard-convex-body reference term.	Yes , via chain term from Wertheim with hard-convex-body RDF.	Yes , via dispersion term from Chen and Kreglewski.	Yes , via dispersion term of Chen and Mi.	No.	Yes , via a polar term that is based on a molecular approach.	4	5	6
SAFT-VR Mie	Yes , via hard-sphere reference term.	Yes , via chain term from Wertheim with cavity function that is obtained by doing a first-order high temperature expansion on the hard-sphere RDF.	Yes , via dispersion term developed by Lafitte that is based on Mie potential.	No.	Yes , via association term from Wertheim with cavity function that is obtained by doing a first-order high temperature expansion on the hard-sphere RDF.	No , but accounted for via <i>Van der Waals</i> approach.	4	4	6

Model	Repulsive interactions	Chain formation	Dispersion interactions	Influence of chain formation on dispersion	Association interactions	Dipolar interactions	Parameters		
							NP	P	HB
CPA	Yes, via SRK repulsive term.	No.	Yes, via SRK attractive term.	No.	Yes, via association term from Wertheim with simplified RDF.	No, but accounted for via <i>Van der Waals</i> approach.	3	3	5

From Table C-1, it is clear which molecular interaction are explicitly accounted for by the different models. This of course does not imply that all models are equally accurate, since the accuracy of the models depends on the extent to which the models are able to account for the different types of interactions. It should be mentioned that all of the models are fairly capable to give a good representation of the pure component phase equilibria properties (saturated vapour pressure and liquid density) with the parameters available to correlate them. Some of the models, however, give better representation of mixture phase equilibria properties of complex properties, but this comes at the expense of an additional pure component parameter, while models such as PC-SAFT and CPA need larger binary interaction parameters values to correlate mixture phase equilibria. Some models such as SAFT-VR Mie and SAFT-CP does not explicitly account for polar interactions, but requires an additional pure component parameter to correlate repulsive and *Van der Waals* interactions (dispersive and polar lumped together).

As mentioned in the performance criteria (section A.3), a goal for theoretical EOS is to provide good description of pure component properties with as few parameters as possible.

CPA, sPC-SAFT and PC-SAFT require the least amount of pure component parameter and have not yet been extensively applied to especially second-order properties. They possibly serve as a good starting point to investigate how much thermodynamic properties can be accurately correlated with as few pure component model parameters as possible. In the event that unsatisfactory results are obtained, the EOS models may then either be extended by including a polar term or a more complex model such as SAFT-VR Mie may be adopted.

In Table C-2 comments are made regarding the various applications of the models surrounding phase equilibria and other derivative properties.

Table C-2: Comments on application of SAFT type models to derivative properties

Model	Phase equilibria applications	Derivative property applications
PC-SAFT	<ul style="list-style-type: none"> Wide application to non-polar, polar and hydrogen bonding components and their mixtures with fair accuracy. Relatively large values of binary interaction parameters required for highly non-ideal systems. 	<ul style="list-style-type: none"> Very limited application to other thermodynamic properties, especially second-order properties.
sPC-SAFT	<ul style="list-style-type: none"> Wide application to non-polar, polar and hydrogen bonding components and their mixtures. Relatively large values of binary interaction parameters required for highly non-ideal systems. Simplification from PC-SAFT does not influence accuracy of phase equilibria calculations in mixtures. 	<ul style="list-style-type: none"> No applications to mixture second-order properties could be found.
Soft-SAFT and Cross-over soft-SAFT	<ul style="list-style-type: none"> Phase equilibria considered were primarily for <i>n</i>-alkanes and alcohols and their binary mixtures. Polar (non-HB) fluids not considered. Good accuracy in critical region with cross-over treatment. Binary interaction parameters required to model mixture. 	<ul style="list-style-type: none"> Various derivative properties of a few selected <i>n</i>-alkanes and alcohols and their binary mixtures. Properties modelled include speed of sound, isochoric & isobaric heat capacities and Joule-Thomson inversion curves. Model is able to capture trends in the critical region of properties that show singularities, but with limited accuracy.
SAFT-CP + polar	<ul style="list-style-type: none"> Phase behaviour of non-polar, polar and hydrogen bonding of selected components with good accuracy in the critical region. Very limited application to mixtures. 	<ul style="list-style-type: none"> Various derivative properties modelled including speed of sound and Joule-Thomson inversion curves for limited number of <i>n</i>-alkanes and alcohols. No application to mixtures properties.
SAFT-VR Mie	<ul style="list-style-type: none"> Phase behaviour of <i>n</i>-alkanes, alcohols and hydrofluoro ethers. Polar (non-HB) components not considered. Binary mixtures of <i>n</i>-alkanes/1-alcohols also considered. Selectec fluorocarbons also considered. 	<ul style="list-style-type: none"> Speed of sound, thermal expansion, isobaric heat capacities for <i>n</i>-alkanes and alkanols reported, but with limited accuracy. SAFT-VR Mie seems to give an improved description compared to other models. Limited application to mixtures properties could be found.

Model	Phase equilibria applications	Derivative property applications
CPA	<ul style="list-style-type: none"> • Wide application to non-polar, polar and hydrogen bonding component and their mixtures with good accuracy. • Relatively large values of binary interaction parameters required for highly non-ideal systems. 	<ul style="list-style-type: none"> • Only speed of sound for methanol and water and their binary mixture with limited accuracy.

Table C-2 emphasizes the following points:

- Models such as CPA, PC-SAFT and sPC-SAFT have been successfully applied to the phase equilibria of a wide range of pure components and their mixtures, but not to other thermodynamic derivative properties.
- Newer models such as SAFT-CP, soft-SAFT and SAFT-VR Mie have been applied to the pure components phase equilibria and derivative properties, but usually only *n*-alkanes and alcohols were considered. Very limited application to mixtures and to polar components that do not self-associate.

Based on the information presented in this section, it was decided to further investigate the performance of sPC-SAFT and CPA in this project. The two main reasons that can be extracted from this section are:

- The models have not yet been extensively applied to other derivative properties than those utilized in phase equilibria calculations.
- The models require the least amount of pure component model parameters.

Appendix D

Validation of model reliability & accuracy

The aim of this appendix is to validate the correctness of the EOS models programmed coded for this project.

Numerical differentiation was carried out by means of central differences:

$$\frac{\partial f(\mathbf{x})}{\partial x_i} = \frac{f(\mathbf{x}, x_i + \varepsilon) - f(\mathbf{x}, x_i - \varepsilon)}{2\varepsilon} \quad (D-1)$$

With $\mathbf{x} \in \{n_i, \dots, n_c, T, V\}$

A comparison between the numerical and analytical derivatives for a one components system is presented below for each EOS used in this study. Water was used as sample component at $T = 300$ K and $V = 0.015$ l/mol. Parameters based on the 4C association scheme was used.

Table D-1: Numerical and analytical derivatives of sPC-SAFT

Derivative	Numerical	Analytical	% difference
F	-8.747165	-8.747165	
$\partial F / \partial V$	-660.6700	-660.6700	-6.783E-08
$\partial F / \partial T$	0.053480	0.053480	-1.069E-07
$\partial^2 F / \partial V^2$	434757.3	434757.35	-1.159E-07
$\partial^2 F / \partial V \partial T$	1.027172	1.027172	-6.851E-08
$\partial^2 F / \partial T^2$	-0.000400	-0.000400	-2.363E-08
$\partial F / \partial n_i$	1.162886	1.162886	-2.628E-07
$\partial^2 F / \partial V \partial n_i$	-6521.360	-6521.360	-6.646E-08
$\partial^2 F / \partial T \partial n_i$	0.038072	0.038072	9.079E-09
$\partial^2 F / \partial n_i \partial n_j$	97.820404	97.820404	-2.69E-08

Table D-2: Numerical and analytical derivatives of sPC-SAFT-GV

Derivative	Numerical	Analytical	% difference
F	-8.972419	-8.972419	
$\partial F/\partial V$	-519.9174	-519.9174	-6.796E-08
$\partial F/\partial T$	0.053551	0.053551	-1.121E-07
$\partial^2 F/\partial V^2$	363471.26	363471.26	-1.186E-07
$\partial^2 F/\partial V\partial T$	0.828419	0.828419	-3.441E-08
$\partial^2 F/\partial T^2$	-0.000395	-0.000395	-3.164E-08
$\partial F/\partial n_i$	-1.173658	-1.173658	2.518E-07
$\partial^2 F/\partial V\partial n_i$	-5452.0689	-5452.0689	-6.978E-08
$\partial^2 F/\partial T\partial n_i$	0.041124	0.041124	-1.000E-08
$\partial^2 F/\partial n_i\partial n_j$	81.7810341	81.7810341	-3.19E-08

Table D-3: Numerical and analytical derivatives of sPC-SAFT-JC

Derivative	Numerical	Analytical	% difference
F	-9.050048	-9.050048	
$\partial F/\partial V$	-467.213644	-467.213644	-6.918E-08
$\partial F/\partial T$	0.053563	0.053563	-1.151E-07
$\partial^2 F/\partial V^2$	337301.57	337301.57	-1.166E-07
$\partial^2 F/\partial V\partial T$	0.719498	0.719498	1.161E-07
$\partial^2 F/\partial T^2$	-0.000397	-0.000397	-5.609E-08
$\partial F/\partial n_i$	-2.041843	-2.041843	1.112E-07
$\partial^2 F/\partial V\partial n_i$	-5059.523	-5059.523	-6.911E-08
$\partial^2 F/\partial T\partial n_i$	0.042770	0.042770	-3.857E-08
$\partial^2 F/\partial n_i\partial n_j$	75.89285	75.89285	-3.06E-08

Table D-4: Numerical and analytical derivatives of CPA

Derivative	Numerical	Analytical	% difference
F	-8.799212	-8.799212	
$\partial F/\partial V$	-1601.306	-1601.306	-4.100E-06
$\partial F/\partial T$	0.057062	0.057062	-1.124E-07
$\partial^2 F/\partial V^2$	4200945	4200945	-9.680E-06
$\partial^2 F/\partial V\partial T$	-0.936029	-0.936029	3.893E-08
$\partial^2 F/\partial T^2$	-0.000422	-0.000422	1.044E-08
$\partial F/\partial n_i$	15.22038	15.22038	-6.160E-06
$\partial^2 F/\partial V\partial n_i$	-63014.1	-63014.1	-9.268E-06
$\partial^2 F/\partial T\partial n_i$	0.071103	0.071103	1.378E-09
$\partial^2 F/\partial n_i\partial n_j$	945.2126	945.2127	-8.87E-06

Table D-5: Numerical and analytical derivatives of CPA-GV

Derivative	Numerical	Analytical	% difference
F	-9.155205	-9.155205	
$\partial F/\partial V$	-796.9755	-796.9755	-1.785E-06
$\partial F/\partial T$	0.056559	0.056559	-1.066E-07
$\partial^2 F/\partial V^2$	1490059.2	1490059.2	-3.573E-06
$\partial^2 F/\partial V\partial T$	-0.820978	-0.820978	4.863E-08
$\partial^2 F/\partial T^2$	-0.000423	-0.000423	7.594E-09
$\partial F/\partial n_i$	2.799429	2.799429	-7.028E-06
$\partial^2 F/\partial V\partial n_i$	-22350.88	-22350.88	-3.323E-06
$\partial^2 F/\partial T\partial n_i$	0.068873	0.068873	1.210E-09
$\partial^2 F/\partial n_i\partial n_j$	335.2633	335.2633	-3.08E-06

Table D-6: Numerical and analytical derivatives of CPA-JC

Derivative	Numerical	Analytical	% difference
F	-9.152251	-9.152251	
$\partial F/\partial V$	-888.5955	-888.5955	-2.112E-06
$\partial F/\partial T$	0.057396	0.057396	-9.285E-08
$\partial^2 F/\partial V^2$	1796954	1796954	-4.281E-06
$\partial^2 F/\partial V\partial T$	-1.143766	-1.143766	2.006E-08
$\partial^2 F/\partial T^2$	-0.000434	-0.000434	8.899E-10
$\partial F/\partial n_i$	4.176682	4.176682	-6.260E-06
$\partial^2 F/\partial V\partial n_i$	-26954.31	-26954.31	-4.007E-06
$\partial^2 F/\partial T\partial n_i$	0.074552	0.074552	-7.838E-10
$\partial^2 F/\partial n_i\partial n_j$	404.3147	404.3147	-3.74E-06

Further verification included comparing how well published model parameter correlate saturated vapour pressure and liquid densities when used with the coded models. The predictions of the models coded were also graphically compared to the VLE of binary mixtures in published articles, specifically comparisons were made for CPA and sPC-SAFT, since results are widely available for these models.

Appendix E

%AAD values of associating components and VLE results for CPA-GV and CPA-JC with the 2B scheme

E.1 %AAD values of associating components

The %AAD values obtained with the model parameters determined in Chapter 8 for the polar sPC-SAFT and CPA are presented in this subsection. The %AAD values for sPC-SAFT-GV and sPC-SAFT-JC are presented in Table E-1. The results show that both sPC-SAFT-GV and sPC-SAFT-JC provide the same measure of accuracy with all three association schemes.

Table E-1: %AADs of pure component properties obtained with parameters determined in Chapter 8 for sPC-SAFT-GV and sPC-SAFT-JC based on different association schemes

Component	Sch.	sPC-SAFT-GV			sPC-SAFT-JC		
		ΔP^{sat} [%]	$\Delta \rho^{sat}$ [%]	Δh^{vap} [%]	ΔP^{sat} [%]	$\Delta \rho^{sat}$ [%]	Δh^{vap} [%]
methanol	2B	0.45	0.17	0.92	0.45	0.19	0.45
ethanol	2B	0.07	0.10	0.89	0.10	0.07	1.15
1-propanol	2B	0.18	0.25	1.24	0.27	0.25	1.38
1-butanol	2B	0.19	0.19	1.14	0.26	0.22	1.34
1-pentanol	2B	0.05	0.16	0.79	0.08	0.13	1.02
1-hexanol	2B	0.12	0.69	0.79	0.15	0.49	1.00
1-heptanol	2B	1.22	1.50	1.42	1.36	2.51	1.83
1-octanol	2B	0.23	0.35	0.75	0.24	0.49	0.88
Average		0.31	0.43	1.00	0.36	0.54	1.13
methanol	2C	0.64	0.48	0.70	0.57	0.51	1.99
Ethanol	2C	0.09	0.11	1.74	0.07	0.09	2.56
1-propanol	2C	0.22	0.14	1.11	0.29	0.18	1.29
1-butanol	2C	0.14	0.22	1.16	0.27	0.24	1.41
1-pentanol	2C	0.14	0.21	0.85	0.10	0.16	1.00
1-hexanol	2C	0.07	0.60	0.78	0.15	0.46	1.00
1-heptanol	2C	0.23	1.05	0.66	0.56	1.42	1.08

Component	Sch.	sPC-SAFT-GV			sPC-SAFT-JC		
		ΔP^{sat} [%]	$\Delta \rho^{sat}$ [%]	Δh^{vap} [%]	ΔP^{sat} [%]	$\Delta \rho^{sat}$ [%]	Δh^{vap} [%]
1-octanol	2C	0.23	0.32	0.73	0.25	0.49	0.88
Average		0.22	0.39	0.96	0.28	0.44	1.40
methanol	3B	1.02	1.22	5.10	1.02	1.22	5.10
ethanol	3B	0.15	0.72	1.20	0.20	0.78	1.24
1-propanol	3B	0.13	0.46	1.44	0.16	0.27	1.42
1-butanol	3B	0.15	0.25	1.32	0.16	0.26	1.44
1-pentanol	3B	0.10	0.18	0.87	0.07	0.13	1.00
1-hexanol	3B	0.14	0.63	0.90	0.14	0.55	0.98
1-heptanol	3B	0.29	1.06	0.69	0.30	1.12	0.79
1-octanol	3B	0.23	0.36	0.89	0.23	0.41	0.90
Average		0.28	0.61	1.55	0.29	0.59	1.61
water	4C	1.13	2.20	3.37	1.10	1.94	3.25

The %AAD values obtained for pure component properties included in the regression function with CPA-GV and CPA-JC are presented in Table E-2:

Table E-2: %AADs of pure component properties obtained with parameters determined in Chapter 8 for CPA-GV and CPA-JC based on different association schemes

Component	Sch.	CPA-GV			CPA-JC		
		ΔP^{sat} [%]	$\Delta \rho^{sat}$ [%]	Δh^{vap} [%]	ΔP^{sat} [%]	$\Delta \rho^{sat}$ [%]	Δh^{vap} [%]
methanol	2B	0.77	0.39	2.89	0.82	0.46	3.34
ethanol	2B	0.35	0.35	2.95	0.36	0.38	2.89
1-propanol	2B	0.09	0.56	0.73	0.10	0.52	0.81
1-butanol	2B	0.09	0.74	1.26	0.09	0.74	1.4
1-pentanol	2B	0.05	0.71	0.99	0.06	0.69	1.2
1-hexanol	2B	0.11	0.74	1.11	0.08	0.67	1.29
1-heptanol	2B	0.69	1.38	1.47	0.65	1.75	1.7
1-octanol	2B	0.21	1.01	1.28	0.18	1.08	1.37
Average		0.30	0.74	1.59	0.29	0.79	1.75
methanol	3B	0.42	0.23	2.40	0.26	0.61	1.48
ethanol	3B	0.07	0.37	0.67	0.07	0.36	0.67
1-propanol	3B	0.12	0.67	1.22	0.13	0.68	1.29
1-butanol	3B	0.13	0.77	1.47	1.80	1.44	2.82
1-pentanol	3B	0.11	0.74	1.12	2.34	0.88	3.01
1-hexanol	3B	0.12	0.77	1.21	0.16	0.69	1.42
1-heptanol	3B	0.81	1.42	1.63	1.02	3.85	2.28
1-octanol	3B	0.54	0.87	1.24	0.19	1.10	1.42
Average		0.29	0.73	1.37	0.74	1.20	1.80

Component	Sch.	CPA-GV			CPA-JC		
		ΔP^{sat} [%]	$\Delta \rho^{sat}$ [%]	Δh^{vap} [%]	ΔP^{sat} [%]	$\Delta \rho^{sat}$ [%]	Δh^{vap} [%]
water	4C	0.24	0.60	2.88	0.17	0.67	3.22

E.2 VLE results with CPA-GV and CPA-JC with the 2B scheme

A summary of alkane/alcohol VLE investigated in this study is presented Table E-3 and the results show that both CPA-GV and CPA-JC provide improved VLE predictions for the systems considered here, if compared to normal CPA. Although these improvements are slightly less pronounced compared to non-associating polar/alkane systems, they are nonetheless still significant.

Table E-3: VLE predictions of alcohol/*n*-alkane mixtures with CPA, CPA-GV and CPA-JC

Mixture	<i>T</i> or <i>P</i>	CPA-2B		CPA-GV-2B		CPA-JC-2B		<i>np</i>	ref.
		Δy ($\times 10^2$) ^a	$\frac{\Delta P(\%)^b}{\Delta T(K)^a}$	Δy ($\times 10^2$) ^a	$\frac{\Delta P(\%)^b}{\Delta T(K)^a}$	Δy ($\times 10^2$) ^a	$\frac{\Delta P(\%)^b}{\Delta T(K)^a}$		
methanol/ <i>n</i> -butane	323.15 K	1.14	7.80	0.75	3.17	0.76	3.03	11	(162)
methanol/ <i>n</i> -pentane	372.7 K	4.02	7.72	2.74	4.56	2.71	4.40	11	(163)
methanol/ <i>n</i> -hexane	343.15 K	2.90	7.00	1.93	2.24	1.86	1.98	24	(164)
methanol/ <i>n</i> -hexane	348.15 K	2.94	7.54	2.60	2.89	2.69	2.64	24	(241)
ethanol/ <i>n</i> -pentane	372.7 K	2.82	7.45	1.66	3.94	1.57	3.75	10	(165)
ethanol/ <i>n</i> -hexane	298.15 K	1.20	4.22	0.18	1.01	0.34	1.80	9	(245)
ethanol/ <i>n</i> -hexane	323.15 K	2.74	6.03	1.56	2.82	1.41	2.41	20	(166)
ethanol/ <i>n</i> -heptane	333.15 K	2.41	4.05	0.71	0.71	0.62	0.63	16	(167)
ethanol/ <i>n</i> -octane	318.15 K	1.74	3.64	0.99	2.73	1.11	3.24	17	(168)
1-propanol/ <i>n</i> -hexane	323.15 K	1.77	7.77	0.53	1.28	0.54	1.29	22	(169)
1-propanol/ <i>n</i> -heptane	333.15 K	2.45	5.39	0.98	1.12	0.95	1.08	33	(169)
1-propanol/ <i>n</i> -octane	358.15 K	2.52	8.46	0.92	2.75	0.89	2.78	25	(170)
1-propanol/ <i>n</i> -octane	363.15 K	2.04	6.34	0.84	1.11	0.80	1.11	24	(247)
1-butanol/ <i>n</i> -hexane	323.15 K	0.46	5.52	0.43	3.46	0.45	3.40	10	(248)
1-butanol/ <i>n</i> -heptane	333.15 K	1.74	5.90	0.77	2.72	0.74	2.53	19	(249)
1-butanol/ <i>n</i> -nonane	323.15 K	1.34	3.24	0.92	1.36	0.93	1.42	15	(171)
1-butanol/ <i>n</i> -decane	373.15 K	2.60	6.53	1.67	3.38	1.72	3.41	22	(241)
1-butanol/ <i>n</i> -decane	383.15 K	2.34	6.02	1.40	2.74	1.44	2.79	22	(241)
1-pentanol/ <i>n</i> -heptane	348.15 K	2.94	7.10	0.99	1.54	1.03	1.67	19	(240)
1-pentanol/ <i>n</i> -heptane	368.15 K	2.99	6.96	1.18	2.16	1.22	2.29	20	(240)
1-hexanol/ <i>n</i> -hexane	342.82 K	1.36	10.3	0.24	2.43	0.24	2.50	22	(241)
1-heptanol/ <i>n</i> -decane	0.1359 bar	6.05	2.65	1.17	0.22	1.17	0.23	15	(242)
1-octanol/ <i>n</i> -decane	383.15 K	3.37	10.6	0.60	0.98	0.67	1.48	14	(243)
Average		2.43	6.44	1.12	2.23	1.12	2.25		

Table E-4 presents VLE results for alcohol/alcohol systems when alcohols are modelled with the 2B scheme. Generally, the same measure of accuracy is obtained with all three CPA variants.

Table E-4: VLE predictions of alcohol/n-alcohol mixtures with CPA, CPA-GV and CPA-JC

Mixture	<i>T</i> or <i>P</i>	CPA		CPA-GV		CPA-JC		<i>np</i>	ref.
		Δy ($\times 10^2$) ^a	$\frac{\Delta P(\%)^b}{\Delta T(K)^a}$	Δy ($\times 10^2$) ^a	$\frac{\Delta P(\%)^b}{\Delta T(K)^a}$	Δy ($\times 10^2$) ^a	$\frac{\Delta P(\%)^b}{\Delta T(K)^a}$		
methanol/ethanol	298.15 K	0.25	0.36	0.52	0.55	0.58	0.59	11	(155)
methanol/ethanol	373.15 K	0.27	0.79	0.29	0.62	0.29	0.56	10	(156)
methanol/1-propanol	333.35 K	0.59	1.58	0.61	0.76	0.61	0.77	26	(157)
ethanol/1-propanol	333.15 K	1.22	4.02	1.52	4.43	1.51	4.34	9	(159)
ethanol/1-butanol	343.15 K	0.80	1.56	0.87	1.40	0.83	1.30	8	(160)
ethanol/1-octanol	1.013 bar	1.59	1.36	3.44	2.50	3.34	2.34	25	(158)
1-propanol/1-pentanol	1.013 bar	0.58	0.29	0.57	0.36	0.57	0.40	19	(161)
Average		0.76	1.42	1.11	1.51	1.10	1.47		

Appendix F

Working equations of models

This appendix contains the working equations of the EOS models used in this project. The terms are first transformed to an expression for the reduced residual Helmholtz energy in terms of the independent variable which is temperature, volume and mole numbers. The working equations of first- and second-order partial derivatives with respects to the independent variables are provided. These derivatives were calculated using the WOLFRAM Mathematica package:

F.1 Simplified hard-sphere term working equations

F.1.1 State function

The dimensionless form of the equation is:

$$\frac{a_{mix}^{hs}}{RT} = m_{mix} a_0^{hs} = m_{mix} \frac{4\eta - 3\eta^2}{(1-\eta)^2} \quad (F-1)$$

$$m_{mix} = \frac{1}{n_{total}} \sum_i^{nc} n_i m_i \quad (F-2)$$

Multiply with total moles to obtain units of mole which is consistent with the thermodynamic framework:

$$\frac{A_{mix}^{hs}}{RT} = m_{mix} n_{total} \frac{4\eta - 3\eta^2}{(1-\eta)^2} \quad (F-3)$$

Write all function in terms of the independent variables:

$$\eta = \frac{\pi \rho}{6} \sum_i^{nc} x_i m_i d_i^3 = \frac{N_{av} \pi d_{mix}^3}{6V} \sum_i^{nc} n_i m_i \quad (F-4)$$

$$d_{mix} = \left(\frac{\sum_i^{nc} n_i m_i d_i^3}{\sum_i^{nc} n_i m_i} \right)^{1/3} \quad (F-5)$$

$$d_i = \sigma_i \left[1 - 0.12 \exp\left(-\frac{3\varepsilon_i}{kT}\right) \right] \quad (F-6)$$

F.1.2 First-order derivatives

ii) Composition

$$\begin{aligned} \frac{\partial F_{mix}^{hs}}{\partial n_k} = & n_{total} \frac{(4\eta - 3\eta^2)}{(1-\eta)^2} \cdot \frac{\partial m_{mix}}{\partial n_k} + m_{mix} \frac{4\eta - 3\eta^2}{(1-\eta)^2} + \frac{2m_{mix} n_{total} (4\eta - 3\eta^2)}{(1-\eta)^3} \cdot \frac{\partial \eta}{\partial n_k} \\ & + \frac{m_{mix} n_{total} \left(4 \frac{\partial \eta}{\partial n_k} - 6\eta \frac{\partial \eta}{\partial n_k} \right)}{(1-\eta)^2} \end{aligned} \quad (F-7)$$

$$\frac{\partial m_{mix}}{\partial n_k} = \frac{m_k}{n_{total}} - \frac{1}{(n_{total})^2} \sum_i^{nc} n_i m_i \quad (F-8)$$

$$\frac{\partial \eta}{\partial n_k} = \frac{N_{av} \pi d_{mix}^3}{6V} m_k + \frac{N_{av} \pi d_{mix}^2}{2V} \cdot \frac{\partial d_{mix}}{\partial n_k} \cdot \sum_i^{nc} n_i m_i \quad (F-9)$$

$$\begin{aligned} \frac{\partial d_{mix}}{\partial n_k} = & \frac{\frac{m_k d_k^3}{\sum_i^{nc} n_i m_i} - m_k \frac{\sum_i^{nc} n_i m_i d_i^3}{\left(\sum_i^{nc} m_i n_i \right)^2}}{3 \left(\frac{\sum_i^{nc} n_i m_i d_i^3}{\sum_i^{nc} m_i n_i} \right)^{2/3}} \end{aligned} \quad (F-10)$$

iii) Temperature

$$\frac{\partial F_{mix}^{hs}}{\partial T} = \frac{2m_{mix} n_{total} (4\eta - 3\eta^2)}{(1-\eta)^3} \cdot \frac{\partial \eta}{\partial T} + \frac{m_{mix} n_{total} \left(4 \frac{\partial \eta}{\partial T} - 6\eta \frac{\partial \eta}{\partial T} \right)}{(1-\eta)^2} \quad (F-11)$$

$$\frac{\partial \eta}{\partial T} = \frac{N_{av} \pi d_{mix}^2}{2V} \cdot \sum_i^{nc} n_i m_i \cdot \frac{\partial d_{mix}}{\partial T} \quad (F-12)$$

$$\frac{\partial d_{mix}}{\partial T} = \frac{\sum_i^{nc} n_i m_i d_i^2 \frac{\partial d_i}{\partial T}}{\left(\sum_i^{nc} n_i m_i \right) \left(\frac{\sum_i^{nc} n_i m_i d_i^3}{\sum_i^{nc} n_i m_i} \right)^{2/3}} \quad (F-13)$$

$$\frac{\partial d_i}{\partial T} = \sigma_i \left(-0.36 \exp \left[\frac{-3\epsilon_i}{kT} \right] \right) \left(\frac{\epsilon_i}{kT^2} \right) \quad (F-14)$$

iv) Volume

$$\frac{\partial F_{mix}^{hs}}{\partial V} = \frac{2m_{mix} n_{total} (4\eta - 3\eta^2)}{(1-\eta)^3} \cdot \frac{\partial \eta}{\partial V} + \frac{m_{mix} n_{total} \left(4 \frac{\partial \eta}{\partial V} - 6\eta \frac{\partial \eta}{\partial V} \right)}{(1-\eta)^2} \quad (F-15)$$

$$\frac{\partial \eta}{\partial V} = - \frac{N_{av} \pi d_{mix}^3}{6V^2} \cdot \sum_i^{nc} n_i m_i \quad (F-16)$$

F.1.3 Second-order derivatives

i) Composition - Composition

$$\begin{aligned}
 \frac{\partial^2 F_{mix}^{hs}}{\partial n_k \partial n_l} = & \frac{(4\eta - 3\eta^2)}{(1-\eta)^2} \cdot \frac{\partial m_{mix}}{\partial n_k} + \frac{(4\eta - 3\eta^2)}{(1-\eta)^2} \cdot \frac{\partial m_{mix}}{\partial n_l} + \frac{n_{total} (4\eta - 3\eta^2)}{(1-\eta)^2} \cdot \frac{\partial^2 m_{mix}}{\partial n_k \partial n_l} + \\
 & + \frac{2n_{total} (4\eta - 3\eta^2)}{(1-\eta)^3} \cdot \frac{\partial m_{mix}}{\partial n_k} \cdot \frac{\partial \eta}{\partial n_l} + \frac{2n_{total} (4\eta - 3\eta^2)}{(1-\eta)^3} \cdot \frac{\partial m_{mix}}{\partial n_l} \cdot \frac{\partial \eta}{\partial n_k} \\
 & + \frac{2m_{mix} (4\eta - 3\eta^2)}{(1-\eta)^3} \cdot \frac{\partial \eta}{\partial n_l} + \frac{2m_{mix} (4\eta - 3\eta^2)}{(1-\eta)^3} \cdot \frac{\partial \eta}{\partial n_k} \\
 & + \frac{n_{total} \left(4 \frac{\partial \eta}{\partial n_l} - 6\eta \frac{\partial \eta}{\partial n_l} \right)}{(1-\eta)^2} \cdot \frac{\partial m_{mix}}{\partial n_k} + \frac{n_{total} \left(4 \frac{\partial \eta}{\partial n_k} - 6\eta \frac{\partial \eta}{\partial n_k} \right)}{(1-\eta)^2} \cdot \frac{\partial m_{mix}}{\partial n_l} \\
 & + \frac{m_{mix} \left(4 \frac{\partial \eta}{\partial n_l} - 6\eta \frac{\partial \eta}{\partial n_l} \right)}{(1-\eta)^2} + \frac{m_{mix} \left(4 \frac{\partial \eta}{\partial n_k} - 6\eta \frac{\partial \eta}{\partial n_k} \right)}{(1-\eta)^2} \\
 & + \frac{2m_{mix} n_{total} \left(4 \frac{\partial \eta}{\partial n_k} - 6\eta \frac{\partial \eta}{\partial n_k} \right)}{(1-\eta)^3} \cdot \frac{\partial \eta}{\partial n_l} + \frac{2m_{mix} n_{total} \left(4 \frac{\partial \eta}{\partial n_l} - 6\eta \frac{\partial \eta}{\partial n_l} \right)}{(1-\eta)^3} \cdot \frac{\partial \eta}{\partial n_k} \\
 & + \frac{6m_{mix} n_{total} (4\eta - 3\eta^2)}{(1-\eta)^4} \cdot \frac{\partial \eta}{\partial n_k} \cdot \frac{\partial \eta}{\partial n_l} + \frac{2m_{mix} n_{total} (4\eta - 3\eta^2)}{(1-\eta)^3} \frac{\partial^2 \eta}{\partial n_k \partial n_l} \\
 & + \frac{m_{mix} n_{total} \left(-6 \frac{\partial \eta}{\partial n_l} \cdot \frac{\partial \eta}{\partial n_k} + 4 \frac{\partial^2 \eta}{\partial n_k \partial n_l} - 6\eta \frac{\partial^2 \eta}{\partial n_k \partial n_l} \right)}{(1-\eta)^2}
 \end{aligned} \tag{F-17}$$

$$\frac{\partial^2 m_{mix}}{\partial n_k \partial n_l} = -\frac{m_k}{(n_{total})^2} - \frac{m_l}{(n_{total})^2} + \frac{2}{(n_{total})^3} \sum_i^{nc} n_i m_i \tag{F-18}$$

$$\begin{aligned}
 \frac{\partial^2 \eta}{\partial n_k \partial n_l} = & \frac{N_{av} \pi d_{mix}^2 m_k}{2V} \cdot \frac{\partial d_{mix}}{\partial n_l} + \frac{N_{av} \pi d_{mix}^2 m_l}{2V} \cdot \frac{\partial d_{mix}}{\partial n_k} + \sum_i^{nc} n_i m_i \\
 & + \frac{N_{av} \pi d_{mix}}{V} \cdot \sum_i^{nc} n_i m_i \cdot \frac{\partial d_{mix}}{\partial n_k} \cdot \frac{\partial d_{mix}}{\partial n_l} + \frac{N_{av} \pi d_{mix}^2}{2V} \cdot \sum_i^{nc} n_i m_i \cdot \frac{\partial^2 d_{mix}}{\partial n_k \partial n_l}
 \end{aligned} \tag{F-19}$$

$$\frac{\partial^2 d_{mix}}{\partial n_k \partial n_l} = \left[\frac{-\frac{(m_k m_l d_k^3)}{\left(\sum_i^{nc} n_i m_i\right)^2} - \frac{(m_k m_l d_l^3)}{\left(\sum_i^{nc} n_i m_i\right)^2} + \frac{2m_k m_l \left(\sum_i^{nc} n_i m_i d_i^3\right)}{\left(\sum_i^{nc} m_i n_i\right)^3}}{3 \left(\frac{\sum_i^{nc} n_i m_i d_i^3}{\sum_i^{nc} m_i n_i} \right)^{2/3}} \right] - \left[\frac{2 \left(\frac{m_k d_k^3}{\sum_i^{nc} m_i n_i} - \frac{m_k \left(\sum_i^{nc} n_i m_i d_i^3\right)}{\left(\sum_i^{nc} n_i m_i\right)^2} \right) \left(\frac{m_l d_l^3}{\sum_i^{nc} m_i n_i} - \frac{m_l \left(\sum_i^{nc} n_i m_i d_i^3\right)}{\left(\sum_i^{nc} n_i m_i\right)^2} \right)}{9 \left(\frac{\sum_i^{nc} n_i m_i d_i^3}{\sum_i^{nc} m_i n_i} \right)^{5/3}} \right] \quad (F-20)$$

ii) Composition - Volume

$$\begin{aligned} \frac{\partial^2 F_{mix}^{hc}}{\partial V \partial n_k} &= \frac{2n_{total} (4\eta - 3\eta^2)}{(1-\eta)^3} \cdot \frac{\partial m_{mix}}{\partial n_k} \cdot \frac{\partial \eta}{\partial V} + \frac{2m_{mix} (4\eta - 3\eta^2)}{(1-\eta)^3} \cdot \frac{\partial \eta}{\partial V} \\ &+ \frac{6m_{mix} n_{total} (4\eta - 3\eta^2)}{(1-\eta)^4} \cdot \frac{\partial \eta}{\partial n_k} \cdot \frac{\partial \eta}{\partial V} + \frac{2m_{mix} n_{total} \left(4 \frac{\partial \eta}{\partial n_k} - 6\eta \frac{\partial \eta}{\partial n_k} \right)}{(1-\eta)^3} \cdot \frac{\partial \eta}{\partial V} \\ &+ \frac{n_{total} \left(4 \frac{\partial \eta}{\partial V} - 6\eta \frac{\partial \eta}{\partial V} \right)}{(1-\eta)^2} \cdot \frac{\partial m_{mix}}{\partial n_k} + \frac{m_{mix} \left(4 \frac{\partial \eta}{\partial V} - 6\eta \frac{\partial \eta}{\partial V} \right)}{(1-\eta)^2} \\ &+ \frac{2m_{mix} n_{total} \left(4 \frac{\partial \eta}{\partial V} - 6\eta \frac{\partial \eta}{\partial V} \right)}{(1-\eta)^3} \cdot \frac{\partial \eta}{\partial n_k} + \frac{2m_{mix} n_{total} (4\eta - 3\eta^2)}{(1-\eta)^3} \cdot \frac{\partial^2 \eta}{\partial V \partial n_k} \\ &+ \frac{m_{mix} n_{total} \left(-6 \frac{\partial \eta}{\partial n_k} \cdot \frac{\partial \eta}{\partial V} + 4 \frac{\partial^2 \eta}{\partial V \partial n_k} - 6\eta \frac{\partial^2 \eta}{\partial V \partial n_k} \right)}{(1-\eta)^2} \end{aligned} \quad (F-21)$$

$$\frac{\partial^2 \eta}{\partial V \partial n_k} = -\frac{N_{av} \pi m_k}{6V^2} d_{mix}^3 - \frac{N_{av} \pi d_{mix}^2}{2V^2} \cdot \frac{\partial d_{mix}}{\partial n_k} \cdot \sum_i^{nc} n_i m_i \quad (F-22)$$

iii) Composition - Temperature

$$\frac{\partial^2 F_{mix}^{hc}}{\partial T \partial n_k} = \frac{2n_{total}(4\eta - 3\eta^2)}{(1-\eta)^3} \cdot \frac{\partial m_{mix}}{\partial n_k} \cdot \frac{\partial \eta}{\partial T} + \frac{2m_{mix}(4\eta - 3\eta^2)}{(1-\eta)^3} \cdot \frac{\partial \eta}{\partial V} \quad (F-23)$$

$$\begin{aligned} & + \frac{6m_{mix}n_{total}(4\eta - 3\eta^2)}{(1-\eta)^4} \cdot \frac{\partial \eta}{\partial n_k} \cdot \frac{\partial \eta}{\partial T} + \frac{2m_{mix}n_{total}\left(4\frac{\partial \eta}{\partial n_k} - 6\eta\frac{\partial \eta}{\partial n_k}\right)}{(1-\eta)^3} \cdot \frac{\partial \eta}{\partial T} \\ & + \frac{n_{total}\left(4\frac{\partial \eta}{\partial T} - 6\eta\frac{\partial \eta}{\partial T}\right)}{(1-\eta)^2} \cdot \frac{\partial m_{mix}}{\partial n_k} + \frac{m_{mix}\left(4\frac{\partial \eta}{\partial T} - 6\eta\frac{\partial \eta}{\partial T}\right)}{(1-\eta)^2} \\ & + \frac{2m_{mix}n_{total}\left(4\frac{\partial \eta}{\partial T} - 6\eta\frac{\partial \eta}{\partial T}\right)}{(1-\eta)^3} \cdot \frac{\partial \eta}{\partial n_k} + \frac{2m_{mix}n_{total}(4\eta - 3\eta^2)}{(1-\eta)^3} \cdot \frac{\partial^2 \eta}{\partial T \partial n_k} \\ & + \frac{m_{mix}n_{total}\left(-6\frac{\partial \eta}{\partial n_k} \cdot \frac{\partial \eta}{\partial T} + 4\frac{\partial^2 \eta}{\partial T \partial n_k} - 6\eta\frac{\partial^2 \eta}{\partial T \partial n_k}\right)}{(1-\eta)^2} \end{aligned}$$

$$\frac{\partial^2 \eta}{\partial T \partial n_k} = \frac{N_{av}m_k\pi d_{mix}^2}{2V} \cdot \frac{\partial d_{mix}}{\partial T} + \frac{N_{av}\pi d_{mix}}{V} \cdot \sum_i^{nc} n_i m_i \cdot \frac{\partial d_{mix}}{\partial T} \cdot \frac{\partial d_{mix}}{\partial n_k} + \frac{N_{av}\pi d_{mix}^2}{2V} \cdot \sum_i^{nc} n_i m_i \cdot \frac{\partial^2 d_{mix}}{\partial T \partial n_k} \quad (F-24)$$

$$\begin{aligned} \frac{\partial^2 d_{mix}}{\partial T \partial n_k} = & \left[\frac{\left(m_k d_k^2 \frac{\partial d_k}{\partial T}\right)}{\left(\sum_i^{nc} m_i n_i\right) \left(\frac{\sum_i^{nc} n_i m_i d_i^3}{\sum_i^{nc} m_i n_i}\right)^{2/3}} - \frac{m_k \left(3 \sum_i^{nc} n_i m_i d_i^2 \frac{\partial d_i}{\partial T}\right)}{3 \left(\sum_i^{nc} m_i n_i\right)^2 \left(\frac{\sum_i^{nc} n_i m_i d_i^3}{\sum_i^{nc} m_i n_i}\right)^{2/3}} \right] \\ & - \left[\frac{2 \left(\frac{m_k d_k^3}{\sum_i^{nc} m_i n_i} - \frac{m_k \left(\sum_i^{nc} n_i m_i d_i^3\right)}{\left(\sum_i^{nc} n_i m_i\right)^2} \right) \left(3 \sum_i^{nc} n_i m_i d_i^2 \frac{\partial d_i}{\partial T}\right)}{9 \left(\sum_i^{nc} m_i n_i\right) \left(\frac{\sum_i^{nc} n_i m_i d_i^3}{\sum_i^{nc} m_i n_i}\right)^{5/3}} \right] \end{aligned} \quad (F-25)$$

iv) Volume – Volume

$$\frac{\partial^2 F_{mix}^{hs}}{\partial V \partial V} = \frac{6m_{mix} n_{total} (4\eta - 3\eta^2) \left(\frac{\partial \eta}{\partial V} \right)^2}{(1-\eta)^4} + \frac{4m_{mix} n_{total} \left(4 \frac{\partial \eta}{\partial V} - 6\eta \frac{\partial \eta}{\partial V} \right)}{(1-\eta)^3} \cdot \frac{\partial \eta}{\partial V} \quad (F-26)$$

$$+ \frac{2m_{mix} n_{total} (4\eta - 3\eta^2)}{(1-\eta)^3} \cdot \frac{\partial^2 \eta}{\partial V^2} + \frac{m_{mix} n_{total} \left(-6 \left(\frac{\partial \eta}{\partial V} \right)^2 + 4 \frac{\partial^2 \eta}{\partial V^2} - 6\eta \frac{\partial^2 \eta}{\partial V^2} \right)}{(1-\eta)^2}$$

$$\frac{\partial^2 \eta}{\partial V^2} = \frac{N_{av} \pi d_{mix}^3}{3V^3} \cdot \sum_i^{nc} n_i m_i \quad (F-27)$$

v) Temperature – Temperature

$$\frac{\partial^2 F_{mix}^{hs}}{\partial T \partial T} = \frac{6m_{mix} n_{total} (4\eta - 3\eta^2) \left(\frac{\partial \eta}{\partial T} \right)^2}{(1-\eta)^4} + \frac{4m_{mix} n_{total} \left(4 \frac{\partial \eta}{\partial T} - 6\eta \frac{\partial \eta}{\partial T} \right)}{(1-\eta)^3} \cdot \frac{\partial \eta}{\partial T} \quad (F-28)$$

$$+ \frac{2m_{mix} n_{total} (4\eta - 3\eta^2)}{(1-\eta)^3} \cdot \frac{\partial^2 \eta}{\partial T^2} + \frac{m_{mix} n_{total} \left(-6 \left(\frac{\partial \eta}{\partial T} \right)^2 + 4 \frac{\partial^2 \eta}{\partial T^2} - 6\eta \frac{\partial^2 \eta}{\partial T^2} \right)}{(1-\eta)^2}$$

$$\frac{\partial^2 \eta}{\partial T^2} = \frac{N_{av} \pi d_{mix}}{V} \cdot \sum_i^{nc} n_i m_i \cdot \left(\frac{\partial d_{mix}}{\partial T} \right)^2 + \frac{N_{av} \pi d_{mix}^2}{2V} \cdot \sum_i^{nc} n_i m_i \cdot \frac{\partial^2 d_{mix}}{\partial T^2} \quad (F-29)$$

$$\frac{\partial^2 d_{mix}}{\partial T^2} = - \frac{2 \left(3 \sum_i^{nc} n_i m_i d_i^2 \frac{\partial d_i}{\partial T} \right)^2}{9 \left(\sum_i^{nc} n_i m_i \right)^2 \left(\frac{\sum_i^{nc} n_i m_i d_i^3}{\sum_i^{nc} n_i m_i} \right)^{5/3}} + \frac{\left(6 \sum_i^{nc} n_i m_i d_i \left(\frac{\partial d_i}{\partial T} \right)^2 + 3 \sum_i^{nc} n_i m_i d_i^2 \left(\frac{\partial^2 d_i}{\partial T^2} \right) \right)}{\left(\left(3 \sum_i^{nc} n_i m_i \right) \left(\frac{\sum_i^{nc} n_i m_i d_i^3}{\sum_i^{nc} n_i m_i} \right)^{2/3} \right)} \quad (F-30)$$

$$\frac{\partial^2 d_i}{\partial T^2} = \frac{0.72 \exp \left[\frac{-3\epsilon_i}{kT} \right] \epsilon_i \sigma_i}{kT^3} - \frac{1.08 \exp \left[\frac{-3\epsilon_i}{kT} \right] (\epsilon_i)^2 \sigma_i}{k^2 T^4} \quad (F-31)$$

vi) Volume – Temperature

$$\begin{aligned}
 \frac{\partial^2 F_{mix}^{hs}}{\partial T \partial V} = & \frac{6m_{mix} n_{total} (4\eta - 3\eta^2)}{(1-\eta)^4} \cdot \frac{\partial \eta}{\partial V} \cdot \frac{\partial \eta}{\partial T} + \frac{2m_{mix} n_{total} \left(4 \frac{\partial \eta}{\partial V} - 6\eta \frac{\partial \eta}{\partial V} \right)}{(1-\eta)^3} \cdot \frac{\partial \eta}{\partial T} \\
 & + \frac{2m_{mix} n_{total} \left(4 \frac{\partial \eta}{\partial T} - 6\eta \frac{\partial \eta}{\partial T} \right)}{(1-\eta)^3} \cdot \frac{\partial \eta}{\partial V} + \frac{2m_{mix} n_{total} (4\eta - 3\eta^2)}{(1-\eta)^3} \cdot \frac{\partial^2 \eta}{\partial V \partial T} \\
 & + \frac{m_{mix} n_{total} \left(-6 \frac{\partial \eta}{\partial V} \cdot \frac{\partial \eta}{\partial T} + 4 \frac{\partial^2 \eta}{\partial V \partial T} - 6\eta \frac{\partial^2 \eta}{\partial V \partial T} \right)}{(1-\eta)^2}
 \end{aligned} \tag{F-32}$$

$$\frac{\partial^2 \eta}{\partial T \partial V} = - \frac{N_{av} \pi d_{mix}^2}{2V^2} \cdot \sum_i^{nc} n_i m_i \cdot \frac{\partial d_{mix}}{\partial T} \tag{F-33}$$

F.2 Simplified chain term working equations

F.2.1 State function

The reduced form of the equation is presented below:

$$\frac{a_{mix}^{chain}}{RT} = \sum_i^{nc} x_i (1 - m_i) \ln(g^{hs}) \tag{F-34}$$

Multiply with total mole numbers and convert to mole fractions to mole numbers in order to transform the equation in terms of the independent variables stated:

$$\frac{A_{mix}^{chain}}{RT} = \frac{n_{total}}{n_{total}} \sum_i^{nc} n_i (1 - m_i) \ln(g^{hs}) \tag{F-35}$$

$$\frac{A_{mix}^{chain}}{RT} = \sum_i^{nc} n_i (1 - m_i) \ln(g^{hs}) = F_{mix}^{chain} \tag{F-36}$$

$$g^{hs} = \frac{1 - 0.5\eta}{(1-\eta)^3} \tag{F-37}$$

F.2.2 First-order derivatives

i) Composition

$$\frac{\partial F_{mix}^{chain}}{\partial n_k} = (1 - m_k) \ln(g^{hs}) + \frac{\sum_i^{nc} n_i (1 - m_i)}{g^{hs}} \cdot \frac{\partial g^{hs}}{\partial n_k} \quad (F-38)$$

$$\frac{\partial g^{hs}}{\partial n_k} = -\frac{0.5}{(1-\eta)^3} \cdot \frac{\partial \eta}{\partial n_k} + \frac{3(1-0.5\eta)}{(1-\eta)^4} \cdot \frac{\partial \eta}{\partial n_k} \quad (F-39)$$

ii) Temperature

$$\frac{\partial F_{mix}^{chain}}{\partial T} = \frac{\sum_i^{nc} n_i (1 - m_i)}{g^{hs}} \cdot \frac{\partial g^{hs}}{\partial T} \quad (F-40)$$

$$\frac{\partial g^{hs}}{\partial T} = -\frac{0.5}{(1-\eta)^3} \cdot \frac{\partial \eta}{\partial T} + \frac{3(1-0.5\eta)}{(1-\eta)^4} \cdot \frac{\partial \eta}{\partial T} \quad (F-41)$$

iii) Volume

$$\frac{\partial F_{mix}^{chain}}{\partial V} = \frac{\sum_i^{nc} n_i (1 - m_i)}{g^{hs}} \cdot \frac{\partial g^{hs}}{\partial V} \quad (F-42)$$

$$\frac{\partial g^{hs}}{\partial V} = -\frac{0.5}{(1-\eta)^3} \cdot \frac{\partial \eta}{\partial V} + \frac{3(1-0.5\eta)}{(1-\eta)^4} \cdot \frac{\partial \eta}{\partial V} \quad (F-43)$$

F.2.3 Second-order derivatives

i) Composition – Composition

$$\begin{aligned} \frac{\partial^2 F_{mix}^{chain}}{\partial n_k \partial n_l} &= \frac{(1 - m_k)}{g^{hs}} \cdot \frac{\partial g^{hs}}{\partial n_l} + \frac{(1 - m_l)}{g^{hs}} \cdot \frac{\partial g^{hs}}{\partial n_k} \\ &\quad - \frac{\sum_i^{nc} n_i (1 - m_i)}{(g^{hs})^2} \cdot \frac{\partial g^{hs}}{\partial n_k} \cdot \frac{\partial g^{hs}}{\partial n_l} + \frac{\sum_i^{nc} n_i (1 - m_i)}{g^{hs}} \cdot \frac{\partial^2 g^{hs}}{\partial n_k \partial n_l} \end{aligned} \quad (F-44)$$

$$\begin{aligned} \frac{\partial^2 g^{hs}}{\partial n_k \partial n_l} &= -\frac{3}{(1-\eta)^4} \cdot \frac{\partial \eta}{\partial n_k} \cdot \frac{\partial \eta}{\partial n_l} + \frac{12(1-0.5\eta)}{(1-\eta)^5} \cdot \frac{\partial \eta}{\partial n_k} \cdot \frac{\partial \eta}{\partial n_l} \\ &\quad - \frac{0.5}{(1-\eta)^3} \cdot \frac{\partial^2 \eta}{\partial n_k \partial n_l} + \frac{3(1-0.5\eta)}{(1-\eta)^4} \cdot \frac{\partial^2 \eta}{\partial n_k \partial n_l} \end{aligned} \quad (F-45)$$

ii) Composition – Volume

$$\frac{\partial^2 F_{mix}^{chain}}{\partial n_k \partial V} = \frac{(1-m_k)}{g^{hs}} \cdot \frac{\partial g^{hs}}{\partial V} - \frac{\sum_i^{nc} n_i (1-m_i)}{(g^{hs})^2} \cdot \frac{\partial g^{hs}}{\partial V} \cdot \frac{\partial g^{hs}}{\partial n_k} + \frac{\sum_i^{nc} n_i (1-m_i)}{g^{hs}} \cdot \frac{\partial^2 g^{hs}}{\partial V \partial n_k} \quad (F-46)$$

$$\begin{aligned} \frac{\partial^2 g^{hs}}{\partial V \partial n_k} = & -\frac{3}{(1-\eta)^4} \cdot \frac{\partial \eta}{\partial V} \cdot \frac{\partial \eta}{\partial n_k} + \frac{12(1-0.5\eta)}{(1-\eta)^5} \cdot \frac{\partial \eta}{\partial V} \cdot \frac{\partial \eta}{\partial n_k} \\ & - \frac{0.5}{(1-\eta)^3} \cdot \frac{\partial^2 \eta}{\partial V \partial n_k} + \frac{3(1-0.5\eta)}{(1-\eta)^4} \cdot \frac{\partial^2 \eta}{\partial V \partial n_k} \end{aligned} \quad (F-47)$$

iii) Composition – Temperature

$$\frac{\partial^2 F_{mix}^{chain}}{\partial n_k \partial T} = \frac{(1-m_k)}{g^{hs}} \cdot \frac{\partial g^{hs}}{\partial T} - \frac{\sum_i^{nc} n_i (1-m_i)}{(g^{hs})^2} \cdot \frac{\partial g^{hs}}{\partial T} \cdot \frac{\partial g^{hs}}{\partial n_k} + \frac{\sum_i^{nc} n_i (1-m_i)}{g^{hs}} \cdot \frac{\partial^2 g^{hs}}{\partial T \partial n_k} \quad (F-48)$$

$$\begin{aligned} \frac{\partial^2 g^{hs}}{\partial T \partial n_k} = & -\frac{3}{(1-\eta)^4} \cdot \frac{\partial \eta}{\partial T} \cdot \frac{\partial \eta}{\partial n_k} + \frac{12(1-0.5\eta)}{(1-\eta)^5} \cdot \frac{\partial \eta}{\partial T} \cdot \frac{\partial \eta}{\partial n_k} \\ & - \frac{0.5}{(1-\eta)^3} \cdot \frac{\partial^2 \eta}{\partial T \partial n_k} + \frac{3(1-0.5\eta)}{(1-\eta)^4} \cdot \frac{\partial^2 \eta}{\partial T \partial n_k} \end{aligned} \quad (F-49)$$

iv) Volume – Volume

$$\frac{\partial^2 F_{mix}^{chain}}{\partial V^2} = -\frac{\sum_i^{nc} n_i (1-m_i)}{(g^{hs})^2} \cdot \left(\frac{\partial g^{hs}}{\partial V} \right)^2 + \frac{\sum_i^{nc} n_i (1-m_i)}{g^{hs}} \cdot \frac{\partial^2 g^{hs}}{\partial V^2} \quad (F-50)$$

$$\begin{aligned} \frac{\partial^2 g^{hs}}{\partial V^2} = & -\frac{3}{(1-\eta)^4} \cdot \left(\frac{\partial \eta}{\partial V} \right)^2 + \frac{12(1-0.5\eta)}{(1-\eta)^5} \cdot \left(\frac{\partial \eta}{\partial V} \right)^2 \\ & - \frac{0.5}{(1-\eta)^3} \cdot \frac{\partial^2 \eta}{\partial V^2} + \frac{3(1-0.5\eta)}{(1-\eta)^4} \cdot \frac{\partial^2 \eta}{\partial V^2} \end{aligned} \quad (F-51)$$

v) Temperature – Temperature

$$\frac{\partial^2 F_{mix}^{chain}}{\partial T^2} = -\frac{\sum_i^{nc} n_i (1-m_i)}{(g^{hs})^2} \cdot \left(\frac{\partial g^{hs}}{\partial T} \right)^2 + \frac{\sum_i^{nc} n_i (1-m_i)}{g^{hs}} \cdot \frac{\partial^2 g^{hs}}{\partial T^2} \quad (F-52)$$

$$\begin{aligned} \frac{\partial^2 g^{hs}}{\partial T^2} = & -\frac{3}{(1-\eta)^4} \cdot \left(\frac{\partial \eta}{\partial T} \right)^2 + \frac{12(1-0.5\eta)}{(1-\eta)^5} \cdot \left(\frac{\partial \eta}{\partial T} \right)^2 \\ & - \frac{0.5}{(1-\eta)^3} \cdot \frac{\partial^2 \eta}{\partial T^2} + \frac{3(1-0.5\eta)}{(1-\eta)^4} \cdot \frac{\partial^2 \eta}{\partial T^2} \end{aligned} \quad (F-53)$$

vi) Volume – Temperature

$$\frac{\partial^2 F_{mix}^{chain}}{\partial V \partial T} = -\frac{\sum_i^{nc} n_i (1-m_i)}{(g^{hs})^2} \cdot \frac{\partial g^{hs}}{\partial T} \cdot \frac{\partial g^{hs}}{\partial V} + \frac{\sum_i^{nc} n_i (1-m_i)}{g^{hs}} \cdot \frac{\partial^2 g^{hs}}{\partial T \partial V} \quad (F-54)$$

$$\begin{aligned} \frac{\partial^2 g^{hs}}{\partial V \partial T} = & -\frac{3}{(1-\eta)^4} \cdot \frac{\partial \eta}{\partial T} \cdot \frac{\partial \eta}{\partial V} + \frac{12(1-0.5\eta)}{(1-\eta)^5} \cdot \frac{\partial \eta}{\partial T} \cdot \frac{\partial \eta}{\partial V} \\ & - \frac{0.5}{(1-\eta)^3} \cdot \frac{\partial^2 \eta}{\partial T \partial V} + \frac{3(1-0.5\eta)}{(1-\eta)^4} \cdot \frac{\partial^2 \eta}{\partial T \partial V} \end{aligned} \quad (F-55)$$

F.3 PC-SAFT dispersion term working equations

F.3.1 State function

The published from the PC-SAFT dispersion term is presented below:

$$\frac{a_{mix}^{disp}}{RT} = -2\pi \rho I_1(\eta, m_{mix}) \left(m^2 \frac{\epsilon}{kT} \sigma^3 \right)_{mix} - \pi \rho m_{mix} C_1 I_2(\eta, m_{mix}) \left(m^2 \left(\frac{\epsilon}{kT} \right)^2 \sigma^3 \right)_{mix} \quad (F-56)$$

Transform to volume by utilizing the following relationship between number density and total volume:

$$\rho_{number} = \frac{N_{av} n_{total}}{V} \quad (F-57)$$

$$\frac{a_{mix}^{disp}}{RT} = -2\pi \frac{N_{av} n_{total}}{V} I_1(\eta, m_{mix}) \left(m^2 \frac{\epsilon}{kT} \sigma^3 \right)_{mix} - \pi \frac{N_{av} n_{total}}{V} m_{mix} C_1 I_2(\eta, m_{mix}) \left(m^2 \left(\frac{\epsilon}{kT} \right)^2 \sigma^3 \right)_{mix} \quad (F-58)$$

Multiply with total moles to obtain expression in correct form:

$$\begin{aligned} \frac{A_{mix}^{disp}}{RT} = & -2\pi \frac{N_{av} n_{total}^2}{V} I_1(\eta, m_{mix}) \left(m^2 \frac{\epsilon}{kT} \sigma^3 \right)_{mix} \\ & - \pi \frac{N_{av} n_{total}^2}{V} m_{mix} C_1 I_2(\eta, m_{mix}) \left(m^2 \left(\frac{\epsilon}{kT} \right)^2 \sigma^3 \right)_{mix} = F_{mix}^{disp} \end{aligned} \quad (F-59)$$

The mixing rules and remaining expression are presented below:

$$\left(m^2 \frac{\varepsilon}{kT} \sigma^3 \right)_{mix} = \sum_i^{nc} \sum_j^{nc} x_i x_j m_i m_j \left(\frac{\varepsilon_{ij}}{kT} \right) \sigma_{ij}^3 \quad (F-60)$$

$$\left(m^2 \frac{\varepsilon}{kT} \sigma^3 \right)_{mix} = \frac{1}{(n_{total})^2} \sum_i^{nc} \sum_j^{nc} n_i n_j m_i m_j \left(\frac{\varepsilon_{ij}}{kT} \right) \sigma_{ij}^3 \quad (F-61)$$

$$\left(m^2 \left(\frac{u^o}{kT} \right)^2 \sigma^3 \right)_{mix} = \sum_i^{nc} \sum_j^{nc} x_i x_j m_i m_j \left(\frac{u_{ij}^o}{kT} \right)^2 \sigma_{ij}^3 \quad (F-62)$$

$$\left(m^2 \left(\frac{\varepsilon}{kT} \right)^2 \sigma^3 \right)_{mix} = \frac{1}{(n_{total})^2} \sum_i^{nc} \sum_j^{nc} n_i n_j m_i m_j \left(\frac{\varepsilon_{ij}}{kT} \right)^2 \sigma_{ij}^3 \quad (F-63)$$

$$I_1(\eta, m_{mix}) = \sum_{i=0}^6 a_i(m_{mix}) \eta^i \quad (F-64)$$

$$I_2(\eta, m_{mix}) = \sum_{i=0}^6 b_i(m_{mix}) \eta^i \quad (F-65)$$

$$C_0 = 1 + m_{mix} \frac{8\eta - 2\eta^2}{(1-\eta)^4} + (1 - m_{mix}) \frac{20\eta - 27\eta^2 + 12\eta^3 - 2\eta^4}{[(1-\eta)(2-\eta)]^2} \quad (F-66)$$

$$C_1 = \left(1 + m_{mix} \frac{8\eta - 2\eta^2}{(1-\eta)^4} + (1 - m_{mix}) \frac{20\eta - 27\eta^2 + 12\eta^3 - 2\eta^4}{[(1-\eta)(2-\eta)]^2} \right)^{-1} \quad (F-67)$$

$$C_1 = (C_0)^{-1} \quad (F-68)$$

Introducing the C_0 intermediate function makes the derivatives easier.

$$a_i(m_{mix}) = a_{0i} + \frac{m_{mix} - 1}{m_{mix}} a_{1i} + \frac{m_{mix} - 1}{m_{mix}} \frac{m_{mix} - 2}{m_{mix}} a_{2i} \quad (F-69)$$

$$b_i(m_{mix}) = b_{0i} + \frac{m_{mix} - 1}{m_{mix}} b_{1i} + \frac{m_{mix} - 1}{m_{mix}} \frac{m_{mix} - 2}{m_{mix}} b_{2i} \quad (F-70)$$

$$\eta = \zeta_3 = \frac{\pi}{6} \rho \sum_i^{nc} x_i m_i d_i^3 = \frac{N_{av} \pi}{6V} \sum_i^{nc} n_i m_i d_i^3 \quad (F-71)$$

F.3.2 First-order derivatives

i) Composition

$$\frac{\partial F_{mix}^{disp}}{\partial n_k} = \frac{\partial}{\partial n_k} (F_{mix}^{disp}) = \frac{\partial}{\partial n_k} (F_{mix}^{disp,1}) + \frac{\partial}{\partial n_k} (F_{mix}^{disp,2}) \quad (F-72)$$

Perturbation term 1

$$\begin{aligned} \frac{\partial F_{mix}^{disp,1}}{\partial n_k} = & -4\pi \frac{N_{av} n_{total}}{V} I_1(\eta, m_{mix}) \left(m^2 \frac{\epsilon}{kT} \sigma^3 \right)_{mix} - 2\pi \frac{N_{av} n_{total}^2}{V} I_1(\eta, m_{mix}) \frac{\partial \left(m^2 \frac{\epsilon}{kT} \sigma^3 \right)_{mix}}{\partial n_k} \\ & - 2\pi \frac{N_{av} n_{total}^2}{V} \left(m^2 \frac{\epsilon}{kT} \sigma^3 \right)_{mix} \frac{\partial I_1(\eta, m_{mix})}{\partial n_k} \end{aligned} \quad (F-73)$$

$$\frac{\partial \left(m^2 \frac{\epsilon}{kT} \sigma^3 \right)_{mix}}{\partial n_k} = \frac{2}{(n_{total})^2} \sum_j^{nc} n_j m_k m_j \left(\frac{\epsilon_{kj}}{kT} \right) \sigma_{kj}^3 - \frac{2}{(n_{total})^3} \sum_i^{nc} \sum_j^{nc} n_i n_j m_i m_j \left(\frac{\epsilon_{ij}}{kT} \right) \sigma_{ij}^3 \quad (F-74)$$

$$\frac{\partial I_1(\eta, m_{mix})}{\partial n_k} = \sum_{i=0}^6 \left[i \times a_i(m_{mix}) \frac{\partial \eta}{\partial n_k} \eta^{i-1} + \eta^i \frac{\partial a_i}{\partial n_k} \right] \quad (F-75)$$

$$\frac{\partial a_i}{\partial n_k} = \frac{(-4a_{2i} + (a_{1i} + 3a_{2i}) m_{mix})}{(m_{mix})^3} \cdot \frac{\partial m_{mix}}{\partial n_k} \quad (F-76)$$

$$\frac{\partial \eta}{\partial n_k} = \frac{\partial \zeta_3}{\partial n_k} = \frac{N_{av} \pi}{6V} m_k d_k^3 \quad (F-77)$$

Perturbation term 2

$$\begin{aligned} \frac{\partial F_{mix}^{disp,2}}{\partial n_k} = & -\pi \frac{N_{av} n_{total}^2}{V} C_1 I_2(\eta, m_{mix}) \left(m^2 \left(\frac{\epsilon}{kT} \right)^2 \sigma^3 \right)_{mix} \cdot \frac{\partial m_{mix}}{\partial n_k} \\ & - 2\pi \frac{N_{av} n_{total}}{V} C_1 I_2(\eta, m_{mix}) m_{mix} \left(m^2 \left(\frac{\epsilon}{kT} \right)^2 \sigma^3 \right)_{mix} \\ & - \pi \frac{N_{av} n_{total}^2}{V} C_1 I_2(\eta, m_{mix}) m_{mix} \frac{\partial \left(m^2 \left(\frac{\epsilon}{kT} \right)^2 \sigma^3 \right)_{mix}}{\partial n_k} \\ & - \pi \frac{N_{av} n_{total}^2}{V} I_2(\eta, m_{mix}) m_{mix} \left(m^2 \left(\frac{\epsilon}{kT} \right)^2 \sigma^3 \right)_{mix} \cdot \frac{\partial C_1}{\partial n_k} \\ & - \pi \frac{N_{av} n_{total}^2}{V} C_1 m_{mix} \left(m^2 \left(\frac{\epsilon}{kT} \right)^2 \sigma^3 \right)_{mix} \cdot \frac{\partial I_2(\eta, m_{mix})}{\partial n_k} \end{aligned} \quad (F-78)$$

$$\frac{\partial \left(m^2 \left(\frac{\varepsilon}{kT} \right)^2 \sigma^3 \right)}{\partial n_k} \Big|_{mix} = \frac{2}{(n_{total})^2} \sum_j^{nc} n_j m_k m_j \left(\frac{\varepsilon_{kj}}{kT} \right)^2 \sigma_{kj}^3 - \frac{2}{(n_{total})^3} \sum_i^{nc} \sum_j^{nc} n_i n_j m_i m_j \left(\frac{\varepsilon_{ij}}{kT} \right)^2 \sigma_{ij}^3 \quad (F-79)$$

$$\begin{aligned} \frac{\partial C_0}{\partial n_k} &= \frac{8\eta - 2\eta^2}{(1-\eta)^4} \cdot \frac{\partial m_{mix}}{\partial n_k} - \frac{20\eta - 27\eta^2 + 12\eta^3 - 2\eta^4}{[(1-\eta)(2-\eta)]^2} \cdot \frac{\partial m_{mix}}{\partial n_k} \\ &+ 2(1-m_{mix}) \frac{20\eta - 27\eta^2 + 12\eta^3 - 2\eta^4}{(1-\eta)^2 (2-\eta)^3} \cdot \frac{\partial \eta}{\partial n_k} + 2(1-m_{mix}) \frac{20\eta - 27\eta^2 + 12\eta^3 - 2\eta^4}{(1-\eta)^3 (2-\eta)^2} \cdot \frac{\partial \eta}{\partial n_k} \\ &+ 4m_{mix} \frac{8\eta - 2\eta^2}{(1-\eta)^5} \cdot \frac{\partial \eta}{\partial n_k} + m_{mix} \frac{8 \frac{\partial \eta}{\partial n_k} - 4\eta \frac{\partial \eta}{\partial n_k}}{(1-\eta)^4} + (1-m_{mix}) \frac{20 \frac{\partial \eta}{\partial n_k} - 54\eta \frac{\partial \eta}{\partial n_k} + 36\eta^2 \frac{\partial \eta}{\partial n_k} - 8\eta^3 \frac{\partial \eta}{\partial n_k}}{[(1-\eta)(2-\eta)]^2} \end{aligned} \quad (F-80)$$

$$\frac{\partial C_1}{\partial n_k} = \frac{\partial}{\partial n_k} (C_1) = -\frac{1}{C_0^2} \cdot \frac{\partial C_0}{\partial n_k} \quad (F-81)$$

$$\frac{\partial I_2(\eta, m_{mix})}{\partial n_k} = \sum_{i=0}^6 \left[i \times b_i(m_{mix}) \frac{\partial \eta}{\partial n_k} \eta^{i-1} + \eta^i \frac{\partial b_i}{\partial n_k} \right] \quad (F-82)$$

$$\frac{\partial b_i}{\partial n_k} = \frac{(-4b_{2i} + (b_{1i} + 3b_{2i})m_{mix})}{(m_{mix})^3} \cdot \frac{\partial m_{mix}}{\partial n_k} \quad (F-83)$$

ii) Temperature

$$\frac{\partial F_{mix}^{disp}}{\partial T} = \frac{\partial}{\partial T} (F_{mix}^{disp}) = \frac{\partial}{\partial T} (F_{mix}^{disp,1}) + \frac{\partial}{\partial T} (F_{mix}^{disp,2}) \quad (F-84)$$

Perturbation term 1

$$\frac{\partial F_{mix}^{disp,1}}{\partial T} = -2\pi \frac{N_{av} n_{total}^2}{V} I_1(\eta, m_{mix}) \frac{\partial \left(m^2 \frac{\varepsilon}{kT} \sigma^3 \right)}{\partial T} \Big|_{mix} - 2\pi \frac{N_{av} n_{total}^2}{V} \left(m^2 \frac{\varepsilon}{kT} \sigma^3 \right)_{mix} \frac{\partial I_1(\eta, m_{mix})}{\partial T} \quad (F-85)$$

$$\frac{\partial \left(m^2 \frac{\varepsilon}{kT} \sigma^3 \right)}{\partial T} \Big|_{mix} = -\frac{1}{(n_{total})^2} \sum_i^{nc} \sum_j^{nc} n_i n_j m_i m_j \left(\frac{\varepsilon_{ij}}{kT^2} \right) \sigma_{ij}^3 \quad (F-86)$$

$$\frac{\partial I_1(\eta, m_{mix})}{\partial T} = \sum_{i=0}^6 i \times a_i(m_{mix}) \eta^{i-1} \cdot \frac{\partial \eta}{\partial T} \quad (F-87)$$

$$\frac{\partial \eta}{\partial T} = \frac{\partial \zeta_3}{\partial T} = \frac{N_{av} \pi}{2V} \sum_i^{nc} n_i m_i d_i^2 \cdot \frac{\partial d_i}{\partial T} \quad (F-88)$$

Perturbation term 2

$$\frac{\partial F_{mix}^{disp,2}}{\partial T} = -\pi \frac{N_{av} n_{total}^2}{V} m_{mix} C_1 I_2(\eta, m_{mix}) \cdot \frac{\partial \left(m^2 \left(\frac{\epsilon}{kT} \right)^2 \sigma^3 \right)}{\partial T} \quad (F-89)$$

$$- \pi \frac{N_{av} n_{total}^2}{V} m_{mix} I_2(\eta, m_{mix}) \left(m^2 \left(\frac{\epsilon}{kT} \right)^2 \sigma^3 \right)_{mix} \cdot \frac{\partial C_1}{\partial T}$$

$$- \pi \frac{N_{av} n_{total}^2}{V} m_{mix} C_1 \left(m^2 \left(\frac{\epsilon}{kT} \right)^2 \sigma^3 \right)_{mix} \frac{\partial I_2(\eta, m_{mix})}{\partial T}$$

$$\frac{\partial \left(m^2 \left(\frac{\epsilon}{kT} \right)^2 \sigma^3 \right)}{\partial T} = - \frac{2}{(n_{total})^2} \sum_i^{nc} \sum_j^{nc} n_i n_j m_i m_j \left(\frac{(\epsilon_{ij})^2}{k^2 T^3} \right) \sigma_{ij}^3 \quad (F-90)$$

$$\frac{\partial C_0}{\partial T} = 2(1-m_{mix}) \frac{20\eta - 27\eta^2 + 12\eta^3 - 2\eta^4}{(1-\eta)^2 (2-\eta)^3} \cdot \frac{\partial \eta}{\partial T} + 2(1-m_{mix}) \frac{20\eta - 27\eta^2 + 12\eta^3 - 2\eta^4}{(1-\eta)^3 (2-\eta)^2} \cdot \frac{\partial \eta}{\partial T} \quad (F-91)$$

$$+ 4m_{mix} \frac{8\eta - 2\eta^2}{(1-\eta)^5} \cdot \frac{\partial \eta}{\partial T} + m_{mix} \frac{8 \frac{\partial \eta}{\partial T} - 4\eta \frac{\partial \eta}{\partial T}}{(1-\eta)^4} + (1-m_{mix}) \frac{20 \frac{\partial \eta}{\partial T} - 54\eta \frac{\partial \eta}{\partial T} + 36\eta^2 \frac{\partial \eta}{\partial T} - 8\eta^3 \frac{\partial \eta}{\partial T}}{[(1-\eta)(2-\eta)]^2}$$

$$\frac{\partial C_1}{\partial T} = \frac{\partial}{\partial T}(C_1) = - \frac{1}{C_0^2} \cdot \frac{\partial C_0}{\partial T} \quad (F-92)$$

$$\frac{\partial I_2(\eta, m_{mix})}{\partial T} = \sum_{i=0}^6 i \times b_i (m_{mix}) \eta^{i-1} \cdot \frac{\partial \eta}{\partial T} \quad (F-93)$$

iii) Volume

$$\frac{\partial F_{mix}^{disp}}{\partial V} = \frac{\partial}{\partial V}(F_{mix}^{disp}) = \frac{\partial}{\partial V}(F_{mix}^{disp,1}) + \frac{\partial}{\partial V}(F_{mix}^{disp,2}) \quad (F-94)$$

Perturbation term1

$$\frac{\partial F_{mix}^{disp,1}}{\partial V} = 2\pi \frac{N_{av} n_{total}^2}{V^2} I_1(\eta, m_{mix}) \left(m^2 \frac{\epsilon}{kT} \sigma^3 \right)_{mix} - 2\pi \frac{N_{av} n_{total}^2}{V} \left(m^2 \frac{\epsilon}{kT} \sigma^3 \right)_{mix} \frac{\partial I_1(\eta, m_{mix})}{\partial V} \quad (F-95)$$

$$\frac{\partial I_1(\eta, m_{mix})}{\partial V} = \sum_{i=0}^6 i \times a_i (m_{mix}) \eta^{i-1} \cdot \frac{\partial \eta}{\partial V} \quad (F-96)$$

$$\frac{\partial \eta}{\partial V} = \frac{\partial \zeta_3}{\partial V} = - \frac{N_{av} \pi}{6V^2} \sum_i^{nc} n_i m_i d_i^3 \quad (F-97)$$

Perturbation term2

$$\begin{aligned} \frac{\partial F_{mix}^{disp,2}}{\partial V} = & \pi \frac{N_{av} n_{total}^2}{V^2} m_{mix} C_1 I_2(\eta, m_{mix}) \left(m^2 \left(\frac{\epsilon}{kT} \right)^2 \sigma^3 \right)_{mix} \\ & - \pi \frac{N_{av} n_{total}^2}{V} m_{mix} I_2(\eta, m_{mix}) \left(m^2 \left(\frac{\epsilon}{kT} \right)^2 \sigma^3 \right)_{mix} \cdot \frac{\partial C_1}{\partial V} \\ & - \pi \frac{N_{av} n_{total}^2}{V} m_{mix} C_1 \left(m^2 \left(\frac{\epsilon}{kT} \right)^2 \sigma^3 \right)_{mix} \cdot \frac{\partial I_2(\eta, m_{mix})}{\partial V} \end{aligned} \quad (F-98)$$

$$\begin{aligned} \frac{\partial C_0}{\partial V} = & 2(1-m_{mix}) \frac{20\eta - 27\eta^2 + 12\eta^3 - 2\eta^4}{(1-\eta)^2 (2-\eta)^3} \cdot \frac{\partial \eta}{\partial V} + 2(1-m_{mix}) \frac{20\eta - 27\eta^2 + 12\eta^3 - 2\eta^4}{(1-\eta)^3 (2-\eta)^2} \cdot \frac{\partial \eta}{\partial V} \\ & + 4m_{mix} \frac{8\eta - 2\eta^2}{(1-\eta)^5} \cdot \frac{\partial \eta}{\partial V} + m_{mix} \frac{8\frac{\partial \eta}{\partial V} - 4\eta \frac{\partial \eta}{\partial V}}{(1-\eta)^4} + (1-m_{mix}) \frac{20\frac{\partial \eta}{\partial V} - 54\eta \frac{\partial \eta}{\partial V} + 36\eta^2 \frac{\partial \eta}{\partial V} - 8\eta^3 \frac{\partial \eta}{\partial V}}{[(1-\eta)(2-\eta)]^2} \end{aligned} \quad ((F-99)$$

$$\frac{\partial C_1}{\partial V} = \frac{\partial}{\partial V}(C_1) = -\frac{1}{C_0^2} \cdot \frac{\partial C_0}{\partial V} \quad (F-100)$$

$$\frac{\partial I_2(\eta, m_{mix})}{\partial V} = \sum_{i=0}^6 i \times b_i(m_{mix}) \eta^{i-1} \cdot \frac{\partial \eta}{\partial V} \quad (F-101)$$

F.3.3 Second-order derivatives

i) Composition – Composition

$$\frac{\partial^2 F_{mix}^{disp}}{\partial n_k \partial n_i} = \frac{\partial^2}{\partial n_k \partial n_k} (F_{mix}^{disp}) = \frac{\partial^2}{\partial n_k \partial n_k} (F_{mix}^{disp,1}) + \frac{\partial^2}{\partial n_k \partial n_k} (F_{mix}^{disp,2}) \quad (F-102)$$

Perturbation term 1

$$\begin{aligned}
 \frac{\partial^2 F_{mix}^{disp,1}}{\partial n_k \partial n_l} = & -4\pi \frac{N_{av}}{V} I_1(\eta, m_{mix}) \left(m^2 \frac{\epsilon}{kT} \sigma^3 \right)_{mix} - 4\pi \frac{N_{av} n_{total}}{V} \cdot I_1(\eta, m_{mix}) \cdot \frac{\partial \left(m^2 \frac{\epsilon}{kT} \sigma^3 \right)_{mix}}{\partial n_k} \\
 & - 4\pi \frac{N_{av} n_{total}}{V} \cdot I_1(\eta, m_{mix}) \cdot \frac{\partial \left(m^2 \frac{\epsilon}{kT} \sigma^3 \right)_{mix}}{\partial n_l} - 2\pi \frac{N_{av} n_{total}^2}{V} \cdot I_1(\eta, m_{mix}) \cdot \frac{\partial^2 \left(m^2 \frac{\epsilon}{kT} \sigma^3 \right)_{mix}}{\partial n_k \partial n_l} \\
 & - 4\pi \frac{N_{av} n_{total}}{V} \cdot \left(m^2 \frac{\epsilon}{kT} \sigma^3 \right)_{mix} \cdot \frac{\partial I_1(\eta, m_{mix})}{\partial n_k} - 4\pi \frac{N_{av} n_{total}}{V} \cdot \left(m^2 \frac{\epsilon}{kT} \sigma^3 \right)_{mix} \cdot \frac{\partial I_1(\eta, m_{mix})}{\partial n_l} \\
 & - 2\pi \frac{N_{av} n_{total}^2}{V} \cdot \frac{\partial \left(m^2 \frac{\epsilon}{kT} \sigma^3 \right)_{mix}}{\partial n_k} \cdot \frac{\partial I_1(\eta, m_{mix})}{\partial n_l} - 2\pi \frac{N_{av} n_{total}^2}{V} \cdot \frac{\partial \left(m^2 \frac{\epsilon}{kT} \sigma^3 \right)_{mix}}{\partial n_l} \cdot \frac{\partial I_1(\eta, m_{mix})}{\partial n_k} \\
 & - 2\pi \frac{N_{av} n_{total}^2}{V} \cdot \left(m^2 \frac{\epsilon}{kT} \sigma^3 \right)_{mix} \cdot \frac{\partial^2 I_1(\eta, m_{mix})}{\partial n_k \partial n_l}
 \end{aligned}
 \tag{F-103}$$

$$\begin{aligned}
 \frac{\partial^2 \left(m^2 \frac{\epsilon}{kT} \sigma^3 \right)_{mix}}{\partial n_k \partial n_l} = & \frac{2}{(n_{total})^2} m_k m_l \left(\frac{\epsilon_{kl}}{kT} \right) \sigma_{kl}^3 - \frac{4}{(n_{total})^3} \sum_j^{nc} n_j m_k m_j \left(\frac{\epsilon_{kj}}{kT} \right) \sigma_{kj}^3 \\
 & - \frac{4}{(n_{total})^3} \sum_j^{nc} n_j m_l m_j \left(\frac{\epsilon_{lj}}{kT} \right) \sigma_{lj}^3 + \frac{6}{(n_{total})^4} \sum_i^{nc} \sum_j^{nc} n_i n_j m_i m_j \left(\frac{\epsilon_{ij}}{kT} \right) \sigma_{ij}^3
 \end{aligned}
 \tag{F-104}$$

$$\frac{\partial I_1(\eta, m_{mix})}{\partial n_k \partial n_l} = \sum_{i=0}^6 \left[\eta^i \frac{\partial^2 a_i}{\partial n_k \partial n_l} + i \times \frac{\partial \eta^i}{\partial n_l} \cdot \frac{\partial a_i}{\partial n_k} \eta^{i-1} + i \times \frac{\partial \eta^i}{\partial n_k} \cdot \frac{\partial a_i}{\partial n_l} \eta^{i-1} \right. \\
 \left. + i \times (i-1) a_i \frac{\partial \eta}{\partial n_k} \cdot \frac{\partial \eta}{\partial n_l} \eta^{i-2} + i \times a_i \frac{\partial^2 \eta}{\partial n_k \partial n_l} \eta^{i-1} \right]
 \tag{F-105}$$

$$\frac{\partial^2 \eta}{\partial n_k \partial n_l} = \frac{\partial^2 \zeta_3}{\partial n_k \partial n_l} = \frac{\partial}{\partial n_l} \left(\frac{\partial \zeta_3}{\partial n_k} \right) = \frac{\partial}{\partial n_l} \left(\frac{N_{av} \pi}{6V} m_k d_k^3 \right) = 0
 \tag{F-106}$$

$$\frac{\partial^2 a_i}{\partial n_k \partial n_l} = \frac{-2(-6a_{2i} + (a_{1i} + 3a_{2i})m_{mix}) \frac{\partial m_{mix}}{\partial n_k} \cdot \frac{\partial m_{mix}}{\partial n_l} + m_{mix}(-4a_{2i} + (a_{1i} + 3a_{2i})m_{mix}) \frac{\partial^2 m_{mix}}{\partial n_k \partial n_l}}{(m_{mix})^4}
 \tag{F-107}$$

Perturbation term 2

$$\begin{aligned}
 \frac{\partial^2 F_{mix}^{dis,2}}{\partial n_k \partial n_l} = & -2\pi \frac{N_{av} n_{total}}{V} C_{12}(\eta, m_{mix}) \left(m^2 \left(\frac{\epsilon}{kT} \right)^2 \sigma^3 \right)_{mix} \cdot \frac{\partial m_{mix}}{\partial n_k} - 2\pi \frac{N_{av} n_{total}}{V} C_{12}(\eta, m_{mix}) \left(m^2 \left(\frac{\epsilon}{kT} \right)^2 \sigma^3 \right)_{mix} \cdot \frac{\partial m_{mix}}{\partial n_l} \\
 & - 2\pi \frac{N_{av}}{V} C_{12}(\eta, m_{mix}) m_{mix} \left(m^2 \left(\frac{\epsilon}{kT} \right)^2 \sigma^3 \right)_{mix} - \pi \frac{N_{av} n_{total}^2}{V} C_{12}(\eta, m_{mix}) \left(m^2 \left(\frac{\epsilon}{kT} \right)^2 \sigma^3 \right)_{mix} \cdot \frac{\partial^2 m_{mix}}{\partial n_k \partial n_l} \\
 & - \pi \frac{N_{av} n_{total}^2}{V} C_{12}(\eta, m_{mix}) \cdot \frac{\partial \left(m^2 \left(\frac{\epsilon}{kT} \right)^2 \sigma^3 \right)_{mix}}{\partial n_l} \cdot \frac{\partial m_{mix}}{\partial n_k} - 2\pi \frac{N_{av} n_{total}}{V} C_{12}(\eta, m_{mix}) m_{mix} \cdot \frac{\partial \left(m^2 \left(\frac{\epsilon}{kT} \right)^2 \sigma^3 \right)_{mix}}{\partial n_l} \\
 & - \pi \frac{N_{av} n_{total}^2}{V} C_{12}(\eta, m_{mix}) \cdot \frac{\partial \left(m^2 \left(\frac{\epsilon}{kT} \right)^2 \sigma^3 \right)_{mix}}{\partial n_k} \cdot \frac{\partial m_{mix}}{\partial n_l} - 2\pi \frac{N_{av} n_{total}}{V} C_{12}(\eta, m_{mix}) m_{mix} \cdot \frac{\partial \left(m^2 \left(\frac{\epsilon}{kT} \right)^2 \sigma^3 \right)_{mix}}{\partial n_k} \\
 & - \pi \frac{N_{av} n_{total}^2}{V} C_{12}(\eta, m_{mix}) m_{mix} \cdot \frac{\partial^2 \left(m^2 \left(\frac{\epsilon}{kT} \right)^2 \sigma^3 \right)_{mix}}{\partial n_k \partial n_l} - \pi \frac{N_{av} n_{total}^2}{V} I_2(\eta, m_{mix}) \left(m^2 \left(\frac{\epsilon}{kT} \right)^2 \sigma^3 \right)_{mix} \cdot \frac{\partial m_{mix}}{\partial n_k} \cdot \frac{\partial C_1}{\partial n_l} \\
 & - 2\pi \frac{N_{av} n_{total}}{V} I_2(\eta, m_{mix}) m_{mix} \left(m^2 \left(\frac{\epsilon}{kT} \right)^2 \sigma^3 \right)_{mix} \cdot \frac{\partial C_1}{\partial n_l} - \pi \frac{N_{av} n_{total}^2}{V} I_2(\eta, m_{mix}) m_{mix} \cdot \frac{\partial \left(m^2 \left(\frac{\epsilon}{kT} \right)^2 \sigma^3 \right)_{mix}}{\partial n_k} \cdot \frac{\partial C_1}{\partial n_l} \\
 & - \pi \frac{N_{av} n_{total}^2}{V} C_1 \left(m^2 \left(\frac{\epsilon}{kT} \right)^2 \sigma^3 \right)_{mix} \cdot \frac{\partial m_{mix}}{\partial n_k} \cdot \frac{\partial I_2(\eta, m_{mix})}{\partial n_l} - 2\pi \frac{N_{av} n_{total}}{V} C_1 m_{mix} \left(m^2 \left(\frac{\epsilon}{kT} \right)^2 \sigma^3 \right)_{mix} \cdot \frac{\partial I_2(\eta, m_{mix})}{\partial n_l} \\
 & - \pi \frac{N_{av} n_{total}^2}{V} C_1 m_{mix} \cdot \frac{\partial \left(m^2 \left(\frac{\epsilon}{kT} \right)^2 \sigma^3 \right)_{mix}}{\partial n_k} \cdot \frac{\partial I_2(\eta, m_{mix})}{\partial n_l} - \pi \frac{N_{av} n_{total}^2}{V} I_2(\eta, m_{mix}) \left(m^2 \left(\frac{\epsilon}{kT} \right)^2 \sigma^3 \right)_{mix} \cdot \frac{\partial m_{mix}}{\partial n_l} \cdot \frac{\partial C_1}{\partial n_k} \\
 & - 2\pi \frac{N_{av} n_{total}}{V} I_2(\eta, m_{mix}) m_{mix} \left(m^2 \left(\frac{\epsilon}{kT} \right)^2 \sigma^3 \right)_{mix} \cdot \frac{\partial C_1}{\partial n_k} - \pi \frac{N_{av} n_{total}^2}{V} I_2(\eta, m_{mix}) m_{mix} \cdot \frac{\partial \left(m^2 \left(\frac{\epsilon}{kT} \right)^2 \sigma^3 \right)_{mix}}{\partial n_l} \cdot \frac{\partial C_1}{\partial n_k} \\
 & - \pi \frac{N_{av} n_{total}^2}{V} \left(m^2 \left(\frac{\epsilon}{kT} \right)^2 \sigma^3 \right)_{mix} m_{mix} \frac{\partial I_2(\eta, m_{mix})}{\partial n_l} \cdot \frac{\partial C_1}{\partial n_k} - \pi \frac{N_{av} n_{total}^2}{V} C_1 \left(m^2 \left(\frac{\epsilon}{kT} \right)^2 \sigma^3 \right)_{mix} \cdot \frac{\partial m_{mix}}{\partial n_l} \cdot \frac{\partial I_2(\eta, m_{mix})}{\partial n_k} \\
 & - 2\pi \frac{N_{av} n_{total}}{V} C_1 m_{mix} \left(m^2 \left(\frac{\epsilon}{kT} \right)^2 \sigma^3 \right)_{mix} \cdot \frac{\partial I_2(\eta, m_{mix})}{\partial n_k} - \pi \frac{N_{av} n_{total}}{V} C_1 m_{mix} \cdot \frac{\partial \left(m^2 \left(\frac{\epsilon}{kT} \right)^2 \sigma^3 \right)_{mix}}{\partial n_l} \cdot \frac{\partial I_2(\eta, m_{mix})}{\partial n_k} \\
 & - \pi \frac{N_{av} n_{total}^2}{V} \left(m^2 \left(\frac{\epsilon}{kT} \right)^2 \sigma^3 \right)_{mix} m_{mix} \frac{\partial I_2(\eta, m_{mix})}{\partial n_k} \cdot \frac{\partial C_1}{\partial n_l} - \pi \frac{N_{av} n_{total}^2}{V} I_2(\eta, m_{mix}) \left(m^2 \left(\frac{\epsilon}{kT} \right)^2 \sigma^3 \right)_{mix} m_{mix} \cdot \frac{\partial^2 C_1}{\partial n_k \partial n_l} \\
 & - \pi \frac{N_{av} n_{total}^2}{V} \left(m^2 \left(\frac{\epsilon}{kT} \right)^2 \sigma^3 \right)_{mix} C_1 m_{mix} \frac{\partial^2 I_2(\eta, m_{mix})}{\partial n_k \partial n_l}
 \end{aligned}
 \tag{F-108}$$

$$\frac{\partial^2 \left(m^2 \left(\frac{\epsilon_{kl}}{kT} \right)^2 \sigma^3 \right)}{\partial n_k \partial n_l}_{mix} = \frac{2}{(n_{total})^2} m_k m_l \left(\frac{\epsilon_{kl}}{kT} \right)^2 \sigma_{kl}^3 - \frac{4}{(n_{total})^3} \sum_j^{nc} n_j m_k m_j \left(\frac{\epsilon_{kj}}{kT} \right)^2 \sigma_{kj}^3$$

$$- \frac{4}{(n_{total})^3} \sum_j^{nc} n_j m_l m_j \left(\frac{\epsilon_{lj}}{kT} \right)^2 \sigma_{lj}^3 + \frac{6}{(n_{total})^4} \sum_i^{nc} \sum_j^{nc} n_i n_j m_i m_j \left(\frac{\epsilon_{ij}}{kT} \right)^2 \sigma_{ij}^3$$
(F-109)

$$\frac{\partial^2 C_0}{\partial n_k \partial n_l} = \frac{\partial}{\partial n_l} \left(\frac{\partial C_0}{\partial n_k} \right) = \frac{\partial}{\partial n_l} \left(\begin{aligned} & \frac{8\eta - 2\eta^2}{(1-\eta)^4} \cdot \frac{\partial m_{mix}}{\partial n_k} - \frac{20\eta - 27\eta^2 + 12\eta^3 - 2\eta^4}{[(1-\eta)(2-\eta)]^2} \cdot \frac{\partial m_{mix}}{\partial n_k} \\ & + 2(1-m_{mix}) \frac{20\eta - 27\eta^2 + 12\eta^3 - 2\eta^4}{(1-\eta)^2 (2-\eta)^3} \cdot \frac{\partial \eta}{\partial n_k} \\ & + 2(1-m_{mix}) \frac{20\eta - 27\eta^2 + 12\eta^3 - 2\eta^4}{(1-\eta)^3 (2-\eta)^2} \cdot \frac{\partial \eta}{\partial n_k} \\ & + 4m_{mix} \frac{8\eta - 2\eta^2}{(1-\eta)^5} \cdot \frac{\partial \eta}{\partial n_k} + m_{mix} \frac{8 \frac{\partial \eta}{\partial n_k} - 4\eta \frac{\partial \eta}{\partial n_k}}{(1-\eta)^4} \\ & + (1-m_{mix}) \frac{20 \frac{\partial \eta}{\partial n_k} - 54\eta \frac{\partial \eta}{\partial n_k} + 36\eta^2 \frac{\partial \eta}{\partial n_k} - 8\eta^3 \frac{\partial \eta}{\partial n_k}}{[(1-\eta)(2-\eta)]^2} \end{aligned} \right)$$
(F-110)

The second-order compositional derivative is estimate the numerically, because the author was unable to code the correct analytical expression. This does not influence the results presented, since the derivative is only in phase equilibria calculations.

$$\frac{\partial I_2(\eta, m_{mix})}{\partial n_k \partial n_l} = \sum_{i=0}^6 \left[\begin{aligned} & \eta^i \frac{\partial^2 b_i}{\partial n_k \partial n_l} + i \times \frac{\partial \eta^i}{\partial n_l} \cdot \frac{\partial b_i}{\partial n_k} \eta^{i-1} + i \times \frac{\partial \eta^i}{\partial n_k} \cdot \frac{\partial b_i}{\partial n_l} \eta^{i-1} \\ & + i \times (i-1) b_i \frac{\partial \eta}{\partial n_k} \cdot \frac{\partial \eta}{\partial n_l} \eta^{i-2} + i \times b_i \frac{\partial^2 \eta}{\partial n_k \partial n_l} \eta^{i-1} \end{aligned} \right]$$
(F-111)

$$\frac{\partial^2 b_i}{\partial n_k \partial n_l} = \frac{-2(-6b_{2i} + (b_{1i} + 3b_{2i})m_{mix}) \frac{\partial m_{mix}}{\partial n_k} \cdot \frac{\partial m_{mix}}{\partial n_l} + m_{mix} (-4b_{2i} + (b_{1i} + 3b_{2i})m_{mix}) \frac{\partial^2 m_{mix}}{\partial n_k \partial n_l}}{(m_{mix})^4}$$
(F-112)

ii) Composition – Volume

$$\frac{\partial^2 F_{mix}^{disp}}{\partial V \partial n_k} = \frac{\partial^2}{\partial V \partial n_k} (F_{mix}^{disp}) = \frac{\partial^2}{\partial V \partial n_k} (F_{mix}^{disp,1}) + \frac{\partial^2}{\partial V \partial n_k} (F_{mix}^{disp,2})$$
(F-113)

Perturbation term 1

$$\frac{\partial^2 F_{mix}^{disp,1}}{\partial V \partial n_k} = 4\pi \frac{N_{av} n_{total}}{V^2} I_1(\eta, m_{mix}) \left(m^2 \frac{\epsilon}{kT} \sigma^3 \right)_{mix} + 2\pi \frac{N_{av} n_{total}^2}{V^2} I_1(\eta, m_{mix}) \frac{\partial \left(m^2 \frac{\epsilon}{kT} \sigma^3 \right)_{mix}}{\partial n_k} \quad (F-114)$$

$$\begin{aligned} & - 4\pi \frac{N_{av} n_{total}}{V} \left(m^2 \frac{\epsilon}{kT} \sigma^3 \right)_{mix} \cdot \frac{\partial I_1(\eta, m_{mix})}{\partial V} - 2\pi \frac{N_{av} n_{total}^2}{V} \cdot \frac{\partial \left(m^2 \frac{\epsilon}{kT} \sigma^3 \right)_{mix}}{\partial n_k} \cdot \frac{\partial I_1(\eta, m_{mix})}{\partial V} \\ & + 2\pi \frac{N_{av} n_{total}^2}{V^2} \left(m^2 \frac{\epsilon}{kT} \sigma^3 \right)_{mix} \cdot \frac{\partial I_1(\eta, m_{mix})}{\partial n_k} - 2\pi \frac{N_{av} n_{total}^2}{V} \left(m^2 \frac{\epsilon}{kT} \sigma^3 \right)_{mix} \cdot \frac{\partial^2 I_1(\eta, m_{mix})}{\partial V \partial n_k} \end{aligned}$$

$$\frac{\partial^2 I_1(\eta, m_{mix})}{\partial V \partial n_k} = \sum_{i=0}^6 \left[i \times \frac{\partial a_i}{\partial n_k} \cdot \eta^{i-1} \cdot \frac{\partial \eta}{\partial V} + i \times (i-1) a_i \frac{\partial \eta}{\partial n_k} \cdot \frac{\partial \eta}{\partial V} \eta^{i-2} + i \times a_i \frac{\partial^2 \eta}{\partial n_k \partial V} \eta^{i-1} \right] \quad (F-115)$$

$$\frac{\partial^2 \eta}{\partial n_k \partial V} = \frac{\partial^2 \zeta_3}{\partial n_k \partial V} = -\frac{N_{av} \pi}{6V^2} m_k d_k^3 \quad (F-116)$$

Perturbation term 2

$$\frac{\partial^2 F_{mix}^{disp,2}}{\partial V \partial n_k} = \pi \frac{N_{av} n_{total}^2}{V^2} C_1 I_2(\eta, m_{mix}) \left(m^2 \left(\frac{\epsilon}{kT} \right)^2 \sigma^3 \right)_{mix} \frac{\partial m_{mix}}{\partial n_k} + 2\pi \frac{N_{av} n_{total}^2}{V^2} m_{mix} C_1 I_2(\eta, m_{mix}) \left(m^2 \left(\frac{\epsilon}{kT} \right)^2 \sigma^3 \right)_{mix} \quad (F-117)$$

$$\begin{aligned} & + \pi \frac{N_{av} n_{total}^2}{V^2} m_{mix} C_1 I_2(\eta, m_{mix}) \frac{\partial \left(m^2 \left(\frac{\epsilon}{kT} \right)^2 \sigma^3 \right)_{mix}}{\partial n_k} - \pi \frac{N_{av} n_{total}^2}{V} I_2(\eta, m_{mix}) \left(m^2 \left(\frac{\epsilon}{kT} \right)^2 \sigma^3 \right)_{mix} \cdot \frac{\partial C_1}{\partial V} \cdot \frac{\partial m_{mix}}{\partial n_k} \\ & - 2\pi \frac{N_{av} n_{total}}{V} m_{mix} I_2(\eta, m_{mix}) \left(m^2 \left(\frac{\epsilon}{kT} \right)^2 \sigma^3 \right)_{mix} \cdot \frac{\partial C_1}{\partial V} - \pi \frac{N_{av} n_{total}^2}{V^2} m_{mix} I_2(\eta, m_{mix}) \frac{\partial \left(m^2 \left(\frac{\epsilon}{kT} \right)^2 \sigma^3 \right)_{mix}}{\partial n_k} \cdot \frac{\partial C_1}{\partial V} \\ & - \pi \frac{N_{av} n_{total}^2}{V} C_1 \left(m^2 \left(\frac{\epsilon}{kT} \right)^2 \sigma^3 \right)_{mix} \cdot \frac{\partial I_2(\eta, m_{mix})}{\partial V} \cdot \frac{\partial m_{mix}}{\partial n_k} - 2\pi \frac{N_{av} n_{total}}{V} C_1 m_{mix} \left(m^2 \left(\frac{\epsilon}{kT} \right)^2 \sigma^3 \right)_{mix} \cdot \frac{\partial I_2(\eta, m_{mix})}{\partial V} \\ & - \pi \frac{N_{av} n_{total}^2}{V} C_1 m_{mix} \frac{\partial \left(m^2 \left(\frac{\epsilon}{kT} \right)^2 \sigma^3 \right)_{mix}}{\partial n_k} \cdot \frac{\partial I_2(\eta, m_{mix})}{\partial V} + \pi \frac{N_{av} n_{total}^2}{V^2} m_{mix} I_2(\eta, m_{mix}) \left(m^2 \left(\frac{\epsilon}{kT} \right)^2 \sigma^3 \right)_{mix} \cdot \frac{\partial C_1}{\partial n_k} \\ & - \pi \frac{N_{av} n_{total}^2}{V} m_{mix} \left(m^2 \left(\frac{\epsilon}{kT} \right)^2 \sigma^3 \right)_{mix} \cdot \frac{\partial C_1}{\partial n_k} \cdot \frac{\partial I_2(\eta, m_{mix})}{\partial V} + \pi \frac{N_{av} n_{total}^2}{V^2} m_{mix} C_1 \left(m^2 \left(\frac{\epsilon}{kT} \right)^2 \sigma^3 \right)_{mix} \cdot \frac{\partial I_2(\eta, m_{mix})}{\partial n_k} \\ & - \pi \frac{N_{av} n_{total}^2}{V} m_{mix} \left(m^2 \left(\frac{\epsilon}{kT} \right)^2 \sigma^3 \right)_{mix} \cdot \frac{\partial C_1}{\partial V} \cdot \frac{\partial I_2(\eta, m_{mix})}{\partial n_k} - \pi \frac{N_{av} n_{total}^2}{V} m_{mix} I_2(\eta, m_{mix}) \left(m^2 \left(\frac{\epsilon}{kT} \right)^2 \sigma^3 \right)_{mix} \cdot \frac{\partial^2 C_1}{\partial V \partial n_k} \\ & - \pi \frac{N_{av} n_{total}^2}{V} m_{mix} C_1 \left(m^2 \left(\frac{\epsilon}{kT} \right)^2 \sigma^3 \right)_{mix} \cdot \frac{\partial^2 I_2(\eta, m_{mix})}{\partial V \partial n_k} \end{aligned}$$

$$\begin{aligned}
 \frac{\partial^2 C_0}{\partial V \partial n_k} = & 4 \frac{8\eta - 2\eta^2}{(1-\eta)^5} \cdot \frac{\partial m_{mix}}{\partial n_k} \cdot \frac{\partial \eta}{\partial V} - 2 \frac{20\eta - 27\eta^2 + 12\eta^3 - 2\eta^4}{(1-\eta)^2 (2-\eta)^3} \cdot \frac{\partial m_{mix}}{\partial n_k} \cdot \frac{\partial \eta}{\partial V} \\
 & - 2 \frac{20\eta - 27\eta^2 + 12\eta^3 - 2\eta^4}{(1-\eta)^3 (2-\eta)^2} \cdot \frac{\partial m_{mix}}{\partial n_k} \cdot \frac{\partial \eta}{\partial V} + \frac{\left(8 \frac{\partial \eta}{\partial V} - 4\eta \frac{\partial \eta}{\partial V}\right)}{(1-\eta)^4} \cdot \frac{\partial m_{mix}}{\partial n_k} \\
 & - \frac{20 \frac{\partial \eta}{\partial V} - 54\eta \frac{\partial \eta}{\partial V} + 36\eta^2 \frac{\partial \eta}{\partial V} - 8\eta^3 \frac{\partial \eta}{\partial V}}{(1-\eta)^2 (2-\eta)^2} \cdot \frac{\partial m_{mix}}{\partial n_k} + 6(1-m_{mix}) \frac{20\eta - 27\eta^2 + 12\eta^3 - 2\eta^4}{(1-\eta)^2 (2-\eta)^4} \cdot \frac{\partial \eta}{\partial V} \cdot \frac{\partial \eta}{\partial n_k} \\
 & + 8(1-m_{mix}) \frac{20\eta - 27\eta^2 + 12\eta^3 - 2\eta^4}{(1-\eta)^3 (2-\eta)^3} \cdot \frac{\partial \eta}{\partial V} \cdot \frac{\partial \eta}{\partial n_k} + 6(1-m_{mix}) \frac{20\eta - 27\eta^2 + 12\eta^3 - 2\eta^4}{(1-\eta)^4 (2-\eta)^2} \cdot \frac{\partial \eta}{\partial V} \cdot \frac{\partial \eta}{\partial n_k} \\
 & + 20m_{mix} \frac{(8\eta - 2\eta^2)}{(1-\eta)^6} \cdot \frac{\partial \eta}{\partial V} \cdot \frac{\partial \eta}{\partial n_k} + 4m_{mix} \frac{\left(8 \frac{\partial \eta}{\partial V} - 4\eta \frac{\partial \eta}{\partial V}\right)}{(1-\eta)^5} \cdot \frac{\partial \eta}{\partial n_k} \\
 & + 2(1-m_{mix}) \frac{20 \frac{\partial \eta}{\partial V} - 54\eta \frac{\partial \eta}{\partial V} + 36\eta^2 \frac{\partial \eta}{\partial V} - 8\eta^3 \frac{\partial \eta}{\partial V}}{(1-\eta)^2 (2-\eta)^3} \cdot \frac{\partial \eta}{\partial n_k} \\
 & + 2(1-m_{mix}) \frac{20 \frac{\partial \eta}{\partial V} - 54\eta \frac{\partial \eta}{\partial V} + 36\eta^2 \frac{\partial \eta}{\partial V} - 8\eta^3 \frac{\partial \eta}{\partial V}}{(1-\eta)^3 (2-\eta)^2} \cdot \frac{\partial \eta}{\partial n_k} \\
 & + 4m_{mix} \frac{\left(8 \frac{\partial \eta}{\partial n_k} - 4\eta \frac{\partial \eta}{\partial n_k}\right)}{(1-\eta)^5} \cdot \frac{\partial \eta}{\partial V} + 2(1-m_{mix}) \frac{20 \frac{\partial \eta}{\partial n_k} - 54\eta \frac{\partial \eta}{\partial n_k} + 36\eta^2 \frac{\partial \eta}{\partial n_k} - 8\eta^3 \frac{\partial \eta}{\partial n_k}}{(1-\eta)^2 (2-\eta)^3} \cdot \frac{\partial \eta}{\partial V} \\
 & + 2(1-m_{mix}) \frac{20 \frac{\partial \eta}{\partial n_k} - 54\eta \frac{\partial \eta}{\partial n_k} + 36\eta^2 \frac{\partial \eta}{\partial n_k} - 8\eta^3 \frac{\partial \eta}{\partial n_k}}{(1-\eta)^3 (2-\eta)^2} \cdot \frac{\partial \eta}{\partial V} \\
 & + 2(1-m_{mix}) \frac{20\eta - 27\eta^2 + 12\eta^3 - 2\eta^4}{(1-\eta)^2 (2-\eta)^3} \cdot \frac{\partial^2 \eta}{\partial n_k \partial V} \\
 & + 2(1-m_{mix}) \frac{20\eta - 27\eta^2 + 12\eta^3 - 2\eta^4}{(1-\eta)^3 (2-\eta)^2} \cdot \frac{\partial^2 \eta}{\partial n_k \partial V} + 4m_{mix} \frac{8\eta - 2\eta^2}{(1-\eta)^5} \cdot \frac{\partial^2 \eta}{\partial n_k \partial V} \\
 & + (1-m_{mix}) \frac{\left(-54 \frac{\partial \eta}{\partial V} \cdot \frac{\partial \eta}{\partial n_k} + 72\eta \frac{\partial \eta}{\partial V} \cdot \frac{\partial \eta}{\partial n_k} - 24\eta^2 \frac{\partial \eta}{\partial V} \cdot \frac{\partial \eta}{\partial n_k} \right.}{(1-\eta)^2 (2-\eta)^2} \\
 & \quad \left. + 20 \frac{\partial^2 \eta}{\partial n_k \partial V} - 54\eta \frac{\partial^2 \eta}{\partial n_k \partial V} + 36\eta^2 \frac{\partial^2 \eta}{\partial n_k \partial V} - 8\eta^3 \frac{\partial^2 \eta}{\partial n_k \partial V} \right)
 \end{aligned}
 \tag{F-118}$$

$$\frac{\partial^2 C_1}{\partial V \partial n_k} = \frac{\partial}{\partial n_k} \left(\frac{\partial C_1}{\partial V} \right) = \frac{2}{C_0^3} \cdot \frac{\partial C_0}{\partial V} \cdot \frac{\partial C_0}{\partial n_k} - \frac{1}{C_0^2} \cdot \frac{\partial^2 C_0}{\partial V \partial n_k}
 \tag{F-119}$$

$$\frac{\partial^2 I_2(\eta, m_{mix})}{\partial V \partial n_k} = \sum_{i=0}^6 \left[i \times \frac{\partial b_i}{\partial n_k} \cdot \eta^{i-1} \cdot \frac{\partial \eta}{\partial V} + i \times (i-1) b_i \frac{\partial \eta}{\partial n_k} \cdot \frac{\partial \eta}{\partial V} \eta^{i-2} + i \times b_i \frac{\partial^2 \eta}{\partial n_k \partial V} \eta^{i-1} \right] \quad (F-120)$$

iii) Composition – Temperature

$$\frac{\partial^2 F_{mix}^{disp}}{\partial T \partial n_k} = \frac{\partial^2}{\partial T \partial n_k} (F_{mix}^{disp}) = \frac{\partial^2}{\partial T \partial n_k} (F_{mix}^{disp,1}) + \frac{\partial^2}{\partial T \partial n_k} (F_{mix}^{disp,2}) \quad (F-121)$$

Perturbation term 1

$$\begin{aligned} \frac{\partial^2 F_{mix}^{disp,1}}{\partial T \partial n_k} = & -4\pi \frac{N_{av} n_{total}}{V} I_1(\eta, m_{mix}) \cdot \frac{\partial \left(m^2 \frac{\epsilon}{kT} \sigma^3 \right)_{mix}}{\partial T} \\ & - 2\pi \frac{N_{av} n_{total}^2}{V} I_1(\eta, m_{mix}) \cdot \frac{\partial^2 \left(m^2 \frac{\epsilon}{kT} \sigma^3 \right)_{mix}}{\partial T \partial n_k} \\ & - 4\pi \frac{N_{av} n_{total}}{V} \cdot \left(m^2 \frac{\epsilon}{kT} \sigma^3 \right)_{mix} \cdot \frac{\partial I_1(\eta, m_{mix})}{\partial T} \\ & - 2\pi \frac{N_{av} n_{total}^2}{V} \cdot \frac{\partial \left(m^2 \frac{\epsilon}{kT} \sigma^3 \right)_{mix}}{\partial n_k} \cdot \frac{\partial I_1(\eta, m_{mix})}{\partial T} \\ & - 2\pi \frac{N_{av} n_{total}^2}{V} \frac{\partial \left(m^2 \frac{\epsilon}{kT} \sigma^3 \right)_{mix}}{\partial T} \cdot \frac{\partial I_1(\eta, m_{mix})}{\partial n_k} \\ & - 2\pi \frac{N_{av} n_{total}^2}{V} \left(m^2 \frac{\epsilon}{kT} \sigma^3 \right)_{mix} \cdot \frac{\partial^2 I_1(\eta, m_{mix})}{\partial T \partial n_k} \end{aligned} \quad (F-122)$$

$$\frac{\partial^2 \left(m^2 \frac{\epsilon}{kT} \sigma^3 \right)_{mix}}{\partial T \partial n_k} = -\frac{2}{(n_{total})^2} \sum_j^{nc} n_j m_k m_j \left(\frac{\epsilon_{kj}}{kT^2} \right) \sigma_{kj}^3 + \frac{2}{(n_{total})^3} \sum_i^{nc} \sum_j^{nc} n_i n_j m_i m_j \left(\frac{\epsilon_{ij}}{kT^2} \right) \sigma_{ij}^3 \quad (F-123)$$

$$\frac{\partial^2 I_1(\eta, m_{mix})}{\partial T \partial n_k} = \sum_{i=0}^6 \left[i \times \frac{\partial a_i}{\partial n_k} \cdot \eta^{i-1} \cdot \frac{\partial \eta}{\partial T} + i \times (i-1) a_i \frac{\partial \eta}{\partial n_k} \cdot \frac{\partial \eta}{\partial T} \eta^{i-2} + i \times a_i \frac{\partial^2 \eta}{\partial n_k \partial T} \eta^{i-1} \right] \quad (F-124)$$

$$\frac{\partial^2 \eta}{\partial n_k \partial T} = \frac{\partial^2 \zeta_3}{\partial n_k \partial T} = \frac{N_{av} \pi}{2V} m_k d_k^2 \cdot \frac{\partial d_k}{\partial T} \quad (F-125)$$

Perturbation term 2

$$\begin{aligned}
 \frac{\partial^2 F_{mix}^{disp,2}}{\partial T \partial n_k} = & -\pi \frac{N_{av} n_{total}^2}{V} C_1 I_2(\eta, m_{mix}) \cdot \frac{\partial \left(m^2 \left(\frac{\epsilon}{kT} \right)^2 \sigma^3 \right)_{mix}}{\partial T} \cdot \frac{\partial m_{mix}}{\partial n_k} \\
 & - 2\pi \frac{N_{av} n_{total}}{V} m_{mix} C_1 I_2(\eta, m_{mix}) \cdot \frac{\partial \left(m^2 \left(\frac{\epsilon}{kT} \right)^2 \sigma^3 \right)_{mix}}{\partial T} \\
 & - \pi \frac{N_{av} n_{total}^2}{V} m_{mix} C_1 I_2(\eta, m_{mix}) \cdot \frac{\partial^2 \left(m^2 \left(\frac{\epsilon}{kT} \right)^2 \sigma^3 \right)_{mix}}{\partial T \partial n_k} - \pi \frac{N_{av} n_{total}^2}{V} I_2(\eta, m_{mix}) \left(m^2 \left(\frac{\epsilon}{kT} \right)^2 \sigma^3 \right)_{mix} \cdot \frac{\partial C_1}{\partial T} \cdot \frac{\partial m_{mix}}{\partial n_k} \\
 & - 2\pi \frac{N_{av} n_{total}}{V} m_{mix} I_2(\eta, m_{mix}) \left(m^2 \left(\frac{\epsilon}{kT} \right)^2 \sigma^3 \right)_{mix} \cdot \frac{\partial C_1}{\partial T} - \pi \frac{N_{av} n_{total}^2}{V} m_{mix} I_2(\eta, m_{mix}) \cdot \frac{\partial \left(m^2 \left(\frac{\epsilon}{kT} \right)^2 \sigma^3 \right)_{mix}}{\partial n_k} \cdot \frac{\partial C_1}{\partial T} \\
 & - \pi \frac{N_{av} n_{total}^2}{V} C_1 \left(m^2 \left(\frac{\epsilon}{kT} \right)^2 \sigma^3 \right)_{mix} \cdot \frac{\partial I_2(\eta, m_{mix})}{\partial T} \cdot \frac{\partial m_{mix}}{\partial n_k} - 2\pi \frac{N_{av} n_{total}}{V} m_{mix} C_1 \left(m^2 \left(\frac{\epsilon}{kT} \right)^2 \sigma^3 \right)_{mix} \cdot \frac{\partial I_2(\eta, m_{mix})}{\partial T} \\
 & - \pi \frac{N_{av} n_{total}^2}{V} m_{mix} C_1 \cdot \frac{\partial \left(m^2 \left(\frac{\epsilon}{kT} \right)^2 \sigma^3 \right)_{mix}}{\partial n_k} \cdot \frac{\partial I_2(\eta, m_{mix})}{\partial T} - \pi \frac{N_{av} n_{total}^2}{V} m_{mix} I_2(\eta, m_{mix}) \cdot \frac{\partial \left(m^2 \left(\frac{\epsilon}{kT} \right)^2 \sigma^3 \right)_{mix}}{\partial T} \cdot \frac{\partial C_1}{\partial n_k} \\
 & - \pi \frac{N_{av} n_{total}^2}{V} m_{mix} \left(m^2 \left(\frac{\epsilon}{kT} \right)^2 \sigma^3 \right)_{mix} \cdot \frac{\partial I_2(\eta, m_{mix})}{\partial T} \cdot \frac{\partial C_1}{\partial n_k} - \pi \frac{N_{av} n_{total}^2}{V} m_{mix} C_1 \cdot \frac{\partial \left(m^2 \left(\frac{\epsilon}{kT} \right)^2 \sigma^3 \right)_{mix}}{\partial T} \cdot \frac{\partial I_2(\eta, m_{mix})}{\partial n_k} \\
 & - \pi \frac{N_{av} n_{total}^2}{V} m_{mix} \left(m^2 \left(\frac{\epsilon}{kT} \right)^2 \sigma^3 \right)_{mix} \cdot \frac{\partial I_2(\eta, m_{mix})}{\partial n_k} \cdot \frac{\partial C_1}{\partial T} \\
 & - \pi \frac{N_{av} n_{total}^2}{V} m_{mix} I_2(\eta, m_{mix}) \left(m^2 \left(\frac{\epsilon}{kT} \right)^2 \sigma^3 \right)_{mix} \cdot \frac{\partial^2 C_1}{\partial T \partial n_k} \\
 & - \pi \frac{N_{av} n_{total}^2}{V} m_{mix} C_1 \left(m^2 \left(\frac{\epsilon}{kT} \right)^2 \sigma^3 \right)_{mix} \cdot \frac{\partial I_2(\eta, m_{mix})}{\partial T \partial n_k}
 \end{aligned}$$

$$\frac{\partial^2 I_2(\eta, m_{mix})}{\partial T \partial n_k} = \sum_{i=0}^6 \left[i \times \frac{\partial b_i}{\partial n_k} \cdot \eta^{i-1} \cdot \frac{\partial \eta}{\partial T} + i \times (i-1) b_i \frac{\partial \eta}{\partial n_k} \cdot \frac{\partial \eta}{\partial T} \eta^{i-2} + i \times b_i \frac{\partial^2 \eta}{\partial n_k \partial T} \eta^{i-1} \right] \quad (F-127)$$

$$\frac{\partial^2 \left(m^2 \left(\frac{\epsilon}{kT} \right)^2 \sigma^3 \right)_{mix}}{\partial T \partial n_k} = -\frac{4}{(n_{total})^2} \sum_j^{nc} n_j m_k m_j \left(\frac{\epsilon_{kj}}{kT} \right)^2 \frac{1}{T} \sigma_{kj}^3 + \frac{4}{(n_{total})^3} \sum_i^{nc} \sum_j^{nc} n_i n_j m_i m_j \left(\frac{\epsilon_{ij}}{kT} \right)^2 \frac{1}{T} \sigma_{ij}^3 \quad (F-128)$$

$$\begin{aligned}
 \frac{\partial^2 C_0}{\partial T \partial n_k} = & 4 \frac{8\eta - 2\eta^2}{(1-\eta)^5} \cdot \frac{\partial m_{mix}}{\partial n_k} \cdot \frac{\partial \eta}{\partial T} - 2 \frac{20\eta - 27\eta^2 + 12\eta^3 - 2\eta^4}{(1-\eta)^2 (2-\eta)^3} \cdot \frac{\partial m_{mix}}{\partial n_k} \cdot \frac{\partial \eta}{\partial T} \\
 & - 2 \frac{20\eta - 27\eta^2 + 12\eta^3 - 2\eta^4}{(1-\eta)^3 (2-\eta)^2} \cdot \frac{\partial m_{mix}}{\partial n_k} \cdot \frac{\partial \eta}{\partial T} + \frac{\left(8 \frac{\partial \eta}{\partial T} - 4\eta \frac{\partial \eta}{\partial T}\right)}{(1-\eta)^4} \cdot \frac{\partial m_{mix}}{\partial n_k} \\
 & - \frac{20 \frac{\partial \eta}{\partial T} - 54\eta \frac{\partial \eta}{\partial T} + 36\eta^2 \frac{\partial \eta}{\partial T} - 8\eta^3 \frac{\partial \eta}{\partial T}}{(1-\eta)^2 (2-\eta)^2} \cdot \frac{\partial m_{mix}}{\partial n_k} + 6(1-m_{mix}) \frac{20\eta - 27\eta^2 + 12\eta^3 - 2\eta^4}{(1-\eta)^2 (2-\eta)^4} \cdot \frac{\partial \eta}{\partial T} \cdot \frac{\partial \eta}{\partial n_k} \\
 & + 8(1-m_{mix}) \frac{20\eta - 27\eta^2 + 12\eta^3 - 2\eta^4}{(1-\eta)^3 (2-\eta)^3} \cdot \frac{\partial \eta}{\partial T} \cdot \frac{\partial \eta}{\partial n_k} + 6(1-m_{mix}) \frac{20\eta - 27\eta^2 + 12\eta^3 - 2\eta^4}{(1-\eta)^4 (2-\eta)^2} \cdot \frac{\partial \eta}{\partial T} \cdot \frac{\partial \eta}{\partial n_k} \\
 & + 20m_{mix} \frac{(8\eta - 2\eta^2)}{(1-\eta)^6} \cdot \frac{\partial \eta}{\partial T} \cdot \frac{\partial \eta}{\partial n_k} + 4m_{mix} \frac{\left(8 \frac{\partial \eta}{\partial T} - 4\eta \frac{\partial \eta}{\partial T}\right)}{(1-\eta)^5} \cdot \frac{\partial \eta}{\partial n_k} \\
 & + 2(1-m_{mix}) \frac{20 \frac{\partial \eta}{\partial T} - 54\eta \frac{\partial \eta}{\partial T} + 36\eta^2 \frac{\partial \eta}{\partial T} - 8\eta^3 \frac{\partial \eta}{\partial T}}{(1-\eta)^2 (2-\eta)^3} \cdot \frac{\partial \eta}{\partial n_k} \\
 & + 2(1-m_{mix}) \frac{20 \frac{\partial \eta}{\partial T} - 54\eta \frac{\partial \eta}{\partial T} + 36\eta^2 \frac{\partial \eta}{\partial T} - 8\eta^3 \frac{\partial \eta}{\partial T}}{(1-\eta)^3 (2-\eta)^2} \cdot \frac{\partial \eta}{\partial n_k} \\
 & + 4m_{mix} \frac{\left(8 \frac{\partial \eta}{\partial n_k} - 4\eta \frac{\partial \eta}{\partial n_k}\right)}{(1-\eta)^5} \cdot \frac{\partial \eta}{\partial T} + 2(1-m_{mix}) \frac{20 \frac{\partial \eta}{\partial n_k} - 54\eta \frac{\partial \eta}{\partial n_k} + 36\eta^2 \frac{\partial \eta}{\partial n_k} - 8\eta^3 \frac{\partial \eta}{\partial n_k}}{(1-\eta)^2 (2-\eta)^3} \cdot \frac{\partial \eta}{\partial T} \\
 & + 2(1-m_{mix}) \frac{20 \frac{\partial \eta}{\partial n_k} - 54\eta \frac{\partial \eta}{\partial n_k} + 36\eta^2 \frac{\partial \eta}{\partial n_k} - 8\eta^3 \frac{\partial \eta}{\partial n_k}}{(1-\eta)^3 (2-\eta)^2} \cdot \frac{\partial \eta}{\partial T} \\
 & + 2(1-m_{mix}) \frac{20\eta - 27\eta^2 + 12\eta^3 - 2\eta^4}{(1-\eta)^2 (2-\eta)^3} \cdot \frac{\partial^2 \eta}{\partial n_k \partial T} \\
 & + 2(1-m_{mix}) \frac{20\eta - 27\eta^2 + 12\eta^3 - 2\eta^4}{(1-\eta)^3 (2-\eta)^2} \cdot \frac{\partial^2 \eta}{\partial n_k \partial T} + 4m_{mix} \frac{8\eta - 2\eta^2}{(1-\eta)^5} \cdot \frac{\partial^2 \eta}{\partial n_k \partial T} \\
 & + (1-m_{mix}) \frac{\left(\begin{aligned} & -54 \frac{\partial \eta}{\partial T} \cdot \frac{\partial \eta}{\partial n_k} + 72\eta \frac{\partial \eta}{\partial T} \cdot \frac{\partial \eta}{\partial n_k} - 24\eta^2 \frac{\partial \eta}{\partial T} \cdot \frac{\partial \eta}{\partial n_k} \\ & + 20 \frac{\partial^2 \eta}{\partial n_k \partial T} - 54\eta \frac{\partial^2 \eta}{\partial n_k \partial T} + 36\eta^2 \frac{\partial^2 \eta}{\partial n_k \partial T} - 8\eta^3 \frac{\partial^2 \eta}{\partial n_k \partial T} \end{aligned} \right)}{(1-\eta)^2 (2-\eta)^2}
 \end{aligned}
 \tag{F-129}$$

$$\frac{\partial^2 C_1}{\partial T \partial n_k} = \frac{\partial}{\partial n_k} \left(\frac{\partial C_1}{\partial T} \right) = \frac{2}{C_0^3} \cdot \frac{\partial C_0}{\partial T} \cdot \frac{\partial C_0}{\partial n_k} - \frac{1}{C_0^2} \cdot \frac{\partial^2 C_0}{\partial T \partial n_k}
 \tag{F-130}$$

iv) Volume – Volume

$$\frac{\partial^2 F_{mix}^{disp}}{\partial V \partial V} = \frac{\partial^2}{\partial V \partial V} (F_{mix}^{disp}) = \frac{\partial^2}{\partial V \partial V} (F_{mix}^{disp,1}) + \frac{\partial^2}{\partial V \partial V} (F_{mix}^{disp,2}) \quad (F-132)$$

Perturbation term 1

$$\begin{aligned} \frac{\partial^2 F_{mix}^{disp,1}}{\partial V^2} = & -4\pi \frac{N_{av} n_{total}^2}{V^3} I_1(\eta, m_{mix}) \left(m^2 \frac{\epsilon}{kT} \sigma^3 \right)_{mix} + 4\pi \frac{N_{av} n_{total}^2}{V^2} \left(m^2 \frac{\epsilon}{kT} \sigma^3 \right)_{mix} \frac{\partial I_1(\eta, m_{mix})}{\partial V} \\ & - 2\pi \frac{N_{av} n_{total}^2}{V} \left(m^2 \frac{\epsilon}{kT} \sigma^3 \right)_{mix} \frac{\partial^2 I_1(\eta, m_{mix})}{\partial V^2} \end{aligned} \quad (F-133)$$

$$\frac{\partial^2 I_1(\eta, m_{mix})}{\partial V^2} = \sum_{i=0}^6 \left[i \times (i-1) \times a_i(m_{mix}) \eta^{i-2} \cdot \left(\frac{\partial \eta}{\partial V} \right)^2 + i \times a_i(m_{mix}) \eta^{i-1} \frac{\partial^2 \eta}{\partial V^2} \right] \quad (F-134)$$

$$\frac{\partial^2 \eta}{\partial V^2} = \frac{\partial^2 \zeta_3}{\partial V^2} = \frac{N_{av} \pi}{3V^3} \sum_i^{nc} n_i m_i d_i^3 \quad (F-135)$$

Perturbation term 2

$$\begin{aligned} \frac{\partial^2 F_{mix}^{disp,2}}{\partial^2 V} = & -2\pi \frac{N_{av} n_{total}^2}{V^3} m_{mix} C_1 I_2(\eta, m_{mix}) \left(m^2 \left(\frac{\epsilon}{kT} \right)^2 \sigma^3 \right)_{mix} \\ & + 2\pi \frac{N_{av} n_{total}^2}{V^2} m_{mix} I_2(\eta, m_{mix}) \left(m^2 \left(\frac{\epsilon}{kT} \right)^2 \sigma^3 \right)_{mix} \cdot \frac{\partial C_1}{\partial V} \\ & + 2\pi \frac{N_{av} n_{total}^2}{V^2} m_{mix} C_1 \left(m^2 \left(\frac{\epsilon}{kT} \right)^2 \sigma^3 \right)_{mix} \cdot \frac{\partial I_2(\eta, m_{mix})}{\partial V} \\ & - 2\pi \frac{N_{av} n_{total}^2}{V} m_{mix} \left(m^2 \left(\frac{\epsilon}{kT} \right)^2 \sigma^3 \right)_{mix} \cdot \frac{\partial C_1}{\partial V} \cdot \frac{\partial I_2(\eta, m_{mix})}{\partial V} \\ & - \pi \frac{N_{av} n_{total}^2}{V} m_{mix} C_1 \left(m^2 \left(\frac{\epsilon}{kT} \right)^2 \sigma^3 \right)_{mix} \cdot \frac{\partial^2 I_2(\eta, m_{mix})}{\partial V^2} \\ & - \pi \frac{N_{av} n_{total}^2}{V} m_{mix} I_2(\eta, m_{mix}) \left(m^2 \left(\frac{\epsilon}{kT} \right)^2 \sigma^3 \right)_{mix} \cdot \frac{\partial^2 C_1}{\partial V^2} \end{aligned} \quad (F-136)$$

$$\frac{\partial^2 I_2(\eta, m_{mix})}{\partial V^2} = \sum_{i=0}^6 \left[i \times (i-1) \times b_i(m_{mix}) \eta^{i-2} \cdot \left(\frac{\partial \eta}{\partial V} \right)^2 + i \times b_i(m_{mix}) \eta^{i-1} \frac{\partial^2 \eta}{\partial V^2} \right]$$

$$\begin{aligned}
 \frac{\partial^2 C_0}{\partial V^2} = & 6(1-m_{mix}) \frac{20\eta - 27\eta^2 + 12\eta^3 - 2\eta^4}{(1-\eta)^2 (2-\eta)^4} \cdot \left(\frac{\partial \eta}{\partial V}\right)^2 + 8(1-m_{mix}) \frac{20\eta - 27\eta^2 + 12\eta^3 - 2\eta^4}{(1-\eta)^3 (2-\eta)^3} \cdot \left(\frac{\partial \eta}{\partial V}\right)^2 \\
 & + 6(1-m_{mix}) \frac{20\eta - 27\eta^2 + 12\eta^3 - 2\eta^4}{(1-\eta)^4 (2-\eta)^2} \cdot \left(\frac{\partial \eta}{\partial V}\right)^2 + 20m_{mix} \frac{8\eta - 2\eta^2}{(1-\eta)^6} \cdot \left(\frac{\partial \eta}{\partial V}\right)^2 \\
 & + 8m_{mix} \frac{\left(8\frac{\partial \eta}{\partial V} - 4\eta\frac{\partial \eta}{\partial V}\right)}{(1-\eta)^5} \cdot \frac{\partial \eta}{\partial V} + 4(1-m_{mix}) \frac{20\frac{\partial \eta}{\partial V} - 54\eta\frac{\partial \eta}{\partial V} + 36\eta^2\frac{\partial \eta}{\partial V} - 8\eta^3\frac{\partial \eta}{\partial V}}{(1-\eta)^2 (2-\eta)^3} \cdot \frac{\partial \eta}{\partial V} \\
 & + 4(1-m_{mix}) \frac{20\frac{\partial \eta}{\partial V} - 54\eta\frac{\partial \eta}{\partial V} + 36\eta^2\frac{\partial \eta}{\partial V} - 8\eta^3\frac{\partial \eta}{\partial V}}{(1-\eta)^3 (2-\eta)^2} \cdot \frac{\partial \eta}{\partial V} \\
 & + 2(1-m_{mix}) \frac{20\eta - 27\eta^2 + 12\eta^3 - 2\eta^4}{(1-\eta)^2 (2-\eta)^3} \cdot \frac{\partial^2 \eta}{\partial V^2} + 2(1-m_{mix}) \frac{20\eta - 27\eta^2 + 12\eta^3 - 2\eta^4}{(1-\eta)^3 (2-\eta)^2} \cdot \frac{\partial^2 \eta}{\partial V^2} \\
 & + 4m_{mix} \frac{8\eta - 2\eta^2}{(1-\eta)^5} \cdot \frac{\partial^2 \eta}{\partial V^2} + m_{mix} \frac{\left(-4\left(\frac{\partial \eta}{\partial V}\right)^2 + 8\frac{\partial^2 \eta}{\partial V^2} - 4\eta\frac{\partial^2 \eta}{\partial V^2}\right)}{(1-\eta)^4} \\
 & + (1-m_{mix}) \frac{\left(-54\left(\frac{\partial \eta}{\partial V}\right)^2 + 72\eta\left(\frac{\partial \eta}{\partial V}\right)^2 - 24\eta^2\left(\frac{\partial \eta}{\partial V}\right)^2\right)}{(1-\eta)^2 (2-\eta)^2} \\
 & + (1-m_{mix}) \frac{\left(+20\frac{\partial^2 \eta}{\partial V^2} - 54\eta\frac{\partial^2 \eta}{\partial V^2} + 36\eta^2\frac{\partial^2 \eta}{\partial V^2} - 8\eta^3\frac{\partial^2 \eta}{\partial V^2}\right)}{(1-\eta)^2 (2-\eta)^2}
 \end{aligned} \tag{F-137}$$

$$\frac{\partial^2 C_1}{\partial V \partial V} = \frac{\partial}{\partial V} \left(\frac{\partial C_1}{\partial V} \right) = \frac{2}{C_0^3} \cdot \frac{\partial C_0}{\partial V} \cdot \frac{\partial C_0}{\partial V} - \frac{1}{C_0^2} \cdot \frac{\partial^2 C_0}{\partial V \partial V} \tag{F-138}$$

v) Temperature – Temperature

$$\frac{\partial^2 F_{mix}^{disp}}{\partial T \partial T} = \frac{\partial^2}{\partial T \partial T} (F_{mix}^{disp}) = \frac{\partial^2}{\partial T \partial T} (F_{mix}^{disp,1}) + \frac{\partial^2}{\partial T \partial T} (F_{mix}^{disp,2}) \tag{F-139}$$

Perturbation term 1

$$\begin{aligned}
 \frac{\partial^2 F_{mix}^{disp,1}}{\partial T^2} = & -2\pi \frac{N_{av} n_{total}^2}{V} I_1(\eta, m_{mix}) \cdot \frac{\partial^2 \left(m^2 \frac{\epsilon}{kT} \sigma^3 \right)_{mix}}{\partial T^2} \\
 & - 4\pi \frac{N_{av} n_{total}^2}{V} \cdot \frac{\partial \left(m^2 \frac{\epsilon}{kT} \sigma^3 \right)_{mix}}{\partial T} \cdot \frac{\partial I_1(\eta, m_{mix})}{\partial T} \\
 & - 2\pi \frac{N_{av} n_{total}^2}{V} \left(m^2 \frac{\epsilon}{kT} \sigma^3 \right)_{mix} \cdot \frac{\partial^2 I_1(\eta, m_{mix})}{\partial T^2}
 \end{aligned} \tag{F-140}$$

$$\frac{\partial^2 \left(m^2 \frac{\epsilon}{kT} \sigma^3 \right)_{mix}}{\partial T^2} = \frac{2}{(n_{total})^2} \sum_i^{nc} \sum_j^{nc} n_i n_j m_i m_j \left(\frac{\epsilon_{ij}}{kT^3} \right) \sigma_{ij}^3 \quad (F-141)$$

$$\frac{\partial^2 I_1(\eta, m_{mix})}{\partial T^2} = \sum_{i=0}^6 \left[i \times (i-1) \times a_i (m_{mix}) \eta^{i-2} \cdot \left(\frac{\partial \eta}{\partial T} \right)^2 + i \times a_i (m_{mix}) \eta^{i-1} \frac{\partial^2 \eta}{\partial T^2} \right] \quad (F-142)$$

$$\frac{\partial^2 \eta}{\partial T^2} = \frac{\partial^2 \zeta_3}{\partial T^2} = \frac{N_{av} \pi}{V} \sum_i^{nc} n_i m_i d_i \cdot \frac{\partial d_i^2}{\partial T} + \frac{N_{av} \pi}{2V} \sum_i^{nc} n_i m_i d_i^2 \cdot \frac{\partial^2 d_i}{\partial T^2} \quad (F-143)$$

Perturbation term 2

$$\begin{aligned} \frac{\partial^2 F_{mix}^{disp,2}}{\partial T^2} = & -\pi \frac{N_{av} n_{total}^2}{V} m_{mix} C_{12}(\eta, m_{mix}) \cdot \frac{\partial^2 \left(m^2 \left(\frac{\epsilon}{kT} \right)^2 \sigma^3 \right)_{mix}}{\partial T^2} \\ & - 2\pi \frac{N_{av} n_{total}^2}{V} m_{mix} I_2(\eta, m_{mix}) \cdot \frac{\partial \left(m^2 \left(\frac{\epsilon}{kT} \right)^2 \sigma^3 \right)_{mix}}{\partial T} \cdot \frac{\partial C_1}{\partial T} \\ & - 2\pi \frac{N_{av} n_{total}^2}{V} m_{mix} C_1 \cdot \frac{\partial \left(m^2 \left(\frac{\epsilon}{kT} \right)^2 \sigma^3 \right)_{mix}}{\partial T} \cdot \frac{\partial I_2(\eta, m_{mix})}{\partial T} \\ & - 2\pi \frac{N_{av} n_{total}^2}{V} m_{mix} \left(m^2 \left(\frac{\epsilon}{kT} \right)^2 \sigma^3 \right)_{mix} \cdot \frac{\partial C_1}{\partial T} \cdot \frac{\partial I_2(\eta, m_{mix})}{\partial T} \\ & - \pi \frac{N_{av} n_{total}^2}{V} m_{mix} I_2(\eta, m_{mix}) \left(m^2 \left(\frac{\epsilon}{kT} \right)^2 \sigma^3 \right)_{mix} \cdot \frac{\partial^2 C_1}{\partial T^2} \\ & - \pi \frac{N_{av} n_{total}^2}{V} m_{mix} C_1 \left(m^2 \left(\frac{\epsilon}{kT} \right)^2 \sigma^3 \right)_{mix} \cdot \frac{\partial^2 I_2(\eta, m_{mix})}{\partial T^2} \end{aligned} \quad (F-144)$$

$$\frac{\partial^2 \left(m^2 \left(\frac{\epsilon}{kT} \right)^2 \sigma^3 \right)_{mix}}{\partial T^2} = \frac{6}{(n_{total})^2} \sum_i^{nc} \sum_j^{nc} n_i n_j m_i m_j \left(\frac{(\epsilon_{ij})^2}{k^2 T^4} \right) \sigma_{ij}^3 \quad (F-145)$$

$$\frac{\partial^2 I_1(\eta, m_{mix})}{\partial T^2} = \sum_{i=0}^6 \left[i \times (i-1) \times b_i (m_{mix}) \eta^{i-2} \cdot \left(\frac{\partial \eta}{\partial T} \right)^2 + i \times b_i (m_{mix}) \eta^{i-1} \frac{\partial^2 \eta}{\partial T^2} \right] \quad (F-146)$$

$$\begin{aligned}
 \frac{\partial^2 C_0}{\partial T^2} = & 6(1-m_{mix}) \frac{20\eta - 27\eta^2 + 12\eta^3 - 2\eta^4}{(1-\eta)^2 (2-\eta)^4} \cdot \left(\frac{\partial \eta}{\partial T}\right)^2 + 8(1-m_{mix}) \frac{20\eta - 27\eta^2 + 12\eta^3 - 2\eta^4}{(1-\eta)^3 (2-\eta)^3} \cdot \left(\frac{\partial \eta}{\partial T}\right)^2 \\
 & + 6(1-m_{mix}) \frac{20\eta - 27\eta^2 + 12\eta^3 - 2\eta^4}{(1-\eta)^4 (2-\eta)^2} \cdot \left(\frac{\partial \eta}{\partial T}\right)^2 + 20m_{mix} \frac{8\eta - 2\eta^2}{(1-\eta)^6} \cdot \left(\frac{\partial \eta}{\partial T}\right)^2 \\
 & + 8m_{mix} \frac{\left(8\frac{\partial \eta}{\partial T} - 4\eta\frac{\partial \eta}{\partial T}\right)}{(1-\eta)^5} \cdot \frac{\partial \eta}{\partial T} + 4(1-m_{mix}) \frac{20\frac{\partial \eta}{\partial T} - 54\eta\frac{\partial \eta}{\partial T} + 36\eta^2\frac{\partial \eta}{\partial T} - 8\eta^3\frac{\partial \eta}{\partial T}}{(1-\eta)^2 (2-\eta)^3} \cdot \frac{\partial \eta}{\partial T} \\
 & + 4(1-m_{mix}) \frac{20\frac{\partial \eta}{\partial T} - 54\eta\frac{\partial \eta}{\partial T} + 36\eta^2\frac{\partial \eta}{\partial T} - 8\eta^3\frac{\partial \eta}{\partial T}}{(1-\eta)^3 (2-\eta)^2} \cdot \frac{\partial \eta}{\partial T} \\
 & + 2(1-m_{mix}) \frac{20\eta - 27\eta^2 + 12\eta^3 - 2\eta^4}{(1-\eta)^2 (2-\eta)^3} \cdot \frac{\partial^2 \eta}{\partial T^2} + 2(1-m_{mix}) \frac{20\eta - 27\eta^2 + 12\eta^3 - 2\eta^4}{(1-\eta)^3 (2-\eta)^2} \cdot \frac{\partial^2 \eta}{\partial T^2} \\
 & + 4m_{mix} \frac{8\eta - 2\eta^2}{(1-\eta)^5} \cdot \frac{\partial^2 \eta}{\partial T^2} + m_{mix} \frac{\left(-4\left(\frac{\partial \eta}{\partial T}\right)^2 + 8\frac{\partial^2 \eta}{\partial T^2} - 4\eta\frac{\partial^2 \eta}{\partial T^2}\right)}{(1-\eta)^4} \\
 & + (1-m_{mix}) \frac{\left(-54\left(\frac{\partial \eta}{\partial T}\right)^2 + 72\eta\left(\frac{\partial \eta}{\partial T}\right)^2 - 24\eta^2\left(\frac{\partial \eta}{\partial T}\right)^2 + 20\frac{\partial^2 \eta}{\partial T^2} - 54\eta\frac{\partial^2 \eta}{\partial T^2} + 36\eta^2\frac{\partial^2 \eta}{\partial T^2} - 8\eta^3\frac{\partial^2 \eta}{\partial T^2}\right)}{(1-\eta)^2 (2-\eta)^2}
 \end{aligned} \tag{F-147}$$

$$\frac{\partial^2 C_1}{\partial T \partial T} = \frac{\partial}{\partial T} \left(\frac{\partial C_1}{\partial T} \right) = \frac{2}{C_0^3} \cdot \frac{\partial C_0}{\partial T} \cdot \frac{\partial C_0}{\partial T} - \frac{1}{C_0^2} \cdot \frac{\partial^2 C_0}{\partial T \partial T} \tag{F-148}$$

vi) Volume - Temperature

$$\frac{\partial^2 F_{mix}^{disp}}{\partial T \partial V} = \frac{\partial^2}{\partial T \partial V} (F_{mix}^{disp}) = \frac{\partial^2}{\partial T \partial V} (F_{mix}^{disp,1}) + \frac{\partial^2}{\partial T \partial V} (F_{mix}^{disp,2}) \tag{F-149}$$

Perturbation term 1

$$\begin{aligned}
 \frac{\partial^2 F_{mix}^{disp,1}}{\partial T \partial V} = & 2\pi \frac{N_{av} n_{total}^2}{V^2} I_1(\eta, m_{mix}) \frac{\partial \left(m^2 \frac{\epsilon}{kT} \sigma^3 \right)_{mix}}{\partial T} \\
 & - 2\pi \frac{N_{av} n_{total}^2}{V} I_1(\eta, m_{mix}) \cdot \frac{\partial \left(m^2 \frac{\epsilon}{kT} \sigma^3 \right)_{mix}}{\partial T} \cdot \frac{\partial I_1(\eta, m_{mix})}{\partial V} \\
 & + 2\pi \frac{N_{av} n_{total}^2}{V^2} \left(m^2 \frac{\epsilon}{kT} \sigma^3 \right)_{mix} \frac{\partial I_1(\eta, m_{mix})}{\partial T} \\
 & - 2\pi \frac{N_{av} n_{total}^2}{V} \left(m^2 \frac{\epsilon}{kT} \sigma^3 \right)_{mix} \frac{\partial^2 I_1(\eta, m_{mix})}{\partial T \partial V}
 \end{aligned} \tag{F-150}$$

$$\frac{\partial^2 I_1(\eta, m_{mix})}{\partial T \partial V} = \sum_{i=0}^6 \left[i \times (i-1) a_i \frac{\partial \eta}{\partial V} \cdot \frac{\partial \eta}{\partial T} \eta^{i-2} + i \times a_i \frac{\partial^2 \eta}{\partial V \partial T} \eta^{i-1} \right] \tag{F-151}$$

$$\frac{\partial^2 \eta}{\partial V \partial T} = \frac{\partial^2 \zeta_3}{\partial V \partial T} = -\frac{N_{av} \pi}{2V^2} \sum_i^{nc} n_i m_i d_i^2 \cdot \frac{\partial d_i}{\partial T} \tag{F-152}$$

Perturbation term 2

$$\begin{aligned}
 \frac{\partial^2 F_{mix}^{disp,2}}{\partial T \partial V} = & \pi \frac{N_{av} n_{total}^2}{V^2} m_{mix} C_{I_2}(\eta, m_{mix}) \cdot \frac{\partial \left(m^2 \left(\frac{\epsilon}{kT} \right)^2 \sigma^3 \right)_{mix}}{\partial T} - \pi \frac{N_{av} n_{total}^2}{V} m_{mix} I_2(\eta, m_{mix}) \cdot \frac{\partial \left(m^2 \left(\frac{\epsilon}{kT} \right)^2 \sigma^3 \right)_{mix}}{\partial T} \cdot \frac{\partial C_{I_1}}{\partial V} \\
 & - \pi \frac{N_{av} n_{total}^2}{V} m_{mix} C_{I_1} \cdot \frac{\partial \left(m^2 \left(\frac{\epsilon}{kT} \right)^2 \sigma^3 \right)_{mix}}{\partial T} \cdot \frac{\partial I_2(\eta, m_{mix})}{\partial V} + \pi \frac{N_{av} n_{total}^2}{V^2} m_{mix} I_2(\eta, m_{mix}) \left(m^2 \left(\frac{\epsilon}{kT} \right)^2 \sigma^3 \right)_{mix} \cdot \frac{\partial C_{I_1}}{\partial T} \\
 & - \pi \frac{N_{av} n_{total}^2}{V} m_{mix} \left(m^2 \left(\frac{\epsilon}{kT} \right)^2 \sigma^3 \right)_{mix} \frac{\partial I_2(\eta, m_{mix})}{\partial V} \cdot \frac{\partial C_{I_1}}{\partial T} + \pi \frac{N_{av} n_{total}^2}{V^2} m_{mix} C_{I_1} \left(m^2 \left(\frac{\epsilon}{kT} \right)^2 \sigma^3 \right)_{mix} \frac{\partial I_2(\eta, m_{mix})}{\partial T} \\
 & - \pi \frac{N_{av} n_{total}^2}{V} m_{mix} \left(m^2 \left(\frac{\epsilon}{kT} \right)^2 \sigma^3 \right)_{mix} \frac{\partial I_2(\eta, m_{mix})}{\partial T} \cdot \frac{\partial C_{I_1}}{\partial V} - \pi \frac{N_{av} n_{total}^2}{V} m_{mix} I_2(\eta, m_{mix}) \left(m^2 \left(\frac{\epsilon}{kT} \right)^2 \sigma^3 \right)_{mix} \cdot \frac{\partial^2 C_{I_1}}{\partial T \partial V} \\
 & - \pi \frac{N_{av} n_{total}^2}{V} m_{mix} C_{I_1} \left(m^2 \left(\frac{\epsilon}{kT} \right)^2 \sigma^3 \right)_{mix} \cdot \frac{\partial^3 I_2(\eta, m_{mix})}{\partial T \partial V}
 \end{aligned} \tag{F-153}$$

$$\frac{\partial^2 I_2(\eta, m_{mix})}{\partial T \partial V} = \sum_{i=0}^6 \left[i \times (i-1) b_i \frac{\partial \eta}{\partial V} \cdot \frac{\partial \eta}{\partial T} \eta^{i-2} + i \times b_i \frac{\partial^2 \eta}{\partial V \partial T} \eta^{i-1} \right] \tag{F-154}$$

$$\begin{aligned}
 \frac{\partial^2 C_0}{\partial T \partial V} = & 6(1-m_{mix}) \frac{20\eta - 27\eta^2 + 12\eta^3 - 2\eta^4}{(1-\eta)^2 (2-\eta)^4} \cdot \frac{\partial \eta}{\partial T} \cdot \frac{\partial \eta}{\partial V} + 8(1-m_{mix}) \frac{20\eta - 27\eta^2 + 12\eta^3 - 2\eta^4}{(1-\eta)^3 (2-\eta)^3} \cdot \frac{\partial \eta}{\partial T} \cdot \frac{\partial \eta}{\partial V} \\
 & + 6(1-m_{mix}) \frac{20\eta - 27\eta^2 + 12\eta^3 - 2\eta^4}{(1-\eta)^4 (2-\eta)^2} \cdot \frac{\partial \eta}{\partial T} \cdot \frac{\partial \eta}{\partial V} \\
 & + 20m_{mix} \frac{(8\eta - 2\eta^2)}{(1-\eta)^6} \cdot \frac{\partial \eta}{\partial T} \cdot \frac{\partial \eta}{\partial V} + 4m_{mix} \frac{\left(8 \frac{\partial \eta}{\partial V} - 4\eta \frac{\partial \eta}{\partial V}\right)}{(1-\eta)^5} \cdot \frac{\partial \eta}{\partial T} \\
 & + 2(1-m_{mix}) \frac{20 \frac{\partial \eta}{\partial V} - 54\eta \frac{\partial \eta}{\partial V} + 36\eta^2 \frac{\partial \eta}{\partial V} - 8\eta^3 \frac{\partial \eta}{\partial V}}{(1-\eta)^2 (2-\eta)^3} \cdot \frac{\partial \eta}{\partial T} \\
 & + 2(1-m_{mix}) \frac{20 \frac{\partial \eta}{\partial V} - 54\eta \frac{\partial \eta}{\partial V} + 36\eta^2 \frac{\partial \eta}{\partial V} - 8\eta^3 \frac{\partial \eta}{\partial V}}{(1-\eta)^3 (2-\eta)^2} \cdot \frac{\partial \eta}{\partial T} \\
 & + 4m_{mix} \frac{\left(8 \frac{\partial \eta}{\partial T} - 4\eta \frac{\partial \eta}{\partial T}\right)}{(1-\eta)^5} \cdot \frac{\partial \eta}{\partial V} + 2(1-m_{mix}) \frac{20 \frac{\partial \eta}{\partial T} - 54\eta \frac{\partial \eta}{\partial T} + 36\eta^2 \frac{\partial \eta}{\partial T} - 8\eta^3 \frac{\partial \eta}{\partial T}}{(1-\eta)^2 (2-\eta)^3} \cdot \frac{\partial \eta}{\partial V} \\
 & + 2(1-m_{mix}) \frac{20 \frac{\partial \eta}{\partial T} - 54\eta \frac{\partial \eta}{\partial T} + 36\eta^2 \frac{\partial \eta}{\partial T} - 8\eta^3 \frac{\partial \eta}{\partial T}}{(1-\eta)^3 (2-\eta)^2} \cdot \frac{\partial \eta}{\partial V} \\
 & + 2(1-m_{mix}) \frac{20\eta - 27\eta^2 + 12\eta^3 - 2\eta^4}{(1-\eta)^2 (2-\eta)^3} \cdot \frac{\partial^2 \eta}{\partial V \partial T} \\
 & + 2(1-m_{mix}) \frac{20\eta - 27\eta^2 + 12\eta^3 - 2\eta^4}{(1-\eta)^3 (2-\eta)^2} \cdot \frac{\partial^2 \eta}{\partial V \partial T} + 4m_{mix} \frac{8\eta - 2\eta^2}{(1-\eta)^5} \cdot \frac{\partial^2 \eta}{\partial V \partial T} \\
 & + \frac{m_{mix} \left(-4 \frac{\partial \eta}{\partial V} \cdot \frac{\partial \eta}{\partial T} + 8 \frac{\partial^2 \eta}{\partial V \partial T} - 4\eta \frac{\partial^2 \eta}{\partial V \partial T} \right)}{(1-\eta)^4} \\
 & + (1-m_{mix}) \frac{\left(-54 \frac{\partial \eta}{\partial T} \cdot \frac{\partial \eta}{\partial V} + 72\eta \frac{\partial \eta}{\partial T} \cdot \frac{\partial \eta}{\partial V} - 24\eta^2 \frac{\partial \eta}{\partial T} \cdot \frac{\partial \eta}{\partial V} \right.}{(1-\eta)^2 (2-\eta)^2} \\
 & \quad \left. + 20 \frac{\partial^2 \eta}{\partial V \partial T} - 54\eta \frac{\partial^2 \eta}{\partial V \partial T} + 36\eta^2 \frac{\partial^2 \eta}{\partial V \partial T} - 8\eta^3 \frac{\partial^2 \eta}{\partial V \partial T} \right)
 \end{aligned}
 \tag{F-155}$$

$$\frac{\partial^2 C_1}{\partial T \partial V} = \frac{\partial}{\partial V} \left(\frac{\partial C_1}{\partial T} \right) = \frac{2}{C_0^3} \cdot \frac{\partial C_0}{\partial T} \cdot \frac{\partial C_0}{\partial V} - \frac{1}{C_0^2} \cdot \frac{\partial^2 C_0}{\partial T \partial V}
 \tag{F-156}$$

F.4 General association term working equations

The Q -function expressions developed by Michelsen and Hendriks (30) are used to calculate the contribution from association to the system.

F.4.1 State function

Consider the Q -function which is equal to the contribution due to association to the reduced Helmholtz energy as derived from Wertheim's theory:

$$Q(T, V, \mathbf{n}, \bar{X}) = \sum_i^{nc} n_i \sum_{A_i}^{ns} (\ln X_{A_i} - X_{A_i} + 1) - \frac{1}{2V} \sum_i^{nc} \sum_j^{nc} n_i n_j \sum_{A_i}^{ns} \sum_{B_j}^{ns} X_{A_i} X_{B_j} \Delta^{A_i B_j} \quad (F-157)$$

F.4.2 First-order derivatives

The solution of Q is always a maximum as a function of the non-bonded fractions. This means that at the stationary point, the derivatives of Q with respect to the fraction of non-bonded molecules is zero. Knowing this we may write the first-order derivatives as follows:

$$\left. \frac{\partial Q}{\partial \alpha} \right|_X = \left. \frac{\partial Q}{\partial \alpha} \right|_X + \sum_i^{nc} \sum_{A_i}^{ns} \frac{\partial Q}{\partial X_{A_i}} \cdot \frac{\partial X_{A_i}}{\partial \alpha} \quad (F-158)$$

At the maximum, the solution is at a stationary point and the derivatives $\frac{\partial Q}{\partial X_{A_i}}$ are by definition

zero. This implies that the first-order derivatives can now be calculated as explicit derivatives of Q with respects to the independent variables.

i) Composition

$$\left(\frac{\partial Q}{\partial n_k} \right)_{T,V} = \sum_{A_k} \ln X_{A_k} - \frac{1}{2V} \sum_i^{nc} \sum_j^{nc} n_i n_j \sum_{A_i} \sum_{B_j} X_{A_i} X_{B_j} \frac{\partial \Delta^{A_i B_j}}{\partial n_k} = Q_n \quad (F-159)$$

ii) Volume

$$\left(\frac{\partial Q}{\partial V} \right)_{n,T} = -\frac{1}{2V} \left(-h + \sum_i^{nc} \sum_j^{nc} n_i n_j \sum_{A_i} \sum_{B_j} X_{A_i} X_{B_j} \frac{\partial \Delta^{A_i B_j}}{\partial V} \right) = Q_V \quad (F-160)$$

$$h = \sum_i^{nc} n_i \sum_{A_i} (1 - X_{A_i}) \quad (F-161)$$

iii) Temperature

$$\left(\frac{\partial Q}{\partial T} \right)_{n,V} = -\frac{1}{2V} \sum_i^{nc} \sum_j^{nc} n_i n_j \sum_{A_i} \sum_{B_j} X_{A_i} X_{B_j} \frac{\partial \Delta^{A_i B_j}}{\partial T} = Q_T \quad (F-162)$$

F.4.3 Second-order derivatives

Second-order derivatives are calculated in the following way:

$$\left(\frac{\partial^2 Q}{\partial \alpha \partial \beta} \right) = \frac{\partial}{\partial \beta} \left(\frac{\partial Q}{\partial \alpha} \right)_{X, opt} \quad (F-163)$$

Then by using the chain rule:

$$\left(\frac{\partial^2 Q}{\partial \alpha \partial \beta} \right) = \frac{\partial^2 Q}{\partial \alpha \partial \beta} \Big|_X + \sum_i^{nc} \sum_{A_i} \frac{\partial^2 Q}{\partial \alpha \partial X_{A_i}} \cdot \frac{\partial X_{A_i}}{\partial \beta} \quad (F-164)$$

However, the expression for $\frac{\partial X_{A_i}}{\partial \beta}$ is now required:

At the optimum or solution it is known that:

$$\left(\frac{\partial Q}{\partial X_{A_i}} \right)_{opt} = 0 \quad (F-165)$$

Then the following can be written:

$$\frac{\partial}{\partial \beta} \left(\frac{\partial Q}{\partial X_{A_i}} \right)_{opt} = \frac{\partial^2 Q}{\partial \beta \partial X_{A_i}} \Big|_X + \sum_i^{nc} \sum_j^{nc} \sum_{X_{A_i}} \sum_{X_{B_j}} \frac{\partial^2 Q}{\partial X_{A_i} \partial X_{B_j}} \cdot \frac{\partial X_{B_j}}{\partial \beta} = 0 \quad (F-166)$$

In simpler notation:

$$\frac{\partial}{\partial \beta} \left(\frac{\partial Q}{\partial X_{A_i}} \right)_{opt} = Q_{\beta X} + Q_{XX} \frac{\partial X_{B_i}}{\partial \beta} = 0 \quad (F-167)$$

From this equation, analytic expression for $\frac{\partial X_{A_i}}{\partial \beta}$ can be obtained:

$$\frac{\partial X_{B_j}}{\partial \beta} = \frac{\partial X_{A_i}}{\partial \beta} = -Q_{XX}^{-1} Q_{X\beta} \quad (F-168)$$

Substitute this into the above equation and in simpler notation, the following is obtained:

$$\left(\frac{\partial^2 Q}{\partial \alpha \partial \beta} \right) = Q_{\alpha\beta} - Q_{\alpha X} \cdot Q_{XX}^{-1} Q_{X\beta} \quad (F-169)$$

$$\text{Or } \left(\frac{\partial^2 Q}{\partial \alpha \partial \beta} \right) = Q_{\alpha\beta} - Q_{\beta X} \cdot Q_{XX}^{-1} Q_{X\alpha} \quad (F-170)$$

Also the matrix Q_{XX} is given by:

$$Q_{XX} = -\frac{n_i}{X_{A_i}^2} \delta_{AB} \delta_{ij} - \frac{n_i n_j \Delta^{AB_j}}{V} \quad (F-171)$$

i) Composition – Composition

Constant un-bonded fractions

$$\left(\frac{\partial^2 Q}{\partial n_k \partial n_l} \right) \Big|_X = -\frac{1}{2V} \left(2 \sum_j^{nc} n_j \sum_{A_i} \sum_{B_j} X_{A_i} X_{B_j} \frac{\partial \Delta^{A_i B_j}}{\partial n_k} + \sum_i^{nc} \sum_j^{nc} n_i n_j \sum_{A_i} \sum_{B_j} X_{A_i} X_{B_j} \frac{\partial^2 \Delta^{A_i B_j}}{\partial n_k \partial n_l} \right) \quad (F-172)$$

$$\begin{aligned} \left(\frac{\partial^2 Q}{\partial n_k \partial n_l} \right) \Big|_X &= -\frac{1}{V} \sum_{A_i} \sum_{B_j} X_{A_i} X_{B_j} \Delta^{A_i B_j} - \frac{1}{V} \sum_j n_j \sum_{A_i} \sum_{B_j} X_{A_i} X_{B_j} \frac{\partial \Delta^{A_i B_j}}{\partial n_l} \\ &\quad - \frac{1}{V} \sum_j^{nc} n_j \sum_{A_i} \sum_{B_j} X_{A_i} X_{B_j} \frac{\partial \Delta^{A_i B_j}}{\partial n_k} - \frac{1}{2V} \sum_i^{nc} \sum_j^{nc} n_i n_j \sum_{A_i} \sum_{B_j} X_{A_i} X_{B_j} \frac{\partial \Delta^{A_i B_j}}{\partial n_i \partial n_k} \end{aligned} \quad (F-173)$$

Composition – unbounded fraction

$$\left(\frac{\partial^2 Q}{\partial n_l \partial X_{C_i}} \right) \Big|_{T,V} = \sum_{A_i} \frac{1}{X_{A_i}} \delta_{AC} \delta_{kl} - \frac{n_k}{V} \sum_j^{nc} n_j \sum_{B_j} X_{B_j} \frac{\partial \Delta^{C_i B_j}}{\partial n_l} = Q_{nX} \quad (F-174)$$

ii) Composition – Volume

Constant un-bonded fractions

$$\left(\frac{\partial^2 Q}{\partial n_k \partial V} \right) \Big|_X = \frac{1}{2V} \left[\frac{1}{V} \sum_i^{nc} \sum_j^{nc} n_i n_j \sum_{A_i} \sum_{B_j} X_{A_i} X_{B_j} \frac{\partial \Delta^{A_i B_j}}{\partial n_k} - \sum_i^{nc} \sum_j^{nc} n_i n_j \sum_{A_i} \sum_{B_j} X_{A_i} X_{B_j} \frac{\partial \Delta^{A_i B_j}}{\partial V \partial n_k} \right] \quad (F-175)$$

Volume – un-bonded fraction

$$\left(\frac{\partial^2 Q}{\partial X_{C_i} \partial V} \right) \Big|_{T,n} = \frac{n_k}{2V} \left(1 - 2 \sum_j^{nc} n_j \sum_{B_j} X_{B_j} \frac{\partial \Delta^{C_i B_j}}{\partial V} \right) = Q_{XV} \quad (F-176)$$

$$\left(\frac{\partial^2 Q}{\partial X_{C_i} \partial V} \right) \Big|_{T,n} = \frac{n_k}{V^2} \sum_j^{nc} n_j \sum_{B_j} X_{B_j} \Delta^{C_i B_j} - \frac{n_k}{V} \sum_j^{nc} n_j \sum_{B_j} X_{B_j} \frac{\partial \Delta^{C_i B_j}}{\partial V} \quad (F-177)$$

iii) Composition – Temperature

Constant un-bonded fraction

$$\left(\frac{\partial^2 Q}{\partial n_k \partial T} \right) \Big|_X = -\frac{1}{2V} \sum_i^{nc} \sum_j^{nc} n_i n_j \sum_{A_i} \sum_{B_j} X_{A_i} X_{B_j} \frac{\partial^2 \Delta^{A_i B_j}}{\partial n_k \partial T} = Q_{nT} \quad (F-178)$$

Temperature – un-bonded fractions

$$\left(\frac{\partial^2 Q}{\partial X_{C_i} \partial T} \right)_{n,V} = -\frac{n_k}{V} \sum_j^{nc} n_j \sum_{B_j} X_{B_j} \frac{\partial \Delta^{C_i B_j}}{\partial T} = Q_{XT} \quad (F-179)$$

iv) Volume - Volume

Constant un-bonded fractions

$$\begin{aligned} \left(\frac{\partial^2 Q}{\partial V \partial V} \right) \Big|_X &= -\frac{1}{V^3} \sum_i \sum_j^{nc} n_i n_j \sum_{A_i} \sum_{B_j} X_{A_i} X_{B_j} \Delta^{A_i B_j} \\ &\quad + \frac{1}{V^2} \sum_i \sum_j^{nc} n_i n_j \sum_{A_i} \sum_{B_j} X_{A_i} X_{B_j} \frac{\partial \Delta^{A_i B_j}}{\partial V} \\ &\quad - \frac{1}{2V} \sum_i \sum_j^{nc} n_i n_j \sum_{A_i} \sum_{B_j} X_{A_i} X_{B_j} \frac{\partial^2 \Delta^{A_i B_j}}{\partial V \partial V} = Q_{VV} \end{aligned} \quad (F-180)$$

v) Temperature – Temperature

Constant un-bonded fractions

$$\left(\frac{\partial^2 Q}{\partial T \partial T} \right) \Big|_X = -\frac{1}{2V} \sum_i \sum_j^{nc} n_i n_j \sum_{A_i} \sum_{B_j} X_{A_i} X_{B_j} \frac{\partial^2 \Delta^{A_i B_j}}{\partial T^2} = Q_{TT} \quad (F-181)$$

vi) Volume – Temperature

Constant un-bonded fractions

$$\begin{aligned} \left(\frac{\partial^2 Q}{\partial T \partial V} \right) \Big|_X &= \frac{1}{2V^2} \sum_i \sum_j^{nc} n_i n_j \sum_{A_i} \sum_{B_j} X_{A_i} X_{B_j} \frac{\partial \Delta^{A_i B_j}}{\partial T} \\ &\quad - \frac{1}{2V} \sum_i \sum_j^{nc} n_i n_j \sum_{A_i} \sum_{B_j} X_{A_i} X_{B_j} \frac{\partial^2 \Delta^{A_i B_j}}{\partial T \partial V} = Q_{TV} \end{aligned} \quad (F-182)$$

$$\begin{aligned} \left(\frac{\partial^2 Q}{\partial T \partial V} \right) \Big|_X &= \frac{1}{2V^2} \sum_i \sum_j^{nc} n_i n_j \sum_{A_i} \sum_{B_j} X_{A_i} X_{B_j} \frac{\partial \Delta^{A_i B_j}}{\partial T} \\ &\quad - \frac{1}{2V} \sum_i \sum_j^{nc} n_i n_j \sum_{A_i} \sum_{B_j} X_{A_i} X_{B_j} \frac{\partial^2 \Delta^{A_i B_j}}{\partial T \partial V} \end{aligned} \quad (F-183)$$

F.5 CPA- CR1 combining rules used in association term

There are two mixing rules commonly employed in the association term, CR1 and ECR. The derivatives of these two mixing rules are different and the derivative required for the CR1 mixing rules for CPA are presented below:

$$\Delta^{A,B_j} = g(n, V) \left[\exp\left(\frac{\varepsilon^{A,B_j}}{RT}\right) - 1 \right] b_{ij} \beta^{A,B_j} = g(n, V) \cdot \lambda(T) \quad (F-184)$$

$$g(n, V) = \frac{1}{1 - 1.9\eta} \quad (F-185)$$

$$\eta = \frac{B}{4V} \quad (F-186)$$

$$B = \frac{\sum_i^{nc} \sum_j^{nc} n_j n_i b_{ij}}{n_i} \quad (F-187)$$

F.5.1 First-order derivative

i) Composition

$$\frac{\partial \Delta^{A,B_j}}{\partial n_k} = \lambda(T) \cdot \frac{\partial g}{\partial \eta} \cdot \frac{\partial \eta}{\partial B} \cdot \frac{\partial B}{\partial n_k} \quad (F-188)$$

$$\frac{\partial g}{\partial \eta} = \frac{1.9}{(1 - 1.9\eta)^2} \quad (F-189)$$

$$\frac{\partial \eta}{\partial B} = \frac{1}{4V} \quad (F-190)$$

ii) Volume

$$\frac{\partial \Delta^{A,B_j}}{\partial V} = \lambda(T) \cdot \frac{\partial(g)}{\partial V} = \lambda(T) \cdot \frac{\partial g}{\partial \eta} \cdot \frac{\partial \eta}{\partial V} \quad (F-191)$$

$$\frac{\partial \eta}{\partial V} = \frac{-B}{4V^2} \quad (F-192)$$

iii) Temperature

$$\frac{\partial \Delta^{A,B_j}}{\partial T} = g \cdot \frac{\partial \lambda}{\partial T} \quad (F-193)$$

$$\frac{\partial \lambda}{\partial T} = -\exp \left[\frac{\varepsilon^{A,B_j}}{RT} \right] b_{ij} \beta^{\Lambda_{B_j}} \frac{\varepsilon^{A,B_j}}{RT^2} \quad (F-194)$$

F.5.2 Second-order derivatives

i) Composition – Composition

$$\left(\frac{\partial^2 \Delta^{A,B_j}}{\partial n_k \partial n_l} \right) = \frac{\partial}{\partial n_l} \left(\frac{\partial \Delta^{A,B_j}}{\partial n_k} \right) = \frac{\partial}{\partial n_l} \left(\lambda(T) \cdot \frac{\partial g}{\partial \eta} \cdot \frac{\partial \eta}{\partial B} \cdot \frac{\partial B}{\partial n_k} \right) \quad (F-195)$$

$$\begin{aligned} \left(\frac{\partial^2 \Delta^{A,B_j}}{\partial n_k \partial n_l} \right) &= \lambda(T) \cdot \frac{\partial^2 g}{\partial \eta^2} \cdot \frac{\partial B}{\partial n_l} \cdot \left(\frac{\partial \eta}{\partial B} \right)^2 \cdot \frac{\partial B}{\partial n_k} + \lambda(T) \cdot \frac{\partial g}{\partial \eta} \cdot \frac{\partial B}{\partial n_l} \cdot \frac{\partial^2 \eta}{\partial B^2} \cdot \frac{\partial B}{\partial n_k} \\ &\quad + \lambda(T) \cdot \frac{\partial g}{\partial \eta} \cdot \frac{\partial \eta}{\partial B} \cdot \frac{\partial^2 B}{\partial n_k \partial n_l} \end{aligned} \quad (F-196)$$

$$\frac{\partial^2 g}{\partial \eta^2} = \frac{\partial}{\partial \eta} \left(\frac{\partial g}{\partial \eta} \right) = \frac{\partial}{\partial \eta} \left(\frac{1.9}{(1-1.9\eta)^2} \right) = \frac{2(1.9^2)}{(1-1.9\eta)^3} \quad (F-197)$$

$$\frac{\partial^2 \eta}{\partial B^2} = \frac{\partial}{\partial B} \left(\frac{\partial \eta}{\partial B} \right) = \frac{\partial}{\partial B} \left(\frac{1}{4V} \right) = 0 \quad (F-198)$$

ii) Composition – Volume

$$\left(\frac{\partial^2 \Delta^{A,B_j}}{\partial V \partial n_l} \right) = \lambda(T) \cdot \frac{\partial B}{\partial n_k} \cdot \frac{\partial^2 g}{\partial \eta^2} \cdot \frac{\partial \eta}{\partial B} \cdot \frac{\partial \eta}{\partial V} + \lambda(T) \cdot \frac{\partial B}{\partial n_k} \cdot \frac{\partial g}{\partial \eta} \cdot \frac{\partial^2 \eta}{\partial V \partial B} \quad (F-199)$$

$$\left(\frac{\partial^2 \eta}{\partial V \partial B} \right) = \frac{\partial}{\partial B} \left(\frac{\partial \eta}{\partial V} \right) = \frac{\partial}{\partial B} \left(\frac{-B}{4V^2} \right) \quad (F-200)$$

$$\left(\frac{\partial^2 \eta}{\partial V \partial B} \right) = \frac{-1}{4V^2} \quad (F-201)$$

iii) Composition – Temperature

$$\left(\frac{\partial^2 \Delta^{A,B_j}}{\partial n_i \partial T} \right) = \left(\frac{\partial \lambda(T)}{\partial T} \cdot \frac{\partial g}{\partial \eta} \cdot \frac{\partial \eta}{\partial B} \cdot \frac{\partial B}{\partial n_i} \right) \quad (F-202)$$

iv) Volume – Volume

$$\left(\frac{\partial^2 \Delta^{A,B_j}}{\partial V^2} \right) = \frac{\partial}{\partial V} \left(\frac{\partial \Delta^{A,B_j}}{\partial V} \right) = \frac{\partial}{\partial V} \left(\lambda(T) \cdot \frac{\partial g}{\partial \eta} \cdot \frac{\partial \eta}{\partial V} \right) \quad (F-203)$$

$$\left(\frac{\partial^2 \Delta^{A,B_j}}{\partial V^2} \right) = \lambda(T) \cdot \frac{\partial^2 g}{\partial \eta^2} \cdot \left(\frac{\partial \eta}{\partial V} \right)^2 + \lambda(T) \cdot \frac{\partial g}{\partial \eta} \cdot \frac{\partial^2 \eta}{\partial V^2} \quad (F-204)$$

$$\frac{\partial^2 \eta}{\partial V^2} = \frac{\partial}{\partial V} \left(\frac{\partial \eta}{\partial V} \right) = \frac{\partial}{\partial V} \left(\frac{-B}{4V^2} \right) \quad (F-205)$$

$$\frac{\partial^2 \eta}{\partial V^2} = \frac{B}{2V^3} \quad (F-206)$$

v) Temperature – Temperature

$$\left(\frac{\partial^2 \Delta^{A,B_j}}{\partial T^2} \right) = \frac{\partial}{\partial T} \left(\frac{\partial \Delta^{A,B_j}}{\partial T} \right) = g \cdot \frac{\partial}{\partial T} \left(\frac{\partial \lambda}{\partial T} \right) = g \cdot \frac{\partial^2 \lambda}{\partial T^2} \quad (F-207)$$

$$\left(\frac{\partial^2 \lambda}{\partial T^2} \right) = 2 \exp \left[\frac{\epsilon^{A,B_j}}{RT} \right] b_{ij} \beta^{\gamma_{A,B_j}} \frac{\epsilon^{A,B_j}}{RT^3} + \exp \left[\frac{\epsilon^{A,B_j}}{RT} \right] b_{ij} \beta^{\gamma_{A,B_j}} \frac{(\epsilon^{A,B_j})^2}{R^2 T^4} \quad (F-208)$$

vi) Volume – Temperature

$$\left(\frac{\partial^2 \Delta^{A,B_j}}{\partial T \partial V} \right) = \frac{\partial}{\partial V} \left(\frac{\partial \Delta^{A,B_j}}{\partial T} \right) = \frac{\partial}{\partial V} \left(g \cdot \frac{\partial \lambda}{\partial T} \right) = \frac{\partial g}{\partial V} \cdot \frac{\partial \lambda}{\partial T} = \frac{\partial g}{\partial \eta} \cdot \frac{\partial \eta}{\partial V} \cdot \frac{\partial \lambda}{\partial T} \quad (F-209)$$

F.6 CPA- ECR combining rules used in association term

The ECR rule and its derivatives is presented below:

$$\Delta^{A,B_j} = \sqrt{\Delta^{A,B_i} \Delta^{A,B_j}} \quad (F-210)$$

F.6.1 First-order derivatives

i) Composition

$$\frac{\partial \Delta^{A_j B_j}}{\partial n_k} = \frac{0.5 \left(\Delta^{A_j B_j} \cdot \frac{\partial \Delta^{A_j B_i}}{\partial n_k} + \Delta^{A_j B_i} \cdot \frac{\partial \Delta^{A_j B_j}}{\partial n_k} \right)}{\left(\Delta^{A_j B_i} \Delta^{A_j B_j} \right)^{0.5}} \quad (F-211)$$

ii) Volume

$$\frac{\partial \Delta^{A_j B_j}}{\partial V} = \frac{0.5 \left(\Delta^{A_j B_j} \cdot \frac{\partial \Delta^{A_j B_i}}{\partial V} + \Delta^{A_j B_i} \cdot \frac{\partial \Delta^{A_j B_j}}{\partial V} \right)}{\left(\Delta^{A_j B_i} \Delta^{A_j B_j} \right)^{0.5}} \quad (F-212)$$

iii) Temperature

$$\frac{\partial \Delta^{A_j B_j}}{\partial T} = \frac{0.5 \left(\Delta^{A_j B_j} \cdot \frac{\partial \Delta^{A_j B_i}}{\partial T} + \Delta^{A_j B_i} \cdot \frac{\partial \Delta^{A_j B_j}}{\partial T} \right)}{\left(\Delta^{A_j B_i} \Delta^{A_j B_j} \right)^{0.5}} \quad (F-213)$$

F.6.2 Second-order derivatives

i) Composition – Composition

$$\begin{aligned} \frac{\partial^2 \Delta^{A_j B_j}}{\partial n_k \partial n_l} = & \frac{-0.25 \left(\Delta^{A_j B_j} \cdot \frac{\partial \Delta^{A_j B_i}}{\partial n_l} + \Delta^{A_j B_i} \cdot \frac{\partial \Delta^{A_j B_j}}{\partial n_l} \right) \left(\Delta^{A_j B_j} \cdot \frac{\partial \Delta^{A_j B_i}}{\partial n_k} + \Delta^{A_j B_i} \cdot \frac{\partial \Delta^{A_j B_j}}{\partial n_k} \right)}{\left(\Delta^{A_j B_i} \Delta^{A_j B_j} \right)^{1.5}} \\ & + \frac{0.5 \left(\frac{\partial \Delta^{A_j B_j}}{\partial n_l} \cdot \frac{\partial \Delta^{A_j B_i}}{\partial n_k} + \frac{\partial \Delta^{A_j B_j}}{\partial n_k} \cdot \frac{\partial \Delta^{A_j B_i}}{\partial n_l} + \Delta^{A_j B_j} \cdot \frac{\partial^2 \Delta^{A_j B_i}}{\partial n_k \partial n_l} + \Delta^{A_j B_i} \cdot \frac{\partial^2 \Delta^{A_j B_j}}{\partial n_k \partial n_l} \right)}{\left(\Delta^{A_j B_i} \Delta^{A_j B_j} \right)^{0.5}} \end{aligned} \quad (F-214)$$

ii) Composition – Volume

$$\frac{\partial^2 \Delta^{A_i B_j}}{\partial n_k \partial V} = \frac{-0.25 \left(\Delta^{A_i B_j} \cdot \frac{\partial \Delta^{A_i B_i}}{\partial V} + \Delta^{A_i B_i} \cdot \frac{\partial \Delta^{A_j B_j}}{\partial V} \right) \left(\Delta^{A_i B_j} \cdot \frac{\partial \Delta^{A_i B_i}}{\partial n_k} + \Delta^{A_i B_i} \cdot \frac{\partial \Delta^{A_j B_j}}{\partial n_k} \right)}{\left(\Delta^{A_i B_i} \Delta^{A_j B_j} \right)^{1.5}} \quad (F-215)$$

$$+ \frac{0.5 \left(\frac{\partial \Delta^{A_i B_j}}{\partial V} \cdot \frac{\partial \Delta^{A_i B_i}}{\partial n_k} + \frac{\partial \Delta^{A_j B_j}}{\partial n_k} \cdot \frac{\partial \Delta^{A_i B_i}}{\partial V} + \Delta^{A_j B_j} \cdot \frac{\partial^2 \Delta^{A_i B_i}}{\partial n_k \partial V} + \Delta^{A_i B_i} \cdot \frac{\partial^2 \Delta^{A_j B_j}}{\partial n_k \partial V} \right)}{\left(\Delta^{A_i B_i} \Delta^{A_j B_j} \right)^{0.5}}$$

iii) Composition – Temperature

$$\frac{\partial^2 \Delta^{A_i B_j}}{\partial n_k \partial T} = \frac{-0.25 \left(\Delta^{A_i B_j} \cdot \frac{\partial \Delta^{A_i B_i}}{\partial T} + \Delta^{A_i B_i} \cdot \frac{\partial \Delta^{A_j B_j}}{\partial T} \right) \left(\Delta^{A_i B_j} \cdot \frac{\partial \Delta^{A_i B_i}}{\partial n_k} + \Delta^{A_i B_i} \cdot \frac{\partial \Delta^{A_j B_j}}{\partial n_k} \right)}{\left(\Delta^{A_i B_i} \Delta^{A_j B_j} \right)^{1.5}} \quad (F-216)$$

$$+ \frac{0.5 \left(\frac{\partial \Delta^{A_i B_j}}{\partial T} \cdot \frac{\partial \Delta^{A_i B_i}}{\partial n_k} + \frac{\partial \Delta^{A_j B_j}}{\partial n_k} \cdot \frac{\partial \Delta^{A_i B_i}}{\partial T} + \Delta^{A_j B_j} \cdot \frac{\partial^2 \Delta^{A_i B_i}}{\partial n_k \partial T} + \Delta^{A_i B_i} \cdot \frac{\partial^2 \Delta^{A_j B_j}}{\partial n_k \partial T} \right)}{\left(\Delta^{A_i B_i} \Delta^{A_j B_j} \right)^{0.5}}$$

iv) Volume – Volume

$$\frac{\partial^2 \Delta^{A_i B_j}}{\partial V \partial V} = \frac{-0.25 \left(\Delta^{A_i B_j} \cdot \frac{\partial \Delta^{A_i B_i}}{\partial V} + \Delta^{A_i B_i} \cdot \frac{\partial \Delta^{A_j B_j}}{\partial V} \right) \left(\Delta^{A_i B_j} \cdot \frac{\partial \Delta^{A_i B_i}}{\partial V} + \Delta^{A_i B_i} \cdot \frac{\partial \Delta^{A_j B_j}}{\partial V} \right)}{\left(\Delta^{A_i B_i} \Delta^{A_j B_j} \right)^{1.5}} \quad (F-217)$$

$$+ \frac{0.5 \left(\frac{\partial \Delta^{A_i B_j}}{\partial V} \cdot \frac{\partial \Delta^{A_i B_i}}{\partial V} + \frac{\partial \Delta^{A_j B_j}}{\partial V} \cdot \frac{\partial \Delta^{A_i B_i}}{\partial V} + \Delta^{A_j B_j} \cdot \frac{\partial^2 \Delta^{A_i B_i}}{\partial V \partial V} + \Delta^{A_i B_i} \cdot \frac{\partial^2 \Delta^{A_j B_j}}{\partial V \partial V} \right)}{\left(\Delta^{A_i B_i} \Delta^{A_j B_j} \right)^{0.5}}$$

v) Temperature – Temperature

$$\frac{\partial^2 \Delta^{A_i B_j}}{\partial T \partial T} = \frac{-0.25 \left(\Delta^{A_i B_j} \cdot \frac{\partial \Delta^{A_i B_i}}{\partial T} + \Delta^{A_i B_i} \cdot \frac{\partial \Delta^{A_j B_j}}{\partial T} \right) \left(\Delta^{A_i B_j} \cdot \frac{\partial \Delta^{A_i B_i}}{\partial T} + \Delta^{A_i B_i} \cdot \frac{\partial \Delta^{A_j B_j}}{\partial T} \right)}{\left(\Delta^{A_i B_i} \Delta^{A_j B_j} \right)^{1.5}} \quad (F-218)$$

$$+ \frac{0.5 \left(\frac{\partial \Delta^{A_i B_j}}{\partial T} \cdot \frac{\partial \Delta^{A_i B_i}}{\partial T} + \frac{\partial \Delta^{A_j B_j}}{\partial T} \cdot \frac{\partial \Delta^{A_i B_i}}{\partial T} + \Delta^{A_j B_j} \cdot \frac{\partial^2 \Delta^{A_i B_i}}{\partial T \partial T} + \Delta^{A_i B_i} \cdot \frac{\partial^2 \Delta^{A_j B_j}}{\partial T \partial T} \right)}{\left(\Delta^{A_i B_i} \Delta^{A_j B_j} \right)^{0.5}}$$

vi) Volume – Temperature

$$\begin{aligned} \frac{\partial^2 \Delta^{A_i B_j}}{\partial V \partial T} = & \frac{-0.25 \left(\Delta^{A_i B_j} \cdot \frac{\partial \Delta^{A_i B_j}}{\partial V} + \Delta^{A_i B_j} \cdot \frac{\partial \Delta^{A_i B_j}}{\partial V} \right) \left(\Delta^{A_i B_j} \cdot \frac{\partial \Delta^{A_i B_j}}{\partial T} + \Delta^{A_i B_j} \cdot \frac{\partial \Delta^{A_i B_j}}{\partial T} \right)}{\left(\Delta^{A_i B_j} \Delta^{A_i B_j} \right)^{1.5}} \\ & + \frac{0.5 \left(\frac{\partial \Delta^{A_i B_j}}{\partial T} \cdot \frac{\partial \Delta^{A_i B_j}}{\partial V} + \frac{\partial \Delta^{A_i B_j}}{\partial V} \cdot \frac{\partial \Delta^{A_i B_j}}{\partial T} + \Delta^{A_i B_j} \cdot \frac{\partial^2 \Delta^{A_i B_j}}{\partial T \partial V} + \Delta^{A_i B_j} \cdot \frac{\partial^2 \Delta^{A_i B_j}}{\partial T \partial V} \right)}{\left(\Delta^{A_i B_j} \Delta^{A_i B_j} \right)^{0.5}} \end{aligned} \quad (F-219)$$

F.7 SAFT-CR1 combining rule used in association term

The general association equations are also used to calculate the association contribution in sPC-SAFT. The only difference compared to CPA is the expression used for the association strength which is slightly different. The derivative take on the same form as the CR1 derivatives. The ECR rule may also be employed in sPC-SAFT. The derivatives are naturally the same as already presented for CPA.

$$\Delta^{A_i B_j} = \frac{N_{av} \pi}{6} \sigma_{ij}^3 \kappa^{A_i B_j} \left[\exp \left(\frac{\epsilon^{A_i B_j}}{kT} \right) - 1 \right] g^{hs} = \lambda(T) g^{hs}(T, V, \mathbf{n}) \quad (F-220)$$

$$\lambda(T) = \frac{N_{av} \pi}{6} \sigma_{ij}^3 \kappa^{A_i B_j} \left[\exp \left(\frac{\epsilon^{A_i B_j}}{kT} \right) - 1 \right] \quad (F-221)$$

F.7.1 First-order derivatives

i) Composition

$$\frac{\partial \Delta^{A_i B_j}}{\partial n_k} = \lambda(T) \cdot \frac{\partial g^{hs}(T, V, \mathbf{n})}{\partial n_k} \quad (F-222)$$

ii) Volume

$$\frac{\partial \Delta^{A_i B_j}}{\partial V} = \lambda(T) \cdot \frac{\partial g^{hs}(T, V, \mathbf{n})}{\partial V} \quad (F-223)$$

iii) Temperature

$$\frac{\partial \Delta^{A,B_j}}{\partial T} = \lambda(T) \cdot \frac{\partial g^{hs}}{\partial T} + g^{hs} \cdot \frac{\partial \lambda(T)}{\partial T} \quad (F-224)$$

$$\frac{\partial \lambda(T)}{\partial T} = -\frac{N_{av}\pi}{6} \sigma_{ij}^3 \kappa^{A,B_j} \exp\left(\frac{\epsilon^{A,B_j}}{kT}\right) \frac{\epsilon^{A,B_j}}{kT^2} \quad (F-225)$$

F.7.2 Second-order derivatives

i) Composition - Composition

$$\frac{\partial^2 \Delta^{A,B_j}}{\partial n_k \partial n_l} = \lambda(T) \cdot \frac{\partial^2 g^{hs}(T, V, \mathbf{n})}{\partial n_k \partial n_l} \quad (F-226)$$

ii) Composition - Volume

$$\frac{\partial^2 \Delta^{A,B_j}}{\partial V \partial n_k} = \lambda(T) \cdot \frac{\partial^2 g^{hs}(T, V, \mathbf{n})}{\partial n_k \partial V} \quad (F-227)$$

iii) Composition Temperature

$$\frac{\partial^2 \Delta^{A,B_j}}{\partial T \partial n_k} = \lambda(T) \cdot \frac{\partial^2 g^{hs}}{\partial T \partial n_k} + \frac{\partial g^{hs}}{\partial n_k} \cdot \frac{\partial \lambda(T)}{\partial T} \quad (F-228)$$

iv) Volume - Volume

$$\frac{\partial^2 \Delta^{A,B_j}}{\partial V \partial V} = \lambda(T) \cdot \frac{\partial^2 g^{hs}(T, V, \mathbf{n})}{\partial V \partial V} \quad (F-229)$$

v) Temperature - Temperature

$$\frac{\partial^2 \Delta^{A,B_j}}{\partial T \partial T} = \lambda(T) \cdot \frac{\partial^2 g^{hs}}{\partial T^2} + 2 \frac{\partial g^{hs}}{\partial T} \cdot \frac{\partial \lambda(T)}{\partial T} + g^{hs} \cdot \frac{\partial^2 \lambda(T)}{\partial T^2} \quad (F-230)$$

$$\frac{\partial^2 \lambda(T)}{\partial T^2} = 2 \frac{N_{av}\pi}{6} \sigma_{ij}^3 \kappa^{A,B_j} \exp\left(\frac{\epsilon^{A,B_j}}{kT}\right) \frac{\epsilon^{A,B_j}}{kT^3} + \frac{N_{av}\pi}{6} \sigma_{ij}^3 \kappa^{A,B_j} \exp\left(\frac{\epsilon^{A,B_j}}{kT}\right) \frac{(\epsilon^{A,B_j})^2}{k^2 T^4} \quad (F-231)$$

vi) Volume - Temperature

$$\frac{\partial^2 \Delta^{A,B_j}}{\partial V \partial T} = \lambda(T) \cdot \frac{\partial^2 g^{hs}(T, V, \mathbf{n})}{\partial T \partial V} + \frac{\partial \lambda(T)}{\partial T} \cdot \frac{\partial g^{hs}(T, V, \mathbf{n})}{\partial V} \quad (F-232)$$

F.8 Jog and Chapman's Polar term

F.8.1 State function

The Pade approximate used to calculate the polar term is presented below:

$$\frac{a^{\text{dipolar}}}{RT} = \frac{\frac{a_2^{\text{dipolar}}}{RT}}{1 - \frac{a_3^{\text{dipolar}}}{a_2^{\text{dipolar}}}} \quad (\text{F-233})$$

Where a_2^{dipolar} is the second-order term in u -expansion and a_3^{dipolar} is the third-order term in u -expansion.

Multiply with total moles to make the equations extensive:

$$\frac{A^{\text{dipolar}}}{RT} = \frac{\frac{A_2^{\text{dipolar}}}{RT}}{1 - \frac{A_3^{\text{dipolar}}}{A_2^{\text{dipolar}}}} \quad (\text{F-234})$$

This may also be written as:

$$\frac{A_{\text{mix}}^{\text{dipolar}}}{RT} = \frac{F_{2,\text{mix}}^{\text{dipolar}}}{1 - F_{3,\text{mix}}^{\text{dipolar}} / F_{2,\text{mix}}^{\text{dipolar}}} \quad (\text{F-235})$$

The published form of the second- and third-order are given below:

$$\frac{a_2^{\text{dipolar}}}{RT} = -\frac{2\pi}{9} \frac{\rho}{(kT)^2} m^2 x_p^2 \frac{\mu^4}{d^3} I_2(\rho^*) \quad (\text{F-236})$$

$$\frac{a_3^{\text{dipolar}}}{RT} = \frac{5\pi^2}{162} \frac{\rho^2}{(kT)^3} m^3 x_p^3 \frac{\mu^6}{d^3} I_3(\rho^*) \quad (\text{F-237})$$

Multiply with moles and convert density to total volume to obtain:

$$\frac{A_{2,\text{mix}}^{\text{dipolar}}}{RT} = F_{2,\text{mix}}^{\text{dipolar}} = -\frac{2\pi}{9} \frac{N_{\text{av}}}{V} \frac{1}{(kT)^2} \sum_i^{nc} \sum_j^{nc} n_i n_j m_i m_j x_{pi} x_{pj} \frac{\mu_i^2 \mu_j^2}{d_{ij}^3} I_{2,ij} \quad (\text{F-238})$$

$$\frac{A_{3,\text{mix}}^{\text{dipolar}}}{RT} = F_{3,\text{mix}}^{\text{dipolar}} = \frac{5}{162} \pi^2 N_{\text{av}}^2 \left(\frac{1}{V}\right)^2 \frac{1}{(kT)^3} \sum_i^{nc} \sum_j^{nc} \sum_k^{nc} n_i n_j n_k m_i m_j m_k x_{pi} x_{pj} x_{pk} \frac{\mu_i^2 \mu_j^2 \mu_k^2}{d_{ij} d_{jk} d_{ik}} I_{3,ijk} \quad (\text{F-239})$$

The remaining equations used are given below:

$$I_2(\rho^*) = \frac{1 - 0.3618\rho^* - 0.3205(\rho^*)^2 + 0.1078(\rho^*)^3}{(1 - 0.5236\rho^*)^2} \quad (\text{F-240})$$

$$I_3(\rho^*) = \frac{1 + 0.62378\rho^* - 0.11658(\rho^*)^2}{1 - 0.59056\rho^* + 0.20059(\rho^*)^2} \quad (\text{F-241})$$

$$I_2(\rho^*) = \frac{1 - A\rho^* - B(\rho^*)^2 + C(\rho^*)^3}{(1 - D\rho^*)^2} \quad (F-242)$$

$$I_3(\rho^*) = \frac{1 + E\rho^* - F(\rho^*)^2}{1 - G\rho^* + H(\rho^*)^2} \quad (F-243)$$

$$\rho_{mix}^* = \frac{N_{av}}{V} \sum_i^{nc} m_i n_i d_i^3 \quad (F-244)$$

F.8.2 First-order derivatives

$$F_{JC} = \frac{A_{mix}^{dipolar}}{RT} = \frac{F_{2,mix}^{dipolar}}{1 - F_{3,mix}^{dipolar} / F_{2,mix}^{dipolar}} \quad (F-245)$$

i) Temperature

$$\begin{aligned} \frac{\partial F_{JC}}{\partial T} &= \frac{\frac{\partial}{\partial T}(F_{2,mix}^{dipolar})}{\left(1 - F_{3,mix}^{dipolar} / F_{2,mix}^{dipolar}\right)} \quad (F-246) \\ &= \frac{F_{2,mix}^{dipolar} \left(\frac{F_{3,mix}^{dipolar} \cdot \frac{\partial}{\partial T}(F_{2,mix}^{dipolar})}{(F_{2,mix}^{dipolar})^2} - \frac{\frac{\partial}{\partial T}(F_{3,mix}^{dipolar})}{F_{2,mix}^{dipolar}} \right)}{\left(1 - F_{3,mix}^{dipolar} / F_{2,mix}^{dipolar}\right)^2} \end{aligned}$$

$$\begin{aligned} \frac{\partial}{\partial T}(F_{2,mix}^{dipolar}) &= \frac{2 \cdot (2) \pi N_{av}}{9} \frac{1}{(kT)^2 \cdot T} \sum_i^{nc} \sum_j^{nc} n_i n_j m_i m_j x_{pi} x_{pj} \frac{\mu_i^2 \mu_j^2}{d_{ij}^3} I_{2,ij} \quad (F-247) \\ &+ \frac{2 \cdot (3) \pi N_{av}}{9} \frac{1}{(kT)^2} \sum_i^{nc} \sum_j^{nc} n_i n_j m_i m_j x_{pi} x_{pj} \frac{\mu_i^2 \mu_j^2}{d_{ij}^4} \cdot \frac{\partial}{\partial T}(d_{ij}) I_{2,ij} \\ &- \frac{2 \pi N_{av}}{9} \frac{1}{(kT)^2} \sum_i^{nc} \sum_j^{nc} n_i n_j m_i m_j x_{pi} x_{pj} \frac{\mu_i^2 \mu_j^2}{d_{ij}^3} \cdot \frac{\partial}{\partial T}(I_{2,ij}) \end{aligned}$$

$$\begin{aligned} \frac{\partial}{\partial T}(F_{3,mix}^{dipolar}) &= -\frac{5 \cdot (3)}{162} \pi^2 N_{av}^2 \left(\frac{1}{V}\right)^2 \frac{1}{(kT)^3 \cdot T} \sum_i^{nc} \sum_j^{nc} \sum_k^{nc} n_i n_j n_k m_i m_j m_k x_{pi} x_{pj} x_{pk} \frac{\mu_i^2 \mu_j^2 \mu_k^2}{d_{ij} d_{jk} d_{ik}} I_{3,ijk} \quad (F-248) \\ &- \frac{5 \cdot (3)}{162} \pi^2 N_{av}^2 \left(\frac{1}{V}\right)^2 \frac{1}{(kT)^3} \sum_i^{nc} \sum_j^{nc} \sum_k^{nc} n_i n_j n_k m_i m_j m_k x_{pi} x_{pj} x_{pk} \frac{\mu_i^2 \mu_j^2 \mu_k^2}{(d_{ij})^2 d_{jk} d_{ik}} \cdot \frac{\partial}{\partial T}(d_{ij}) \cdot I_{3,ijk} \\ &+ \frac{5}{162} \pi^2 N_{av}^2 \left(\frac{1}{V}\right)^2 \frac{1}{(kT)^3} \sum_i^{nc} \sum_j^{nc} \sum_k^{nc} n_i n_j n_k m_i m_j m_k x_{pi} x_{pj} x_{pk} \frac{\mu_i^2 \mu_j^2 \mu_k^2}{d_{ij} d_{jk} d_{ik}} \cdot \frac{\partial}{\partial T}(I_{3,ijk}) \end{aligned}$$

$$\frac{\partial}{\partial T}(I_2(\rho^*)) = \frac{2D \cdot (1 - A\rho^* - B(\rho^*)^2 + C(\rho^*)^3)}{(1 - D\rho^*)^3} \cdot \frac{\partial}{\partial T}(\rho^*) \quad (F-249)$$

$$- \frac{A \frac{\partial}{\partial T}(\rho^*) - 2B(\rho^*) \cdot \frac{\partial}{\partial T}(\rho^*) + 3C(\rho^*)^2 \cdot \frac{\partial}{\partial T}(\rho^*)}{(1 - D\rho^*)^2}$$

$$\frac{\partial}{\partial T}(I_3(\rho^*)) = \frac{E \cdot \frac{\partial}{\partial T}(\rho^*) - 2F\rho^* \cdot \frac{\partial}{\partial T}(\rho^*)}{1 - G\rho^* + H(\rho^*)^2} \quad (F-250)$$

$$- \frac{(1 + E\rho^* - F(\rho^*)^2) \left(-G \cdot \frac{\partial}{\partial T}(\rho^*) + 2H\rho^* \cdot \frac{\partial}{\partial T}(\rho^*) \right)}{(1 - G\rho^* + H(\rho^*)^2)^2}$$

$$\frac{\partial}{\partial T}(\rho_{mix}^*) = 3 \frac{N_{av}}{V} \sum_i^{nc} m_i n_i d_i^2 \cdot \frac{\partial}{\partial T}(d_i) \quad (F-251)$$

ii) Volume

$$\frac{\partial F_{JC}}{\partial V} = \frac{\frac{\partial}{\partial V}(F_{2,mix}^{dipolar})}{(1 - F_{3,mix}^{dipolar} / F_{2,mix}^{dipolar})} \quad (F-252)$$

$$- \frac{F_{2,mix}^{dipolar} \left(\frac{F_{3,mix}^{dipolar} \cdot \frac{\partial}{\partial V}(F_{2,mix}^{dipolar})}{(F_{2,mix}^{dipolar})^2} - \frac{\frac{\partial}{\partial V}(F_{3,mix}^{dipolar})}{F_{2,mix}^{dipolar}} \right)}{(1 - F_{3,mix}^{dipolar} / F_{2,mix}^{dipolar})^2}$$

$$\frac{\partial}{\partial V}(F_{2,mix}^{dipolar}) = \frac{2\pi}{9} \frac{N_{av}}{V^2} \frac{1}{(kT)^2} \sum_i^{nc} \sum_j^{nc} n_i n_j m_i m_j x_{pi} x_{pj} \frac{\mu_i^2 \mu_j^2}{d_{ij}^3} I_{2,ij} \quad (F-253)$$

$$- \frac{2\pi}{9} \frac{N_{av}}{V} \frac{1}{(kT)^2} \sum_i^{nc} \sum_j^{nc} n_i n_j m_i m_j x_{pi} x_{pj} \frac{\mu_i^2 \mu_j^2}{d_{ij}^3} \cdot \frac{\partial}{\partial V}(I_{2,ij})$$

$$\frac{\partial}{\partial V}(F_{3,mix}^{dipolar}) = - \frac{5 \cdot (2)}{162} \pi^2 N_{av}^2 \left(\frac{1}{V} \right)^3 \frac{1}{(kT)^3} \sum_i^{nc} \sum_j^{nc} \sum_k^{nc} n_i n_j n_k m_i m_j m_k x_{pi} x_{pj} x_{pk} \frac{\mu_i^2 \mu_j^2 \mu_k^2}{d_{ij} d_{jk} d_{ik}} I_{3,ijk} \quad (F-254)$$

$$+ \frac{5}{162} \pi^2 N_{av}^2 \left(\frac{1}{V} \right)^2 \frac{1}{(kT)^3} \sum_i^{nc} \sum_j^{nc} \sum_k^{nc} n_i n_j n_k m_i m_j m_k x_{pi} x_{pj} x_{pk} \frac{\mu_i^2 \mu_j^2 \mu_k^2}{d_{ij} d_{jk} d_{ik}} \cdot \frac{\partial}{\partial V}(I_{3,ijk})$$

$$\frac{\partial}{\partial V}(I_2(\rho^*)) = \frac{2D \cdot (1 - A\rho^* - B(\rho^*)^2 + C(\rho^*)^3)}{(1 - D\rho^*)^3} \cdot \frac{\partial}{\partial V}(\rho^*) \quad (F-255)$$

$$- \frac{A \frac{\partial}{\partial V}(\rho^*) - 2B(\rho^*) \cdot \frac{\partial}{\partial V}(\rho^*) + 3C(\rho^*)^2 \cdot \frac{\partial}{\partial V}(\rho^*)}{(1 - D\rho^*)^2}$$

$$\frac{\partial}{\partial V}(I_3(\rho^*)) = \frac{E \cdot \frac{\partial}{\partial V}(\rho^*) - 2F\rho^* \cdot \frac{\partial}{\partial V}(\rho^*)}{1 - G\rho^* + H(\rho^*)^2} \quad (F-256)$$

$$- \frac{(1 + E\rho^* - F(\rho^*)^2) \left(-G \cdot \frac{\partial}{\partial V}(\rho^*) + 2H\rho^* \cdot \frac{\partial}{\partial V}(\rho^*) \right)}{(1 - G\rho^* + H(\rho^*)^2)^2}$$

$$\frac{\partial}{\partial V}(\rho_{mix}^*) = - \frac{N_{av}}{V^2} \sum_i^{nc} m_i n_i d_i^3 \quad (F-257)$$

iii) Composition

$$\frac{\partial F_{JC}}{\partial n_i} = \frac{\frac{\partial}{\partial n_i}(F_{2,mix}^{dipolar})}{(1 - F_{3,mix}^{dipolar} / F_{2,mix}^{dipolar})} \quad (F-258)$$

$$- \frac{F_{2,mix}^{dipolar} \left(\frac{F_{3,mix}^{dipolar} \cdot \frac{\partial}{\partial n_i}(F_{2,mix}^{dipolar})}{(F_{2,mix}^{dipolar})^2} - \frac{\frac{\partial}{\partial n_i}(F_{3,mix}^{dipolar})}{F_{2,mix}^{dipolar}} \right)}{(1 - F_{3,mix}^{dipolar} / F_{2,mix}^{dipolar})^2}$$

$$\frac{\partial}{\partial n_k}(F_{2,mix}^{dipolar}) = - \frac{2 \cdot (2) \pi}{9} \frac{N_{av}}{V} \frac{1}{(kT)^2} \sum_i^{nc} n_i m_i x_{pi} x_{pk} \frac{\mu_i^2 \mu_k^2}{d_{ik}^3} I_{2,ik} \quad (F-259)$$

$$- \frac{2\pi}{9} \frac{N_{av}}{V} \frac{1}{(kT)^2} \sum_i^{nc} \sum_j^{nc} n_i n_j m_i m_j x_{pi} x_{pj} \frac{\mu_i^2 \mu_j^2}{d_{ij}^3} \cdot \frac{\partial}{\partial n_k}(I_{2,ij})$$

$$\frac{\partial}{\partial n_f}(F_{3,mix}^{dipolar}) = \frac{5 \cdot (3)}{162} \pi^2 N_{av}^2 \left(\frac{1}{V} \right)^2 \frac{1}{(kT)^3} \sum_i^{nc} \sum_j^{nc} n_i n_j m_i m_j m_f x_{pi} x_{pj} x_{pf} \frac{\mu_i^2 \mu_j^2 \mu_f^2}{d_{ij} d_{jf} d_{if}} I_{3,ijf} \quad (F-260)$$

$$+ \frac{5}{162} \pi^2 N_{av}^2 \left(\frac{1}{V} \right)^2 \frac{1}{(kT)^3} \sum_i^{nc} \sum_j^{nc} \sum_k^{nc} n_i n_j n_k m_i m_j m_k x_{pi} x_{pj} x_{pk} \frac{\mu_i^2 \mu_j^2 \mu_k^2}{d_{ij} d_{jk} d_{ik}} \cdot \frac{\partial}{\partial n_f}(I_{3,ijk})$$

$$\frac{\partial}{\partial n_k} (I_2(\rho^*)) = \frac{2D \cdot (1 - A\rho^* - B(\rho^*)^2 + C(\rho^*)^3)}{(1 - D\rho^*)^3} \cdot \frac{\partial}{\partial n_k} (\rho^*) \quad (F-261)$$

$$\begin{aligned} & - \frac{A \frac{\partial}{\partial n_k} (\rho^*) - 2B(\rho^*) \cdot \frac{\partial}{\partial n_k} (\rho^*) + 3C(\rho^*)^2 \cdot \frac{\partial}{\partial n_k} (\rho^*)}{(1 - D\rho^*)^2} \\ & \frac{\partial}{\partial n_k} (I_3(\rho^*)) = \frac{E \cdot \frac{\partial}{\partial n_k} (\rho^*) - 2F\rho^* \cdot \frac{\partial}{\partial n_k} (\rho^*)}{1 - G\rho^* + H(\rho^*)^2} \quad (F-262) \\ & - \frac{(1 + E\rho^* - F(\rho^*)^2) \left(-G \cdot \frac{\partial}{\partial n_k} (\rho^*) + 2H\rho^* \cdot \frac{\partial}{\partial n_k} (\rho^*) \right)}{(1 - G\rho^* + H(\rho^*)^2)^2} \end{aligned}$$

$$\frac{\partial}{\partial n_k} (\rho_{mix}^*) = \frac{N_{av}}{V} m_k d_k^3 \quad (F-263)$$

F.8.3 Second-order derivatives

i) Temperature – Temperature

$$\begin{aligned} & \frac{\partial}{\partial T} (F_{2,mix}^{dipolar}) \left(\frac{F_{3,mix}^{dipolar} \cdot \frac{\partial}{\partial T} (F_{2,mix}^{dipolar})}{(F_{2,mix}^{dipolar})^2} - \frac{\frac{\partial}{\partial T} (F_{3,mix}^{dipolar})}{F_{2,mix}^{dipolar}} \right) - \frac{\partial}{\partial T} (F_{2,mix}^{dipolar}) \left(\frac{F_{3,mix}^{dipolar} \cdot \frac{\partial}{\partial T} (F_{2,mix}^{dipolar})}{(F_{2,mix}^{dipolar})^2} - \frac{\frac{\partial}{\partial T} (F_{3,mix}^{dipolar})}{F_{2,mix}^{dipolar}} \right) \quad (F-264) \\ & \frac{\partial^2 F_{JC}}{\partial T^2} = - \frac{\left(1 - F_{3,mix}^{dipolar} / F_{2,mix}^{dipolar} \right)^2}{2F_{2,mix}^{dipolar} \left(\frac{F_{3,mix}^{dipolar} \cdot \frac{\partial}{\partial T} (F_{2,mix}^{dipolar})}{(F_{2,mix}^{dipolar})^2} - \frac{\frac{\partial}{\partial T} (F_{3,mix}^{dipolar})}{F_{2,mix}^{dipolar}} \right) \cdot \left(\frac{F_{3,mix}^{dipolar} \cdot \frac{\partial}{\partial T} (F_{2,mix}^{dipolar})}{(F_{2,mix}^{dipolar})^2} - \frac{\frac{\partial}{\partial T} (F_{3,mix}^{dipolar})}{F_{2,mix}^{dipolar}} \right)} \\ & + \frac{\left(1 - F_{3,mix}^{dipolar} / F_{2,mix}^{dipolar} \right)^3}{\frac{\partial^2}{\partial T^2} (F_{2,mix}^{dipolar})} \\ & - \frac{\left(1 - F_{3,mix}^{dipolar} / F_{2,mix}^{dipolar} \right)}{F_{2,mix}^{dipolar} \left(- \frac{2F_{3,mix}^{dipolar} \cdot \frac{\partial}{\partial T} (F_{2,mix}^{dipolar}) \cdot \frac{\partial}{\partial V} (F_{2,mix}^{dipolar})}{(F_{2,mix}^{dipolar})^3} + \frac{\frac{\partial}{\partial T} (F_{3,mix}^{dipolar}) \cdot \frac{\partial}{\partial V} (F_{2,mix}^{dipolar})}{(F_{2,mix}^{dipolar})^2} \right.} \\ & \left. + \frac{\frac{\partial}{\partial T} (F_{3,mix}^{dipolar}) \cdot \frac{\partial}{\partial T} (F_{2,mix}^{dipolar})}{(F_{2,mix}^{dipolar})^2} + \frac{F_{3,mix}^{dipolar} \cdot \frac{\partial^2}{\partial T^2} (F_{2,mix}^{dipolar})}{(F_{2,mix}^{dipolar})^2} - \frac{\frac{\partial^2}{\partial T^2} (F_{3,mix}^{dipolar})}{F_{2,mix}^{dipolar}} \right) \end{aligned}$$

(F-265)

$$\begin{aligned}
 \frac{\partial^2}{\partial T^2} (F_{2,mix}^{dipolar}) = & -\frac{2 \cdot (6) \pi N_{av}}{9} \frac{1}{V (kT)^2 \cdot T^2} \sum_i^{nc} \sum_j^{nc} n_i n_j m_i m_j x_{pi} x_{pj} \frac{\mu_i^2 \mu_j^2}{d_{ij}^3} I_{2,ij} a \\
 & -\frac{2 \cdot (12) \pi N_{av}}{9} \frac{1}{V (kT)^2 \cdot T} \sum_i^{nc} \sum_j^{nc} n_i n_j m_i m_j x_{pi} x_{pj} \frac{\mu_i^2 \mu_j^2}{d_{ij}^4} \cdot \frac{\partial}{\partial T} (d_{ij}) \\
 & +\frac{2 \cdot (4) \pi N_{av}}{9} \frac{1}{V (kT)^2 \cdot T} \sum_i^{nc} \sum_j^{nc} n_i n_j m_i m_j x_{pi} x_{pj} \frac{\mu_i^2 \mu_j^2}{d_{ij}^3} \cdot \frac{\partial}{\partial T} (I_{2,ij}) \\
 & -\frac{2 \cdot (12) \pi N_{av}}{9} \frac{1}{V (kT)^2} \sum_i^{nc} \sum_j^{nc} n_i n_j m_i m_j x_{pi} x_{pj} \frac{\mu_i^2 \mu_j^2}{d_{ij}^5} \cdot \frac{\partial}{\partial T} (d_{ij})^2 I_{2,ij} \\
 & +\frac{2 \cdot (3) \pi N_{av}}{9} \frac{1}{V (kT)^2} \sum_i^{nc} \sum_j^{nc} n_i n_j m_i m_j x_{pi} x_{pj} \frac{\mu_i^2 \mu_j^2}{d_{ij}^4} \cdot \frac{\partial^2}{\partial T^2} (d_{ij}) I_{2,ij} \\
 & +\frac{2 \cdot (6) \pi N_{av}}{9} \frac{1}{V (kT)^2} \sum_i^{nc} \sum_j^{nc} n_i n_j m_i m_j x_{pi} x_{pj} \frac{\mu_i^2 \mu_j^2}{d_{ij}^4} \cdot \frac{\partial}{\partial T} (d_{ij}) \cdot \frac{\partial}{\partial T} (I_{2,ij}) \\
 & -\frac{2 \pi N_{av}}{9} \frac{1}{V (kT)^2} \sum_i^{nc} \sum_j^{nc} n_i n_j m_i m_j x_{pi} x_{pj} \frac{\mu_i^2 \mu_j^2}{d_{ij}^3} \cdot \frac{\partial^2}{\partial T^2} (I_{2,ij})
 \end{aligned}$$

(F-266)

$$\begin{aligned}
 \frac{\partial^2}{\partial T^2} (F_{3,mix}^{dipolar}) = & \frac{5 \cdot (12)}{162} \pi^2 N_{av}^2 \left(\frac{1}{V} \right)^2 \frac{1}{(kT)^3 \cdot T^2} \sum_i^{nc} \sum_j^{nc} \sum_k^{nc} n_i n_j n_k m_i m_j m_k x_{pi} x_{pj} x_{pk} \frac{\mu_i^2 \mu_j^2 \mu_k^2}{d_{ij} d_{jk} d_{ik}} I_{3,ijk} \\
 & +\frac{5 \cdot (6) \cdot (3)}{162} \pi^2 N_{av}^2 \left(\frac{1}{V} \right)^2 \frac{1}{(kT)^3 \cdot T} \sum_i^{nc} \sum_j^{nc} \sum_k^{nc} n_i n_j n_k m_i m_j m_k x_{pi} x_{pj} x_{pk} \frac{\mu_i^2 \mu_j^2 \mu_k^2}{(d_{ij})^2 d_{jk} d_{ik}} \cdot \frac{\partial}{\partial T} (d_{ij}) \cdot I_{3,ijk} \\
 & -\frac{5 \cdot (6)}{162} \pi^2 N_{av}^2 \left(\frac{1}{V} \right)^2 \frac{1}{(kT)^3 \cdot T} \sum_i^{nc} \sum_j^{nc} \sum_k^{nc} n_i n_j n_k m_i m_j m_k x_{pi} x_{pj} x_{pk} \frac{\mu_i^2 \mu_j^2 \mu_k^2}{d_{ij} d_{jk} d_{ik}} \cdot \frac{\partial}{\partial T} (I_{3,ijk}) \\
 & +\frac{5 \cdot (12)}{162} \pi^2 N_{av}^2 \left(\frac{1}{V} \right)^2 \frac{1}{(kT)^3} \sum_i^{nc} \sum_j^{nc} \sum_k^{nc} n_i n_j n_k m_i m_j m_k x_{pi} x_{pj} x_{pk} \frac{\mu_i^2 \mu_j^2 \mu_k^2}{(d_{ij})^2 (d_{jk})^2 d_{ik}} \cdot \frac{\partial}{\partial T} (d_{ij}) \cdot \frac{\partial}{\partial T} (d_{ik}) \cdot I_{3,ijk} \\
 & -\frac{5 \cdot (3)}{162} \pi^2 N_{av}^2 \left(\frac{1}{V} \right)^2 \frac{1}{(kT)^3} \sum_i^{nc} \sum_j^{nc} \sum_k^{nc} n_i n_j n_k m_i m_j m_k x_{pi} x_{pj} x_{pk} \frac{\mu_i^2 \mu_j^2 \mu_k^2}{(d_{ij})^2 d_{jk} d_{ik}} \cdot \frac{\partial^2}{\partial T^2} (d_{ij}) \cdot I_{3,ijk} \\
 & -\frac{5 \cdot (6)}{162} \pi^2 N_{av}^2 \left(\frac{1}{V} \right)^2 \frac{1}{(kT)^3} \sum_i^{nc} \sum_j^{nc} \sum_k^{nc} n_i n_j n_k m_i m_j m_k x_{pi} x_{pj} x_{pk} \frac{\mu_i^2 \mu_j^2 \mu_k^2}{(d_{ij})^2 d_{jk} d_{ik}} \cdot \frac{\partial}{\partial T} (d_{ij}) \cdot \frac{\partial}{\partial T} (I_{3,ijk}) \\
 & +\frac{5}{162} \pi^2 N_{av}^2 \left(\frac{1}{V} \right)^2 \frac{1}{(kT)^3} \sum_i^{nc} \sum_j^{nc} \sum_k^{nc} n_i n_j n_k m_i m_j m_k x_{pi} x_{pj} x_{pk} \frac{\mu_i^2 \mu_j^2 \mu_k^2}{d_{ij} d_{jk} d_{ik}} \cdot \frac{\partial^2}{\partial T^2} (I_{3,ijk})
 \end{aligned}$$

(F-267)

$$\begin{aligned}
 \frac{\partial^2}{\partial T^2}(I_2(\rho^*)) &= \frac{6D^2 \cdot (1 - A\rho^* - B(\rho^*)^2 + C(\rho^*)^3)}{(1 - D\rho^*)^4} \cdot \frac{\partial}{\partial T}(\rho^*) \cdot \frac{\partial}{\partial T}(\rho^*) \\
 &+ \frac{4D \cdot \left(-A \cdot \frac{\partial}{\partial T}(\rho^*) - 2B(\rho^*) \cdot \frac{\partial}{\partial T}(\rho^*) + 3C(\rho^*)^2 \cdot \frac{\partial}{\partial T}(\rho^*) \right)}{(1 - D\rho^*)^3} \cdot \frac{\partial}{\partial T}(\rho^*) \\
 &+ \frac{2D \cdot (1 - A\rho^* - B(\rho^*)^2 + C(\rho^*)^3)}{(1 - D\rho^*)^3} \cdot \frac{\partial^2}{\partial T^2}(\rho^*) \\
 &+ \frac{\left(\begin{aligned} &-2B \frac{\partial}{\partial T}(\rho^*) \cdot \frac{\partial}{\partial T}(\rho^*) + 6C(\rho^*) \cdot \frac{\partial}{\partial T}(\rho^*) \cdot \frac{\partial}{\partial T}(\rho^*) \\ &-A \cdot \frac{\partial^2}{\partial T^2}(\rho^*) - 2B(\rho^*) \cdot \frac{\partial^2}{\partial T^2}(\rho^*) + 3(\rho^*)^2 \cdot \frac{\partial^2}{\partial T^2}(\rho^*) \end{aligned} \right)}{(1 - D\rho^*)^2}
 \end{aligned}$$

(F-268)

$$\begin{aligned}
 \frac{\partial^2}{\partial T^2}(I_3(\rho^*)) &= -2 \frac{\left(-G \cdot \frac{\partial}{\partial T}(\rho^*) + 2H\rho^* \cdot \frac{\partial}{\partial T}(\rho^*) \right) \left(E \frac{\partial}{\partial T}(\rho^*) - 2F(\rho^*) \cdot \frac{\partial}{\partial T}(\rho^*) \right)}{(1 - G\rho^* + H(\rho^*)^2)^2} \\
 &+ \frac{2(1 + E\rho^* - F(\rho^*)^2) \left(-G \cdot \frac{\partial}{\partial T}(\rho^*) + 2H\rho^* \cdot \frac{\partial}{\partial T}(\rho^*) \right) \left(-G \cdot \frac{\partial}{\partial T}(\rho^*) + 2H\rho^* \cdot \frac{\partial}{\partial T}(\rho^*) \right)}{(1 - G\rho^* + H(\rho^*)^2)^3} \\
 &+ \frac{-2F \cdot \frac{\partial}{\partial T}(\rho^*) \cdot \frac{\partial}{\partial T}(\rho^*) + E \cdot \frac{\partial^2}{\partial T^2}(\rho^*) - 2F\rho^* \cdot \frac{\partial^2}{\partial T^2}(\rho^*)}{(1 - G\rho^* + H(\rho^*)^2)} \\
 &- \frac{(1 + E\rho^* - F(\rho^*)^2) \left(2H \frac{\partial}{\partial T}(\rho^*) \cdot \frac{\partial}{\partial T}(\rho^*) - G \frac{\partial^2}{\partial T^2}(\rho^*) + 2H\rho^* \cdot \frac{\partial^2}{\partial T^2}(\rho^*) \right)}{(1 - G\rho^* + H(\rho^*)^2)^2}
 \end{aligned}$$

(F-269)

$$\frac{\partial^2}{\partial T^2}(\rho_{mix}^*) = 6 \frac{N_{av}}{V} \sum_i^{nc} m_i n_i d_i \cdot \frac{\partial}{\partial T}(d_i)^2 + 3 \frac{N_{av}}{V} \sum_i^{nc} m_i n_i d_i^2 \cdot \frac{\partial^2}{\partial T^2}(d_i)$$

ii) Temperature – Volume

$$\begin{aligned}
 \frac{\partial^2 F_{JC}}{\partial V \partial T} = & - \frac{\frac{\partial}{\partial V} \left(F_{2,mix}^{dipolar} \right) \left(\frac{F_{3,mix}^{dipolar} \cdot \frac{\partial}{\partial T} (F_{2,mix}^{dipolar})}{(F_{2,mix}^{dipolar})^2} - \frac{\frac{\partial}{\partial T} (F_{3,mix}^{dipolar})}{F_{2,mix}^{dipolar}} \right) - \frac{\partial}{\partial T} \left(F_{2,mix}^{dipolar} \right) \left(\frac{F_{3,mix}^{dipolar} \cdot \frac{\partial}{\partial V} (F_{2,mix}^{dipolar})}{(F_{2,mix}^{dipolar})^2} - \frac{\frac{\partial}{\partial V} (F_{3,mix}^{dipolar})}{F_{2,mix}^{dipolar}} \right)}{(1 - F_{3,mix}^{dipolar} / F_{2,mix}^{dipolar})^2} \\
 & + \frac{2 F_{2,mix}^{dipolar} \left(\frac{F_{3,mix}^{dipolar} \cdot \frac{\partial}{\partial n_i} (F_{2,mix}^{dipolar})}{(F_{2,mix}^{dipolar})^2} - \frac{\frac{\partial}{\partial T} (F_{3,mix}^{dipolar})}{F_{2,mix}^{dipolar}} \right) \cdot \left(\frac{F_{3,mix}^{dipolar} \cdot \frac{\partial}{\partial V} (F_{2,mix}^{dipolar})}{(F_{2,mix}^{dipolar})^2} - \frac{\frac{\partial}{\partial V} (F_{3,mix}^{dipolar})}{F_{2,mix}^{dipolar}} \right)}{(1 - F_{3,mix}^{dipolar} / F_{2,mix}^{dipolar})^3} \\
 & - \frac{\frac{\partial^2}{\partial V \partial T} (F_{2,mix}^{dipolar})}{(1 - F_{3,mix}^{dipolar} / F_{2,mix}^{dipolar})} \\
 & - \frac{F_{2,mix}^{dipolar} \left(- \frac{2 F_{3,mix}^{dipolar} \cdot \frac{\partial}{\partial T} (F_{2,mix}^{dipolar}) \cdot \frac{\partial}{\partial V} (F_{2,mix}^{dipolar})}{(F_{2,mix}^{dipolar})^3} + \frac{\frac{\partial}{\partial T} (F_{3,mix}^{dipolar}) \cdot \frac{\partial}{\partial V} (F_{2,mix}^{dipolar})}{(F_{2,mix}^{dipolar})^2} \right.}{(1 - F_{3,mix}^{dipolar} / F_{2,mix}^{dipolar})^2} \\
 & \quad \left. + \frac{\frac{\partial}{\partial V} (F_{3,mix}^{dipolar}) \cdot \frac{\partial}{\partial T} (F_{2,mix}^{dipolar})}{(F_{2,mix}^{dipolar})^2} + \frac{F_{3,mix}^{dipolar} \cdot \frac{\partial^2}{\partial V \partial T} (F_{2,mix}^{dipolar})}{(F_{2,mix}^{dipolar})^2} - \frac{\frac{\partial^2}{\partial V \partial T} (F_{3,mix}^{dipolar})}{F_{2,mix}^{dipolar}} \right)
 \end{aligned}
 \tag{F-270}$$

$$\begin{aligned}
 \frac{\partial^2}{\partial T \partial V} (F_{2,mix}^{dipolar}) = & - \frac{2 \cdot (2) \pi N_{av}}{9 V^2} \frac{1}{(kT)^2 \cdot T} \sum_i^{nc} \sum_j^{nc} n_i n_j m_i m_j x_{pi} x_{pj} \frac{\mu_i^2 \mu_j^2}{d_{ij}^3} I_{2,ij} \\
 & + \frac{2 \cdot (2) \pi N_{av}}{9 V} \frac{1}{(kT)^2 \cdot T} \sum_i^{nc} \sum_j^{nc} n_i n_j m_i m_j x_{pi} x_{pj} \frac{\mu_i^2 \mu_j^2}{d_{ij}^3} \cdot \frac{\partial}{\partial V} (I_{2,ij}) \\
 & - \frac{2 \cdot (3) \pi N_{av}}{9 V^2} \frac{1}{(kT)^2} \sum_i^{nc} \sum_j^{nc} n_i n_j m_i m_j x_{pi} x_{pj} \frac{\mu_i^2 \mu_j^2}{d_{ij}^4} \cdot \frac{\partial}{\partial T} (d_{ij}) I_{2,ij} \\
 & + \frac{2 \pi N_{av}}{9 V^2} \frac{1}{(kT)^2} \sum_i^{nc} \sum_j^{nc} n_i n_j m_i m_j x_{pi} x_{pj} \frac{\mu_i^2 \mu_j^2}{d_{ij}^3} \cdot \frac{\partial}{\partial T} (I_{2,ij}) \\
 & + \frac{2 \cdot (3) \pi N_{av}}{9 V} \frac{1}{(kT)^2} \sum_i^{nc} \sum_j^{nc} n_i n_j m_i m_j x_{pi} x_{pj} \frac{\mu_i^2 \mu_j^2}{d_{ij}^4} \cdot \frac{\partial}{\partial T} (d_{ij}) \cdot \frac{\partial}{\partial V} (I_{2,ij}) \\
 & - \frac{2 \pi N_{av}}{9 V} \frac{1}{(kT)^2} \sum_i^{nc} \sum_j^{nc} n_i n_j m_i m_j x_{pi} x_{pj} \frac{\mu_i^2 \mu_j^2}{d_{ij}^3} \cdot \frac{\partial^2}{\partial T \partial V} (I_{2,ij})
 \end{aligned}
 \tag{F-271}$$

$$\begin{aligned}
 \frac{\partial}{\partial T \partial V} (F_{3,mix}^{dipolar}) = & \frac{5 \cdot (6)}{162} \pi^2 N_{av}^2 \left(\frac{1}{V} \right)^3 \frac{1}{(kT)^3 \cdot T} \sum_i^{nc} \sum_j^{nc} \sum_k^{nc} n_i n_j n_k m_i m_j m_k x_{p_i} x_{p_j} x_{p_k} \frac{\mu_i^2 \mu_j^2 \mu_k^2}{d_{ij} d_{jk} d_{ik}} I_{3,ijk} \\
 & - \frac{5 \cdot (3)}{162} \pi^2 N_{av}^2 \left(\frac{1}{V} \right)^2 \frac{1}{(kT)^3 \cdot T} \sum_i^{nc} \sum_j^{nc} \sum_k^{nc} n_i n_j n_k m_i m_j m_k x_{p_i} x_{p_j} x_{p_k} \frac{\mu_i^2 \mu_j^2 \mu_k^2}{d_{ij} d_{jk} d_{ik}} \cdot \frac{\partial}{\partial V} (I_{3,ijk}) \\
 & + \frac{5 \cdot (2) \cdot (3)}{162} \pi^2 N_{av}^2 \left(\frac{1}{V} \right)^3 \frac{1}{(kT)^3} \sum_i^{nc} \sum_j^{nc} \sum_k^{nc} n_i n_j n_k m_i m_j m_k x_{p_i} x_{p_j} x_{p_k} \frac{\mu_i^2 \mu_j^2 \mu_k^2}{(d_{ij})^2 d_{jk} d_{ik}} \cdot \frac{\partial}{\partial T} (d_{ij}) \cdot I_{3,ijk} \\
 & - \frac{5 \cdot (2)}{162} \pi^2 N_{av}^2 \left(\frac{1}{V} \right)^3 \frac{1}{(kT)^3} \sum_i^{nc} \sum_j^{nc} \sum_k^{nc} n_i n_j n_k m_i m_j m_k x_{p_i} x_{p_j} x_{p_k} \frac{\mu_i^2 \mu_j^2 \mu_k^2}{d_{ij} d_{jk} d_{ik}} \cdot \frac{\partial}{\partial T} (I_{3,ijk}) \\
 & - \frac{5 \cdot (3)}{162} \pi^2 N_{av}^2 \left(\frac{1}{V} \right)^2 \frac{1}{(kT)^3} \sum_i^{nc} \sum_j^{nc} \sum_k^{nc} n_i n_j n_k m_i m_j m_k x_{p_i} x_{p_j} x_{p_k} \frac{\mu_i^2 \mu_j^2 \mu_k^2}{(d_{ij})^2 d_{jk} d_{ik}} \cdot \frac{\partial}{\partial T} (d_{ij}) \cdot \frac{\partial}{\partial V} (I_{3,ijk}) \\
 & + \frac{5 \cdot (2)}{162} \pi^2 N_{av}^2 \left(\frac{1}{V} \right)^2 \frac{1}{(kT)^3} \sum_i^{nc} \sum_j^{nc} \sum_k^{nc} n_i n_j n_k m_i m_j m_k x_{p_i} x_{p_j} x_{p_k} \frac{\mu_i^2 \mu_j^2 \mu_k^2}{d_{ij} d_{jk} d_{ik}} \cdot \frac{\partial^2}{\partial T \partial V} (I_{3,ijk})
 \end{aligned}
 \tag{F-272}$$

$$\begin{aligned}
 \frac{\partial^2}{\partial V \partial T} (I_2(\rho^*)) = & \frac{6D^2 \cdot (1 - A\rho^* - B(\rho^*)^2 + C(\rho^*)^3)}{(1 - D\rho^*)^4} \cdot \frac{\partial}{\partial V}(\rho^*) \cdot \frac{\partial}{\partial T}(\rho^*) \\
 & + \frac{2D \cdot \left(-A \cdot \frac{\partial}{\partial V}(\rho^*) - 2B(\rho^*) \cdot \frac{\partial}{\partial V}(\rho^*) + 3C(\rho^*)^2 \cdot \frac{\partial}{\partial V}(\rho^*) \right)}{(1 - D\rho^*)^3} \cdot \frac{\partial}{\partial T}(\rho^*) \\
 & + \frac{2D \cdot \left(-A \cdot \frac{\partial}{\partial T}(\rho^*) - 2B(\rho^*) \cdot \frac{\partial}{\partial T}(\rho^*) + 3C(\rho^*)^2 \cdot \frac{\partial}{\partial T}(\rho^*) \right)}{(1 - D\rho^*)^3} \cdot \frac{\partial}{\partial V}(\rho^*) \\
 & + \frac{2D \cdot (1 - A\rho^* - B(\rho^*)^2 + C(\rho^*)^3)}{(1 - D\rho^*)^3} \cdot \frac{\partial^2}{\partial V \partial T}(\rho^*) \\
 & + \frac{\left(-2B \frac{\partial}{\partial V}(\rho^*) \cdot \frac{\partial}{\partial T}(\rho^*) + 6C(\rho^*) \cdot \frac{\partial}{\partial V}(\rho^*) \cdot \frac{\partial}{\partial T}(\rho^*) \right)}{(1 - D\rho^*)^2} \\
 & + \frac{\left(-A \cdot \frac{\partial^2}{\partial V \partial T}(\rho^*) - 2B(\rho^*) \cdot \frac{\partial^2}{\partial V \partial T}(\rho^*) + 3(\rho^*)^2 \cdot \frac{\partial^2}{\partial V \partial T}(\rho^*) \right)}{(1 - D\rho^*)^2}
 \end{aligned}
 \tag{F-273}$$

(F-274)

$$\begin{aligned}
 \frac{\partial^2}{\partial T \partial V} (I_3(\rho^*)) = & - \frac{\left(-G \cdot \frac{\partial}{\partial V}(\rho^*) + 2H\rho^* \cdot \frac{\partial}{\partial V}(\rho^*) \right) \left(E \frac{\partial}{\partial T}(\rho^*) - 2F(\rho^*) \cdot \frac{\partial}{\partial T}(\rho^*) \right)}{\left(1 - G\rho^* + H(\rho^*)^2 \right)^2} \\
 & - \frac{\left(-G \cdot \frac{\partial}{\partial T}(\rho^*) + 2H\rho^* \cdot \frac{\partial}{\partial T}(\rho^*) \right) \left(E \frac{\partial}{\partial V}(\rho^*) - 2F(\rho^*) \cdot \frac{\partial}{\partial V}(\rho^*) \right)}{\left(1 - G\rho^* + H(\rho^*)^2 \right)^2} \\
 & + \frac{2 \left(1 + E\rho^* - F(\rho^*)^2 \right) \left(-G \cdot \frac{\partial}{\partial V}(\rho^*) + 2H\rho^* \cdot \frac{\partial}{\partial V}(\rho^*) \right) \left(-G \cdot \frac{\partial}{\partial T}(\rho^*) + 2H\rho^* \cdot \frac{\partial}{\partial T}(\rho^*) \right)}{\left(1 - G\rho^* + H(\rho^*)^2 \right)^3} \\
 & + \frac{-2F \cdot \frac{\partial}{\partial V}(\rho^*) \cdot \frac{\partial}{\partial T}(\rho^*) + E \cdot \frac{\partial}{\partial T \partial V}(\rho^*) - 2F\rho^* \cdot \frac{\partial}{\partial T \partial V}(\rho^*)}{\left(1 - G\rho^* + H(\rho^*)^2 \right)} \\
 & - \frac{\left(1 + E\rho^* - F(\rho^*)^2 \right) \left(2H \frac{\partial}{\partial V}(\rho^*) \cdot \frac{\partial}{\partial T}(\rho^*) - G \frac{\partial}{\partial T \partial V}(\rho^*) + 2H\rho^* \cdot \frac{\partial}{\partial T \partial V}(\rho^*) \right)}{\left(1 - G\rho^* + H(\rho^*)^2 \right)^2}
 \end{aligned}$$

(F-275)

$$\frac{\partial^2}{\partial T \partial V} (\rho_{mix}^*) = -3 \frac{N_{av}}{V^2} \sum_i^{nc} m_i n_i d_i^2 \cdot \frac{\partial}{\partial T} (d_i)$$

iii) Temperature – Composition

$$\begin{aligned}
 \frac{\partial^2 F_{JC}}{\partial T \partial n_i} = & - \frac{\frac{\partial}{\partial T} (F_{2,mix}^{dipolar}) \left(\frac{F_{3,mix}^{dipolar} \cdot \frac{\partial}{\partial n_i} (F_{2,mix}^{dipolar})}{(F_{2,mix}^{dipolar})^2} - \frac{\partial}{\partial n_i} (F_{3,mix}^{dipolar}) \right)}{\left(1 - F_{3,mix}^{dipolar} / F_{2,mix}^{dipolar} \right)^2} - \frac{\partial}{\partial n_i} (F_{2,mix}^{dipolar}) \left(\frac{F_{3,mix}^{dipolar} \cdot \frac{\partial}{\partial T} (F_{2,mix}^{dipolar})}{(F_{2,mix}^{dipolar})^2} - \frac{\partial}{\partial T} (F_{3,mix}^{dipolar}) \right)}{F_{2,mix}^{dipolar}} \\
 & + \frac{2F_{2,mix}^{dipolar} \left(\frac{F_{3,mix}^{dipolar} \cdot \frac{\partial}{\partial n_i} (F_{2,mix}^{dipolar})}{(F_{2,mix}^{dipolar})^2} - \frac{\partial}{\partial n_i} (F_{3,mix}^{dipolar}) \right) \left(\frac{F_{3,mix}^{dipolar} \cdot \frac{\partial}{\partial T} (F_{2,mix}^{dipolar})}{(F_{2,mix}^{dipolar})^2} - \frac{\partial}{\partial T} (F_{3,mix}^{dipolar}) \right)}{\left(1 - F_{3,mix}^{dipolar} / F_{2,mix}^{dipolar} \right)^3} \\
 & - \frac{\frac{\partial^2}{\partial T \partial n_i} (F_{2,mix}^{dipolar})}{\left(1 - F_{3,mix}^{dipolar} / F_{2,mix}^{dipolar} \right)} \\
 & - \frac{F_{2,mix}^{dipolar} \left(- \frac{2F_{3,mix}^{dipolar} \cdot \frac{\partial}{\partial n_i} (F_{2,mix}^{dipolar}) \cdot \frac{\partial}{\partial T} (F_{2,mix}^{dipolar})}{(F_{2,mix}^{dipolar})^3} + \frac{\frac{\partial}{\partial n_i} (F_{3,mix}^{dipolar}) \cdot \frac{\partial}{\partial T} (F_{2,mix}^{dipolar})}{(F_{2,mix}^{dipolar})^2} \right.}{\left(1 - F_{3,mix}^{dipolar} / F_{2,mix}^{dipolar} \right)^2} \\
 & \left. + \frac{\frac{\partial}{\partial T} (F_{3,mix}^{dipolar}) \cdot \frac{\partial}{\partial n_i} (F_{2,mix}^{dipolar})}{(F_{2,mix}^{dipolar})^2} + \frac{F_{3,mix}^{dipolar} \cdot \frac{\partial^2}{\partial T \partial n_i} (F_{2,mix}^{dipolar})}{(F_{2,mix}^{dipolar})^2} - \frac{\frac{\partial^2}{\partial T \partial n_i} (F_{3,mix}^{dipolar})}{F_{2,mix}^{dipolar}} \right)
 \end{aligned} \tag{F-276}$$

$$\begin{aligned}
 \frac{\partial^2}{\partial T \partial n_k} (F_{2,mix}^{dipolar}) = & \frac{2 \cdot (4) \pi N_{av}}{9 V} \frac{1}{(kT)^2 \cdot T} \sum_i^{nc} n_i m_i m_k x_{pi} x_{pk} \frac{\mu_i^2 \mu_j^2}{d_{ik}^3} I_{2,ik} \\
 & + \frac{2 \cdot (2) \pi N_{av}}{9 V} \frac{1}{(kT)^2 \cdot T} \sum_i^{nc} \sum_j^{nc} n_i n_j m_i m_j x_{pi} x_{pj} \frac{\mu_i^2 \mu_j^2}{d_{ij}^3} \cdot \frac{\partial}{\partial n_k} (I_{2,ij}) \\
 & + \frac{2 \cdot (6) \pi N_{av}}{9 V} \frac{1}{(kT)^2} \sum_i^{nc} n_i m_i m_k x_{pi} x_{pk} \frac{\mu_i^2 \mu_j^2}{d_{ik}^4} \cdot \frac{\partial}{\partial T} (d_{ik}) \cdot I_{2,ik} \\
 & + \frac{2 \cdot (3) \pi N_{av}}{9 V} \frac{1}{(kT)^2} \sum_i^{nc} \sum_j^{nc} n_i n_j m_i m_j x_{pi} x_{pj} \frac{\mu_i^2 \mu_j^2}{d_{ij}^4} \cdot \frac{\partial}{\partial T} (d_{ij}) \cdot \frac{\partial}{\partial n_k} (I_{2,ij}) \\
 & - \frac{2 \cdot (2) \pi N_{av}}{9 V} \frac{1}{(kT)^2} \sum_i^{nc} n_i m_i m_k x_{pi} x_{pk} \frac{\mu_i^2 \mu_k^2}{d_{ik}^3} \cdot \frac{\partial}{\partial T} (I_{2,ik}) \\
 & - \frac{2 \pi N_{av}}{9 V} \frac{1}{(kT)^2} \sum_i^{nc} \sum_j^{nc} n_i n_j m_i m_j x_{pi} x_{pj} \frac{\mu_i^2 \mu_j^2}{d_{ij}^3} \cdot \frac{\partial^2}{\partial T \partial n_k} (I_{2,ij})
 \end{aligned} \tag{F-277}$$

$$\begin{aligned}
 \frac{\partial^2}{\partial T \partial n_f} (F_{3,mix}^{dipolar}) = & -\frac{5 \cdot (3) \cdot (3)}{162} \pi^2 N_{av}^2 \left(\frac{1}{V} \right)^2 \frac{1}{(kT)^3} \sum_i^{nc} \sum_j^{nc} n_i n_j m_i m_j m_f x_{p_i} x_{p_j} x_{pf} \frac{\mu_i^2 \mu_j^2 \mu_f^2}{d_{ij} d_{jf} d_{if}} I_{3,ijk} \\
 & -\frac{5 \cdot (3)}{162} \pi^2 N_{av}^2 \left(\frac{1}{V} \right)^2 \frac{1}{(kT)^3} \sum_i^{nc} \sum_j^{nc} \sum_k^{nc} n_i n_j n_k m_i m_j m_k x_{p_i} x_{p_j} x_{p_k} \frac{\mu_i^2 \mu_j^2 \mu_k^2}{d_{ij} d_{jk} d_{ik}} \cdot \frac{\partial}{\partial n_f} (I_{3,ijk}) \\
 & -\frac{5 \cdot (9)}{162} \pi^2 N_{av}^2 \left(\frac{1}{V} \right)^2 \frac{1}{(kT)^3} \sum_i^{nc} \sum_j^{nc} n_i n_j m_i m_j m_f x_{p_i} x_{p_j} x_{pf} \frac{\mu_i^2 \mu_j^2 \mu_f^2}{(d_{ij})^2 d_{jf} d_{if}} \cdot \frac{\partial}{\partial T} (d_{ij}) \cdot I_{3,ijk} \\
 & -\frac{5 \cdot (3)}{162} \pi^2 N_{av}^2 \left(\frac{1}{V} \right)^2 \frac{1}{(kT)^3} \sum_i^{nc} \sum_j^{nc} \sum_k^{nc} n_i n_j n_k m_i m_j m_k x_{p_i} x_{p_j} x_{p_k} \frac{\mu_i^2 \mu_j^2 \mu_k^2}{(d_{ij})^2 d_{jk} d_{ik}} \cdot \frac{\partial}{\partial n_f} (I_{3,ijk}) \cdot \frac{\partial}{\partial T} (d_{ij}) \\
 & +\frac{5 \cdot (3)}{162} \pi^2 N_{av}^2 \left(\frac{1}{V} \right)^2 \frac{1}{(kT)^3} \sum_i^{nc} \sum_j^{nc} n_i n_j m_i m_j m_f x_{p_i} x_{p_j} x_{pf} \frac{\mu_i^2 \mu_j^2 \mu_k^2}{d_{ij} d_{jf} d_{if}} \cdot \frac{\partial}{\partial T} (I_{3,ijk}) \\
 & +\frac{5}{162} \pi^2 N_{av}^2 \left(\frac{1}{V} \right)^2 \frac{1}{(kT)^3} \sum_i^{nc} \sum_j^{nc} \sum_k^{nc} n_i n_j n_k m_i m_j m_k x_{p_i} x_{p_j} x_{p_k} \frac{\mu_i^2 \mu_j^2 \mu_k^2}{d_{ij} d_{jk} d_{ik}} \cdot \frac{\partial^2}{\partial T \partial n_f} (I_{3,ijk})
 \end{aligned}
 \tag{F-278}$$

$$\begin{aligned}
 \frac{\partial^2}{\partial n_k \partial T} (I_2(\rho^*)) = & \frac{6D^2 \cdot (1 - A\rho^* - B(\rho^*)^2 + C(\rho^*)^3)}{(1 - D\rho^*)^4} \cdot \frac{\partial}{\partial n_k} (\rho^*) \cdot \frac{\partial}{\partial T} (\rho^*) \\
 & + \frac{2D \cdot \left(-A \cdot \frac{\partial}{\partial n_k} (\rho^*) - 2B(\rho^*) \cdot \frac{\partial}{\partial n_k} (\rho^*) + 3C(\rho^*)^2 \cdot \frac{\partial}{\partial V} (\rho^*) \right)}{(1 - D\rho^*)^3} \cdot \frac{\partial}{\partial T} (\rho^*) \\
 & + \frac{2D \cdot \left(-A \cdot \frac{\partial}{\partial T} (\rho^*) - 2B(\rho^*) \cdot \frac{\partial}{\partial T} (\rho^*) + 3C(\rho^*)^2 \cdot \frac{\partial}{\partial T} (\rho^*) \right)}{(1 - D\rho^*)^3} \cdot \frac{\partial}{\partial n_k} (\rho^*) \\
 & + \frac{2D \cdot (1 - A\rho^* - B(\rho^*)^2 + C(\rho^*)^3)}{(1 - D\rho^*)^3} \cdot \frac{\partial^2}{\partial n_k \partial T} (\rho^*) \\
 & + \frac{\left(\begin{aligned} & -2B \frac{\partial}{\partial n_k} (\rho^*) \cdot \frac{\partial}{\partial T} (\rho^*) + 6C(\rho^*) \cdot \frac{\partial}{\partial n_k} (\rho^*) \cdot \frac{\partial}{\partial T} (\rho^*) \\ & -A \cdot \frac{\partial^2}{\partial n_k \partial T} (\rho^*) - 2B(\rho^*) \cdot \frac{\partial^2}{\partial n_k \partial T} (\rho^*) + 3(\rho^*)^2 \cdot \frac{\partial^2}{\partial n_k \partial T} (\rho^*) \end{aligned} \right)}{(1 - D\rho^*)^2}
 \end{aligned}
 \tag{F-279}$$

(F-280)

$$\begin{aligned}
 \frac{\partial^2}{\partial T \partial n_k} (I_3(\rho^*)) = & - \frac{\left(-G \cdot \frac{\partial}{\partial n_k}(\rho^*) + 2H\rho^* \cdot \frac{\partial}{\partial n_k}(\rho^*) \right) \left(E \frac{\partial}{\partial T}(\rho^*) - 2F(\rho^*) \cdot \frac{\partial}{\partial T}(\rho^*) \right)}{\left(1 - G\rho^* + H(\rho^*)^2 \right)^2} \\
 & - \frac{\left(-G \cdot \frac{\partial}{\partial T}(\rho^*) + 2H\rho^* \cdot \frac{\partial}{\partial T}(\rho^*) \right) \left(E \frac{\partial}{\partial n_k}(\rho^*) - 2F(\rho^*) \cdot \frac{\partial}{\partial n_k}(\rho^*) \right)}{\left(1 - G\rho^* + H(\rho^*)^2 \right)^2} \\
 & + \frac{2 \left(1 + E\rho^* - F(\rho^*)^2 \right) \left(-G \cdot \frac{\partial}{\partial n_k}(\rho^*) + 2H\rho^* \cdot \frac{\partial}{\partial n_k}(\rho^*) \right) \left(-G \cdot \frac{\partial}{\partial T}(\rho^*) + 2H\rho^* \cdot \frac{\partial}{\partial T}(\rho^*) \right)}{\left(1 - G\rho^* + H(\rho^*)^2 \right)^3} \\
 & + \frac{-2F \cdot \frac{\partial}{\partial V}(\rho^*) \cdot \frac{\partial}{\partial T}(\rho^*) + E \cdot \frac{\partial}{\partial T \partial n_k}(\rho^*) - 2F\rho^* \cdot \frac{\partial}{\partial T \partial n_k}(\rho^*)}{\left(1 - G\rho^* + H(\rho^*)^2 \right)} \\
 & - \frac{\left(1 + E\rho^* - F(\rho^*)^2 \right) \left(2H \frac{\partial}{\partial n_k}(\rho^*) \cdot \frac{\partial}{\partial T}(\rho^*) - G \frac{\partial}{\partial T \partial n_k}(\rho^*) + 2H\rho^* \cdot \frac{\partial}{\partial T \partial n_k}(\rho^*) \right)}{\left(1 - G\rho^* + H(\rho^*)^2 \right)^2}
 \end{aligned}$$

(F-281)

$$\frac{\partial^2}{\partial T \partial n_k} (\rho_{mix}^*) = 3 \frac{N_{av}}{V} m_k d_k^2 \cdot \frac{\partial}{\partial T} (d_k)$$

iv) Volume – Volume

$$\begin{aligned}
 \frac{\partial^2 F_{JC}}{\partial V^2} = & - \frac{\frac{\partial}{\partial V} (F_{2,mix}^{dipolar}) \left(\frac{F_{3,mix}^{dipolar} \cdot \frac{\partial}{\partial V} (F_{2,mix}^{dipolar})}{(F_{2,mix}^{dipolar})^2} - \frac{\frac{\partial}{\partial n_i} (F_{3,mix}^{dipolar})}{F_{2,mix}^{dipolar}} \right) - \frac{\partial}{\partial V} (F_{2,mix}^{dipolar}) \left(\frac{F_{3,mix}^{dipolar} \cdot \frac{\partial}{\partial V} (F_{2,mix}^{dipolar})}{(F_{2,mix}^{dipolar})^2} - \frac{\frac{\partial}{\partial V} (F_{3,mix}^{dipolar})}{F_{2,mix}^{dipolar}} \right)}{(1 - F_{3,mix}^{dipolar} / F_{2,mix}^{dipolar})^2} \\
 & + \frac{2F_{2,mix}^{dipolar} \left(\frac{F_{3,mix}^{dipolar} \cdot \frac{\partial}{\partial n_i} (F_{2,mix}^{dipolar})}{(F_{2,mix}^{dipolar})^2} - \frac{\frac{\partial}{\partial n_i} (F_{3,mix}^{dipolar})}{F_{2,mix}^{dipolar}} \right) \cdot \left(\frac{F_{3,mix}^{dipolar} \cdot \frac{\partial}{\partial V} (F_{2,mix}^{dipolar})}{(F_{2,mix}^{dipolar})^2} - \frac{\frac{\partial}{\partial V} (F_{3,mix}^{dipolar})}{F_{2,mix}^{dipolar}} \right)}{(1 - F_{3,mix}^{dipolar} / F_{2,mix}^{dipolar})^3} \\
 & - \frac{\frac{\partial^2}{\partial V^2} (F_{2,mix}^{dipolar})}{(1 - F_{3,mix}^{dipolar} / F_{2,mix}^{dipolar})} \\
 & - \frac{F_{2,mix}^{dipolar} \left(\begin{aligned} & - \frac{2F_{3,mix}^{dipolar} \cdot \frac{\partial}{\partial V} (F_{2,mix}^{dipolar}) \cdot \frac{\partial}{\partial V} (F_{2,mix}^{dipolar})}{(F_{2,mix}^{dipolar})^3} + \frac{\frac{\partial}{\partial V} (F_{3,mix}^{dipolar}) \cdot \frac{\partial}{\partial V} (F_{2,mix}^{dipolar})}{(F_{2,mix}^{dipolar})^2} \\ & + \frac{\frac{\partial}{\partial V} (F_{3,mix}^{dipolar}) \cdot \frac{\partial}{\partial V} (F_{2,mix}^{dipolar})}{(F_{2,mix}^{dipolar})^2} + \frac{F_{3,mix}^{dipolar} \cdot \frac{\partial^2}{\partial V^2} (F_{2,mix}^{dipolar})}{(F_{2,mix}^{dipolar})^2} - \frac{\frac{\partial^2}{\partial V^2} (F_{3,mix}^{dipolar})}{F_{2,mix}^{dipolar}} \end{aligned} \right)}{(1 - F_{3,mix}^{dipolar} / F_{2,mix}^{dipolar})^2}
 \end{aligned} \tag{F-282}$$

$$\begin{aligned}
 \frac{\partial^2}{\partial V^2} (F_{2,mix}^{dipolar}) = & - \frac{2 \cdot (2) \pi N_{av}}{9 V^3} \frac{1}{(kT)^2} \sum_i^{nc} \sum_j^{nc} n_i n_j m_i m_j x_{pi} x_{pj} \frac{\mu_i^2 \mu_j^2}{d_{ij}^3} I_{2,ij} \\
 & + \frac{2 \cdot (2) \pi N_{av}}{9 V^2} \frac{1}{(kT)^2} \sum_i^{nc} \sum_j^{nc} n_i n_j m_i m_j x_{pi} x_{pj} \frac{\mu_i^2 \mu_j^2}{d_{ij}^3} \cdot \frac{\partial}{\partial V} (I_{2,ij}) \\
 & - \frac{2\pi N_{av}}{9 V} \frac{1}{(kT)^2} \sum_i^{nc} \sum_j^{nc} n_i n_j m_i m_j x_{pi} x_{pj} \frac{\mu_i^2 \mu_j^2}{d_{ij}^3} \cdot \frac{\partial^2}{\partial V \partial V} (I_{2,ij})
 \end{aligned} \tag{F-283}$$

$$\begin{aligned}
 \frac{\partial^2}{\partial V^2} (F_{3,mix}^{dipolar}) = & \frac{5 \cdot (6)}{162} \pi^2 N_{av}^2 \left(\frac{1}{V} \right)^4 \frac{1}{(kT)^3} \sum_i^{nc} \sum_j^{nc} \sum_k^{nc} n_i n_j n_k m_i m_j m_k x_{pi} x_{pj} x_{pk} \frac{\mu_i^2 \mu_j^2 \mu_k^2}{d_{ij} d_{jk} d_{ik}} I_{3,ijk} \\
 & - \frac{5 \cdot (4)}{162} \pi^2 N_{av}^2 \left(\frac{1}{V} \right)^3 \frac{1}{(kT)^3} \sum_i^{nc} \sum_j^{nc} \sum_k^{nc} n_i n_j n_k m_i m_j m_k x_{pi} x_{pj} x_{pk} \frac{\mu_i^2 \mu_j^2 \mu_k^2}{d_{ij} d_{jk} d_{ik}} \cdot \frac{\partial}{\partial V} (I_{3,ijk}) \\
 & + \frac{5}{162} \pi^2 N_{av}^2 \left(\frac{1}{V} \right)^2 \frac{1}{(kT)^3} \sum_i^{nc} \sum_j^{nc} \sum_k^{nc} n_i n_j n_k m_i m_j m_k x_{pi} x_{pj} x_{pk} \frac{\mu_i^2 \mu_j^2 \mu_k^2}{d_{ij} d_{jk} d_{ik}} \cdot \frac{\partial^2}{\partial V^2} (I_{3,ijk})
 \end{aligned} \tag{F-284}$$

(F-285)

$$\begin{aligned}
 \frac{\partial^2}{\partial V^2}(I_2(\rho^*)) &= \frac{6D^2 \cdot (1 - A\rho^* - B(\rho^*)^2 + C(\rho^*)^3)}{(1 - D\rho^*)^4} \cdot \frac{\partial}{\partial V}(\rho^*) \cdot \frac{\partial}{\partial V}(\rho^*) \\
 &+ \frac{4D \cdot \left(-A \cdot \frac{\partial}{\partial V}(\rho^*) - 2B(\rho^*) \cdot \frac{\partial}{\partial V}(\rho^*) + 3C(\rho^*)^2 \cdot \frac{\partial}{\partial V}(\rho^*) \right)}{(1 - D\rho^*)^3} \cdot \frac{\partial}{\partial V}(\rho^*) \\
 &+ \frac{2D \cdot (1 - A\rho^* - B(\rho^*)^2 + C(\rho^*)^3)}{(1 - D\rho^*)^3} \cdot \frac{\partial^2}{\partial V^2}(\rho^*) \\
 &+ \frac{\left(\begin{aligned} &-2B \frac{\partial}{\partial V}(\rho^*) \cdot \frac{\partial}{\partial V}(\rho^*) + 6C(\rho^*) \cdot \frac{\partial}{\partial V}(\rho^*) \cdot \frac{\partial}{\partial V}(\rho^*) \\ &-A \cdot \frac{\partial^2}{\partial V^2}(\rho^*) - 2B(\rho^*) \cdot \frac{\partial^2}{\partial V^2}(\rho^*) + 3(\rho^*)^2 \cdot \frac{\partial^2}{\partial V^2}(\rho^*) \end{aligned} \right)}{(1 - D\rho^*)^2}
 \end{aligned}$$

(F-286)

$$\begin{aligned}
 \frac{\partial^2}{\partial V^2}(I_3(\rho^*)) &= -2 \frac{\left(-G \cdot \frac{\partial}{\partial V}(\rho^*) + 2H\rho^* \cdot \frac{\partial}{\partial V}(\rho^*) \right) \left(E \frac{\partial}{\partial V}(\rho^*) - 2F(\rho^*) \cdot \frac{\partial}{\partial V}(\rho^*) \right)}{(1 - G\rho^* + H(\rho^*)^2)^2} a \\
 &+ \frac{2(1 + E\rho^* - F(\rho^*)^2) \left(-G \cdot \frac{\partial}{\partial V}(\rho^*) + 2H\rho^* \cdot \frac{\partial}{\partial V}(\rho^*) \right) \left(-G \cdot \frac{\partial}{\partial V}(\rho^*) + 2H\rho^* \cdot \frac{\partial}{\partial V}(\rho^*) \right)}{(1 - G\rho^* + H(\rho^*)^2)^3} \\
 &+ \frac{-2F \cdot \frac{\partial}{\partial V}(\rho^*) \cdot \frac{\partial}{\partial V}(\rho^*) + E \cdot \frac{\partial^2}{\partial V^2}(\rho^*) - 2F\rho^* \cdot \frac{\partial^2}{\partial V^2}(\rho^*)}{(1 - G\rho^* + H(\rho^*)^2)} \\
 &- \frac{(1 + E\rho^* - F(\rho^*)^2) \left(2H \frac{\partial}{\partial V}(\rho^*) \cdot \frac{\partial}{\partial V}(\rho^*) - G \frac{\partial^2}{\partial V^2}(\rho^*) + 2H\rho^* \cdot \frac{\partial^2}{\partial V^2}(\rho^*) \right)}{(1 - G\rho^* + H(\rho^*)^2)^2}
 \end{aligned}$$

(F-287)

$$\frac{\partial^2}{\partial V^2}(\rho_{mix}^*) = 2 \frac{N_{av}}{V^3} \sum_i^{nc} m_i n_i d_i^3$$

v) Volume – composition

$$\begin{aligned}
 \frac{\partial^2 F_{JC}}{\partial V \partial n_i} = & - \frac{\frac{\partial}{\partial V} (F_{2,mix}^{dipolar}) \left(\frac{F_{3,mix}^{dipolar} \cdot \frac{\partial}{\partial n_i} (F_{2,mix}^{dipolar})}{(F_{2,mix}^{dipolar})^2} - \frac{\partial}{\partial n_i} (F_{3,mix}^{dipolar}) \right) - \frac{\partial}{\partial n_i} (F_{2,mix}^{dipolar}) \left(\frac{F_{3,mix}^{dipolar} \cdot \frac{\partial}{\partial V} (F_{2,mix}^{dipolar})}{(F_{2,mix}^{dipolar})^2} - \frac{\partial}{\partial V} (F_{3,mix}^{dipolar})}{F_{2,mix}^{dipolar}} \right)}{\left(1 - F_{3,mix}^{dipolar} / F_{2,mix}^{dipolar} \right)^2} \\
 & + \frac{2F_{2,mix}^{dipolar} \left(\frac{F_{3,mix}^{dipolar} \cdot \frac{\partial}{\partial n_i} (F_{2,mix}^{dipolar})}{(F_{2,mix}^{dipolar})^2} - \frac{\partial}{\partial n_i} (F_{3,mix}^{dipolar}) \right) \cdot \left(\frac{F_{3,mix}^{dipolar} \cdot \frac{\partial}{\partial V} (F_{2,mix}^{dipolar})}{(F_{2,mix}^{dipolar})^2} - \frac{\partial}{\partial V} (F_{3,mix}^{dipolar})}{F_{2,mix}^{dipolar}} \right)}{\left(1 - F_{3,mix}^{dipolar} / F_{2,mix}^{dipolar} \right)^3} \\
 & - \frac{\frac{\partial^2}{\partial V \partial n_i} (F_{2,mix}^{dipolar})}{\left(1 - F_{3,mix}^{dipolar} / F_{2,mix}^{dipolar} \right)} \\
 & - \frac{F_{2,mix}^{dipolar} \left(- \frac{2F_{3,mix}^{dipolar} \cdot \frac{\partial}{\partial n_i} (F_{2,mix}^{dipolar}) \cdot \frac{\partial}{\partial V} (F_{2,mix}^{dipolar})}{(F_{2,mix}^{dipolar})^3} + \frac{\frac{\partial}{\partial n_i} (F_{3,mix}^{dipolar}) \cdot \frac{\partial}{\partial V} (F_{2,mix}^{dipolar})}{(F_{2,mix}^{dipolar})^2} \right.}{\left(1 - F_{3,mix}^{dipolar} / F_{2,mix}^{dipolar} \right)^2} \\
 & \left. + \frac{\frac{\partial}{\partial V} (F_{3,mix}^{dipolar}) \cdot \frac{\partial}{\partial n_i} (F_{2,mix}^{dipolar})}{(F_{2,mix}^{dipolar})^2} + \frac{F_{3,mix}^{dipolar} \cdot \frac{\partial^2}{\partial V \partial n_i} (F_{2,mix}^{dipolar})}{(F_{2,mix}^{dipolar})^2} - \frac{\frac{\partial^2}{\partial V \partial n_i} (F_{3,mix}^{dipolar})}{F_{2,mix}^{dipolar}} \right)}{\left(1 - F_{3,mix}^{dipolar} / F_{2,mix}^{dipolar} \right)^2}
 \end{aligned} \tag{F-288}$$

$$\begin{aligned}
 \frac{\partial^2}{\partial V \partial n_k} (F_{2,mix}^{dipolar}) = & \frac{2 \cdot (2) \pi}{9} \frac{N_{av}}{V^2} \frac{1}{(kT)^2} \sum_i^{nc} n_i m_i m_k x_{pi} x_{pk} \frac{\mu_i^2 \mu_j^2}{d_{ik}^3} I_{2,ik} a \\
 & + \frac{2\pi}{9} \frac{N_{av}}{V^2} \frac{1}{(kT)^2} \sum_i^{nc} \sum_j^{nc} n_i n_j m_i m_j x_{pi} x_{pj} \frac{\mu_i^2 \mu_j^2}{d_{ij}^3} \cdot \frac{\partial}{\partial n_k} (I_{2,ij}) \\
 & - \frac{2 \cdot (2) \pi}{9} \frac{N_{av}}{V} \frac{1}{(kT)^2} \sum_i^{nc} n_i m_i m_k x_{pi} x_{pk} \frac{\mu_i^2 \mu_k^2}{d_{ik}^3} \cdot \frac{\partial}{\partial V} (I_{2,ik}) \\
 & - \frac{2\pi}{9} \frac{N_{av}}{V} \frac{1}{(kT)^2} \sum_i^{nc} \sum_j^{nc} n_i n_j m_i m_j x_{pi} x_{pj} \frac{\mu_i^2 \mu_j^2}{d_{ij}^3} \cdot \frac{\partial^2}{\partial V \partial n_k} (I_{2,ij})
 \end{aligned} \tag{F-289}$$

$$\begin{aligned}
 \frac{\partial^2}{\partial V \partial n_f} (F_{3,mix}^{dipolar}) = & -\frac{5 \cdot (2) \cdot (3)}{162} \pi^2 N_{av}^2 \left(\frac{1}{V} \right)^3 \frac{1}{(kT)^3} \sum_i^{nc} \sum_j^{nc} n_i n_j m_i m_j m_f x_{p_i} x_{p_j} x_{p_f} \frac{\mu_i^2 \mu_j^2 \mu_f^2}{d_{ij} d_{jf} d_{if}} I_{3,ijk} \\
 & -\frac{5 \cdot (2)}{162} \pi^2 N_{av}^2 \left(\frac{1}{V} \right)^3 \frac{1}{(kT)^3} \sum_i^{nc} \sum_j^{nc} \sum_k^{nc} n_i n_j n_k m_i m_j m_k x_{p_i} x_{p_j} x_{p_k} \frac{\mu_i^2 \mu_j^2 \mu_k^2}{d_{ij} d_{jk} d_{ik}} \cdot \frac{\partial}{\partial n_f} (I_{3,ijk}) \\
 & +\frac{5 \cdot (3)}{162} \pi^2 N_{av}^2 \left(\frac{1}{V} \right)^2 \frac{1}{(kT)^3} \sum_i^{nc} \sum_j^{nc} n_i n_j m_i m_j m_f x_{p_i} x_{p_j} x_{p_f} \frac{\mu_i^2 \mu_j^2 \mu_f^2}{d_{ij} d_{jf} d_{if}} \cdot \frac{\partial}{\partial V} (I_{3,ijk}) \\
 & +\frac{5}{162} \pi^2 N_{av}^2 \left(\frac{1}{V} \right)^2 \frac{1}{(kT)^3} \sum_i^{nc} \sum_j^{nc} \sum_k^{nc} n_i n_j n_k m_i m_j m_k x_{p_i} x_{p_j} x_{p_k} \frac{\mu_i^2 \mu_j^2 \mu_k^2}{d_{ij} d_{jk} d_{ik}} \cdot \frac{\partial^2}{\partial V \partial n_f} (I_{3,ijk})
 \end{aligned} \tag{F-290}$$

$$\begin{aligned}
 \frac{\partial^2}{\partial n_k \partial V} (I_2(\rho^*)) = & \frac{6D^2 \cdot (1 - A\rho^* - B(\rho^*)^2 + C(\rho^*)^3)}{(1 - D\rho^*)^4} \cdot \frac{\partial}{\partial n_k}(\rho^*) \cdot \frac{\partial}{\partial V}(\rho^*) \\
 & + \frac{2D \cdot \left(-A \cdot \frac{\partial}{\partial n_k}(\rho^*) - 2B(\rho^*) \cdot \frac{\partial}{\partial n_k}(\rho^*) + 3C(\rho^*)^2 \cdot \frac{\partial}{\partial V}(\rho^*) \right)}{(1 - D\rho^*)^3} \cdot \frac{\partial}{\partial V}(\rho^*) \\
 & + \frac{2D \cdot \left(-A \cdot \frac{\partial}{\partial V}(\rho^*) - 2B(\rho^*) \cdot \frac{\partial}{\partial V}(\rho^*) + 3C(\rho^*)^2 \cdot \frac{\partial}{\partial V}(\rho^*) \right)}{(1 - D\rho^*)^3} \cdot \frac{\partial}{\partial n_k}(\rho^*) \\
 & + \frac{2D \cdot (1 - A\rho^* - B(\rho^*)^2 + C(\rho^*)^3)}{(1 - D\rho^*)^3} \cdot \frac{\partial^2}{\partial n_k \partial V}(\rho^*) \\
 & + \frac{\left(\begin{aligned} & -2B \frac{\partial}{\partial n_k}(\rho^*) \cdot \frac{\partial}{\partial V}(\rho^*) + 6C(\rho^*) \cdot \frac{\partial}{\partial n_k}(\rho^*) \cdot \frac{\partial}{\partial V}(\rho^*) \\ & -A \cdot \frac{\partial^2}{\partial n_k \partial V}(\rho^*) - 2B \cdot (\rho^*) \cdot \frac{\partial^2}{\partial n_k \partial V}(\rho^*) + 3(\rho^*)^2 \cdot \frac{\partial^2}{\partial n_k \partial V}(\rho^*) \end{aligned} \right)}{(1 - D\rho^*)^2}
 \end{aligned} \tag{F-291}$$

(F-292)

$$\begin{aligned}
 \frac{\partial^2}{\partial V \partial n_k} (I_3(\rho^*)) = & - \frac{\left(-G \cdot \frac{\partial}{\partial n_k}(\rho^*) + 2H\rho^* \cdot \frac{\partial}{\partial n_k}(\rho^*) \right) \left(E \frac{\partial}{\partial V}(\rho^*) - 2F(\rho^*) \cdot \frac{\partial}{\partial V}(\rho^*) \right)}{\left(1 - G\rho^* + H(\rho^*)^2 \right)^2} \\
 & - \frac{\left(-G \cdot \frac{\partial}{\partial V}(\rho^*) + 2H\rho^* \cdot \frac{\partial}{\partial V}(\rho^*) \right) \left(E \frac{\partial}{\partial n_k}(\rho^*) - 2F(\rho^*) \cdot \frac{\partial}{\partial n_k}(\rho^*) \right)}{\left(1 - G\rho^* + H(\rho^*)^2 \right)^2} \\
 & + \frac{2 \left(1 + E\rho^* - F(\rho^*)^2 \right) \left(-G \cdot \frac{\partial}{\partial n_k}(\rho^*) + 2H\rho^* \cdot \frac{\partial}{\partial n_k}(\rho^*) \right) \left(-G \cdot \frac{\partial}{\partial V}(\rho^*) + 2H\rho^* \cdot \frac{\partial}{\partial V}(\rho^*) \right)}{\left(1 - G\rho^* + H(\rho^*)^2 \right)^3} \\
 & + \frac{-2F \cdot \frac{\partial}{\partial n_k}(\rho^*) \cdot \frac{\partial}{\partial V}(\rho^*) + E \cdot \frac{\partial}{\partial T \partial n_k}(\rho^*) - 2F\rho^* \cdot \frac{\partial}{\partial V \partial n_k}(\rho^*)}{\left(1 - G\rho^* + H(\rho^*)^2 \right)} \\
 & - \frac{\left(1 + E\rho^* - F(\rho^*)^2 \right) \left(2H \frac{\partial}{\partial n_k}(\rho^*) \cdot \frac{\partial}{\partial V}(\rho^*) - G \frac{\partial}{\partial V \partial n_k}(\rho^*) + 2H\rho^* \cdot \frac{\partial}{\partial V \partial n_k}(\rho^*) \right)}{\left(1 - G\rho^* + H(\rho^*)^2 \right)^2}
 \end{aligned}$$

(F-293)

$$\frac{\partial^2}{\partial V \partial n_k} (\rho_{mix}^*) = - \frac{N_{av}}{V^2} m_k d_k^3$$

vi) Composition – composition

$$\begin{aligned}
 \frac{\partial^2 F_{JC}}{\partial n_i \partial n_j} = & - \frac{\frac{\partial}{\partial n_j} \left(F_{2,mix}^{dipolar} \right) \left(\frac{F_{3,mix}^{dipolar} \cdot \frac{\partial}{\partial n_i} (F_{2,mix}^{dipolar})}{(F_{2,mix}^{dipolar})^2} - \frac{\frac{\partial}{\partial n_i} (F_{3,mix}^{dipolar})}{F_{2,mix}^{dipolar}} \right) - \frac{\partial}{\partial n_i} \left(F_{2,mix}^{dipolar} \right) \left(\frac{F_{3,mix}^{dipolar} \cdot \frac{\partial}{\partial n_j} (F_{2,mix}^{dipolar})}{(F_{2,mix}^{dipolar})^2} - \frac{\frac{\partial}{\partial n_j} (F_{3,mix}^{dipolar})}{F_{2,mix}^{dipolar}} \right)}{\left(1 - F_{3,mix}^{dipolar} / F_{2,mix}^{dipolar} \right)^2} \\
 & + \frac{2 F_{2,mix}^{dipolar} \left(\frac{F_{3,mix}^{dipolar} \cdot \frac{\partial}{\partial n_i} (F_{2,mix}^{dipolar})}{(F_{2,mix}^{dipolar})^2} - \frac{\frac{\partial}{\partial n_i} (F_{3,mix}^{dipolar})}{F_{2,mix}^{dipolar}} \right) \cdot \left(\frac{F_{3,mix}^{dipolar} \cdot \frac{\partial}{\partial n_j} (F_{2,mix}^{dipolar})}{(F_{2,mix}^{dipolar})^2} - \frac{\frac{\partial}{\partial n_j} (F_{3,mix}^{dipolar})}{F_{2,mix}^{dipolar}} \right)}{\left(1 - F_{3,mix}^{dipolar} / F_{2,mix}^{dipolar} \right)^3} \\
 & - \frac{\frac{\partial^2}{\partial n_i \partial n_j} (F_{2,mix}^{dipolar})}{\left(1 - F_{3,mix}^{dipolar} / F_{2,mix}^{dipolar} \right)} \\
 & - \frac{F_{2,mix}^{dipolar} \left(\begin{aligned} & - \frac{2 F_{3,mix}^{dipolar} \cdot \frac{\partial}{\partial n_i} (F_{2,mix}^{dipolar}) \cdot \frac{\partial}{\partial n_j} (F_{2,mix}^{dipolar})}{(F_{2,mix}^{dipolar})^3} + \frac{\frac{\partial}{\partial n_i} (F_{3,mix}^{dipolar}) \cdot \frac{\partial}{\partial n_j} (F_{2,mix}^{dipolar})}{(F_{2,mix}^{dipolar})^2} \\ & + \frac{\frac{\partial}{\partial n_j} (F_{3,mix}^{dipolar}) \cdot \frac{\partial}{\partial n_i} (F_{2,mix}^{dipolar})}{(F_{2,mix}^{dipolar})^2} + \frac{F_{3,mix}^{dipolar} \cdot \frac{\partial^2}{\partial n_i \partial n_j} (F_{2,mix}^{dipolar})}{(F_{2,mix}^{dipolar})^2} - \frac{\frac{\partial^2}{\partial n_i \partial n_j} (F_{3,mix}^{dipolar})}{F_{2,mix}^{dipolar}} \end{aligned} \right)}{\left(1 - F_{3,mix}^{dipolar} / F_{2,mix}^{dipolar} \right)^2}
 \end{aligned} \tag{F-294}$$

$$\begin{aligned}
 \frac{\partial^2}{\partial n_k \partial n_l} (F_{2,mix}^{dipolar}) = & - \frac{4\pi}{9} \frac{N_{av}}{V} \frac{1}{(kT)^2} m_k m_l x_{pk} x_{pl} \frac{\mu_k^2 \mu_l^2}{d_{kl}^3} I_{2,ij} \\
 & - \frac{4\pi}{9} \frac{N_{av}}{V} \frac{1}{(kT)^2} \sum_i^{nc} n_i m_i m_k x_{pi} x_{pk} \frac{\mu_i^2 \mu_k^2}{d_{ik}^3} \cdot \frac{\partial}{\partial n_l} (I_{2,ij}) \\
 & - \frac{4\pi}{9} \frac{N_{av}}{V} \frac{1}{(kT)^2} \sum_i^{nc} n_i m_i m_l x_{pi} x_{pl} \frac{\mu_i^2 \mu_l^2}{d_{il}^3} \cdot \frac{\partial}{\partial n_k} (I_{2,ij}) \\
 & - \frac{2\pi}{9} \frac{N_{av}}{V} \frac{1}{(kT)^2} \sum_i^{nc} \sum_j^{nc} n_i n_j m_i m_j x_{pi} x_{pj} \frac{\mu_i^2 \mu_j^2}{d_{ij}^3} \cdot \frac{\partial^2}{\partial n_k \partial n_l} (I_{2,ij})
 \end{aligned} \tag{F-295}$$

$$\begin{aligned}
 \frac{\partial^2}{\partial n_f \partial n_g} (F_{3,mix}^{dipolar}) = & \frac{5 \cdot (2)}{162} \pi^2 N_{av}^2 \left(\frac{1}{V} \right)^3 \frac{1}{(kT)^3} \sum_i^{nc} n_i m_i m_f m_g x_{pi} x_{pf} x_{pg} \frac{\mu_i^2 \mu_f^2 \mu_g^2}{d_{if} d_{ig} d_{fg}} I_{3,ifg} \\
 & + \frac{5 \cdot (3)}{162} \pi^2 N_{av}^2 \left(\frac{1}{V} \right)^2 \frac{1}{(kT)^3} \sum_i^{nc} \sum_j^{nc} n_i n_j m_i m_j m_f x_{pi} x_{pj} x_{pf} \frac{\mu_i^2 \mu_j^2 \mu_f^2}{d_{ij} d_{jf} d_{if}} \cdot \frac{\partial}{\partial n_g} (I_{3,ijk}) \\
 & + \frac{5 \cdot (3)}{162} \pi^2 N_{av}^2 \left(\frac{1}{V} \right)^2 \frac{1}{(kT)^3} \sum_i^{nc} \sum_j^{nc} n_i n_j m_i m_j m_g x_{pi} x_{pj} x_{pg} \frac{\mu_i^2 \mu_j^2 \mu_g^2}{d_{ij} d_{ig} d_{jg}} \cdot \frac{\partial}{\partial n_f} (I_{3,ijk}) \\
 & + \frac{5}{162} \pi^2 N_{av}^2 \left(\frac{1}{V} \right)^2 \frac{1}{(kT)^3} \sum_i^{nc} \sum_j^{nc} \sum_k^{nc} n_i n_j n_k m_i m_j m_k x_{pi} x_{pj} x_{pk} \frac{\mu_i^2 \mu_j^2 \mu_k^2}{d_{ij} d_{jk} d_{ik}} \cdot \frac{\partial^2}{\partial n_f \partial n_g} (I_{3,ijk})
 \end{aligned} \tag{F-296}$$

(F-297)

$$\begin{aligned}
 \frac{\partial^2}{\partial n_k \partial n_l} (I_2(\rho^*)) &= \frac{6D^2 \cdot (1 - A\rho^* - B(\rho^*)^2 + C(\rho^*)^3)}{(1 - D\rho^*)^4} \cdot \frac{\partial}{\partial n_k}(\rho^*) \cdot \frac{\partial}{\partial n_l}(\rho^*) \\
 &+ \frac{2D \cdot \left(-A \cdot \frac{\partial}{\partial n_k}(\rho^*) - 2B(\rho^*) \cdot \frac{\partial}{\partial n_k}(\rho^*) + 3C(\rho^*)^2 \cdot \frac{\partial}{\partial n_k}(\rho^*) \right)}{(1 - D\rho^*)^3} \cdot \frac{\partial}{\partial n_l}(\rho^*) \\
 &+ \frac{2D \cdot \left(-A \cdot \frac{\partial}{\partial n_l}(\rho^*) - 2B(\rho^*) \cdot \frac{\partial}{\partial n_l}(\rho^*) + 3C(\rho^*)^2 \cdot \frac{\partial}{\partial n_l}(\rho^*) \right)}{(1 - D\rho^*)^3} \cdot \frac{\partial}{\partial n_k}(\rho^*) \\
 &+ \frac{2D \cdot (1 - A\rho^* - B(\rho^*)^2 + C(\rho^*)^3)}{(1 - D\rho^*)^3} \cdot \frac{\partial^2}{\partial n_k \partial n_l}(\rho^*) \\
 &+ \frac{\left(\begin{aligned} &-2B \frac{\partial}{\partial n_k}(\rho^*) \cdot \frac{\partial}{\partial n_l}(\rho^*) + 6C(\rho^*) \cdot \frac{\partial}{\partial n_k}(\rho^*) \cdot \frac{\partial}{\partial n_l}(\rho^*) \\ &-A \cdot \frac{\partial^2}{\partial n_k \partial n_l}(\rho^*) - 2B \cdot (\rho^*) \cdot \frac{\partial^2}{\partial n_k \partial n_l}(\rho^*) + 3(\rho^*)^2 \cdot \frac{\partial^2}{\partial n_k \partial n_l}(\rho^*) \end{aligned} \right)}{(1 - D\rho^*)^2}
 \end{aligned}$$

(F-298)

$$\begin{aligned}
 \frac{\partial^2}{\partial n_k \partial n_l} (I_3(\rho^*)) &= - \frac{\left(-G \cdot \frac{\partial}{\partial n_k}(\rho^*) + 2H\rho^* \cdot \frac{\partial}{\partial n_k}(\rho^*) \right) \left(E \frac{\partial}{\partial n_l}(\rho^*) - 2F(\rho^*) \cdot \frac{\partial}{\partial n_l}(\rho^*) \right)}{(1 - G\rho^* + H(\rho^*)^2)^2} \\
 &- \frac{\left(-G \cdot \frac{\partial}{\partial n_l}(\rho^*) + 2H\rho^* \cdot \frac{\partial}{\partial n_l}(\rho^*) \right) \left(E \frac{\partial}{\partial n_k}(\rho^*) - 2F(\rho^*) \cdot \frac{\partial}{\partial n_k}(\rho^*) \right)}{(1 - G\rho^* + H(\rho^*)^2)^2} \\
 &+ \frac{2(1 + E\rho^* - F(\rho^*)^2) \left(-G \cdot \frac{\partial}{\partial n_k}(\rho^*) + 2H\rho^* \cdot \frac{\partial}{\partial n_k}(\rho^*) \right) \left(-G \cdot \frac{\partial}{\partial n_l}(\rho^*) + 2H\rho^* \cdot \frac{\partial}{\partial n_l}(\rho^*) \right)}{(1 - G\rho^* + H(\rho^*)^2)^3} \\
 &+ \frac{-2F \cdot \frac{\partial}{\partial n_k}(\rho^*) \cdot \frac{\partial}{\partial n_l}(\rho^*) + E \cdot \frac{\partial}{\partial n_l \partial n_k}(\rho^*) - 2F\rho^* \cdot \frac{\partial}{\partial n_l \partial n_k}(\rho^*)}{(1 - G\rho^* + H(\rho^*)^2)} \\
 &- \frac{(1 + E\rho^* - F(\rho^*)^2) \left(2H \frac{\partial}{\partial n_k}(\rho^*) \cdot \frac{\partial}{\partial n_l}(\rho^*) - G \frac{\partial}{\partial n_l \partial n_k}(\rho^*) + 2H\rho^* \cdot \frac{\partial}{\partial n_l \partial n_k}(\rho^*) \right)}{(1 - G\rho^* + H(\rho^*)^2)^2}
 \end{aligned}$$

(F-299)

$$\frac{\partial^2}{\partial n_k \partial n_l} (\rho_{mix}^*) = 0$$

F.9 Gross and Vrabec's dipolar term

F.9.1 State function

$$\frac{a^{dipolar}}{RT} = \frac{a_2^{dd}/RT}{1 - a_3^{dd}/a_2^{dd}} \quad (F-300)$$

Multiply with total mole numbers:

$$\frac{A_{mix}^{dipolar}}{RT} = \frac{A_{2,mix}^{dd}/RT}{1 - A_{3,mix}^{dd}/A_{2,mix}^{dd}} \quad (F-301)$$

The second- and third-order perturbation terms are evaluated from:

$$\frac{a_2^{dd}}{RT} = -\frac{\pi\rho}{(kT)^2} \sum_i^{nc} \sum_j^{nc} x_i x_j \frac{n_{pi} n_{pj}}{m_i m_j} \frac{\mu_i^2 \mu_j^2}{\sigma_{ij}^3} J_{2,ij}^{dd} \quad (F-302)$$

$$\frac{a_3^{dd}}{RT} = -\frac{4\pi^2}{3} \frac{\rho^2}{(kT)^3} \sum_i^{nc} \sum_j^{nc} \sum_k^{nc} x_i x_j x_k \frac{n_{pi} n_{pj} n_{pk}}{m_i m_j m_k} \frac{\mu_i^2 \mu_j^2 \mu_k^2}{\sigma_{ij} \sigma_{jk} \sigma_{ik}} J_{3,ijk}^{dd} \quad (F-303)$$

Multiply with total moles:

$$\frac{A_2^{dd}}{RT} = -n_{total} \frac{\pi\rho}{(kT)^2} \sum_i^{nc} \sum_j^{nc} x_i x_j \frac{n_{pi} n_{pj}}{m_i m_j} \frac{\mu_i^2 \mu_j^2}{\sigma_{ij}^3} J_{2,ij}^{dd} \quad (F-304)$$

$$\frac{A_3^{dd}}{RT} = -n_{total} \frac{4\pi^2}{3} \frac{\rho^2}{(kT)^3} \sum_i^{nc} \sum_j^{nc} \sum_k^{nc} x_i x_j x_k \frac{n_{pi} n_{pj} n_{pk}}{m_i m_j m_k} \frac{\mu_i^2 \mu_j^2 \mu_k^2}{\sigma_{ij} \sigma_{jk} \sigma_{ik}} J_{3,ijk}^{dd} \quad (F-305)$$

Convert number density to total volume and simplify:

$$\frac{A_2^{dd}}{RT} = F_2^{dd} = -\frac{N_{av}}{V} \frac{\pi}{(kT)^2} \sum_i^{nc} \sum_j^{nc} n_i n_j \frac{n_{pi} n_{pj}}{m_i m_j} \frac{\mu_i^2 \mu_j^2}{\sigma_{ij}^3} J_{2,ij}^{dd} \quad (F-306)$$

$$\quad (F-307)$$

$$\frac{A_3^{dd}}{RT} = F_3^{dd} = -\frac{4N_{av}^2 \pi^2}{3} \left(\frac{1}{V}\right)^2 \frac{1}{(kT)^3} \sum_i^{nc} \sum_j^{nc} \sum_k^{nc} n_i n_j n_k \frac{n_{pi} n_{pj} n_{pk}}{m_i m_j m_k} \frac{\mu_i^2 \mu_j^2 \mu_k^2}{\sigma_{ij} \sigma_{jk} \sigma_{ik}} J_{3,ijk}^{dd} \quad (F-308)$$

$$J_{2,ij}^{dd} = \sum_{w=0}^4 \left(a_{n,ij} + b_{n,ij} \frac{\varepsilon_{ij}}{kT} \right) \eta^w \quad (F-309)$$

$$\quad (F-309)$$

$$J_{3,ijk}^{dd} = \sum_{w=0}^4 c_{n,ijk} \eta^w \quad (F-310)$$

$$a_{n,ij} = a_{0n} + \frac{m_{ij} - 1}{m_{ij}} a_{1n} + \left(\frac{m_{ij} - 1}{m_{ij}} \right) \left(\frac{m_{ij} - 2}{m_{ij}} \right) a_{2n} \quad (F-311)$$

$$\quad (F-311)$$

$$b_{n,ij} = b_{0n} + \frac{m_{ij} - 1}{m_{ij}} b_{1n} + \left(\frac{m_{ij} - 1}{m_{ij}} \right) \left(\frac{m_{ij} - 2}{m_{ij}} \right) b_{2n}$$

(F-312)

$$c_{n,ijk} = c_{0n} + \frac{m_{ijk} - 1}{m_{ijk}} c_{1n} + \left(\frac{m_{ijk} - 1}{m_{ijk}} \right) \left(\frac{m_{ijk} - 2}{m_{ijk}} \right) c_{2n}$$

(F-313)

$$m_{ij} = (m_i m_j)^{1/2} \quad \text{with } m_{ij} \leq 2$$

(F-314)

$$m_{ijk} = (m_i m_j m_k)^{1/3} \quad \text{with } m_{ijk} \leq 2$$

(F-315)

$$\eta = \frac{N_{av} \pi}{6V} \sum_i^{nc} n_i m_i d_i^3$$

F.9.2 First-order derivatives

i) Temperature

(F-316)

$$\begin{aligned} \frac{\partial}{\partial T} (F_{2,mix}^{dd}) &= \frac{2N_{av}}{V} \frac{\pi}{(kT)^2} \sum_i^{nc} \sum_j^{nc} n_i n_j \frac{n_{pi} n_{pj}}{m_i m_j} \frac{\mu_i^2 \mu_j^2}{\sigma_{ij}^3} J_{2,ij}^{dd} \\ &\quad - \frac{N_{av}}{V} \frac{\pi}{(kT)^2} \sum_i^{nc} \sum_j^{nc} n_i n_j \frac{n_{pi} n_{pj}}{m_i m_j} \frac{\mu_i^2 \mu_j^2}{\sigma_{ij}^3} \cdot \frac{\partial}{\partial T} (J_{2,ij}^{dd}) \end{aligned}$$

(F-317)

$$\begin{aligned} \frac{\partial}{\partial T} (F_{3,mix}^{dd}) &= \frac{4 \cdot 3 \cdot N_{av}^2 \pi^2}{3} \left(\frac{1}{V} \right)^2 \frac{1}{(kT)^3} \sum_i^{nc} \sum_j^{nc} \sum_k^{nc} n_i n_j n_k \frac{n_{pi} n_{pj} n_{pk}}{m_i m_j m_k} \frac{\mu_i^2 \mu_j^2 \mu_k^2}{\sigma_{ij} \sigma_{jk} \sigma_{ik}} J_{3,ijk}^{dd} \\ &\quad - \frac{4N_{av}^2 \pi^2}{3} \left(\frac{1}{V} \right)^2 \frac{1}{(kT)^3} \sum_i^{nc} \sum_j^{nc} \sum_k^{nc} n_i n_j n_k \frac{n_{pi} n_{pj} n_{pk}}{m_i m_j m_k} \frac{\mu_i^2 \mu_j^2 \mu_k^2}{\sigma_{ij} \sigma_{jk} \sigma_{ik}} \cdot \frac{\partial}{\partial T} (J_{3,ijk}^{dd}) \end{aligned}$$

(F-318)

$$\frac{\partial}{\partial T} (J_{2,ij}^{dd}) = - \sum_{w=0}^4 \left(b_{n,ij} \frac{\varepsilon_{ij}}{kT^2} \right) \eta^w + w \cdot \sum_{w=0}^4 \left(a_{n,ij} + b_{n,ij} \frac{\varepsilon_{ij}}{kT} \right) \eta^{w-1} \cdot \frac{\partial}{\partial T} (\eta)$$

(F-319)

$$\frac{\partial}{\partial T} J_{3,ijk}^{dd} = w \cdot \sum_{w=0}^4 c_{n,ijk} \eta^{w-1} \cdot \frac{\partial}{\partial T} (\eta)$$

ii) Volume

(F-320)

$$\begin{aligned} \frac{\partial}{\partial V} (F_{2,mix}^{dd}) &= \frac{N_{av}}{V^2} \frac{\pi}{(kT)^2} \sum_i^{nc} \sum_j^{nc} n_i n_j \frac{n_{pi} n_{pj}}{m_i m_j} \frac{\mu_i^2 \mu_j^2}{\sigma_{ij}^3} J_{2,ij}^{dd} \\ &\quad - \frac{N_{av}}{V} \frac{\pi}{(kT)^2} \sum_i^{nc} \sum_j^{nc} n_i n_j \frac{n_{pi} n_{pj}}{m_i m_j} \frac{\mu_i^2 \mu_j^2}{\sigma_{ij}^3} \cdot \frac{\partial}{\partial V} (J_{2,ij}^{dd}) \end{aligned}$$

$$\frac{\partial}{\partial V} (F_{3,mix}^{dd}) = \frac{4 \cdot 2 \cdot N_{av}^2 \pi^2}{3} \left(\frac{1}{V} \right)^3 \frac{1}{(kT)^3} \sum_i^{nc} \sum_j^{nc} \sum_k^{nc} n_i n_j n_k \frac{n_{pi} n_{pj} n_{pk}}{m_i m_j m_k} \frac{\mu_i^2 \mu_j^2 \mu_k^2}{\sigma_{ij} \sigma_{jk} \sigma_{ik}} J_{3,ijk}^{dd} \quad (F-321)$$

$$- \frac{4 N_{av}^2 \pi^2}{3} \left(\frac{1}{V} \right)^2 \frac{1}{(kT)^3} \sum_i^{nc} \sum_j^{nc} \sum_k^{nc} n_i n_j n_k \frac{n_{pi} n_{pj} n_{pk}}{m_i m_j m_k} \frac{\mu_i^2 \mu_j^2 \mu_k^2}{\sigma_{ij} \sigma_{jk} \sigma_{ik}} \cdot \frac{\partial}{\partial V} (J_{3,ijk}^{dd}) \quad (F-322)$$

$$\frac{\partial}{\partial V} (J_{2,ij}^{dd}) = w \cdot \sum_{w=0}^4 \left(a_{n,ij} + b_{n,ij} \frac{\epsilon_{ij}}{kT} \right) \eta^{w-1} \cdot \frac{\partial}{\partial V} (\eta) \quad (F-323)$$

$$\frac{\partial}{\partial V} J_{3,ijk}^{dd} = w \cdot \sum_{w=0}^4 c_{n,ijk} \eta^{w-1} \cdot \frac{\partial}{\partial V} (\eta) \quad (F-324)$$

iii) Composition

$$\begin{aligned} \frac{\partial}{\partial n_k} (F_{2,mix}^{dipolar}) &= - \frac{N_{av}}{V} \frac{\pi}{(kT)^2} \sum_i^{nc} n_i \frac{n_{pi} n_{pk}}{m_i m_k} \frac{\mu_i^2 \mu_k^2}{\sigma_{ik}^3} J_{2,ij}^{dd} \\ &\quad - \frac{N_{av}}{V} \frac{\pi}{(kT)^2} \sum_i^{nc} \sum_j^{nc} n_i n_j \frac{n_{pi} n_{pj}}{m_i m_j} \frac{\mu_i^2 \mu_j^2}{\sigma_{ij}^3} \cdot \frac{\partial}{\partial n_k} (J_{2,ij}^{dd}) \end{aligned} \quad (F-325)$$

$$\begin{aligned} \frac{\partial^2}{\partial n_f \partial n_g} (F_{3,mix}^{dd}) &= - \frac{4 \cdot 2 N_{av}^2 \pi^2}{3} \left(\frac{1}{V} \right)^2 \frac{1}{(kT)^3} \sum_i^{nc} n_i \frac{n_{pi} n_{pg} n_{pf}}{m_i m_g m_f} \frac{\mu_i^2 \mu_g^2 \mu_f^2}{\sigma_{ig} \sigma_{jg} \sigma_{if}} J_{3,ijk}^{dd} \\ &\quad - \frac{3 \cdot 4 N_{av}^2 \pi^2}{3} \left(\frac{1}{V} \right)^2 \frac{1}{(kT)^3} \sum_i^{nc} \sum_j^{nc} n_i n_j \frac{n_{pi} n_{pj} n_{pf}}{m_i m_j m_f} \frac{\mu_i^2 \mu_j^2 \mu_f^2}{\sigma_{ij} \sigma_{jf} \sigma_{if}} \cdot \frac{\partial}{\partial n_g} (J_{3,ijk}^{dd}) \\ &\quad - \frac{3 \cdot 4 N_{av}^2 \pi^2}{3} \left(\frac{1}{V} \right)^2 \frac{1}{(kT)^3} \sum_i^{nc} \sum_j^{nc} n_i n_j \frac{n_{pi} n_{pj} n_{pg}}{m_i m_j m_g} \frac{\mu_i^2 \mu_j^2 \mu_g^2}{\sigma_{ij} \sigma_{jg} \sigma_{ig}} \cdot \frac{\partial}{\partial n_f} (J_{3,ijk}^{dd}) \\ &\quad - \frac{4 N_{av}^2 \pi^2}{3} \left(\frac{1}{V} \right)^2 \frac{1}{(kT)^3} \sum_i^{nc} \sum_j^{nc} \sum_k^{nc} n_i n_j n_k \frac{n_{pi} n_{pj} n_{pk}}{m_i m_j m_k} \frac{\mu_i^2 \mu_j^2 \mu_k^2}{\sigma_{ij} \sigma_{jk} \sigma_{ik}} \cdot \frac{\partial^2}{\partial n_f \partial n_g} (J_{3,ijk}^{dd}) \end{aligned} \quad (F-326)$$

$$\frac{\partial}{\partial n_k} (J_{2,ij}^{dd}) = w \cdot \sum_{w=0}^4 \left(a_{n,ij} + b_{n,ij} \frac{\epsilon_{ij}}{kT} \right) \eta^{w-1} \cdot \frac{\partial}{\partial n_k} (\eta) \quad (F-327)$$

$$\frac{\partial}{\partial n_k} (J_{3,ijk}^{dd}) = w \cdot \sum_{w=0}^4 c_{n,ijk} \eta^{w-1} \cdot \frac{\partial}{\partial n_k} (\eta)$$

F.9.3 Second-order derivatives

i) Temperature – Temperature

$$\frac{\partial^2}{\partial T^2} (F_{2,mix}^{dipolar}) = -\frac{6 \cdot N_{av}}{V} \frac{\pi}{(kT)^2 \cdot T^2} \sum_i^{nc} \sum_j^{nc} n_i n_j \frac{n_{pi} n_{pj}}{m_i m_j} \frac{\mu_i^2 \mu_j^2}{\sigma_{ij}^3} J_{2,ij}^{dd} \quad (F-328)$$

$$+ \frac{4 \cdot N_{av}}{V} \frac{\pi}{(kT)^2 \cdot T} \sum_i^{nc} \sum_j^{nc} n_i n_j \frac{n_{pi} n_{pj}}{m_i m_j} \frac{\mu_i^2 \mu_j^2}{\sigma_{ij}^3} \cdot \frac{\partial}{\partial T} (J_{2,ij}^{dd})$$

$$- \frac{N_{av}}{V} \frac{\pi}{(kT)^2} \sum_i^{nc} \sum_j^{nc} n_i n_j \frac{n_{pi} n_{pj}}{m_i m_j} \frac{\mu_i^2 \mu_j^2}{\sigma_{ij}^3} \cdot \frac{\partial^2}{\partial T^2} (J_{2,ij}^{dd})$$

$$\frac{\partial^2}{\partial T^2} (F_{3,ijk}^{dd}) = -\frac{4 \cdot 12 \cdot N_{av}^2 \pi^2}{3} \left(\frac{1}{V} \right)^2 \frac{1}{(kT)^3 \cdot T^2} \sum_i^{nc} \sum_j^{nc} \sum_k^{nc} n_i n_j n_k \frac{n_{pi} n_{pj} n_{pk}}{m_i m_j m_k} \frac{\mu_i^2 \mu_j^2 \mu_k^2}{\sigma_{ij} \sigma_{jk} \sigma_{ik}} J_{3,ijk}^{dd} \quad (F-329)$$

$$+ \frac{4 \cdot 6 \cdot N_{av}^2 \pi^2}{3} \left(\frac{1}{V} \right)^2 \frac{1}{(kT)^3 \cdot T} \sum_i^{nc} \sum_j^{nc} \sum_k^{nc} n_i n_j n_k \frac{n_{pi} n_{pj} n_{pk}}{m_i m_j m_k} \frac{\mu_i^2 \mu_j^2 \mu_k^2}{\sigma_{ij} \sigma_{jk} \sigma_{ik}} \cdot \frac{\partial}{\partial T} (J_{3,ijk}^{dd})$$

$$- \frac{4 \cdot N_{av}^2 \pi^2}{3} \left(\frac{1}{V} \right)^2 \frac{1}{(kT)^3} \sum_i^{nc} \sum_j^{nc} \sum_k^{nc} n_i n_j n_k \frac{n_{pi} n_{pj} n_{pk}}{m_i m_j m_k} \frac{\mu_i^2 \mu_j^2 \mu_k^2}{\sigma_{ij} \sigma_{jk} \sigma_{ik}} \cdot \frac{\partial^2}{\partial T^2} (J_{3,ijk}^{dd})$$

$$\frac{\partial^2}{\partial T^2} (J_{2,ij}^{dd}) = 2 \cdot \sum_{w=0}^4 \left(b_{n,ij} \frac{\mathcal{E}_{ij}}{kT^3} \right) \eta^w - 2 \cdot w \cdot \sum_{w=0}^4 \left(b_{n,ij} \frac{\mathcal{E}_{ij}}{kT^2} \right) \eta^{w-1} \cdot \frac{\partial}{\partial T} (\eta) \quad (F-330)$$

$$+ w \cdot (w-1) \cdot \sum_{w=0}^4 \left(a_{n,ij} + b_{n,ij} \frac{\mathcal{E}_{ij}}{kT} \right) \eta^{w-2} \cdot \frac{\partial}{\partial T} (\eta)^2$$

$$+ w \cdot \sum_{w=0}^4 \left(a_{n,ij} + b_{n,ij} \frac{\mathcal{E}_{ij}}{kT} \right) \eta^{w-1} \cdot \frac{\partial}{\partial T} (\eta)$$

$$\frac{\partial^2}{\partial T \partial T} (J_{3,ijk}^{dd}) = (w-1) \cdot w \cdot \sum_{w=0}^4 c_{n,ijk} \eta^{w-2} \cdot \frac{\partial}{\partial T} (\eta) \cdot \frac{\partial}{\partial T} (\eta) \quad (F-331)$$

$$+ w \cdot \sum_{w=0}^4 c_{n,ijk} \eta^{w-1} \cdot \frac{\partial^2}{\partial T \partial T} (\eta)$$

ii) Temperature – Volume

$$\frac{\partial^2}{\partial T \partial V} (F_{2,mix}^{dd}) = -\frac{2 \cdot N_{av}}{V^2} \frac{\pi}{(kT)^2 \cdot T} \sum_i^{nc} \sum_j^{nc} n_i n_j \frac{n_{pi} n_{pj}}{m_i m_j} \frac{\mu_i^2 \mu_j^2}{\sigma_{ij}^3} J_{2,ij}^{dd} \quad (F-332)$$

$$+ \frac{2 \cdot N_{av}}{V} \frac{\pi}{(kT)^2 \cdot T} \sum_i^{nc} \sum_j^{nc} n_i n_j \frac{n_{pi} n_{pj}}{m_i m_j} \frac{\mu_i^2 \mu_j^2}{\sigma_{ij}^3} \cdot \frac{\partial}{\partial V} (J_{2,ij}^{dd})$$

$$+ \frac{N_{av}}{V^2} \frac{\pi}{(kT)^2} \sum_i^{nc} \sum_j^{nc} n_i n_j \frac{n_{pi} n_{pj}}{m_i m_j} \frac{\mu_i^2 \mu_j^2}{\sigma_{ij}^3} \cdot \frac{\partial}{\partial T} (J_{2,ij}^{dd})$$

$$- \frac{N_{av}}{V} \frac{\pi}{(kT)^2} \sum_i^{nc} \sum_j^{nc} n_i n_j \frac{n_{pi} n_{pj}}{m_i m_j} \frac{\mu_i^2 \mu_j^2}{\sigma_{ij}^3} \cdot \frac{\partial^2}{\partial T \partial V} (J_{2,ij}^{dd})$$

$$\frac{\partial^2}{\partial T \partial V} (F_{3,mix}^{dd}) = -\frac{4 \cdot 6 \cdot N_{av}^2 \pi^2}{3} \left(\frac{1}{V} \right)^3 \frac{1}{(kT)^3 \cdot T} \sum_i^{nc} \sum_j^{nc} \sum_k^{nc} n_i n_j n_k \frac{n_{pi} n_{pj} n_{pk}}{m_i m_j m_k} \frac{\mu_i^2 \mu_j^2 \mu_k^2}{\sigma_{ij} \sigma_{jk} \sigma_{ik}} J_{3,ijk}^{dd} \quad (F-333)$$

$$+ \frac{4 \cdot 3 \cdot N_{av}^2 \pi^2}{3} \left(\frac{1}{V} \right)^2 \frac{1}{(kT)^3 \cdot T} \sum_i^{nc} \sum_j^{nc} \sum_k^{nc} n_i n_j n_k \frac{n_{pi} n_{pj} n_{pk}}{m_i m_j m_k} \frac{\mu_i^2 \mu_j^2 \mu_k^2}{\sigma_{ij} \sigma_{jk} \sigma_{ik}} \cdot \frac{\partial}{\partial V} (J_{3,ijk}^{dd})$$

$$+ \frac{4 \cdot 2 \cdot N_{av}^2 \pi^2}{3} \left(\frac{1}{V} \right)^3 \frac{1}{(kT)^3} \sum_i^{nc} \sum_j^{nc} \sum_k^{nc} n_i n_j n_k \frac{n_{pi} n_{pj} n_{pk}}{m_i m_j m_k} \frac{\mu_i^2 \mu_j^2 \mu_k^2}{\sigma_{ij} \sigma_{jk} \sigma_{ik}} \cdot \frac{\partial}{\partial T} (J_{3,ijk}^{dd})$$

$$- \frac{4 N_{av}^2 \pi^2}{3} \left(\frac{1}{V} \right)^3 \frac{1}{(kT)^3} \sum_i^{nc} \sum_j^{nc} \sum_k^{nc} n_i n_j n_k \frac{n_{pi} n_{pj} n_{pk}}{m_i m_j m_k} \frac{\mu_i^2 \mu_j^2 \mu_k^2}{\sigma_{ij} \sigma_{jk} \sigma_{ik}} \cdot \frac{\partial^2}{\partial T \partial V} (J_{3,ijk}^{dd})$$

$$\frac{\partial^2}{\partial T \partial V} (J_{2,ij}^{dd}) = -w \cdot \sum_{w=0}^4 \left(b_{n,ij} \frac{\varepsilon_{ij}}{kT^2} \right) \eta^{w-1} \cdot \frac{\partial}{\partial V} (\eta) \quad (F-334)$$

$$+ w \cdot (w-1) \cdot \sum_{w=0}^4 \left(a_{n,ij} + b_{n,ij} \frac{\varepsilon_{ij}}{kT} \right) \eta^{w-2} \cdot \frac{\partial}{\partial T} (\eta) \cdot \frac{\partial}{\partial V} (\eta)$$

$$+ w \cdot \sum_{w=0}^4 \left(a_{n,ij} + b_{n,ij} \frac{\varepsilon_{ij}}{kT} \right) \eta^{w-1} \cdot \frac{\partial^2}{\partial V \partial T} (\eta)$$

$$\frac{\partial^2}{\partial T \partial V} (J_{3,ijk}^{dd}) = (w-1) \cdot w \cdot \sum_{w=0}^4 c_{n,ijk} \eta^{w-2} \cdot \frac{\partial}{\partial T} (\eta) \cdot \frac{\partial}{\partial V} (\eta) \quad (F-335)$$

$$+ w \cdot \sum_{w=0}^4 c_{n,ijk} \eta^{w-1} \cdot \frac{\partial^2}{\partial T \partial V} (\eta)$$

iii) Temperature – Composition

$$\frac{\partial^2}{\partial T \partial n_k} (F_{2,mix}^{dipolar}) = \frac{2 \cdot 2 \cdot N_{av}}{V} \frac{\pi}{(kT)^2 \cdot T} \sum_i^{nc} n_i \frac{n_{pi} n_{pk}}{m_i m_k} \frac{\mu_i^2 \mu_k^2}{\sigma_{ik}^3} J_{2,ij}^{dd} \quad (F-336)$$

$$+ \frac{2 \cdot N_{av}}{V} \frac{\pi}{(kT)^2 \cdot T} \sum_i^{nc} \sum_j^{nc} n_i n_j \frac{n_{pi} n_{pj}}{m_i m_j} \frac{\mu_i^2 \mu_j^2}{\sigma_{ij}^3} \cdot \frac{\partial}{\partial n_k} (J_{2,ij}^{dd})$$

$$- \frac{2 \cdot N_{av}}{V} \frac{\pi}{(kT)^2} \sum_i^{nc} n_i \frac{n_{pi} n_{pk}}{m_i m_k} \frac{\mu_i^2 \mu_k^2}{\sigma_{ik}^3} \cdot \frac{\partial}{\partial T} (J_{2,ij}^{dd})$$

$$- \frac{N_{av}}{V} \frac{\pi}{(kT)^2} \sum_i^{nc} \sum_j^{nc} n_i n_j \frac{n_{pi} n_{pj}}{m_i m_j} \frac{\mu_i^2 \mu_j^2}{\sigma_{ij}^3} \cdot \frac{\partial^2}{\partial T \partial n_k} (J_{2,ij}^{dd})$$

$$\frac{\partial^2}{\partial T \partial n_f} (F_{3,mix}^{dd}) = \frac{4 \cdot 3 \cdot 3 \cdot N_{av}^2 \pi^2}{3} \left(\frac{1}{V} \right)^2 \frac{1}{(kT)^3 \cdot T} \sum_i^{nc} \sum_j^{nc} n_i n_j \frac{n_{pi} n_{pj} n_{pf}}{m_i m_j m_f} \frac{\mu_i^2 \mu_j^2 \mu_f^2}{\sigma_{ij} \sigma_{jf} \sigma_{if}} J_{3,ijk}^{dd} \quad (F-337)$$

$$+ \frac{4 \cdot 3 N_{av}^2 \pi^2}{3} \left(\frac{1}{V} \right)^2 \frac{1}{(kT)^3 \cdot T} \sum_i^{nc} \sum_j^{nc} \sum_k^{nc} n_i n_j n_k \frac{n_{pi} n_{pj} n_{pk}}{m_i m_j m_k} \frac{\mu_i^2 \mu_j^2 \mu_k^2}{\sigma_{ij} \sigma_{jk} \sigma_{ik}} \cdot \frac{\partial}{\partial n_f} (J_{3,ijk}^{dd})$$

$$- \frac{4 \cdot 3 \cdot N_{av}^2 \pi^2}{3} \left(\frac{1}{V} \right)^2 \frac{1}{(kT)^3} \sum_i^{nc} \sum_j^{nc} n_i n_j \frac{n_{pi} n_{pj} n_{pf}}{m_i m_j m_f} \frac{\mu_i^2 \mu_j^2 \mu_f^2}{\sigma_{ij} \sigma_{jf} \sigma_{if}} \cdot \frac{\partial}{\partial T} (J_{3,ijk}^{dd})$$

$$- \frac{4 N_{av}^2 \pi^2}{3} \left(\frac{1}{V} \right)^2 \frac{1}{(kT)^3} \sum_i^{nc} \sum_j^{nc} \sum_k^{nc} n_i n_j n_k \frac{n_{pi} n_{pj} n_{pk}}{m_i m_j m_k} \frac{\mu_i^2 \mu_j^2 \mu_k^2}{\sigma_{ij} \sigma_{jk} \sigma_{ik}} \cdot \frac{\partial^2}{\partial T \partial n_f} (J_{3,ijk}^{dd})$$

$$\frac{\partial^2}{\partial T \partial n_k} (J_{2,ij}^{dd}) = -w \cdot \sum_{w=0}^4 \left(b_{n,ij} \frac{\epsilon_{ij}}{kT^2} \right) \eta^{w-1} \cdot \frac{\partial}{\partial n_k} (\eta) \quad (F-338)$$

$$+ w \cdot (w-1) \cdot \sum_{w=0}^4 \left(a_{n,ij} + b_{n,ij} \frac{\epsilon_{ij}}{kT} \right) \eta^{w-2} \cdot \frac{\partial}{\partial T} (\eta) \cdot \frac{\partial}{\partial n_k} (\eta)$$

$$+ w \cdot \sum_{w=0}^4 \left(a_{n,ij} + b_{n,ij} \frac{\epsilon_{ij}}{kT} \right) \eta^{w-1} \cdot \frac{\partial^2}{\partial n_k \partial T} (\eta)$$

$$\frac{\partial^2}{\partial T \partial n_k} (J_{3,ijk}^{dd}) = (w-1) \cdot w \cdot \sum_{w=0}^4 c_{n,ijk} \eta^{w-2} \cdot \frac{\partial}{\partial T} (\eta) \cdot \frac{\partial}{\partial n_k} (\eta) \quad (F-339)$$

$$+ w \cdot \sum_{w=0}^4 c_{n,ijk} \eta^{w-1} \cdot \frac{\partial^2}{\partial T \partial n_k} (\eta)$$

iv) Volume – Volume

$$\frac{\partial^2}{\partial V^2} (F_{2,mix}^{dd}) = -\frac{2 \cdot N_{av}}{V^3} \frac{\pi}{(kT)^2} \sum_i^{nc} \sum_j^{nc} n_i n_j \frac{n_{pi} n_{pj}}{m_i m_j} \frac{\mu_i^2 \mu_j^2}{\sigma_{ij}^3} J_{2,ij}^{dd} \quad (F-340)$$

$$+ \frac{2 \cdot N_{av}}{V^2} \frac{\pi}{(kT)^2} \sum_i^{nc} \sum_j^{nc} n_i n_j \frac{n_{pi} n_{pj}}{m_i m_j} \frac{\mu_i^2 \mu_j^2}{\sigma_{ij}^3} \cdot \frac{\partial}{\partial V} (J_{2,ij}^{dd})$$

$$- \frac{N_{av}}{V} \frac{\pi}{(kT)^2} \sum_i^{nc} \sum_j^{nc} n_i n_j \frac{n_{pi} n_{pj}}{m_i m_j} \frac{\mu_i^2 \mu_j^2}{\sigma_{ij}^3} \cdot \frac{\partial^2}{\partial V^2} (J_{2,ij}^{dd})$$

$$\frac{\partial^2}{\partial V^2} (F_{3,mix}^{dd}) = -\frac{6 \cdot 4 \cdot N_{av}^2 \pi^2}{3} \left(\frac{1}{V} \right)^4 \frac{1}{(kT)^3} \sum_i^{nc} \sum_j^{nc} \sum_k^{nc} n_i n_j n_k \frac{n_{pi} n_{pj} n_{pk}}{m_i m_j m_k} \frac{\mu_i^2 \mu_j^2 \mu_k^2}{\sigma_{ij} \sigma_{jk} \sigma_{ik}} J_{3,ijk}^{dd} \quad (F-341)$$

$$+ \frac{4 \cdot 4 \cdot N_{av}^2 \pi^2}{3} \left(\frac{1}{V} \right)^3 \frac{1}{(kT)^3} \sum_i^{nc} \sum_j^{nc} \sum_k^{nc} n_i n_j n_k \frac{n_{pi} n_{pj} n_{pk}}{m_i m_j m_k} \frac{\mu_i^2 \mu_j^2 \mu_k^2}{\sigma_{ij} \sigma_{jk} \sigma_{ik}} \cdot \frac{\partial}{\partial V} (J_{3,ijk}^{dd})$$

$$- \frac{4 N_{av}^2 \pi^2}{3} \left(\frac{1}{V} \right)^2 \frac{1}{(kT)^3} \sum_i^{nc} \sum_j^{nc} \sum_k^{nc} n_i n_j n_k \frac{n_{pi} n_{pj} n_{pk}}{m_i m_j m_k} \frac{\mu_i^2 \mu_j^2 \mu_k^2}{\sigma_{ij} \sigma_{jk} \sigma_{ik}} \cdot \frac{\partial^2}{\partial V^2} (J_{3,ijk}^{dd})$$

$$\frac{\partial^2}{\partial V^2} (J_{2,ij}^{dd}) = w \cdot (w-1) \sum_{w=0}^4 \left(a_{n,ij} + b_{n,ij} \frac{\epsilon_{ij}}{kT} \right) \eta^{w-2} \cdot \frac{\partial}{\partial V} (\eta)^2 \quad (F-342)$$

$$+ w \cdot \sum_{w=0}^4 \left(a_{n,ij} + b_{n,ij} \frac{\epsilon_{ij}}{kT} \right) \eta^{w-1} \cdot \frac{\partial^2}{\partial V^2} (\eta)$$

(F-343)

$$\frac{\partial^2}{\partial V \partial V} (J_{3,ijk}^{dd}) = (w-1) \cdot w \cdot \sum_{w=0}^4 c_{n,ijk} \eta^{w-2} \cdot \frac{\partial}{\partial V} (\eta) \cdot \frac{\partial}{\partial V} (\eta)$$

$$+ w \cdot \sum_{w=0}^4 c_{n,ijk} \eta^{w-1} \cdot \frac{\partial^2}{\partial V \partial V} (\eta)$$

v) Volume – composition

$$\frac{\partial^2}{\partial V \partial n_k} (F_{2,mix}^{dd}) = \frac{2 \cdot N_{av}}{V^2} \frac{\pi}{(kT)^2} \sum_i^{nc} n_i \frac{n_{pi} n_{pk}}{m_i m_k} \frac{\mu_i^2 \mu_k^2}{\sigma_{ik}^3} J_{2,ij}^{dd} \quad (F-344)$$

$$+ \frac{N_{av}}{V^2} \frac{\pi}{(kT)^2} \sum_i^{nc} \sum_j^{nc} n_i n_j \frac{n_{pi} n_{pj}}{m_i m_j} \frac{\mu_i^2 \mu_j^2}{\sigma_{ij}^3} \cdot \frac{\partial}{\partial n_k} (J_{2,ij}^{dd})$$

$$- \frac{2 \cdot N_{av}}{V} \frac{\pi}{(kT)^2} \sum_i^{nc} n_i \frac{n_{pi} n_{pk}}{m_i m_k} \frac{\mu_i^2 \mu_k^2}{\sigma_{ik}^3} \cdot \frac{\partial}{\partial V} (J_{2,ij}^{dd})$$

$$- \frac{N_{av}}{V} \frac{\pi}{(kT)^2} \sum_i^{nc} \sum_j^{nc} n_i n_j \frac{n_{pi} n_{pj}}{m_i m_j} \frac{\mu_i^2 \mu_j^2}{\sigma_{ij}^3} \cdot \frac{\partial^2}{\partial V \partial n_k} (J_{2,ij}^{dd})$$

$$\begin{aligned}
 \frac{\partial^2}{\partial V \partial n_f} (F_{3,mix}^{dipolar}) = & \frac{4 \cdot 2 \cdot 3 \cdot N_{av}^2 \pi^2}{3} \left(\frac{1}{V} \right)^3 \frac{1}{(kT)^3} \sum_i^{nc} \sum_j^{nc} n_i n_j \frac{n_{pi} n_{pj} n_{pf}}{m_i m_j m_f} \frac{\mu_i^2 \mu_j^2 \mu_f^2}{\sigma_{ij} \sigma_{jf} \sigma_{if}} J_{3,ijk}^{dd} \\
 & + \frac{4 \cdot 2 \cdot N_{av}^2 \pi^2}{3} \left(\frac{1}{V} \right)^3 \frac{1}{(kT)^3} \sum_i^{nc} \sum_j^{nc} \sum_k^{nc} n_i n_j n_k \frac{n_{pi} n_{pj} n_{pk}}{m_i m_j m_k} \frac{\mu_i^2 \mu_j^2 \mu_k^2}{\sigma_{ij} \sigma_{jk} \sigma_{ik}} \cdot \frac{\partial}{\partial n_f} (J_{3,ijk}^{dd}) \\
 & - \frac{4 \cdot 3 \cdot N_{av}^2 \pi^2}{3} \left(\frac{1}{V} \right)^2 \frac{1}{(kT)^3} \sum_i^{nc} \sum_j^{nc} n_i n_j \frac{n_{pi} n_{pj} n_{pf}}{m_i m_j m_f} \frac{\mu_i^2 \mu_j^2 \mu_f^2}{\sigma_{ij} \sigma_{jf} \sigma_{if}} \cdot \frac{\partial}{\partial V} (J_{3,ijk}^{dd}) \\
 & - \frac{4 N_{av}^2 \pi^2}{3} \left(\frac{1}{V} \right)^2 \frac{1}{(kT)^3} \sum_i^{nc} \sum_j^{nc} \sum_k^{nc} n_i n_j n_k \frac{n_{pi} n_{pj} n_{pk}}{m_i m_j m_k} \frac{\mu_i^2 \mu_j^2 \mu_k^2}{\sigma_{ij} \sigma_{jk} \sigma_{ik}} \cdot \frac{\partial^2}{\partial V \partial n_f} (J_{3,ijk}^{dd})
 \end{aligned} \tag{F-345}$$

$$\begin{aligned}
 \frac{\partial^2}{\partial V \partial n_k} (J_{2,ij}^{dd}) = & w \cdot (w-1) \sum_{w=0}^4 \left(a_{n,ij} + b_{n,ij} \frac{\varepsilon_{ij}}{kT} \right) \eta^{w-2} \cdot \frac{\partial}{\partial V} (\eta) \cdot \frac{\partial}{\partial n_k} (\eta) \\
 & + w \cdot \sum_{w=0}^4 \left(a_{n,ij} + b_{n,ij} \frac{\varepsilon_{ij}}{kT} \right) \eta^{w-1} \cdot \frac{\partial^2}{\partial V \partial n_k} (\eta)
 \end{aligned} \tag{F-346}$$

$$\begin{aligned}
 \frac{\partial^2}{\partial T \partial n_k} (J_{3,ijk}^{dd}) = & (w-1) \cdot w \cdot \sum_{w=0}^4 c_{n,ijk} \eta^{w-2} \cdot \frac{\partial}{\partial T} (\eta) \cdot \frac{\partial}{\partial n_k} (\eta) \\
 & + w \cdot \sum_{w=0}^4 c_{n,ijk} \eta^{w-1} \cdot \frac{\partial^2}{\partial T \partial n_k} (\eta)
 \end{aligned} \tag{F-347}$$

vi) Composition - composition

$$\begin{aligned}
 \frac{\partial^2}{\partial n_k \partial n_l} (F_{2,mix}^{dd}) = & - \frac{2 \cdot N_{av}}{V} \frac{\pi}{(kT)^2} \frac{n_{pk} n_{pl}}{m_k m_l} \frac{\mu_k^2 \mu_l^2}{\sigma_{kl}^3} J_{2,ij}^{dd} \\
 & - \frac{2 \cdot N_{av}}{V} \frac{\pi}{(kT)^2} \sum_i^{nc} n_i \frac{n_{pi} n_{pk}}{m_i m_k} \frac{\mu_i^2 \mu_k^2}{\sigma_{ik}^3} \cdot \frac{\partial}{\partial n_l} (J_{2,ij}^{dd}) \\
 & - \frac{2 \cdot N_{av}}{V} \frac{\pi}{(kT)^2} \sum_i^{nc} n_i \frac{n_{pi} n_{pl}}{m_i m_l} \frac{\mu_i^2 \mu_l^2}{\sigma_{il}^3} \cdot \frac{\partial}{\partial n_k} (J_{2,ij}^{dd}) \\
 & - \frac{N_{av}}{V} \frac{\pi}{(kT)^2} \sum_i^{nc} \sum_j^{nc} n_i n_j \frac{n_{pi} n_{pj}}{m_i m_j} \frac{\mu_i^2 \mu_j^2}{\sigma_{ij}^3} \cdot \frac{\partial^2}{\partial n_k \partial n_l} (J_{2,ij}^{dd})
 \end{aligned} \tag{F-348}$$

$$\begin{aligned}
 \frac{\partial^2}{\partial n_f \partial n_g} (F_{3,mix}^{dipolar}) = & \frac{5 \cdot (2)}{162} \pi^2 N_{av}^2 \left(\frac{1}{V} \right)^3 \frac{1}{(kT)^3} \sum_i^{nc} n_i m_i m_f m_g x_{pi} x_{pf} x_{pg} \frac{\mu_i^2 \mu_f^2 \mu_g^2}{d_{if} d_{ig} d_{fg}} I_{3,ifg} \\
 & + \frac{5 \cdot (3)}{162} \pi^2 N_{av}^2 \left(\frac{1}{V} \right)^2 \frac{1}{(kT)^3} \sum_i^{nc} \sum_j^{nc} n_i n_j m_i m_j m_f x_{pi} x_{pf} x_{pj} \frac{\mu_i^2 \mu_j^2 \mu_f^2}{d_{ij} d_{jf} d_{if}} \cdot \frac{\partial}{\partial n_g} (I_{3,ijk}) \\
 & + \frac{5 \cdot (3)}{162} \pi^2 N_{av}^2 \left(\frac{1}{V} \right)^2 \frac{1}{(kT)^3} \sum_i^{nc} \sum_j^{nc} n_i n_j m_i m_j m_g x_{pi} x_{pg} x_{pj} \frac{\mu_i^2 \mu_j^2 \mu_g^2}{d_{ij} d_{ig} d_{jg}} \cdot \frac{\partial}{\partial n_f} (I_{3,ijk}) \\
 & + \frac{5}{162} \pi^2 N_{av}^2 \left(\frac{1}{V} \right)^2 \frac{1}{(kT)^3} \sum_i^{nc} \sum_j^{nc} \sum_k^{nc} n_i n_j n_k m_i m_j m_k x_{pi} x_{pj} x_{pk} \frac{\mu_i^2 \mu_j^2 \mu_k^2}{d_{ij} d_{jk} d_{ik}} \cdot \frac{\partial^2}{\partial n_f \partial n_g} (I_{3,ijk})
 \end{aligned} \tag{F-349}$$

$$\begin{aligned} \frac{\partial^2}{\partial n_f \partial n_g} (J_{2,ij}^{dd}) &= w \cdot (w-1) \sum_{w=0}^4 \left(a_{n,ij} + b_{n,ij} \frac{\mathcal{E}_{ij}}{kT} \right) \eta^{w-2} \cdot \frac{\partial}{\partial n_f} (\eta) \cdot \frac{\partial}{\partial n_g} (\eta) \\ &+ w \cdot \sum_{w=0}^4 \left(a_{n,ij} + b_{n,ij} \frac{\mathcal{E}_{ij}}{kT} \right) \eta^{w-1} \cdot \frac{\partial^2}{\partial n_f \partial n_g} (\eta) \end{aligned} \quad (F-350)$$

$$\begin{aligned} \frac{\partial^2}{\partial n_k \partial n_l} (J_{3,ijk}^{dd}) &= (w-1) \cdot w \cdot \sum_{w=0}^4 c_{n,ijk} \eta^{w-2} \cdot \frac{\partial}{\partial n_k} (\eta) \cdot \frac{\partial}{\partial n_l} (\eta) \\ &+ w \cdot \sum_{w=0}^4 c_{n,ijk} \eta^{w-1} \cdot \frac{\partial^2}{\partial n_k \partial n_l} (\eta) \end{aligned} \quad (F-351)$$

Nomenclature

Abbreviations

CPA	Cubic-Plus-Association
EOS	Equation-of-state
GV	Gross and Vrabec
hcb	Hard-convex-body
JC	Jog and Chapman
KSE	Karakatsani , Spyriouni, Economou
OPLS	Optimized Intermolecular Potential Functions for Liquid Alcohols
PC-SAFT	Perturbed Chain - Statistical Associating Fluid Theory
PR	Peng-Robinson
RDF	Radial Distribution Function
SAFT	Statistical Associating Fluid Theory
SAFT-CP	Statistical Associating Fluid Theory across Critical Points
SAFT-VR Mie	Statistical Associating Fluid Theory Variable range Mie potential
Soft-SAFT	Soft Statistical Associating Fluid Theory
sPC-SAFT	Simplified Perturbed Chain - Statistical Associating Fluid Theory
SRK	Soave-Redlich-Kwong
TIP4P	Transferable intermolecular potential function with 4 sites
TIP5P	Transferable intermolecular potential function with 5 sites
tKE	Truncated Karakatsani and Economou
%AAD	Percentage Absolute Average Deviation

Symbols

A	Helmholtz free energy
B	Parameter in general cubic equation of state
C_1	Compressibility expression in PC-SAFT
C_p	Isobaric heat capacity
C_v	Isochoric heat capacity
D	Parameter in general cubic equation-of-state
F	Reduced residual Helmholtz free energy Force between molecule
H	Enthalpy
H_{kl}	Hessian in Michelsen's solution to fraction non-bonded molecules
$I_1(\eta, m), I_2(\eta, m)$	Perturbation theory integrals in PC-SAFT
$I_{2,ii}(\rho^*), I_{3,iii}(\rho^*)$	Angular pair and triplet correlations function in the dipolar term of Jog and Chapman
$J_{2,ij}^{dd}, J_{3,ijk}^{dd}$	Angular pair and triplet correlations function in the dipolar term of Gross and Co-workers
M	Number of association sites on a molecule
M_w	Molecular weight
N_{av}	Avogadro's number = 6.0221415×10^{23}
OF	Objective function in regression procedure
P	Pressure
P_c	Critical pressure
Q	Quadrupole moment
\tilde{Q}	Reduced quadrupole moment
$Q(T, V, \mathbf{X}, \mathbf{n})$	Michelsen's function to account for association
R	Universal gas constant
S	Entropy
T	Temperature
\tilde{T}	Reduced temperature

Symbols

T_c	Critical temperature
V	Total molar volume
X_{Ai}	Fraction on non-bonded molecules at site A on molecule i
Z	Compressibility factor
a	Attraction energy parameter in general cubic equation-of-state
a_0	Temperature independent energy parameter in CPA
$a_{n,ij}$	Model constants used in PC-SAFT and polar terms of Gross-and Co-workers
$a_i(m)$	Used in perturbation theory integrals in PC-SAFT
b	Co-volume energy parameter in general cubic equation-of-state
$b_{n,ij}$	Model constants used in PC-SAFT and polar terms of Gross-and Co-workers
$b_i(m)$	Used in perturbation theory integrals in PC-SAFT
c_1	Parameter characterising temperature dependency of energy parameter in CPA
$c_{n,ijk}$	Model constants used in PC-SAFT and polar terms of Gross-and Co-workers
d	Temperature dependent segment diameter in SAFT
f	Fugacity
g	Radial distribution function
k	Boltzmann constant
k_{ij}	Binary interaction parameter between component i and j
m	Segment number in SAFT models Function Peng-Robinson based CPA
n	Mole numbers
np	Number of data points
n_{pi}	Number of dipolar segments on chain molecule in dipole term of Gross and Co-workers
n_{qi}	Number of dipolar segments on chain molecule in quadrupole term of Gross and Co-workers
r	Separation distance between molecules

Symbols

u	Speed of sound
w	Regression weight in objective function
x	Mole fraction Experimental data point in %ADD definition
x_p^2	Fraction of dipolar segments on the chain molecule in Jog and Chapman's polar term

Greek symbols

α	Polarizability
$\tilde{\alpha}$	Reduced polarizability
α_p	Isobaric thermal expansivity
$\alpha(T)_{SRK}, \alpha(T)_{PR}, \alpha_{CPA,PR}(T)$	Temperature function in energy parameter of SRK and Peng-Robinson and Peng-Robinson based CPA
β_T	Isothermal compressibility
β_s	Isentropic compressibility
γ	Adiabatic index (heat capacity ratio)
$\Delta^{A_i B_j}$	Association strength between site A on molecule i and site B on molecule j
$\epsilon^{A_i B_j}$	Association energy between site A on molecule i and site B on molecule j in SAFT and CPA
ϵ	Dispersion energy parameter in PC-SAFT
η	Reduced density in SAFT models Joule-Thomson coefficient
$\kappa^{A_i B_j}$	Association volume between site A on molecule i and site B on molecule j in SAFT
μ	Dipole moment
$\tilde{\mu}$	Reduced dipole moment
ζ_n	Used in mixture hard-sphere term of PC-SAFT
π	Pi = 3.14159
ρ	Molar density
σ	Temperature independent segment diameter in SAFT

Greek symbols

σ_p	Effective polar interaction diameter in polar term of Karakatsani and Economou
ν	Specific molar volume
$\hat{\phi}_i$	Fugacity coefficient of component i in mixture.
ω	Acentric factor Regression weights Damping factor in $Q(T, V, \mathbf{X}, \mathbf{n})$

Superscripts

E	Indicates excess property
$assoc$	Indicates contribution due to association
$calc$	Calculated value in %AAD definition
$chain$	Indicates contribution due to chain formation
$comp$	Indicates property in the compressed liquid phase
$dipolar$	Indicates contribution due dipolar interactions
$dipole - quadrupole$	Indicates contribution due to dipole-quadrupole forces
exp	Experimental data point in %AAD definition
hcb	Indicates hard-convex-body contribution
hs	Indicates hard-sphere contribution
$ideal$	Indicates ideal property
ind	Indicate scontribution due to induction forces
$polar$	Indicates polar contribution
$quadrupolar$	Indicates contribution due to quadrupolar forces
ref	Indicates reference contribution
r	Indicates residual property
sat	Indicates property at saturated conditions
seg	Indicates segment contribution
$vaporization$	Indicates heat of vapourisation

Subscripts

i, j	Indicates property of component i, j
mix	Indicates property in mixture
$total$	Indicates total moles in system